frontiers | Research Topics

Innovative solutions for next-generation fertilizers

Edited by
Mohamed Ait-El-Mokhtar, Marouane Baslam and Raffaella Maria Balestrini

Published in
Frontiers in Sustainable Food Systems

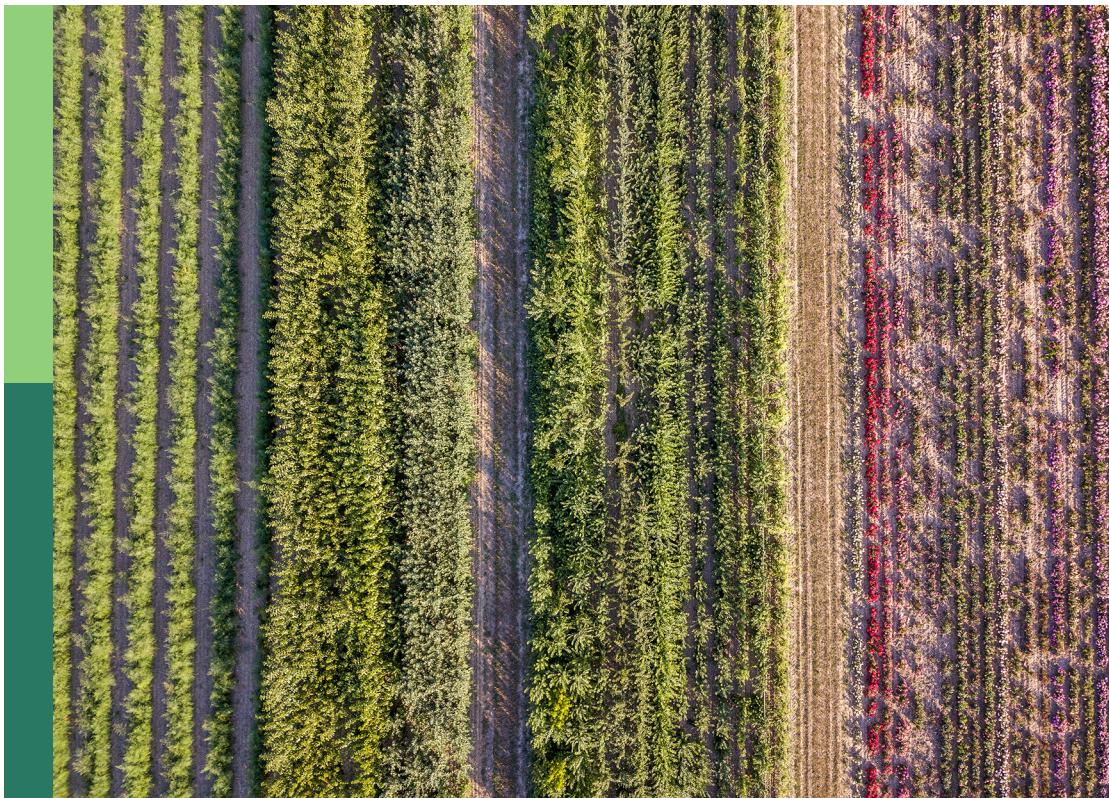

FRONTIERS EBOOK COPYRIGHT STATEMENT

The copyright in the text of individual articles in this ebook is the property of their respective authors or their respective institutions or funders. The copyright in graphics and images within each article may be subject to copyright of other parties. In both cases this is subject to a license granted to Frontiers.

The compilation of articles constituting this ebook is the property of Frontiers.

Each article within this ebook, and the ebook itself, are published under the most recent version of the Creative Commons CC-BY licence. The version current at the date of publication of this ebook is CC-BY 4.0. If the CC-BY licence is updated, the licence granted by Frontiers is automatically updated to the new version.

When exercising any right under the CC-BY licence, Frontiers must be attributed as the original publisher of the article or ebook, as applicable.

Authors have the responsibility of ensuring that any graphics or other materials which are the property of others may be included in the CC-BY licence, but this should be checked before relying on the CC-BY licence to reproduce those materials. Any copyright notices relating to those materials must be complied with.

Copyright and source acknowledgement notices may not be removed and must be displayed in any copy, derivative work or partial copy which includes the elements in question.

All copyright, and all rights therein, are protected by national and international copyright laws. The above represents a summary only. For further information please read Frontiers' Conditions for Website Use and Copyright Statement, and the applicable CC-BY licence.

ISSN 1664-8714
ISBN 978-2-8325-6945-0
DOI 10.3389/978-2-8325-6945-0

Generative AI statement
Any alternative text (Alt text) provided alongside figures in the articles in this ebook has been generated by Frontiers with the support of artificial intelligence and reasonable efforts have been made to ensure accuracy, including review by the authors wherever possible. If you identify any issues, please contact us.

About Frontiers

Frontiers is more than just an open access publisher of scholarly articles: it is a pioneering approach to the world of academia, radically improving the way scholarly research is managed. The grand vision of Frontiers is a world where all people have an equal opportunity to seek, share and generate knowledge. Frontiers provides immediate and permanent online open access to all its publications, but this alone is not enough to realize our grand goals.

Frontiers journal series

The Frontiers journal series is a multi-tier and interdisciplinary set of open-access, online journals, promising a paradigm shift from the current review, selection and dissemination processes in academic publishing. All Frontiers journals are driven by researchers for researchers; therefore, they constitute a service to the scholarly community. At the same time, the *Frontiers journal series* operates on a revolutionary invention, the tiered publishing system, initially addressing specific communities of scholars, and gradually climbing up to broader public understanding, thus serving the interests of the lay society, too.

Dedication to quality

Each Frontiers article is a landmark of the highest quality, thanks to genuinely collaborative interactions between authors and review editors, who include some of the world's best academicians. Research must be certified by peers before entering a stream of knowledge that may eventually reach the public - and shape society; therefore, Frontiers only applies the most rigorous and unbiased reviews. Frontiers revolutionizes research publishing by freely delivering the most outstanding research, evaluated with no bias from both the academic and social point of view. By applying the most advanced information technologies, Frontiers is catapulting scholarly publishing into a new generation.

What are Frontiers Research Topics?

Frontiers Research Topics are very popular trademarks of the *Frontiers journals series*: they are collections of at least ten articles, all centered on a particular subject. With their unique mix of varied contributions from Original Research to Review Articles, Frontiers Research Topics unify the most influential researchers, the latest key findings and historical advances in a hot research area.

Find out more on how to host your own Frontiers Research Topic or contribute to one as an author by contacting the Frontiers editorial office: frontiersin.org/about/contact

Innovative solutions for next-generation fertilizers

Topic editors

Mohamed Ait-El-Mokhtar — University of Hassan II Casablanca, Morocco

Marouane Baslam — Niigata University, Japan

Raffaella Maria Balestrini — Institute for Sustainable Plant Protection, National Research Council (CNR), Italy

Citation

Ait-El-Mokhtar, M., Baslam, M., Balestrini, R. M., eds. (2025). *Innovative solutions for next-generation fertilizers*. Lausanne: Frontiers Media SA. doi: 10.3389/978-2-8325-6945-0

Table of contents

frontiers | Frontiers in Sustainable Food Systems

TYPE Editorial
PUBLISHED 16 October 2025
DOI 10.3389/fsufs.2025.1711141

Check for updates

OPEN ACCESS

EDITED AND REVIEWED BY
Maryke T. Labuschagne,
University of the Free State, South Africa

*CORRESPONDENCE
Mohamed Ait-El-Mokhtar
✉ mohamed.aitelmokhtar@univh2c.ma
Raffaella Balestrini
✉ raffaellamaria.balestrini@cnr.it
Marouane Baslam
✉ mmm.baslam@gmail.com

RECEIVED 23 September 2025
ACCEPTED 03 October 2025
PUBLISHED 16 October 2025

CITATION
Ait-El-Mokhtar M, Balestrini R and Baslam M (2025) Editorial: Innovative solutions for next-generation fertilizers.
Front. Sustain. Food Syst. 9:1711141.
doi: 10.3389/fsufs.2025.1711141

COPYRIGHT
© 2025 Ait-El-Mokhtar, Balestrini and Baslam. This is an open-access article distributed under the terms of the Creative Commons Attribution License (CC BY). The use, distribution or reproduction in other forums is permitted, provided the original author(s) and the copyright owner(s) are credited and that the original publication in this journal is cited, in accordance with accepted academic practice. No use, distribution or reproduction is permitted which does not comply with these terms.

Editorial: Innovative solutions for next-generation fertilizers

Mohamed Ait-El-Mokhtar[1]*, Raffaella Balestrini[2,3]* and Marouane Baslam[4,5]*

[1]Laboratory of Biotechnology, Agri-Food, Materials, and Environment (LBAME), Department of Biology, Faculty of Science and Techniques—Mohammedia, Hassan II University of Casablanca, Mohammedia, Morocco, [2]Institute for Sustainable Plant Protection, National Research Council (CNR-IPSP), Torino, Italy, [3]Institute of Biosciences and Bioresources, National Research Council (CNR-IBBR), Bari, Italy, [4]Center of Agrobiotechnology and Bioengineering, Research Unit labelled CNRST (Centre AgroBiotech-URL-7 CNRST-05), Cadi Ayyad University, Marrakesh, Morocco, [5]GrowSmart, Paul van Vlissingenstraat 10 F, Amsterdam, Netherlands

KEYWORDS

next-generation fertilizers, nutrient use efficiency, microbial biofertilizers, biostimulants, controlled/slow release fertilizers, nano-fertilizers, nanotechnology in agriculture, sustainable crop production

Editorial on the Research Topic
Innovative solutions for next-generation fertilizers

Feeding a global population approaching 10 billion by 2050 requires not only more food but smarter ways of producing it. Fertilizers remain at the heart of agricultural intensification, yet their current forms contribute heavily to nutrient losses, greenhouse gas emissions, and soil degradation. The challenge is clear: to develop next-generation fertilizers that are efficient, affordable, and environmentally responsible, thereby aligning productivity with sustainability.

The Research Topic "*Innovative Solutions for Next-Generation Fertilizers*" assembled 14 contributions-−13 original research articles and one review—reflecting the breadth of strategies being developed worldwide. Collectively, these studies span microbial biotechnology, nanotechnology, soil amendments, and bioactive inputs for stress tolerance. Together, they form a broad, interdisciplinary picture of how fertilizer research is evolving toward resilient, climate-smart agriculture.

One of the strongest themes in this collection is the role of microbial and bio-based fertilizers. The review by Alori et al. set the stage by discussing the potential of cell-free supernatants (CFS) derived from plant growth-promoting microbes. Unlike live inoculants, which often fail due to survival and formulation challenges, CFS retain bioactive metabolites capable of enhancing plant growth, conferring stress tolerance, and suppressing pathogens. This positions CFS as an underexplored yet promising avenue for sustainable agriculture. Building on this microbial focus, Khattak et al. reported the isolation of *Bacillus velezensis* strain ARF4, which proved highly effective against *Verticillium* wilt in eggplants. The strain produced a suite of antifungal metabolites and hydrolytic enzymes, visibly deforming fungal hyphae, and ultimately reduced disease severity by nearly 70% in greenhouse trials. Such results highlight how biological alternatives can displace fungicides in disease management. Bitire et al. evaluated the inoculation of *Bradyrhizobium japonicum* in Bambara groundnut across two Nigerian regions and cropping seasons. Their findings showed that rhizobial inoculation not only improved plant height and biomass but also significantly increased yields compared with

urea fertilization, demonstrating that biofertilizers can provide affordable, environmentally friendly options for smallholder farmers. Similarly, de Andrade da Silva et al. tested soybean co-inoculation with several plant growth-promoting bacteria, including *Bacillus subtilis* and Streptomyces species. While the yield differences were modest compared with mineral fertilization, the inoculated plants displayed profound shifts in root microbiome composition, particularly enhanced colonization by *Bradyrhizobium*. This suggests that microbial consortia may exert their benefits by reshaping rhizosphere communities rather than direct yield gains. Finally, Barua et al. pioneered a high-throughput microwell recovery array (MRA) platform to identify beneficial microbial consortia within the maize rhizobiome. Using this approach, they uncovered combinations of bacteria—mainly from *Acinetobacter*, *Enterobacter*, and *Serratia* genera—that improved *Azospirillum brasilense* colonization and accelerated maize seedling growth. This study demonstrates a scalable route for assembling robust microbial consortia as next-generation biofertilizers. Together, these works illustrate how the frontier of microbial fertilization lies not in single strains but in engineered communities and metabolite-based solutions designed to deliver consistent results in the field.

Another prominent theme is the development of advanced delivery systems and nanotechnology-enabled fertilizers. Baral et al. investigated nano-ZnO–coated urea combined with green manuring in Basmati rice. Their field trials showed yield increases of over 30% compared to conventional practices, along with improvements in grain quality and nutrient uptake, revealing how nanomaterials can work synergistically with organic soil amendments to optimize nutrient use efficiency. Elshayb et al. took a different approach by formulating chitosan-based NPK nanostructures as foliar applications. Remarkably, they demonstrated that applying chitosan-NPK at 300 ppm allowed for a 30% reduction in synthetic fertilizer use without compromising rice yield or nutrient content. Hu et al., meanwhile, focused on fertilizer application methods by testing localized nitrogen supply (LNS) with controlled-release urea in rice paddies. They showed that root-zone fertilization dramatically increased nitrogen uptake and chlorophyll content while reducing nitrogen leaching by half compared to farmer practices. These findings collectively demonstrate how nanotechnology, controlled-release coatings, and spatially optimized application methods are redefining fertilizer efficiency, moving away from bulk nutrient application toward precision nutrient management.

Soil amendments and nutrient cycling also featured prominently in this Research Topic, reflecting the growing recognition that sustainable fertilization must be rooted in long-term soil health. Zhang et al. investigated the integration of soybean green manure with moderate reductions in synthetic N and P inputs. Their two-season pot study revealed that wheat yields were maintained while soil organic C increased by more than 12%, alongside significant gains in microbial biomass and labile C fractions. Adhikari et al. evaluated the impact of reduced rates of mustard meal and dried molasses in strawberry systems in North Carolina. Even at half the conventional application rates, these organic amendments improved soil bacterial diversity and produced marketable yields comparable to chemical fumigation, demonstrating both economic and ecological benefits. In sugarcane, Bhatt et al. tested polyhalite, a multi-nutrient mineral fertilizer rich in potassium, calcium, magnesium, and sulfur. Their trials showed improved cane yield, better juice quality, and reduced pest incidence compared with muriate of potash, particularly under nutrient-deficient semiarid soils. These contributions underscore the importance of reintroducing organic matter, diversifying nutrient sources, and balancing multi-nutrient deficiencies as part of next-generation fertilizer strategies.

A fourth cluster of studies focused on how innovative fertilizers can confer stress resilience and improve crop quality. Xiao et al. examined silicon foliar sprays during strawberry propagation under high-temperature stress. Their results showed that continuous silicon application improved photosynthesis, enhanced antioxidant enzyme activity, and increased sugar accumulation, with sprayed daughter plants performing best under 43 °C heat stress. In greenhouse sweet pepper, Tahmasebi et al. compared microbial-based fertilizers with conventional chemical programs and found that biological treatments significantly enriched the fruits' nutritional and nutraceutical qualities, including higher antioxidant activity and mineral content. Oddi et al. tested the combined use of arbuscular mycorrhizal fungi inoculation and chito-oligosaccharides in meadow restoration. They observed not only higher root colonization and improved early plant establishment but also greater species evenness and long-term productivity, demonstrating the ecological potential of bioactive fertilizers in biodiversity-based systems. These studies highlight how fertilizers can be designed not only as nutrient suppliers but also as enhancers of resilience, quality, and ecosystem function.

Taken together, the 14 contributions in this Research Topic make clear that next-generation fertilizers are not defined by a single innovation but by the convergence of multiple approaches: microbial inoculants and metabolites, nanostructured carriers, controlled-release formulations, organic and mineral amendments, and bioactives that confer stress tolerance and quality benefits. A unifying message is that the fertilizers of the future must not only feed crops but also regenerate soils, strengthen resilience, and reduce environmental impacts.

Looking ahead, the central challenge lies in scaling these solutions. Laboratory and greenhouse successes must be validated under real-world conditions, adapted to diverse agro-ecological zones, and made affordable for smallholder farmers. Policy frameworks, farmer-centered innovation, and interdisciplinary collaboration will be critical to ensure that these technologies are not only developed but also deployed at scale.

We thank all contributing authors and reviewers for their invaluable efforts. This Research Topic demonstrates that fertilizers can no longer be regarded as simple yield enhancers but must be seen as tools for sustainability, resilience, and food security in the decades ahead.

Author contributions

MA-E-M: Writing – original draft. RB: Writing – review & editing. MB: Writing – review & editing.

Conflict of interest

The authors declare that the research was conducted in the absence of any commercial or financial relationships that could be construed as a potential conflict of interest.

The author(s) declared that they were an editorial board member of Frontiers, at the time of submission. This had no impact on the peer review process and the final decision.

Generative AI statement

The author(s) declare that no Gen AI was used in the creation of this manuscript.

Any alternative text (alt text) provided alongside figures in this article has been generated by Frontiers with the support of artificial intelligence and reasonable efforts have been made to ensure accuracy, including review by the authors wherever possible. If you identify any issues, please contact us.

Publisher's note

All claims expressed in this article are solely those of the authors and do not necessarily represent those of their affiliated organizations, or those of the publisher, the editors and the reviewers. Any product that may be evaluated in this article, or claim that may be made by its manufacturer, is not guaranteed or endorsed by the publisher.

frontiers | Frontiers in Sustainable Food Systems

ORIGINAL RESEARCH
published: 23 June 2022
doi: 10.3389/fsufs.2022.913239

Effect of *Bradyrhizobium japonicum* Strains and Inorganic Nitrogen Fertilizer on the Growth and Yield of Bambara Groundnut (*Vigna subterranea (L.) Verdc)* Accessions

Tope Daniel Bitire[1,2], *Michael Abberton*[2], *Olaniyi Oyatomi*[2] *and Olubukola Oluranti Babalola*[1]*

[1] *Food Security and Safety Focus Area, Faculty of Natural and Agricultural Sciences, North-West University, Mmabatho, South Africa,* [2] *Genetic Resources Center, International Institute of Tropical Agriculture (IITA), Ibadan, Nigeria*

OPEN ACCESS

Edited by:
Everlon Cid Rigobelo, São Paulo State University, Brazil

Reviewed by:
Yusuf Y. Muhammad, Bayero University Kano, Nigeria
Takudzwa Mandizvo, University of KwaZulu-Natal, South Africa
Doris Kanvenaa Puozaa, CSIR-Savanna Agricultural Research Institute, Ghana

***Correspondence:**
Olubukola Oluranti Babalola
Olubukola.babalola@nwu.ac.za

Specialty section:
This article was submitted to Crop Biology and Sustainability, a section of the journal Frontiers in Sustainable Food Systems

Received: *05 April 2022*
Accepted: *18 May 2022*
Published: *23 June 2022*

Citation:
Bitire TD, Abberton M, Oyatomi O and Babalola OO (2022) Effect of Bradyrhizobium japonicum Strains and Inorganic Nitrogen Fertilizer on the Growth and Yield of Bambara Groundnut (Vigna subterranea (L.) Verdc) Accessions. Front. Sustain. Food Syst. 6:913239. doi: 10.3389/fsufs.2022.913239

This study was set up to compare the inoculation of *Bradyrhizobium japonicum* strains and the application of nitrogen (N) fertilizers (urea with 46% nitrogen) on the growth and yield of Bambara groundnut accessions. The study results suggest that the benefits of *Bradyrhizobium japonicum* (*B. japonicum*) strain inoculation are greater and that the strain could reduce reliance and the excess amount spent by farmers to procure inorganic fertilizers and avoid the negative effect of *N* fertilizer on the environment after its use. Field studies were conducted in two different geographical locations, in Ibadan (Ib) and Ikenne (Ik), Nigeria, during the rainy season between August and December in 2019 and 2020. The experiment was arranged in a randomized complete block design (RCBD) in both locations and seasons and was replicated three times, with each block representing each replicate. It had a 10 × 6 factorial arrangement with one block holding the 10 accessions of Bambara groundnut inoculated with four *B. japonicum* strains. The second block had *N* fertilizer application and the third control block was without inoculation or fertilizer application. The 10 accessions of Bambara groundnut used in the study were as follows: TVSu-378, TVSu-506, TVSu-787, TVSu-1606, TVSu-1698, TVSu-1739, TVSu-710, TVSu-365, TVSu-475, and TVSu-305. Six seeds of each accession were coated with each of the four *B. japonicum* strains, namely, FA3, USDA110, IRJ2180A, and RACA6, before planting them in the field in both locations during the rainy season. In the next block, urea as *N* fertilizer (46% nitrogen) was applied to the uninoculated seedlings of accessions of Bambara groundnut 2 weeks after planting (WAP). The third block was the control with zero inoculation and zero fertilizer application. Data collected were subjected to an analysis of variance and mean and were separated using Duncan's Multiple Range Test (DMRT) at a $p > 0.05$ level of probability. It was found that FA3 inoculation significantly enhanced the growth traits of the accessions than other strains and *N* fertilizer application. In both locations and seasons, at 7 weeks after planting (WAP) and 12 WAP, plant height (19.54 and 22.71 cm), number of branches (33.63 and 62.77), number of leaves (116.54 and 209.25), terminal leaf length (5.62 and 6.00 cm), and width (2.09 and 2.56 cm) were recorded. The yield and yield components recorded at harvest

were as follows: pod length (13.27 cm), pod width (9.08 mm), seed length (9.39 mm), seed width (6.92 mm), weight of 100 seeds (56.85 g), and yield/ha (750.72 kg). The yield and yield components were also significantly influenced by the inoculation of FA3 and RACA6 than other inoculated strains and *N* fertilizer application in both locations and seasons.

Keywords: underutilized legume, inoculation, plant trait, bacterial strains, inorganic fertilizer

INTRODUCTION

Bambara groundnut (*Vigna subterranea* (L.) Verdc) is a leguminous crop usually cultivated in sub-Saharan Africa and some parts of Asia but is now grown all over the world. It can thrive in all kinds of soil, especially in marginal soil (Mandizvo and Odindo, 2019; Mayes et al., 2019; Soropa et al., 2019). *Bradyrhizobium* usually establishes mutual symbiosis with legumes by creating root nodules and fixing atmospheric nitrogen for the host plant and can be used as an inoculant for improving crop productivity (Jaiswal and Dakora, 2019). Also, inexpensive microbial inoculants help in improving plant growth, reducing heavy metal contaminations, and controlling phytopathogens to enhance sustainable agriculture (Fasusi and Babalola, 2021). However, bacterial strains used in inoculation may not dominate during nodule formation due to competition with indigenous strains in the crop field (Suzuki et al., 2014). On the other hand, applying *N* fertilizers helps improve the nutrition of the plant (Islam et al., 2018). It is also very essential for optimum growth and development and a constituent of various organic compounds such as protein, nucleic acid, and hence part of protoplasm. It encourages rapid vegetative growth and regulates the utilization of phosphorus and potassium uptake by the plant from the soil (Tyoakoso et al., 2019). Some agricultural practices which involve the use of agrochemicals are very harmful to human health due to their residue on food crops being consumed by humans (Enagbonma and Babalola, 2019). The application of *N* fertilizer at the seedling stage usually increases the growth and yield of Bambara groundnut (Hasan et al., 2018). However, its negative effect on the environment includes soil acidification and compaction (Guo et al., 2010; Cai et al., 2015), eutrophication of surface water (Zhang et al., 2011), accelerating global warming by greenhouse gases emission (Battye et al., 2017), and decreasing crop leaf area, photosynthetic assimilation, and seed growth.

Although urea is the most suitable source of *N* fertilizer recommended for Bambara groundnut (Hasan et al., 2019), leguminous crops usually live in association with Rhizobium bacteria which helps to improve the soil status (Sarr et al., 2016). Therefore, successful rhizobial inoculation in the field is usually measured by the extent of nodulation, nitrogen fixation (N_2), plant growth, and grain yield when compared with the uninoculated control (Kyei-Boahen et al., 2017). Also, bacteria play a vital role in the decomposition of organic matter, transformation of nutrients, and regulation of soil productivity for plant growth and development (Oburger and Schmidt, 2016). The inoculation of bacterial strains to enhance the productivity of leguminous crops commenced with discovering the beneficial effects of the plant growth-promoting rhizobacteria and the method to use it by applying it to the seed. The most common methods include seed treatments, soil treatments, and root dipping of the bacteria in suspension before transplanting (Mahmood et al., 2016; Ikenganyia et al., 2017). Farmers usually experience difficulty procuring inorganic *N* fertilizer due to its high cost, and those who can afford it typically apply it below the manufacturer-recommended levels. Therefore, the aim of this study was to compare the effect of the inoculation of *B. japonicum* strains and *N* fertilizer application on the field performance of Bambara groundnut accessions.

MATERIALS AND METHODS

An experiment was carried out in 2019 and 2020 during the rainy season between August and December in two different geographical locations, Ibadan (Ib) and Ikenne, in Nigeria. Ikenne can be characterized as a tropical savanna, with a latitude (lat) of 6° 51′ 56″ *N* and a longitude (long) of 3° 42′ 54″ E, while Ibadan can be characterized as subhumid, with a lat of 7° 22' 30 *N* and a long of 3° 45' 54 E.

The experiment was arranged in a randomized complete block design (RCBD) and was replicated three times in the field, with each block representing each replicate. The first block had accession seeds coated with the bacterial strains. The 10 accessions of Bambara groundnut used in this study were randomly selected from the gene bank of the International Institute of Tropical Agriculture (IITA), while the *B. japonicum* strains were type strains readily available at the soil microbiology unit at IITA. The randomly selected 10 accessions from the gene bank were as follows: TVSu-378, TVSu-506, TVSu-787, TVSu-1606, TVSu-1698, TVSu-1739, TVSu-710, TVSu-365, TVSu-475, and TVSu-305. Six sets of seeds of each accession were coated with each of the four *Bradyrhizobium japonicum* strains (FA3, RACA6, USDA110, and IRJ2180A) and with gum Arabic 20% (w/v) to attach the strain to the seed before planting. The seeds were carefully dipped into the mixture of gum Arabic and *B. japonicum* strains, carefully stirred and allowed to stick firmly to the seeds, carefully spread and labeled to prevent mix up and allowed to dry properly before the commencement of the planting operation. The seeds coated with the bacterial strains were sown into a 2-m plot with 25 cm between each plot and 1 m between each replicate block.

In the second block, *N* fertilizer (20kg/ha) was applied to uninoculated seedlings at 2 WAP (Tyoakoso et al., 2019). The

third block had the control which had no bacterial strain-coated seeds or seedlings administered with urea.

Each block was identified with a plastic peg showing the accession number and bacteria strains and *N* fertilizer application. Data were collected on the percentage of germination after planting seeds at 2 WAP, on growth traits at 7 and 12 WAP in the flowering stage, and on yield and yield components at harvest in both locations and seasons.

Land Preparation

The field was prepared mechanically using a tractor-driven plow in both locations. It was carefully pulverized and harrowed to remove debris. Afterward, plots of 2 m with spacing of 25 cm between the plot and 1 m between the blocks were prepared.

Gum Arabic Preparation

A total of 20 g of gum Arabic was suspended in 100 ml of hot sterile water (22°C) to enable the gum Arabic to dissolve instantly. It was then mixed with 10 g of peat inoculant of *B. japonicum* strains, which was eventually used to inoculate 1 kg of the accessions of Bambara groundnut (Ogbuehi, 2020).

Planting Operation

The seeds of the 10 accessions were coated with the *Bradyrhizobium japonicum* strains and allowed to dry before planting to ensure the strains were firmly coated on the seeds. Six coated seeds were sown on each plot with one seed per stand and were replicated three times in the field and prepared for the treatment (bacteria and *N* fertilizer) and uninoculated control.

Fertilizer Application

Urea was applied to seedlings at 2 WAP to compare the effect of the nitrogen-fixing bacteria, *B. japonicum*, strains with the urea. Approximately 20 kg ha^{-1} of urea was applied to each accession of the Bambara groundnut (Tyoakoso et al., 2019) and planted separately in the field without bacteria inoculation.

Weeding Operation

Weeding of the plot was carried out using chemical herbicides before their pre-emergence (lifeline 3 L/ha and metaforce 2 L/ha according to manufacturers' instructions) and manually using a hoe to weed at 6 WAP and 10 WAP to ensure optimum yield.

Insecticide Application

Spraying of insecticides was carried out post-emergence using Karate and Termex 1 L/ha according to manufacturers' instructions in both locations and seasons to control whiteflies sucking the leaves of Bambara groundnut.

Data Collection

Data on percentage germination and growth parameters at 7 WAP and 12 WAP, which include plant height (cm), number of leaves, number of stems, plant spread (cm), number of branches, leaf area, terminal leaf length (cm), terminal leaf width (cm), chlorophyll content of leaf (mg/L), number of days to 1st flowering and to 50% flowering, and fresh and dry shoot at 50% flowering and at harvest, were collected in both locations (Ib and Ik). Additionally, the number of nodules, the weight of nodules (g), and the size and shape of nodules were also recorded. At harvest, the number of pods, the weight of pods (g), pod length (g), pod width (g), seed length (g), seed width (g), yield/plot (g), yield/ha (kg/ha), and weight of 100 seeds were further recorded.

Data Analysis

Data collected were subjected to the analysis of variance (ANOVA) using a four-way ANOVA, and DMRT at $p>0.05$ was used for mean comparison.

Soil Analysis

The pH of the soil in the Ikenne field was acidic in nature with values of 4.46 ± 0.08 and 4.91 ± 0.09 in both seasons, while, in Ibadan, the pH was neutral with values of 6.84 ± 0.1 and 7.13 ± 0.11 in both seasons. The percentage of organic carbon was analyzed following the procedure of Walkley and Black (1934). It ranged from 0.29 to 0.40 in both locations and seasons, which showed that the soil used was normal. The percentages of nitrogen (N), phosphorus (P), and potassium (K) ranged from 0.04 to 0.15, 2.55 to 52.84, and 0.22 to 0.56, respectively. The percentage of *N* was determined using the Kjeldahl method (Mulvaney and Page, 1982). The available P (ppm) was determined using Bray's method. A higher percentage of P was recorded in the soil in both locations and seasons (**Table 1**). The exchangeable potassium, sodium, and calcium were determined by ammonium acetate (Black et al., 1965). The percentage of K present in the soil in both locations and seasons showed that it was available in moderate quantities. The calcium (Ca, Cmol/kg) in the soil from the Ibadan field in 2019 had a value of 1.216 ± 0.10, which is, according to Walkley and Black (1934), considered normal. However, the soil in Ikenne for the 2019 season had a very high value of 3.53 ± 2.50, which is considered abnormal. Higher magnesium (Mg, Cmol/kg) values were obtained in Ikenne, 0.80 ± 0.37 and 0.404 ± 0.02 for 2019 and 2020, respectively, while lower quantities of Mg were obtained in Ibadan, 0.075 ± 0.01 and 0.158 ± 0.05 for 2019 and 2020, respectively (**Table 1**). The particle size analysis was determined by the hydrometer method. The texture class of the soil on the field showed that it was loamy sand because it ranged from 76.00 to 83.00% sand, 8.00 to 19.00% clay, and 3.00 to 10.00% silt. The mycorrhizal spore count was low in Ibadan with mean values of 382 and 392 in both 2019 and 2020, respectively, compared to that in Ikenne, which had mean values of 412 and 432 for 2019 and 2020, respectively (**Table 1**).

Crop Establishment

The coated Bambara groundnut seeds after planting in both locations and seasons developed into seedlings with multiple stems and branches and increased in growth every week. During flowering, the increase in the number of flowers was recorded from the number of days to first flowering to the number of days to 50% flowering. The space occupied by the plant, its canopy spread until when its growth ceased, and the commencement of reproductive stages (pod formation) were also calculated.

TABLE 1 | Physiochemical and biological properties of soil used for the studies.

Planting season properties/location	2019 Ikenne	2020 Ikenne	2019 Ibadan	2020 Ibadan
pH (H_2O) 1:1	4.46 ± 0.08	4.91 ± 0.09	6.84 ± 0.1	7.13 ± 0.11
N (%)	0.073 ± 0.02	0.121 ± 0.01	0.150 ± 0.013	0.119 ± 0.02
OC (%)	0.329 ± 0.07	0.297 ± 0.01	0.407 ± 0.10	0.336 ± 0.06
Bray *P* (ppm)	13.23 ± 4.26	22.46 ± 3.43	15.352 ± 3.74	52.84 ± 6.67
Sand (%)	76.00 ± 1.16	76.00 ± 1.16	83.00 ± 1.16	82.00 ± 0.00
Clay (%)	16.00 ± 1.16	20.00 ± 2.00	10.00 ± 0.00	8.00 ± 0.00
Silt (%)	6.00 ± 1.15	3.00 ± 1.15	7.00 ± 1.15	10.00 ± 0.0
Ca (Cmol/kg)	3.530 ± 2.50	1.505 ± 0.24	1.216 ± 0.10	1.101 ± 0.30
Mg (Cmol/kg)	0.80 ± 0.37	0.404 ± 0.02	0.075 ± 0.01	0.158 ± 0.05
K (Cmol/kg)	0.560 ± 0.24	0.242 ± 0.06	0.137 ± 0.02	0.201 ± 0.02
Na (Cmol/kg)	0.076 ± 0.01	0.082 ± 0.00	0.055 ± 0.02	0.057 ± 0.01
ECEC (Cmol/kg)	4.96 ± 1.56	2.23 ± 0.57	1.29 ± 0.56	1.47 ± 0.48
Zn (ppm)	1.964 ± 1.67	1.196 ± 0.19	1.19 ± 0.10	0.66 ± 0.04
Cu (ppm)	1.167 ± 0.62	2.045 ± 0.19	0.86 ± 0.11	0.97 ± 0.22
Mn (ppm)	12.15 ± 10.5	116.7 ± 3.31	244.20 ± 18.4	383.6 ± 33.4
Fe (ppm)	25.58 ± 7.47	88.29 ± 4.08	133.33 ± 3.33	114.4 ± 3.85
Glomus	106	117	135	152
Acaulospora	192	185	202	208
Enthrophospora	25	28	34	32
Spore/100 gdwt	380	392	412	432
Soil textural class	Loamy sand	Loamy sand	Loamy sand	Loamy sand

RESULTS

Interplay Between *B. japonicum* Strains and *N* Fertilizer Application on Growth Traits, Flowering Stages, and Biomass Yield of Bambara Groundnut Accessions

Table 2 shows the comparison of the effect of *B. japonicum* strains and urea (46% *N* fertilizer) application on growth traits and flowering stages of inoculated accessions of Bambara groundnut at 7 WAP in Ibadan and Ikenne in the first season. As seen in **Table 2**, the IRJ2180A bacterial strain had a significantly enhanced germination percentage with a mean value of 67.32% compared to other inoculated strains and *N* fertilizers. Bacterial strains, FA3 and IRJ2180A, significantly enhanced plant height of the accessions with mean values of 19.88 and 19.89 cm, respectively, compared to all other accessions, whether inoculated with *N* fertilizer or uninoculated control. On the other hand, *N* fertilizer significantly enhanced the number of leaves and number of stems compared to other inoculated accessions and uninoculated control. However, FA3-inoculated accessions and uninoculated control showed a significantly enhanced number of days to first flowering compared to other accessions inoculated with USDA110, IRJ2180A, and RACA6 strains or applied with *N* fertilizer. Significant differences were, however, observed in the number of branches among accessions inoculated with FA3 and RACA6 strains, with *N* fertilizer applied, compared to USDA110 and IRJ2180A inoculated accessions and the uninoculated control.

Impact of *B. japonicum* Strains and *N* Fertilizer on Growth Traits at 7 WAP and 12 WAP of Bambara Groundnut Accessions

The comparison of the effect of *B. japonicum* strains and urea on the growth traits and biomass yield of Bambara groundnut accessions at 12 WAP in both locations in the first season revealed that the FA3 strain significantly enhanced plant height, canopy spread, petiole length, terminal leaf width, number of leaves, number of stems, and peduncle length compared to accessions inoculated with other bacterial strains or when *N* fertilizer was applied, or under uninoculated control (**Table 3**). Similarly, the IRJ2180A strain significantly enhanced the terminal leaf length of the accessions of Bambara groundnut more than other bacterial strains, or *N* fertilizer, and the uninoculated control. Furthermore, the number of branches was significantly enhanced by the inoculation with FA3, USDA110, and RACA6 compared to IRJ2180A inoculation, *N* fertilizer application, or uninoculated control. Similarly, RACA6 significantly enhanced the leaf area compared to other inoculated strains and application of *N* fertilizer. However, there were no significant differences observed in chlorophyll content of leaf, fresh and dry shoots at flowering and fresh and dry roots at flowering.

The comparison of the effect of bacterial strains and urea on growth traits at flowering at 7 WAP in both locations in the second season is shown in **Table 4**. At 7 WAP there were no significant differences in germination percentage, petiole length, chlorophyll content of leaf, and peduncle length

TABLE 2 | Effect of *N* fertilizer and *B. japonicum* strains on the percentage of germination at 2 WAP, growth traits of accessions of Bambara groundnut at 7 WAP, and flowering in the first season in Ibadan and Ikenne 2019.

Treatment	% GM	PLH (cm)	NOL	NOB	NOS	TLL (cm)	TLW (cm)	CPYL (mg/L)	GH	D50% Flw	D1st Flw	PL (cm)	PEL (cm)	CS (cm)	LA (cm2)
FA3	56.17^{d}	19.89^{a}	118.97^{ab}	35.41^{a}	39.83^{ab}	5.28^{a}	2.17^{a}	43.52^{a}	2.08^{a}	54.97^{bc}	41.63^{a}	7.74^{a}	1.77^{a}	10.44^{a}	11.79^{a}
USDA110	58.33^{cd}	19.66^{ab}	111.20^{b}	32.22^{b}	37.78bb	5.51^{a}	2.13^{a}	44.86^{a}	2.12^{a}	55.43^{ab}	42.54^{b}	7.91^{a}	1.67^{a}	10.70^{a}	12.38^{a}
N	63.75^{ab}	19.53^{ab}	129.36^{a}	37.89^{a}	43.52^{a}	5.37^{a}	2.13^{a}	44.85^{a}	2.14^{a}	54.71^{bc}	42.14^{b}	7.72^{a}	1.72^{a}	10.52^{a}	11.74^{a}
IRJ2180A	67.32^{a}	19.88^{a}	120.93^{ab}	33.18^{b}	39.46^{ab}	5.26^{a}	2.28^{a}	44.50^{a}	2.11^{a}	54.71^{bc}	41.82^{b}	7.61^{a}	1.82^{a}	10.48^{a}	12.24^{a}
RACA6	62.32^{bc}	19.69^{ab}	123.44^{ab}	36.14^{a}	42.04^{ab}	5.35^{a}	2.22^{a}	42.41^{a}	2.12^{a}	54.49^{c}	41.86^{b}	8.03^{a}	1.73^{a}	10.16^{a}	12.13^{a}
CONTROL	54.17^{d}	18.29^{b}	109.75^{b}	32.57^{b}	37.89^{b}	5.23^{a}	2.21^{a}	40.75^{a}	2.09^{a}	55.78^{a}	43.55^{a}	6.63^{b}	1.76^{a}	10.09^{a}	12.10^{a}

Means with the same letter are not significantly different at a P > 0.05 level of probability using the Duncan multiple range test (DMRT).%GM, percentage of germination; PLH, plant height; NOL, number of leaves; NOS, number of stems; NOB, number of branches; TLL, terminal leaf length; TLW, terminal leaf width; CPYL, chlorophyll; GH, growth habit; D50% Flw, days to 50% flowering; D1st Flw, days to first flowering; PL, peduncle length; PEL, petiole length; CS, canopy spread; LA, leaf area; WAP, weeks after planting.

[a]highly significant.

[b]significant.

[c]less significant.

[d]not significant.

TABLE 3 | Effect of *N* fertilizer and *B. japonicum* strains on growth trait and biomass yield of accessions of B. groundnut at 12 WAP in Ibadan and Ikenne in the first season, 2019.

Treatment	PLH (cm)	CS (cm)	PEL (cm)	TLL (cm)	TLW (cm)	NOB	NOL	NOS	LA (cm^2)	CPYL (mg/L)	PL (cm)	FSF (g)	DSF (g)	FRF (g)	DRF (g)
FA3	22.61^{a}	12.21^{a}	1.76^{a}	5.98^{b}	2.55^{a}	62.77^{a}	215.88^{a}	72.68^{a}	15.39^{b}	35.74^{a}	14.12^{a}	33.05^{a}	12.22^{a}	10.07^{a}	3.39^{a}
USDA110	21.68^{bc}	11.24^{b}	1.61^{b}	5.79^{b}	2.35^{b}	59.03^{a}	195.00^{b}	64.85^{b}	13.74^{b}	35.76^{a}	10.94^{b}	28.42^{a}	10.82^{a}	9.39^{a}	3.39^{a}
N	21.64^{bc}	11.39^{ab}	1.69^{ab}	5.90^{b}	2.46^{ab}	54.30^{b}	162.33^{b}	62.00^{b}	14.59^{b}	37.29^{a}	10.35^{b}	30.41^{a}	10.76^{a}	9.86^{a}	3.33^{a}
IRJ2180A	22.42^{ab}	11.53^{ab}	1.59^{b}	11.12^{a}	2.45^{ab}	56.59^{b}	190.77^{b}	63.59^{b}	14.89^{b}	36.40^{a}	10.73^{b}	31.59^{a}	11.71^{a}	9.69^{a}	3.48^{a}
RACA6	21.69^{bc}	11.62^{ab}	1.65^{ab}	5.69^{b}	2.47^{ab}	57.08^{a}	188.26^{b}	64.54^{b}	21.34^{a}	36.21^{a}	10.83^{b}	34.79^{a}	12.77^{a}	12.12^{a}	4.14^{a}
CONTROL	20.90^{c}	11.14^{b}	1.64^{ab}	5.84^{b}	2.44^{ab}	49.21^{c}	182.71^{b}	56.48^{c}	14.44^{b}	33.97^{a}	9.74^{b}	24.77^{b}	10.91^{a}	9.51^{a}	3.76^{a}

Means with the same letter are not significantly different at P > 0.05 level of probability using the Duncan multiple range test (Dmrt). PLH, plant height; NOL, number of leaves; NOS, number of stems; NOB, number of branches; TLL, terminal leaf length; TLW, terminal leaf width; CPYL, chlorophyll; PL, peduncle length; PEL, petiole length; CS, canopy spread; LA, leaf area; WAP, weeks after planting. FSF, fresh shoot at flowering; DSF, dry shoot at flowering; FRF, fresh root at flowering; DRF, dry root at flowering.

[a]highly significant.

[b]significant.

[c]less significant.

[d]not significant.

among strains inoculated on accessions, application of *N* fertilizer, and uninoculated control. Similarly, there were no significant differences in the number of leaves, number of branches, and number of stems in all accessions barring those that were treated with RACA6 or urea. Plant height was significantly enhanced by FA3 and USDA110 strains compared to those inoculated with IRJ2180A and RACA6. Accessions with *N* fertilizer application had the lowest mean value in plant height. Also, terminal leaf length was significantly enhanced with the inoculation of FA3 and USDA110 strains compared to that of IRJ2180A and RACA6 strains and uninoculated control. On the other hand, *N* fertilizer-applied accessions recorded the lowest terminal leaf length. It was further noted that terminal leaf width and days to 50% flowering significantly decreased with *N* fertilizer application compared to the bacterial strain-inoculated accessions or the uninoculated control.

Impact of *B. japonicum* Strain Inoculation and *N* Fertilizer Application on Growth Traits, Flowering, and Biomass Yield at 7 WAP and 12 WAP

Table 4 shows that FA3 significantly enhanced the number of days to the first flowering of accessions compared to other strains or uninoculated control; *N* fertilizer had the lowest mean value. Similarly, analyzing the growth traits and biomass yield at 12 WAP in both locations in the first season revealed that FA3 significantly enhanced plant height, petiole length, terminal leaf width, number of branches, number of leaves, chlorophyll content of leaf, and peduncle length more than other strains (**Table 5**); *N* fertilizer recorded the lowest mean value on the growth traits. Also, RACA6 significantly enhanced biomass yield (dry shoot at flowering, and fresh and dry roots at flowering) compared to other strains, or when *N* fertilizer was applied, or uninoculated control. The FA3 strain also significantly enhanced plant height while *N* fertilizer had the lowest mean value (**Table 6**). It was further revealed that USDA110 significantly enhanced terminal leaf length compared to other strains, when *N* fertilizer was applied, or uninoculated control. **Table 6** demonstrates that, though there were no significant differences in terminal leaf length between inoculated accessions and uninoculated control in both seasons, there was a significant difference between the inoculated strains and *N* fertilizer-applied accessions. The peduncle length was significantly enhanced among FA3 and USDA110-inoculated accessions in both seasons, and the leaf area was significantly enhanced by USDA110 compared to *N* fertilizer. A comparison of the effect of the bacterial strains and *N* fertilizer on growth traits and biomass yield at 12 WAP in both locations and seasons shows no significant differences. However, as seen in **Table 7**, FA3 significantly enhanced all growth traits at 12 WAP except for terminal leaf length and leaf areas, which were significantly enhanced by IRJ2180A and RACA6.

Impact of *B. japonicum* Strains and *N* Fertilizer Application on the Yield and Yield Components of Bambara Groundnut Accessions

Significant differences were recorded in the seed length, yield/plot, yield/ha, pod/plant, pod/plot, weight of pod/plot, seed/plot, seed weight/plot, and shelling percentage at harvest among the strains inoculated, the *N* fertilizer applied, and uninoculated control in both locations in the first season (**Table 8**). The application of nitrogen fertilizer and inoculation of IRJ2180A were found to significantly enhance yield/plot at harvest. On the other hand, RACA6 strains significantly enhanced yield/ha, pod/plant, weight of pod/plot, and seed weight/plot at harvest compared to other strains, *N* fertilizer application, and uninoculated control in the first season. Similarly, in both locations in the second season, significant differences were recorded in the pod width, seed width, 100 seed weight, yield/plot, yield/ha, pod/plant, pod/plot, weight of pod/plot, seed/plant, seed/plot, seed weight/plot, and shelling percentage at harvest between accessions inoculated with bacterial strains, application of *N* fertilizer, and uninoculated control. While inoculation with FA3 strain was found to significantly enhance pod width, seed width, 100 seed weight, pod/plant, and seed/plant at harvest compared to inoculations with other strains and application with *N* fertilizer in the second season. Yield/plot, yield/ha, pod/plot, weight of pod/plot, and seed weight/plot at harvest were found to be significantly enhanced when inoculated with USDA110 strains (**Table 9**). Significant differences were also recorded in all other yield and yield components after harvest between accessions inoculated with bacterial strains, *N* fertilizer application, and uninoculated control in both locations in both seasons. Interestingly, pod width, seed length, seed width, and weight of pod/plot at harvest were found to be significantly enhanced in the uninoculated control compared to inoculated accessions or those applied with *N* fertilizer (**Table 10**). The FA3 strain significantly enhanced 100 seed weight, seed/plant, and seed weight/plot of accessions at harvest in both seasons, while the RACA6 strain significantly enhanced yield/plot and yield/ha. Among bacterial strains, FA3, RACA6, and USDA110 significantly enhanced pod/plant and seed/plot of the accessions. **Table 11** provides a cumulative overview of the significant differences recorded among accessions inoculated with different *B. japonicum* strains in different seasons, locations, and its yield and yield components.

DISCUSSION

Response of Bambara Groundnut to Inoculation and *N* Fertilizer Application

The differences in the impact recorded in the growth and yield of the Bambara groundnut accessions due to the inoculation of *B. japonicum* strains coated to the seeds before planting in both locations and seasons are similar to the result obtained by Sanginga et al. (1996) and Houngnandan et al. (2000), which

TABLE 4 | Effect of *N* fertilizer and *B. japonicum* strains on the percentage of germination at 2 WAP, growth traits of accessions of Bambara groundnut at 7 WAP, and flowering in Ibadan and Ikenne in the second season, 2020.

Treatment	% GM	PEL (cm)	PLH (cm)	NOL	NOB	NOS	TLL (cm)	TLW (cm)	CPYL (mg/L)	D50% Flw	D1st Flw	PL (cm)	LA (cm^2)
FA3	78.17[a]	1.43[a]	19.62[a]	116.10[a]	38.45[a]	38.92[a]	6.06[a]	2.06[a]	42.37[a]	54.93[a]	45.83[a]	7.99[a]	12.56[ab]
USDA110	80.38[a]	1.42[a]	19.63[a]	118.32[a]	39.13[a]	39.68[a]	5.99[a]	2.08[a]	43.73[a]	49.03[b]	44.18[ab]	7.16[a]	13.02[a]
N	70.75[a]	1.57[a]	17.18[b]	97.78[b]	32.38[b]	32.83[b]	5.18[b]	1.75[b]	39.67[a]	44.82[c]	38.83[c]	6.78[a]	10.75[b]
IRJ2180A	78.17[a]	1.39[a]	18.79[ab]	114.88[a]	37.04[a]	38.30[ab]	5.76[ab]	2.04[a]	43.78[a]	52.95[ab]	44.28[ab]	6.72[a]	12.24[ab]
RACA6	77.00[a]	1.41[a]	18.01[ab]	110.20[ab]	36.30[ab]	36.57[ab]	5.48[ab]	2.15[a]	40.29[a]	51.67[ab]	41.63[bc]	6.37[a]	12.89[a]
CONTROL	78.55[a]	1.80[a]	19.97[a]	119.82[a]	39.33[a]	39.73[a]	5.74[ab]	2.13[a]	43.80[a]	54.87[a]	43.27[ab]	6.45[a]	12.93[a]

Means with the same letter are not significantly different at $P < 0.05$ level of probability using the Duncan multiple range test (DMRT).%GM, percentage of germination; PLH, plant height; NOL, number of leaves; NOS, number of stems; NOB, number of branches; TLL, terminal leaf length; TLW, terminal leaf width; CPYL, chlorophyll content of leaf; GH, growth habit; D50% Flw, days to 50% flowering; $D1^{st}$ Flw, days to first flowering; PL, peduncle length; PEL, petiole length; CS, canopy spread; LA, leaf area; WAP, weeks after planting.

[a] *highly significant.*

[b] *significant.*

[c] *less significant.*

[d] *not significant.*

TABLE 5 | Effect of *N* fertilizer and *B. japonicum* strains on growth traits and biomass yield of accessions of Bambara groundnut at 12 WAP in Ibadan and Ikenne in the second season, 2020.

Treatment	PLH (cm)	PEL (cm)	TLL (cm)	TLW (cm)	NOB	NOL	NOS	LA (cm^2)	CPYL (mg/L)	PL (cm)	FSF (g)	DSF (g)	FRF (g)	DRF (g)
FA3	22.80[a]	1.69[a]	6.02[b]	2.56[a]	62.70[a]	202.62[a]	67.53[a]	33.92[a]	28.15[a]	11.26[a]	20.38[a]	6.76[ab]	6.21[ab]	1.25[ab]
USDA110	19.51[c]	1.43[bc]	5.29[cd]	2.17[c]	52.28[b]	166.45[b]	58.97[a]	31.95[a]	12.59[d]	9.22[ab]	19.42[a]	6.73[ab]	6.42[ab]	1.16[ab]
N	17.79[d]	1.36[c]	4.86[d]	2.12[c]	45.72[c]	143.12[c]	49.31[b]	28.15[b]	12.41[d]	8.39[b]	18.76[a]	5.97[ab]	6.08[ab]	1.00[ab]
IRJ2180A	21.71[ab]	1.56[ab]	10.06[a]	2.37[b]	54.05[b]	171.98[b]	63.63[a]	30.99[ab]	14.24[bc]	9.81[ab]	19.48[a]	6.83[ab]	5.98[b]	1.28[ab]
RACA6	20.95[bc]	1.55[ab]	5.42[c]	2.37[b]	57.05[ab]	177.17[b]	60.98[a]	32.29[a]	13.91[c]	9.47[ab]	23.19[a]	7.55[a]	8.08[a]	1.37[a]
CONTROL	21.25[ab]	1.63[a]	5.96[a]	2.49[ab]	55.15b	172.55[b]	59.58[a]	34.22[a]	15.23[a]	9.22[ab]	17.34[a]	5.13[b]	6.66[ab]	0.85[b]

Means with the same letter are not significantly different at $P < 0.05$ level of probability using the Duncan multiple range test (DMRT). PLH, plant height; NOL, number of leaves; NOS, number of stems; NOB, number of branches; TLL, terminal leaf length; TLW, terminal leaf width; CPYL, chlorophyll content of leaf; PL, peduncle length; PEL, petiole length; CS, canopy spread; LA, leaf area; WAP, weeks after planting. FSF, fresh shoot at flowering; DSF, dry shoot at flowering; FRF, fresh root at flowering; DRF, dry root at flowering.

[a] *highly significant.*

[b] *significant.*

[c] *less significant.*

[d] *not significant.*

TABLE 6 | Effect of *N* fertilizer and *B. japonicum* strains on the percentage of germination at 2 WAP, growth traits of accessions of Bambara groundnut at 7 WAP, and flowering in Ibadan and Ikenne during both seasons.

Treatment	%GM	PLH (cm)	NOL (cm)	NOB	NOS	TLL (cm)	TLW (cm)	CPYL (mg/L)	D1st Flw	D50% Flw	PL (cm)	PEL (cm)	CS (cm)	LA (cm^2)
FA3	67.17[a]	19.59[a]	116.54[a]	36.63[a]	39.04[a]	5.62[ab]	2.09[a]	42.22[a]	43.38[a]	54.95[a]	7.80[a]	1.58[a]	10.74[a]	12.08[ab]
USDA110	69.36[a]	19.47[ab]	113.83[a]	35.41[a]	38.42[a]	5.70[a]	2.09[a]	43.54[a]	43.00[ab]	51.31[b]	7.47[a]	1.53[a]	10.65[ab]	12.59[a]
N	65.13[a]	18.03[b]	111.42[a]	34.51[a]	37.89[a]	5.18[b]	1.91[b]	41.14[a]	39.78[c]	49.73[c]	7.12[ab]	1.62[a]	9.72[c]	11.05[b]
IRJ2180A	70.50[a]	18.84[ab]	114.88[a]	34.28[a]	37.89[a]	5.38[ab]	2.10[a]	43.03[a]	42.00[abc]	49.73[b]	6.98[ab]	1.56[a]	10.37[abc]	11.93[ab]
RACA6	67.58[a]	18.36[ab]	113.73[a]	35.32[a]	38.25[a]	5.28[ab]	2.13[a]	40.29[a]	40.70[bc]	51.72[b]	6.99[ab]	1.52[a]	9.91[bc]	12.20[ab]
CONTROL	66.36[a]	18.52[ab]	111.13[a]	34.87[a]	37.55[a]	5.31[ab]	2.09[a]	40.92[a]	41.96[abc]	55.33[a]	6.32[b]	1.72[a]	10.05[abc]	12.11[ab]

Means with the same letter are not significantly different at P < 0.05 level of probability using the Duncan multiple range test (DMRT).%GM, percentage of germination; PLH, plant height; NOL, number of leaves; NOS, number of stems; NOB, number of branches; TLL, terminal leaf length; TLW, terminal leaf width; CPYL, chlorophyll content of leaf; GH, growth habit; D50% Flw, days to 50% flowering; D1st Flw, days to first flowering; PL, peduncle length; PEL, petiole length; CS, canopy spread; LA, leaf area; WAP, weeks after planting.

[a]highly significant.

[b]significant.

[c]less significant.

[d]not significant.

TABLE 7 | Effect of *N* fertilizer and *B. japonicum* strains on growth traits and biomass yield of accessions of Bambara groundnut at 12 WAP in Ibadan and Ikenne during both seasons.

Treatment	PLH (cm)	CS (cm)	PEL (cm)	TLL (cm)	TLW (cm)	NOB	NOL	NOS	LA (cm^2)	CPYL (SPAD)	PL (cm)	FSF (g)	DSF (g)	FRF (g)	DRF (g)
FA3	22.71[a]	12.21[a]	1.73[a]	6.00[b]	2.56[a]	62.73[a]	209.25[a]	70.10[a]	15.74[ab]	34.53[a]	12.69[a]	21.68[a]	6.31[a]	8.38[a]	1.90[a]
USDA110	20.23[b]	10.37[bc]	1.49[c]	5.44[b]	2.22[c]	54.68[b]	177.48[b]	60.83[b]	12.94[b]	33.26[abc]	9.89[b]	19.53[a]	6.46[a]	7.73[a]	1.72[a]
N	18.99[c]	10.37[c]	1.47[c]	5.18[b]	2.20[c]	48.20[c]	156.83[c]	53.59[c]	13.02[b]	31.48[bc]	9.025[b]	18.29[a]	5.94[a]	7.54[a]	1.80[a]
IRJ2180A	20.38[b]	10.46[bc]	1.46[c]	9.75[a]	2.22[c]	51.08[bc]	167.07[bc]	58.84[bc]	13.45[b]	30.96[c]	9.46[b]	19.55[a]	6.41[a]	7.78[a]	1.83[a]
RACA6	20.78[b]	10.99[b]	1.56[bc]	5.42[b]	2.36[b]	55.64[b]	178.01[b]	61.15[b]	17.09[a]	33.35[abc]	9.88[b]	20.65[a]	6.45[a]	8.39[a]	1.77[a]
CONTROL	21.07[b]	11.07[b]	1.64[ab]	5.90[b]	2.46[ab]	52.18[bc]	167.44[bc]	58.03[bc]	14.83[ab]	34.09[ab]	9.48[b]	19.74[a]	5.86[a]	8.15[a]	1.68[a]

Means with the same letter are not significantly different at P < 0.05 level of probability using the Duncan multiple range test (DMRT). PLH, plant height; NOL, number of leaves; NOS, number of stems; NOB, number of branches; TLL, terminal leaf length; TLW, terminal leaf width; CPYL, chlorophyll content of leaf; PL, peduncle length; PEL, petiole length; CS, canopy spread; LA, leaf area; WAP, weeks after planting. FSF, fresh shoot at flowering; DSF, dry shoot at flowering; FRF, fresh root at flowering; DRF, dry root at flowering.

[a]highly significant.

[b]significant.

[c]less significant.

[d]not significant.

TABLE 8 | Effect of *N* fertilizer and *B. japonicum* strains on yield and yield components of Bambara groundnut accessions at harvest in Ibadan and Ikenne in the first season, 2019.

Treatment	Pod length (mm)	Pod width (mm)	Seed length (mm)	Seed width (mm)	100seed wgt (g)	Yield /Plot (g)	yield/ha (kg)	Pod /Plant	Pod/plot (g)	Wgt of pod/plot (g)	Seed/plant	Seed/ plot	Seed wgt/plot (g)	Shelling %
FA3	17.12[a]	11.49[a]	12.64[b]	9.23[a]	55.79[a]	70.25[ab]	1,401.8[b]	29.39[b]	100.25[ab]	73.24[ab]	27.23[a]	93.89[a]	41.61[ab]	41.42[ab]
USDA110	17.28[a]	11.69[a]	12.38[b]	9.63[a]	53.32[a]	63.54[b]	1,367.7[c]	27.65[b]	95.20[c]	67.62[b]	27.01[a]	96.13[a]	38.14[b]	44.49[a]
N	17.85[a]	12.02[a]	13.59[ab]	9.63[a]	55.29[a]	75.61[a]	1,394.9[c]	31.26[a]	109.39[a]	73.71[ab]	25.29[a]	97.47[a]	42.86[ab]	42.86[ab]
IRJ2180A	17.11[a]	11.93[a]	12.47[b]	9.53[a]	58.19[a]	75.05[a]	1,459.9b	28.80[b]	95.43[c]	74.44[ab]	27.61[a]	88.68[b]	42.38[ab]	39.48[b]
RACA6	16.89[a]	11.78[a]	13.39[ab]	9.72[a]	54.31[a]	81.19[ab]	1,582.7[a]	30.53[a]	102.26[ab]	86.08[a]	27.74[a]	96.72[a]	44.66[a]	45.38[a]
CONTROL	17.34[a]	11.76[a]	14.78[a]	9.85[a]	55.19[a]	64.41[b]	1,201.6[d]	21.79[c]	80.35[d]	78.37[ab]	28.47[a]	70.82[c]	38.99[b]	41.89[ab]

Means with the same letter are not significantly different at a P < 0.05 level of probability using the Duncan multiple range test (DMRT).
[a]*highly significant.*
[b]*significant.*
[c]*less significant.*
[d]*not significant.*

TABLE 9 | Effect of *N* fertilizer and *B. japonicum* strains on yield and yield components of Bambara groundnut accessions at harvest in Ibadan and Ikenne in the second season, 2020.

Treatment	Pod length (mm)	Pod width (mm)	Seed length (mm)	Seed width (mm)	100seed wgt (g)	Yield/plot (g)	yield/ha (kg)	Pod /Plant	Pod/plot (g)	Wgt of spod/plot (g)	Seed/ plant	Seed/ plot	Seed wgt/plot (g)	Shelling %
FA3	10.29[a]	7.24[a]	6.79[a]	5.07[a]	60.70[a]	34.71[ab]	125.04[ab]	16.06[a]	42.17[ab]	32.02[ab]	16.03[a]	41.11[a]	24.39[ab]	26.79[a]
USDA110	10.80[a]	7.36[ab]	6.66[a]	5.01[ab]	56.51[ab]	43.85[a]	130.59[a]	12.88[abc]	44.08[a]	34.51[a]	14.81[ab]	42.91[a]	27.10[a]	23.20[a]
N	9.74[a]	6.30[b]	5.78[a]	4.23[b]	45.05[b]	25.04[b]	118.58[b]	9.26[c]	28.65[b]	22.23[c]	10.97[c]	27.48[b]	16.01[c]	24.51[ab]
IRJ2180A	9.923[a]	7.08[b]	6.23[a]	4.74[ab]	54.84[ab]	33.92[ab]	106.56[b]	12.15[bc]	40.04[ab]	28.29[b]	12.99[b]	39.26[ab]	19.86[bc]	23.24[a]
RACA6	9.74[a]	7.00[b]	6.33[a]	4.82[ab]	56.46[ab]	31.29[b]	103.39[b]	12.14[bc]	37.12[ab]	27.67[b]	12.96[b]	35.87[ab]	20.49[abc]	22.04[b]
CONTROL	10.29[a]	9.36[a]	6.76[a]	4.91[ab]	42.09[b]	26.69[b]	80.47[c]	14.19[ab]	24.15[c]	31.29[ab]	6.50[d]	20.62[c]	23.61[ab]	24.00[ab]

Means with the same letter are not significantly different at a P < 0.05 level of probability using the Duncan multiple range test (DMRT).
[a]*highly significant.*
[b]*significant.*
[c]*less significant.*
[d]*not significant.*

TABLE 10 | Effect of *N* fertilizer and *B. japonicum* strains on yield and yield components of Bambara groundnut accessions at harvest in Ibadan and Ikenne during both seasons.

Treatment	Pod length (mm)	Pod width (mm)	Seed length (mm)	Seed width (mm)	100seed wgt (g)	Yield/plot (g)	yield/ha (kg)	Pod /plant	Pod/plot (g)	Wgt of pod/plot (g)	Seed/ plant	Seed/plot	Seed wgt/plot (g)	Shelling %
FA3	13.27^{a}	9.08^{ab}	9.39^{ab}	6.92^{ab}	56.85^{a}	50.72^{ab}	728.39^{ab}	21.99^{a}	68.70^{a}	50.79^{ab}	20.95^{a}	65.16^{a}	31.96^{a}	33.07^{b}
USDA110	13.18^{a}	8.94^{b}	8.90^{b}	6.84^{ab}	52.25^{ab}	50.52^{ab}	680.75^{b}	18.88^{ab}	64.88^{ab}	47.68^{ab}	19.56^{ab}	64.72^{a}	30.72^{ab}	31.62^{b}
N	12.01^{a}	8.26^{b}	8.67^{b}	6.21^{b}	46.03^{b}	44.66^{b}	633.07^{c}	17.91^{b}	63.73^{ab}	42.44^{b}	17.22^{b}	55.16^{b}	26.22^{b}	30.47^{b}
IRJ2180A	12.52^{a}	8.81^{b}	8.62^{b}	6.58^{ab}	53.12^{ab}	50.11^{ab}	698.06^{b}	18.79^{ab}	62.17^{b}	47.03^{ab}	17.67^{b}	58.79^{b}	28.65^{ab}	29.11^{c}
RACA6	12.33^{a}	8.70^{b}	9.07^{ab}	6.70^{ab}	52.22^{ab}	51.51^{a}	750.72^{a}	19.56^{a}	63.73^{ab}	51.86^{ab}	18.73^{ab}	60.65^{ab}	29.97^{ab}	31.06^{b}
CONTROL	13.39^{a}	10.27^{a}	10.40^{a}	7.135^{a}	47.26^{b}	48.44^{b}	533.82^{d}	12.20^{c}	54.97^{c}	32.87^{a}	11.78^{c}	46.78^{c}	25.07^{b}	41.90^{a}

Means with the same letter are not significantly different at a P < 0.05 level of probability using the Duncan multiple range test (DMRT).
[a]highly significant.
[b]significant.
[c]less significant.
[d]not significant.

TABLE 11 | Analysis of accessions inoculated with *B. japonicum* strains in Ibadan and Ikenne locations during both seasons.

Source	DF	Pod length (mm)	Pod width (mm)	Seed length (mm)	Seed width (mm)	Wgt100 seed	Yield/plot (g)	yield/ha (kg/ha)	Pod/plot	Wgt pod/plot (g)	Seed/plot	Wgt seed/plot (g)
Accessions	9	157.89**	80.14**	66.29**	41.33**	11,572**	19,516.19**	4,516,451**	25,275.49**	23,518.6**	39,987.39**	10,103.8**
Strains	5	37.89^{ns}	53.94**	52.68**	12.15*	1,987.91*	2,327.35*	565,048.9*	3,253.76**	1,794.03*	2,373.35*	1,083.01*
Season	1	4,238.9**	1,278.9*	5,296.93*	2,696.2^{ns}	6,422.29^{ns}	201,741.8**	2.6833**	505,919.5**	272,160.4**	414,765.6**	52,271.9**
Location	1	2,966.4**	2,231.0*	4,875.5**	4,066.9^{ns}	21,817.9*	230,306.6**	1.0923**	554,858.6**	401,441.3**	510,664.9**	102,848.9**
Rep	2	201.59**	43.00^{ns}	211.75**	43.02**	574.42^{ns}	693.39^{ns}	13.4^{ns}	360.86^{ns}	356.96^{ns}	7,352.33^{ns}	160.69^{ns}
Accessions*strain	45	26.61^{ns}	25.44^{ns}	21.94^{ns}	7.71^{ns}	759.33^{ns}	1,665.43^{ns}	570,363.7^{ns}	2,968.66**	2,138.72**	5,237.34**	789.09^{ns}
Accessions*season	9	60.06*	35.15^{ns}	39.23^{ns}	17.50**	986.93^{ns}	6,257.61**	3,649,903**	20,459.03**	12,296.21**	26,870.41**	4,297.76**
Accessions*location	9	47.89^{ns}	29.73^{ns}	41.97^{ns}	10.92^{ns}	510.95^{ns}	9,438.24**	2,705,124**	15,403.54**	10,086.17**	28,445.74**	4,562.71**
Strains*season	5	19.15^{ns}	17.53^{ns}	29.23^{ns}	2.77^{ns}	591.48^{ns}	3,546.55^{ns}	473,516.6^{ns}	2,457.12^{ns}	1,628.54^{ns}	1,047.16^{ns}	900.31^{ns}
Season*location	1	51.37^{ns}	1,016.4*	125.96^{ns}	686.91*	8.01^{ns}	332,521.6**	1.1322**	569,157.2**	459,783.1**	462,964.6**	128,785.2**
Ace*stra*sea*loc	131	20.41^{ns}	18.81^{ns}	18.43^{ns}	5.83^{ns}	445.15^{ns}	2,296.82**	889,695.4^{ns}	2,822.56**	2,493.77**	5,679.69**	1,005.93**

**P < 0.01 Significant, **P < 0.05 highly significant, ns, not significant.*

indicated that response to inoculation is likely to occur when the indigenous rhizobia population is less than 5 or 10 rhizobia cells g^{-1} soil. Furthermore, significant differences observed in the biomass yield in this study show that *B. japonicum* strains enhance the biomass yield more than the *N* fertilizer (Soe et al., 2010). This is in agreement with the research conducted by Hungria and Mendes (2015), where, compared to *N* fertilizers, bacterial strains enhanced the growth traits and the biomass yield.

The low yield recorded in the second season in both locations resulted from inadequate rainfall in Nigeria. Our study demonstrated that the growth traits, biomass yield, number of days to flowering, and yield and yield components in Bambara groundnut accessions were significantly enhanced due to the inoculation of *B. japonicum* strains compared to *N* fertilizers. This is in agreement with a study conducted by Solomon et al. (2012), which revealed that inoculation of *B. japonicum* enhanced nodulation, nitrogen fixation, and yield of soybean in Ethiopia. The results of our study will help farmers increase their profitability due to the low procuring cost of bacterial strains compared to inorganic *N* fertilizers, which are very expensive and lead to environmental contamination and adverse soil health (Igiehon and Babalola, 2018).

Role of Bacterial Strains in Improving Legume Productivity

This study revealed the importance of the inoculation of bacterial strains (*B. japonicum*) over *N* fertilizers. The Bambara groundnut accessions in both locations inoculated with four bacterial strains in this study showed a significant difference in growth, yield, and yield components compared to the *N* fertilizers applied. This indicates that the bacterial strains possessed a greater advantage over the *N* fertilizers. It is of paramount importance to introduce this technique to the end-users—the farmers—to improve their legume production and reduce the amount spent annually on inorganic fertilizers, which adversely affect the soil. The inoculation of bacterial strains to legumes is inexpensive and easily accessible.

Further Studies on Improving Legume Production Using Inoculation

In a research conducted in Chad and Cameroon, the inoculation of Bambara groundnut and groundnut in the field shows that inoculation contributed to the improvement of growth traits and biomass yield of the two legumes as well as their yield and yield components with a mean value of 63.73 kg/ha for groundnut and 72.71 kg/ha for Bambara groundnut, which is related to the results recorded in this study (Gomoung et al., 2017). In another study conducted in South Africa, inoculating *B. japonicum* and *Bacillus subtilis* strains on Bambara groundnut and cowpea revealed that co-inoculation of *B. japonicum* and *Bacillus subtilis* strains had the potential to improve the yield of both Bambara groundnut and cowpea (Nelwamondo, 2020).

CONCLUSION

The bacterial strains inoculated in this study significantly influenced the growth traits, biomass yield, and yield traits of Bambara groundnut accessions during both seasons and both locations. The results revealed that it is important to promote the use of biofertilizers over inorganic *N* fertilizers, which most farmers may not be able to afford due to their high cost, and those who can afford them usually apply *N* fertilizers below manufacturer-recommended levels. Rhizobia inoculants are readily available and farmers need to be informed about this new technique because the results of research such as this one tend to remain within the research community and do not reach the farmers. Therefore, more efforts are needed to disseminate new innovations to farmers in rural settlements and introduce this cheap and friendly technique to the poor farming community to improve the production of their legumes and increase their profit. For alternative use, FA3, USDA110, and RACA6 can be recommended for Bambara groundnut inoculations.

DATA AVAILABILITY STATEMENT

The original contributions presented in the study are included in the article/supplementary material, further inquiries can be directed to the corresponding author/s.

AUTHOR CONTRIBUTIONS

TB undertook conceptualization, methodology, and original draft preparation. OB and OO undertook supervision and the formal analysis and editing. MA handled project administration and funding acquisition. All the authors discussed the result and contributed to the final manuscript.

FUNDING

This research was funded by Global Crop Diversity Trust through Genetic Resources Center, International Institute of Tropical Agriculture, Ibadan, Nigeria.

ACKNOWLEDGMENTS

The authors are grateful to the Genetic Resources Center of the International Institute of Tropical Agriculture, Ibadan, Nigeria for germplasm, facilities, and financial support.

REFERENCES

Battye, W., Aneja, V. P., and Schlesinger, W. H. (2017). Is nitrogen the next carbon? *J. Earth's Fut.* 5, 894–904. doi: 10.1002/2017EF000592

Black, C. A., Evans, D., and White, J. (1965). *Methods of Soil Analysis: Chemical and Microbiological Properties*. New York, NY: ASA.

Cai, Z., Wang, B., Xu, M., Zhang, H., He, X., Zhang, L., et al. (2015). Intensified soil acidification from chemical *N* fertilization and prevention by manure in an

18-year field experiment in the red soil of southern China. *J. Soils Sediment.* 15, 260–270. doi: 10.1007/s11368-014-0989-y

Enagbonma, B. J., and Babalola, O. O. (2019). Potentials of termite mound soil bacteria in ecosystem engineering for sustainable agriculture. *Annals Microbiol.* 69, 211–219. doi: 10.1007/s13213-019-1439-2

Fasusi, O. A., and Babalola, O. O. (2021). The multifaceted plant-beneficial rhizobacteria toward agricultural sustainability. *Plant Protect. Sci.* 57, 95–111. doi: 10.17221/130/2020-PPS

Gomoung, D., Mbailao, M., Toukam, S. T., and Ngakou, A. (2017). Influence of cross-inoculation on groundnut and bambara groundnut-rhizobium symbiosis: contribution to Plant growth and yield in the field at Sarh (Chad) and Ngaoundere (Cameroon). *Am. J. Plant Sci.* 8, 1953–1966. doi: 10.4236/ajps.2017.88131

Guo, J. H., Liu, X. J., Zhang, Y., Shen, J. L., Han, W. X., Zhang, W. F., et al. (2010). Significant acidification in major Chinese croplands. *J. Sci.* 327, 1008–1010. doi: 10.1126/science.1182570

Hasan, M., Uddin, M. K., Mohammed, M. T. M., and Zuan, A. T. K. (2019). impact of nitrogen and phosphorus fertilizer on growth and yield of bambara groundnut. *J. Plant Archiv.* 19, 501–504. doi: 10.3329/bjb.v48i4.48932

Hasan, M., Uddin, M. K., Muda Mohamed, M. T., and Kee Zuan, A. T. (2018). Nitrogen and phosphorus management for Bambara groundnut (Vigna subterranea) production-a review. *J. Legume Res. Int. J.* 41, 4. doi: 10.18805/LR-379

Houngnandan, P., Sanginga, N., Woomer, P., Vanlauwe, B., and Van Cleemput, O. (2000). Response of Mucuna pruriens to symbiotic nitrogen fixation by rhizobia following inoculation in farmers' fields in the derived savanna. *Benin.* 30, 558–565. doi: 10.1007/s003740050036

Hungria, M., and Mendes, I. C. (2015). Nitrogen fixation with soybean: the perfect symbiosis? *Symbiosis* 10, 99. doi: 10.1002/9781119053095.ch99

Igiehon, N. O., and Babalola, O. O. (2018). Rhizosphere microbiome modulators: contributions of nitrogen fixing bacteria towards sustainable agriculture. *Int. J. Environ. Res. Public Health* 15, 574. doi: 10.3390/ijerph15040574

Ikenganyia, E., Anikwe, M., and Ngwu, O. S. S. (2017). Responses of Bambara groundnut [Vigna subterranea (L.) Verdc.] to phosphate fertilizer rates and plant spacing and effects on soil nutrient statues in a degraded tropical ultisol Agbani Enugu South East Nigeria. *J. Int. J. Plant.* 17, 1–17. doi: 10.9734/IJPSS/2017/32606

Islam, S. M., Gaihre, Y. K., Biswas, J. C., Jahan, M. S., Singh, U., Adhikary, S. K., et al. (2018). Different nitrogen rates and methods of application for dry season rice cultivation with alternate wetting and drying irrigation: fate of nitrogen and grain yield. *J. Agricult. Water Manage.* 196, 144–153. doi: 10.1016/j.agwat.2017.11.002

Jaiswal, S. K., and Dakora, F. D. (2019). Widespread distribution of highly adapted Bradyrhizobium species nodulating diverse legumes in Africa. *Front. Microbiol.* 9, 310. doi: 10.3389/fmicb.2019.00310

Kyei-Boahen, S., Savala, C. E., Chikoye, D., and Abaidoo, R. (2017). Growth and yield responses of cowpea to inoculation and phosphorus fertilization in different environments. *J. Front. Plant Sci.* 8, 646. doi: 10.3389/fpls.2017.00646

Mahmood, A., Turgay, O. C., Farooq, M., and Hayat, R. (2016). Seed biopriming with plant growth promoting rhizobacteria: a review. *J. FEMS Microbiol. Ecol.* 92, fiw112. doi: 10.1093/femsec/fiw112

Mandizvo, T., and Odindo, A. (2019). Seed mineral reserves and vigour of Bambara groundnut (Vigna subterranea L.) landraces differing in seed coat colour. *Heliyon* 5, e01635. doi: 10.1016/j.heliyon.2019.e01635

Mayes, S., Ho, W. K., Chai, H. H., Gao, X., Kundy, A. C., Mateva, K. I., et al. (2019). Bambara groundnut: AN exemplar underutilised legume for resilience under climate change. *Planta* 250, 803–820. doi: 10.1007/s00425-019-03191-6

Mulvaney, B. J., and Page, A. (1982). Nitrogen-total. *Meth. Soil Anal.* 2, 595–624.

Nelwamondo, A. M. (2020). *Assessment of co-inoculation of Bradyrhizobium Japonicum and Bacillus subtilis on yield and metabolic profile of Bambara groundnut and cowpea under glasshouse conditions* (Doctoral dissertation). University of South Africa, Pretoria, South Africa. Available online at: https://uir.unisa.ac.za/bitstream/handle/10500/27023/dissertation_nelwamondo_am.pdf?sequence=1&isAllowed=y

Oburger, E., and Schmidt, H. (2016). New methods to unravel rhizosphere processes. *J. Trends Plant Sci.* 21, 243–255. doi: 10.1016/j.tplants.2015.12.005

Ogbuehi, H. C. (2020). Effect of nodumax inoculant on morpho-physiological parameters, nutrient content and yield of soybean (Glycine max. *L). J. Agricult. Food Sci.* 18, 54–72. doi: 10.4314/jafs.v18i2.4

Sanginga, N., Ibewiro, B., Houngnandan, P., Vanlauwe, B., Okogun, J., Akobundu, I., et al. (1996). Evaluation of symbiotic properties and nitrogen contribution of mucuna to maize grown in the derived savanna of West Africa. *J. Plant Soil* 179, 119–129. doi: 10.1007/BF00011649

Sarr, P. S., Okon, J. W., Begoude, D. A. B., Araki, S., Ambang, Z., Shibata, M., et al. (2016). Symbiotic N2-fixation estimated by the 15N tracer technique and growth of Pueraria phaseoloides (Roxb.) Benth. inoculated with Bradyrhizobium strain in field conditions. *J. Scientifica* 2016, 2689. doi: 10.1155/2016/7026859

Soe, K. M., Bhromsiri, A., and Karladee, D. (2010). Effects of selected endophytic actinomycetes (Streptomyces sp.) and Bradyrhizobia from Myanmar on growth, nodulation, nitrogen fixation and yield of different soybean varieties. *CMU J. Nat. Sci.* 9, 95–109.

Solomon, T., Pant, L. M., and Angaw, T. (2012). Effects of inoculation by Bradyrhizobium japonicum strains on nodulation, nitrogen fixation, and yield of soybean (Glycine max L. *Merill)* varieties on nitisols of Bako, Western Ethiopia. *Int. Scholar. Res. Notic.* 2012, 475. doi: 10.5402/2012/261475

Soropa, G., Nyamangara, J., and Nyakatawa, E. Z. (2019). Nutrient status of sandy soils in smallholder areas of Zimbabwe and the need to develop site-specific fertiliser recommendations for sustainable crop intensification. *South Afric. J. Plant Soil* 36, 149–151. doi: 10.1080/02571862.2018.1517901

Suzuki, Y., Adhikari, D., Itoh, K., and Suyama, K. (2014). Effects of temperature on competition and relative dominance of Bradyrhizobium japonicum and Bradyrhizobium elkanii in the process of soybean nodulation. *Plant Soil* 374, 915–924. doi: 10.1007/s11104-013-1924-5

Tyoakoso, M., Toungos, M., and Babayola, M. (2019). Effects of nitrogen rate on growth and yield of bambara groundnut (vigna subterranea (l.) verdc.) in jalingo, taraba state, nigeria. *J. Int. J. Res. granthaalayah* 7, 67–76. doi: 10.29121/granthaalayah.v7.i12.2019.301

Walkley, A., and Black, I. A. (1934). An examination of the Degtjareff method for determining soil organic matter, and a proposed modification of the chromic acid titration method. *Soil Sci.* 37, 29–38. doi: 10.1097/00010694-193401000-00003

Zhang, F., Cui, Z., Fan, M., Zhang, W., Chen, X., and Jiang, R. (2011). Integrated soil–crop system management: reducing environmental risk while increasing crop productivity and improving nutrient use efficiency in China. *J. Environ. Qual.* 40, 1051–1057. doi: 10.2134/jeq2010.0292

Conflict of Interest: The authors declare that the research was conducted in the absence of any commercial or financial relationships that could be construed as a potential conflict of interest.

Publisher's Note: All claims expressed in this article are solely those of the authors and do not necessarily represent those of their affiliated organizations, or those of the publisher, the editors and the reviewers. Any product that may be evaluated in this article, or claim that may be made by its manufacturer, is not guaranteed or endorsed by the publisher.

Copyright © 2022 Bitire, Abberton, Oyatomi and Babalola. This is an open-access article distributed under the terms of the Creative Commons Attribution License (CC BY). The use, distribution or reproduction in other forums is permitted, provided the original author(s) and the copyright owner(s) are credited and that the original publication in this journal is cited, in accordance with accepted academic practice. No use, distribution or reproduction is permitted which does not comply with these terms.

frontiers | Frontiers in Sustainable Food Systems

ORIGINAL RESEARCH
published: 27 June 2022
doi: 10.3389/fsufs.2022.938128

Foliar Silicon Spray to Strawberry Plants During Summer Cutting Propagation Enhances Resistance of Transplants to High Temperature Stresses

Jie Xiao[1], *Yali Li*[1] *and Byoung Ryong Jeong*[1,2,3]*

[1] Division of Applied Life Science (BK21 Four), Department of Horticulture, Graduate School, Gyeongsang National University, Jinju, South Korea, [2] Institute of Agriculture and Life Science, Gyeongsang National University, Jinju, South Korea, [3] Research Institute of Life Science, Gyeongsang National University, Jinju, South Korea

OPEN ACCESS

Edited by:
Joerg Schaller,
Leibniz Center for Agricultural Landscape Research (ZALF), Germany

Reviewed by:
Lyudmila Petrova Simova-Stoilova, Institute of Plant Physiology and Genetics (BAS), Bulgaria
Ou Sheng,
Guangdong Academy of Agricultural Sciences (GDAAS), China

***Correspondence:**
Byoung Ryong Jeong
brjeong@gnu.ac.kr

Specialty section:
This article was submitted to Crop Biology and Sustainability, a section of the journal Frontiers in Sustainable Food Systems

Received: 07 May 2022
Accepted: 02 June 2022
Published: 27 June 2022

Citation:
Xiao J, Li Y and Jeong BR (2022) Foliar Silicon Spray to Strawberry Plants During Summer Cutting Propagation Enhances Resistance of Transplants to High Temperature Stresses. Front. Sustain. Food Syst. 6:938128. doi: 10.3389/fsufs.2022.938128

Silicon (Si) has been reported to benefit plant growth and stress resistance. This work aimed to find out an optimal method of Si application to enhance the resistance of strawberry (*Fragaria* × *ananassa* Duch.) transplants to high temperatures, commonly experienced in the summer when strawberries are propagated for greenhouse production in Korea. Plants of strawberry "Sulhyang", "Maehyang", and "Kuemsil" were subjected to one of five treatments before the cutting propagation: no treatment (control), substrate dressing of a water-soluble silicate fertilizer, substrate drench of 75 mg·L^{-1} Si (from potassium silicate) to the mother plants, or foliar spray of 75 mg·L^{-1} Si to either the mother plants or daughter plants. Half of the daughter plants in each Si treatment received continued application of Si through either substrate dressing of a water-soluble silicate fertilizer, substrate drench, or foliar spray after the cutting propagation. A high temperature (43°C) resistance test was conducted in plant growth chambers for 7 days with a 16-h photoperiod with a light intensity of 300 mmol·m^{-2}·s^{-1} PPFD. During the high temperature test, the rate of decline in the photosynthesis was lower in plants treated with Si than in the control. After the high temperature test, it was observed that Si application significantly increased the shoot fresh weight of transplants. Moreover, the contents of sugars, proteins, and enzymatic (CAT, SOD, POD, and APX) and non-enzymatic (anthocyanin and proline) antioxidants were higher in plants treated with Si throughout the entire propagation period, compared to the control and plants only treated with Si before or after the cutting propagation. Overall, the Si application improved the growth of the transplants regardless of the application method used. Moreover, spraying the daughter plants with Si, and continually spraying the transplants were found to be the best and is recommended to increase the resistance of strawberries to high temperatures during propagation.

Keywords: abiotic stress, anthocyanin, antioxidant enzyme, chlorophyll fluorescence, photosynthesis pigment, reactive oxygen species

INTRODUCTION

Strawberry (*Fragaria* × *ananassa*, Duchesne) is a major economical fruit crop. In Korea, strawberry is cultivated on 6,057 hectares as of 2021. Of those, the open-field cultivation area was 519 hectares, while most of the strawberry cultivation was through facility cultivation (Korean Statistical Information Service, KOSIS, The Area of Facility Crop Cultivation https://kosis.kr/statHtml/statHtml.do?orgId=101&tblId=DT_1ET0017&conn_path=I2 accessed on 7 April 2022). Almost all strawberry plants are commercially propagated by using daughter plants from the runners (Caruana et al., 2018). The mother plants begin growing into unrooted runners in March, and the runner grows to daughter plants and are transferred to trays for rooting in June. Lastly, these plants are kept in a greenhouse until September, then established in the field or greenhouses (Takeda et al., 2004; Li et al., 2020). During this period, the temperature inside the greenhouse reaches 45°C with natural ventilation (Kim et al., 2020). In the last decade, abnormally high-temperature weather occurred from spring to late autumn in Korea (Korea Meteorological Administration, Report of Abnormal Climate http://www.climate.go.kr/home/bbs/list.php?code=93&bname=abnormal accessed on 7 April 2022). Furthermore, excessively high temperature frequently occurs due to global warming, and the Fifth Assessment Report presented by the Intergovernmental Panel on Climate Change (IPCC) suggests that there is a long-term increase in the global temperature (IPCC, 2014). Using cooling devices may be a heavy burden for farmers, therefore, researchers are recently trending toward improving the resistance of strawberries to high temperatures.

Silicon (Si) is the second most abundant element in the earth's crust (Epstein, 1994). It is present in the form of silicic acid (H_4SiO_4) in the soil solution and is absorbed by plants (Etesami and Jeong, 2018). Si has been demonstrated to be beneficial for the growth and development of plants, and the accumulation and deposition of Si can form a cuticle-Si double silicate layer in the leaves, decreasing the evapotranspiration and improving the photosynthesis rate (Park et al., 2018). Additionally, the variation can reinforce the morphological structures of the cell wall, and maintain the integrity of the cell membrane by creating a physical barrier (Nasircilar, 2021). It was reported that Si improves the N use efficiency and adjusts the absorption of P and micronutrients (Pavlovic et al., 2021). Besides, Si was involved in the stomatal regulation and the antioxidant enzyme system, and alleviated damages by preventing lipid peroxidation and hydrogen peroxide (H_2O_2) formation (Hu et al., 2020).

Many researchers have concluded that Si plays an important role in mitigating high temperature stresses in plants. The Si helps maintain photosynthesis in high-temperature environments by improving the abundance of photosynthetic proteins, especially the photosystem I P700 apoprotein A (PsaA) and photosystem II protein D1 (PsbA) (Soundararajan et al., 2014; Muneer et al., 2017; Moradtalab et al., 2019). Moreover, Si application can mitigate the electrolyte leakage of leaf tissues (Agarie et al., 1998), and alleviate heat-induced oxidative membrane damages by improving the antioxidant enzyme activities (Sattar et al., 2020). Furthermore, Si is the only element that can be translocated and accumulated in massive amounts in plants without toxic symptoms, and it is non-corrosive and pollution-free (Ma et al., 2001; Wang et al., 2016). Therefore, Si can be used as a profitable and effective fertilizer for strawberry facility cultivation.

However, Si fertilization in agricultural production is in its infancy, and it has yet to be determined how silicon affects specific internal mechanisms in plants. The concentration of Si in the shoots greatly varies among different plants. Plants are classified as either Si excluders or non-accumulators, Si intermediates, and Si accumulators according to the

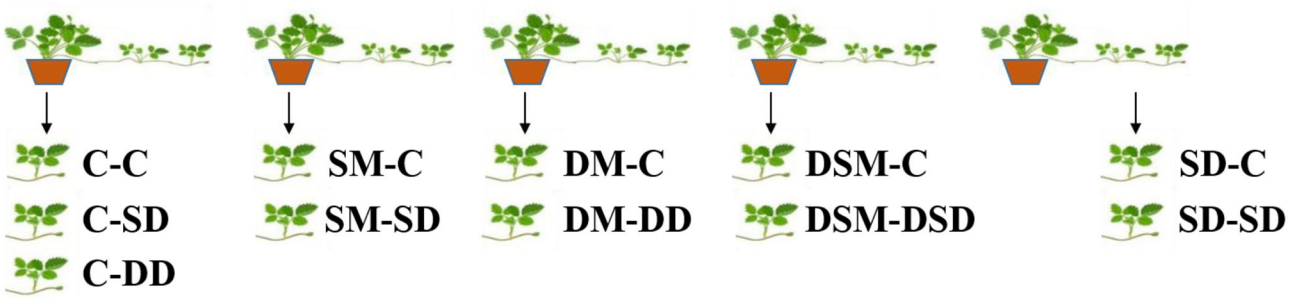

FIGURE 1 | Methods of Si application for strawberries. Respectively: C-C, no Si application during cutting propagation; C-SD, no Si application before cutting propagation and the daughter plants sprayed with the Si solution after cutting propagation; C-DD, no Si application before cutting propagation and the daughter plants drenched with the Si solution after cutting propagation; SM-C, the mother plants sprayed with the Si solution before cutting propagation and no Si application after cutting propagation; SM-SD, the mother plants sprayed with the Si solution before cutting propagation and the daughter plants sprayed with the Si solution after cutting propagation; DM-C, the mother plants drenched with the Si solution before cutting propagation and no Si application after cutting propagation; DM-DD, the mother plants drenched with the Si solution before cutting propagation and the daughter plants drenched with the Si solution after cutting propagation; DSM-C, the mother plants dressed with the soluble Si fertilizer before cutting propagation and no Si application after cutting propagation; DSM-DSD, the mother plants dressed with the soluble Si fertilizer before cutting propagation and the daughter plants dressed with the soluble Si fertilizer after cutting propagation; SD-C, the daughter plants sprayed with the Si solution before cutting propagation and no Si application after cutting propagation; or SD-SD, the daughter plants sprayed the Si solution before and after cutting propagation.

TABLE 1 | Methods of Si application for strawberries.

Treatment	Application of Si before cutting propagation	Application of Si after cutting propagation
C-C	No Si application	No Si application
C-SD	No Si application	The daughter plants sprayed with the Si solution
C-DD	No Si application	The daughter plants drenched with the Si solution
SM-C	The mother plants sprayed with the Si solution	No Si application
SM-SD	The mother plants sprayed with the Si solution	The daughter plants sprayed with the Si solution
DM-C	The mother plants drenched with the Si solution	No Si application
DM-DD	The mother plants drenched with the Si solution	The daughter plants drenched with the Si solution
DSM-C	The mother plants dressed with the soluble Si fertilizer	No Si application
DSM-DSD	The mother plants dressed with the soluble Si fertilizer	The daughter plants dressed with the soluble Si fertilizer
SD-C	The daughter plants sprayed with the Si solution	No Si application
SD-SD	The daughter plants sprayed with the Si solution	The daughter plants sprayed with the Si solution

concentration of Si ranging from <0.5, 0.5–0.1, and more than 1.0% (v/v), respectively (Takahashi et al., 1990). All monocots are Si accumulators, and most dicots belong to the excluders or intermediates. The absorption of Si includes radial transport and release of Si. Firstly, it depends on a proteinaceous transporter for the Si transport to the cortical cells of the root from the exterior (Tamai and Ma, 2003). For instance, tomato, cucumber, and rice, respectively, represent Si non-accumulators, Si intermediates, and Si accumulators. Rice had the highest density of the Si transporter, followed by cucumbers. Therefore, the accumulation of Si in shoots depends on the ability of the roots to absorb Si (Mitani and Ma, 2005). Following absorption to the root, Si is transported into the xylem of the shoot as silicic acid. Those two processes are involved in two different types of Si transporters. Roots absorb Si into the symplast via the influx transporter low silicon rice 1 (Lsi1), and the efflux transporter Lsi2 loads the Si into the apoplast (Ma and Takahashi, 2002). In higher plants, rice *Lsi1* was the first gene that was isolated by a low-Si rice mutant, and was identified to encode the Si transporter (Ma et al., 2006). In contrast to rice, little information is available in the research on Si transport in dicots, and the gene encoding the silicon transporter in strawberries was not identified until 2017 (Ouellette et al., 2017). In addition to transporter proteins, Si uptake is related to transpiration, and with the loss of water. The Si is deposited as the "phytoliths" in the leaves, stem, leaf sheath, and hull (Ma, 2003). And the "phytoliths" are able to recycle into the soil to form a soil-Si-plant mechanisms in ecosystems (Katz et al., 2021). Compared to non-agricultural soils, the agricultural soils showed lower Si concentrations due to desilication during the soil-Si-plant cycle (Puppe et al., 2021). Therefore, it is necessary to explore improved utilization of Si in limited sources. Researchers found that the method of Si application and plant conditions can greatly influence the benefits that strawberry can obtain from Si (Dallagnol et al., 2020). Combining soil and foliar Si application resulted in the greatest yield in wheat (Kowalska et al., 2021). Soil Si application was the most effective in alleviating cadmium stress (Howladar et al., 2018). Furthermore, it was reported that potassium silicate (K_2SiO_3) is more efficient than Na_2SiO_3 or $CaSiO_3$ (Sivanesan et al., 2013). The commercial soluble silicate fertilizer 'Keunson' also showed beneficial effects on plant growth (Vu et al., 2017; Song et al., 2021). Therefore, we are still working on finding the most suitable Si application method for enhancing the growth and stress tolerance in strawberry.

In this study, the three most common strawberry cultivars "Sulhyang", "Maehyang", and "Kuemsil" in Korea were investigated. "Sulhyang" was registered in 2005 and originated from the "Akihime" and "Red Pearl", and its cultivation area occupies more than 80% of strawberries in Korea (Jun et al., 2017). "Maehyang" was bred from "Tochinomine" and "Akihime", and showed high growth, yield, and quality (Kim et al., 2004). "Kuemsil" was derived from "Sulhyang" and "Maehyang" with the general characteristics of early flower bud differentiation and first harvest (Yoon et al., 2020). The optimum growth temperature range for strawberries is between 10 and 26°C (Strik, 1985). And it has been established that the critical temperature range for strawberry growth inhibition is 35–40°C (Kadir et al., 2006). Previous research has reported oxidative damages in "Sulhyang" and "Maehyang" under 33 and 41°C, and showed a decrease in the abundance of PSI-A core protein of PSI (PsaA) and D1 protein of PSII (PsbA) (Muneer et al., 2017). Moreover, "Sulhyang" showed necrotic leaves after subjection to 42°C (Li et al., 2020). Although there is no research on heat tolerance of "Kuemsil", its antioxidative properties are lower than "Sulhyang" and "Maehyang" (Kim et al., 2012). Therefore, the three cultivars are thought to be sensitive to high temperatures. We applied Si for strawberry plants during the summer cutting propagation, and evaluated the growth parameters, antioxidant enzymes, and reactive oxygen species of transplants after Si application under high temperatures to preliminarily dissect the response of strawberry transplants incurred by high temperatures, and to find the optimal Si application method to enhance the resistance to high temperature stresses in strawberry transplants during hot summer seasons.

TABLE 2 | The growth parameters as affected by the Si treatment in strawberry transplants after subjection to 43°C for 7 days.

Treatment before cutting (A)	Treatment after cutting (B)	Sulhyang						Maehyang						Kuemsil					
		Shoot				Leaf		Shoot				Leaf		Shoot				Leaf	
		Height (cm)	Crown diameter (mm)	Fresh weight (g)	Dry weight (g)	Length (cm)	Width (cm)	Height (cm)	Crown diameter (mm)	Fresh weight (g)	Dry weight (g)	Length (cm)	Width (cm)	Height (cm)	Crown diameter (mm)	Fresh weight (g)	Dry weight (g)	Length (cm)	Width (cm)
C	C	17.8 f[z]	5.63 e	5.55 e	1.83 c	8.1 a	5.7 b	21.4 e	5.9 cd	3.92 e	1.90 c	7.2 c	4.3 e	22.0 e	6.93 d	6.44 h	2.16 c	8.9 de	7.8 f
C	SD	27.0 a	7.35 c-e	7.14 bc	2.07 b	9.4 a	6.9 a	28.6 ab	7.2 bc	5.94 b-b	2.81 a	9.3 ab	7.1 a	23.6 cd	7.49 cd	8.71 cd	2.64 ab	10.1 cd	9.6 cd
C	DD	20.2 d-f	8.38 a-c	7.52 bc	2.24 b	8.8 a	7.3 a	25.8 b-d	8.8 ab	6.23 bc	2.62 ab	8.7 a-c	5.3 b-e	25.8 b	7.77 bc	9.68 b	2.62 ab	9.7 c-e	9.7 cd
SM	C	22.1 c-e	6.27 de	5.87 de	2.03 b	8.3 a	5.8 b	25.3 b-e	4.7 d	4.61 de	2.11 bc	7.5 bc	4.5 de	23.0 c-e	7.17 d	7.82 fg	2.18 c	8.5 e	8.4 ef
SM	SD	27.1 a	7.70 b-d	7.21 bc	2.18 b	8.8 a	7.3 a	28.2 a-c	7.7 bc	6.82 b	2.32 a-c	9.7 a	5.9 a-d	26.6 ab	7.82 bc	9.72 b	2.64 ab	12.2 b	10.6 b
DM	C	22.2 c-e	7.16 c-e	6.79 cd	2.14 b	8.6 a	5.7 b	24.1 c-e	6.8 bc	4.83 c-e	2.13 bc	7.8 a-c	5.1 c-e	23.5 cd	7.15 d	7.81 fg	2.26 c	10.6 c	9.0 de
DM	DD	23.3 bc	9.78 a	9.67 a	2.59 a	8.8 a	5.7 b	24.4 b-e	10.2 a	8.31 a	2.85 a	9.6 a	6.8 ab	27.1 a	8.93 a	10.33 a	2.89 a	12.4 b	12.1 a
DSM	C	19.5 ef	7.83 b-d	7.55 bc	2.25 b	8.2 a	5.4 b	23.3 de	7.7 bc	4.90 c-e	2.44 a-c	8.7 a-c	5.7 a-e	23.0 de	7.33 cd	7.56 g	2.39 bc	10.0 cd	10.2 bc
DSM	DSD	23.0 b-d	9.39 ab	7.50 bc	2.20 b	8.7 a	7.3 a	26.9 a-d	8.8 ab	6.72 b	2.64 ab	8.5 a-c	5.2 c-e	24.1 c	7.82 bc	8.57 de	2.58 ab	10.9 c	11.9 a
SD	C	21.9 c-e	6.82 c-e	7.35 bc	2.19 b	9.3 a	7.0 a	27.4 a-d	6.1 cd	6.90 b	2.20 bc	7.6 bc	5.1 c-e	25.9 b	7.82 bc	8.18 ef	2.63 ab	12.3 b	11.6 a
SD	SD	25.4 ab	6.96 c-e	7.87 b	2.25 b	9.0 a	6.8 a	31.0 a	7.3 bc	8.42 a	2.63 ab	8.1 a-c	6.3 a-c	27.4 a	8.32 b	9.09 c	2.74 a	14.2 a	12.1 a
F-test [y]	A	**	*	***	*	NS	*	**	**	***	**	NS	**	***	***	***	***	NS	***
	B	***	**	***	*	NS	***	***	***	***	*	*	**	***	***	***	***	***	***
	A × B	***	***	***	***	***	***	**	NS	*	NS	NS	NS	***	***	***	***	NS	***

[z] *Lowercase letters indicate significant differences calculated by the Duncan's multiple range test at $p \leq 0.05$.*

[y] *NS, *, **, and *** represent non-significant or significant at $p \leq 0.05$, 0.01, and 0.001, respectively: C, no Si application; SM, the mother plants sprayed with the Si solution; DM, the mother plants drenched with the Si solution; DSM, the mother plants dressed with the soluble Si fertilizer; SD, the daughter plants sprayed with the Si solution; DD, the daughter plants drenched with the Si solution; and DSD, the daughter plants dressed with the soluble Si fertilizer.*

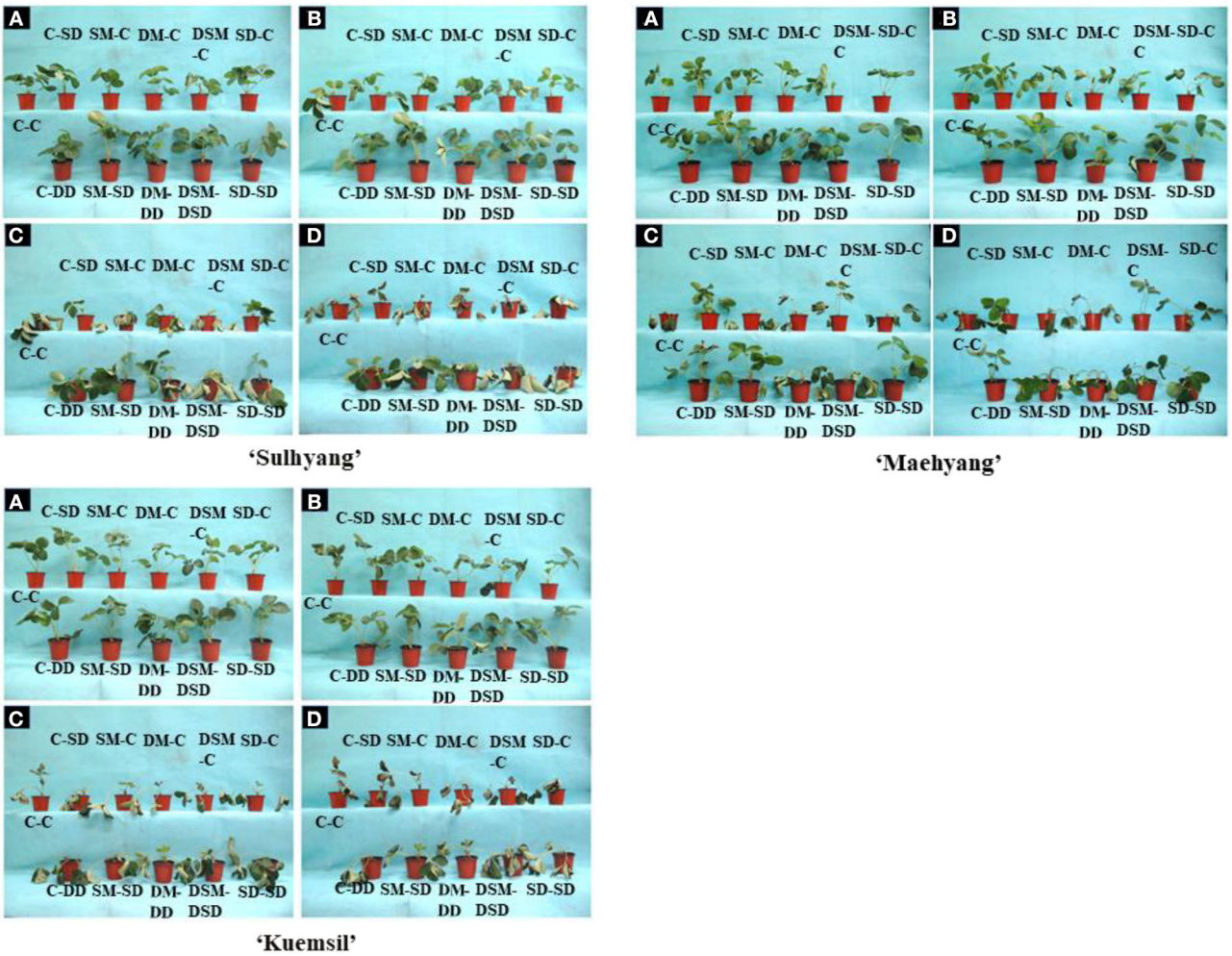

FIGURE 2 | Morphophysiological state as affected by the Si treatment in strawberry transplants after subjection to 43°C for 1 **(A)**, 3 **(B)**, 5 **(C)**, and 7 **(D)** days. See **Figure 1** for descriptions of treatment codes.

MATERIALS AND METHODS

Plant Materials and Silicon Treatments

The strawberry cultivars used were "Sulhyang", "Maehyang", and "Kuemsil". Daughter plants were selected from a strawberry farm (Sugok-myeon, Jinju, Gyeongsangnam-do, Korea) and transplanted in a hydroponic gutter system filled with the BVB medium (Bas Van Buuren Substrate, EN-12580, De Lier, Westland, The Netherlands) on January 10, 2021. The plants was drip-irrigated with a multipurpose nutrient solution composed of NH_4NO_3 80.0, KNO_3 232.3, KH_2PO_4 272.0, K_2SO_4 17.4, $Ca(NO_3)_2{\cdot}4H_2O$ 467.6, $MgSO_4{\cdot}H_2O$ 209.1, H_3BO_3 1.4, $NaMoO_4{\cdot}2H_2O$ 0.12, $MnSO_4{\cdot}4H_2O$ 2.10, $ZnSO_4{\cdot}7H_2O$ 0.80, and $CuSO_4{\cdot}5H_2O$ 0.20 ($mg{\cdot}L^{-1}$).

The axillary buds of mother plants developed into runners and gradually grew into daughter plants after 2 months. The Si treatments were started on March 10, 2021. Strawberry plants were subjected to one of five treatments before the cutting propagation: C, no treatments (control); SM, foliar spray of a Si solution (from K_2SiO_3 at a final concentration of 75 $mg{\cdot}L^{-1}$) to the mother plants; DM, substrate drenching with a Si solution to the mother plants; DSM, substrate dressing with a commercial soluble silicon fertilizer "Keunson" (equivalent to 0.075 g of pure Na_2SiO_3) (Saturn Bio Tech Co., Ltd., Gangwon-do, Korea) to the mother plants; or SD, foliar spraying of Si solution to the daughter plants. All daughter plants were stuck in 21-cell zigzag trays (21-Zigpot/21 cell tray, Daeseung, Jeonju, Korea) filled with the BVB medium (Bas Van Buuren Substrate, EN-12580, De Lier, Westland, The Netherlands) on April 30, 2020. The plants were then put into a fogging system (UH-303, JB Natural Co. Ltd., Gunpo, Korea) on a propagation bench for rooting. Two weeks later, the plants were moved out from the fogging tunnel, and the control group was separated into three groups: C-C, no Si application during cutting propagation; C-SD, no Si application before cutting propagation and the daughter plants sprayed with the Si solution after cutting propagation; C-DD, no

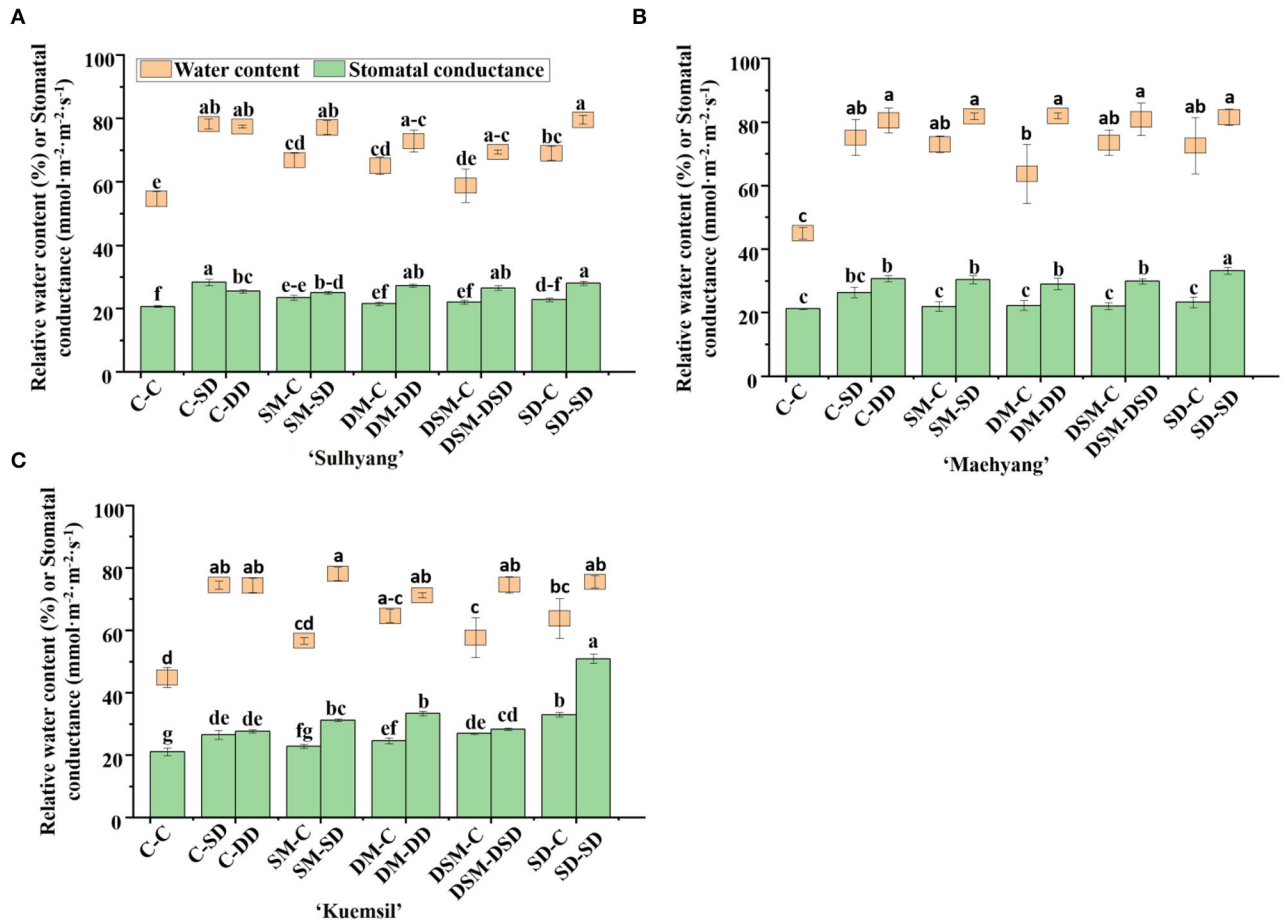

FIGURE 3 | Leaves relative water content and stomatal conductance of strawberry transplants **(A)** "Sulhyang"; **(B)** "Maehyang"; and **(C)** "Kuemsil" as affected by the Si treatment after subjection to 43°C for 7 days. Lowercase letters indicate significant differences calculated by the Duncan's multiple range test at $p \leq 0.05$. See **Figure 1** for descriptions of treatment codes.

Si application before cutting propagation and the daughter plants drenched with the Si solution after cutting propagation. The daughter plants from other treatments were separated into two groups and continued application Si: SM-C, the mother plants sprayed with the Si solution before cutting propagation and no Si application after cutting propagation; SM-SD, the mother plants sprayed with the Si solution before cutting propagation and the daughter plants sprayed with the Si solution after cutting propagation; DM-C, the mother plants drenched with the Si solution before cutting propagation and no Si application after cutting propagation; DM-DD, the mother plants drenched with the Si solution before cutting propagation and the daughter plants drenched with the Si solution; DSM-C, the mother plants dressed with soluble Si fertilizer before cutting propagation and no Si application after cutting propagation; DSM-DSD, the mother plants dressed with the soluble Si fertilizer before cutting propagation and the daughter plants dressed with the soluble Si fertilizer; SD-C, the daughter plants spray with the Si solution before cutting propagation and no Si application after cutting propagation; or SD-SD, the daughter plants sprayed with the Si solution before and after cutting propagation (**Figure 1** and **Table 1**).

High Temperature Stress Treatments and Measurements of the Chlorophyll Fluorescence Parameters

The daughter plants were transplanted into 10 cm plastic pots for high temperature experiments on 11 June 2021. Two weeks later, transplants were randomly placed in plant growth chambers (C1200H3, FC Poibe Co. Ltd., Seoul, Korea) for 1 week under a condition of 43°C, a 16-hour photoperiod with a light intensity of 300 $mmol \cdot m^{-2} \cdot s^{-1}$ PPFD, and 65% relative humidity. The plants were fertigated with 50 mL per plant of a multipurpose nutrient solution everyday. There were 3 replicates and each replicate had 3 transplants, a total of 9 plants for each treatment. All plants were randomly placed in the growth chambers. The chlorophyll fluorescence parameters were measured every 48

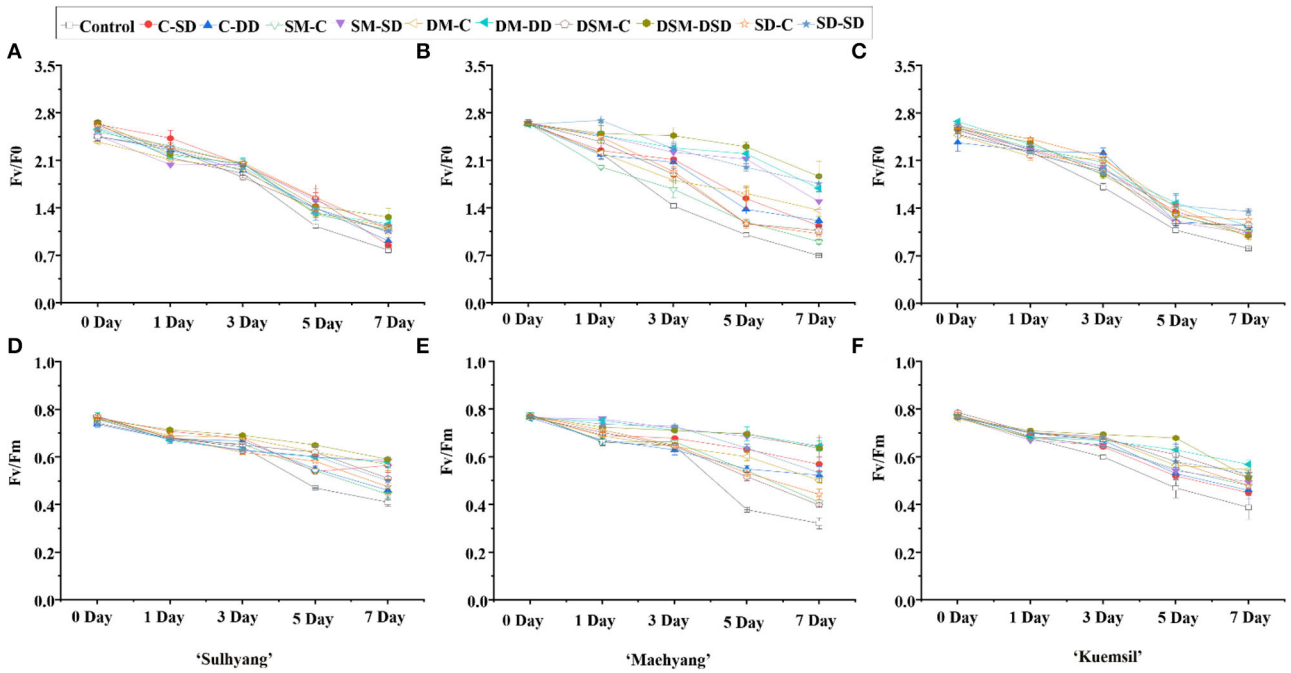

FIGURE 4 | Chlorophyll fluorescence Fv/F0 and Fv/Fm of strawberry transplants **(A,D)** "Sulhyang"; **(B,E)** "Maehyang"; and **(C,F)** "Kuemsil" as affected by the Si treatment after subjection to 43°C for 0, 1, 3, 5, and 7 days. See **Figure 1** for descriptions of treatment codes.

hours using a portable fluorometer (FluorPen FP110, Photon Systems Instruments, Drásov, Czech Republic).

Measurement of the Growth Parameters

The plant height, crown diameter, fresh and dry weights of the shoot, length and width and stomatal conductance of leaves of the transplants were measured. The stomatal conductance was determined using a Decagon Leaf Porometer SC-1 (Decagon Device Inc., Pullman, WA, USA). The fresh weight was measured with an electronic scale (EW 220-3NM, Kern and Sohn GmbH., Balingen, Germany), The dry weights of shoot and roots were measured after drying for 72 hours in a drying oven (Venticell-222, MMM Medcenter Einrichtungen GmbH., Munich, Germany) at 70°C. The relative water content (LRWC) was determined using the following formula (González and González-Vilar, 2001):

$$\text{Relative water content}\ (\%) = \frac{(\text{Fresh weight} - \text{Dry weight}) \times 100}{\text{Saturated weight} - \text{Dry weight}}$$

Determination of the Contents of Chlorophyll, Carotenoid, and Total Anthocyanin

The content of chlorophyll was measured according to Sükran et al. (1998). A 0.1 g leaf sample was submerged in 80% (*v*/*v*) acetone for 12 hours, which was then centrifuged (Centrifuge 5428, Eppendorf, Hamburg, Germany) at 13,000 rpm for 15 min at 4°C, and the absorbance of the liquid supernatant was measured at 645 and 663 nm using a UV-spectrophotometer (Libra S22, Biochrom Ltd., Cambridge, UK). The contents of chlorophyll a and b were determined using the following formulae:

$$\text{Chlorophyll a} = \frac{(11.75 \times \text{OD at 663 nm} - 2.35 \times \text{OD at 645 nm}) \times \text{V}*}{\text{Sample fresh weight}}$$

$$\text{Chlorophyll b} = \frac{(27.05 \times \text{OD at 645 nm} - 11.21 \times \text{OD at 663 nm}) \times \text{V}}{\text{Sample fresh weight}}$$

$$\text{Carotenoid} = \frac{1000 \times \text{OD at 470 nm} - 2.27 \times \text{Chlorophyll a} - 81.4 \times \text{Chlorophyll b}}{227}$$

(*V, the volume of the extraction solution. The pigment content was expressed as mg of chlorophyll a and b, and carotenoid per gram of fresh leaf weight).

The total anthocyanin content was determined according to Pirie and Mullins (1976). Briefly, 0.5 g leaf tissue was extracted in 2 mL of 1% (*v*/*v*) HCl-ethanol and centrifuged at 13,000 rpm for 20 min at 4°C. Then the liquid supernatant was acidified to approximately pH 1.0 using 0.1 N HCl, and the absorbance was measured at 530 nm.

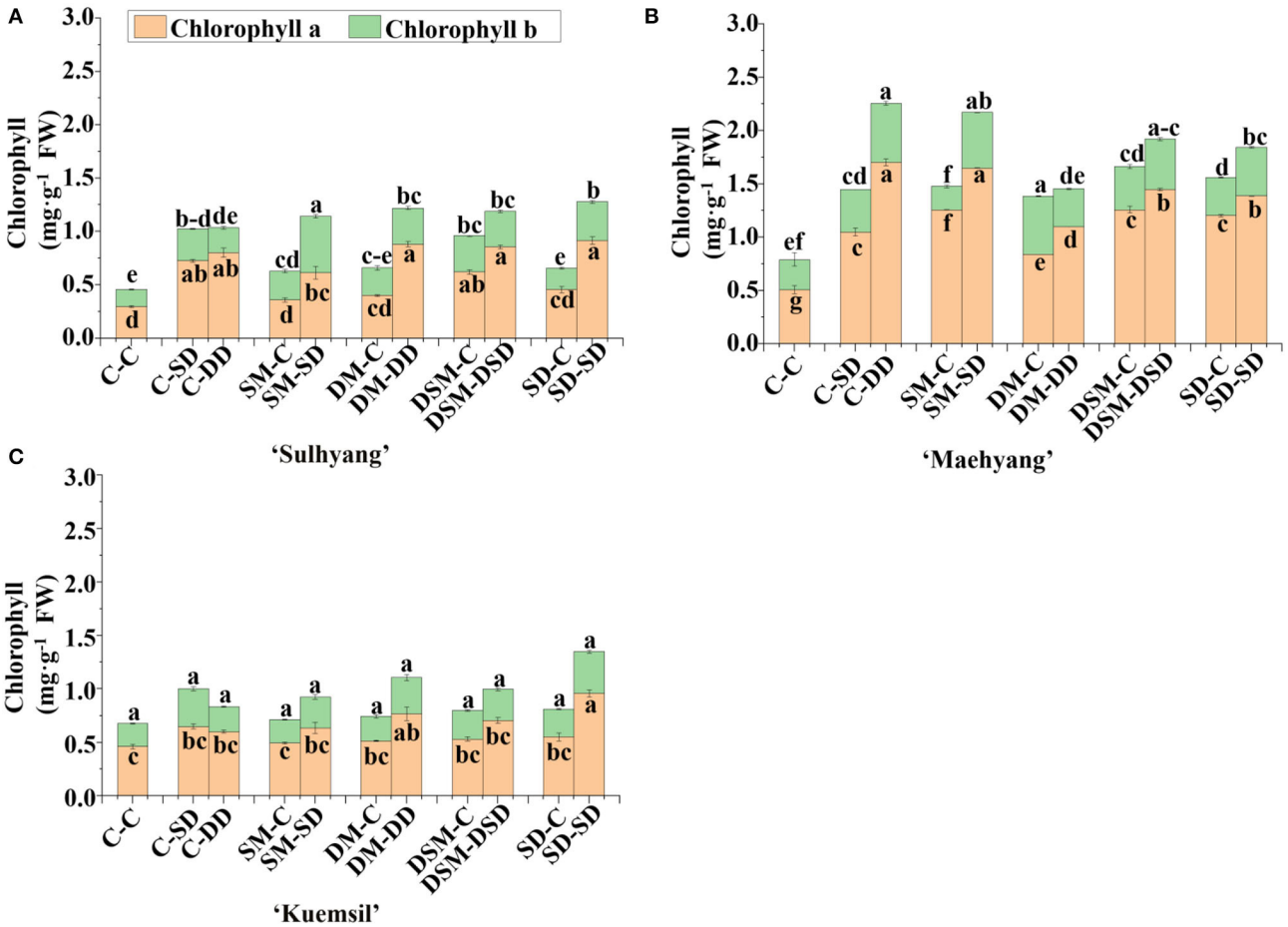

FIGURE 5 | Chlorophyll content of strawberry transplants **(A)** "Sulhyang"; **(B)** "Maehyang"; and **(C)** "Kuemsil" as affected by Si treatment after subjection to 43°C for 7 days. Lowercase letters indicate significant differences calculated by the Duncan's multiple range test at $p \leq 0.05$. See **Figure 1** for descriptions of treatment codes.

Determination of the Contents of Micro- and Macro-Nutrients

The Si content was determined according to the methods of Zhang and Dotson (1994). Briefly, dried leaves and roots in an oven at 60°C and ground, then 0.5 g samples were ashed using a nabertherm muffle furnace (Model LV 5/11/B180, Lilienthal, Breman, Germany) at 525°C for 4 h. Afterward, the ash was dissolved into 5 mL 25% (*v*/*v*) HCl, and then diluted with 15 mL of warm distilled water and 10 mL of room temperature distilled water. The nutrient contents of Si, potassium (K), calcium (Ca), phosphorus (P), sulfur (S), magnesium (Mg), iron (Fe), zinc (Zn), copper (Cu), and manganese (Mn) were measured using the inductively coupled plasma spectrometer (Optima 4300DV/5300DV, Perkin Elmer, Germany).

Determination of the Hydrogen Peroxide (H_2O_2) Content and Lipid Peroxidation

To estimate the content of H_2O_2, 0.1 g leaf samples were homogenized and extracted in a 5 mL 10 mM phosphate buffer (pH 5.8) containing 0.1% (*w*/*v*) trichloroacetic acid (TCA), which was then centrifuged at 10,000 rpm for 30 min at 4°C. 2 mL of the liquid supernatant was mixed with a 0.2 mL 10 mM phosphate buffer (pH 5.8) and 0.2 mL 1 M potassium iodide (KI). After incubation in the dark for 30 min, the absorbance was measured at 350 nm (Junglee et al., 2014).

Lipid peroxidation was measured according to Sun et al. (2015). 0.5 g leaf samples were extracted in 5 mL 0.1% (*w*/*v*) TCA and then centrifuged at 10,000 g for 5 min. 1 mL of the liquid supernatant was mixed with 0.6% (*w*/*v*) thiobarbituric acid and 10% (*w*/*v*) TCA, which were subsequently placed in a boiling water bath for 30 min to react and rapidly cooled. The absorbance was measured at 450, 532, and 600 nm, and the lipid peroxidation was estimated by the malondialdehyde (MDA) level:

$$\mathbf{MDA^{*}=6.45\times(OD\ at\ 532\ nm-OD\ at\ 600\ nm)-0.56\times OD\ at\ 450\ nm}$$

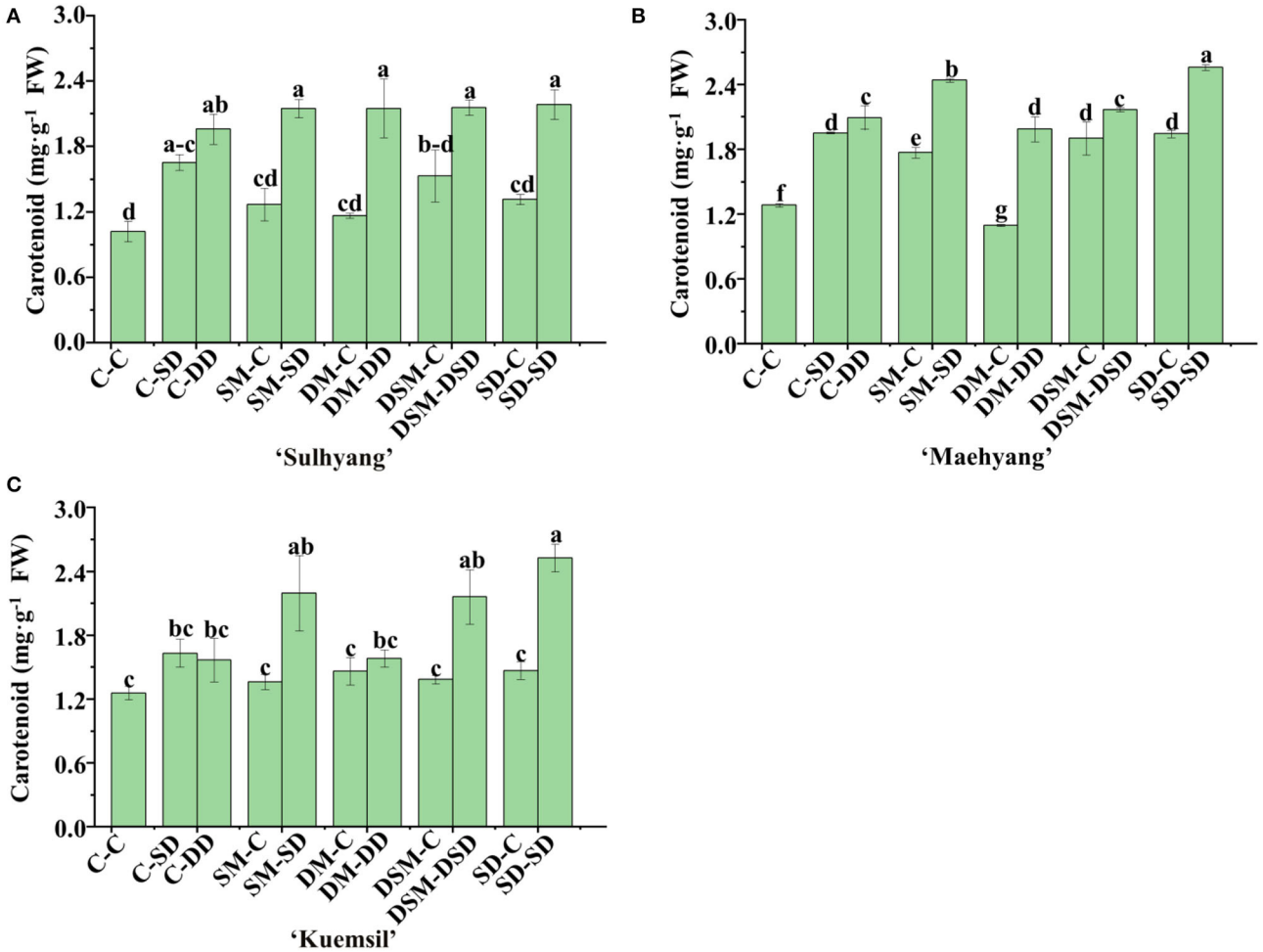

FIGURE 6 | Carotenoid content of strawberry transplants **(A)** "Sulhyang"; **(B)** "Maehyang"; and **(C)** "Kuemsil" as affected by the Si treatment after subjection to 43°C for 7 days. Lowercase letters indicate significant differences calculated by the Duncan's multiple range test at $p \leq 0.05$. See **Figure 1** for descriptions of treatment codes.

(The content of MDA was expressed as μmol per gram of fresh leaf weight).

Determination of Proline and Soluble Sugar Contents

To estimate the proline content, 1.0 g leaf samples were homogenized and extracted in 10 mL 3% (*w/v*) sulfosalicylic acid. 1 mL of the liquid supernatant was then mixed with 1 mL acid ninhydrin and 1 mL glacial acetic acid, and reacted in a 95°C water bath for 1 h. After natural cooling at room temperature, 2 mL cold toluene was added and the absorbance was measured at 520 nm (Bates et al., 1973).

To estimate the soluble sugar contents, 0.5 g leaf samples were homogenized and extracted in a 10 mL 20 mM phosphate buffer (pH 7.0), and centrifuged at 10,000 rpm for 30 min at 4°C. 0.2 mL of the liquid supernatant was then mixed with 5 mL H_2SO_4 and 1.8 mL distilled H_2O, and reacted in a boiling water bath for 10 min. After natural cooling, the absorbance was measured at 620 nm (Sun et al., 2015).

Determination of the Total Soluble Protein Content and Antioxidant Enzyme Activities

To estimate the total soluble protein content, the 0.5 g leaf samples were homogenized with liquid nitrogen and extracted in a 1.5 mL ice-cold 50 mM phosphate buffer (pH 7.0) containing 1 mM ethylenediaminetetraacetic acid (EDTA), 0.05% (*v/v*) Triton X-100, and 1 mM polyvinylpyrrolidone (PVP), which was then centrifuged at 13,000 rpm for 20 min at 4°C, and the liquid supernatant was used in assaying the

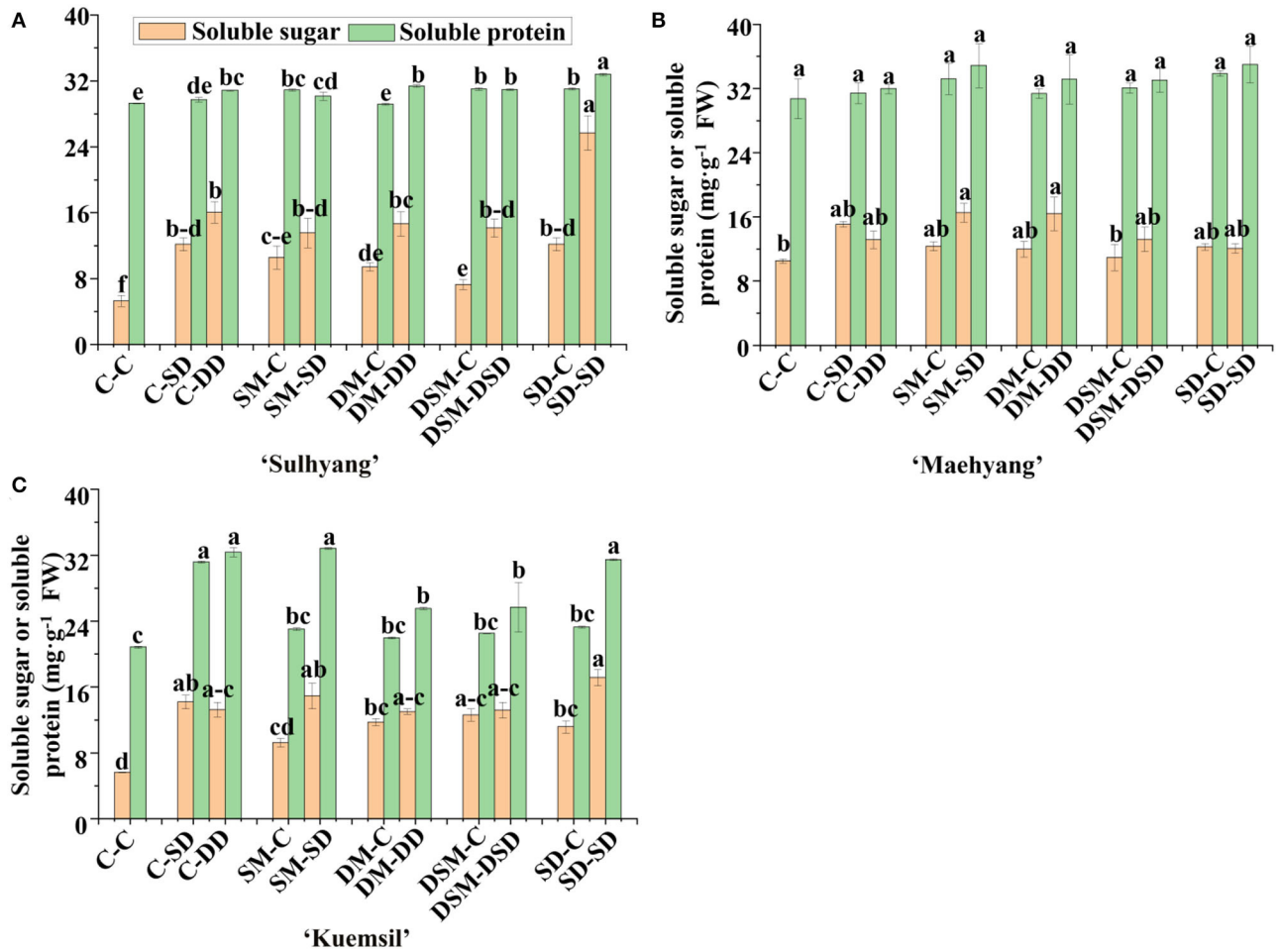

FIGURE 7 | Soluble sugar and protein contents in leaves of strawberry transplants **(A)** "Sulhyang"; **(B)** "Maehyang"; and **(C)** "Kuemsil" as affected by the Si treatment after subjection to 43°C for 7 days. Lowercase letters indicate significant differences calculated by the Duncan's multiple range test at $p \leq 0.05$. See **Figure 1** for descriptions of treatment codes.

antioxidant enzyme activities, namely of superoxide dismutase (SOD), guaiacol peroxidase (GPX), ascorbate peroxidase (APX), and catalase (CAT) according to Soundararajan et al. (2019).

Data Collection and Analysis

The experimental results were subjected to an analysis of variance (ANOVA) and the Duncan's multiple range test ($p \leq 0.05$) for comparison within a cultivar, and the *F*-test was calculated according to Fisher's least significant difference test at a threshold of $p = 0.05$. The Statistical Analysis Program (SAS 9.1, SAS Institute Inc., Cary, NC, USA) was used for the statistical analysis. Graphing was performed with the OriginPro software (version 9.0, OriginLab Co. Ltd., Northampton, MA, USA).

RESULTS

Growth and Development of Strawberry Transplants

In the present experiment, the height, fresh and dry weights, and shoot crown diameter of the three strawberry cultivars all significantly increased with Si treatments when compared with the control (**Table 2**). The maximal shoot fresh and dry weights were observed when plants were drenched in the Si solution both before and after the cutting propagation (DM-DD). The *F*-test results revealed that the supplemental Si significantly affected the shoot height, crown diameter, and fresh weight. However, Si treatments had no significant effects on the leaf length. Furthermore, as shown in **Figure 2**, the morphophysiological state is affected by the Si treatments in 'Sulhyang", "Maehyang", and "Kuemsil' strawberry transplants subjected to 43°C on different days. The leaves of transplants began to slightly roll from

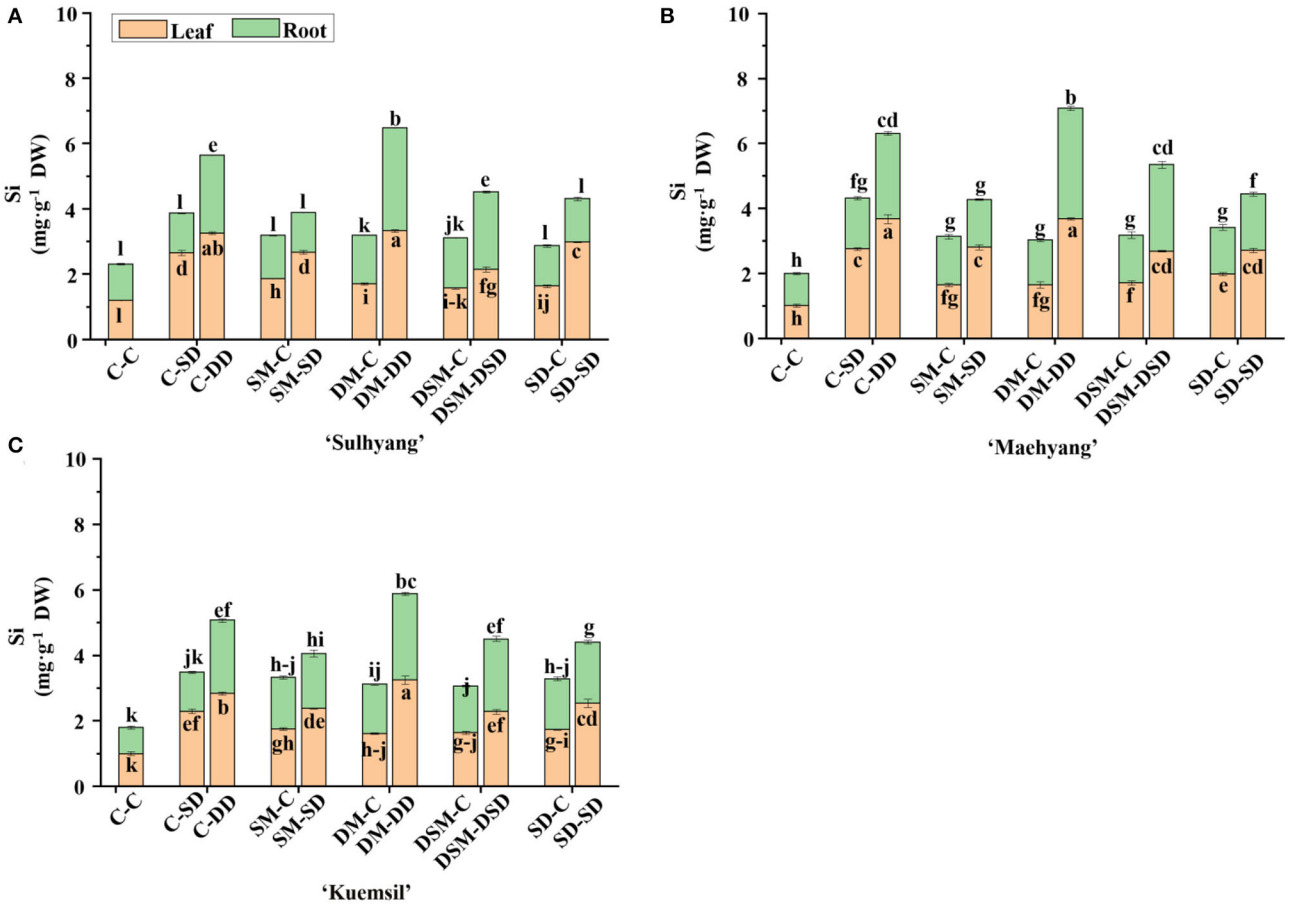

FIGURE 8 | The Si content in leaves and root of strawberry transplants **(A)** "Sulhyang"; **(B)** "Maehyang"; and **(C)** "Kuemsil" as affected by the Si treatments subjected to 43°C for 7 days. Lowercase letters indicate significant differences calculated by the Duncan's multiple range test at $p \leq 0.05$. See **Figure 1** for descriptions of treatment codes.

the third day of the high temperature stress. On the fifth day of the high temperature stress, varying degrees of wilting were observed on the transplants. It is noteworthy that the plants in the control were severely stressed and gradually died, while the Si-treated plants remained alive on the seventh day of the high temperature stress.

Relative Water Content and Stomatal Conductance

The LRWC in leaves is considered as a degree of stress expressed under high temperatures. As compared with the control (**Figure 3**), the LRWC values increased by 26–45%, 56–75%, and 70–84% in "Sulhyang", "Maehyang", and "Kuemsil" cultivars, respectively, with Si (+, +) application. Meanwhile, we found that Si treatments increased the stomatal conductance of leaves compared to the control, and the greatest stomatal conductance was obtained with the SD-SD.

Chlorophyll Fluorescence Parameters and Photosynthetic Pigment Contents

We further studied the changes in the chlorophyll fluorescence parameters of the photosystem II (PS II) under high temperature stress (**Figure 4**). The maximum primary yield of PS II photochemistry (Fv/F0) and the chlorophyll fluorescence parameters of the maximum/potential quantum efficiency of PS II (Fv/Fm) significantly decreased. The Fv/F0 and Fv/Fm decreased relatively slowly for the first three days, and then rapidly decreased until the fifth day. Interestingly, there were no significant differences in the Fv/F0 and Fv/Fm values between the control and Si-treated transplants on the first and third day, whereafter, the Fv/F0 and Fv/Fm of the control transplants (0.92 and 0.43), were 58% and 48% lower than that of Si-treated transplants (1.42 and 0.64), respectively.

To further explore the influence of the Si and high temperature stress on photosynthesis, the chlorophyll contents of leaves were investigated in this study (**Figure 5**). The

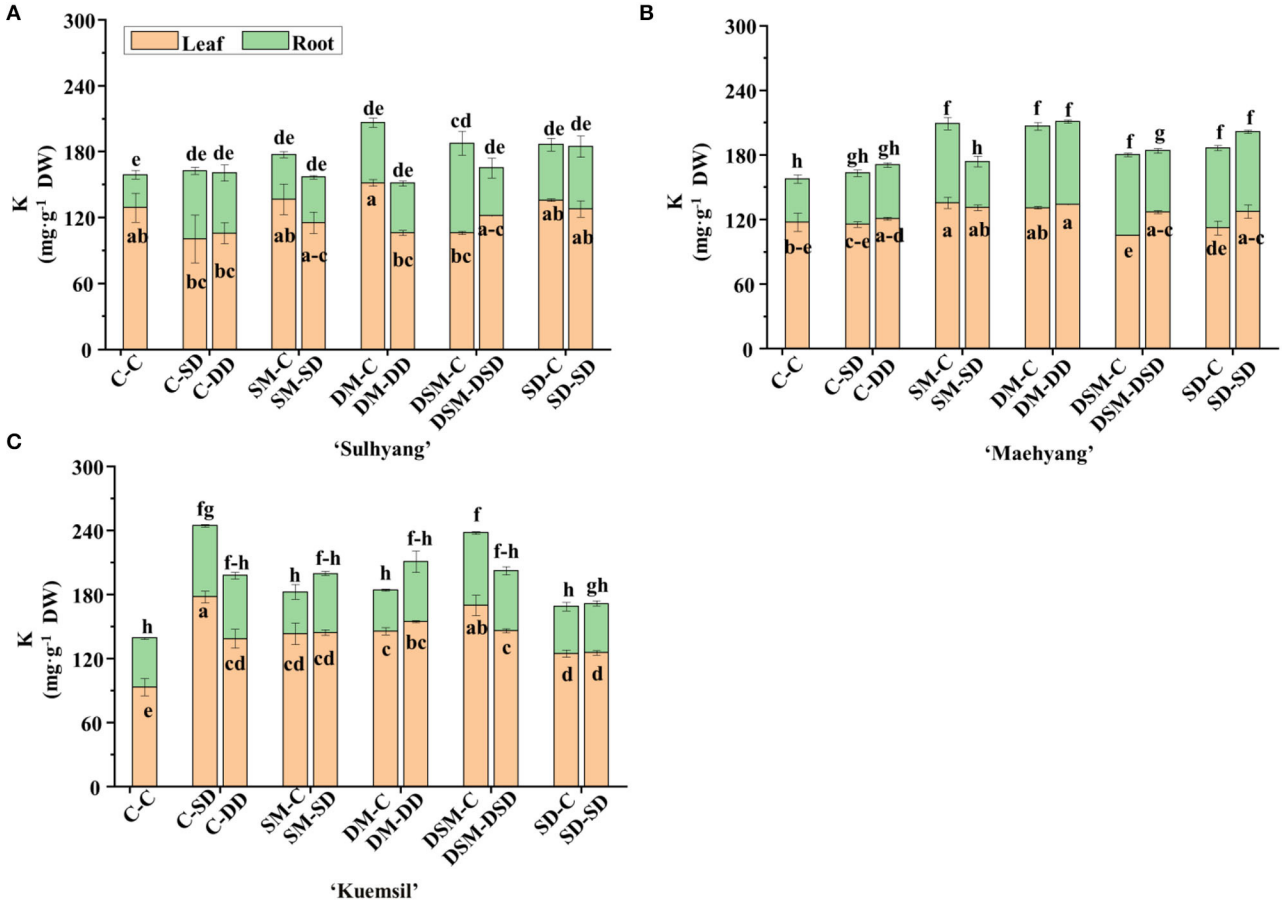

FIGURE 9 | The K content in leaves and root of strawberry transplants **(A)** "Sulhyang"; **(B)** "Maehyang"; and **(C)** "Kuemsil" as affected by the Si treatments subjected to 43°C for 7 days. Lowercase letters indicate significant differences calculated by the Duncan's multiple range test at $p \leq 0.05$. See **Figure 1** for descriptions of treatment codes.

lowest total chlorophyll contents were observed in the control, regardless of the cultivar. Similarly, the chlorophyll a content in "Sulhyang" (0.39–0.91 mg·g^{-1}), "Maehyang" (0.68–2.29 mg·g^{-1}), and "Kuemsil" (0.54∼0.95 mg·g^{-1}) transplants with Si application were, respectively, 1.3–3.1, 1.3–4.5, and 1.2–2.0 times those in the control (0.29, 0.50, and 0.46 mg·g^{-1}). In addition, the chlorophyll b content in "Sulhyang" and "Maehyang" leaves were found to be significantly affected by the Si application. However, for "Kuemsil" transplants exposed to the high temperature stress, there were no significant differences in the chlorophyll a content with or without the Si treatments.

Moreover, there were significant differences in the carotenoid content (**Figure 6**). In "Sulhyang", "Maehyang", and "Kuemsil", the carotenoid content with Si (+, +) treatments (2.12, 2.24, and 2.07 mg·g^{-1}) were, respectively, 1.1, 1.0, and 0.6 times higher than those of the control transplants (1.02, 1.09, and 1.26 mg·g^{-1}). However, there were no significant differences in the content of carotenoids in transplants Si (+,–) and Si (–,–).

Soluble Sugars and Soluble Proteins

The results related to the accumulation of soluble sugars and proteins showed significant effects of Si application (**Figure 7**). Si application promoted the soluble sugar contents, and SD-SD led to the highest soluble sugar contents in "Sulhyang" and "Kuemsil". However, there were no significant differences in the content of soluble proteins in transplants treated with or without Si after subjection to the high temperature in "Maehyang".

Contents of Micro- and Macro-Nutrients

The contents of micro- and macro-nutrients in leaves and roots were measured (**Figures 8**, **9** and **Tables 3**–**5**). Si application promoted the Si content both in leaves and roots, and the maximum Si content was obtained in DM-DD, followed by C-DD and SD-SD. Furthermore, the Si content in leaves was higher than that of roots in transplants treated with Si, for all three cultivars. However, in "Sulhyang", the Si content of the roots was no differences compared with those in the control after the foliar spray. The results of *F*-test showed

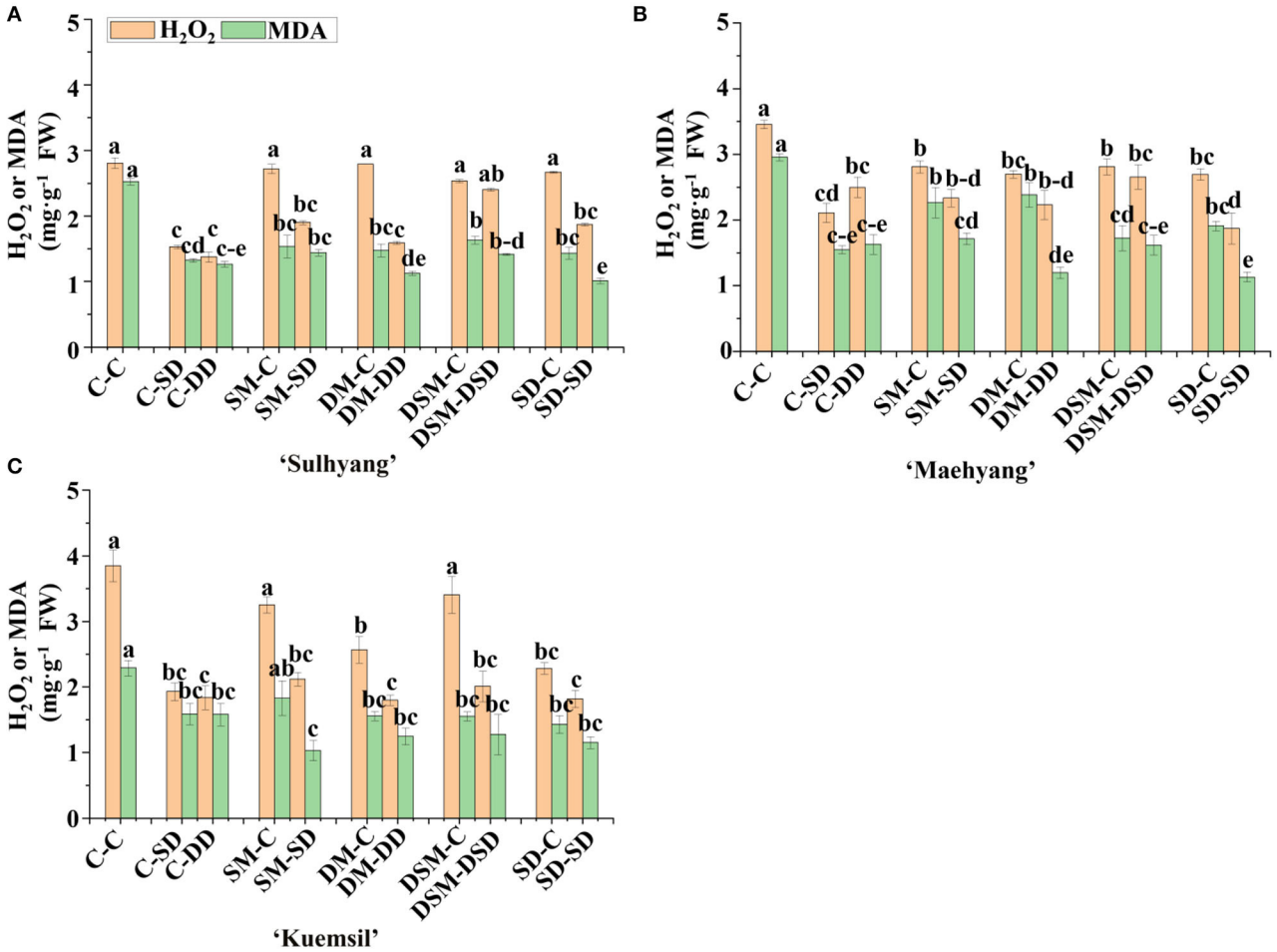

FIGURE 10 | The H_2O_2 and MDA contents in leaves of strawberry transplants **(A)** "Sulhyang"; **(B)** "Maehyang"; and **(C)** "Kuemsil" as affected by the Si treatment after subjection to 43°C for 7 days. Lowercase letters indicate significant differences calculated by the Duncan's multiple range test at $p \leq 0.05$. See **Figure 1** for descriptions of treatment codes.

that Si application significantly affected the macro-nutrient contents in "Maehyang" and "Kuemsil", and Si increased the absorption and transport of K, P, S, and Mg. For micro-nutrients, Si significantly affected Fe transport from roots to leaves.

Reactive Oxygen Species

ROS is closely related to the degree of damage caused by stresses. **Figure 8** presents the H_2O_2 and MDA contents of the strawberry transplants measured after the high temperature stress. On average, Si application substantially reduced the MDA content of transplants (by about 85, 72, and 62%, respectively, compared to the control). Differently, although the H_2O_2 content decreased in the Si (+, +) treatments, there were no significant differences in the ROS contents between Si (+, −) and Si (−, −) treatments in "Sulhyang" and "Kuemsil".

Antioxidant Enzyme Activities

Significant differences in the activities of certain key enzymes were found in the transplants with Si application (**Figures 10–13**). All Si treatments lead to significantly higher SOD activities than in the control (by 33–62%) in "Maehyang" (**Figure 12D**). Moreover, the CAT and APX activities as affected by the Si (+, +) treatments in "Sulhyang" (0.23 and 0.52 U·mg^{-1}), "Maehyang" (1.05 and 0.37 U·mg^{-1}), and "Kuemsil" (0.26 and 0.47 U·mg^{-1}) were, respectively, 1.0 and 0.9, 3.8 and 1.65, and 0.9 and 0.76 times higher than those of the control (0.11 and 0.27, 0.21 and 0.14, and 0.14 and 0.26 U·mg^{-1}) (**Figures 11A,B**). Overall, Si application resulted in higher activities of antioxidant enzymes.

Anthocyanin and Proline

The trend of anthocyanin and proline contents was opposite to that of H_2O_2 and MDA contents (**Figures 14**, **15**). The anthocyanin content in Si (+, +) (2.74, 3.20, and 2.40 mg·g^{-1})

TABLE 3 | Mineral contents in leaves and root of "Sulhyang" transplants as affected by different Si treatments.

Tissue (A)	Si treatment (B)	Macro-nutrient (mg·g^{-1} DW)				Micro-nutrient (mg·g^{-1} DW)			
		Ca	P	S	Mg	Fe	Zn	Cu	Mn
Shoot	C-C	180.6 a	14.9 bc	1.9 c-e	18.5 b	0.75 d	0.17 ef	0.10 bc	0.69 a-d
	C-SD	157.1 a-d	13.2 cd	2.1 bc	29.0 a	0.65 d	0.16 ef	0.12 ab	0.47 b-f
	C-DD	135.4 b-g	13.5 cd	1.6 c-g	25.9 a	0.85 d	0.14 f	0.08 d	0.80 a
	SM-C	161.8 a-d	23.5 a	3.0 a	28.0 a	0.90 d	0.20 ef	0.12 ab	0.72 a-c
	SM-SD	154.7 a-e	13.6 cd	2.1 cd	20.5 b	0.92 d	0.13 f	0.12 a	0.60 a-e
	DM-C	110.3 fg	17.3 b	1.8 c-f	20.7 b	0.66 d	0.14 f	0.11 a-c	0.41 d-h
	DM-DD	112.0 e-g	15.0 bc	1.1 g	26.8 a	0.62 d	0.12 f	0.10 c	0.51 a-e
	DSM-C	107.3 g	12.1 d	1.8 c-f	19.5 b	0.85 d	0.10 f	0.10 bc	0.67 a-d
	DSM-DSD	109.2 fg	14.6 cd	2.9 a	20.2 b	0.65 d	0.12 f	0.10 c	0.56 a-e
	SD-C	112.4 e-g	15.0 bc	1.8 c-f	21.6 b	0.72 d	0.13 f	0.12 ab	0.77 a
	SD-SD	132.4 c-g	13.4 cd	2.7 ab	27.2 a	0.59 d	0.12 f	0.10 bc	0.75 ab
Root	C-C	147.8 a-g	4.7 e	1.4 e-g	4.6 c	2.63 ab	0.46 cd	0.11 a-c	0.33 e-h
	C-SD	133.7 b-g	6.0 e	1.7 c-f	7.1 c	2.75 ab	0.40 de	0.11 a-c	0.45 b-g
	C-DD	174.7 a-c	6.3 e	1.4 e-g	5.9 c	2.83 ab	0.53 b-d	0.11 a-c	0.43 c-h
	SM-C	176.3 ab	5.9 e	1.5 d-g	5.3 c	2.62 ab	0.41 de	0.10 bc	0.31 e-h
	SM-SD	159.2 a-d	5.6 e	1.6 c-g	5.7 c	2.60 ab	0.70 a-c	0.11 a-c	0.15 gh
	DM-C	119.9 d-g	5.6 e	1.3 fg	6.4 c	2.87 ab	0.79 a	0.13 a	0.15 gh
	DM-DD	121.2 d-g	7.4 e	1.6 c-g	6.2 c	2.93 a	0.74 ab	0.13 a	0.14 h
	DSM-C	151.1 a-f	5.7 e	1.5 e-g	5.4 c	1.47 c	0.48 cd	0.11 a-c	0.20 f-h
	DSM-DSD	161.6 a-d	7.4 e	2.2 bc	5.6 c	2.50 b	0.76 ab	0.13 a	0.18 f-h
	SD-C	128.1 d-g	5.3 e	1.8 c-f	5.5 c	2.66 ab	0.63 a-d	0.13 a	0.17 f-h
	SD-SD	140.2 a-g	6.4 e	1.6 c-g	4.9 c	2.51 b	0.59 a-d	0.11 a-c	0.17 f-h
F-test [y]	A	*	***	***	***	***	***	**	***
	B	NS	***	***	***	***	NS	**	*
	A × B	*	***	***	***	***	*	***	NS

[z] *Lowercase letters indicate significant differences calculated by the Duncan's multiple range test at $p \leq 0.05$.*

[y] *NS, *, **, and *** represent non-significant or significant at $p \leq 0.05$, 0.01, and 0.001, respectively: C-C, no Si application during cutting propagation; C-SD, no Si application before cutting propagation and the daughter plants sprayed with the Si solution after cutting propagation; C-DD, no Si application before cutting propagation and the daughter plants drenched with the Si solution after cutting propagation; SM-C, the mother plants sprayed with the Si solution before cutting propagation and no Si application after cutting propagation; SM-SD, the mother plants sprayed with the Si solution before cutting propagation and the daughter plants sprayed with the Si solution after cutting propagation; DM-C, the mother plants drenched with the Si solution before cutting propagation and no Si application after cutting propagation; DM-DD, the mother plants drenched with the Si solution before cutting propagation and the daughter plants drenched with the Si solution after cutting propagation; DSM-C, the mother plants dressed with the soluble Si fertilizer before cutting propagation and no Si application after cutting propagation; DSM-DSD, the mother plants dressed with the soluble Si fertilizer before cutting propagation and the daughter plants dressed with the soluble Si fertilizer after cutting propagation; SD-C, the daughter plants sprayed with the Si solution before cutting propagation and no Si application after cutting propagation; or SD-SD, the daughter plants sprayed the Si solution before and after cutting propagation.*

were, respectively, 1.45, 1.34, and 0.53 times higher than that of the control (1.11, 1.37, and 1.57 mg·g^{-1}). Similarly, the Si (+, +) treatments led to higher proline contents than the Si (+, –) treatments, and the SD-SD resulted in the maximum proline value for all three cultivars. However, the proline content of the treatments SM-C, SM-C, and DSM-C were significantly decreased than the control in "Sulhyang".

DISCUSSION

Temperature affects the membrane properties, enzyme activity levels, and chemical reactions of life processes, and plants adapt to high temperature stresses by modifying photosynthesis, synthesis and accumulation of primary and secondary metabolites, and induction of stress proteins (Wahid et al., 2012). It is considered that Si induces high temperature stress tolerance by enhancing these abilities (Chen et al., 2011).

Analysis of the High Temperature and Si Application on Strawberry Photosynthesis, Growth, and Development

The growth, development, and survival of plants depend on the temperature. In general, high temperature damages the balance in photosynthesis and respiration, as the rate of photosynthesis decreases while the dark- and photo-respiration rates increase (Wahid et al., 2007). Extensive studies have shown that high temperature leads to a decrease in net photosynthesis (Pn) (Su and Liu, 2005). In cotton, high temperature inhibited the photosynthetic electron transport and Rubisco regeneration

TABLE 4 | Mineral contents in leaves and root of "Maehyang" transplants as affected by different Si treatments.

Tissue (A)	Si treatment (B)	Macro-nutrient (mg·g^{-1} DW)				Micro-nutrient (mg·g^{-1} DW)			
		Ca	P	S	Mg	Fe	Zn	Cu	Mn
Shoot	C-C	75.9 g	14.7 c	1.2 i	18.5 d	0.48 e	0.12 d	0.02 e	0.47 f-k
	C-SD	163.4 a-d	15.7 c	2.8 c-f	30.8 a	1.20 c	0.16 cd	0.11 a-c	1.48 a
	C-DD	185.3 ab	19.0 ab	4.0 a	32.5 a	0.66 de	0.16 d	0.09 bc	1.66 a
	SM-C	175.0 a-c	19.0 ab	3.1 b-d	20.2 d	0.50 e	0.18 cd	0.04 e	0.48 e-k
	SM-SD	96.9 g	16.4 c	3.3 a-c	20.3 d	0.63 de	0.18 cd	0.03 e	0.65 c-g
	DM-C	132.7 d-f	15.2 c	3.7 ab	18.6 d	0.82 d	0.13 d	0.04 e	1.15 b
	DM-DD	111.5 e-g	19.5 a	3.7 ab	24.1 bc	0.75 de	0.20 cd	0.05 de	0.66 c-g
	DSM-C	87.7 g	16.8 bc	1.7 g-i	20.0 d	0.50 e	0.14 d	0.03 e	0.58 c-i
	DSM-DSD	82.8 g	18.9 ab	2.1 e-h	23.5 c	0.74 de	0.15 d	0.03 e	1.49 a
	SD-C	86.7 g	15.9 c	2.2 e-h	23.1 c	1.32 bc	0.16 d	0.04 e	0.64 c-h
	SD-SD	100.2 fg	18.6 ab	2.3 d-h	26.3 b	0.61 de	0.15 d	0.11 a-c	0.86 c
Root	C-C	184.6 ab	4.5 g	1.5 hi	4.7 e	1.33 bc	0.29 b-d	0.08 cd	0.20 k
	C-SD	147.8 b-e	7.9 d-f	2.1 e-h	5.7 e	1.49 bc	0.56 a-d	0.11 a-c	0.26 jk
	C-DD	137.7 c-e	8.9 d	2.7 c-f	6.6 e	1.44 bc	0.32 a-d	0.11 a-c	0.56 c-j
	SM-C	151.5 b-d	7.4 d-f	2.3 d-h	6.1 e	1.47 bc	0.43 a-d	0.13 a	0.69 c-f
	SM-SD	169.6 a-d	6.4 e-g	1.7 g-i	6.4 e	1.22 c	0.42 a-d	0.10 a-c	0.33 h-k
	DM-C	197.9 a	6.4 e-g	2.0 f-h	6.8 e	1.46 bc	0.74 ab	0.12 ab	0.81 cd
	DM-DD	158.9 b-d	8.4 de	2.9 b-e	6.0 e	2.28 a	0.53 a-d	0.09 bc	0.80 c-e
	DSM-C	160.9 a-d	4.6 g	1.6 g-i	4.7 e	1.41 bc	0.63 a-c	0.10 a-c	0.37 f-k
	DSM-DSD	139.9 c-e	5.7 fg	2.4 d-g	5.3 e	1.47 bc	0.33 a-d	0.10 a-c	0.27 i-k
	SD-C	144.6 c-e	6.3 e-g	2.7 c-f	5.2 e	1.36 bc	0.36 a-d	0.12 a-c	0.36 g-k
	SD-SD	136.9 c-e	5.8 fg	2.7 c-f	6.4 e	1.55 b	0.78 a	0.10 a-c	0.52 d-k
F-test[y]	A	***	***	***	***	***	***	***	***
	B	***	***	***	***	***	***	NS	***
	A × B	***	***	***	***	***	*	NS	***

[z] *Lowercase letters indicate significant differences calculated by the Duncan's multiple range test at $p \leq 0.05$.*

[y] *NS, *, and *** represent non-significant or significant at $p \leq 0.05$, 0.01, and 0.001, respectively: C-C, no Si application during cutting propagation; C-SD, no Si application before cutting propagation and the daughter plants sprayed with the Si solution after cutting propagation; C-DD, no Si application before cutting propagation and the daughter plants drenched with the Si solution after cutting propagation; SM-C, the mother plants sprayed with the Si solution before cutting propagation and no Si application after cutting propagation; SM-SD, the mother plants sprayed with the Si solution before cutting propagation and the daughter plants sprayed with the Si solution after cutting propagation; DM-C, the mother plants drenched with the Si solution before cutting propagation and no Si application after cutting propagation; DM-DD, the mother plants drenched with the Si solution before cutting propagation and the daughter plants drenched with the Si solution after cutting propagation; DSM-C, the mother plants dressed with the soluble Si fertilizer before cutting propagation and no Si application after cutting propagation; DSM-DSD, the mother plants dressed with the soluble Si fertilizer before cutting propagation and the daughter plants dressed with the soluble Si fertilizer after cutting propagation; SD-C, the daughter plants sprayed with the Si solution before cutting propagation and no Si application after cutting propagation; or SD-SD, the daughter plants sprayed the Si solution before and after cutting propagation.*

capacity, which simultaneously reduced chlorophyll biosynthesis (Wise et al., 2004). High temperature stress (38/28°C) for 14 days was observed to result in pigment loss and thylakoid membrane damage in soybean (Djanaguiraman et al., 2011). In this study, Si application increased the chlorophyll and carotenoid contents (**Figures 5**, **6**). This demonstrated that Si effectively protects photosynthetic pigments. Similarly, in ryegrass (*Lolium perenne* L.), exogenous Si induced chlorophyll synthesis and reduced membrane injury under saline-alkali stresses. Photosynthetic apparatuses, especially PSII, water splitting, and oxygen-evolving complex (OEC) are highly susceptible to high temperature (Edwards and Walker, 1983). High temperature directly inactivates the OEC in PSII by dissociating the divalent Ca^{2+} and Mn^{2+} cations (Nash et al., 1985). This simultaneously dislodges PSII complexes from the thylakoid membrane by increasing the fluidity of thylakoid membranes (Mathur et al., 2014). Maize seedlings grown above 40°C had sharply decreased Fv/Fm and Pn was completely inhibited (Crafts-Brandner and Salvucci, 2002). Therefore, the Fv/Fm is regarded as a common tool to detect and quantify damages in photosynthesis (particularly PSII) in response to temperature stresses and has been widely used in various crops (Shangguan et al., 2000; Sinsawat et al., 2004). In this study, the Fv/Fm decreased with the duration of the high temperature stress, while from the fifth day, the Si (+) slowed down the decline of Fv/Fm (**Figure 4**). This is in good agreement well agreed with the report where Si application was useful to enhance photochemical efficiency in rice plants (Chen et al., 2011).

It is noteworthy that there is always a risk the high temperature effects get confounded with drought and light effects

TABLE 5 | Mineral contents in leaves and root of "Kuemsil" transplants as affected by different Si treatments.

Tissue (A)	Si treatment (B)	Macro-nutrient (mg·g^{-1} DW)				Micro-nutrient (mg·g^{-1} DW)			
		Ca	P	S	Mg	Fe	Zn	Cu	Mn
Shoot	C-C	99.2 h	10.4 f	2.2 e-h	22.8 f	0.47 c	0.11 g	0.03 f	0.80 f
	C-SD	221.2 a	14.7 de	3.3 b-e	36.2 a	0.78 c	0.13 g	0.11 a-d	1.70 b
	C-DD	153.8 c-g	12.9 e	2.5 d-h	29.6 b-d	0.88 c	0.13 g	0.13 ab	1.34 c
	SM-C	213.8 ab	12.34 ef	2.3 d-h	23.5 ef	0.94 c	0.13 g	0.10 b-e	1.99 a
	SM-SD	116.0 gh	17.8 a-c	3.4 b-d	27.5 b-f	0.71 c	0.18 fg	0.11 a-e	0.87 ef
	DM-C	137.7 d-h	19.0 ab	4.1 ab	31.5 b	0.62 c	0.19 fg	0.09 de	1.07 d
	DM-DD	136.2 e-h	19.2 ab	3.6 bc	30.7 bc	0.70 c	0.18 fg	0.10 c-e	0.98 de
	DSM-C	102.7 h	19.4 a	4.9 a	26.4 c-f	0.59 c	0.22 fg	0.12 a-d	1.28 c
	DSM-DSD	115.0 gh	16.7 b-d	3.3 b-e	25.1 d-f	0.66 c	0.15 fg	0.09 c-e	0.99 de
	SD-C	189.3 a-c	16.1 cd	3.2 b-f	29.2 b-d	1.05 c	0.15 fg	0.12 a-c	1.67 b
	SD-SD	192.5 a-c	16.7 b-d	2.6 c-g	28.4 b-e	0.90 c	0.15 fg	0.12 a-c	1.27 c
Root	C-C	99.8 h	4.6 h	1.4 h	6.5 g	2.41 b	0.33 ef	0.08 e	0.12 g
	C-SD	139.0 d-h	7.3 gh	2.9 c-g	7.4 g	2.93 ab	0.62 b-d	0.11 a-d	0.14 g
	C-DD	157.5 c-f	5.5 gh	2.4 d-h	7.6 g	3.03 ab	0.50 c-e	0.11 a-e	0.14 g
	SM-C	174.6 c-e	4.1 h	2.4 d-h	6.3 g	2.46 b	0.51 c-e	0.11 a-d	0.13 g
	SM-SD	123.6 f-h	5.6 gh	2.5 c-h	6.6 g	3.19 a	0.57 b-d	0.09 c-e	0.18 g
	DM-C	129.0 f-h	5.9 gh	2.1 f-h	7.2 g	2.63 ab	0.80 a	0.10 b-e	0.18 g
	DM-DD	180.2 bc	7.8 g	2.6 c-g	7.1 g	2.86 ab	0.71 ab	0.10 a-e	0.14 g
	DSM-C	130.0 f-h	6.6 gh	1.9 gh	6.4 g	2.78 ab	0.65 a-c	0.13 a	0.23 g
	DSM-DSD	177.2 b-d	7.9 g	2.6 c-g	6.5 g	3.18 a	0.55 b-d	0.11 a-e	0.18 g
	SD-C	136.9 e-h	5.3 gh	2.3 d-h	5.9 g	3.25 a	0.45 de	0.11 a-d	0.19 g
	SD-SD	152.9 c-g	6.2 gh	2.8 c-g	5.2 g	2.72 ab	0.53 b-d	0.10 a-e	0.17 g
F-test[y]	A	***	***	***	***	***	***	***	NS
	B	***	***	***	***	**	NS	*	***
	A × B	***	***	***	*	**	NS	NS	***

[z] *Lowercase letters indicate significant differences calculated by the Duncan's multiple range test at $p \leq 0.05$.*

[y] *NS, *, **, and *** represent non-significant or significant at $p \leq 0.05$, 0.01, and 0.001, respectively: C-C, no Si application during cutting propagation; C-SD, no Si application before cutting propagation and the daughter plants sprayed with the Si solution after cutting propagation; C-DD, no Si application before cutting propagation and the daughter plants drenched with the Si solution after cutting propagation; SM-C, the mother plants sprayed with the Si solution before cutting propagation and no Si application after cutting propagation; SM-SD, the mother plants sprayed with the Si solution before cutting propagation and the daughter plants sprayed with the Si solution after cutting propagation; DM-C, the mother plants drenched with the Si solution before cutting propagation and no Si application after cutting propagation; DM-DD, the mother plants drenched with the Si solution before cutting propagation and the daughter plants drenched with the Si solution after cutting propagation; DSM-C, the mother plants dressed with the soluble Si fertilizer before cutting propagation and no Si application after cutting propagation; DSM-DSD, the mother plants dressed with the soluble Si fertilizer before cutting propagation and the daughter plants dressed with the soluble Si fertilizer after cutting propagation; SD-C, the daughter plants sprayed with the Si solution before cutting propagation and no Si application after cutting propagation; or SD-SD, the daughter plants sprayed the Si solution before and after cutting propagation.*

in high temperature experiments. Therefore, special attention to watering during this trial. In order to maintain normal leaf temperature, plants intensive transpiration and lose a number of water under high temperature (Sadok et al., 2021). In this study, the leaf relative water content and stomatal conductance analysis showed application Si both increased the LRWC and stomatal conductance (**Figure 3**), it help plants to increase the rate of photosynthesis evaporative cooling (Urban et al., 2017). Likewise, exogenous Ca or 2,4-epibrassinolide helps relieve high-temperature-induced inhibition of the stomatal conductance (Tan et al., 2011; Zhang et al., 2014).

Moreover, high temperature tolerance is also generally defined as the ability of the plant to grow and produce. High temperature reduced cell wall elongation and cell differentiation, and decreased the shoot dry weight and net assimilation rates (Potters et al., 2007). Si is involved in growth stimulation and increases plant vigor and stress resistance. In leaves, Si is deposited as amorphous silica and forms a cuticle-Si double layer, such as hemicellulose, pectin, and lignin (He et al., 2015). This cuticle-Si double layer is beneficial for cell wall synthesis and remodeling, and maintains the mesophyll cells relatively intact under stresses (Sheng and Chen, 2020). As expected, Si application increased the fresh and dry weights of strawberry shoots (**Table 1**). This agrees with many previous findings in grass and soybean (Eneji et al., 2008; Lee et al., 2010). It is a positive cycle for plants: the increased biomass accumulation contributed to increased photosynthesis (Frazão et al., 2020).

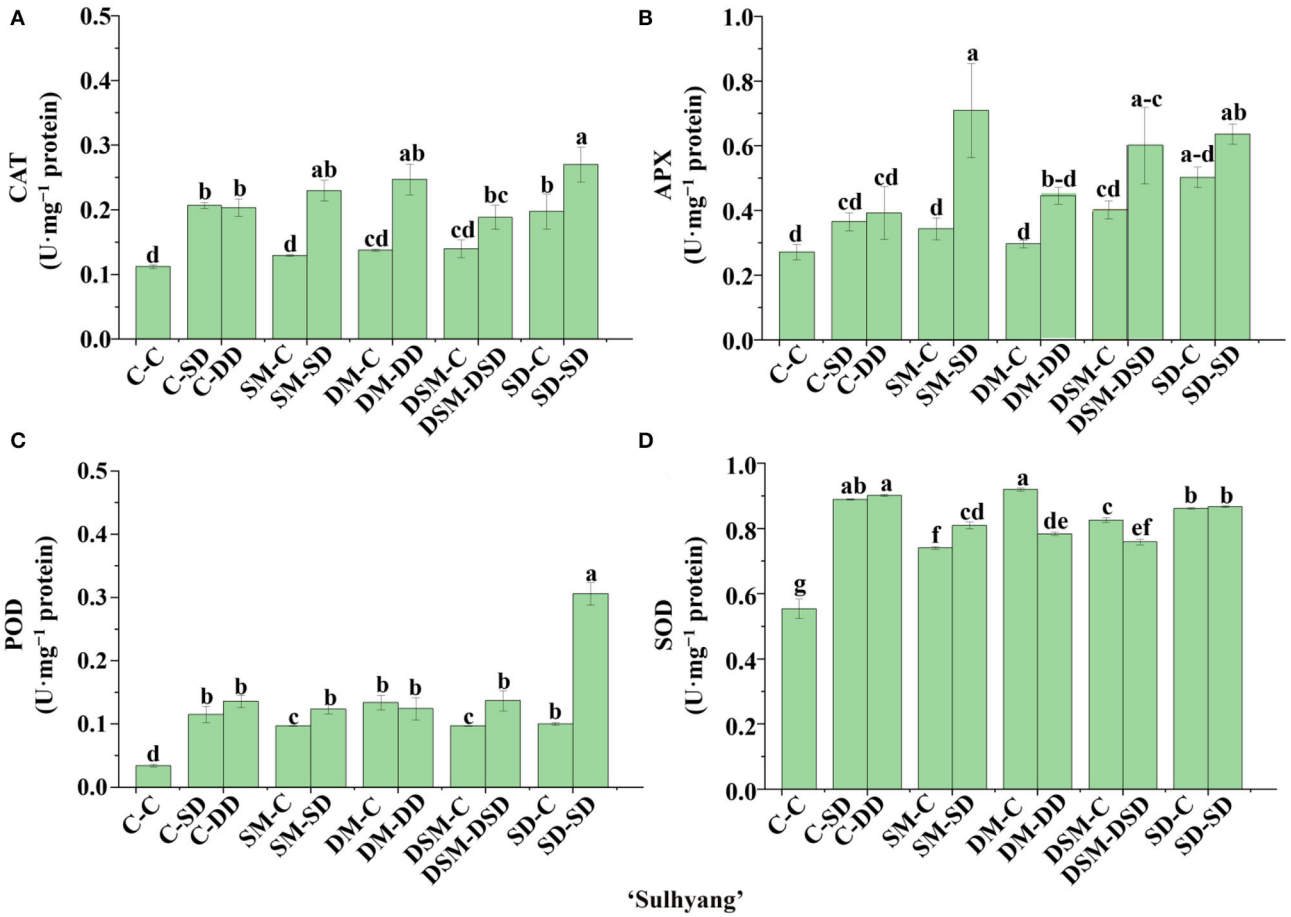

FIGURE 11 | Activities of CAT **(A)**, APX **(B)**, POD **(C)**, and SOD **(D)** in leaves of "Sulhyang" as affected by the Si treatment after subjection to 43°C for 7 days. Lowercase letters indicate significant differences calculated by the Duncan's multiple range test at $p \leq 0.05$. See **Figure 1** for descriptions of treatment codes.

Analysis of Nutrients

A positive response of nutrients to Si application was observed. The K is able to induce the activation of enzymes and maintains the balance of ionic among the cells, in addition to increasing the mechanical strength of plants (Amtmann et al., 2008). The effect of Si application on K depends on the plant species (Rea et al., 2022). In lettuce, the content of K decreased with the application of Si, while Si application increased the K concentration in maize and rice (Greger et al., 2018). It is worth noting that the content of K in the root of the DSM-DSD is higher than the DSM-C, despite the Na_2SiO_3 being the main component of soluble Si fertilizer. It is illustrated that the Si application increased the absorption of K by the root. As expected, the application of Si increased the accumulation of P in the root of transplants, and it was reported that Si binds with Fe and Mn, and increased the availability of P (Owino and Gascho, 2005). Overall, Si is beneficial for nutrient utilization and enhances absorption by the root.

Analysis of High Temperature and Si Application on Strawberry ROS Regulation

The chemical energy expended in a mass metabolic processes is originates from photosynthesis (Ashraf and Harris, 2013). ROS is an inevitable result of electron transport chains during normal metabolic processes. In fact, the chloroplast and mitochondria are the main sites for ROS production, and stress leads to excessive ROS production and accumulation (Bhattacharjee, 2005). For example, superoxide radicals (O_2^-) are produced by NADPH oxidases and cell wall peroxidases, then SOD turns O_2^- into H_2O_2 through the disproportionation reaction. Because H_2O_2 can freely diffuse through the biological membranes, it is cell-damaging and relatively long-living (Plaine, 1955; Møller et al., 2007). Individual aldehydic lipids break down into MDA and alter proteins, DNA, RNA, and other biomolecules (Alscher et al., 1997). Overall, ROS are reactive and can cause the peroxidation of membrane lipids and the destruction of pigments (Sewelam et al., 2016). It is noteworthy that MDA

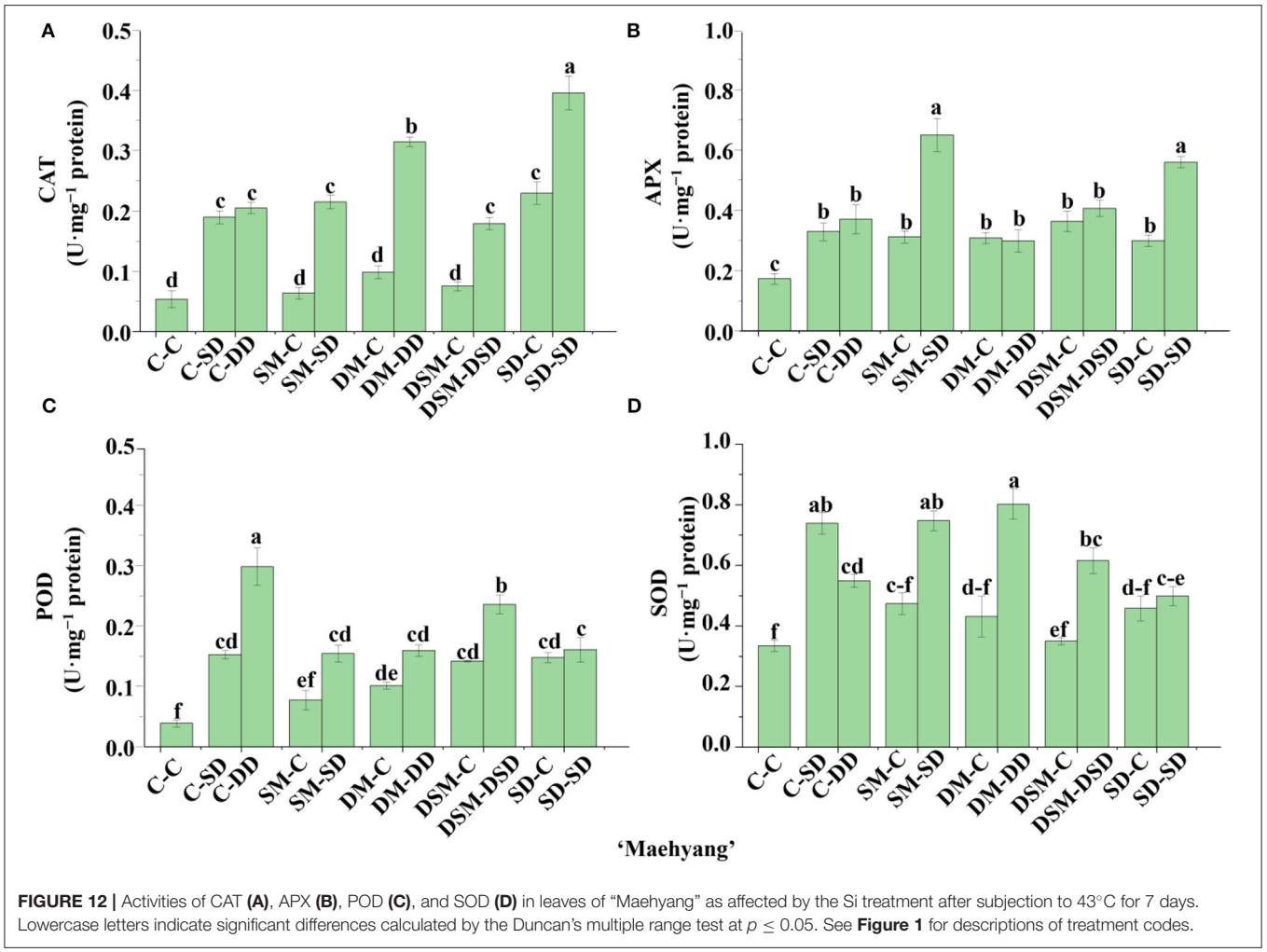

FIGURE 12 | Activities of CAT **(A)**, APX **(B)**, POD **(C)**, and SOD **(D)** in leaves of "Maehyang" as affected by the Si treatment after subjection to 43°C for 7 days. Lowercase letters indicate significant differences calculated by the Duncan's multiple range test at $p \leq 0.05$. See **Figure 1** for descriptions of treatment codes.

and H_2O_2 play important signaling roles in stress response pathways. Several studies have indicated that H_2O_2 interacted with other signaling molecules such as abscisic acid (ABA), calcium (Ca^{2+}), nitric oxide, salicylic acid (SA), as well as the ethylene signaling pathways in plants (Saxena et al., 2016). On the other hand, MDA signaling does not require jasmonic acid (JA), SA, or ethylene due to MDA is able to directly induce a series of stress relative genes such as cell wall metabolism, beta-oxidation, drought stress, and lipid metabolism (Weber et al., 2004). In general, according to these signaling molecules, plants are able to maintain a dynamic equilibrium of the production and scavenging of ROS with osmoregulation, phytohormones, and antioxidant enzymes (Huang et al., 2019). ROS scavenging mechanisms can be classified as enzymatic and non-enzymatic antioxidant defense systems (Apel and Hirt, 2004). In this study, the control group had higher ROS contents and lower antioxidant enzyme activities (**Figures 10**–**13**). The enzymatic antioxidant systems increased with the Si application (**Figure 8**). It was reported that Si played a role not only as a mechanical barrier in the resistance process (Samuels et al., 1991). Likewise, it was frequently observed that Si application induced higher activities of antioxidant enzymes in plants such as barely, rice, cucumber, and strawberry (Liang et al., 2003; Zhu et al., 2004; Farooq et al., 2019; Xiao et al., 2022). Therefore, Si is able to regulate ROS with antioxidant proteins.

Although the regulation of ROS by Si focuses on enzymatic systems, it was reported that Si application is beneficial to osmoregulation and production of secondary metabolites subjection to abiotic stresses (Maghsoudi et al., 2019; El-Beltagi et al., 2020). Proline is an important amino acid and considered to be an osmo-protectant (Abdelaal et al., 2020). It can generate turgor, scavenge ROS, and regulate the cytosolic pH (Smirnoff and Cumbes, 1989). Anthocyanin in plants has also been proposed as an effective antioxidant (Yamasaki et al., 1996). In this study, Si application increased the proline and total anthocyanin contents (**Figures 14**, **15**). Similar results were observed in wheat, where Si application alleviates the losses of yield caused by high temperatures through improvements in the

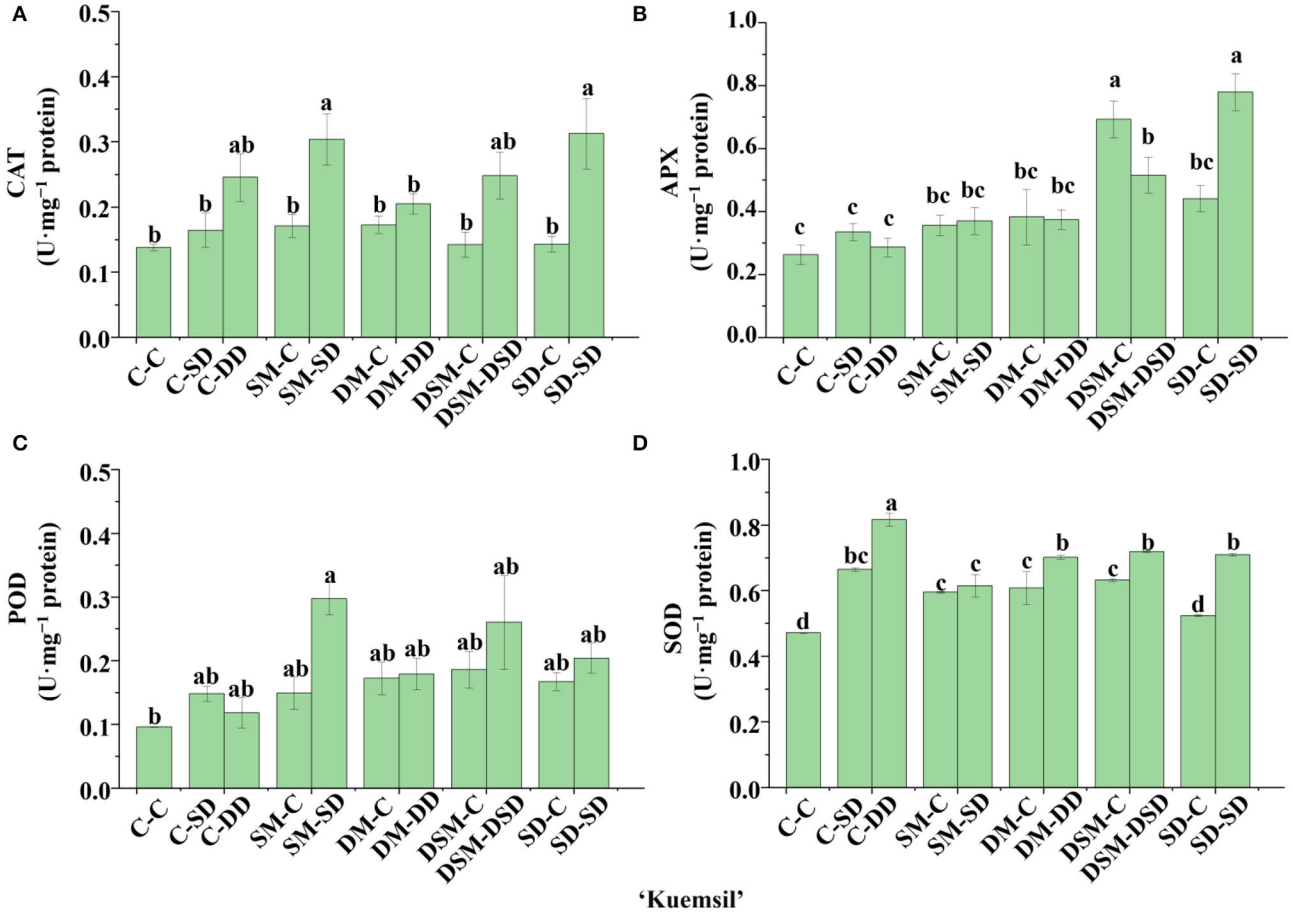

FIGURE 13 | Activities of CAT **(A)**, APX **(B)**, POD **(C)**, and SOD **(D)** in leaves of "Kuemsil" as affected by the Si treatment after subjection to 43°C for 7 days. Lowercase letters indicate significant differences calculated by the Duncan's multiple range test at $p \leq 0.05$. See **Figure 1** for descriptions of treatment codes.

production of proline and anthocyanin (Mustafa et al., 2021). Interestingly, the proline content in plants treated with Si (+, –) approached that of the control (**Figure 13**), which leads to the speculation that the effects of Si on the proline will decrease over time.

Method of Si Application Affects the Quality of Strawberry Transplants

Although the beneficial effects of Si fertilization are observed in agriculture, a common use for Si application is its infancy because many plant species are unable to benefit from Si application, and optimizing Si fertilization methods is still controversial (Tubana et al., 2016). Previous studies have shown that the transfer direction of Si in strawberry was unidirectional, there are only two ways: from the root to the shoot or from the mother plants to the daughter plants (Li et al., 2020). The results of this study show that the Si contents in the roots did not show differences between the control and after the foliar spray in "Sulhyang" (**Figure 8**). Interestingly, although strawberry plants absorbed more Si through root drench than with foliar spray, the Si content in the roots of foliar-sprayed plants was higher than in the control in "Maehyang" and "Kuemsil". It has been shown that Si must be transported by specific Lsi6 transporters in shoots. Furthermore, some tissues with low transpiration can accumulate high levels of Si despite the fact that Si transport in the xylem is driven by transpiration (Yang et al., 2018). Therefore, it is not excluded that Si is redistributed from the leaf to the shoot and root before deposition. Far more research is needed to understand whether or not there are any transport mechanisms after foliar Si spray. Moreover, organosilicon is a nonionic surfactant and has been found to enhance stomatal infiltration (Fernández and Eichert, 2009). In this study, the stomatal conductance in SD-SD was higher than in DM-DD (**Figure 3**) in "Maehyang" and "Kuemsil". Furthermore, compared with the substrate Si drench, foliar spray increased the plant resistance to wilting; this was not replicated when foliar Si spray was combined with substrate Si drench (Tebow et al., 2021). Trials on a variety of crops have led to the "Silicic Acid Agro Technology (SAAT)", which indicates that foliar Si sprays are only effective when they start early in

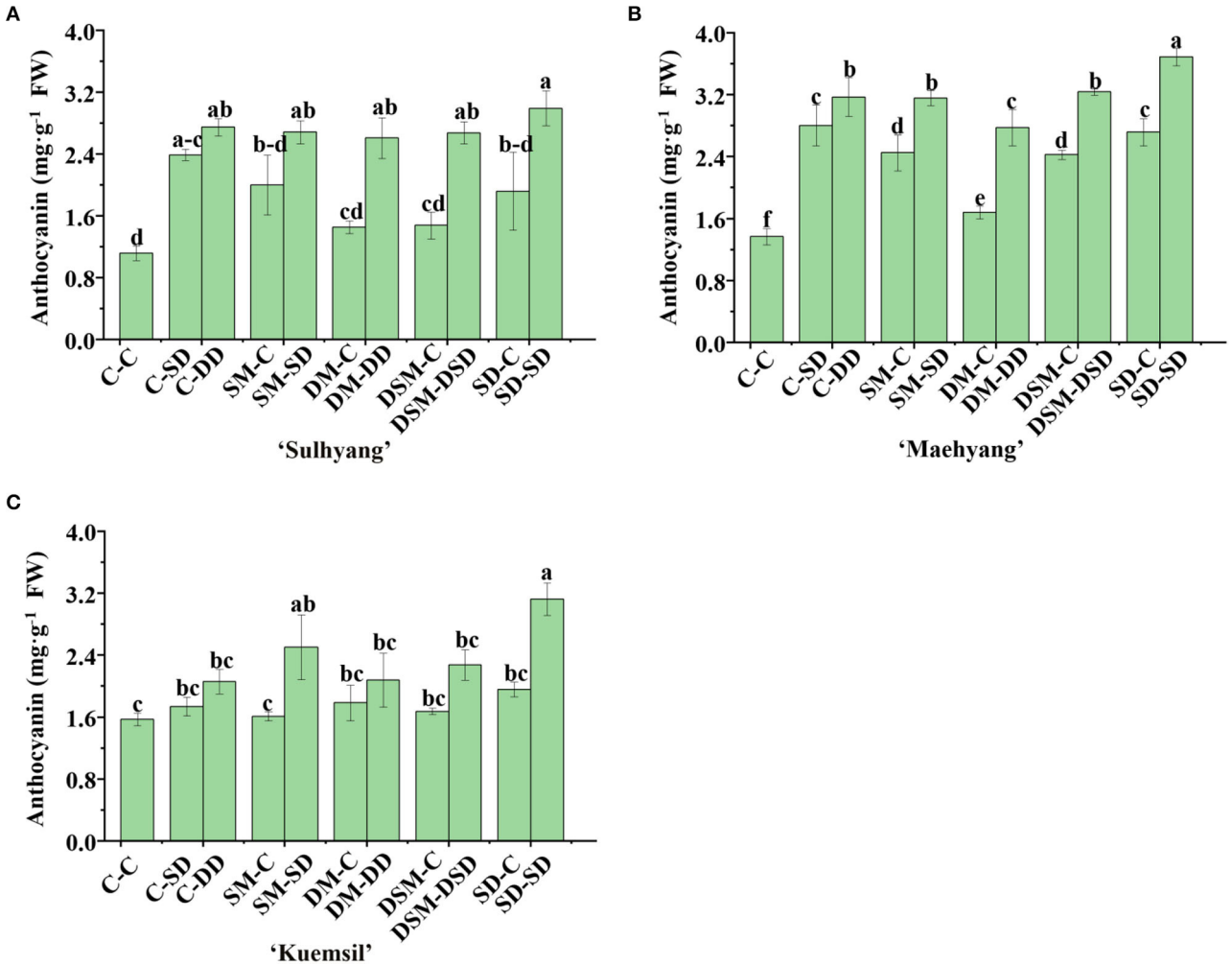

FIGURE 14 | Anthocyanin content in leaves of strawberry transplants **(A)** "Sulhyang"; **(B)** "Maehyang"; and **(C)** "Kuemsil" as affected by the Si treatment after subjection to 43°C for 7 days. Lowercase letters indicate significant differences calculated by the Duncan's multiple range test at $p \leq 0.05$. See **Figure 1** for descriptions of treatment codes.

the vegetative stage and follow a specific spray schedule (Laane, 2017). Moreover, the amount of Si in the edible parts of higher plants varies widely. For fruits and vegetables, the trichomes or ultrafine hairs of fruits are the potential location for Si depositions (Powell et al., 2005). However, the Si hardly accumulates in edible parts of strawberries and the Si rather enhanced the vegetative growth and fruit quality by stimulating growth and modifying the phenolic metabolism (Hajiboland et al., 2018). It was reported that the Si concentration of the fruit never reached the level of detection and was undetectable after subjection to Si treatment for 5 months in six strawberry cultivars (Ouellette et al., 2017). Furthermore, Si increased the shelf-life of berries (Peris et al., 2020). Therefore, the absorption and efficiency of Si are affected by the species, plant age, application method, and frequency.

CONCLUSION

The significant effects of Si application on plants have been extensively investigated, but researchers have rarely studied the optimal method for better growth, development, and resistance to high temperature during strawberry cutting propagation. Our results suggest that Si increased the plant growth during the cutting propagation. DM-DD (the mother plants drenched with the Si solution before cutting propagation and the daughter plants drenched with the Si solution after cutting propagation) and SD-SD (the daughter plants sprayed with the Si solution before and after cutting propagation) were especially effective, compared to applying Si only before or after the cutting propagation. SD-SD (the daughter plants sprayed with the Si solution before and after cutting propagation) was the best

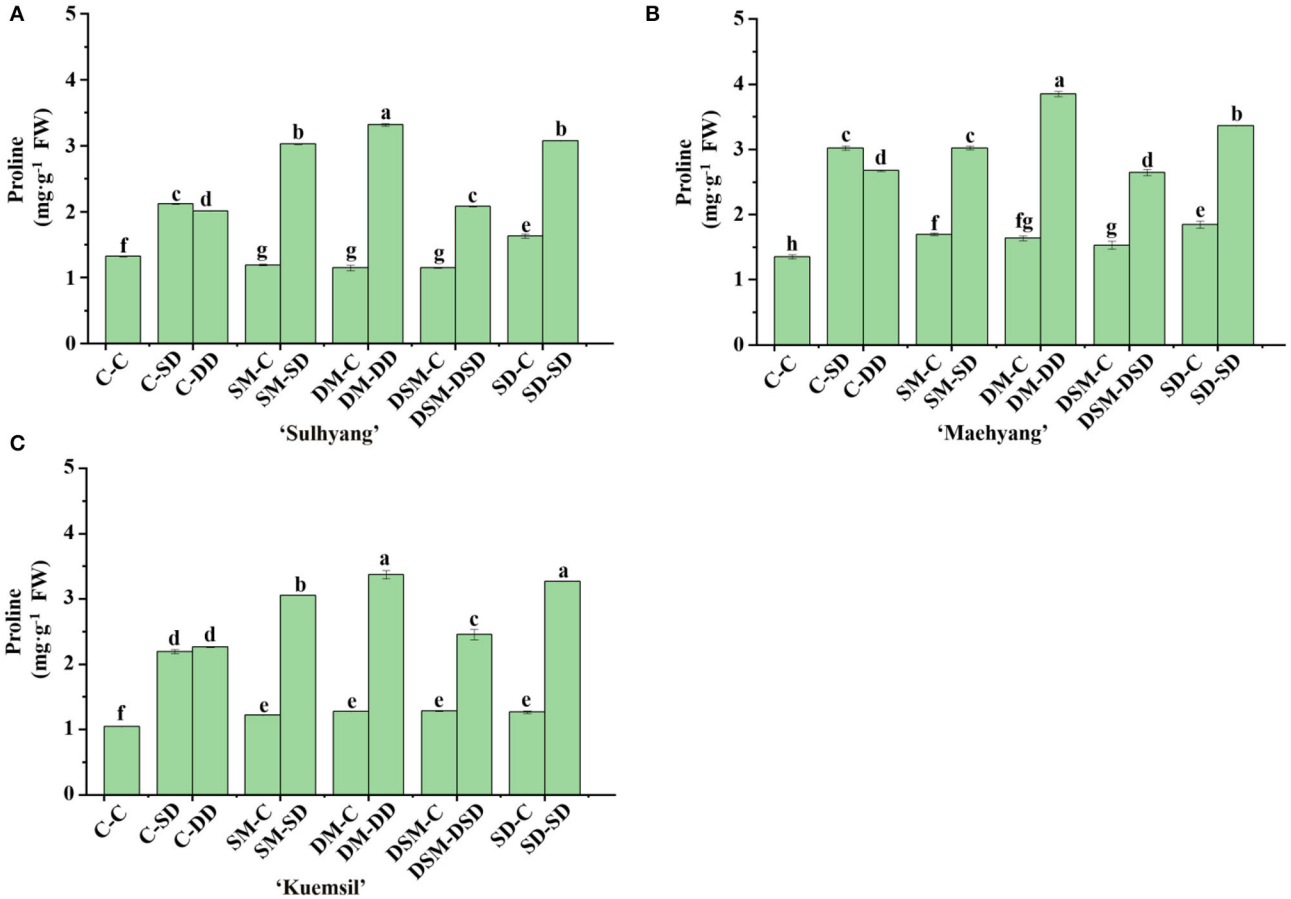

FIGURE 15 | Proline content in leaves of strawberry transplants **(A)** "Sulhyang"; **(B)** "Maehyang"; and **(C)** "Kuemsil" as affected by the Si treatment after subjection to 43°C for 7 days. Lowercase letters indicate significant differences calculated by the Duncan's multiple range test at $p \leq 0.05$. See **Figure 1** for descriptions of treatment codes.

for enhancing the resistance to high temperature stresses in strawberry transplants because photosynthesis and stomatal conductance were less affected by the high temperature, and the strawberry transplants were able to accumulate more sugars, proteins, and enzymatic and non-enzymatic antioxidants.

DATA AVAILABILITY STATEMENT

The original contributions presented in the study are included in the article/supplementary material, further inquiries can be directed to the corresponding author/s.

AUTHOR CONTRIBUTIONS

JX, YL, and BRJ conceived and designed this study. JX performed the experiments, analyzed the data, and drafted the manuscript. JX and BRJ edited and finalized the manuscript. All authors read and approved the submitted version.

FUNDING

JX and YL were supported by the BK21 Four Program, Ministry of Education, Republic of Korea.

REFERENCES

Abdelaal, K. A., Attia, K. A., Alamery, S. F., ElAfry, M. M., Ghazy, A. I., and Tantawy, D. S. (2020). Exogenous application of proline and salicylic acid can mitigate the injurious impacts of drought stress on barley plants associated with physiological and histological characters. *Sustainability.* 12, 1736. doi: 10.3390/su12051736

Agarie, S., Hanaoka, N., Ueno, O., Miyazaki, A., Kubota, F., and Agata, W. (1998). Effects of silicon on tolerance to water deficit and heat stress in rice plants (*Oryza sativa* L.), monitored by electrolyte leakage. *Plant. Prod. Sci.* 1, 96–103. doi: 10.1626/pps.1.96

Alscher, R. G., Donahue, J. L., and Cramer, C. L. (1997). Reactive oxygen species and antioxidants: relationships in green cells. *Physiol. Plant.* 100, 224–233. doi: 10.1111/j.1399-3054.1997.tb04778.x

Amtmann, A., Troufflard, S., and Armengaud, P. (2008). The effect of potassium nutrition on pest and disease resistance in plants. *Physiol. Plant.* 133, 682–691. doi: 10.1111/j.1399-3054.2008.01075.x

Apel, K., and Hirt, H. (2004). Reactive oxygen species: Metabolism, oxidative stress, and signal transduction. *Annu. Rev. Plant Biol.* 55, 373–399. doi: 10.1146/annurev.arplant.55.031903.141701

Ashraf, M., and Harris, P. J. (2013). Photosynthesis under stressful environments: An overview. *Photosynthetica*. 51, 163–190. doi: 10.1007/s11099-013-0021-6

Bates, L. S., Waldren, R. P., and Teare, I. (1973). Rapid determination of free proline for water-stress studies. *Plant Soil*. 39205–207. doi: 10.1007/BF00018060

Bhattacharjee, S. (2005). Reactive oxygen species and oxidative burst: Roles in stress, senescence and signal transducation in plants. *Curr. Sci.* 11, 13–1121.

Caruana, J. C., Sittmann, J. W., Wang, W., and Liu, Z. (2018). Suppressor of runnerless encodes a DELLA protein that controls runner formation for asexual reproduction in strawberry. *Mol. Plant*. 11, 230–233. doi: 10.1016/j.molp.2017.11.001

Chen, W., Yao, X., Cai, K., and Chen, J. (2011). Silicon alleviates drought stress of rice plants by improving plant water status, photosynthesis and mineral nutrient absorption. *Biol. Trace Elem. Res.* 142, 67–76. doi: 10.1007/s12011-010-8742-x

Crafts-Brandner, S. J., and Salvucci, M. E. (2002). Sensitivity of photosynthesis in a C4 plant, maize, to heat stress. *Plant Physiol.* 129, 1773–1780. doi: 10.1104/pp.002170

Dallagnol, L. J., Ramos, A. E. R., and da Rosa Dorneles, K. (2020). Silicon use in the integrated disease management of wheat: Current knowledge. *Curr. Trends Wheat Res*. 10, 95285.

Djanaguiraman, M., Prasad, P., and Al-Khatib, K. (2011). Ethylene perception inhibitor 1-MCP decreases oxidative damage of leaves through enhanced antioxidant defense mechanisms in soybean plants grown under high temperature stress. *Environ. Exp. Bot.* 71, 215–223. doi: 10.1016/j.envexpbot.2010.12.006

Edwards, G., and Walker, D. (1983). "The reduction pentose phosphate pathway and associated reaction," in *C*3, C4. *Mechanisms, Cellular and Environmental Regulation of Photosynthesis*, eds G. Edwards, and D. Walker (Berkeley: University of California Press), 107–156.

El-Beltagi, H. S., Sofy, M. R., Aldaej, M. I., and Mohamed, H. I. (2020). Silicon alleviates copper toxicity in flax plants by up-regulating antioxidant defense and secondary metabolites and decreasing oxidative damage. *Sustainability*. 12, 4732. doi: 10.3390/su12114732

Eneji, A. E., Inanaga, S., Muranaka, S., Li, J., Hattori, T., and An, P. (2008). Growth and nutrient use in four grasses under drought stress as mediated by silicon fertilizers. *J. Plant Nutr.* 31, 355–365. doi: 10.1080/01904160801894913

Epstein, E. (1994). The anomaly of silicon in plant biology. *Proc. Natl. Acad. Sci.* 91, 11–17. doi: 10.1073/pnas.91.1.11

Etesami, H., and Jeong, B. R. (2018). Silicon (Si): Review and future prospects on the action mechanisms in alleviating biotic and abiotic stresses in plants. *Ecotoxicol. Environ. Saf.* 147, 881–896. doi: 10.1016/j.ecoenv.2017.09.063

Farooq, M. A., Saqib, Z. A., Akhtar, J., Bakhat, H. F., Pasala, R.-., K., et al. (2019). Protective role of silicon (Si) against combined stress of salinity and boron (B) toxicity by improving antioxidant enzymes activity in rice. *Silicon*. 11, 2193–2197. doi: 10.1007/s12633-015-9346-z

Fernández, V., and Eichert, T. (2009). Uptake of hydrophilic solutes through plant leaves: current state of knowledge and perspectives of foliar fertilization. *Crit. Rev. Plant Sci.* 28, 36–68. doi: 10.1080/07352680902743069

Frazão, J. J., de Mello Prado, R., de Souza Júnior, J. P., and Rossatto, D.R. (2020). Silicon changes C: N: P stoichiometry of sugarcane and its consequences for photosynthesis, biomass partitioning and plant growth. *Sci. Rep.* 10, 1–10. doi: 10.1038/s41598-020-69310-6

González, L., and González-Vilar, M. (2001). "Determination of relative water content," in *Handbook of Plant Ecophysiology Techniques*, ed M. J. R. Roger (New York: Springer), 207–212. doi: 10.1007/0-306-48057-3_14

Greger, M., Landberg, T., and Vaculík, M. (2018). Silicon influences soil availability and accumulation of mineral nutrients in various plant species. *Plants*. 7, 41. doi: 10.3390/plants7020041

Hajiboland, R., Moradtalab, N., Eshaghi, Z., and Feizy, J. (2018). Effect of silicon supplementation on growth and metabolism of strawberry plants at three developmental stages. *N. Z. J. Crop Hortic. Sci.* 46, 144–161. doi: 10.1080/01140671.2017.1373680

He, C., Ma, J., and Wang, L. (2015). A hemicellulose-bound form of silicon with potential to improve the mechanical properties and regeneration of the cell wall of rice. *New Phytol.* 206, 1051–1062. doi: 10.1111/nph.13282

Howladar, S. M., Al-Robai, S. A., Alzahrani, F. S., Howladar, M. M., and Aldhebiani, A. Y. (2018). Silicon and its application method effects on modulation of cadmium stress responses in *Triticum aestivum* (L.) through improving the antioxidative defense system and polyamine gene expression. *Ecotoxicol. Environ. Saf.* 159, 143–152. doi: 10.1016/j.ecoenv.2018.05.004

Hu, J., Li, Y., and Jeong, B. R. (2020). Silicon alleviates temperature stresses in poinsettia by regulating stomata, photosynthesis, and oxidative damages. *Agronomy.* 10, 1419. doi: 10.3390/agronomy10091419

Huang, H., Ullah, F., Zhou, D. X., Yi, M., and Zhao, Y. (2019). Mechanisms of ROS regulation of plant development and stress responses. *Front. Plant Sci.* 10, 800. doi: 10.3389/fpls.2019.00800

IPCC (2014). "Climate Change 2014: Synthesis Report," in *Proceedings of the Contribution of Working Groups I, II and III to the Fifth Assessment Report of the Intergovernmental Panel on Climate Change*, eds Core Writing Team, R. K. Pachauri, and L. A. Meyer (Geneva: IPCC), 151.

Jun, H., Jung, H., and Imai, K. (2017). Gas exchange characteristics of a leading cultivar of Korean strawberry (Fragaria × ananassa,"Sulhyang"). *Sci. Hortic.* 221, 10–15. doi: 10.1016/j.scienta.2017.04.009

Junglee, S., Urban, L., Sallanon, H., and Lopez-Lauri, F. (2014). Optimized assay for hydrogen peroxide determination in plant tissue using potassium iodide. *Am. J. Anal. Chem.* 5, 730. doi: 10.4236/ajac.2014.511081

Kadir, S., Sidhu, G., and Al-Khatib, K. (2006). Strawberry (*Fragaria* × *ananassa* Duch.) growth and productivity as affected by temperature. *HortScience*. 41, 1423–1430. doi: 10.21273/HORTSCI.41.6.1423

Katz, O., Puppe, D., Kaczorek, D., Prakash, N. B., and Schaller, J. (2021). Silicon in the soil-plant continuum: intricate feedback mechanisms within ecosystems. *Plants* 10, 652. doi: 10.3390/plants10040652

Kim, D. E., Kwon, J. K., Hong, S. J., Lee, J. W., and Woo, Y. H. (2020). The effect of greenhouse climate change by temporary shading at summer on photo respiration, leaf temperature and growth of cucumber. *Protected Hortic. Plant Fact.* 29, 306–312. doi: 10.12791/KSBEC.2020.29.3.306

Kim, S. K., Bae, R., Na, H., Song, J. H., Kang, H. J., and Chun, C. (2012). Changes in fruit physicochemical characteristics by fruit clusters in June-bearing strawberry cultivars. *Kor. J. Sci. Technol.* 30, 378–384. doi: 10.7235/hort.2012.12027

Kim, T. I., Jang, W. S., Choi, J. H., Nam, M. H., Kim, W. S., and Lee, S. S. (2004). Breeding of strawberry 'Maehyang' for forcing culture. *Horticul. Sci. Technol.* 22, 434–437.

Kowalska, J., Tyburski, J., Jakubowska, M., and Krzymińska, J. (2021). Effect of different forms of silicon on growth of spring wheat cultivated in organic farming system. *Silicon*. 13, 211–217. doi: 10.1007/s12633-020-00414-4

Laane, H. (2017). The effects of the application of foliar sprays with stabilized silicic acid: an overview of the results from 2003-2014. *Silicon* 9, 803–807. doi: 10.1007/s12633-016-9466-0

Lee, S., Sohn, E., Hamayun, M., Yoon, J., and Lee, I. (2010). Effect of silicon on growth and salinity stress of soybean plant grown under hydroponic system. *Agrofor. Syst.* 80, 333–340. doi: 10.1007/s10457-010-9299-6

Li, Y., Xiao, J., Hu, J., and Jeong, B. R. (2020). Method of silicon application affects quality of strawberry daughter plants during cutting propagation in hydroponic substrate system. *Agronomy*. 10, 1753. doi: 10.3390/agronomy10111753

Liang, Y., Chen, Q., Liu, Q., Zhang, W., and Ding, R. (2003). Exogenous silicon (Si) increases antioxidant enzyme activity and reduces lipid peroxidation in roots of salt-stressed barley (*Hordeum vulgare* L.). *J. Plant Physiol.* 160, 1157–1164. doi: 10.1078/0176-1617-01065

Ma, J. F. (2003). "Functions of silicon in higher plants," in *Silicon biomineralization,* ed. E. G. Werner (New York: Springer), 127–147.

Ma, J. F., Miyake, Y., and Takahashi, E. (2001). Silicon as a beneficial element for crop plants. *Stud. Plant Sci.* 8, 17–39. doi: 10.1016/S0928-3420(01)80006-9

Ma, J. F., and Takahashi, E. (2002). "Silicon uptake and accumulation in plants," in *Soil, Fertilizer, and Plant Silicon Research in Japan,* eds. J. F. Ma, and E. Takahashi (Amsterdam: Elsevier), 73–100.

Ma, J. F., Tamai, K., Yamaji, N., Mitani, N., Konishi, S., and Katsuhara, M. (2006). A silicon transporter in rice. *Nature*. 440, 688–691. doi: 10.1038/nature04590

Maghsoudi, K., Emam, Y., Ashraf, M., Pessarakli, M., and Arvin, M. J. (2019). Silicon application positively alters pollen grain area, osmoregulation and

antioxidant enzyme activities in wheat plants under water deficit conditions. *J. Plant Nutr.* 42, 2121–2132. doi: 10.1080/01904167.2019.1648677

Mathur, S., Agrawal, D., and Jajoo, A. (2014). Photosynthesis: response to high temperature stress. *J. Photochem. Photobiol. B.* 137, 116–126. doi: 10.1016/j.jphotobiol.2014.01.010

Mitani, N., and Ma, J. F. (2005). Uptake system of silicon in different plant species. *J. Exp. Bot.* 56, 1255–1261. doi: 10.1093/jxb/eri121

Møller, I. M., Jensen, P. E., and Hansson, A. (2007). Oxidative modifications to cellular components in plants. *Annu. Rev. Plant Biol.* 58, 459–481. doi: 10.1146/annurev.arplant.58.032806.103946

Moradtalab, N., Hajiboland, R., Aliasgharzad, N., Hartmann, T. E., and Neumann, G. (2019). Silicon and the association with an arbuscular-mycorrhizal fungus (*Rhizophagus clarus*) mitigate the adverse effects of drought stress on strawberry. *Agronomy.* 9, 41. doi: 10.3390/agronomy9010041

Muneer, S., Park, Y. G., Kim, S., and Jeong, B. R. (2017). Foliar or subirrigation silicon supply mitigates high temperature stress in strawberry by maintaining photosynthetic and stress-responsive proteins. *J. Plant Growth Regul.* 36, 836–845. doi: 10.1007/s00344-017-9687-5

Mustafa, T., Sattar, A., Sher, A., Ul-Allah, S., Ijaz, M., and Irfan, M. (2021). Exogenous application of silicon improves the performance of wheat under terminal heat stress by triggering physio-biochemical mechanisms. *Sci. Rep.* 1, 11–12. doi: 10.1038/s41598-021-02594-4

Nash, D., Miyao, M., and Murata, N. (1985). Heat inactivation of oxygen evolution in photosystem II particles and its acceleration by chloride depletion and exogenous manganese. *Biochim. Biophys. Acta. Bioenerg.* 807, 127–133. doi: 10.1016/0005-2728(85)90115-X

Nasircilar, A. P. D. A. G. (2021). "The role of silicone applications in tolerance to abiotic stress conditions," in *Highly Interconnected and Endless Puzzle: Agriculture,* ed A. B. Özçinar (Ankara: Iksad), 23–44.

Ouellette, S., Goyette, M. H., Labb,é, C., Laur, J., Gaudreau, L., and Gosselin, A. (2017). Silicon transporters and effects of silicon amendments in strawberry under high tunnel and field conditions. *Front. Plant Sci.* 8, 949. doi: 10.3389/fpls.2017.00949

Owino, G. C., and Gascho, G. J. (2005). Effect of silicon on low pH soil phosphorus sorption and on uptake and growth of maize. *Commun. Soil Sci. Plant Anal.* 35, 2369–2378. doi: 10.1081/LCSS-200030686

Park, Y. G., Muneer, S., Kim, S., Hwang, S. J., and Jeong, B. R. (2018). Silicon application during vegetative propagation affects photosynthetic protein expression in strawberry. *Hortic. Environ. Biotechnol.* 59, 167–177. doi: 10.1007/s13580-018-0022-2

Pavlovic, J., Kostic, L., Bosnic, P., Kirkby, E. A., and Nikolic, M. (2021). Interactions of silicon with essential and beneficial elements in plants. *Front. Plant Sci.* 12, 1224. doi: 10.3389/fpls.2021.697592

Peris, F. J., Benavent-Gil, Y., and Hernández-Apaolaza, L. (2020). Silicon beneficial effects on yield, fruit quality and shelf-life of strawberries grown in different culture substrates under different iron status. *Plant Physiol. Biochem.* 152, 23–31. doi: 10.1016/j.plaphy.2020.04.026

Pirie, A., and Mullins, M. G. (1976). Changes in anthocyanin and phenolics content of grapevine leaf and fruit tissues treated with sucrose, nitrate, and abscisic acid. *Plant Physiol.* 58468–472. doi: 10.1104/pp.58.4.468

Plaine, H. L. (1955). The effect of oxygen and of hydrogen peroxide on the action of a specific gene and on tumor induction in *Drosophila melanogaster*. *Genetics*. 40, 268. doi: 10.1093/genetics/40.2.268

Potters, G., Pasternak, T. P., Guisez, Y., Palme, K. J., and Jansen, M. A. (2007). Stress-induced morphogenic responses: growing out of trouble? *Trends Plant Sci.* 12, 98–105. doi: 10.1016/j.tplants.2007.01.004

Powell, J. J., McNaughton, S. A., Jugdaohsingh, R., Anderson, S. H. C., Dear, J., Khot, F., et al. (2005). A provisional database for the silicon content of foods in the United Kingdom. *Br. J. Nutr.* 94, 804–812. doi: 10.1079/BJN20051542

Puppe, D., Kaczorek, D., Schaller, J., Barkusky, D., and Sommer, M. (2021). Crop straw recycling prevents anthropogenic desilication of agricultural soil-plant systems in the temperate zone–results from a long-term field experiment in NE Germany. *Geoderma*. 403, 115187. doi: 10.1016/j.geoderma.2021.115187

Rea, R. S., Islam, M. R., Rahman, M. M., Nath, B., and Mix, K. (2022). Growth, nutrient accumulation, and drought tolerance in crop plants with silicon application: a review. *Sustainability*. 14, 4525. doi: 10.3390/su14084525

Sadok, W., Lopez, J. R., and Smith, K. P. (2021). Transpiration increase under high-temperature stress: Potential mechanisms, trade-offs and prospects for crop resilience in a warming world. *Plant Cell Environ.* 44, 2102–2116. doi: 10.1111/pce.13970

Samuels, A., Glass, A., Ehret, D., and Menzies, J. (1991). Distribution of silicon in cucumber leaves during infection by powdery mildew fungus (*Sphaerotheca fuliginea*). *Can. J. Bot.* 69, 140–146. doi: 10.1139/b91-020

Sattar, A., Cheema, M. A., Sher, A., Ijaz, M., Wasaya, A., and Yasir, T. A. (2020). Foliar applied silicon improves water relations, stay green and enzymatic antioxidants activity in late sown wheat. *Silicon*. 12, 223–230. doi: 10.1007/s12633-019-00115-7

Saxena, I., Srikanth, S., and Chen, Z. (2016). Cross talk between H_2O_2 and interacting signal molecules under plant stress response. *Front. Plant Sci.* 7, 570. doi: 10.3389/fpls.2016.00570

Sewelam, N., Kazan, K., and Schenk, P. M. (2016). Global plant stress signaling: reactive oxygen species at the cross-road. *Front. Plant Sci.* 7, 187. doi: 10.3389/fpls.2016.00187

Shangguan, Z., Shao, M., and Dyckmans, J. (2000). Effects of nitrogen nutrition and water deficit on net photosynthetic rate and chlorophyll fluorescence in winter wheat. *J. Plant Physiol.* 156, 46–51. doi: 10.1016/S0176-1617(00)80271-0

Sheng, H., and Chen, S. (2020). Plant silicon-cell wall complexes: Identification, model of covalent bond formation and biofunction. *Plant Physiol. Biochem.* 155, 13–19. doi: 10.1016/j.plaphy.2020.07.020

Sinsawat, V., Leipner, J., Stamp, P., and Fracheboud, Y. (2004). Effect of heat stress on the photosynthetic apparatus in maize (*Zea mays* L.) grown at control or high temperature. *Environ. Exp. Bot.* 52, 123–129. doi: 10.1016/j.envexpbot.2004.01.010

Sivanesan, I., Son, M. S., Soundararajan, P., and Jeong, B. R. (2013). Growth of chrysanthemum cultivars as affected by silicon source and application method. *Horticul. Sci. Technol.* 31, 544–551. doi: 10.7235/hort.2013.13046

Smirnoff, N., and Cumbes, Q. J. (1989). Hydroxyl radical scavenging activity of compatible solutes. *Phytochemistry*. 28, 1057–1060. doi: 10.1016/0031-9422(89)80182-7

Song, J., Li, Y., Hu, J., Lee, J., and Jeong, B. R. (2021). Pre-and/or postharvest silicon application prolongs the vase life and enhances the quality of cut peony (*Paeonia lactiflora* Pall.) flowers. *Plants*. 10, 1742. doi: 10.3390/plants10081742

Soundararajan, P., Manivannan, A., Ko, C. H., Park, J. E., and Jeong, B. R. (2019). Evaluation of relative toxicity caused by deicing agents on photosynthesis, redox homeostasis, and the osmoregulatory system in creeper-type plants. *Hortic. Environ. Biotechnol.* 60, 175–186. doi: 10.1007/s13580-018-0117-9

Soundararajan, P., Sivanesan, I., Jana, S., and Jeong, B. R. (2014). Influence of silicon supplementation on the growth and tolerance to high temperature in *Salvia splendens*. *Hortic. Environ. Biotechnol.* 55271–279. doi: 10.1007/s13580-014-0023-8

Strik, B. (1985). Flower bud initiation in strawberry cultivars. *Fruit Var. J.* 39, 5–9.

Su, P., and Liu, X. (2005). Photosynthetic characteristics of linze jujube in conditions of high temperature and irradiation. *Sci. Hortic.*104, 339–350. doi: 10.1016/j.scienta.2004.08.012

Sükran, D., GÜNES, T., and Sivaci, R. (1998). Spectrophotometric determination of chlorophyll-a, b and total carotenoid contents of some algae species using different solvents. *Turk. J. Bot.* 2213–18.

Sun, C., Li, X., Hu, Y., Zhao, P., Xu, T., and Sun, J. (2015). Proline, sugars, and antioxidant enzymes respond to drought stress in the leaves of strawberry plants. *Hortic. Sci. Biotechnol.* 33625–632. doi: 10.7235/hort.2015.15054

Takahashi, E., Ma, J., and Miyake, Y. (1990). The possibility of silicon as an essential element for higher plants. *Comments Agric. Food Chem.* 2, 99–122.

Takeda, F., Hokanson, S. C., and Enns, J. M. (2004). Influence of daughter plant weight and position on strawberry transplant production and field performance in annual plasticulture. *HortSci.* 39, 1592–1595. doi: 10.21273/HORTSCI.39.7.1592

Tamai, K., and Ma, J. F. (2003). Characterization of silicon uptake by rice roots. *New Phytol.* 158, 431–436. doi: 10.1046/j.1469-8137.2003.00773.x

Tan, W., wei Meng, Q., Brestic, M., Olsovska, K., and Yang, X. (2011). Photosynthesis is improved by exogenous calcium in heat-stressed tobacco plants. *J. Plant Physiol.* 168, 2063–2071. doi: 10.1016/j.jplph.2011.06.009

Tebow, J. B., Houston, L. L., and Dickson, R. W. (2021). Silicon foliar spray and substrate drench effects on plant growth, morphology, and resistance to wilting with container-grown edible species. *Horticulturae.* 7, 263. doi: 10.3390/horticulturae7090263

Tubana, B. S., Babu, T., and Datnoff, L. E. (2016). A review of silicon in soils and plants and its role in US agriculture: history and future perspectives. *Soil Sci.* 181, 393–411. doi: 10.1097/SS.0000000000000179

Urban, J., Ingwers, M., McGuire, M. A., and Teskey, R. O. (2017). Stomatal conductance increases with rising temperature. *Plant Signaling Behav.* 12, e1356534. doi: 10.1080/15592324.2017.1356534

Vu, N. T., Tran, A. T., Le, T. T. C., Na, J. K., Kim, S. H., Park, J. M., et al. (2017). Improvement of tomato seedling quality under low temperature by application of silicate fertilizer. *J. Bio-Environ. Control.* 26, 158–166. doi: 10.12791/KSBEC.2017.26.3.158

Wahid, A., Farooq, M., Hussain, I., Rasheed, R., and Galani, S. (2012). "Responses and management of heat stress in plants," in *Environmental Adaptations and Stress Tolerance of Plants in The Era of Climate Change,* ed A. Parvaiz (New York: Springer), 135–157. doi: 10.1007/978-1-4614-0815-4_6

Wahid, A., Gelani, S., Ashraf, M., and Foolad, M. R. (2007). Heat tolerance in plants: an overview. *Environ. Exp. Bot.* 61199–223. doi: 10.1016/j.envexpbot.2007.05.011

Wang, Y., Hu, Y., Duan, Y., Feng, R., and Gong, H. (2016). Silicon reduces long-term cadmium toxicities in potted garlic plants. *Acta Physiol. Plant.* 381–9. doi: 10.1007/s11738-016-2231-6

Weber, H., Chételat, A., Reymond, P., and Farmer, E. E. (2004). Selective and powerful stress gene expression in *Arabidopsis* in response to malondialdehyde. *Plant J.* 37, 877–888. doi: 10.1111/j.1365-313X.2003.02013.x

Wise, R., Olson, A., Schrader, S., and Sharkey, T. (2004). Electron transport is the functional limitation of photosynthesis in field-grown Pima cotton plants at high temperature. *Plant Cell Environ.* 27, 717–724. doi: 10.1111/j.1365-3040.2004.01171.x

Xiao, J., Li, Y., and Jeong, B. R. (2022). Foliar silicon spray before summer cutting propagation enhances resistance to powdery mildew of daughter plants. *Int. J. Mol. Sci.* 23, 3803. doi: 10.3390/ijms23073803

Yamasaki, H., Uefuji, H., and Sakihama, Y. (1996). Bleaching of the red anthocyanin induced by superoxide radical. *Arch. Biochem. Biophys.* 332, 183–186. doi: 10.1006/abbi.1996.0331

Yan, C., Nikolic, M., Ye, M., Xiao, Z. and Liang, Y. (2018). Silicon acquisition and accumulation in plant and its significance for agriculture. *J. Integr. Agric.* 17, 2138–2150. doi: 10.1016/S2095-3119(18)62037-4

Yoon, H. S., Jin, H. J., and Oh, J. Y. (2020). "Kuemsil", a strawberry variety suitable for forcing culture. *Kor. Soc. Breed. Sci.* 52, 184–189. (In Korean) doi: 10.9787/KJBS.2020.52.2.184

Zhang, H., and Dotson, P. (1994). The use of microwave muffle furnace for dry ashing plant tissue samples. *Commun. Soil Sci. Plant Anal.* 25, 1321–1327. doi: 10.1080/00103629409369118

Zhang, Y., He, J., Yang, S., and Chen, Y. (2014). Exogenous 24-epibrassinolide ameliorates high temperature-induced inhibition of growth and photosynthesis in *Cucumis melo*. *Biol. Plant.* 58, 311–318. doi: 10.1007/s10535-014-0395-8

Zhu, Z., Wei, G., Li, J., Qian, Q., and Yu, J. (2004). Silicon alleviates salt stress and increases antioxidant enzymes activity in leaves of salt-stressed cucumber (*Cucumis sativus* L.). *Plant Sci.* 167, 527–533. doi: 10.1016/S0168-9452(04)00179-7

Conflict of Interest: The authors declare that the research was conducted in the absence of any commercial or financial relationships that could be construed as a potential conflict of interest.

Publisher's Note: All claims expressed in this article are solely those of the authors and do not necessarily represent those of their affiliated organizations, or those of the publisher, the editors and the reviewers. Any product that may be evaluated in this article, or claim that may be made by its manufacturer, is not guaranteed or endorsed by the publisher.

Copyright © 2022 Xiao, Li and Jeong. This is an open-access article distributed under the terms of the Creative Commons Attribution License (CC BY). The use, distribution or reproduction in other forums is permitted, provided the original author(s) and the copyright owner(s) are credited and that the original publication in this journal is cited, in accordance with accepted academic practice. No use, distribution or reproduction is permitted which does not comply with these terms.

frontiers | Frontiers in Sustainable Food Systems

TYPE Original Research
PUBLISHED 06 April 2023
DOI 10.3389/fsufs.2023.1145972

Check for updates

OPEN ACCESS

EDITED BY
Matteo Balderacchi,
Independent Researcher, Piacenza, Italy

REVIEWED BY
Lin Xu,
Ghent University, Belgium
Giuseppe Mannino,
University of Turin, Italy
Sławomir Swierczyński,
Poznan University of Life Sciences, Poland

*CORRESPONDENCE
Aminallah Tahmasebi
✉ a.tahmasbi@hormozgan.ac.ir

SPECIALTY SECTION
This article was submitted to Crop Biology and Sustainability, a section of the journal Frontiers in Sustainable Food Systems

RECEIVED 18 January 2023
ACCEPTED 24 March 2023
PUBLISHED 06 April 2023

CITATION
Tahmasebi A, Mirzaalian Dastjerdi A and Jamali B (2023) Microbial-based biological treatments improved the nutritional, nutraceutical and functional properties of greenhouse sweet pepper (*Capsicum annuum* L.). *Front. Sustain. Food Syst.* 7:1145972. doi: 10.3389/fsufs.2023.1145972

COPYRIGHT
© 2023 Tahmasebi, Mirzaalian Dastjerdi and Jamali. This is an open-access article distributed under the terms of the Creative Commons Attribution License (CC BY). The use, distribution or reproduction in other forums is permitted, provided the original author(s) and the copyright owner(s) are credited and that the original publication in this journal is cited, in accordance with accepted academic practice. No use, distribution or reproduction is permitted which does not comply with these terms.

Microbial-based biological treatments improved the nutritional, nutraceutical and functional properties of greenhouse sweet pepper (*Capsicum annuum* L.)

Aminallah Tahmasebi[1,2]*, Abdolmajid Mirzaalian Dastjerdi[3] and Babak Jamali[1]

[1]Department of Agriculture, Minab Higher Education Center, University of Hormozgan, Bandar Abbas, Iran, [2]Plant Protection Research Group, University of Hormozgan, Bandar Abbas, Iran, [3]Department of Horticultural Sciences, University of Hormozgan, Bandar Abbas, Iran

Sweet pepper (*Capsicum annum*) is an important vegetable with high economic and nutritional value. The present study was conducted to evaluate the effectiveness of biological treatments on the nutritional, nutraceutical and functional status of greenhouse sweet peppers cv. Nirvin. Plants were divided into two categories: Peppers that were biologically treated included five microbial-based fertilizers and insecticide and those that were chemically treated contained a large number of chemical fertilizers and pesticides. The results showed that the total phenolic content, antioxidant activity, and leaf chlorophyll content were significantly higher (1.16, 1.14, and 1.09-fold) in the biologically treated plants compared to those that received the chemical treatment. The concentration of Fe, K, Mg, P, Ca, Cu, Si, and Mn also increased in the fruits of biologically treated sweet pepper plants. Fe, Mg, and P content of the leaves was higher in the chemically treated plants, while, the concentration of Zn and Cu showed the higher values in the leaves of the biologically treated plants. There was no significant difference between biological and chemical treatments in plant height as well as the number of flowers and fruits per plant. In conclusion, biological treatment could significantly improve the nutritional, nutraceutical and functional values of sweet peppers. Considering the risk of environmental pollution, the high cost of chemical fertilizers and pesticides, as well as their adverse impact on human health and the ecosystem, biological treatment can be a suitable alternative for sweet pepper management programs.

KEYWORDS

beneficial microorganisms, clean production, fruit quality, greenhouse, vegetable crop

Introduction

In recent years, greenhouse crops have gained more attention and importance due to numerous advantages such as high productivity, possibility of out-of-season production, high quality of products, low water consumption, and job creation (Naderi et al., 2019). Sweet pepper (*Capsicum annuum*) belongs to the nightshade family (Solanaceae). It is considered worldwide as an important vegetable plant with high nutritional value, mainly used for fresh consumption, cooking, and processing (Krasnow and Ziv, 2022). In addition, this crop is used in food and cosmetics, pharmaceuticals, as well

as nutraceuticals and has beneficial impact on human health (Murariu et al., 2019; Brezeanu et al., 2022). These beneficial effects of sweet peppers on human health are attributed to the high concentration of ascorbic acid, carotenoids, tocopherols, and phenolic compounds that scavenge free radicals and protect against oxidative damage (Sreeramulu and Raghunath, 2010; Chen and Kang, 2013; Brezeanu et al., 2022). Greenhouse crops have a high commercial value due to production costs. Consequently, the damage caused by pests and pathogens in greenhouses is of great importance from an economic point of view (Nasiri and Nikzadfar, 2007). Chemicals such as pesticides and fertilizers are extensively used yearly in greenhouse production worldwide. However, due to the contamination of water, air, and soil, the increased use of these chemical inputs can pose a significant risk to the environment. These agents can also lead to resistance in insects and pathogens, reduce populations of beneficial insects, contribute to high greenhouse gas emissions and incur high costs (Arias-Estevez et al., 2008; Alvarez et al., 2017; Brezeanu et al., 2022). Due to the environmental and health risks associated with the use of chemical fertilizers and pesticides in agriculture, the production and consumption of safe products have become a practical alternative that attracted the attention of investors in the agricultural sector worldwide (Mishra et al., 2013). Biopesticides and biofertilizers, as environmentally friendly and cost-effective means, contain the natural microflora (beneficial bacteria and fungi). They provide micro- and macronutrients through the varieties of mechanisms including fixation of nitrogen, solubilization of phosphate and potassium and production of plant growth regulators, antibiotics, siderophores, hydrogen cyanide, lytic acid and indole acetic acid (Sinha et al., 2010; Babalola and Glick, 2012). In other words, the biological agents can improve plant diseases and pests control, soil fertility, microflora, plant growth, and yield (Deepak et al., 2014; Fasusi et al., 2021). Recently, a plant protein hydrolysate-based biostimulant increased growth rate and fruit yield and promoted faster and more efficient plant recovery in stressed sweet pepper plants (Agliassa et al., 2021). Additionally, biostimulant treatment improved yield parameters, vitamin C, phenolic contents and antioxidant activities in sweet pepper fruits (Paradiković et al., 2011). Moreover, a seaweed liquid extract biostimulant increased the yield, antioxidant activity and composition of *C. annuum* (Ashour et al., 2021). Therefore, there is increasing consumer demand for safe and residue-free crop production by applying biopesticides and biofertilizers. Hormozgan province is located in the southern region of Iran and is considered the production hub of sweet pepper. Considering the importance of this crop in the agricultural economy of Hormozgan province, the present study aimed to evaluate the effectiveness of the application of biological agents (biofertilizers and biopesticides) in the management program of sweet pepper under greenhouse conditions.

Materials and methods

Study location

The present study was conducted in 2021 and 2022 in a commercial greenhouse in a completely randomized design in the Minab region (longitude and latitude of 57.01758671 and 27.14917768 and 27 m elevation), Hormozgan province, Iran. Healthy and uniform sweet peppers cv. Nirvin transplants with four to five fully expanded leaves were planted with the row spacing and inter-row spacing of 50 and 55 cm, respectively. Three rows (each 55 m long) were selected for each treatment. Plants were irrigated every other day for 6 h using a tape drip irrigation system. Drip irrigation involved distinct tubes for each treatment and the treatments were separated based on a drip-lock end cap. In this case, the special tubes for each treatment were opened and the treatment was applied. After each treatment, tubes were washed with water to eliminate any residual materials. The insolation for growing plants in the greenhouse ranged from 5,000 to 6,000 lux. The average maximum and minimum temperature (October 2021-March 2022) was between 14 and 28°C, respectively. Greenhouse soil and water samples were collected and analyzed before the start of the experiment; their characteristics are shown in Tables 1, 2. The soil sample was taken at a depth of 0–30 cm. Sheep manure was applied to improve the quality of the greenhouse soil.

Treatments and experimental design

Plants were divided into two categories under the same conditions; sweet peppers which received biological treatments and those that were chemically treated. Nature Biotechnology Company (Biorun) products were used as the biological treatment, including: "Probio 96" (a biological fertilizer containing *Bacillus subtilis*), "Biofarm" [a biological fertilizer formulated based on several nitrogen fixing PGPRs, such as *Azospirillum* and *Pseudomonas* (2×10^7 CFU per mL)], "RoshdAfza" (a biological fertilizer formulated based on several phyllosphere bacteria), "Bioguard" [a water-soluble fertilizer based on beneficial microorganisms such as *Trichoderma harzianum* and *Bacillus velezensis*, humic acid

TABLE 1 Characteristics of chemical parameters of the irrigation water sample in the greenhouse used for sweet pepper cultivation.

Alkalinity (ppm)	125
Total hardness (ppm)	305
Sodium adsorption ratio (SAR)	4.02
Soluble sodium percent (SSP)	50.98
pH	7.56
Total dissolved solids (TDS) (mg/L)	625
Electrical conductivity (μS/cm)	1,378
Total cations	13.73
Potassium (K^+)	0.63
Sodium (Na^+)	7
Magnesium (Mg^{2+})	2
Bicarbonate (HCO_3^-)	2.5
Calcium (Ca^{2+})	4.1
Total anions	13.68
Sulfate (SO_4^{2-})	1.98
Chloride (Cl^-)	9.2

TABLE 2 Characteristics of the chemical and structural parameters of the greenhouse soil sample used for sweet pepper cultivation.

Saturation percentage (%)	41
Silt percentage (%)	28
Clay percentage (%)	14
Sand percentage (%)	58
pH	7.65
Absorbable potassium (mg/kg)	150
Absorbable phosphorus (mg/kg)	11.25
Electrical conductivity (ds/m)	5.06
Total nitrogen (%)	0.069
Organic Carbon (%)	0.83
Manganese (ppm)	3.79
Copper (ppm)	0.14
Zinc (ppm)	0.61
Ferrous (ppm)	4.83
Soil depth (cm)	0–30

(potassium humate), and seaweed extract (*Ascophyllum nodosum*, *Laminaria*, and *Sargassum*)], and Biolep (a biological insecticide formulated based on the entomopathogenic bacterium, *Bacillus thuringiensis* subsp. *kurstaki*). Probio 96 (three liters per hectare), Biofarm (one liter per hectare), and Bioguard (1.5 kg per hectare) were added with the adequate volume of water to irrigate plants. RoshdAfza (three liters per hectare) and Biolep (two liters per hectare) were added to the appropriate volume of water and sprayed on sweet pepper plants. Probio 96 and Biofarm fertilizers were used four times during the growth stage. RoshdAfza fertilizer was applied to sweet pepper plants at two stages (30 and 60 days after cultivation). Bioguard was used monthly during the cultivation cycle. Biolep insecticide was applied on a weekly basis once insects started appearing on the plants.

During their growth cycle, plants in the second category received common conventional management programs (application of fertilizers and pesticides). Chemical fertilizers included ammonium sulfate, khazra iron, zinc, and boron chelate fertilizers, humic acid, ammonium nitrate, calcium nitrate, codamin radicular rooting fertilizer, super liquid fertilizer, liquid sulfur fertilizer, frutaliv fertilizer, NPK 20-20-20 (10 Kg per hectare), super micro plus fertilizer, isabion amino acids. Chemical pesticides in this category included beltanol, berdofix, ortiva top, signum, potassium phosphite, dichlorvos, abamectin, starkle, avaunt, acetamiprid, dursban, nissorun, sponsor, chess, methoxyfenozide, and adjuvants.

Leaf chlorophyll content

For each treatment, ten leaf samples were selected from mature leaves and below the growing point with similar growth in ten different places of three rows in the greenhouse at 90 days after transplanting and their leaf chlorophyll concentration was determined using a SPAD meter (Konica-Minolta, Japan).

Plant height, number of flowers and fruits per plant

For each treatment, 10 plants were selected from 10 different places in three rows of each treatment to measure plant height, number of flowers and fruits per plant at the end of the experiment, flowering stage and harvest period, respectively. Their height was determined using a measuring tape. A number of fruits and flowers per plant were counted.

Mineral composition

The plant samples (leaves and fruits) were dried. Then the amount of 0.5 g of the powdered samples from 10 plants in three rows of each treatment were mixed with 12.5 ml of HNO_3 and kept on a heater at a temperature of 100°C for 2 h. A yellow solution was formed, and the residue was filtered through filter paper. Finally, the element concentrations in the leaf and fruit samples of sweet peppers were determined by inductively coupled plasma optical emission spectrometry (ICP-OES, Agilent 700 Series, USA).

Total phenolic content

One gram of sweet pepper fruit tissue was homogenized with 10 ml of distilled water and then filtered. The amount of 700 µl of the extract was mixed with 900 µl sodium carbonate solution (2% w/v). Then 180 µl Folin-Ciocalteau reagent (50%) was added to the mixture and the samples were kept at room temperature for 30 min. The absorbance of the samples was then evaluated using a spectrophotometer (DR3900, Hach, Germany) at 750 nm. The total phenolic content was measured using a calibration curve and expressed as mg gallic acid per 100 g fresh weight (Etemadipoor et al., 2020). Four replicates of each treatment were randomized on the fruits of test plants in three rows at the harvest period.

Antioxidant activity

One gram of sweet pepper fruit tissue was homogenized with 10 ml of methanol (80%) and then filtered. One ml of DPPH (0.1 mM) was added to 100 µl of the methanolic fruit extract and mixed with one ml of Tris-HCl (pH = 7.5). The samples were vortexed and kept in the dark. Four replicates of each treatment were randomized on the fruits of test plants in three rows at the harvest period. The absorbance of the samples was evaluated using a spectrophotometer (DR3900, Hach, Germany) at 517 nm. Antioxidant activity was measured according to the equation (Etemadipoor et al., 2020):

Antioxidant activity (%): [1 – Abs sample/Abs control ×100]

Statistical analysis

The independent-sample *t*-test was used to compare the effects of treatments at 5% probability level (2-tailed) using SPSS 21.0 (SPSS Inc., Chicago, IL, USA).

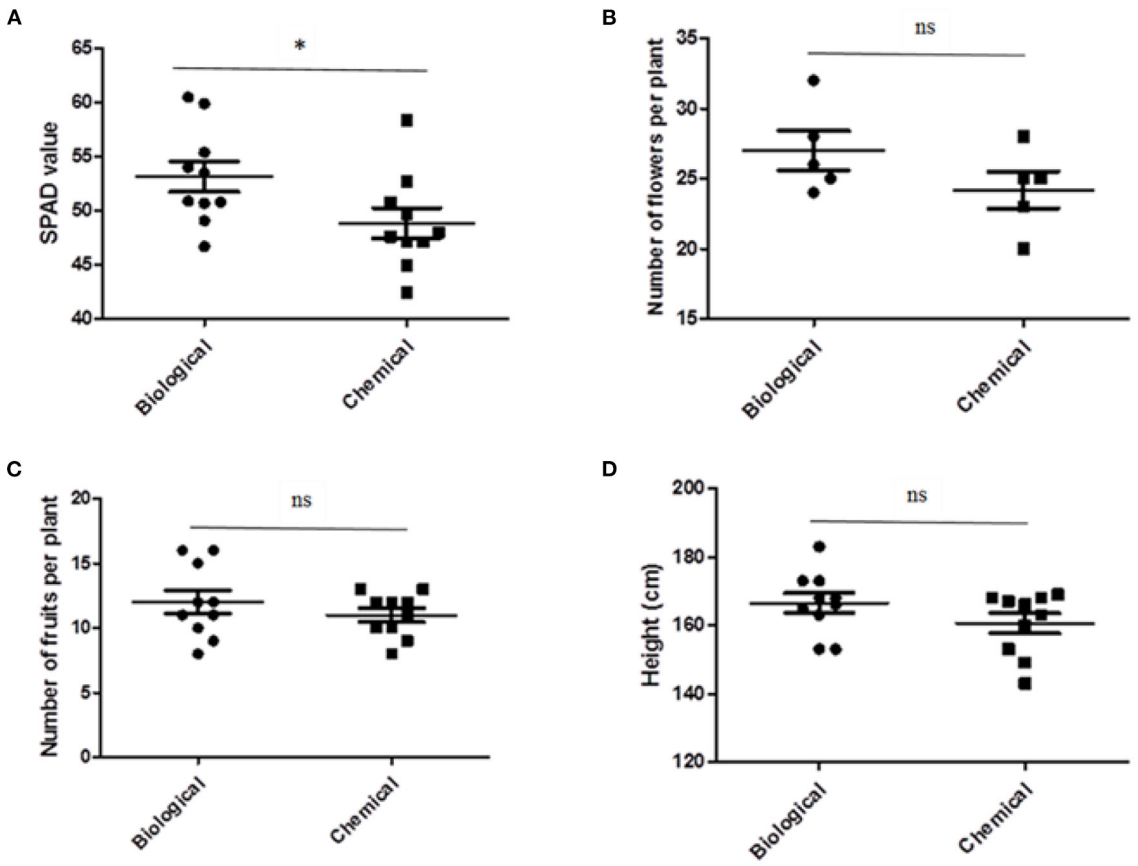

FIGURE 1
The effect of biological and chemical treatments on leaf SPAD value **(A)**, number of flowers **(B)** and fruits **(C)** per plant and height **(D)** of sweet pepper plants. Asterisk indicates a statistically significant effect (*$p < 0.05$), whereas "ns" indicates not significant ($p > 0.05$) between biological and chemical treatments.

Results and discussion

Soil and water analysis

According to soil and water analysis conducted before the start of the experiment (Tables 1, 2), water EC showed an optimum value (1,378 μS/cm). The soil organic carbon, P, Fe, Mn, Zn, and Cu concentrations were relatively low and the soil demonstrated a deficiency in nitrogen element.

Effect of biological and chemical treatments on some growth and physiological parameters

Leaf chlorophyll concentration increased by the biological treatment compared to the chemical treatment (Figure 1A). SPAD values have been shown to be positively correlated with nitrogen concentration and leaf chlorophyll content (Murdock et al., 1997). Lozo et al. (2022) reported that *Bacillus* bacteria can produce indole acetic acid and aminocyclopropane carboxylate deaminase, which increases plant growth and inhibits chlorophyll degradation. Aminocyclopropane carboxylate deaminase reduces the formation of ethylene hormone in plants by degrading aminocyclopropane carboxylate, a precursor of ethylene (Ghorai et al., 2021), which may inhibit plant reactions associated with senescence, such as chlorophyll degradation. There was no significant difference between biological and chemical treatments in plant height and the number of flowers and fruits per plant (Figures 1B–D). Our findings were in accordance with another study that showed the application of biostimulants did not affect marketable yield but improved pepper fruit quality (Arthur et al., 2022). Additionally, the application of microbial-based biostimulants did not improve the morphological characteristics and yield of pepper fruit (Majkowska-Gadomska et al., 2021).

Effect of biological and chemical treatments on the element concentration of sweet pepper plants

The concentration of Fe, K, Mg, P, Ca, Cu, Si, and Mn increased in sweet pepper fruits when the plants were treated with the biological treatment. Satisfactory fruit quality and productivity require the adequate supply of macro- and micronutrients (Gruda,

TABLE 3 Concentration of some macro- and micronutrients in the leaf and fruit of sweet pepper plants.

Element	Leaf		Fruit	
	Biological	Chemical	Biological	Chemical
Fe (mg/Kg)	$6.76^{a} \pm 0.01$	$8.28^{b} \pm 0.01$	$6.04^{a} \pm 0.01$	$4.01^{b} \pm 0.01$
K (mg/Kg)	$2.42^{a} \pm 0.04$	$2.43^{a} \pm 0.03$	$0.92^{a} \pm 0.02$	$0.86^{b} \pm 0.03$
Mg (mg/Kg)	$85.79^{a} \pm 0.61$	$92.92^{b} \pm 0.47$	$10.77^{a} \pm 0.05$	$10.03^{b} \pm 0.08$
P (mg/Kg)	$16.49^{a} \pm 0.24$	$17.70^{b} \pm 0.13$	$18.83^{a} \pm 0.03$	$18.68^{b} \pm 0.03$
Zn (mg/Kg)	$1.57^{a} \pm 0.07$	$1.35^{b} \pm 0.07$	$0.23^{a} \pm 0.02$	$0.19^{a} \pm 0.02$
Ca (mg/Kg)	$139.89^{a} \pm 0.04$	$139.86^{a} \pm 0.05$	$8.20^{a} \pm 0.03$	$6.76^{b} \pm 0.02$
Cu (mg/Kg)	$1.58^{a} \pm 0.06$	$1.28^{b} \pm 0.07$	$2.37^{a} \pm 0.05$	$0.07^{b} \pm 00$
Si (mg/Kg)	$1.26^{a} \pm 0.06$	$1.24^{a} \pm 0.06$	$1.62^{a} \pm 0.02$	$1.23^{b} \pm 0.03$
B (mg/Kg)	$1.45^{a} \pm 0.04$	$1.48^{a} \pm 0.03$	$0.14^{a} \pm 0.01$	$0.14^{a} \pm 0.01$
Mn (mg/Kg)	$0.66^{a} \pm 0.04$	$0.60^{a} \pm 0.03$	$0.19^{a} \pm 0.01$	$0.14^{b} \pm 0.01$

Values are expressed as the mean of three replicates ± SD. Values in each column with different letters are significantly different (t-test at $P < 0.05$) between each mineral composition in the leaf and fruit of sweet pepper plants.

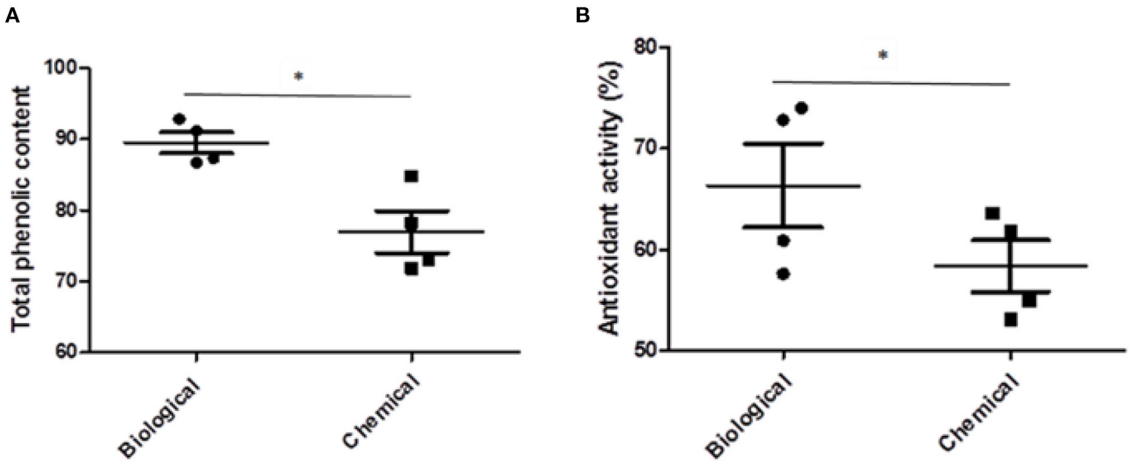

FIGURE 2
The effect of biological and chemical treatments on the total phenolic content **(A)** and antioxidant activity **(B)** of sweet pepper fruits. Asterisk indicates a statistically significant effect (*$p < 0.05$) between biological and chemical treatments.

2005). In our experiment, the higher concentration of macro- and micronutrients in the biologically treated plants demonstrated a beneficial impact of this treatment on fruit quality. Compared with the chemical treatment, the concentration of Zn and Cu was higher in the leaves of the biologically treated plants (Table 3). The beneficial effects of plant growth-promoting bacteria as a significant component of our biological treatments may be due to the induction of phytohormone production, nitrogen fixation, and enhancement of mineral nutrient uptake by plants (Del Amor and Cuadra-Crespo, 2011; Backer et al., 2018). Cisternas-Jamet et al. (2020) indicated that inoculation of the roots of bell pepper plants with *Bacillus amyloliquefaciens* bacteria led to increased Ca and Fe concentrations, antioxidant activity in fruits, and also an improved growth. Similarly, the use of growth-promoting bacteria with a mixture of compost and *Trichoderma harzianum* fungus has been shown to increase the concentration of Cu in tomato (Khan et al., 2017). It has been reported that *B. amyloliquefaciens* can affect Ca transport in plants through the production of auxin (Tadesse, 1997; Salvatierra-Martinez et al., 2018). Application of *B. subtilis* in cauliflower resulted in an increase in Ca concentration (Ekinci et al., 2014). Inoculation of green bell pepper seeds with *B. amyloliquefaciens* resulted in an increase in Ca and Fe concentration (Cisternas-Jamet et al., 2020). The pH of the soil in the greenhouse was 7.65 (Table 2), which could affect the availability of several micronutrients such as Fe, Zn, Mn, etc., which were deficient in this study. Under iron deficiency conditions, chelating compounds such as siderophores are synthesized by some bacteria. These compounds help in the uptake of macronutrients and have a beneficial effect on plant growth and productivity (Shahriari and Moradi, 2018).

Effect of biological and chemical treatments on the total phenols and antioxidant activity of sweet peppers

In our experiment the concentration of total phenols and antioxidant activity showed a significant increase in plants treated with the biological treatment in comparison with the chemical treatment (Figure 2). These results are in agreement with previous investigations, which showed that inoculation of green pepper seeds with *B. amyloliquefaciens* bacteria caused an increase in vitamin C, total phenols and antioxidant activity (Cisternas-Jamet et al., 2020). The results of another study showed that the use of biological agents could lead to a higher yield of sweet pepper (El Arnaouty et al., 2020). Higher concentration of micronutrients such as Fe, Mn, Zn and Cu can increase the antioxidant activity within plant tissues as these essential elements are cofactors of enzymatic antioxidants such as superoxide dismutase. In addition, zinc plays an important role (cofactor of transcription factors) in the expression of genes encoding antioxidant enzymes (Homayoonzadeh et al., 2022). There was a significant positive correlation between total phenolic content and antioxidant activity ($r = 0.983$, significant at the 0.05 level). Therefore, the high antioxidant activity in biologically treated sweet pepper plants in our experiment, could be attributed to the higher concentration of phenolic compounds in the fruit extract.

Conclusion

This study provides new information on the effects of microbial-based biological treatments on the nutritional, nutraceutical and functional properties of greenhouse sweet pepper. Biological treatments significantly improved the nutritional, nutraceutical and functional composition of sweet pepper fruits compared to chemical treatments. These results indicate that biological treatments have great potential to increase the concentration of elements, total phenolic content, and antioxidant activity in sweet pepper fruits, compared with the chemical control program under the same conditions. However, the exact mechanisms of these processes need further investigation. Therefore, biological treatments can be used as a practical, safe, and promising alternative to chemical agents in sweet pepper management programs for growers seeking environmentally friendly strategies to improve sweet pepper fruit quality.

Data availability statement

The original contributions presented in the study are included in the article/supplementary material, further inquiries can be directed to the corresponding author.

Author contributions

AT conceived the study, performed the experiments, analyzed the data, and mainly wrote the manuscript. AM performed some experiments. BJ wrote some parts of the manuscript. All authors edited and approved the final version of the manuscript.

Funding

This study was funded by the Minab Higher Education Center, University of Hormozgan.

Acknowledgments

The authors express their gratitude to Minab Higher Education Center, University of Hormozgan to provide laboratory facilities and equipment.

Conflict of interest

The authors declare that the research was conducted in the absence of any commercial or financial relationships that could be construed as a potential conflict of interest.

Publisher's note

All claims expressed in this article are solely those of the authors and do not necessarily represent those of their affiliated organizations, or those of the publisher, the editors and the reviewers. Any product that may be evaluated in this article, or claim that may be made by its manufacturer, is not guaranteed or endorsed by the publisher.

References

Agliassa, C., Mannino, G., Molino, D., Cavalletto, S., Contartese, V., Bertea, C. M., et al. (2021). A new protein hydrolysate-based biostimulant applied by fertigation promotes relief from drought stress in *Capsicum annuum* L. *Plant Physiol. Biochem.* 166, 1076–1086. doi: 10.1016/j.plaphy.2021.07.015

Alvarez, A., Saez, J. M., Costa, J. S. D., Colin, V. L., Fuentes, M. S., Cuozzo, S. A., et al. (2017). Actinobacteria: current research and perspectives for bioremediation of pesticides and heavy metals. *Chemosphere* 166, 41–62. doi: 10.1016/j.chemosphere.2016.09.070

Arias-Estevez, M., Lopez-Periago, E., Mart'inez-Carballo, E., Simal-G'andara, J., Mejuto, J. C., and Garc'ia-R'io, L. (2008). The mobility and degradation of pesticides in soils and the pollution of groundwater resources. *Agric. Ecosyst. Environ.* 123, 247–260. doi: 10.1016/j.agee.2007.07.011

Arthur, J. D., Li, T., and Bi, G. (2022). Plant Growth, Yield, and quality of containerized heirloom chile pepper cultivars affected by three types of biostimulants. *Horticulturae* 9, 12. doi: 10.3390/horticulturae9010012

Ashour, M., Hassan, S. M., Elshobary, M. E., Ammar, G. A., Gaber, A., Alsanie, W. F., et al. (2021). Impact of commercial seaweed liquid extract (TAM®) biostimulant and its bioactive molecules on growth and antioxidant activities of hot pepper (*Capsicum annuum*). *Plants* 10,1045. doi: 10.3390/plants 10061045

Babalola, O. O., and Glick, B. R. (2012). The use of microbial inoculants in African agriculture: current practice and future prospects. *J. Food Agric. Environ*. 10, 540–549.

Backer, R., Rokem, J. S., Ilangumaran, G., Lamont, J., Praslickova, D., Ricci, E., et al. (2018). Plant growth-promoting rhizobacteria: context, mechanisms of action, and roadmap to commercialization of biostimulants for sustainable agriculture. *Front. Plant Sci*. 9, 1473. doi: 10.3389/fpls.2018.01473

Brezeanu, C., Brezeanu, P. M., Stoleru, V., Irimia, L. M., Lipşa, F. D., Teliban, G. C., et al. (2022). Nutritional value of new sweet pepper genotypes grown in organic system. *Agriculture* 12, 1863. doi: 10.3390/agriculture12111863

Chen, L., and Kang, Y. H. (2013). Anti-inflammatory and antioxidant activities of red pepper (*Capsicum annum* L.) stalk extracts: comparison of pericarp and placenta extract. *J. Funct. Food* 5, 1724–1731. doi: 10.1016/j.jff.2013.07.018

Cisternas-Jamet, J., Salvatierra-Martínez, R., Vega-Gálvez, A., Stoll, A., Uribe, E., and Goñi, M. G. (2020). Biochemical composition as a function of fruit maturity stage of bell pepper (*Capsicum annum*) inoculated with *Bacillus amyloliquefaciens*. *Sci. Hortic*. 263, 109107. doi: 10.1016/j.scienta.2019.109107

Deepak, B., Mohammad, W. A., Ranjan, K. S., and Narendra, T. (2014). Biofertilizers function as a key player in sustainable agriculture by improving soil fertility, plant tolerance, and crop productivity. *Microb. Cell Fact*. 13, 66. doi: 10.1186/1475-2859-13-66

Del Amor, F. M., and Cuadra-Crespo, P. (2011). Plant growth-promoting bacteria as a tool to improve salinity tolerance in sweet pepper. *Funct. Plant Biol*. 39, 82–90. doi: 10.1071/FP11173

Ekinci, M., Turan, M., Yildirim, E., Günes, A., Kotam, R., and Dursun, A. (2014). Effect of plant growth promoting Rhizobacteria on growth, nutrient, organic acid, amino acid and hormone content of cauliflower (*Brassica oleracea* L. var. botrytis) transplants. *Acta Sci. Pol. Hortorum. Cultus*. 13, 71–85.

El Arnaouty, S. A., El-Heneidy, A. H., Afifi, A. I., Heikal, I. H., and Kortam, M. N. (2020). Comparative study between biological and chemical control programs of certain sweet pepper pests in greenhouses. *Egypt J. Biol. Pest Control* 30, 1–7. doi: 10.1186/s41938-020-00226-z

Etemadipoor, R., Dastjerdi, A. M., Ramezanian, A., and Ehteshami, S. (2020). Ameliorative effect of gum arabic, oleic acid and/or cinnamon essential oil on chilling injury and quality loss of guava fruit. *Sci. Hortic*. 266, 109255. doi: 10.1016/j.scienta.2020.109255

Fasusi, O. A., Cruz, C., and Babalola, O. O. (2021). Agricultural sustainability: microbial biofertilizers in rhizosphere management. *Agriculture* 11, 163. doi: 10.3390/agriculture11020163

Ghorai, A. K., Patsa, R., Jash, S., and Dutta, S. (2021). "Microbial secondary metabolites and their role in stress management of plants," in *Biocontrol Agents and Secondary Metabolites* (Cambridge: Woodhead Publishing), 283–319. doi: 10.1016/B978-0-12-822919-4.00012-0

Gruda, N. (2005). Impact of environmental factors on product quality of greenhouse vegetables for fresh consumption. *Crit. Rev. Plant Sci*. 24, 227–274. doi: 10.1080/07352680591008628

Homayoonzadeh, M., Haghighi, S. R., Hosseininaveh, V., Talebi, K., Roessner, U., and Winters, A. (2022). Effect of spirotetramat application on salicylic acid, antioxidative enzymes, amino acids, mineral elements, and soluble carbohydrates in Cucumber (*Cucumis sativus* L.). *Biol. Life Sci Forum* 11, 3. doi: 10.3390/IECPS2021-11921

Khan, Y. M., Manjurul Haque, M., Molla, A. H., Rahman, M., and Alam, M. Z. (2017). Antioxidant compounds and minerals in tomatoes by *Trichoderma* enriched bio- fertilizer and their relationship with the soil environments. *J. Integr. Agric*. 16, 691–703. doi: 10.1016/S2095-3119(16)61350-3

Krasnow, C., and Ziv, C. (2022). Non-chemical approaches to control postharvest gray mold disease in bell peppers. *Agronomy* 12, 216. doi: 10.3390/agronomy12010216

Lozo, J., Danojević, D., Jovanović, Ž., Nenadović, Ž., Fira, D., Stanković, S., et al. (2022). Genotype-Dependent antioxidative response of four sweet pepper cultivars to water deficiency as affected by drought-tolerant *Bacillus safensis* SS-2.7 and *Bacillus thuringiensis* SS-29.2 Strains. *Horticulturae* 8, 236. doi: 10.3390/horticulturae8030236

Majkowska-Gadomska, J., Dobrowolski, A., Jadwisieńczak, K. K., Kaliniewicz, Z., and Francke, A. (2021). Effect of biostimulants on the growth, yield and nutritional value of *Capsicum annuum* grown in an unheated plastic tunnel. *Sci. Rep*. 11, 1–14. doi: 10.1038/s41598-021-01834-x

Mishra, D. J., Singh, R., Mishra, U. K., and Kumar, S. S. (2013). Role of bio-fertilizer in organic agriculture: a review. *Res. J. Recent Sci*. 2, 39–41.

Murariu, F., Voda, A. D., and Murariu, O. C. (2019). Researches on food safety assessment—Supporting a healthy lifestyle for the population from NE of Romania. *J. Biotechnol*. 5, S68. doi: 10.1016/j.jbiotec.2019.05.238

Murdock, L., Jones, S., Bowely, C., Needham, P., James, J., and Howe, P. (1997). *Using a Chlorophyll Meter to Make Nitrogen Recommendations on Wheat*. Louisville, KY: Cooperative Extension Service University of Kentucky-college of Agriculture.

Naderi, S. A., Dehkordi, A. L., and Taki, M. (2019). Energy and environmental evaluation of greenhouse bell pepper production with life cycle assessment approach. *Environ. Sustain. Indic*. 3, 100011. doi: 10.1016/j.indic.2019.100011

Nasiri, A., and Nikzadfar, M. (2007). *Assessment of the Current Situation and Prospects of Greenhouse Cultivation*. Isfahan: The First National Conference of Hydroponics and Greenhouse Production, Isfahan University of Technology.

Paradiković, N., Vinković, T., Vinković Vrček, I., Žuntar, I., Bojić, M., and Medić-Šarić, M. (2011). Effect of natural biostimulants on yield and nutritional quality: an example of sweet yellow pepper (*Capsicum annuum* L.) plants. *J. Sci. Food Agric*. 91, 2146–2152. doi: 10.1002/jsfa.4431

Salvatierra-Martinez, R., Arancibia, W., Araya, M., Aguilera, S., Olalde, V., Bravo, J., et al. (2018). Colonization ability as an indicator of enhanced biocontrol capacity—an example using two *Bacillus amyloliquefaciens* strains and *Botrytis cinerea* infection of tomatoes. *J. Phytopathol*. 166, 601–612. doi: 10.1111/jph.12718

Shahriari, F., and Moradi, R. (2018). Siderophores in environmental research: roles and applications. *J Bio Safety* 12, 1–20.

Sinha, R. K., Valani, D., Chauhan, K., and Agarwal, S. (2010). Embarking on a second green revolution for sustainable agriculture by vermiculture biotechnology using earthworms: reviving the dreams of Sir Charles Darwin. *J. Agric. Biotech. Sustain. Dev*. 2, 113–128. doi: 10.5897/JABSD.9000017

Sreeramulu, D., and Raghunath, M. (2010). Antioxidant activity and phenolic content of roots, tubers and vegetables commonly consumed in India. *Food Res. Int*. 43, 1017–1020. doi: 10.1016/j.foodres.2010.01.009

Tadesse, T. (1997). *Some Factors Affecting the Yield and Quality of Sweet Pepper (Capsicum Annuum L.) cv. Domino*. New Zealand: Massey University.

frontiers | Frontiers in Sustainable Food Systems

TYPE Original Research
PUBLISHED 18 April 2023
DOI 10.3389/fsufs.2023.1106528

Check for updates

OPEN ACCESS

EDITED BY
Micaela Tosi,
University of Guelph, Canada

REVIEWED BY
Expedito Olimi,
Graz University of Technology, Austria
Becky Nancy Aloo,
University of Eldoret, Kenya
Oluwaseyi Samuel Olanrewaju,
North-West University, South Africa

*CORRESPONDENCE
Ryan R. Hansen
✉ rrhansen@ksu.edu

SPECIALTY SECTION
This article was submitted to Crop Biology and Sustainability, a section of the journal Frontiers in Sustainable Food Systems

RECEIVED 23 November 2022
ACCEPTED 27 March 2023
PUBLISHED 18 April 2023

CITATION
Barua N, Clouse KM, Ruiz Diaz DA, Wagner MR, Platt TG and Hansen RR (2023) Screening the maize rhizobiome for consortia that improve *Azospirillum brasilense* root colonization and plant growth outcomes.
Front. Sustain. Food Syst. 7:1106528.
doi: 10.3389/fsufs.2023.1106528

COPYRIGHT
© 2023 Barua, Clouse, Ruiz Diaz, Wagner, Platt and Hansen. This is an open-access article distributed under the terms of the Creative Commons Attribution License (CC BY). The use, distribution or reproduction in other forums is permitted, provided the original author(s) and the copyright owner(s) are credited and that the original publication in this journal is cited, in accordance with accepted academic practice. No use, distribution or reproduction is permitted which does not comply with these terms.

Screening the maize rhizobiome for consortia that improve *Azospirillum brasilense* root colonization and plant growth outcomes

Niloy Barua[1], Kayla M. Clouse[2], Dorivar A. Ruiz Diaz[3], Maggie R. Wagner[2], Thomas G. Platt[4] and Ryan R. Hansen[1]*

[1]Tim Taylor Department of Chemical Engineering, Kansas State University, Manhattan, KS, United States, [2]Department of Ecology and Evolutionary Biology, University of Kansas, Lawrence, KS, United States, [3]Department of Agronomy, Kansas State University, Manhattan, KS, United States, [4]Division of Biology, Kansas State University, Manhattan, KS, United States

Plant growth-promoting bacteria (PGPB) are valuable for supporting sustainable food production and may alleviate the negative impacts of chemical fertilizers on human health and the environment. While single-strain inoculations have proven unreliable due to poor survival and colonization in the rhizosphere, application of PGPB in multispecies consortia has the potential to improve these outcomes. Here, we describe a new approach for screening and identifying bacterial consortia that improve the growth of corn relative to plants inoculated with a single strain. The method uses the microwell recovery array (MRA), a microfabricated high-throughput screening device, to rapidly explore the maize (*Zea mays L.*) rhizobiome for higher-order combinations of bacteria that promote the growth and colonization of the nitrogen-fixing PGPB, *Azospirillum brasilense*. The device simultaneously generates thousands of random, unique combinations of bacteria that include *A. brasilense* and members of the maize rhizobiome, then tracks *A. brasilense* growth in each combination during co-culture. Bacteria that show the highest levels of *A. brasilense* growth promotion are then recovered from the device using a patterned light extraction technique and are identified. With this approach, the screen uncovered growth-promoting consortia consisting primarily of bacteria from the *Acinetobacter-Enterobacter-Serratia* genera, which were then co-inoculated with *A. brasilense* on axenic maize seedlings that were monitored inside a plant growth chamber. Compared to maize plants inoculated with *A. brasilense* alone, plants that were co-inoculated with these consortia showed accelerated growth after 15 days. Follow-up root colonization assays revealed that *A. brasilense* colonized at higher levels on roots from the co-inoculated seedlings. These findings demonstrate a new method for rapid bioprospecting of root and soil communities for complementary PGPB and for developing multispecies consortia with potential use as next-generation biofertilizers.

KEYWORDS

biofertilizers, consortia, *Azospirillum*, plant growth promoting bacteria, microbial interactions, high throughput screening, microwell arrays

1. Introduction

Increasing crop production and enhancing plant health in a sustainable manner is critical in the face of climate change (Farooq et al., 2022), increasing population (Komarek and Msangi, 2019), reduction of cultivable lands (Maranguit et al., 2017), and pest or pathogen mediated diseases in crops (Leisner et al., 2022). While chemical fertilizers and pesticides remain necessary for enhancing food production, their indiscriminate use has proven unsustainable and negatively impacts human and environmental health (Chaudhary et al., 2022). Much effort has focused on exploiting plant growth-promoting bacteria (PGPB) as bioinoculants, i.e., biofertilizers, to enhance plant growth and address the limitations of chemical approaches (Mitter et al., 2021; Bhat et al., 2022). Biofertilizers offer a low-energy, environmentally friendly, and sustainable approach to promoting plant health and increasing biomass production. PGPB can fix nitrogen (Aasfar et al., 2021), produce phytohormones (Egamberdieva et al., 2017), stimulate root development (Gowtham et al., 2022), provide pathogen defense (Zhu et al., 2022), and alleviate environmental and human-induced stresses (Ma et al., 2019; Dodds et al., 2020). However, PGPB are often unreliable and pose a high economic risk amongst agricultural producers, limiting their broad adoption (Nakkeeran et al., 2006; Tabassum et al., 2017).

Currently, the biofertilizer market is dominated by diazotrophic PGPB, such as *Rhizobium spp., Bradyrhizobium spp., Actinorhizobium spp., Azotobacter spp., and Azospirillum spp.* (Stamenković et al., 2018; Pedrosa et al., 2020). *Azospirillum brasilense* is one of the most widely adopted diazotrophs, and it displays versatile C- and N-metabolism. It also promotes plant growth through additional mechanisms, including phytohormone production (Alzate Zuluaga et al., 2022), development of stress tolerance (Pedrosa et al., 2020), siderophore production (Ferreira et al., 2019; Timofeeva et al., 2022), phosphate solubilization (Bargaz et al., 2021), and phytopathogen inhibition (Viejobueno et al., 2021). With this array of benefits, significant effort has been given to understanding the microbial interactions that influence the association and colonization of *A. brasilense* and other diazotrophic bacteria with non-leguminous maize (*Zea mays*) crops (Dent and Cocking, 2017; Oliveira et al., 2018; Van Deynze et al., 2018). Prior studies have also shown that co-inoculation of *A. brasilense* with complementary organisms such as *Bradyrhizobium* (Wang et al., 2018; dos Santos Lima Fagotti et al., 2019) and cyanobacteria isolates (Hungria et al., 2010; Verma et al., 2011; Ferreira et al., 2013; Bashan et al., 2014) improves maize yield. This suggests that *A. brasilense* applied in a symbiotic, multi-species consortium may be key for its improvement as a biofertilizer. However, this requires isolating and identify new collections of complementary bacteria that are also well-adapted to the root environment.

As crop roots harbor diverse collections of beneficial bacteria (Philippot et al., 2013), recent bioprospecting efforts have targeted the rhizosphere and endosphere to uncover new PGPB strains (Mitter et al., 2021). For example, Aloo et al. (2021) recently prospected the potato rhizosphere to uncover isolates with multiple plant growth promoting traits, including bacteria from the *Klebsiella*, *Serratia*, *Enterobacter* and *Citrobacter* genus (2021). Jochum et al. (2019) screened the rhizosphere of perennial grass in semi-arid regions to uncover *Bacillus* and *Enterobacter* strains that improved the drought tolerance of wheat by modifying root architecture (2019). With respect to maize, Ikeda et al. (2020) uncovered *Cellulosimicrobium*, *Bacillus*, *Stenotrophomonas*, and *Enterobacter* strains from the maize root which were found to promote maize growth in greenhouse studies, albeit in a genotype-specific manner (2020). These studies demonstrate that crop roots are a rich resource of bacteria that have potential application as biofertilizers, and motivate screening the maize rhizosphere for bacteria that are interactive and complementary toward *A. brasilense*.

Uncovering favorable PGPB interactions is a daunting task due to the high degree of species diversity in root communities, which depends on soil type/conditioning, irrigation, and climate at different agricultural sites (Lee et al., 2020). Such a task necessitates the application of novel high-throughput screening technologies that can rapidly explore interactions in a microbiome and accelerate the pace of discovery. Here, we apply the microwell recovery array (MRA) (Barua et al., 2021) to rapidly search the maize (*Zea mays L.*) rhizobiome for collections of root-associated bacteria that improve *A. brasilense* growth. Subsequent experiments investigate the impact of these consortia on *A. brasilense's* root colonization and the resulting plant growth. The results demonstrate the unique ability of the MRA as a bioprospecting tool that generates combinations of microbes from root or soil samples that have positive effects on maize growth. The technique has the potential be extended to other plants and offers a new approach to screening plant rhizosphere for multispecies consortia that are potentially useful as biofertilizers.

2. Materials and methods

2.1. Preparation of *Azosprillium brasilense* strain Sp7-GFP and of *Zea mays* rhizobacteria

All bacteria strains and plasmids used in this research are listed in Supplementary Table 1. *A. brasilense* Sp7-GFP, herein referred to as Sp7, was received from the Alexandre lab (University of Tennessee, Knoxville) and was stored in 25% glycerol at −80 °C. Sterile inoculation loops were used to pick cells from the frozen stocks for culture in R2A broth media (pH: 7.2 ± 0.2, Teknova) in sterile test tubes supplemented with ampicillin (100 μg/mL) and tetracycline (5 μg/mL) for 24 hrs (28°C, 215 rpm). For collection of rhizosphere-associated maize (*Zea mays)* microbes, soil and root samples were first collected from a conservation tillage maize field located near Glen Eder, Kansas (Field coordinate: 39.3533616 and −98.362541, 1147 m above sea level). The growth stage at the time of sampling was VT (beginning of flowering). Soil samples from the site were sent to K-State Soil Testing Lab for a complete analysis of carbon, nitrogen, phosphorous content, and soil pH. The comprehensive analysis of the soil samples is listed in Supplementary Table 2. A total of 4 sets of soil and root samples were collected from maize plants, immediately stored on ice, transferred to the laboratory, and stored overnight at 4°C. 200 g of each root sample were washed with 200 mL of sterile, ice-cold 1X phosphate buffer saline (PBS buffer: 8 g/L NaCl, 0.2 g/L KCL,

0.2 g/L KH_2PO_4,1.15 g/L Na_2HPO_4, pH 7) for 20 min (Machado and Colli Mull, 2017). The resulting suspensions were filtered using 0.8 μm sterile filters and centrifuged at 4,400 rpm for 20 min to collect pellets composed of bacteria harvested from maize roots. Extracted cells from each root sample were combined, resuspended in 25% glycerol, and stored at −80°C.

2.2. Media selection

Microbes extracted from maize roots were inoculated from glycerol stocks and incubated in TY Media (10 g/L Bacto-tryptone, 10 g/L NaCl, 5 g/L Yeast Extract, pH: 7 ± 0.2), R2A media (0.50 g/L Yeast extract, 0.50 g/L Proteose Peptone, 0.50 g/L Casamino acids, 0.50 g/L Glucose, 0.50 g/L Soluble starch, 0.30 g/L Na-pyruvate, 0.30 g/L K_2HPO_4, 0.05 g/L $MgSO_4.7H_2O$, pH: 7 ± 0.2), or LB media (10 g/L Tryptone, 10 g/L NaCl, 5 g/L Yeast Extract, pH: 7 ± 0.2), in sterile test tubes for 24 h (28°C, 215 rpm). After incubation, cells grown in each culture media were stored at −80°C in 25% glycerol before the 16S amplicon sequencing used to identify the media that recovered the highest diversity of maize root-associated bacteria (described in Section 2.3).

2.3. 16S rRNA gene community sequencing of maize root isolates

Purified gDNA samples of cells directly extracted from maize roots (Section 2.1) or from cells after culture in TY, R2A, and LB media (Section 2.2) were obtained from the respective glycerol stocks. E.Z.N.A soil DNA kit (Omega Bio-Tek, Norcross, GA) and DNeasy Blood & Tissue Kit (Qiagen, Germantown, MD) were used for DNA extraction. gDNA was diluted to 20 ng/μL in 100 μL aliquots and sent to Integrated Genomics Facility (Department of Plant Pathology, Kansas State University, Manhattan, KS) for library preparation using Nextera XT index Kit v2 (Illumina, Inc., San Diego, CA) and Illumina MiSeq sequencing (2 x 300 bp PE) of the hypervariable V4 region of the 16S rRNA gene (MiSeq platform, PE-300bp format). The following Earth Microbiome Project primers were used to generate amplicons: 515F: 5'-GTGCCAGCMGCCGCGGTAA-3' and 806R: 5'- GGACTACHVGGGTWTCTAAT-3' (Caporaso et al., 2011). Cutadapt was used to remove adapter and primer sequences from raw reads (Martin, 2011), and reads with any ambiguous bases or more than 0.15 expected errors were discarded. The trimmed 16S-v4 reads were further quality-filtered, truncated, de-noised, and merged using DADA2 software (Callahan et al., 2016) to generate an amplicon sequence variant (ASV) table. Bimeric ASVs were identified using the consensus method and removed. ASVs were identified using the Naïve Bayesian Classifier (Wang et al., 2007) trained on the RDP trainset v16. The ASV table and taxonomic assignments were imported into R v.4.1.2 and analyzed using the tidyverse and phyloseq packages (McMurdie and Holmes, 2013; Wickham et al., 2019). After discarding ASVs that could not be confidently identified as either bacteria or archaea, the dataset included 499 ASVs with a mean of 58,962 reads per sample (standard deviation = 12,835).

2.4. MRA design, fabrication, and preparation

MRAs were fabricated by following the protocols described by Barua et al. (2021). Each array was divided into a 7 × 7 grid of sub-arrays, consisting of a 15 × 15 microwell arrays of 10 μm diameter, 20 μm depth, and 30 μm pitch. A total of 11,025 microwells were etched on a single 3-inch diameter N-type silicon wafer (University Wafers), coated with 1 μm thick layer of Parylene N (PDS 2010 Labcoater, Specialty Coating Systems), using standard photolithography techniques described in previous publications (Masigol et al., 2017, 2018). Cells were next seeded into the MRA devices. R2A was selected as the media for use in MRA operation, as this media was found to recover the most diverse collections of bacteria (Section 2.3, Supplementary Figures 1, 2). *A. brasilense* Sp7 and microbes extracted from maize roots were first cultured in R2A media to mid-log phase then resuspended in R2A to an OD_{600} of 0.2. Next, bacteria cells were inoculated in microwell arrays using protocols described previously (Barua et al., 2021). Based on prior MRA screens, we estimate this generated inoculum densities of ∼40 cells per well, where wells are inoculated with a unique combinations of bacteria species (Hansen et al., 2016; Barua et al., 2021). For co-culture studies, cultures of Sp7 (OD_{600} = 0.2) and root-extracted microbes were mixed at a ratio of 1:1 to reach a final OD_{600} of 0.2. 700 μL of each cell suspension was seeded on top of microwell arrays for 1 h at room temperature. Then, the substrates were dried, followed by the parylene lift-off process to remove cells attached to the array's background regions (Hansen et al., 2016). A polyethylene glycol (PEG) photodegradable membrane was attached on top of the MRA seeded with cells. This membrane attachment step has been previously described in detail (van der Vlies et al., 2019; Fattahi et al., 2021), a summary of the protocol is also provided in the Supplementary material.

2.5. Time-lapse fluorescent microscopy and image analysis

Time-lapse fluorescent microscopy (TLFM) images were acquired with a Nikon Eclipse Ti-U inverted microscope equipped with a 20× objective, a motorized XYZ stage, a humidified live-cell incubation chamber (Tokai Hit), a DS-QiMc monochromatic digital camera, and NIS Elements image acquisition software. The prepared microwell arrays were placed in a custom 3D printed scaffold in order to keep them submerged under liquid media while imaging. The design of the scaffold was described previously (Barua et al., 2021). The scaffold was then placed inside a humidified live-cell incubation chamber at 28°C for co-culture and imaging. A FITC filter was used to image Sp7 (20×, 200 ms, 17.1× gain) with a neutral density filter and with 25% standard light intensity to ensure imaging without photobleaching. Brightfield images were also taken at each section of the array after fluorescent imaging. Images of the microwell arrays (3,600 microwells total) were taken every 60 min during culture. GFP fluorescent images from Sp7 were analyzed following the protocol described by Timm et al. (2017). The Protein Array Analyzer tool in ImageJ was used to generate growth profiles for each microwell to identify the

top 2 wells with the highest growth levels for extraction. The time-lapse fluorescent images were imported as image sequences corrected by subtracting darkfield images from illumination field images with the image calculator plugin. Then image backgrounds were removed by selecting a 125-radius sliding paraboloid, and illumination correction was performed using the calculator plus plugin. Finally, the growth of each strain in the microwells was calculated using the ImageJ "Micro Array" plugin (Timm et al., 2017).

2.6. Recovery and storage of isolates from microwell arrays

Cells were extracted from microwell arrays using a Polygon400 patterned illumination tool (Mightex Systems, Pleasanton, CA) following previously described procedures (van der Vlies et al., 2019). The two promoter wells (A, B) showing the greatest final Sp7 growth levels after 24 h of co-culture were opened by exposing the well perimeter to 365 nm UV light in a ring pattern area with a 10 μm inner diameter and a 20 μm outer diameter as described in Fattahi et al. (2021). The extraction process was done sequentially for two promoter wells, the opened wells were then washed from the well using wash buffer (0.05% Tween in R2A media) into a ~ 200 mL volume, and cell suspensions were plated onto agar-R2A for overnight culture (28°C) and recovery of individual colonies. Five colonies from the two wells with unique colony morphologies were sampled from the plates, these colonies were cultured in R2A media and finally stored in 25% glycerol stocks. These consortia were labeled as promoting consortia 1-5 (PC1, PC2, PC3, PC4, and PC5).

2.7. Validation using 96-well plates

It was previously demonstrated that microbe-microbe interactions observed in the MRA microwells can be recapitulated in a 96-well plate validation assay (Barua et al., 2021). This approach was applied here to validate the growth enhancement of *A. brasilense* in co-culture with consortia PC1-PC5. To obtain cell-free culture fluid (CFCF), R2A liquid media was inoculated with each individual consortium directly from glycerol stocks using a sterile loop, and each sample was cultured (28°C, 300 rpm) in 2mL of media overnight. Cells were removed from the media by centrifugation (2000g, 10 min). To obtain conditioned media, the CFCF was then mixed with Sp7 in R2A media at a 1:1 volumetric ratio to reach an initial OD_{600} value of 0.2 (final volume = 100 μL), at which point growth was quantified with a Biotek Epoch 2 Multi-Mode Microplate Reader (28°C, 300 rpm). Unconditioned media (UCM), which represents the Sp7 growth in monoculture, was obtained following the same procedure, except 1X PBS was added to Sp7 in R2A media instead of CFCF. To verify that the OD_{600} measurement was due to Sp7 growth, CFCF from selected isolates without inoculation of Sp7 was also measured. A total of n=3 independent replicates were calculated for each culture condition. Growth rates and carrying capacities for each condition were quantified using Growthcurver (Sprouffske and Wagner, 2016). Statistical tests were performed using Statistical Analysis System (SAS) analytical software. Differences were identified by comparing Sp7 growth metrics in UCM with Sp7 growth metrics in CFCF from each separate consortium (PC1-PC5) using the Wilcoxon two-sample test to demonstrate Sp7 growth promotion with the consortia.

2.8. 16S rRNA gene community sequencing of microwell extracts

Consortia (PC1-PC5) were first cultured in R2A media by direct inoculation from glycerol stocks into R2A media and then incubated overnight (28°C, 215 rpm). Genomic DNA from each culture was then extracted using DNeasy Blood & Tissue Kit (Qiagen, Germantown, MD) following manufacture's protocol and DNA quality and quantity were measured using a NanoDrop spectrophotometer. DNA quantities (Ads260) of 39–47 ng/mL and DNA qualities (Ads260/Ads280) between 1.74 and 1.88 were measured. Genomic DNA samples were temporarily stored at 4°C in TE buffer, then sent to MR DNA (Shallowater, TX, U.S.A.) for 16S diversity analysis using an Illumina MiSeq sequencing (PE-300bp format). Updated Earth Microbiome primers (515F: 5′-GTGYCAGCMGCCGCGGTAA-3′ and 806R: 5′- GGACTACNVGGGTWTCTAAT-3′) were used to amplify the V4 region of the 16S rRNA gene (Apprill et al., 2015; Parada et al., 2016). Raw sequences were processed into ASV tables using the bioinformatic pipeline described above (Section 2.3). After removing reads that were unclassifiable at the kingdom level or classified as mitochondria or chloroplasts, the dataset included 153 ASVs. Rare ASVs (<0.5% relative abundance) were then removed, leaving 10 ASVs that together accounted for 99.1% of the original data. In this final dataset, the number of reads per consortium ranged from 401,854 to 592,830.

2.9. Plant growth studies to validate survival and colonization of *A. brasilense* Sp7

Plant growth studies were conducted to validate the enhancement of maize growth, as well as survival and colonization of Sp7 in maize rhizosphere when Sp7 was combined with five of the promoter consortia using the protocol described by Niu and Kolter (Niu and Kolter, 2018). First, Sp7 and each of one of the five consortia were inoculated in 2 mL of R2A broth and cultured separately overnight (28°C, 215 rpm). 50 μL of each culture was then transferred to 2 mL of fresh R2A broth and cultured for another 8 h at 28°C. Cells were then centrifuged at 4,400 rpm for 10 min and resuspended in 1X PBS. Cell suspensions from each consortium (PC1-PC5) as well as Sp7 were diluted to ~10^8 cells per milliliter. Each consortium was then mixed with Sp7 in 50 mL Falcon tubes in equal volume to prepare the final formulations (Sp7+PC1, Sp7+PC2, Sp7+PC3, Sp7+PC4, Sp7+PC5). Combining Sp7 with the promoting consortia in this way ensured that Sp7 was present at comparable levels for each of the five formulations. 80 surface-sterilized and germinated maize seedlings (genotype B73) were soaked in each formulation. Sp7 monoculture cell suspension and formulations without Sp7 (PC1, PC2, PC3, PC4, PC5), and a sterile 1X PBS control were

included as controls. Seedlings were incubated without shaking at room temperature for 1 hr. Inoculated maize seedlings were then transferred onto 20 ml ½ Murashige and Skoog (MS) agar (0.8%) in 16 x 150 mm glass tubes with sterile forceps. Sterile empty glass tubes of the same size were attached to the tubes containing seeds in a mouth-to-mouth way using air porous tape (Niu and Kolter, 2018). Sealed glass tubes were then placed in test tube racks and were transferred to a plant growth chamber (Carolina Plant Environmental chamber, Carolina Biological Supply Company) under diurnal light under the following conditions: 8 h of light (day) at 27°C and 9,500 lux of light intensity, 16 h of dark (night) at 23°C, and relative humidity of 54%, and the growth of the maize seedlings was measured every 5 days for 15 days to measure plant height and Sp7 rhizosphere colonization in each sample. Plant growth was measured across n=6 replicate plants for each condition. The Wilcoxon two-sample test (SAS software) was used to identify differences in plant growth by comparing plant height after inoculation with Sp7 only to plant height after inoculation with Sp7 plus each separate consortium (PC1 + Sp7 to PC5 + Sp7).

2.10. Quantification of *A. brasilense* Sp7 abundance on maize roots

Roots generated from maize seedlings that were inoculated with Sp7 or with Sp7 and one of the five consortia (PC1-PC5) were sampled on day 15 after inoculation. Roots were then cut and washed with sterile 1x PBS to remove agar adhered to the root surface. A 1-cm long primary root fragment below the maize kernel was then cut, weighed (~20 mg each), and transferred into 1.5 mL centrifuge tubes containing six glass beads (diameter: 3 mm, Propper) and 1 mL sterile 1x PBS buffer. The bacterial cells colonized on the root surfaces were dislodged by sonication (amplitude: 30%; pulse: on 01 sec, off 01 s; time: 30 s) for 1 m, then vortexing for another 1 min. This step was repeated twice, then the tube was put on ice for 1 min. The cell suspensions were collected and sequentially diluted by a dilution factor of 10^8. 10 µL of the diluted suspensions were then spread on R2A agar supplemented with 200 µg/mL of ampicillin and 10 µg/mL of tetracycline to selectively recover Sp7. The plates were air-dried before incubating the plates at 28 °C in the dark for 16 to 60 hrs. The number of the colony-forming units (CFUs) was counted. Sp7 abundance, defined as CFU per mg root, was then calculated using the equation below (Niu and Kolter, 2018):

$$\textit{A. brasilense}\ \text{Sp7 abundance} = \frac{\text{Colony count} \times 100 \times \text{Dilution factor}}{\text{Weight of root fragment (mg)}} \quad (1)$$

Sp7 abundance measurements were performed for n=3 replicates for each condition. The Wilcoxon two-sample test (SAS software) was used to identify differences in Sp7 abundance by comparing roots inoculated with Sp7 only to roots inoculated with Sp7 and each separate consortium (PC1+Sp7 to PC5+Sp7).

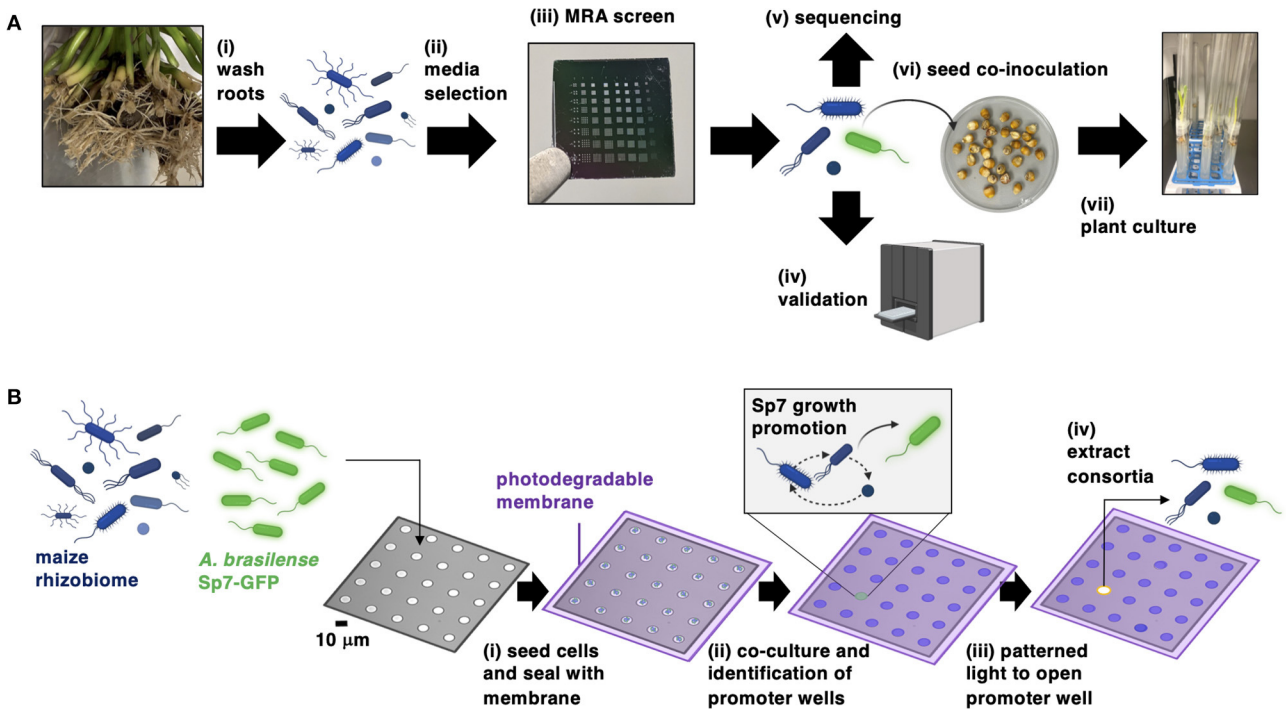

FIGURE 1
(A) Workflow for bioprospecting the maize rhizosphere for isolates (blue cells) that improve the colonization of Sp7 (green cells) in maize roots. **(B)** Operational steps of the MRA device for screening and isolating consortia from the maize rhizosphere that promote the growth of Sp7. Figure was prepared with the assistance of BioRender software.

3. Results and discussion

3.1. Overview of the bioprospecting workflow and MRA device operation

The bioprospecting approach (Figure 1A) involves sampling maize roots to isolate the rhizobiome, then selection of a culture media that recovers rhizobiome isolates at highest taxonomic diversity. The MRA device then uses a co-culture screening process to select a combination of bacteria from the rhizobiome that best promotes the growth of Sp7. The promoting interaction between Sp7 and the consortia found in the MRA is validated in independent 96-well plate assays and the consortia are genomically characterized. After this, Sp7 and the promoting consortia are inoculated onto seedlings to investigate the impact on plant growth. A key step in this workflow is the MRA screening process (Figure 1B), which uses a stochastic cell seeding process characterized previously (Halsted et al., 2016; Hansen et al., 2016, 2021) to generate random collections of rhizobiome isolates and Sp7 cells in small (10 μm diameter) microwells which are compositionally unique from each other. Cells are then sealed into wells with a photodegradable membrane and co-cultured in the selected media. Sp7 growth is monitored in parallel across 3600 microwells using TLFM to reveal the location of individual wells containing consortia that best promote Sp7 growth rate and population size. These wells are tagged as promoter wells. Using a patterned light source, promoting consortia are extracted out of promoter wells (van der Vlies et al., 2019; Fattahi et al., 2020, 2021) and plated for recovery.

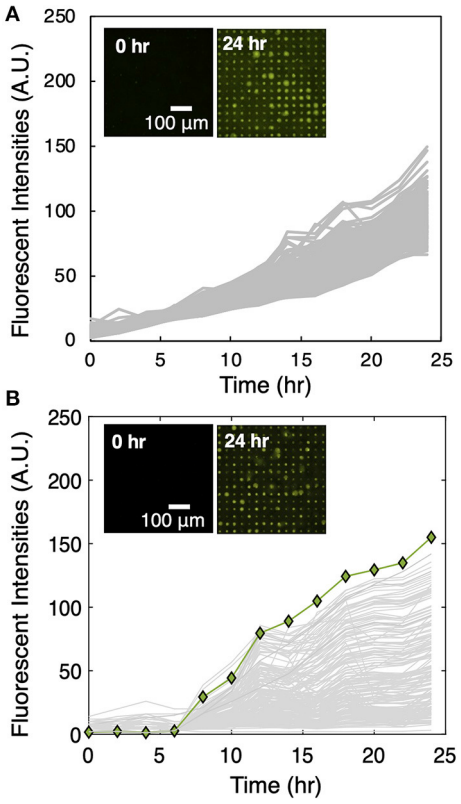

FIGURE 2
(A) Sp7 growth trajectories across a 225 microwell subset in the MRA device during monoculture. (Inset) Corresponding TLFM images of a sample 15 × 15 array of microwells during Sp7 monoculture. **(B)** Sp7 growth trajectories of a sample 15 × 15 array containing a Sp7 promoter well during Sp7 co-culture with microbes recovered from maize rhizosphere. Growth trajectories that result in the highest end-point fluorescent signal (green line) indicate a well where highest levels of Sp7 growth promotion occurred. (Inset) Corresponding TLFM images of the sample 15 × 15 array of microwells during Sp7 co-culture.

3.2. Media selection and MRA screening results

The goal of the media selection was to identify the media that would enable observation of a maximum number of interactions during MRA co-culture screen and that would recover the highest diversity of bacteria from the device. Here, LB, TY, and R2A media were considered and used to culture bacteria from maize rhizosphere, cultures were then characterized with 16S-V4 rRNA gene sequencing. Community analysis for the rhizosphere microbiome showed members of four bacterial phyla (Proteobacteria, Firmicutes, Bacteroidetes, and Actinobacteria), with the genera *Pseudomonas*, *Serratia*, *Acinetobacter*, *Enterobacter*, and *Stenotrophomonas* at high relative abundances (Supplementary Figure 1). As expected, diversity of the original root washes was much higher than the diversity of any of the cultured communities. Of the three media, R2A supported a slightly higher diversity of bacterial ASVs (Supplementary Figure 2) and was selected as the culture media for the MRA screen and for all further cultures.

After media selection, the MRA workflow (Figure 1B) was followed to screen for unknown interactions between the microbes extracted from maize rhizosphere and Sp7. Monoculture control arrays seeded with Sp7 only were first performed (Figure 2A) to generate baseline growth curves. Then co-culture arrays seeded with Sp7 and the root isolates in a 1:1 ratio were performed (Figure 2B). Compared to the monoculture control, significant changes in Sp7 growth metrics were observed with co-culture. Averaged endpoint fluorescence levels of Sp7 monoculture across the measured wells showed relatively low variance ($s^2 = 67$) compared to co-culture ($s^2 = 553$), indicating a wide range of impact due to the addition of the various combinations of rhizobacteria in wells across the array. In the co-culture wells, a noticeable lag time was observed for Sp7 growth compared to the monoculture wells, and low levels of Sp7 growth were most frequently observed, which could be due to competitive and/or antagonistic interactions with many of the rhizobacteria. In fact, relative to the monoculture wells, Sp7 exhibited enhanced population growth in only 16.5% of the co-culture array. Wells with highest Sp7 growth and end-point fluorescence signals were identified in the co-culture array using Grubb's outlier testing, and these "promoter wells" were targeted for selective recovery of the putative promoter isolates.

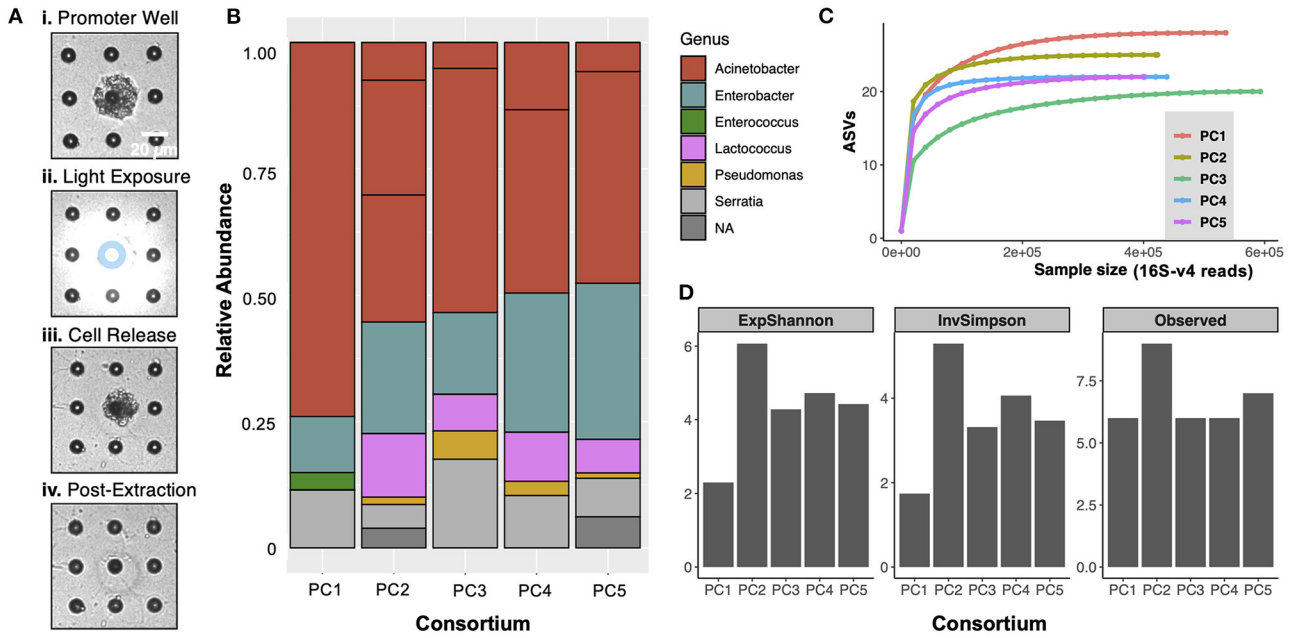

FIGURE 3
(A) Removal of communities from promoter wells. The perimeter of the promoter well was exposed to UV light in a 10 μm inner diameter and 20 μm outer diameter ring pattern (denoted by blue ring in (ii)) to open the photodegradable membrane above the well while also minimizing direct UV exposure to cells. After membrane degradation, cells were released from only the opened well. **(B)** Taxonomic bar plots of the composition of the 5 promoter consortia (PC1-PC5), extracted from promoter wells. 'NA' indicates reads that were not assigned to one of the dominant genera. **(C)** Rarefaction curves generated prior to removal of rare ASVs indicate that the sequencing effort was sufficient to capture the full diversity of each promoter consortium. **(D)** Alpha diversity metrics are presented for the 5 promoter consortia. "ExpShannon" = Shannon diversity, calculated as $e^{[\text{Shannon index}]}$. "InvSimpson" = Inverse Simpson diversity. "Observed" = number of ASVs.

3.3. Extraction, identification, and validation of promoter consortia

Consortia from the top two promoter wells on the co-culture MRA were extracted for characterization using 16S-V4 rRNA gene sequencing and then off-chip validation and application. Cells from the promoter wells became visible with brightfield microscopy after culture, as the cells protruded out of the well boundary due to the high levels of growth (Figure 3A, i). Promoter wells were exposed to ring patterned light (Figure 3A, ii) to remove the membrane from the top of the wells while minimizing cellular exposure to UV light, releasing cells into solution. After exposure, the cell mass could be observed moving out of an opened well (Figure 3A, iii), at which point it was retrieved by washing the arrays with R2A media. After this process, visible cells appeared removed from the promoter wells, and an opening in the membrane around the well was clearly visible (Figure 3A, iv), verifying the successful extraction. During previous development of this extraction protocol, it was demonstrated that minimal cross-contamination from other wells or from the outside environment occurred (van der Vlies et al., 2019), which ensured that the isolates recovered here originated from the promoter well. The extraction process was done sequentially for two promoter wells, and the extract from each individual well was then plated on R2A-agar to recover individual colonies.

After extraction and recovery, 16S-V4 rRNA gene of PC1-PC5 was performed to characterize the taxa present in the promoting consortia extracted from the promoter wells (Figures 3B–D). The analysis revealed that each consortium was dominated with cells from the *Acinetobacter*, *Enterobacter*, and *Serratia* genera, as well as smaller amounts of *Lactococcus* cells (<10%) and some *Pseudomonas* cells (<2%). Measures of alpha diversity for the consortia (Figure 3D) were lower than those of the input (Supplementary Figure 2), demonstrating that the device was able to refine the rhizosphere communities that were input into the device toward interacting members. It should be noted that the compositions of all consortia were similar, with only minor differences in composition at the genus level. This was expected because these consortia originated from one of two wells, which were the top two wells on the array for promoting Sp7 growth. Because of these similarities, it was hypothesized that the five promoting consortia would function similarly to one other. However, with the compositional differences noted, each consortium was still included as independent seedling inoculum in the following studies. It is also notable that some of the genera dominant within these consortia could potentially have inherent plant growth promoting function, independent of Sp7. For example, several species in the *Serratia* genus have been reported to fix nitrogen [e.g., *Serratia nematodiphila*, *Serratia ureilytica* (Tang et al., 2020)] and produce indole-3-acetic acid and siderophores [e.g., *Serratia marcescens* (Khan et al., 2017; Matteoli et al., 2018)].

To verify the on-chip observations, interactions between each PC and Sp7 were recapitulated in an independent off-chip co-culture, following our previous validation assay procedure (Barua

et al., 2021). Culture in CFCF accounts for the PC's diffusive effects on Sp7 in a scaled-up solution volume (from a 1.6 pL microwell volume to a 100 mL volume on the 96 well plate). As a control, a monoculture of Sp7 (OD_{600} = 0.2) in unconditioned media (UCM), which was R2A culture media instead supplemented with a blank solution (1X PBS) at a 1:1 ratio, was also performed and used for comparison. As a negative control, conditioned media from a PC was inoculated without Sp7 to verify that the measured growth in the other experiments was solely due to Sp7 and not due to contaminating microbes. Growth trajectories of each culture reveled that, congruent with microwell observations, higher levels of Sp7 growth occurred when cultured when in CFCF from each promoting consortium (Figure 4A). The corresponding growth metrics show significantly increased the growth rate and carrying capacity of Sp7 compared to the UCM monoculture control (Figures 4B, C, raw data provided in Supplementary Figure 3). This demonstrates that the Sp7 promotion effect from each consortium that was initially identified on the MRA device could be independently recapitulated, and motivated further investigation of the complementary formulations in the context of a root host.

3.4. Effect of *A. brasilense* - isolate co-inoculation on maize growth

With a panel of five consortia with verified growth promotion on Sp7 in liquid co-culture, the effect of co-inoculation with Sp7 and each individual consortium on the growth of axenic maize seedlings was studied in a plant growth chamber environment. After inoculating the surface-sterilized and germinated seeds with a cell suspension containing both Sp7 and each consortium at a Sp7:consortium cellular ratio of 1:1, the axenic seedlings were transferred to a glass tube growth chamber and allowed to grow in ½ MS agar for 15 days (Figure 5A). Two control treatments were included for comparison, these were sterilized seedlings with no inoculation and sterilized seedlings inoculated with Sp7 only. Because several genera of bacteria found in the consortia samples also had known plant growth promoting properties, surface-sterilized and germinated seedlings inoculated only with individual consortia but no Sp7 were added as a final control study. This enabled a distinction between consortia-mediated plant growth due to Sp7 promotion and potential plant growth enhancement due to the promoting consortia alone.

In all the treatments involving Sp7, leaf emergence from all maize seedlings was observed on Day 2. It was therefore concluded that the promoting consortia combined with Sp7 did not have an observed impact on leaf emergence compared to single strain inoculation with Sp7. Co-inoculations also did not significantly impact plant height at Day 5 (Figure 5C). However, significant differences were observed at Day 15 (Figures 5B, D). At this time, seedlings grown after inoculating with Sp7 only showed significantly greater plant height compared to the axenic maize seedlings grown in no-inoculum conditions, demonstrating the positive impact of *A. brasilense* alone. Additionally, axenic seedlings soaked with Sp7 and each promoting consortium showed significantly greater plant height at Day 15 ($p < 0.01$) compared to both control treatments of Sp7 only and no inoculum.

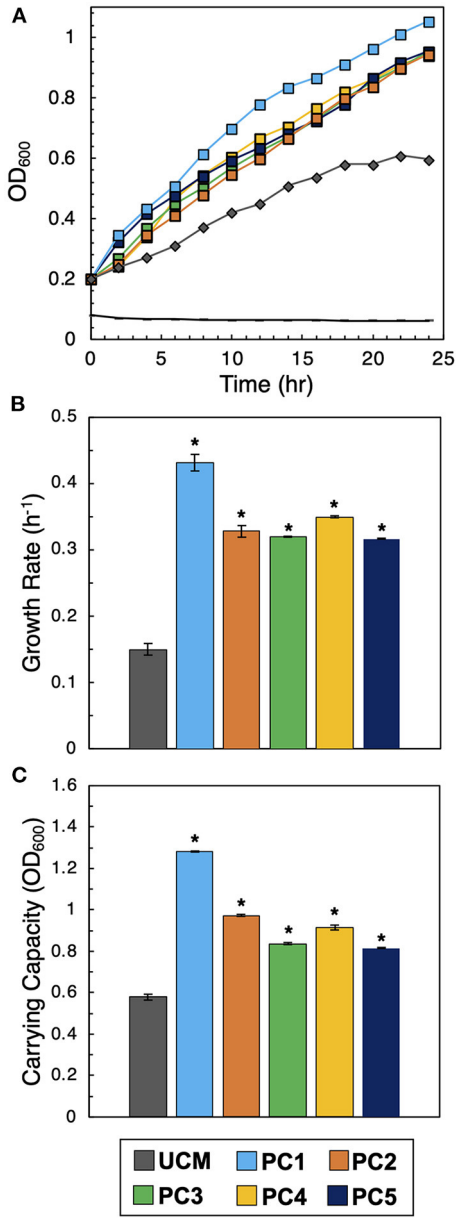

FIGURE 4
Validation of interactions. **(A)** Sp7 growth curves after inoculation into unconditioned media (UCM) or conditioned media from each of the five consortia (PC1-PC5). The black control line represents conditioned media without Sp7. **(B)** Corresponding growth rates and **(C)** carrying capacities of Sp7 in UCM or media conditioned with the promoter consortia (PC1-PC5). Statistical differences were identified by comparing Sp7 growth metrics in consortia-conditioned media with Sp7 monoculture growth metrics in UCM (Wilcoxon two-sample test, $^*P < 0.01$, $n = 3$ independent experiments).

No significant differences in plant height were found between seedlings inoculated with Sp7 plus any one of the five consortia. This was not surprising given the similar composition of each promoting consortium (Figure 3B). Finally, 15-day plant height for the seedlings inoculated only with a promoting consortium but without Sp7 showed diminished growth compared to seedlings inoculated with Sp7 only, and minimal or no improvement relative

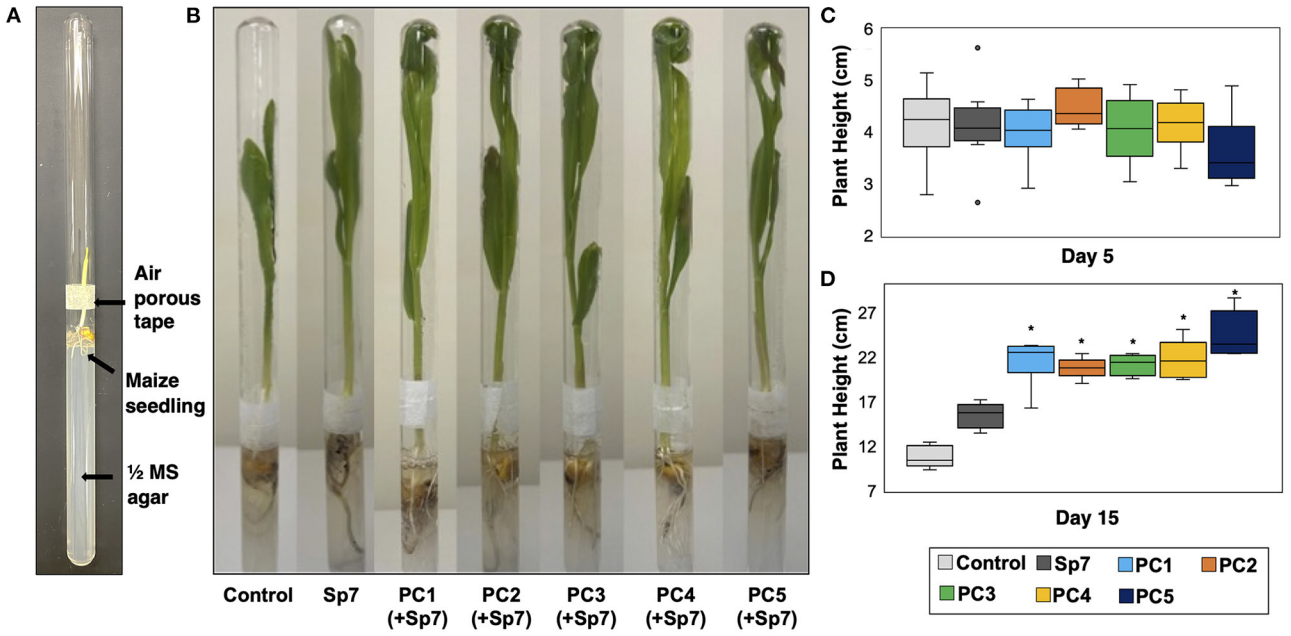

FIGURE 5
Growth of axenic maize seedlings in a growth chamber environment. **(A)** A double-tube growth chamber was used for accomodating surface-sterilized and germinated maize seedlings after inoculation with an ultrapure water blank (control), Sp7, or Sp7 with a promoter consortium (PC1-PC5). Two test tubes were attached in a mouth-to-mouth fashion with air-porous tape. **(B)** Growth of the maize seedlings in the double-tube growth chamber at day 15. **(C)** Comparison of plant heights for each treatment at day 5 and **(D)** at day 15 (*Wilcoxon Rank test: p-value < 0.01). $n = 6$ replicate trials.

to uninoculated seedlings (Figure 6). This demonstrated that the promoter consortia (PC1–PC5) must be combined with Sp7 to provide improvement in plant growth.

3.5. Promoter consortia increase *A. brasilense* population size on maize roots

Given the *A. brasilense* Sp7 growth promotion observed in MRA and 96-well plate co-cultures, combined with improved maize growth outcomes with seedling co-inoculations, we hypothesized that the promoter consortia enhanced plant growth by increasing Sp7 population sizes on root hosts during the plant growth studies. To test this hypothesis, we measured Sp7 abundances on the maize roots used in the plant growth studies by plating on antibiotic-supplemented R2A agar. As a control to verify that only Sp7 would be recovered from these plating experiments, the five consortia (PC1-PC5) were also plated on R2A agar plates supplemented with the Sp7 resistant antibiotics. No cell colonies were observed here (Supplementary Figure 4), verifying that the colonies observed in the plating experiment were Sp7. Quantification of Sp7 abundance from each sample revealed that three of the consortia (PC2, PC3, and PC5) generated the most significant increases in Sp7 root colonization levels ($p < 0.01$), while the other two (PC1, PC4) still generated significantly elevated levels of Sp7 ($p < 0.05$) relative to seedlings inoculated with Sp7 only (Figure 7). The differences in quantified Sp7 abundance levels between the different promoting consortia were mostly likely due to the differences in the consortia composition noted previously (Figure 3B). However, all formulations resulted in elevated Sp7 root colonization to some degree and all led to improved and equivalent plant growth after 15 days (Figure 5D).

4. Discussion

Taken together, the findings show that by using promoting consortia to elevate the level of Sp7 population on the root host, the growth of maize could be accelerated. This suggests that the approach of pairing a well-known PGPB, such as Sp7, with collections of rhizosphere isolates that have positive interactions with the PGPB could be a viable strategy for advancing the formulation of next-generation, consortia-based biofertilizers for improved food production. These findings support a growing body of literature suggesting that applying PGPB as complementary, multi-species consortia instead of single-strain inoculations can improve crop health and development (Backer et al., 2018; Trivedi et al., 2020).

While the much of effort in developing PGPB formulations has focused on identifying and using complementary pair-wise interactions, a key advantage of the MRA platform is the capability to assemble cells at a consortium level and screen multi-membered interactions. By using small wells (10 μm diameter) that only partition a low number of cells, random consortia are generated across the array space, where cells are confined together at a length scale that facilitates intercellular interactions. While small wells are critical to platform design, this feature also presents challenges related to removal of consortia from the wells. Although

10.3389/fsufs.2023.1106528

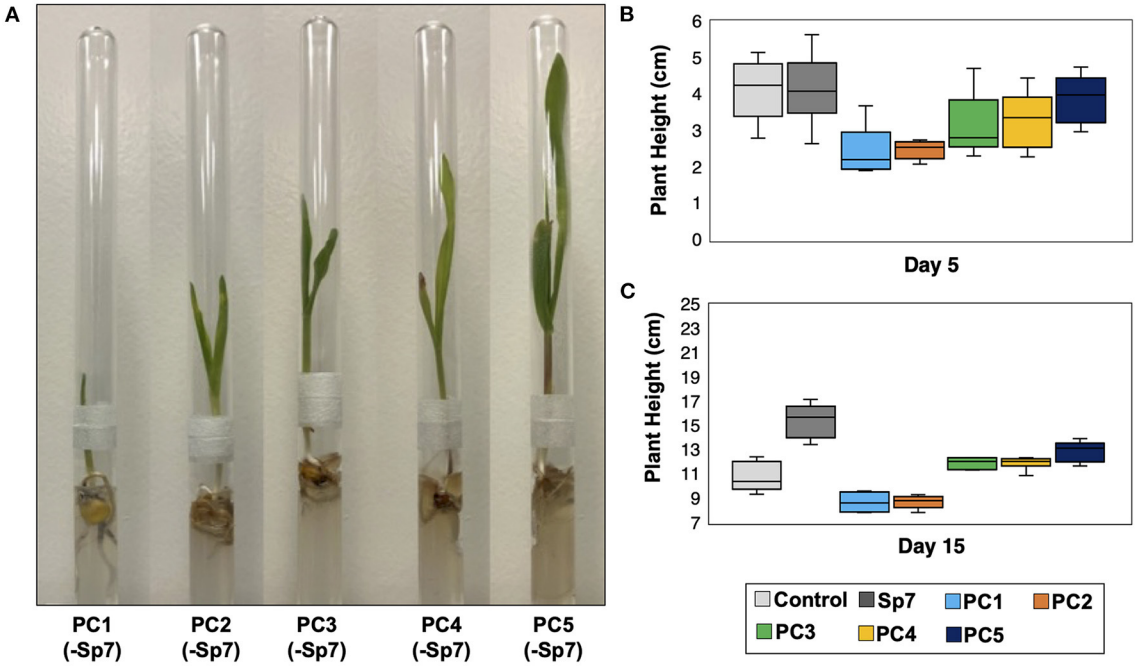

FIGURE 6
Growth of axenic maize seedlings after innoculation with each promoter consortium (PC1-PC5) but without Sp7. **(A)** Plant growth in growth chambers after 15 days. Comparision of plant heights for each consortium at **(B)** day 5 and **(C)** day 15 with sterile seedlings (control) and with seedlings inoculated with Sp7 only. $n = 6$ replicate trials.

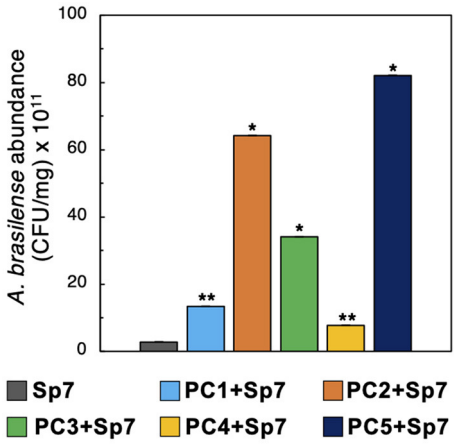

FIGURE 7
Sp7 abundance in maize roots. Sp7 abundance (CFU/mg root) on maize roots inoculated with Sp7 only or co-inoculated with Sp7 and promoter consortia (PC1-PC5). (*Wilcoxon Rank test: p-value $<$ 0.01; **Wilcoxon Rank test: p-value < 0.05). $n = 3$ replicate trials.

an optimized, light-based extraction system is used (van der Vlies et al., 2019), cellular recovery from wells may still be incomplete, which may result in a recovered composition that is modified from the well composition. Likewise, culture-based recovery steps after extraction could shift community compositions from what it was in the promoter well. However, these drawbacks are mitigated by performing 96-well plate co-culturing validation assays that evaluate weather interactions present on the chip recapitulate *in vitro*. This is a critical step in this workflow. If the interaction can be successfully recapitulated, as done here, one can proceed with using the promoting consortium in plant growth studies.

Finally, it should be noted that the platform is reliant on co-culture during the screening and recovery steps, and is therefore only able to screen and recover consortia that consist of bacteria that are culturable in the selected media. This underscores the need to carefully select the media most appropriate to the specific screen. For example, depending on the specific goals of the study, it may be desirable to target the screen toward a specific group of bacteria (e.g., *Rhizobium*), in which case it would be appropriate to select a media that supports the growth of a wide range of isolates of that group. The approach taken here was to consider common culture media and select the one that recovered the highest diversity of bacteria. While this inevitably introduces bias that limits the interactions that can be found and the composition of consortia that can be recovered, from an application standpoint, culturability is a pre-requisite for generating enough inoculant biomass for seed coating. For improvement, one may consider performing the co-cultures in the presence of root exudates, which may contain natural growth factors that fit the metabolic requirements of more diverse collections of isolates.

5. Conclusions

Poor survival and colonization of PGPB after single strain inoculations highlight the need to exploit microbe-microbe interactions to improve the growth, survival, and function of

beneficial microbes in the rhizosphere. Here, we use a new technology platform for high-throughput screening of multispecies consortia that included *A. brasilense*, a well-known diazotrophic PGPB, and thousands of combinations of maize rhizobiome isolates taken from the field. Utilizing the unique capability of the platform to screen microbial interactions at a consortium level, consortia consisting of bacteria primarily of the *Acinetobacter*, *Enterobacter*, and *Serratia* genera that promoted the growth of *A. brasilense* were uncovered from the maize rhizosphere. Furthermore, for the first time, we demonstrated that interactions initially observed in the screening platform can also be observed in the context of root hosts, and that application of these MRA-assembled consortia can be used to elicit improved plant development. By coupling a well-known PGPB with bacteria native to roots that were observationally found to promote its growth and colonization, we present a new bioprospecting approach to discover multispecies consortia that have potential application as next-generation biofertilizers for food production. Future studies involve investigating the effect of these consortia on maize growth in more complex, soil-based systems in larger scale greenhouse studies and expanding the MRA platform capabilities to screening consortia that include fungi, which may further enhance plant responses. Moreover, the workflow developed here—consisting of field sampling, media selection, MRA screening, cross validation, and application—lays a foundation for future bioprospecting endeavors aimed at developing formulations of plant-associated microbes that can improve seedling vigor, crop yield, and tolerance to drought, salinity, and heat stress.

Data availability statement

The datasets presented in this study can be found in online repositories. The names of the repository/repositories and accession number(s) can be found in the article/Supplementary material.

Author contributions

NB, KC, MW, TP, and RH conceived and designed experiments. NB and KC performed experiments. MW and DR developed or contributed analysis tools, samples, reagents, and materials. NB, TP, and RH wrote the paper. All authors contributed to the article and approved the submitted version.

Funding

We acknowledge support from the Global Food Systems Seed Program at Kansas State University and from the National Science Foundation Award 1828571. KC and MW were supported by the National Science Foundation under Award No. IOS-2033621 to MW as well as No. OIA-1656006 to Kristin Bowman-James and matching support from the State of Kansas through the Kansas Board of Regents.

Acknowledgments

We thank Gladys Alexandre and Elena Ganusova (Biochemistry and Cellular and Molecular Biology, University of Tennessee Knoxville) for kindly providing *A. brasilense* Sp7-GFP strains. We also acknowledge the Nebraska Nanoscale Facility at the University of Nebraska Lincoln for assistance in microwell fabrication. A portion of this manuscript has been included in a Ph.D. dissertation that is available online at the Kansas State Research Exchange (K-REx) repository (Barua, 2021).

Conflict of interest

RH and TP currently have a U.S. patent on this technology (Hansen et al., 2022).

The remaining authors declare that the research was conducted in the absence of any commercial or financial relationships that could be construed as a potential conflict of interest.

Publisher's note

All claims expressed in this article are solely those of the authors and do not necessarily represent those of their affiliated organizations, or those of the publisher, the editors and the reviewers. Any product that may be evaluated in this article, or claim that may be made by its manufacturer, is not guaranteed or endorsed by the publisher.

Supplementary material

The Supplementary Material for this article can be found online at: https://www.frontiersin.org/articles/10.3389/fsufs.2023.1106528/full#supplementary-material

References

Aasfar, A., Bargaz, A., Yaakoubi, K., Hilali, A., Bennis, I., Zeroual, Y., et al. (2021). Nitrogen fixing azotobacter species as potential soil biological enhancers for crop nutrition and yield stability. *Front. Microbiol.* 12, 8739. doi: 10.3389/fmicb.2021.628379

Aloo, B. N., Mbega, E. R., Makumba, B. A., Hertel, R., and Daniel, R. (2021). Molecular identification and *in vitro* plant growth-promoting activities of culturable potato (*Solanum tuberosum* L.) Rhizobacteria in Tanzania. *Potato Res.* 64, 67–95. doi: 10.1007/s11540-020-09465-x

Alzate Zuluaga, M. Y., Miras-Moreno, B., Monterisi, S., Rouphael, Y., Colla, G., Lucini, L., et al. (2022). Integrated metabolomics and morpho-biochemical analyses reveal a better performance of azospirillum brasilense over plant-derived biostimulants in counteracting salt stress in tomato. *Int. J. Mol. Sci.* 23, 14216. doi: 10.3390/ijms232214216

Apprill, A., McNally, S. P., Parsons, R. J., and Weber, L. (2015). Minor revision to V4 region SSU rRNA 806R gene primer greatly increases detection of SAR11 bacterioplankton. *Aquatic Microb. Ecol.* 75, 129–137. doi: 10.3354/ame01753

Backer, R., Rokem, J. S., Ilangumaran, G., Lamont, J., Praslickova, D., Ricci, E., et al. (2018). Plant growth-promoting rhizobacteria: context, mechanisms of action,

and roadmap to commercialization of biostimulants for sustainable agriculture. *Front. Plant Sci*. 9, 1473. doi: 10.3389/fpls.2018.01473

Bargaz, A., Elhaissoufi, W., Khourchi, S., Benmrid, B., Borden, K. A., Rchiad, Z., et al. (2021). Benefits of phosphate solubilizing bacteria on belowground crop performance for improved crop acquisition of phosphorus. *Microbiol. Res*. 252, 110. doi: 10.16./j.micres.2021.126842

Barua, N. (2021). *Screening and Discovery of Symbiotic and Antagonistic Microbial Networks Using Microwell Recovery Arrays*. PhD dissertation, Chemical Engineering, Kansas State University.

Barua, N., Herken, A. M., Stern, K. R., Reese, S., Powers, R. L., Morrell-Falvey, J. L., et al. (2021). Simultaneous discovery of positive and negative interactions among rhizosphere bacteria using microwell recovery arrays. *Front. Microbiol*. 11, 6010. doi: 10.3389/fmicb.2020.601788

Bashan, Y. de-Bashan, L.E., Prabhu, S.R., and Hernandez, J. P. (2014). Advances in plant growth-promoting bacterial inoculant technology: formulations and practical perspectives (1998–2013). *Plant Soil* 378, 1–33. doi: 10.1007/s11104-013-1956-x

Bhat, B. A., Tariq, L., Nissar, S., Islam, S. T., Islam, S. U., Mangral, Z., et al. (2022). The role of plant-associated rhizobacteria in plant growth, biocontrol and abiotic stress management. *J. Appl. Microbiol*. 133, 2717–2810. doi: 10.1111/jam.15796

Callahan, B. J., McMurdie, P. J., Rosen, M. J., Han, A. W., Johnson, A. J. A., Holmes, S. P., et al. (2016). DADA2: high-resolution sample inference from illumina amplicon data. *Nat. Methods* 13, 581–583. doi: 10.1038/nmeth.3869

Caporaso, J. G., Lauber, C. L., Walters, W. A., Berg-Lyons, D., Lozupone, C. A., Turnbaugh, P. J., et al. (2011). Global patterns of 16S rRNA diversity at a depth of millions of sequences per sample. *Proceed. Nat. Acad. Sci.* 108(supplement_1), 4516–4522. doi: 10.1073/pnas.1000080107

Chaudhary, P., Singh, S., Chaudhary, A., Sharma, A., and Kumar, G. (2022). Overview of biofertilizers in crop production and stress management for sustainable agriculture. *Front. Plant Sci*. 13, 340. doi: 10.3389/fpls.2022.930340

Dent, D., and Cocking, E. (2017). Establishing symbiotic nitrogen fixation in cereals and other non-legume crops: the greener nitrogen revolution. *Agricult. Food Sec*. 6, 7. doi: 10.1186/s40066-016-0084-2

Dodds, W. K., Zeglin, L. H., Ramos, R. J., Platt, T. G., Pandey, A., Michaels, T., et al. (2020). Connections and feedback: aquatic, plant, and soil microbiomes in heterogeneous and changing environments. *BioScience* 70, 548–562. doi: 10.1093/biosci/biaa046

dos Santos Lima Fagotti, D., Abrantes, J. L. F., Cerezini, P., Fukami, J., Nogueira, M. A. del Cerro, P., et al. (2019). Quorum sensing communication: bradyrhizobium-Azospirillum interaction via N-acyl-homoserine lactones in the promotion of soybean symbiosis. *J. Basic Microb*. 59, 38–53. doi: 10.1002/jobm.201800324

Egamberdieva, D., Wirth, S. J., and Alqarawi, A. A. Abd_Allah, E.F., and Hashem, A. (2017). Phytohormones and beneficial microbes: essential components for plants to balance stress and fitness. *Front. Microbiol*. 8, 2104. doi: 10.3389/fmicb.2017.02104

Farooq, M. S., Uzair, M., Raza, A., Habib, M., Xu, Y., Yousuf, M., et al. (2022). Uncovering the research gaps to alleviate the negative impacts of climate change on food security: a review. *Front. Plant Sci*. 13, 7535. doi: 10.3389/fpls.2022.927535

Fattahi, N., Barua, N., van der Vlies, A. J., and Hansen, R. R. (2021). Photodegradable hydrogel interfaces for bacteria screening, selection, and isolation. *JoVE* 177, e63048. doi: 10.3791/63048

Fattahi, N., Nieves-Otero, P. A., Masigol, M., van der Vlies, A. J., Jensen, R. S., Hansen, R. R., et al. (2020). Photodegradable hydrogels for rapid screening, isolation, and genetic characterization of bacteria with rare phenotypes. *Biomacromolecules* 21, 3140–3151. doi: 10.1021/acs.biomac.0c00543

Ferreira, A. S., Pires, R. R., Rabelo, P. G., Oliveira, R. C., Luz, J. M. Q., Brito, C. H., et al. (2013). Implications of Azospirillum brasilense inoculation and nutrient addition on maize in soils of the Brazilian Cerrado under greenhouse and field conditions. *Appl. Soil Ecol*. 72, 103–108. doi: 10.1016/j.apsoil.2013.05.020

Ferreira, C. M. H., Soares, H. M. V. M., and Soares, E. V. (2019). Promising bacterial genera for agricultural practices: an insight on plant growth-promoting properties and microbial safety aspects. *Sci. Total Environ*. 682, 779–799. doi: 10.1016/j.scitotenv.2019.04.225

Gowtham, H. G., Singh, S. B., Shilpa, N., Aiyaz, M., Nataraj, K., Udayashankar, A. C., et al. (2022). Insight into recent progress and perspectives in improvement of antioxidant machinery upon PGPR augmentation in plants under drought stress: a review. *Antioxidants* 11, 1763. doi: 10.3390/antiox11091763

Halsted, M., Wilmoth, J. L., Briggs, P. A., Hansen, R. R., Briggs, D. P., Timm, A. C., et al. (2016). Development of transparent microwell arrays for optical monitoring and dissection of microbial communities. *J. Vac. Sci. Technol. B* 34, 06KI03. doi: 10.1116/1.4962739

Hansen, R. R., Anderson, A. C., Barua, N., and McGinley, L. M. (2021). Using ongoing laboratory problems as active learning research projects in transport phenomena. *Chem. Engin. Edu*. 55, 51–60. doi: 10.18260/2-1-370.660-120873

Hansen, R. R., Platt, T. G., and van der Vlies, A. J. (2022). *Hydrogel Membrane and Methods for Selective Retrieval of Microbial Targets*. USA Patent 11, 235.330B2.

Hansen, R. R., Timm, A. C., Timm, C. M., Bible, A. N., Morrell-Falvey, J. L., Pelletier, D. A., et al. (2016). Stochastic assembly of bacteria in microwell arrays reveals the importance of confinement in community development. *PLoS ONE* 11, e0155080. doi: 10.1371/journal.pone.0155080

Hungria, M., Campo, R. J., Souza, E. M., and Pedrosa, F. O. (2010). Inoculation with selected strains of *Azospirillum* brasilense and *A. lipoferum* improves yields of maize and wheat in Brazil. *Plant Soil* 331, 413–425. doi: 10.1007/s11104-009-0262-0

Ikeda, A. C., Savi, D. C., Hungria, M., Kava, V., Glienke, C., Galli-Terasawa, L. V., et al. (2020). Bioprospecting of elite plant growth-promoting bacteria for the maize crop. *Acta Scientiarum. Agronomy* 42, 364. doi: 10.4025/actasciagron.v42i1.44364

Jochum, M. D., McWilliams, K. L., Borrego, E. J., Kolomiets, M. V., Niu, G., Pierson, E. A., et al. (2019). Bioprospecting plant growth-promoting rhizobacteria that mitigate drought stress in grasses. *Front. Microbiol*. 10, 2106. doi: 10.3389/fmicb.2019.02106

Khan, A. R., Park, G. S., Asaf, S., Hong, S. J., Jung, B. K., Shin, J. H., et al. (2017). Complete genome analysis of Serratia marcescens RSC-14: a plant growth-promoting bacterium that alleviates cadmium stress in host plants. *PLoS ONE* 12, e01710. doi: 10.1371/journal.pone.0171534

Komarek, A. M., and Msangi, S. (2019). Effect of changes in population density and crop productivity on farm households in Malawi. *Agricult. Econ*. 50, 615–628. doi: 10.1111/agec.12513

Lee, S. A., Kim, J. M., Kim, Y., Joa, J-. H., Kang, S-. S., Ahn, J-. H., et al. (2020). Different types of agricultural land use drive distinct soil bacterial communities. *Sci Rep-Uk* 10, 8. doi: 10.1038/s41598-020-74193-8

Leisner, C. P., Potnis, N., and Sanz-Saez, A. (2022). Crosstalk and trade-offs: plant responses to climate change-associated abiotic and biotic stresses. *Plant Cell Environ*. 4, 1. doi: 10.22541/au.166462027.71310652/v1

Ma, Y., Vosátka, M., and Freitas, H. (2019). Editorial: beneficial microbes alleviate climatic stresses in plants. *Front. Plant Sci*. 10, 595. doi: 10.3389/fpls.2019.00595

Machado, G. P., Colli Mull, P. M. G. JG, Aguero Chapin, G, Riva de la Riva, GA, de la Vargas Samano, C. D. (2017). Plant growth promoting bacteria isolated from a mexican natural ecosystem induce water stress resistance in maize and sorghum plants. *J. Microb. Biochem. Technol*. 9, 209–219. doi: 10.4172/1948-5948.1000367

Maranguit, D., Guillaume, T., and Kuzyakov, Y. (2017). Land-use change affects phosphorus fractions in highly weathered tropical soils. CATENA 149, 385-393. doi: 10.1016/j.catena.2016.10.010

Martin, M. (2011). Cutadapt removes adapter sequences from high-throughput sequencing reads. *EMBnet J*. 17, 3. doi: 10.14806/ej.17.1.200

Masigol, M., Barua, N., Lokitz, B. S., and Hansen, R. R. (2018). Fabricating reactive surfaces with brush-like and crosslinked films of azlactone-functionalized block co-polymers. *Jove-J Vis Exp, ARTN* 5, *e*57562. doi: 10.3791/57562

Masigol, M., Barua, N., Retterer, S. T., Lokitz, B. S., and Hansen, R. R. (2017). Chemical copatterning strategies using azlactone-based block copolymers. *J. Vac. Sci. Technol. B* 35, Artn 06gj01. doi: 10.1116/1.4991881

Matteoli, F. P., Passarelli-Araujo, H., Reis, R. J. A., Rocha, da., de Souza, L. O., Aravind, E. M., et al. (2018). Genome sequencing and assessment of plant growth-promoting properties of a Serratia marcescens strain isolated from vermicompost. *BMC Genom*. 19, 750. doi: 10.1186/s12864-018-5130-y

McMurdie, P. J., and Holmes, S. (2013). phyloseq: an R package for reproducible interactive analysis and graphics of microbiome census data. *PLoS ONE* 8, e610. doi: 10.1371/journal.pone.0061217

Mitter, E. K., Tosi, M., Obregón, D., Dunfield, K. E., and Germida, J. J. (2021). Rethinking crop nutrition in times of modern microbiology: innovative biofertilizer technologies. *Front. Sustain. Food Sys*. 5. doi: 10.3389/fsufs.2021.606815

Nakkeeran, S., Fernando, W. G. D., and Siddiqui, Z. A. (2006). "Plant growth promoting rhizobacteria formulations and its scope in commercialization for the management of pests and diseases," in *PGPR: Biocontrol and Biofertilization*, Z.A. Siddiqui, ed. (Springer Netherlands), pp. 257-296. doi: 10.1007/1-4020-4152-7_10

Niu, B., and Kolter, R. (2018). Quantification of the composition dynamics of a maize root-associated simplified bacterial community and evaluation of its biological control effect. *Bio. Protoc*. 8, 2885. doi: 10.21769/BioProtoc.2885

Oliveira, I. J., Fontes, J. R. A., Pereira, B. F. F., and Muniz, A. W. (2018). Inoculation with Azospirillum brasiliense increases maize yield. *Chem. Biol. Technol. Agricult*. 5, 6. doi: 10.1186/s40538-018-0118-z

Parada, A. E., Needham, D. M., and Fuhrman, J. A. (2016). Every base matters: assessing small subunit rRNA primers for marine microbiomes with mock communities, time series and global field samples. *Environ. Microbiol*. 18, 1403-10. doi: 10.1111/1462-2920.13023

Pedrosa, F. O., Oliveira, A. L. M., Guimarães, V. F., Etto, R. M., Souza, E. M., Furmam, F. G., et al. (2020). The ammonium excreting Azospirillum brasilense strain HM053: a new alternative inoculant for maize. *Plant Soil* 451, 45–56. doi: 10.1007/s11104-019-04124-8

Philippot, L., Raaijmakers, J. M., Lemanceau, P., and van der Putten, W. H. (2013). Going back to the roots: the microbial ecology of the rhizosphere. *Nat. Rev. Microbiol.* 11, 789–799. 10.1038/nrmicro3109. doi: 10.1038/nrmicro3109

Sprouffske, K., and Wagner, A. (2016). Growthcurver: an R package for obtaining interpretable metrics from microbial growth curves. *BMC Bioinform.* 17, 172. doi: 10.1186/s12859-016-1016-7

Stamenković, S., Beškoski, V., Karabegović, I., Lazić, M., and Nikolić, N. (2018). Microbial fertilizers: a comprehensive review of current findings and future perspectives. *Span. J. Agric. Res.* 16, e09R.01. doi: 10.5424/sjar/2018161-12117

Tabassum, B., Khan, A., Tariq, M., Ramzan, M., Iqbal Khan, M. S., Shahid, N., et al. (2017). Bottlenecks in commercialisation and future prospects of PGPR. *Appl. Soil Ecol.* 121, 102–117. doi: 10.1016/j.apsoil.2017.09.030

Tang, A., Haruna, A. O., Majid, N. M. A., and Jalloh, M. B. (2020). Effects of selected functional bacteria on maize growth and nutrient use efficiency. *Microorganisms* 8, 854. doi: 10.3390/microorganisms8060854

Timm, A. C., Halsted, M. C., Wilmoth, J. L., and Retterer, S. T. (2017). Assembly and tracking of microbial community development within a microwell array platform. *J. Vis. Exp.* 124, 55701. doi: 10.3791/55701

Timofeeva, A. M., Galyamova, M. R., and Sedykh, S. E. (2022). Bacterial siderophores: classification, biosynthesis, perspectives of use in agriculture. *Plants* 11, 3065. doi: 10.3390/plants11223065

Trivedi, P., Leach, J. E., Tringe, S. G., Sa, T., and Singh, B. K. (2020). Plant–microbiome interactions: from community assembly to plant health. *Nat. Rev. Microbiol.* 18, 607–621. doi: 10.1038/s41579-020-0412-1

van der Vlies, A. J., Barua, N., Nieves-Otero, P. A., Platt, T. G., and Hansen, R. R. (2019). On demand release and retrieval of bacteria from microwell arrays using photodegradable hydrogel membranes. *Acs. Appl. Bio. Mater.* 2, 266–276. doi: 10.1021/acsabm.8b00592

Van Deynze, A., Zamora, P., Delaux, P-. M., Heitmann, C., Jayaraman, D., Rajasekar, S., et al. (2018). Nitrogen fixation in a landrace of maize is supported by a mucilage-associated diazotrophic microbiota. *PLOS Biol.* 16, e2006352.. doi: 10.1371/journal.pbio.2006352

Verma, R., Chourasia, S. K., and Jha, M. N. (2011). Population dynamics and identification of efficient strains of *Azospirillum* in maize ecosystems of Bihar (India). *3 Biotech* 1, 247–253. doi: 10.1007/s13205-011-0031-7

Viejobueno, J., Albornoz, P. L., and Camacho, M. de los Santos, B., Martínez-Zamora, M.G., and Salazar, S.M. (2021). Protection of strawberry plants against charcoal rot disease (*Macrophomina phaseolina*) induced by *Azospirillum* brasilense. *Agronomy* 11, 195. doi: 10.3390/agronomy11020195

Wang, J., Li, Q., Xu, S., Zhao, W., Lei, Y., Song, C., et al. (2018). Traits-based integration of multi-species inoculants facilitates shifts of indigenous soil bacterial community. *Front. Microbiol.* 9, 1692. doi: 10.3389/fmicb.2018.01692

Wang, Q., Garrity, G. M., Tiedje, J. M., and Cole, J. R. (2007). Naïve bayesian classifier for rapid assignment of rRNA sequences into the new bacterial taxonomy. *Appl. Environ. Microbiol.* 73, 5261–5267. doi: 10.1128/AEM.00062-07

Wickham, H., Averick, M., Bryan, J., Chang, W., D'Agostino McGowan, L., Francois, R., et al. (2019). Welcome to the tidyverse. J. *Open Source Software* 4, 1686. doi: 10.21105/joss.01686

Zhu, L., Huang, J., Lu, X., and Zhou, C. (2022). Development of plant systemic resistance by beneficial rhizobacteria: Recognition, initiation, elicitation and regulation. *Front. Plant Sci.* 13, 2397. doi: 10.3389/fpls.2022.952397

frontiers | Frontiers in Sustainable Food Systems

TYPE Original Research
PUBLISHED 25 August 2023
DOI 10.3389/fsufs.2023.1252324

Check for updates

OPEN ACCESS

EDITED BY
Marouane Baslam,
Niigata University, Japan

REVIEWED BY
Jiban Shrestha,
Nepal Agricultural Research Council, Nepal
Takuji Ohyama,
Tokyo University of Agriculture, Japan
Tian Xiaofei,
Liaocheng University, China

*CORRESPONDENCE
Jun Hou
houjungoodluck1@163.com
Xuexia Wang
wxx0427@163.com

RECEIVED 03 July 2023
ACCEPTED 26 July 2023
PUBLISHED 25 August 2023

CITATION
Hu R, Xiao D, Ding Z, Cao Y, Hou J and Wang X (2023) Effects of local nitrogen supply and nitrogen fertilizer variety coupling on rice nitrogen transport and soil nitrogen balance in paddy fields.
Front. Sustain. Food Syst. 7:1252324.
doi: 10.3389/fsufs.2023.1252324

COPYRIGHT
© 2023 Hu, Xiao, Ding, Cao, Hou and Wang. This is an open-access article distributed under the terms of the Creative Commons Attribution License (CC BY). The use, distribution or reproduction in other forums is permitted, provided the original author(s) and the copyright owner(s) are credited and that the original publication in this journal is cited, in accordance with accepted academic practice. No use, distribution or reproduction is permitted which does not comply with these terms.

Effects of local nitrogen supply and nitrogen fertilizer variety coupling on rice nitrogen transport and soil nitrogen balance in paddy fields

Ren Hu[1], Dakang Xiao[1], Zijuan Ding[1], Yuxian Cao[2], Jun Hou[1]* and Xuexia Wang[3]*

[1]College of Agriculture, Yangtze University, MARA Key Laboratory of Sustainable Crop Production in the Middle Reaches of the Yangtze River (Co-construction by Ministry and Province), Jingzhou, China, [2]College of Life Science, Yangtze University, Jingzhou, China, [3]Institute of Plant Nutrition, Resources and Environment, Beijing Agricultural Forestry Academy Sciences, Beijing, China

Introduction: This study aimed to provide the theoretical basis for formulating scientific and reasonable on-farm nitrogen (N) management measures and efficient strategic fertilization to understand the effects of localized N supply (LNS) and N fertilizer variety coupling on N transport and soil N balance in rice fields.

Methods: A 2-year field experiment (2020 and 2021) was conducted in Jingzhou, Hubei Province, which included the following six treatments: no N application (CK), farmers' fertilizer practice (FFP), and four LNS treatments, including two N application methods including mechanical side-deep fertilization (M) and root-zone fertilization (R), two N fertilizer types with urea (U), and controlled-release urea (CRU).

Results: Compared with FFP, LNS increased the N apparent translocation level from stems, sheathes, and leaves (TNT) and N uptake by 10.70–50.59% and 11.28–29.71%, respectively. In LNS, the levels of nitrite reductase (NR), glutamine synthetase (GS), and glutamate synthase (GOGAT) under R increased by 13.81, 9.56, and 15.59%, respectively, compared with those under M, resulting in a significant increase in TNT by 8.58% and N uptake by 1.87%. Regarding the N fertilizer type, CRU significantly increased chlorophyll content by 7.27%, superoxide dismutase (SOD) and catalase (CAT) by 14.78 and 29.95% ($p < 0.05$), and NR, GS, and GOGAT by 44.41, 16.12, and 28.41% ($p < 0.05$), respectively, compared with that in U, which contributed to N absorption and transport. Moreover, CRUR significantly decreased N apparent loss by 50.04% compared with CRUM ($p < 0.05$).

Discussion: Considering the risk of soil N leaching and environmental protection, R should be selected as the recommended fertilization method. The combination of CRU and R is the most effective fertilization approach.

KEYWORDS

controlled-release urea, mechanical side deep fertilization, rice, root zone fertilization, nitrogen balance

1. Introduction

Rice is the number one food crop in China, with production reaching 146.10 million tons in 2022 and making China the top rice producer worldwide (Food Agriculture Organization of the United Nations, 2022). This record rice production in China is because of the massive application of nitrogen (N) fertilizers (Grafton et al., 2015). Relevant studies showed that

unreasonable N application methods and N fertilizer varieties reduced the efficiency of N fertilizers. Hence, a large amount of N fertilizers that were not absorbed by rice plants flowed into groundwater, significantly impacting the environment (Guo et al., 2017; Jiang et al., 2022). Therefore, improving N uptake and reducing N loss have become important in N fertilizer management.

Localized N supply (LNS) has been the most popular method of N application in recent years compared with the conventional broadcasting method. LNS effectively increases nutrient concentration in the rhizosphere, thereby promoting N absorption by the root system and reducing nutrient loss (Wu et al., 2022). LNS is mainly categorized into mechanical side deep fertilization (M) and root-zone fertilization (R). Zhu et al. (2019) reported that M promoted N uptake in rice by increasing soil ammonium–N concentration and further reducing N loss. Jiang et al. (2017) showed through a field micro-plot experiment that the vertical migration distance of fertilizer-released N under the M was 3–18 cm, while the vertical migration distance under R was 6–15 cm in the soil layer, and the ammonium N content under R was 8.3 times higher than that under M. This indicates that R had a tendency to increase the inorganic N content of the soil and reduce the inorganic N loss. In addition, the higher nutrient concentration could provide sufficient N to seedlings after regreening, promote tillering, reduce ammonia volatilization by 26–93% (Liu et al., 2015; Wu M. et al., 2017), and also reduce N oxide emissions (Yao et al., 2017; Gaihre et al., 2018). Moreover, both M and R can provide a stable supply of available soil N, which may regulate the N-assimilation ability of plants by affecting the activity of N metabolism enzymes (Hu et al., 2023). Therefore, which of these two types of N application is more beneficial to improve N-assimilation enzymes and soil N balance also needs to be further explored.

Urea (U) and controlled-release urea (CRU) are two of the most studied N fertilizers in China that play a vital role in improving rice production (Ye et al., 2013). U, the instant fertilizer used globally, releases all the N rapidly within 20 days of application into the soil (Campos et al., 2018), resulting in insufficient N supply at a later stage and seriously affecting rice growth (i.e., dry matter accumulation and N transfer) (Li et al., 2018). CRU is a new type of highly efficient and environmentally friendly fertilizer. It slows down the release rate of fertilizer nutrients in the soil to achieve the synchronization of fertilizer nutrient release time and intensity with crop nutrient demand (Zhang et al., 2018), thus reducing the volatilization, leaching, and denitrification losses of fertilizer nutrients in the soil and achieving high rice yield and efficiency (Tian et al., 2021; Jiang et al., 2022). Moreover, rice scavenges excess reactive oxygen species by increasing the activity of antioxidant enzymes such as superoxide dismutase (SOD) and catalase (CAT), while malondialdehyde (MDA) is a product of lipid peroxidation of cell membranes that directly affects rice growth (Liao et al., 2019). However, research on N fertilizer varieties has mostly focused on rice yield and N utilization. The effects of antioxidant enzymes and MDA content on N uptake and N transfer in rice need further clarification.

In this study, 2 years of field experiments were conducted to investigate the effects of the combined application of LNS with different N fertilizer varieties (U and CRU) on N uptake and transport by different organs and N balance in paddy soil. The aims were as follows: (1) to study the mechanism of promoting N uptake and transport of rice by comparing the enzymatic characteristics and photosynthetic properties under different N application treatments; (2) to find out the most suitable N fertilizer treatment for the environment through comparing the N balance in paddy soil; and (3) to provide a theoretical basis for the realization of light and simplified fertilization of rice in China in the future.

2. Materials and methods

2.1. Study location

A 2-year field experiment was conducted in the Meteorological Bureau of Jingzhou City, Hubei Province, China, in 2020 and 2021. The study site was located in the Jianghan Plain (N 29° 26′-31° 37′, E 111° 14′-114° 36′), which is a humid subtropical monsoon climate zone suitable for rice cultivation (Zhou et al., 2022). The weather data were provided by the Jingzhou Weather Bureau in Hubei. In 2020/2021, the average temperature and total precipitation during the rice production season were 23.2/23.8°C and 2,130/1,385 mm, respectively (Figure 1). The region has been known for planting rice for years, and the soil is a silty medium loam developed from the deposition of inland and lacustrine sediments. The initial soil test results were as follows: pH, 7.9; soil bulk density, 1.4 g cm^{-3} in the 0–20 cm soil layer; organic carbon, 26.88 g kg^{-1}; total N, 1.09 g kg^{-1}; Olsen-P, 9.4 mg kg^{-1}; and available K, 56.3 mg kg^{-1}.

2.2. Study material

Yang LiangYou No. 6 was used as the test object in this study; the parental source of Yang LiangYou No. 6 is Guangzhan 63-4S (female) and Yangdao No. 6 (male), and the variety type is indica two-series hybrid rice. It is widely grown by local farmers in Jingzhou, Hubei Province. In this study, Yang LiangYou No. 6 was transplanted in late May and harvested in late September in 2020 and 2021. Two types of N fertilizers that were used included U (46% N) and CRU (43% N); CRU is polyolefin-coated urea, which has a static water 25°C parabolic curve release and a release period of 120 days (National Engineering Technology Research Center of Slow and Controlled Release Fertilizer, Linyi, China) (Figure 2).

2.3. Experimental treatments

The field plot experiment was conducted with six treatments: (i) CK: a control treatment without N fertilizer application; (ii) FFP: farmers' fertilizer practice, U was broadcasted manually three times, 50% as basal fertilizer, 30% as tillering fertilizer, and 20% as booting fertilizer; (iii) UM: U was mechanically applied to a band 5 cm away from the rice root system and 10 cm deep; (iv) UR: U was manually applied into a hole 5 cm away from the rice root system and 10 cm deep; (v) CRUM: CRU was mechanically applied to a

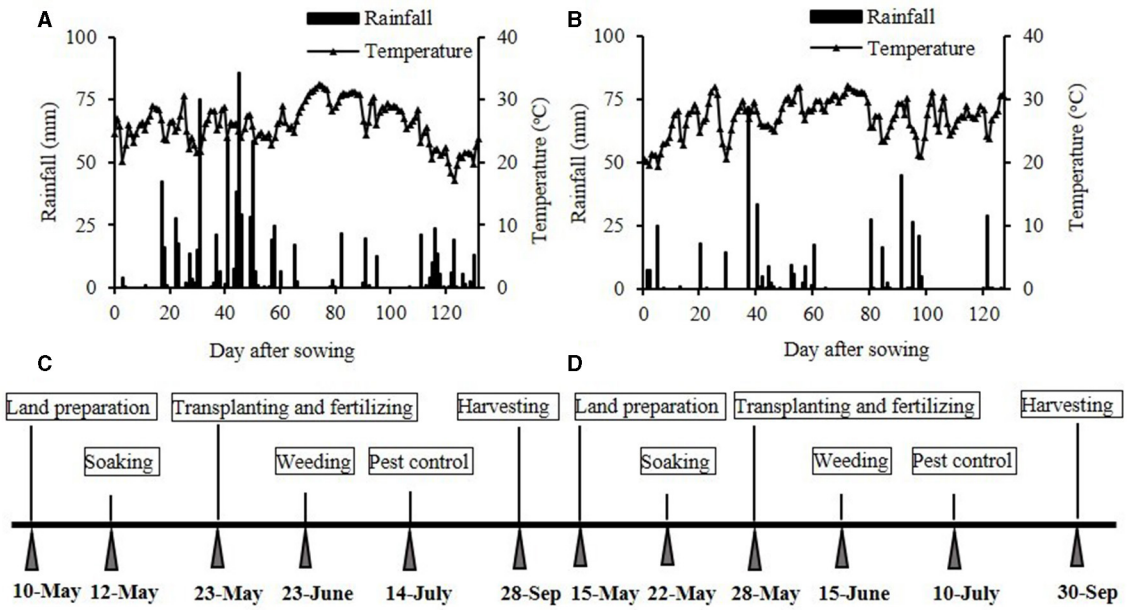

FIGURE 1
The rainfall and average temperatures in 2020 **(A)** and 2021 **(B)** and the rice management details in 2020 **(C)** and 2021 **(D)**.

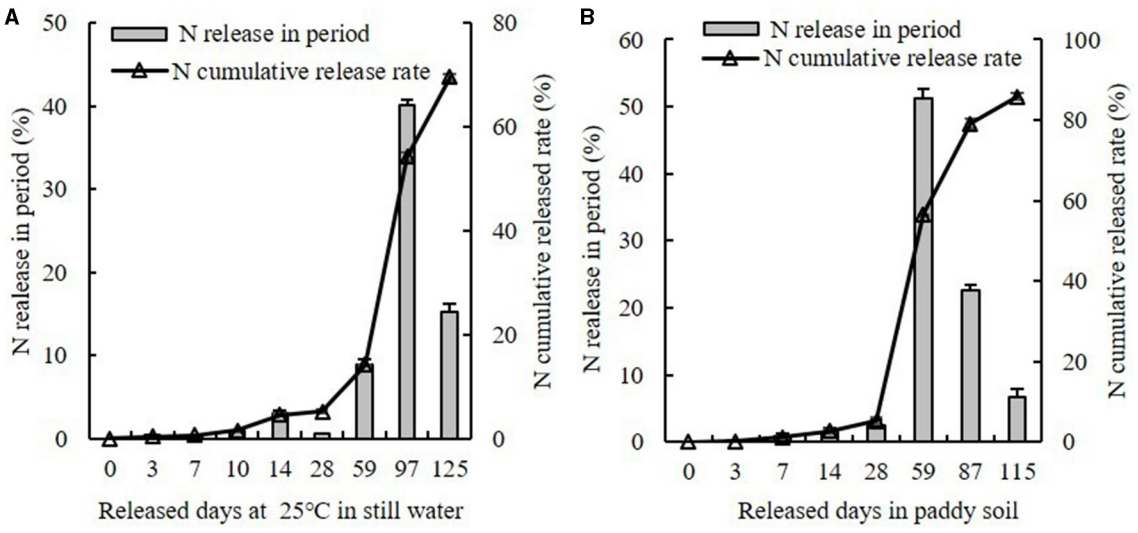

FIGURE 2
The N release in period and N accumulative release rate of CRU in still water **(A)** and paddy soil **(B)**.

band 5 cm away from the rice root system and 10 cm deep; and (vi) CRUR: CRU was manually applied into a hole 5 cm away from the rice root system and 10 cm deep. For LNS (UM, UR, CRUM, and CRUR) treatments, the U and CRU were point-deep-placed once as basal fertilizer after the rice had been transplanted (1.76 g U $hill^{-1}$ for UM and UR and 1.88 g CRU $hill^{-1}$ for CRUM and CRUR). A map of mechanical side deep fertilization (M) and root-zone fertilization (R) is shown in Figure 3. The field experiment was completely randomized with three replicates. The plot dimensions were 5 × 5 m, and each plot was separated by a 30-cm-wide earth bank covered with plastic film to prevent the lateral flow of water and nutrients.

Except for CK (no N fertilizer), all the treatments were administered at the following rates: 180 kg N ha^{-1}, 90 kg P_2O_5 ha^{-1}, and 120 kg K_2O ha^{-1}. The phosphate (12% P_2O_5; Hubei Sanning Chemical Co., Ltd., Hubei, China) and potassium fertilizers (60% K_2O; Sinofert Holdings Limited, Beijing, China) were applied once, following which a small amount of water was added to mix the field soil and fertilizer before transplanting. The transplanting density was 25 × 18 cm for each plot, with

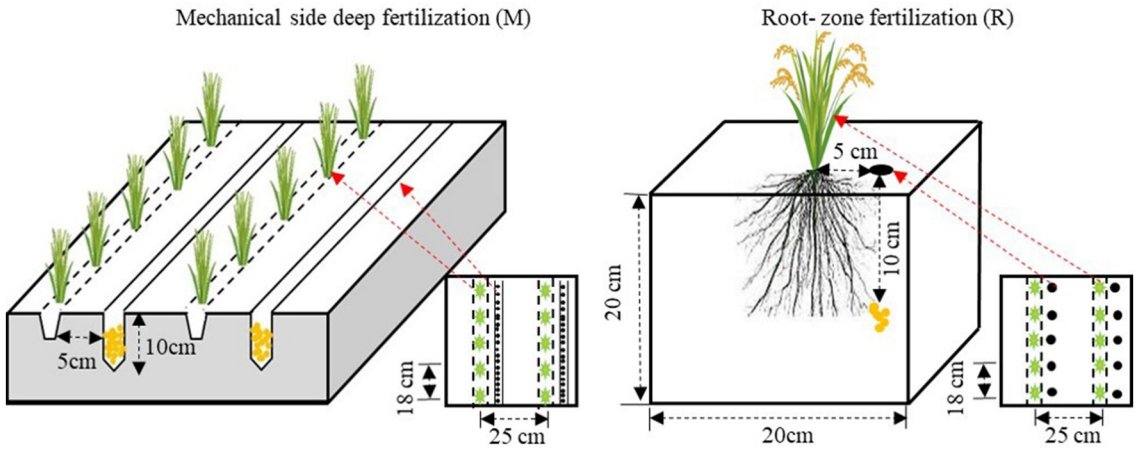

FIGURE 3
The sketch map of mechanical side deep fertilization (M) and root-zone fertilization (R).

three to five seedlings in each hole. All plots were irrigated approximately 1 week prior to transplanting, and the water layer was always maintained at a depth of 3–5 cm (except during the tillering stage and 1 week prior to harvest). The irrigation was coordinated with local precipitation events, and the same irrigation pattern was used in both 2020 and 2021. Herbicide weed control (glufosinate-ammonium) was applied before rice transplanting and at the tillering stage, and insecticide (emamectin benzoate) was sprayed at the booting stage. Glufosinate-ammonium and emamectin benzoate were both purchased at the local pesticide store and applied at the same time in both years.

2.3.1. Measurement of chlorophyll content

The value of soil plant analysis development (SPAD) was measured using a SPAD chlorophyll meter (SPAD 502, Minolta Camera Co., Osaka, Japan) from the six uppermost fully expanded leaves on each plot in the tillering, booting, and heading stages in 2020 and 2021. The chlorophyll content was calculated from the SPAD values using the method of Cao et al. (2001).

2.3.2. Measurement of photosynthetic traits

Three hills of rice were randomly selected in each plot, and five fully expanded flag leaves were selected on the main stem to measure the photosynthetic traits in the tillering and booting stages in 2021. The photosynthetic traits, including net photosynthesis rate (P_n), stomatal conductance (G_s), intercellular CO_2 concentration (C_i), and transpiration rate (T_r), were calculated using the portable Li-COR 6400 Photosynthesis System (LI-COR Inc., USA). The calculation time was from 10.00 a.m. to 12.30 p.m. under sunlit conditions (photosynthetically active radiation, 1,000 μmol m^{-2} s^{-1}; leaf chamber temperature, 30°C; and ambient CO_2 levels, 380 ppm).

2.3.3. Measurement of antioxidant enzymes and malondialdehyde content

Five rice plants were selected from each treatment in the tillering and booting stages, and the uppermost fully expanded leaves were preserved in liquid N for measuring SOD, CAT, and MDA content (Wu and Yang, 2016).

For measuring the SOD activity, fresh rice leaves (1 g), phosphate-buffered saline (PBS) (3 ml, 0.05 mol/L, pH = 7.8), and a small amount of quartz sand were ground into homogenate in an ice bath. The resulting homogenate was then transferred into a 5-ml centrifuge tube, fixed, and centrifuged at 10,000 rpm at 4°C for 15 min. The extracted supernatant was used as the enzyme solution. The enzyme solution was taken in a 10 ml centrifuge tube and immediately illuminated using a fluorescent tube at 4,000 Lx. The reaction was terminated by stopping the light and shading the light after 15 min. The control tube contained PBS and SOD solutions. The colorimetric wavelength was 560 nm.

For measuring the CAT activity, the rice leaves (0.2 g) and PBS (1 ml) were ground at low temperatures. Then, 5 ml of PBS was added, and the mixture was centrifuged at 10,000 rpm at 40°C for 15 min. The supernatant was the enzyme solution. To calculate the enzyme activity, 0.2 ml of the enzyme solution, 1.5 ml of PBS, and 1.5 ml of H_2O_2 were mixed, and colorimetric readings were taken immediately at 240 nm every 30 s for a total of 2 min.

For calculating the MDA content, 0.2 g of rice leaves were ground into a homogenate and transferred to a 10-ml centrifuge tube, and then the mortar was rinsed using 1 ml of 10% TCA solution. The mortar was then centrifuged at 4,000 rpm for 10 min, and the supernatant enzyme solution was obtained (Shahid et al., 2019).

2.3.4. N metabolism enzyme activity assay

The topmost leaves of rice plants were taken at the tillering and booting stages, stored in an ice box, transported, and frozen at −80°C to measure the activities of the N-metabolizing enzymes

nitrate reductase (NR), glutamine synthetase (GS), and glutamate synthase (GOGAT).

To measure NR activity, 0.5 g of rice leaves were added to the test tube with 9 ml of KNO_3, isopropanol, and PBS, and 1.0 ml of trichloroacetic acid was added to the control tube to mix evenly as a control. After draining the air in the tube, the straight leaves settled at the bottom, and the tube was placed in the dark at 3°C for 30 min. Then, 1.0 mmo1/L trichloroacetic acid was added and shaken. After allowing it to stand, 2 ml of the supernatant was extracted, and the control tube was used to determine the chromogenicity for enzyme activity (Wu S. W. et al., 2017).

The GS activity was measured using the method of Zhong et al. (2018). In this experiment, 5 g of rice leaves and 5 ml of the crude enzyme extract were taken and put in the ice bath to make a homogenate. The homogenate was centrifuged at 13,000 rpm at 4°C. The supernatant was the crude enzyme extract. Furthermore, 1 ml of the reaction solution, 0.5 ml of crude enzyme extract, and 0.5 ml of ATP solution were taken in the test tube, mixed well, and kept at 37°C for 30 min. Furthermore, 1 ml of the color developer was added to terminate the reaction, and the mixture was shaken well continuously and centrifuged at 4,000 rpm for 15 min. The supernatant was used to measure the absorbance value at 540 m, and the control solution with 1.0 was used as the control.

The GOGAT activity was determined based on the methods of Shahid et al. (2019). The crude enzyme extract was used for GS. The blank control (a mixture of glutamine, α-ketoglutarate, KCl, and Tris-HCl buffer) and the treatment tube (a mixture of α-ketoglutarate, KCl, and Tris-HCl buffer) were preheated in a constant-temperature water bath at 30°C for some time. Then, 0.2 ml of nicotinamide adenine dinucleotide (NADH), 0.3 ml of crude enzyme solution, and 0.4 ml of glutamine were added sequentially. The mixed GOGAT enzyme activity was defined as one unit of enzyme activity per minute of reaction solution reduction using l μmol NADH at 30°C.

2.3.5. Root sample collection and measurement

The roots were excavated whole from the plot soil using the holistic method during different growth periods (60 and 90 days after transplanting in 2020 and 30 and 60 days after transplanting in 2021) and rinsed well with tap water immediately after excavation. Then, the enzyme was deactivated at 105°C for 30 min, dried to a constant weight at 75°C, and weighed (Sun et al., 2014). The weighed samples were ground and sieved to calculate their total N content using the Kjeldahl method (Li et al., 2011).

2.3.6. Soil sampling and measurement of inorganic n content

Fresh soil samples were collected in different plots from three soil layers (0–20, 20–40, and 40–60 cm) using a steel soil auger before transplanting and after harvest (Zheng et al., 2020). The inorganic N was extracted from the soil using a 2 mol/L KCl solution, which was shaken at 200 rpm for 1 h in an oscillating incubator and filtered using filter paper (Yao et al., 2017). The AUV spectrophotometer was used to measure the concentration of ammonium nitrogen (NH_4^+-N) and nitrate nitrogen (NO_3^--N) (UV-5300PC; Shanghai Mattel Instrument Co., Ltd., Shanghai, China).

2.4. Sampling and analyses

2.4.1. Bi omass and N content in different organs

Three hills of rice were collected from each plot to calculate the biomass in the tillering, booting, and maturity stages. First, the stems, leaves, and panicles were separated, and the fresh samples were dried to deactivate the enzymes at 105°C for 30 min. Then, the samples were further dried to a constant weight at 75°C, which was considered the dry matter accumulation. Subsequently, the weighed samples were milled and sieved to calculate their total N content using the Kjeldahl method (Li et al., 2011).

The biomass transfer amount in different organs (BTA, t/ha), biomass transfer rate (BTR, %), contribution rate of BTA from other organs to grains (GCR, %), total biomass exportation from vegetative organs (BME, t/ha), and transportation rate of biomass from vegetative organs (TRBV, %) were, respectively, calculated using the following equations (Liu et al., 2017; Qi et al., 2020):

$$BTA = BMH - BMM \quad (1)$$

$$BTR = \frac{BTA}{BMH} \times 100\% \quad (2)$$

$$GCR = \frac{BTA}{GDW} \times 100\% \quad (3)$$

$$DME = BMH - BMM \quad (4)$$

$$TRBV = \frac{BME}{BMH} \times 100\% \quad (5)$$

where BMH and BMM represent biomass in organs at the heading and maturity stages, respectively, and GHW represents the grain weight.

2.4.2. N uptake and transportation

The N uptake (kg/ha) was calculated using the following equation (Zhu et al., 2019):

$$N\ uptake = TD \times NC \quad (6)$$

where TD represents the total dry matter accumulation of panicles, leaves, and stems with leaf sheaths. NC represents the content of N in the panicles, leaves, and stems with leaf sheaths.

N apparent translocation amount from stems, sheaths, and leaves (TNT, kg/ha); N apparent translocation efficiency of stems, sheaths, and leaves (TNTE, %); contribution rate of transferred N (NCR, %); N apparent translocation amount from stems and sheaths (SNT, kg/ha); N apparent translocation efficiency of stems and sheaths (SNTE, %); N apparent translocation amount from leaves (LNT, kg/ha); and N apparent translocation efficiency of leaves (LNTE, %) were calculated using the following equations

(Zhu et al., 2019):

$$TNT = TNH - TNM \quad (7)$$

$$TNTE = \frac{TNT}{TNH} \times 100\% \quad (8)$$

$$NCR = \frac{TNT}{TNG} \times 100\% \quad (9)$$

$$SNT = SNH - SNM \quad (10)$$

$$SNTE = \frac{SNT}{SNH} \times 100\% \quad (11)$$

$$LNT = LNH - LNM \quad (12)$$

$$LNTE = \frac{LNT}{LNH} \times 100\% \quad (13)$$

where TNH and TNM represent the total N uptake of aboveground in heading and maturity stages, respectively. TNG represents the total N uptake of grain in the maturity stage. SNH and SNM represent the total N uptake of stems and sheaths in the heading and maturity stages, respectively. LNT and LNM represent the total N uptake of leaves in the heading and maturity stages, respectively.

2.4.3. N balance

The N residual (N_{res}, kg/ha), N initial (N_{ini}, kg/ha), and N mineral (N_{min}, kg/ha) were calculated as follows (Zheng et al., 2020):

$$N_{res} = \frac{C \times B \times H}{10} \quad (14)$$

where C represents the total content of NH_4^+-N and NO_3^--N (mg/kg). B and H represent bulk density and height in the soil, respectively (Kou et al., 2021).

$$N_{ini} = \frac{C0i \times B \times H}{10} \quad (15)$$

$$N_{\min} = Not\ uptake + \frac{C0h \times B \times H}{10} N_{ini} \quad (16)$$

where C_{0i} and C_{0h} represent the total content of NH_4^+-N and NO_3^--N (mg/kg) before transplanting and after harvesting of CK, respectively. N_{ot} uptake represents the total uptake including shoots and roots in the maturity stage of CK.

The N apparent loss (N_{app}, kg/ha) and N surplus (N_{sur}, kg/ha) were calculated as follows (Zheng et al., 2020):

$$N_{app} = N_{fer} + N_{ini} + N_{\min} - N_{res} - N_t\ uptake \quad (17)$$

$$N_{sur} = N_{res} + N_{app} \quad (18)$$

where N_t uptake represents the total N uptake including shoots and roots in the maturity stage.

2.5. Data analysis

Microsoft Excel 2010 (WA, USA) was used for data processing. The pairwise means among treatments were compared using the Tukey's test at the 0.05 level of probability (SAS Institute Inc. 2001). SPSS Statistics 26.0 (IBM, Inc.; NY, USA) was used for statistical analyses, including simple path analyses of the indicators affecting rice yields and the interaction of different N application methods and N fertilizer varieties on each indicator. The graphs were drawn using the Origin 8.5 software (Origin Lab, MA, USA) and Microsoft PowerPoint 2010 (WA, USA).

3. Results

3.1. Chlorophyll content and photosynthesis traits

N application can effectively increase chlorophyll content (Figure 4). The chlorophyll contents under CRUM and CRUR treatments were higher than those under FFP ($p < 0.05$). The chlorophyll content in CRUM significantly increased in LNS by 7.98, 7.90, and 5.70% in 2020 and by 14.42, 13.69, and 11.36% in 2021, respectively ($p < 0.05$), at the tillering, booting, and heading stages compared with that in UM. The chlorophyll content increased by 7.94, 9.71, and 8.45% (2020) and 12.28, 11.35, and 10.13% (2021) in CRUR compared with UR ($p < 0.05$) at the tillering, booting, and heading stages, respectively, indicating that the CRU effectively increased the chlorophyll content. The chlorophyll content of R was slightly higher than that of M when the same amount of N fertilizer was applied.

The photosynthesis traits are shown in Figure 5. The N application was beneficial to increase P_n, G_s, and T_r and decrease Ci. Differences were observed in the net photosynthetic rate and transpiration rate under different N fertilization treatments at different stages, especially in the booting stage. In CRU in the booting stage, P_n, G_s, and T_r levels significantly increased by 11.53, 19.64, and 15.86%, respectively, under CRUM compared with UM. P_n, G_s, and T_r significantly increased by 15.91, 25.22, and 25.49%, respectively, under CRUR compared with UR. Furthermore, the C_i significantly decreased by 12.87 and 58.55% under CRUM compared with UM in the tillering and booting stages, respectively. The C_i decreased by 13.84 and 80.64% in CRUR compared with UR in the tillering and booting stages ($p < 0.05$), respectively, which indicated that CRU application could improve the photosynthesis of rice leaves.

3.2. Levels of antioxidant enzymes, MDA, and N metabolism enzymes

As shown in Figure 6, significant differences were found in antioxidant enzyme and MDA levels under different N fertilization treatments at different stages. Compared with the other N fertilization treatments (FFP, UM, UR, and CRUM) in tillering and booting stages, the SOD and CAT activities under CRUR significantly increased by 14.79–40.36% and 11.76–25.51%, and 14.85–65.44% and 5.44–55.52% ($p < 0.05$), respectively. Moreover, the N application treatments (FFP, UM, UR, and CRUM) significantly increased the MDA content by 42.45–137.49% in 2020 and 45.52–104.20% in 2021 compared to that under CRUR ($p < 0.05$), respectively.

Compared with U, CRU could significantly promote NR, GOGAT, and GS activities when the same N fertilizer was used.

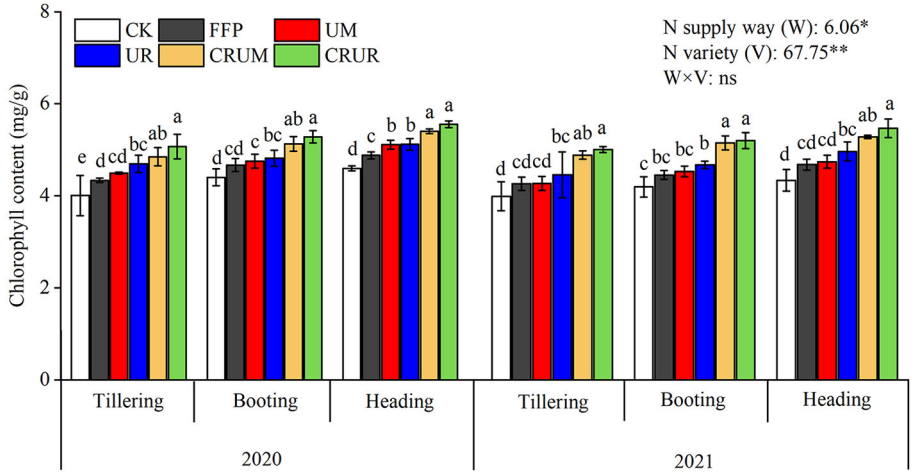

FIGURE 4
Effects of different N fertilizer treatments on chlorophyll content of rice leaves. Values are the means ± SD of three replicates. Means followed by a common letter are not significantly different by the Tukey's test at the 5% level of significance. * and ** represent statistical significance at $p < 0.05$ and $p < 0.01$, respectively. ns indicated statistical significance at $p > 0.05$ within a column.

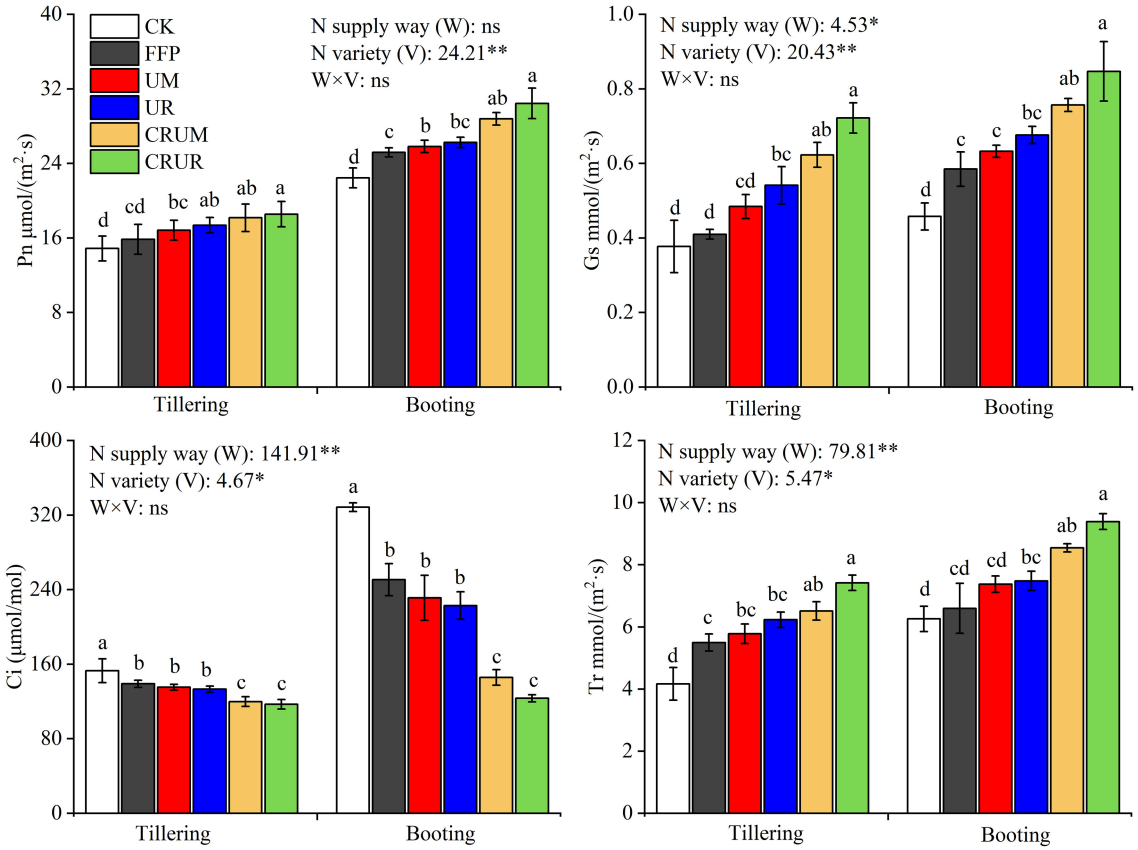

FIGURE 5
Effects of different N fertilizer treatments on photosynthesis traits (P_n, G_s, C_i, and T_r) in 2021. P_n, G_s, C_i, and T_r indicated net photosynthesis rate, stomatal conductance, intercellular CO_2 concentration, and transpiration rate, respectively. Values are the means ± SD of three replicates. Means followed by a common letter are not significantly different by the Tukey's test at the 5% level of significance. *, **, and *** represented the significance levels of $p < 0.05$, $p < 0.01$, and $p < 0.001$, respectively; ns indicated statistical significance at $p > 0.05$ within a column.

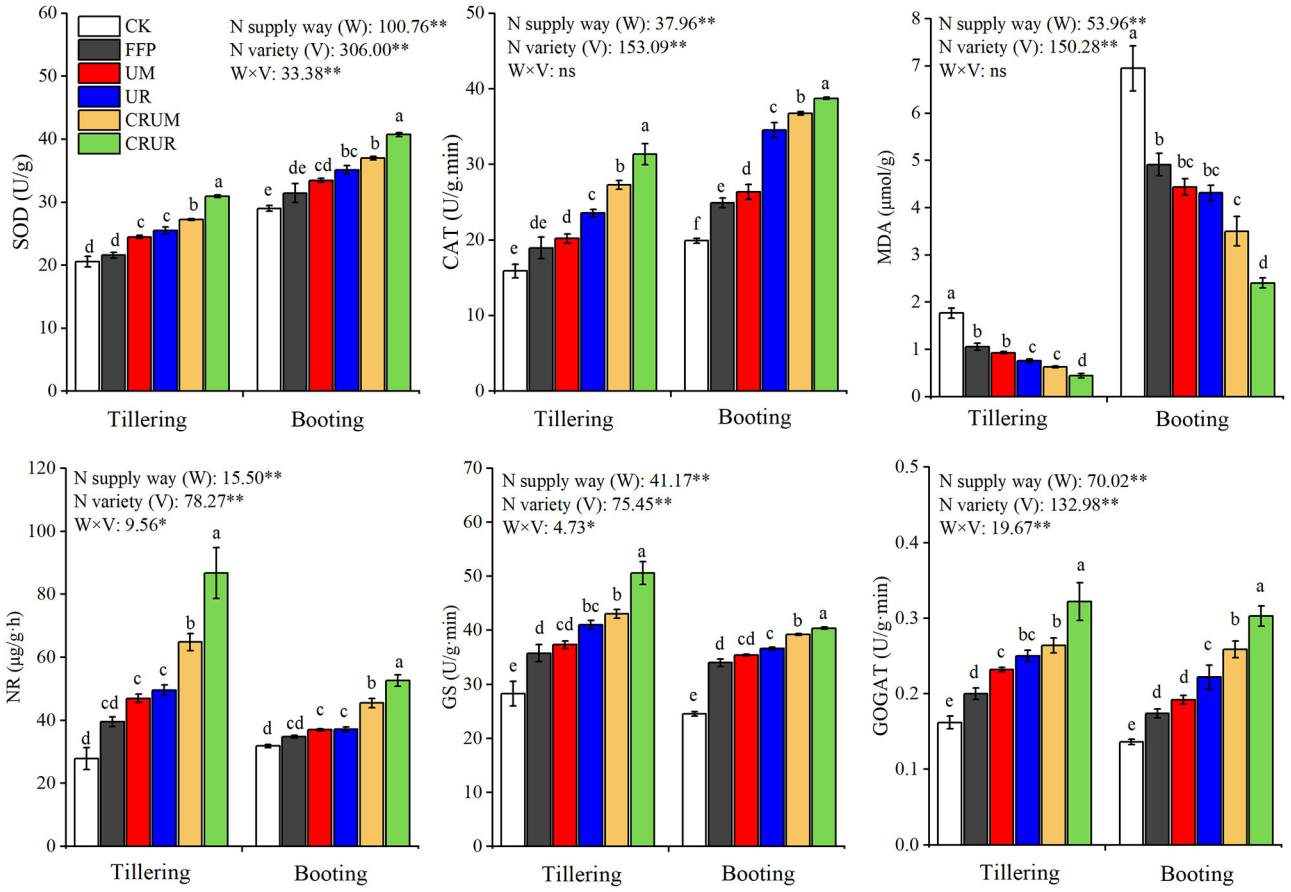

FIGURE 6
Effects of different N fertilizer treatments on antioxidant enzymes, MDA, and N metabolism enzyme of rice leaves at different growth stages in 2021. SOD, CAT, and MDA indicated superoxide dismutase, catalase, and malondialdehyde, respectively. NR, GS, and GOGAT indicated nitrate reductase, glutamine synthetase, and glutamate synthetase, respectively. Values are the means ± SD of three replicates. Means followed by a common letter are not significantly different by the Tukey's test at the 5% level of significance. *, **, and *** represented the significance levels of $p < 0.05$, $p < 0.01$, and $p < 0.001$, respectively; ns indicated statistical significance at $p > 0.05$ within a column.

Furthermore, the NR, GS, and GOGAT levels in CRUR were higher than those under the other N fertilization treatments (FFP, UM, UR, and CRUM), especially in the tillering stage. Compared with the other N fertilization treatments (FFP, UM, UR, and CRUM) in the tillering stage, the NR, GS, and GOGAT levels in CRUR significantly increased by 33.71–119.38%, 17.56–41.56%, and 21.97–61.00% ($p < 0.05$), respectively.

3.3. Biomass and N uptake distribution and translocation in each organ

As depicted in Table 1, the BTA, BTR, and contribution rate of BTA from GCR under all treatments were the highest in stems, followed by leaves, in 2020 and 2021. However, the BTA, BTR, and GCR levels varied among different N treatments. Compared with the UM of stems and leaves in 2021, the BTA and BTR levels under CRUM significantly increased by 37.04 and 23.36% in 2020 and 33.85 and 23.07% in 2021, respectively. The BTA level of stems and leaves significantly increased by 27.42 and 46.16% in 2020 and 33.62 and 39.71% in 2021, respectively, compared with the UR level ($p < 0.05$). Furthermore, the DME of CRU was significantly higher than that of U, indicating that CRU effectively promoted dry matter exportation compared with U.

The N uptake of stems and leaves increased first and then decreased gradually in the rice-growing stage (Table 2). A significant difference was observed between N application treatments of stems, leaves, and panicles in different stages. For example, the N uptake of stems and leaves was significantly higher under CRU treatments (CRUM and CRUR) than under U treatments (FFP, UM, and UR) in the tillering stage but not in the heading and maturity stages. In panicles in the maturity stage, the N uptake significantly increased by 19.19% (2020) and 34.22% (2021) under CRUM compared to UM ($p < 0.05$). The N uptake increased significantly by 17.75% under CRUR (2021) compared to UR ($p < 0.05$).

The TNT, TNTE, and NCR were significantly affected by N applications and varieties (Table 3). In LNS, the CRU treatment could significantly increase the SNT and LNT levels by 28% ($p < 0.05$) compared with the U treatment, which further improved TNT. For M and R application methods, the TNT significantly increased by 4.35% ($p < 0.05$) under UR compared with UM in 2021. The TNT significantly increased by 11.78 and 11.92% under CRUR compared with CRUM in 2021 and 2021, respectively ($p < 0.05$).

TABLE 1 Effects of different N fertilization treatments on biomass translocation in each organ and its contribution rate to grain.

Year	Treatment	Index	Stem			Leave			BME (t/ha)	TRBV (%)
			BTA (t/ha)	BTR (%)	CGR (%)	BTA (t/ha)	BTR (%)	CGR (%)		
2020	CK	Mean ± SD	0.89 ± 0.01e	18.40 ± 0.52c	11.10 ± 0.14b	0.36 ± 0.02c	13.48 ± 0.44c	4.55 ± 0.36b	1.12 ± 0.01b	15.11 ± 0.37b
		CV %	1.12	2.83	1.26	5.56	3.26	7.91	0.89	2.45
	FFP	Mean ± SD	1.03 ± 0.01d	21.11 ± 1.71bc	10.68 ± 0.05b	0.48 ± 0.02bc	15.82 ± 0.93b	4.99 ± 0.24b	1.51 ± 0.03b	18.98 ± 0.88ab
		CV %	0.97	8.10	·0.47	4.17	5.88	4.81	1.99	4.64
	UM	Mean ± SD	1.13 ± 0.02d	18.98 ± 0.99bc	11.44 ± 0.83ab	0.57 ± 0.07b	16.63 ± 0.64ab	5.80 ± 1.08ab	1.42 ± 0.08b	15.66 ± 0.65b
		CV %	1.77	5.22	7.26	12.28	3.85	18.62	5.63	4.15
	UR	Mean ± SD	1.24 ± 0.03c	22.04 ± 0.15ab	11.71 ± 0.96ab	0.62 ± 0.01b	17.97 ± 1.37ab	5.85 ± 0.42ab	1.83 ± 0.03b	20.19 ± 0.48ab
		CV %	2.42	0.68	8.20	1.61	7.62	7.18	1.64	2.38
	CRUM	Mean ± SD	1.44 ± 0.02b	24.65 ± 1.45a	11.77 ± 0.64ab	0.83 ± 0.07a	18.06 ± 0.34a	6.77 ± 0.70a	2.81 ± 0.07a	25.45 ± 0.81a
		CV %	1.39	5.88	5.44	8.43	1.88	10.34	2.49	3.18
	CRUR	Mean ± SD	1.58 ± 0.07a	24.66 ± 1.31a	12.95 ± 0.72a	0.90 ± 0.06a	18.55 ± 0.69a	7.35 ± 0.57a	2.90 ± 0.13a	24.93 ± 0.76a
		CV %	4.43	5.31	5.56	6.67	3.72	7.76	4.48	3.05
2021	CK	Mean ± SD	0.92 ± 0.06c	24.28 ± 2.27ab	12.06 ± 0.54ab	0.51 ± 0.02d	18.75 ± 1.63c	6.72 ± 0.29bc	1.76 ± 0.08b	25.67 ± 1.31b
		CV %	6.52	9.35	4.48	3.92	8.69	4.32	4.55	5.10
	FFP	Mean ± SD	1.12 ± 0.01b	26.66 ± 1.20a	11.14 ± 0.23b	0.61 ± 0.01c	19.41 ± 0.84bc	6.11 ± 0.16c	2.27 ± 0.02b	28.71 ± 0.56ab
		CV %	0.89	4.5	2.06	1.64	4.33	2.62	0.88	1.95
	UM	Mean ± SD	1.08 ± 0.01b	22.05 ± 0.38b	11.98 ± 0.86ab	0.65 ± 0.02c	20.89 ± 1.00bc	7.21 ± 0.64ab	2.32 ± 0.02b	26.96 ± 0.16ab
		CV %	0.93	1.72	7.18	3.08	4.79	8.88	0.86	0.59
	UR	Mean ± SD	1.16 ± 0.06b	23.61 ± 2.97ab	12.13 ± 1.00ab	0.68 ± 0.02c	21.52 ± 0.93b	7.15 ± 0.12ab	2.36 ± 0.04b	27.34 ± 1.52ab
		CV %	5.17	12.58	8.24	2.94	4.32	1.68	1.69	5.56
	CRUM	Mean ± SD	1.48 ± 0.01a	27.20 ± 0.789a	12.51 ± 0.17ab	0.87 ± 0.02b	25.71 ± 0.60a	7.41 ± 0.27ab	3.18 ± 0.03a	32.95 ± 0.48a
		CV %	0.68	2.9	1.36	2.3	2.33	3.64	0.94	1.46
	CRUR	Mean ± SD	1.55 ± 0.06a	27.07 ± 0.50a	12.98 ± 0.42a	0.95 ± 0.03a	27.00 ± 0.73a	7.94 ± 0.36a	3.01 ± 0.07a	30.88 ± 0.45ab
		CV %	3.87	1.85	3.24	3.16	2.7	4.53	2.33	1.46
N supply way (W)			7.41*	4.66*	ns	4.97*	ns	ns	5.71*	5.30*
N variety (V)			86.68**	48.16**	ns	61.58**	ns	7.13*	76.85**	31.79**
W × V			ns	ns	ns	ns	ns	ns	ns	ns

Means followed by a common letter are not significantly different by the Tukey-test at the 5% level of significance. *, **, and *** represented the significance level of $p < 0.05$, $p < 0.01$, and $p < 0.001$, respectively, ns indicated statistical significance at $p > 0.05$ within a column.

10.3389/fsufs.2023.1252324

TABLE 2 Effects of N application treatment on N uptake in different organs of rice at different growth stages (kg/ha).

Year	Treatment	Index	Tillering stage			Heading stage				Maturity stage			
			Stem	Leaf	Total[a]	Stem	Leaf	Panicle	Total[a]	Stem	Leaf	Panicle	Total[a]
2020	CK	Mean ± SD	19.73 ± 0.75c	22.28 ± 0.86d	42.01 ± 1.60d	31.78 ± 1.38d	43.02 ± 2.07b	10.09 ± 1.88d	84.90 ± 2.57d	18.34 ± 1.28b	27.76 ± 2.68a	58.61 ± 4.61d	104.71 ± 7.40e
		CV %	3.80	3.86	3.81	4.34	4.81	18.63	2.57	6.98	9.65	7.87	7.07
	FFP	Mean ± SD	23.60 ± 1.10b	28.41 ± 0.14bc	52.00 ± 0.97c	38.53 ± 4.12cd	46.99 ± 2.33ab	15.62 ± 3.55bc	101.14 ± 9.72cd	22.57 ± 4.22b	30.94 ± 2.31a	97.91 ± 4.37c	151.43 ± 8.17d
		CV %	4.66	0.49	1.87	10.69	4.96	22.73	9.72	18.7	7.47	4.46	5.40
	UM	Mean ± SD	24.01 ± 0.79b	27.04 ± 0.19c	51.05 ± 0.66c	52.40 ± 5.10ab	49.02 ± c6.95ab	14.65 ± 2.17cd	116.06 ± 11.71bc	32.40 ± 0.55a	31.73 ± 6.71a	108.58 ± 4.90bc	172.71 ± 3.31cd
		CV %	3.29	0.70	1.29	9.73	14.18	14.81	11.71	1.70	21.15	4.51	1.92
	UR	Mean ± SD	24.94 ± 0.79b	30.11 ± 1.76b	55.05 ± 0.97b	45.38 ± 1.55bc	50.12 ± c3.83ab	21.87 ± 0.66a	117.38 ± 4.16bc	23.95 ± 2.05c	30.91 ± 4.13a	118.04 ± 10.20ab	172.89 ± 2.81bc
		CV %	3.17	5.85	1.76	3.42	7.64	3.02	4.16	8.56	13.36	8.64	1.63
	CRUM	Mean ± SD	27.41 ± 0.50a	37.87 ± 0.42a	65.29 ± 0.90a	58.01 ± 3.41a	53.92 ± 6.40ab	23.27 ± 0.68a	135.20 ± 9.87ab	35.25 ± 3.73a	31.35 ± 5.90a	129.42 ± 4.90a	196.02 ± 12.70ab
		CV %	1.82	1.11	1.38	5.88	11.87	2.92	9.87	10.58	18.82	3.79	6.48
	CRUR	Mean ± SD	28.22 ± 0.55a	37.51 ± 0.42a	65.74 ± 0.86a	60.44 ± 1.83a	56.13 ± 4.31a	20.40 ± 0.80ab	143.14 ± 2.10a	35.38 ± 1.76a	30.09 ± 3.92a	131.25 ± 10.94a	196.71 ± 16.88a
		CV %	1.95	1.12	1.31	3.03	7.68	3.92	2.10	4.97	13.03	8.34	8.58
2021	CK	Mean ± SD	14.66 ± 0.83c	21.70 ± 1.34c	36.36 ± 1.78d	32.79 ± 2.00c	29.24 ± 1.48c	14.24 ± 0.27c	76.27 ± 5.47e	21.42 ± 2.18b	16.63 ± 4.41b	59.85 ± 5.20d	97.90 ± 9.79e
		CV %	5.66	6.18	4.9	6.10	5.06	1.9	0.47	10.18	26.52	8.69	0.81
	FFP	Mean ± SD	16.68 ± 0.35bc	28.18 ± 2.46b	44.87 ± 2.80c	42.57 ± 2.25b	46.29 ± 1.52b	14.86 ± 0.31c	103.72 ± 0.86d	26.79 ± 2.28ab	21.21 ± 0.85ab	94.18 ± 5.69c	142.18 ± 4.5d0
		CV %	2.1	8.73	6.24	5.29	3.28	2.09	0.86	8.51	4.01	6.04	3.17
	UM	Mean ± SD	17.34 ± 1.40b	32.01 ± 0.14b	49.35 ± 1.26bc	45.68 ± 2.69b	49.64 ± 1.43ab	21.25 ± 0.17b	116.57 ± 2.84c	28.44 ± 2.18a	21.43 ± 0.73ab	104.41 ± 9.98c	154.27 ± 9.10cd
		CV %	8.07	0.44	2.55	5.89	2.88	0.80	2.84	7.67	3.41	9.56	5.90
	UR	Mean ± SD	18.48 ± 0.34b	32.31 ± 0.46b	50.80 ± 0.69b	47.52 ± 4.87ab	50.34 ± 2.99ab	26.59 ± 2.06a	123.85 ± 4.75bc	29.05 ± 1.41a	21.43 ± 3.11ab	110.96 ± 5.73bc	161.44 ± 12.86bc
		CV %	1.84	1.42	1.36	10.25	5.94	7.75	4.75	4.85	14.51	5.16	7.97
	CRUM	Mean ± SD	21.84 ± 0.75a	46.28 ± 0.50a	68.13 ± 0.61a	49.53 ± 4.10ab	55.52 ± 3.87a	27.43 ± 0.81a	132.48 ± 1.03ab	28.58 ± 2.96a	24.86 ± 1.99a	126.41 ± 6.63ab	179.85 ± 16.10ab
		CV %	3.43	1.08	0.90	8.28	6.97	2.95	1.03	10.36	8.00	5.24	8.95
	CRUR	Mean ± SD	23.49 ± 0.54a	43.67 ± 2.44a	67.16 ± 1.99a	55.74 ± 2.19a	55.67 ± 3.37a	20.27 ± 2.26b	138.75 ± 2.77a	30.61 ± 1.93a	22.87 ± 3.98ab	130.66 ± 3.08a	184.14 ± 16.57a
		CV %	2.30	5.59	2.96	3.93	6.05	11.15	2.77	6.31	17.4	2.36	9.00
N supply way (W)			5.09*	6.30*	20.26**	ns	ns	9.14*	ns	9.67*	ns	6.41*	3.01*
N variety (V)			75.00**	286.84**	636.35**	29.57**	ns	24.58**	23.61**	28.44**	ns	12.80**	29.30**
W × V			ns	10.14*	12.90**	6.19*	ns	49.10**	ns	10.24*	ns	6.43*	4.32*

"a" indicated the total N uptake of stem, leaves, and panicle. Means followed by a common letter are not significantly different by the Tukey-test at the 5% level of significance. *, **, and *** represented the significance level of $p < 0.05$, $p < 0.01$, and $p < 0.001$, respectively, ns indicated statistical significance at $p > 0.05$ within a column.

10.3389/fsufs.2023.1252324

TABLE 3 Effects of different N fertilizer treatments on N transport of rice.

Year	Treatment	Index	TNT (kg/ha)	TNTE (%)	NCR (%)	Stem		Leaf	
						SNT (kg/ha)	SNTE (%)	LNT (kg/ha)	LNTE (%)
2020	CK	Mean ± SD	25.11 ± 0.70d	35.31 ± 2.13b	43.07 ± 4.55a	9.84 ± 0.41c	34.95 ± 1.62a	15.27 ± 0.98e	35.57 ± 3.50b
		CV %	2.79	6.03	10.56	4.17	4.64	6.42	9.84
	FFP	Mean ± SD	28.14 ± 1.45d	34.57 ± 1.64b	29.28 ± 1.27b	12.10 ± 1.55c	35.06 ± 1.49a	16.04 ± 0.39de	34.20 ± 1.79b
		CV %	5.15	4.74	4.34	12.81	4.25	2.43	5.23
	UM	Mean ± SD	33.64 ± 2.59c	34.71 ± 3.46b	31.09 ± 3.71b	16.35 ± 2.54b	34.88 ± 6.02a	17.29 ± 0.36d	35.69 ± 4.42b
		CV %	7.7	9.97	11.93	15.54	17.26	2.08	12.38
	UR	Mean ± SD	35.76 ± 0.56c	39.55 ± 2.51ab	30.41 ± 2.15b	16.54 ± 0.17b	40.92 ± 1.94a	19.22 ± 0.39c	38.52 ± 3.56ab
		CV %	1.57	6.35	7.07	1.03	4.74	2.03	9.24
	CRUM	Mean ± SD	45.32 ± 0.44b	40.68 ± 3.19ab	35.67 ± 1.79ab	22.75 ± 0.59a	39.33 ± 2.94a	22.57 ± 0.56b	42.16 ± 3.84ab
		CV %	0.97	7.84	5.02	2.59	7.48	2.48	9.11
	CRUR	Mean ± SD	50.66 ± 1.09a	43.63 ± 0.57a	39.37 ± 2.34a	24.62 ± 1.21a	41.04 ± 2.11a	26.04 ± 0.57a	46.53 ± 2.86a
		CV %	2.15	1.31	5.94	4.92	5.14	2.19	6.15
2021	CK	Mean ± SD	23.95 ± 1.04f	38.78 ± 2.95c	65.34 ± 10.04a	11.37 ± 0.19e	34.80 ± 2.69c	12.58 ± 1.23d	43.62 ± 7.06b
		CV %	4.34	7.61	15.37	1.67	7.73	9.78	16.19
	FFP	Mean ± SD	41.14 ± 0.38e	46.16 ± 1.04b	49.09 ± 2.12b	15.80 ± 0.21d	37.16 ± 1.83bc	25.34 ± 0.45c	54.44 ± 0.61a
		CV %	0.92	2.25	4.32	1.33	4.93	1.78	1.12
	UM	Mean ± SD	45.54 ± 0.02d	47.75 ± 1.09ab	45.97 ± 3.79b	17.26 ± 0.32cd	37.82 ± 1.33bc	28.28 ± 0.34b	56.89 ± 0.85a
		CV %	0.04	2.28	8.25	1.85	3.52	1.2	1.49
	UR	Mean ± SD	47.52 ± 0.29c	48.62 ± 2.99ab	43.97 ± 4.63b	18.47 ± 0.13c	39.11 ± 3.64bc	29.05 ± 0.26b	57.70 ± 3.54a
		CV %	0.61	6.15	10.53	0.7	9.31	0.9	6.14
	CRUM	Mean ± SD	51.77 ± 0.60b	49.21 ± 0.77ab	39.32 ± 4.82b	20.96 ± 1.29b	42.38 ± 1.29ab	30.80 ± 1.87ab	55.36 ± 0.50a
		CV %	1.16	1.57	12.26	6.16	3.04	6.07	0.9
	CRUR	Mean ± SD	57.94 ± 0.29a	52.07 ± 2.22a	39.87 ± 2.22b	25.13 ± 0.64a	45.11 ± 0.93a	32.81 ± 0.57a	59.12 ± 4.10a
		CV %	0.5	4.26	5.57	2.55	2.06	1.74	6.94
N supply way (W)			194.74**	ns	ns	32.76**	ns	6.35*	ns
N variety (V)			1132.80**	ns	5.03*	141.81**	12.61*	38.05**	ns
W × V			51.79**	ns	ns	10.40*	ns	2.09*	ns

"a" indicated the total N uptake of stem, leaves and panicle. Values are means ± SD of three replicates. Means followed by a common letter are not significantly different by the Tukey-test at the 5% level of significance. *, **, and *** represented the significance level of $p < 0.05$, $p < 0.01$, and $p < 0.001$, respectively, ns indicated statistical significance at $p > 0.05$ within a column.

3.4. N uptake in roots

As shown in Figure 7, the N uptake of roots showed similar trends in LNS after 30 and 60 days (d). The treatments were in the order CRUR > CRUM > UR = UM. N uptake significantly increased by 27.68% ($p < 0.05$) after 30 and 60 days under CRU treatment compared with under U treatment. Furthermore, CRUR treatment significantly increased the N uptake of roots by 10.80–34.50% after 60 days and by 15.83–22.92% after 90 days in 2020, and by 16.83–50.49% after 30 days and 10.82–32.56% after 60 days in 2021 ($p < 0.05$), compared with other treatments (UM, UR, and CRUM).

3.5. NH_4^+-N and NO_3^--N concentration in different soil layers

As shown in Figure 8, the NH_4^+-N concentration decreased gradually with the deepening of the soil layer. In LNS, NH_4^+-N concentration was significantly higher under CRU treatment than under U treatment in the 0–20 and 20–40 cm soil layers when the same N application method was used. Moreover, the NH_4^+-N concentration significantly increased by 52.90–94.02% under CRUR treatment compared with other treatments (UM, UR, and CRUM) at a depth of 0–20 cm, indicating that CRUR was most beneficial in increasing soil NH_4^+-N concentration.

The NO_3^--N concentration in different soil layers showed different trends compared with the NH_4^+-N concentration (Figure 8), and it increased first and then decreased with the deepening of the soil layer. The NO_3^--N concentration in different soil layers was significantly higher under N treatment than under CK treatment, indicating that the N treatment resulted in the continuous accumulation of NO_3^--N in the soil. The NO_3^--N concentration in the 0–20 and 20–40 cm soil layers was significantly higher under FFP treatment than under LNS treatment. Furthermore, compared with other treatments (UM, UR, and CRUM) at a depth of 0–20 cm, the NO_3^--N concentration

in the 0–20 cm soil layer under CRUR treatment significantly decreased by 34.31–47.39% ($p < 0.05$).

3.6. N balance

The N varieties and methods significantly affected N uptake, N residual, N apparent loss, and N surplus in the soil–crop system (Table 4). In LNS, the total N uptake and N residual increased under CRU treatment compared with U treatment, especially CRUR. The N residual significantly increased by 17.50–48.07% ($p < 0.05$) under CRUR treatment compared with other LNS treatments (UM, UR, and CRUM). Moreover, the CRU could effectively reduce the N apparent loss and N surplus compared with U, and the CRUR showed the lowest N apparent loss. The N apparent loss significantly decreased by 50.05–75.51% ($p < 0.05$) under CRUR treatment compared with other LNS treatments (UM, UR, and CRUM).

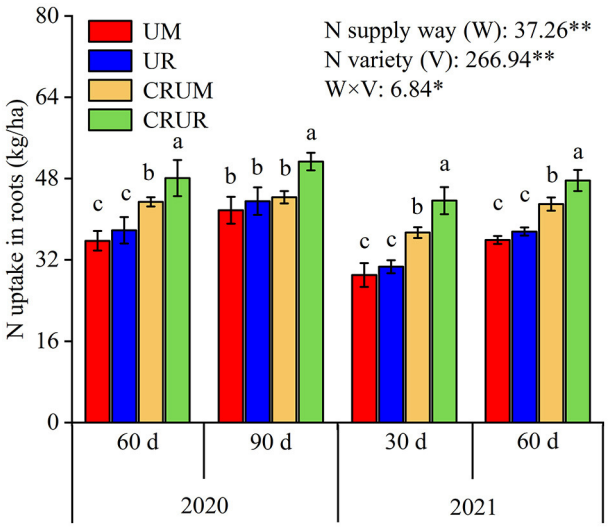

FIGURE 7
Effects of different N fertilizer treatments on N uptake of roots in 2020 and 2021. Values are means ± SD of three replicates. Means followed by a common letter are not significantly different by the Tukey-test at the 5% level of significance. Means followed by a common letter are not significantly different by the Tukey-test at the 5% level of significance. *, **, and *** represented the significance level of $p < 0.05$, $p < 0.01$, and $p < 0.001$, respectively, ns indicated statistical significance at $p > 0.05$ within a column.

3.7. Relationship between N uptake in shoots and roots

Figure 9 shows the path coefficient structural model that describes the important relationships among selected traits. The N uptake in rice shoots directly and positively affected yield and yield components. Moreover, the N metabolism enzyme activity (GS), N residual in soil, and N uptake in roots also directly and positively affected N uptake in shoots. For underground rice plants, the N residual in the 0–20 cm soil layer directly promoted the increase in the N uptake of roots. Furthermore, the N varieties had positive and significant effects on NH_4^+-N and NO_3^--N contents in different soil layers, but the N fertilization modes only had a positive and significant effect on NH_4^+-N in the soil layer of 0–20 cm and on NO_3^--N content in the soil layer of 0–40 cm, respectively.

4. Discussion

4.1. N uptake and transport affected by local n supply

Conventional broadcasting of N fertilizers is considered an inefficient N management method for rice (Nkebiwe et al., 2016). Previous studies indicated that LNS was a more effective alternative to broadcast fertilization to increase the N uptake by rice in paddy fields (Nkebiwe et al., 2016; Zhu et al., 2022). In this

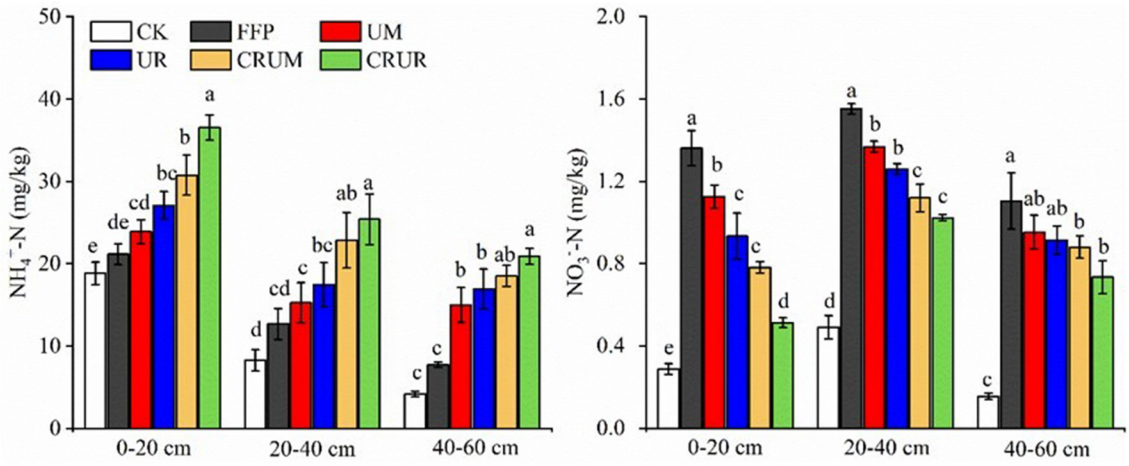

FIGURE 8
Average contents of NH_4^+-N and NO_3^--N in different soil layers in 2021.

TABLE 4 Effects of local nitrogen supply on N balance in rice field system in 2020 (kg/ha).

Treatment	Index	N initial[a]	N fertilizer	N mineral[b]	Total N uptake[c]	N residual	N apparent loss	N surplus
CK	Mean ± SD	101.89	–	87.53	138.55 ± 7.53d	50.87 ± 3.72e	0.00 ± 0.00e	50.87 ± 7.53d
	CV %	–	–	–	5.43	7.31	0.00	14.80
FFP	Mean ± SD	101.89	180.00	87.53	186.57 ± 6.76c	59.93 ± 3.51de	122.92 ± 7.45a	182.85 ± 6.76a
	CV %	–	–	–	3.62	5.86	6.06	3.70
UM	Mean ± SD	101.89	180.00	87.53	214.42 ± 6.84b	66.57 ± 3.99cd	88.43 ± 3.63b	155.00 ± 6.84b
	CV %	–	–	–	3.19	5.99	4.10	4.41
UR	Mean ± SD	101.89	180.00	87.53	216.25 ± 8.63b	74.58 ± 4.66bc	78.59 ± 4.41b	153.17 ± 8.63b
	CV %	–	–	–	3.99	6.25	5.61	5.63
CRUM	Mean ± SD	101.89	180.00	87.53	240.40 ± 1.83a	83.90 ± 6.53b	45.12 ± 5.83c	129.02 ± 1.83c
	CV %	–	–	–	0.76	7.78	12.92	1.42
CRUR	Mean ± SD	101.89	180.00	87.53	248.30 ± 6.26a	98.58 ± 4.04a	22.54 ± 3.29d	121.12 ± 6.26c
	CV %	–	–	–	2.52	4.10	14.60	5.17
N supply way (W)		–	–	–	ns	15.98**	40.71**	ns
N variety (V)		–	–	–	61.67**	52.97**	382.25**	61.67**
W × V		–	–	–	ns	ns	6.29*	ns

"a" indicated that the total of NH_4^+-N and NO_3^--N content before transplanting.
"b" indicated that "the N residual in CK + the total N uptake—the N initial".
"c" indicated the total N uptake indicated "the shoot N uptake + root N uptake". Means followed by a common letter are not significantly different by the Tukey-test at the 5% level of significance. *, **, and *** represented the significance level of $p < 0.05$, $p < 0.01$ and $p < 0.001$, respectively, ns indicated statistical significance at $p > 0.05$ within a column.

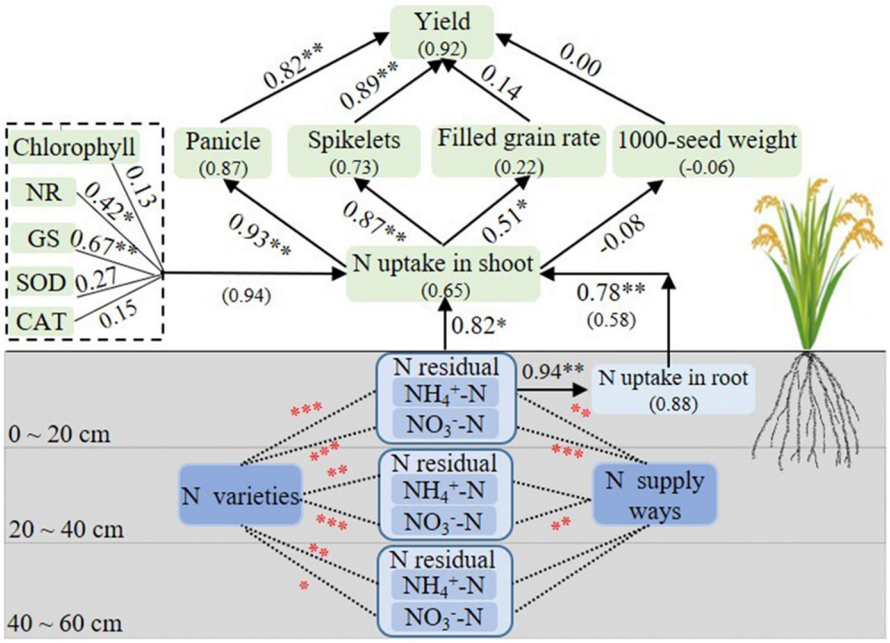

FIGURE 9
Path coefficient structural model of rice yield and the variables, analysis variance of NH_4^+-N and NO_3^--N content under N varieties and N fertilization modes. Boxes indicate the variable name, and the numbers in parentheses indicate the variance explained by the model (R^2). The numbers adjacent to arrows are standardized path coefficients and indicative of the effect size of the relationship. A line with arrowhead indicates a putative causal link between the cause (base of arrow) and effect (point of error). "0–20, 20–40, 40–60" indicated different soil layers. *, **, and *** in black and red colors represent the significance levels of $p < 0.05$, $p < 0.01$, and $p < 0.001$, respectively.

study, LNS increased N uptake in the maturity stage by 11.37–16.48% compared with FFP (Table 3). It is widely believed that LNS provides adequate nutrient concentration near the root zone, facilitating root growth and maintaining root viability (Li et al., 2021), thus improving N uptake (Linquist et al., 2012). The results of this study showed that LNS enhanced the activity of SOD and CAT by 23.13 and 33.33%, respectively, and reduced the MDA content by 66.48%, which was in line with the findings of Pan et al. (2017). A good antioxidant enzyme system can delay plant aging and promote the growth and N uptake of rice (Liao et al., 2019, 2022).

M and R, the two main application methods of LNS, place the fertilizer near the rice root system to ensure N supply while effectively reducing N loss (Zhu et al., 2019; Ding et al., 2022). Previous studies showed that the differences in N availability due to the different ways of placing fertilizers via the two fertilization methods further affected N uptake and transfer (Liu et al., 2017). In this study, R increased the TNT by 8.58% compared with M (Table 3), which was relatively similar to the N metabolism enzyme. R increased the enzyme activities of NR, GS, and GOGAT by 13.81, 9.56, and 15.59%, respectively, compared with M. Generally, NH_4^+-N and NO_3^--N can be absorbed by rice roots, and NO_3^--N can be converted into NH_4^+-N by NR. The NH_4^+-N can be converted into glutamine by GS and glutamic acid by GOGAT (Takabayashi et al., 2016). This is a critical step in converting inorganic N into organic N in plants, which facilitates N transport (Wang et al., 2018). Moreover, according to Figure 9, increased NR and GS activities directly stimulated N uptake in the shoot, which resulted in an increased rice yield. In addition, in rice field fertilization, M is mechanized, while R needs to be realized manually, which is comparatively more time-consuming and labor-intensive (Liu et al., 2020; Min et al., 2021). Therefore, researchers should focus on mechanizing R as soon as possible.

4.2. N transport affected by N varieties

N is the main component of chloroplasts, and N supply significantly increases the N uptake, chlorophyll contents, and photosynthesis of rice leaves (Sun et al., 2016). Studies have shown that the CRU application can prolong N availability in the soil, delay leaf senescence, and further increase N accumulation in the plant (Ding et al., 2022). In this study, the total N uptake and TNT under CRU treatment were significantly higher than those under U treatment (Table 2), which was consistent with the results of previous studies (Li et al., 2017, 2020).

N release rate under CRU treatments is influenced by the N application method. This is because the nutrient release of CRU is mainly influenced by the external ambient temperature and accelerates with increasing temperature. Meanwhile, the soil surface layer is more susceptible to the influence of solar radiation and temperature than the deeper layers. Fertilizers placed on the surface are more susceptible to wind and water erosion than those placed below the ground (Ding et al., 2020). Studies showed that the local CRU supply not only improved N uptake by rice but also reduced greenhouse gas emissions by 9.2% compared with the broadcast CRU supply (Li et al., 2023). This indicated that the application of CRU under LNS was more effective. Furthermore, it was found that N uptake in the roots was significantly higher under CRUR treatment than under other treatments (UM, UR, and CRUM) by 25.74% (Figure 7). This was because root N uptake was influenced by the N concentration around the roots (Ruseani et al., 2022), and the uptake rate was higher in roots grown in nutrient-rich patches than in nutrient-poor patches. Moreover, this study also revealed that N uptake in the root system had a direct and positive effect on aboveground N uptake (Figure 9), which was consistent with the findings of Niu et al. (2019). In addition, the yield and gross return under the CRUR treatment were higher than other treatments (UM, UR, and CRUM) by 2.06–22.86% and 1.92–22.51%, respectively (Supplementary Tables S1, S2).

4.3. Soil N balance affected by the coupling of local n supply and n varieties

The remaining N fertilizer in the soil has three destinations: it is absorbed by the next crop, enters the groundwater of paddy fields by leaching and runoff, and is converted into N_2O and N_2 in the atmosphere by denitrification. The unabsorbed residual N can lead to serious environmental issues, such as the greenhouse effect of rice fields, groundwater nitrate pollution, and biodiversity degradation (Chen et al., 2014; Smith et al., 2016). Thus, maintaining soil apparent N balance is significant to crop yield and environmental protection. In this study, CRUR treatment showed the lowest N apparent loss compared with other N treatments (FFP, UM, UR, and CRUM), besides the higher N uptake of CRUR. Most importantly, the N residual under CRUR was significantly higher than that under other treatments. The continuous N supply from CRUR increased the soil microbial enzyme activity around the root system (Zhang et al., 2017), which facilitated the N conversion of the fertilizer and enhanced the N fixation capacity in the soil, thus increasing the residual N in the soil based on the N application method. The contact area between N fertilizer and soil determines the rate of N fertilizer dilution and release, and the larger the contact area, the higher the rate of N fertilizer dilution and release (Zhou et al., 2020). The contact area between N fertilizer and soil can be in the following order: broadcasting > strip application > cavity application. Therefore, it can be hypothesized that the N fertilizer dilution and release rate are the lowest under R, the N occurs due to leaching, and runoff losses are smaller (Jiang et al., 2017). Interestingly, Ju and Zhang (2003) argued that this residual N was not necessarily lost immediately and might also serve to replenish the soil N pool with good management (Ju and Zhang, 2003; Smith and Chalk, 2018). Therefore, considering rice growth and soil N balance, R should be used as the main N fertilizer application method, and the best effect is achieved with the application of CRU.

5. Conclusion

These results clearly indicated that local N supply significantly improved N transport and reduced N loss in rice compared with

farmers' fertilizer practices. In local N supply, CRU significantly increased the activities of antioxidant enzymes and N metabolism enzymes compared with urea, which contributed to N uptake and transport in rice. Root-zone fertilization significantly reduced N loss compared with mechanical side-deep fertilization. Therefore, considering the risk of soil N leaching and environmental protection, root-zone fertilization should be selected as the recommended fertilization method, and the combination of CRU and root-zone fertilization is the most effective. The government should support the development of simple deep fertilizer application machinery to promote root-zone fertilization with CRU.

Data availability statement

The original contributions presented in the study are included in the article/Supplementary material, further inquiries can be directed to the corresponding authors.

Author contributions

RH: writing—original draft preparation, data curation, and editing. DX: investigation. ZD: investigation and conceptualization. YC: investigation and conceptualization. JH: methodology and reviewing. XW: reviewing. All authors contributed to the article and approved the submitted version.

Funding

This study was supported by Key R&D plan of Hubei Province in 2022 (2022BBA002), Carbon account accounting and carbon reduction and sequestration technology research of Quzhou city of China (2022-31), and Innovation Capacity Construction of Beijing Academy of Agricultural and Forestry Sciences (KJCX20230304, PT2023-47).

Acknowledgments

We particularly appreciate the guidance of the editor and reviewers on the refinement of the study.

Conflict of interest

The authors declare that the research was conducted in the absence of any commercial or financial relationships that could be construed as a potential conflict of interest.

Publisher's note

All claims expressed in this article are solely those of the authors and do not necessarily represent those of their affiliated organizations, or those of the publisher, the editors and the reviewers. Any product that may be evaluated in this article, or claim that may be made by its manufacturer, is not guaranteed or endorsed by the publisher.

Supplementary material

The Supplementary Material for this article can be found online at: https://www.frontiersin.org/articles/10.3389/fsufs.2023.1252324/full#supplementary-material

References

Campos, O. R., Mattiello, E. M., Cantarutti, R. B., and Vergütz, L. (2018). Nitrogen release from urea with different coatings. *J. Sci. Food Agric.* 98, 775–780. doi: 10.1002/jsfa.8525

Cao, S. Q., Lu, W., Zhai, H. Q., Sheng, S. L., Gong, H. B., Yang, T. L., et al. (2001). Research on the method to estimating flag leaf photosynthesis function duration at rice seedling stage by relative steady phase of chlorophyll content. *Chin. J. Rice Sci.* 15, 309–313. doi: 10.3321/j.issn:1001-7216.2001.04.014

Chen, X. P., Cui, Z. L., Fan, M. S., Vitousek, P., Zhao, M., Ma, W. Q., et al. (2014). Producing more grain with lower environmental costs. *Nature* 514, 486–489. doi: 10.1038/nature13609

Ding, X. P., Hao, L. G., Zhang, J. W., Liu, P., Ren, B. Z., and Zhao, B. (2020). Effects of base application depths of controlled release urea on yield and nitrogen utilization of summer maize. *Sci. Agric. Sin.* 53, 4342–4354.

Ding, Z. J., Li, J. T., Hu, R., Xiao, D. K., Huang, F., Peng, S. B., et al. (2022). Root-zone fertilization of controlled-release urea reduces nitrous oxide emissions and ammonia volatilization under two irrigation practices in a ratoon rice field. *Field Crop. Res.* 287, 108673. doi: 10.1016/j.fcr.2022.108673

Food Agriculture Organization of the United Nations. (2022). *Food Outlook Biannual Report on Global Food Markets.* Available online at: https://www.fao.org/giews/reports/food-outlook/en/ (accessed July 07, 2022).

Gaihre, Y. K., Singh, U., Mofijul Islam, S. M., Huda, A., Islam, M. R., Sanabria, J., et al. (2018). Nitrous oxide and nitric oxide emissions and nitrogen use efficiency as affected by nitrogen placement in lowland rice fields. *Nutr. Cycle Agroecosyst.* 110, 277–291. doi: 10.1007/s10705-017-9897-z

Grafton, R. Q., Williams, J., and Jiang, Q. (2015). Food and water gaps to 2050: preliminary results from the global food and water system (GFWS) platform. *Food Secur.* 7, 209–220. doi: 10.1007/s12571-015-0439-8

Guo, J. X., Hu, X. Y., Gao, L. M., Xie, K. L., Ling, N., Shen, Q. R., et al. (2017). The rice production practices of high yield and high nitrogen use efficiency in Jiangsu, China. *Sci. Rep.* 7, 1–10. doi: 10.1038/s41598-017-02338-3

Hu, K. B., Zhao, P., Wu, K. X., Yang, H. L., Yang, Q. X., Fan, M. Q., et al. (2023). Reduced and deep application of controlled-release urea-maintained yield and improved nitrogen-use efficiency. *Field Crop Res.* 295, 108876. doi: 10.1016/j.fcr.2023.108876

Jiang, C. Q., Wang, H. Y., Lu, D. J., Zhou, J. M., Li, D. C., and Zu, C. L. (2017). Effects of fertilizer placement and nitrogen forms on soil nitrogen diffusion and migration of red-yellow soil in China. *Agric. Sci.* 8, 1227–1238. doi: 10.4236/as.2017.811088

Jiang, Z. W., Yang, S. H., Chen, X., Pang, Q. Q., Xu, Y., Qi, S. T., et al. (2022). Controlled release urea improves rice production and reduces environmental pollution: a research based on meta-analysis and machine learning. *Environ. Sci. Pollut. Res.* 29, 3587–3599. doi: 10.1007/s11356-021-15956-2

Ju, X. T., and Zhang, F. S. (2003). Thinking about nitrogen recovery rate. *Ecol. Environ.* 2, 192–197.

Kou, C. L., Luo, X. S., and Ju, X. T. (2021). Effects of optimal nitrogen fertilization on N balance and nitrate-N accumulation in greenhouse tomato fields. *J. Plant Nutr. Fertiliz.* 27, 837–848. doi: 10.11674/zwyf.20456

Li, D., Wang, X., Zheng, H. B., Zhou, K., Yao, X., Tian, Y. C., et al. (2018). Estimation of area-and mass-based leaf nitrogen contents of wheat and rice crops from water-removed spectra using continuous wavelet analysis. *Plant Methods* 14, 1–20. doi: 10.1186/s13007-018-0344-1

Li, G. H., Zhao, B., Dong, S. T., Zhang, J. W., Liu, P., and Lu, W. P. (2020). Controlled-release urea combining with optimal irrigation improved grain yield, nitrogen uptake, and growth of maize. *Agric. Water* 227, 105834–105834. doi: 10.1016/j.agwat.2019.105834

Li, G. H., Zhao, B., Dong, S. T., Zhang, J. W., Liu, P., and Vyn, T. J. (2017). Interactive effects of water and controlled release urea on nitrogen metabolism, accumulation, translocation, and yield in summer maize. *Sci. Nat.* 104, 72. doi: 10.1007/s00114-017-1491-3

Li, G. H., Zhao, L. P., Zhang, S. X., Hosen, Y., and Yagi, K. (2011). Recovery and leaching of 15N labeled coated urea in a lysimeter system in the North China plain. *Pedosphere* 21, 763–772. doi: 10.1016/S1002-0160(11)60180-X

Li, L., Li, Q. K., Lin, Z. H., Zhang, Z., Tian, H., Ashraf, U., et al. (2021). Effects of nitrogen deep placement coupled with straw incorporation on grain quality and root traits from paddy fields. *Crop Sci.* 61, 3675–3686. doi: 10.1002/csc2.20578

Li, W. W., Ahmad, S., Liu, D., Gao, S., Wang, Y. H., Tao, W. K., et al. (2023). Subsurface banding of blended controlled-release urea can optimize rice yields while minimizing yield-scaled greenhouse gas emissions. *Crop. J.* 11, 914–921. doi: 10.1016/j.cj.2022.10.005

Liao, G. X., Yang, Y. H., Xiao, W. M., and Mo, Z. W. (2022). Nitrogen modulates grain yield, nitrogen metabolism, and antioxidant response in different rice genotypes. *J. Plant Growth Regul.* 42, 2103–2114. doi: 10.1007/s00344-022-10684-4

Liao, L., Dong, T. T., Qiu, X., Rong, Y., Sun, G. C., Wang, Z. H., et al. (2019). Antioxidant enzyme activity and growth responses of huangguogan citrus cultivar to nitrogen supplementation. *Biosci. Biotech. Biochem.* 83, 1–13. doi: 10.1080/09168451.2019.1634513

Linquist, B. A., Adviento-Borbe, M. A., Pittelkow, C. M., Kessel, C. V., and Groenigen, K. J. (2012). Fertilizer management practices and greenhouse gas emissions from rice systems: a quantitative review and analysis. *Field Crop Res.* 135, 10–21. doi: 10.1016/j.fcr.2012.06.007

Liu, T. Q., Fan, D. J., Zhang, X. X., Chen, J., Li, C. F., and Cao, C. G. (2015). Deep placement of nitrogen fertilizers reduces ammonia volatilization and increases nitrogen utilization efficiency in no-tillage paddy fields in central China. *Field Crop Res* 184, 80–90. doi: 10.1016/j.fcr.2015.09.011

Liu, T. Q., Li, S. H., Guo, L. G., Cao, C. G., Li, C. F., Zhai, Z. B., et al. (2020). Advantages of nitrogen fertilizer deep placement in greenhouse gas emissions and net ecosystem economic benefits from no-tillage paddy fields. *J. Clean Prod.* 263, 121322. doi: 10.1016/j.jclepro.2020.121322

Liu, X., Xu, G. C., Wang, Q. S., and Hang, Y. H. (2017). Effects of insect–proof net cultivation, rice–duck farming, and organic matter return on rice dry matter accumulation and nitrogen utilization. *Front. Plant Sci.* 8, 47. doi: 10.3389/fpls.2017.00047

Min, J., Sun, H. J., Wang, Y., Pan, Y. F., Kronzucker, H. J., Zhao, D. Q., et al. (2021). Mechanical side-deep fertilization mitigates ammonia volatilization and nitrogen runoff and increases profitability in rice production independent of fertilizer type and split ratio. *J. Clean. Prod.* 316, 128370. doi: 10.1016/j.jclepro.2021.128370

Niu, X. L., Hu, T. T., Zhang, F. C., Duan, A. W., and Zhang, J. Y. (2019). The root nitrogen uptake response to partial nitrogen stress is related to previous nutritional status. *Plant Growth Regul.* 87, 55–67. doi: 10.1007/s10725-018-0451-z

Nkebiwe, P. M., Weinmann, M., Bar-Tal, A., and Müller, T. (2016). Fertilizer placement to improve crop nutrient acquisition and yield: a review and meta-analysis. *Field Crop Res.* 196, 389–401. doi: 10.1016/j.fcr.2016.07.018

Pan, S. G., Wen, X. C., Wang, Z. M., Ashraf, U., Tian, H., Duan, M. Y., et al. (2017). Benefits of mechanized deep placement of nitrogen fertilizer in direct-seeded rice in south China. *Field Crop Res.* 203, 139–149. doi: 10.1016/j.fcr.2016.12.011

Qi, D. L., Hu, T. T., and Liu, T. T. (2020). Biomass accumulation and distribution, yield formation and water use efficiency responses of maize (Zea mays L.) to nitrogen supply methods under partial root-zone irrigation. *Agric. Water Manage.* 230, 105981. doi: 10.1016/j.agwat.2019.105981

Ruseani, N. S., Vanhove, W., Susilo, A. W., and Van Damme, P. (2022). Cocoa clones reveal variation in plant biomass, root nitrogen uptake, and apparent nitrogen recovery at the seedling stage. *J. Soil Sci. Plant Nutr.* 22, 4727–4738. doi: 10.1007/s42729-022-00955-0

Shahid, M. A., Balal, R. M., Khan, N., Zotarelli, L., Liu, G. D., Sarkhosh, A., et al. (2019). Selenium impedes cadmium and arsenic toxicity in potato by modulating carbohydrate and nitrogen metabolism. *Ecotox. Environ. Safe* 180, 588–599. doi: 10.1016/j.ecoenv.2019.05.037

Smith, C. J., and Chalk, P. M. (2018). The residual value of fertilizer N in crop sequences: an appraisal of 60 years of research using 15N tracer. *Field Crop Res.* 217, 66–74. doi: 10.1016/j.fcr.2017.12.006

Smith, P., House, J. I., Bustamante, M., Sobock,á, J., Harper, R., Pan, G., et al. (2016). Global change pressures on soils from land use and management. *Global Change Biol.* 22, 1008–1028. doi: 10.1111/gcb.13068

Sun, H. Y., Li, X. K., Ren, T., Cong, R. T., and Lv, J. T. (2014). Effects of fertilizer in shallow soils on growth and distribution of rice roots at seedling stage. *Sci. Agric. Sin.* 47, 2476–2484. doi: 10.3864/j.issn.0578-1752.2014.12.020

Sun, J. L., Ye, M., Peng, S. B., and Li, Y. (2016). Nitrogen can improve the rapid response of photosynthesis to changing irradiance in rice (*Oryza sativa* L.) plants. *Sci. Rep.* 6, 1–10. doi: 10.1038/srep31305

Takabayashi, A., Niwata, A., and Tanaka, A. (2016). Direct interaction with ACR11 is necessary for post-transcriptional control of GLU1-encoded ferredoxin-dependent glutamate synthase in leaves. *Sci. Rep.* 6. doi: 10.1038/srep 29668

Tian, X. F., Fan, Z., Zhao, Y. X., Sun, S. C., Li, T. Y., Yu, N., et al. (2021). Controlled-release urea improved cotton productivity and nitrogen use efficiency in China: a meta-analysis. *Agron. J.* 113, 2251–2259. doi: 10.1002/agj2.20702

Wang, Y. Y., Cheng, Y. H., Chen, K. E., and Tsay, Y. F. (2018). Nitrate transport, signaling, and use efficiency. *Annu. Rev. Plant Biol.* 69, 85–122. doi: 10.1146/annurev-arplant-042817-040056

Wu, M., Liu, M., Liu, J., Li, W. T., Jiang, C. Y., and Li, Z. P. (2017). Optimize nitrogen fertilization location in root-growing zone to increase grain yield and nitrogen use efficiency of transplanted rice in subtropical China. *J. Integr. Agric.* 16, 2073–2081. doi: 10.1016/S2095-3119(16)61544-7

Wu, S. W., Hu, C. X., Tan, Q. L., Xu, S. J., and Sun, X. (2017). Nitric oxide mediates molybdenum-induced antioxidant defense in wheat under drought stress. *Front. Plant Sci.* 8, 1085. doi: 10.3389/fpls.2017.01085

Wu, X. B., Li, H. B., Rengel, Z., Whalley, W. R., Li, H. G., Zhang, F. S., et al. (2022). Localized nutrient supply can facilitate root proliferation and increase nitrogen–use efficiency in compacted soil. *Soil Till. Res.* 215, 105198. doi: 10.1016/j.still.2021.105198

Wu, Y. S., and Yang, C. Y. (2016). Physiological responses and expression profile of NADPH oxidase in rice (Oryza Sativa) seedlings under different levels of submergence. *Rice* 9, 1–10. doi: 10.1186/s12284-016-0074-9

Yao, Y. L., Zhang, M., Tian, Y. H., Zhao, M., Zhang, B., Zhao, M., et al. (2017). Urea deep placement for minimizing NH_3 loss in an intensive rice cropping system. *Field Crop Res.* 218, 254–266. doi: 10.1016/j.fcr.2017.03.013

Ye, Y. S., Liang, X. Q., Chen, Y. X., Liu, J., Gu, J. T., Guo, R., et al. (2013). Alternate wetting and drying irrigation and controlled–release nitrogen fertilizer in late–season rice. Effects on dry matter accumulation, yield, water and nitrogen use. *Field Crop Res.* 144, 212–224. doi: 10.1016/j.fcr.2012.12.003

Zhang, J. S., Wang, C. Q., Li, B., Liang, J. Y., He, J., Xiang, H., et al. (2017). Effects of controlled release blend bulk urea on soil nitrogen and soil enzyme activity in wheat and rice fields. *Chin. J. Appl. Ecol.* 28, 1899–1908.

Zhang, S. G., Shen, T. L., Yang, Y. C., Li, Y. C., Wan, Y. S., Zhang, M., et al. (2018). Controlled-release urea reduced nitrogen leaching and improved nitrogen use efficiency and yield of direct-seeded rice. *J. Environ. Manage.* 220, 191–197. doi: 10.1016/j.jenvman.2018.05.010

Zheng, Y., Han, X. R., Li, Y. Y., Liu, S. Q., Ji, J. H., and Tong, Y. X. (2020). Effects of mixed controlled release nitrogen fertilizer with rice straw biochar on rice yield and nitrogen balance in northeast China. *Sci. Rep.* 10, 1–10. doi: 10.1038/s41598-020-66300-6

Zhong, C., Cao, X. C., Bai, Z. G., Zhang, J. H., Zhu, L. F., Huang, J. L., et al. (2018). Nitrogen metabolism correlates with the acclimation of photosynthesis to short-term water stress in rice (*Oryza sativa* L.). *Plant Physiol. Biochem.* 125, 52–62. doi: 10.1016/j.plaphy.2018.01.024

Zhou, C. M., Li, Y. C., and Chen, P. P. (2020). Effects of single application of fertilizer on yield and nitrogen utilization of mulching summer maize. *Transact. Chin. Soc. Agric. Machin.* 51, 9. doi: 10.6041/j.issn.1000-1298.2020.10.037

Zhou, Y., Yan, X. Y., Gong, S. L., Li, C. W., Zhu, R., Zhu, B., et al. (2022). Changes in paddy cropping system enhanced economic profit and ecological sustainability in central China. *J. Integr. Agric.* 21, 566–577. doi: 10.1016/S2095-3119(21)63841-8

Zhu, C. H., Xiang, J., Zhang, Y. P., Zhang, Y. K., Zhu, D. F., and Chen, H. Z. (2019). Mechanized transplanting with side deep fertilization increases yield and nitrogen use efficiency of rice in Eastern China. *Sci. Rep.* 9, 5653. doi: 10.1038/s41598-019-42039-7

Zhu, W. B., Zeng, K., Tian, Y. H., and Yin, B. (2022). Coupling side-deep fertilization with azolla to reduce ammonia volatilization while achieving a higher net economic benefits in rice cropping system. *Agric. Ecosyst. Environ.* 333, 107976. doi: 10.1016/j.agee.2022.107976

frontiers | Frontiers in Plant Science

TYPE Original Research
PUBLISHED 08 February 2024
DOI 10.3389/fpls.2024.1303750

Check for updates

OPEN ACCESS

EDITED BY
Raffaella Balestrini,
National Research Council (CNR), Italy

REVIEWED BY
Katarzyna Turnau,
Jagiellonian University, Poland
Luciano Avio,
University of Pisa, Italy

*CORRESPONDENCE
Andrea Genre
andrea.genre@unito.it

†These authors have contributed equally to this work and share first authorship

RECEIVED 03 October 2023
ACCEPTED 08 January 2024
PUBLISHED 08 February 2024

CITATION
Oddi L, Volpe V, Carotenuto G, Politi M, Barni E, Crosino A, Siniscalco C and Genre A (2024) Boosting species evenness, productivity and weed control in a mixed meadow by promoting arbuscular mycorrhizas.
Front. Plant Sci. 15:1303750.
doi: 10.3389/fpls.2024.1303750

COPYRIGHT
© 2024 Oddi, Volpe, Carotenuto, Politi, Barni, Crosino, Siniscalco and Genre. This is an open-access article distributed under the terms of the Creative Commons Attribution License (CC BY). The use, distribution or reproduction in other forums is permitted, provided the original author(s) and the copyright owner(s) are credited and that the original publication in this journal is cited, in accordance with accepted academic practice. No use, distribution or reproduction is permitted which does not comply with these terms.

Boosting species evenness, productivity and weed control in a mixed meadow by promoting arbuscular mycorrhizas

Ludovica Oddi†, Veronica Volpe†, Gennaro Carotenuto†, Mara Politi, Elena Barni, Andrea Crosino, Consolata Siniscalco and Andrea Genre*

Department of Life Sciences and Systems Biology, University of Turin, Turin, Italy

Lowland meadows represent aboveground and belowground biodiversity reservoirs in intensive agricultural areas, improving water retention and filtration, ensuring forage production, contrasting erosion and contributing to soil fertility and carbon sequestration. Besides such major ecosystem services, the presence of functionally different plant species improves forage quality, nutritional value and productivity, also limiting the establishment of weeds and alien species. Here, we tested the effectiveness of a commercial seed mixture in restoring a lowland mixed meadow in the presence or absence of inoculation with arbuscular mycorrhizal (AM) fungi and biostimulation of symbiosis development with the addition of short chain chito-oligosaccharides (CO). Plant community composition, phenology and productivity were regularly monitored alongside AM colonization in control, inoculated and CO-treated inoculated plots. Our analyses revealed that the CO treatment accelerated symbiosis development significantly increasing root colonization by AM fungi. Moreover, the combination of AM fungal inoculation and CO treatment improved plant species evenness and productivity with more balanced composition in forage species. Altogether, our study presented a successful and scalable strategy for the reintroduction of mixed meadows as valuable sources of forage biomass; demonstrated the positive impact of CO treatment on AM development in an agronomic context, extending previous observations developed under controlled laboratory conditions and leading the way to the application in sustainable agricultural practices.

KEYWORDS

arbuscular mycorrhizas, forage plants, fungal inoculum, grass-legume seed mixture, pastoral value, mixed meadow, chito-oligosaccharides, sustainable agriculture

Introduction

In an agricultural context, management intensification is a major driver of biodiversity loss (Sala et al., 2000; Foley et al., 2005; Culman et al., 2010). Despite their importance, lowland meadows are critically endangered habitats in many European countries, because of hydrological perturbation and land-use change leading to the decline of meadow cover

area and distribution, and the alteration of their species composition (Poschlod et al., 2005). The category of 'agricultural grasslands' includes silage and hay fields, pastures under intensive production, and semi-natural grasslands. Over the last decades, silage made from arable crops such as maize has become much more widely adopted in irrigated areas than hay production, due to economic reasons, with serious consequences on biodiversity at different trophic levels, such as high mortality of ground-nesting birds and resource removal for other taxa, especially pollinators (Stoate et al., 2009).

Furthermore, the intensive use of pesticides, herbicides, and fertilizers had a strong impact on soil biodiversity, causing cultivated varieties to become partially reluctant to the development of beneficial interactions with soil-borne microorganisms (Duhamel and Vandenkoornhuyse, 2013). Moreover, humans significantly altered the composition of many natural plant communities through the deliberate or accidental introduction of exotic species (Van der Putten et al., 2007; Milardi et al., 2020), reducing biodiversity and compromising ecosystem functionality (Griffiths and Philippot, 2013; Agathokleous et al., 2020). Several studies reported that repeated monoculture cropping, the inclusion of non-mycorrhizal crops within rotation and fallowing affect mycorrhizal activity and decrease crop yields (Baltruschat and Dehne, 1988; Hetrick et al., 1996; Douds et al., 1997; Arihawa and Karasawa, 2000; Harrier and Watson, 2004).

In addition to their importance for biodiversity, lowland meadows also provide significant ecosystem services: water retention and filtration, forage production, soil protection from erosion and contribution to its fertility, and potential for carbon sequestration (Hopkins and Holz, 2006; Stoate et al., 2009). Finally, lowland grasslands also have a significant aesthetic value and support recreation in the countryside (Boval and Dixon, 2012).

Besides its ecological implications, the biodiversity of lowland meadows also provides several benefits for farmers. Indeed, the presence of functionally different plant species improves forage quality and nutritional value. In this frame, French (2017) demonstrated that forage from species-rich grasslands contained more protein, phosphorus, potassium, and calcium than cereals and conventional hay. Moreover, higher biodiversity, especially in terms of functional dispersion and species evenness, enhances the productivity of plant communities and consequently reduces available space for the establishment of weeds and alien species, representing an effective and low-cost strategy for weed control (Sanderson et al., 2012; Suter et al., 2017).

For all these reasons, the reintroduction of lowland meadows has become a major goal in the last two decades, in particular in cattle farms where both animal health and dairy product quality take advantage of hay-based feeding. Moreover, grasslands management requires lower energy and fertilizer input than cereals, thus supporting more efficient, sustainable, and adaptable agricultural practices with a reduced environmental impact, especially in those farms where grasslands were replaced decades ago by cereal monoculture. Lastly, permanent grasslands constitute no tillage areas, with a major positive impact on the maintenance of the microbial communities in the soil (Guldberg et al., 2022).

When comparing the results of different agronomic techniques in restoring meadow biodiversity, Sengl et al. (2017) found that sod transplantation and hay transfer were more successful than seeding. However, sod transplantation requires the destruction of valuable grassland habitat, whereas hay transfer is often associated with low seed germination rate; furthermore, both approaches require the availability of source sites and are relatively expensive. As a consequence, the use of commercial seed mixtures remains the most convenient technique in highly productive areas, albeit its weak effectiveness in biodiversity restoration needs to be improved.

This goal can be achieved by exploiting the potential of soil microbial biodiversity in influencing plant diversity in grasslands. Although the functional implications for restoration require further investigations, the soil communities of diverse grasslands tend to be dominated by decomposer fungal communities and mycorrhizal networks (Bardgett, 1996; Smith et al., 2003; Walker et al., 2004). In particular, the latter are believed to play a key role in driving ecosystem processes, such as nutrient cycling and plant productivity, as well as controlling community composition and structure during the early phases of succession (Walker et al., 2004).

Arbuscular mycorrhiza (AM), involving root colonization by specialized soil fungi belonging to Glomeromycotina, represents the most widespread plant symbiosis (Genre et al., 2020). Indeed, around 72% of plant species - including the vast majority of forage and crop plants - host AM fungi in their root tissues. By exploring a larger volume of soil, the extraradical mycelium grants roots a more efficient access to mineral nutrients (namely phosphorus and nitrogen) and water (Smith et al., 2010). Furthermore, AM symbiosis increases plant tolerance to water stress and reinforces defense against pathogens (Shi et al., 2023). In return, AM fungi are fed with a percentage of plant metabolites, such as sugars and lipids, that are essential for the completion of their life cycle, in a truly mutualistic relationship (Smith and Read, 2008; Jiang et al., 2017; Keymer et al., 2017; Luginbuehl et al., 2017).

In this frame, due to their broad host range, different AM fungi have been shown to provide different degrees of benefits to different host species, overall generating a complex and versatile exchange mechanism that influences the structure of plant communities (van der Heijden et al., 2015) and has been likened to a biological market (Wyatt et al., 2014). Generally, AM fungal diversity was observed to be positively related to plant species diversity and productivity, due to a relaxation of plant competitive interactions and to the promotion of subordinate species (Bardgett, 1996; Walker et al., 2004). Moreover, mycorrhizas may promote seedling establishment with important advantages in the early stages of development of the plant community (van der Heijden, 2004).

Concerning forage species, evidence is accumulating that their symbiotic status is a basic requirement for sustainable feed production and any advance in the optimization of this symbiotic system may lead to an improvement in forage productivity and nutritional properties (Baslam et al., 2014; Hack et al., 2019). Therefore, due to their ecological and nutritional functions, AM fungi must be seen as an important biotechnology in sustainable agriculture, leading to improved agricultural management of soil and crops (Lanfranco et al., 2016) and eventually increasing the efficiency of lowland meadow restoration.

Currently, the most commonly introduced change in soil management to promote AM associations has been to limit acknowledged harmful practices, such as deep tillage and fungicide use, and introduce AM fungal inocula in crop fields. The main drawback in this approach is related to the lack of information on how a commercial AM fungal strain is performing with each crop species and variety; how it adapts to local soil and climate conditions; how it competes with the native AM fungal community (Douds et al., 2005; Gosling et al., 2006). Furthermore, due to the prolonged selection of crop cultivars for their productivity in highly fertilized soils (with rather limited attention to their symbiotic associations), many cultivated species are recalcitrant to engage in AM symbiosis and AM inoculation alone may have limited effects on their mycorrhizal status (Duhamel and Vandenkoornhuyse, 2013).

An innovative approach to address this problem has been to boost pre-symbiotic signaling by exogenously treating the plants with fungal molecules that promote symbiosis development. Such mycorrhizal factors (or myc-factors) are known to be released by symbiotic fungi and trigger cellular and molecular responses that accelerate symbiosis establishment (Volpe et al., 2023). In this frame, short chain chito-oligosaccharides (COs) have been shown to be recognized as myc-factors in a wide range of host plants, including legumes and monocots (Genre et al., 2013; Sun et al., 2015) and their use as promoters of AM establishment paved the way to possible applications in sustainable agriculture and pasture management (Volpe et al., 2020; Volpe et al., 2023).

In this research we tested the effectiveness of a commercial seed mixture in restoring a lowland mixed meadow in an area of the Po plain, where grasslands have been replaced by cereals for two decades. Furthermore, we evaluated the impact of a commercial AM inoculum combined with myc-factor treatment on the composition of the plant community and its productivity.

Materials and methods

Study area location and soil properties

The present study was carried out in South-Western Piedmont (Italy), in a 5 ha experimental field located in Monasterolo di Savigliano (Lat 44.6894147, Long 7.6196066) (Supplementary Figure S1). In order to prevent soil heterogeneity caused by the edge effect and uneven water distribution during flow irrigation, we decided to locate our experimental area in the central part of the field (Supplementary Figure S1). Soil homogeneity in the selected area was confirmed by the analysis of soil chemical properties (by Camera di Commercio di Torino; www.lab-to.camcom.it) in 5 sampling points distributed along the two diagonals crossing the experimental area.

The same sampling points were used to evaluate the presence and activity of the native AM fungal community at time zero. To this aim, 20x20x20 cm soil samples were collected from the soil surface. Soil samples were pooled and mixed with 20% sterilized sand (0.4-0.8 mm; Valle Po, Revello, CN, Italy) and used to fill 5 plastic pots (biological replicates), where a 2 cm layer of perlite had previously been introduced for draining. Two *Medicago sativa* seeds were planted in each pot and plants were grown in a greenhouse, supplied with tap water as needed and fertilized once per week with a modified Long Ashton nutrient solution (Hewitt, 1966) with a low phosphate content (3.2 μM), to allow AM development. After 4 months, the roots were sampled from each biological replicate and used to quantify AM colonization according to Trouvelot et al. (1986), as described below.

Experimental setup and sampling design

The experimental area (Supplementary Figure S2) was split into three plots, corresponding to an untreated control (CTR, 12.400 m^2), a mycorrhizal (MYC, 23.800 m^2), where seeds were coated with a commercial inoculum, and a CO-treated mycorrhizal plot (MYC+CO, 12.800 m^2), where seed coating was added with a mix of short chain COs (see below).

All samples were collected using the sampling scheme presented in Supplementary Figure S2. For each treatment six circular sampling areas (radius = 4 m) were identified and distributed at regular distances (15 m) along a longitudinal line in the central part of the three experimental plots (Supplementary Figure S2). Within each circular sampling area, soil and plant samples were randomly collected, avoiding previous sampling points. Sample collection was carried out immediately before mowing in three time points covering two productive seasons: April 2017/2018, July 2017/2018 and October 2017/September 2018. Two additional samplings devoted to AM colonization were carried out during winter (December 2016 and February 2018).

Seed mixture and sowing

The field was plowed and sown in October 2016,with a mixture of commercial native species (Supplementary Figure S3), composed of *Dactylis glomerata* cv. Dactyna (40%; 12.3 kg/ha), *Festuca arundinacea* cv. Kora (20%; 13.8 kg/ha), *Trifolium pratense* cv. Krinya o Nike (10%; 3.7 kg/ha), *Poa pratensis* cv. Balin (5%; 0.6 kg/ha), *Medicago sativa* cv. Vogherese Padus (20%; 10.9 kg/ha) and *Festulolium* cv. Becva (5%; 3.7 kg/ha).

AM inoculum and CO treatment

The commercial microbial inoculum Micosat F (Supplementary Table S1; CCS Aosta S.r.l.) was used in MYC and MYC+CO plots. In more detail, the seed mixture used for the MYC plot was coated with 1 kg/ha of Micosat F by mixing the inoculum powder with the seed mixture inside the hopper tank, immediately before sowing. For CO treatments, 100g/ha of powder containing a mixture of short chain chito-oligosaccharides (CO2-CO5; Zhengzhou Sigma Chemical Co., Ltd. Zhengzhou, Henan, China) were added to the seed coating, alongside the inoculum. A second CO treatment was applied in November 2017, by spraying a 1 g/L CO solution in water on the meadow, using a tractor-operated bar sprayer. Specifically,

we sprayed 100 L/ha of CO solution for the MYC+CO plot and 100 L/ha of water for MYC and CTR plots.

Biomass and plant community analyses

To estimate forage productivity, aboveground plant biomass was collected from each sampling point by mowing all the plant material at the soil surface inside a 30x30 cm wooden frame randomly located within the circular sampling area, avoiding previous sampling points. After collection, biomass was immediately transferred to the lab and manually sorted into grasses, forbs and weeds. All the sorted samples were then oven-dried at 65°C for 24 hours and weighed to measure the dry mass.

Plant community composition was analyzed through vegetation surveys based on vertical point quadrat transects (Daget and Poissonet, 1971). Three 15-meter long transects were located alternately between sampling points and records of the plant species contacts were performed every 0.50 m for a total of 30 contact points per transect and 90 contact points per treatment.

These data were used to calculate alpha diversity considering the total number of plant species and evenness Pielou index.

The pastoral value (PV) of the meadows under different experimental conditions (see below) was calculated according to the equation (Daget and Poissonet, 1971):

$$PV = \frac{\sum_{i=1}^{n} SC_i \times ISQ_i}{5}$$

where SC_i is the specific contribution (i.e. the percentage of each species in the total vegetation as derived from the Daget-Poissonet method), and ISQ_i is the Index of Specific Quality (ranging between 0 and 5 as shown in Supplementary Table S2), depending on the preference, morphology, structure, and productivity of the plant species (Cavallero et al., 1992; Cavallero et al., 2002; Cavallero et al., 2007). The resulting PV ranges between 0 and 100.

Quantitative analysis of AM colonization

Roots were isolated by rinsing each soil sample with tap water. Six biological replicates consisting of at least 1 m of root were analyzed for each sampling point and used for morphological and quantitative analyses. Root samples were carefully cleared of adhering soil debris and then stained in 0.1% (W/V) cotton blue in lactic acid for at least 12 h, destained in freshly prepared lactic acid solution for 3-4 times and cut into 1 cm-long segments. The segments were then placed on microscope slides and mounted in glycerol for observation in bright-field microscopy. AM colonization level was quantified in each segment according to Trouvelot et al. (1986).

Statistical analyses

Statistical analysis and figure creation were performed using R 4.3.0 (R Core Team, 2023) and the packages 'betapart', 'devtools', 'dplyr', 'ggplot2', 'ggtern', 'indicspecies', 'mass', 'multcomp', 'pairwiseAdonis', 'Rmisc', and 'vegan'. In the case of data showing normal distribution (i.e., aboveground plant biomass), the differences among treatments were tested for significance using generalized linear models (GLMs) followed by Tukey's HSD *post hoc* test for multiple comparisons, with a single-step method to calculate adjusted p-values (95% CI). When data were not normally distributed (i.e., frequency of AM colonization, species richness, Pielou index, biomass composition, and pastoral value) the non-parametric Kruskal-Wallis test by rank was performed, followed by the pairwise Wilcoxon rank sum tests and p-value Bonferroni adjustment method, to calculate pairwise comparisons between group levels with corrections for multiple testing.

To test the differences in plant community structure and composition multivariate analyses were performed. Firstly, we calculated the beta dispersion of Bray-Curtis dissimilarity matrices and tested it for homogeneity among treatments. Afterwards, since the assumption of homogeneity was verified, we performed a permutational multivariate analysis of variance (PERMANOVA) using the wrapper function 'pairwise.adonis' for multilevel pairwise comparison and p-value Bonferroni adjustment method.

Results

Soil properties

A preliminary chemical analysis of 5 samples was shown in the Supplementary Figure S1, with an average of a pH of 6.3, a 7.36 C/N ratio, 20.4 and 35.2 g/kg content in organic carbon and organic matter, respectively. The soil resulted to be particularly rich in assimilable nitrogen (0.3%) and phosphate (64.8 mg/kg), a condition that does not favor AM development (Balzergue et al., 2013; Wang et al., 2017). Nevertheless, our microcosm experiment resulted in a high level of root colonization in the trap plants of *M. sativa*, with a mycorrhizal frequency (F%) of 50% and arbuscular abundance (A%) close to 10% (Supplementary Figure S4).

AM colonization

The quantification of symbiotic fungal structures in root samples from each experimental plot over time is presented in Figure 1A. The most apparent feature, present in all the three treatments, is a seasonal cycle of mycorrhization intensity, with a progressive increase through winter, a peak in spring-early summer and a subsequent drop. The evident shift in the colonization peak from April (2017) to July (2018) should be ascribed to climate variability between years. In particular, the spring of 2017 was rather dry and warm, whereas relatively low temperatures were registered until May 2018, with abundant rain (Supplementary Figure S5).

MYC treatment did not significantly change this seasonal pattern compared to CTR plants, even if a limited (and statistically significant) increase in root colonization was recorded

10.3389/fpls.2024.1303750

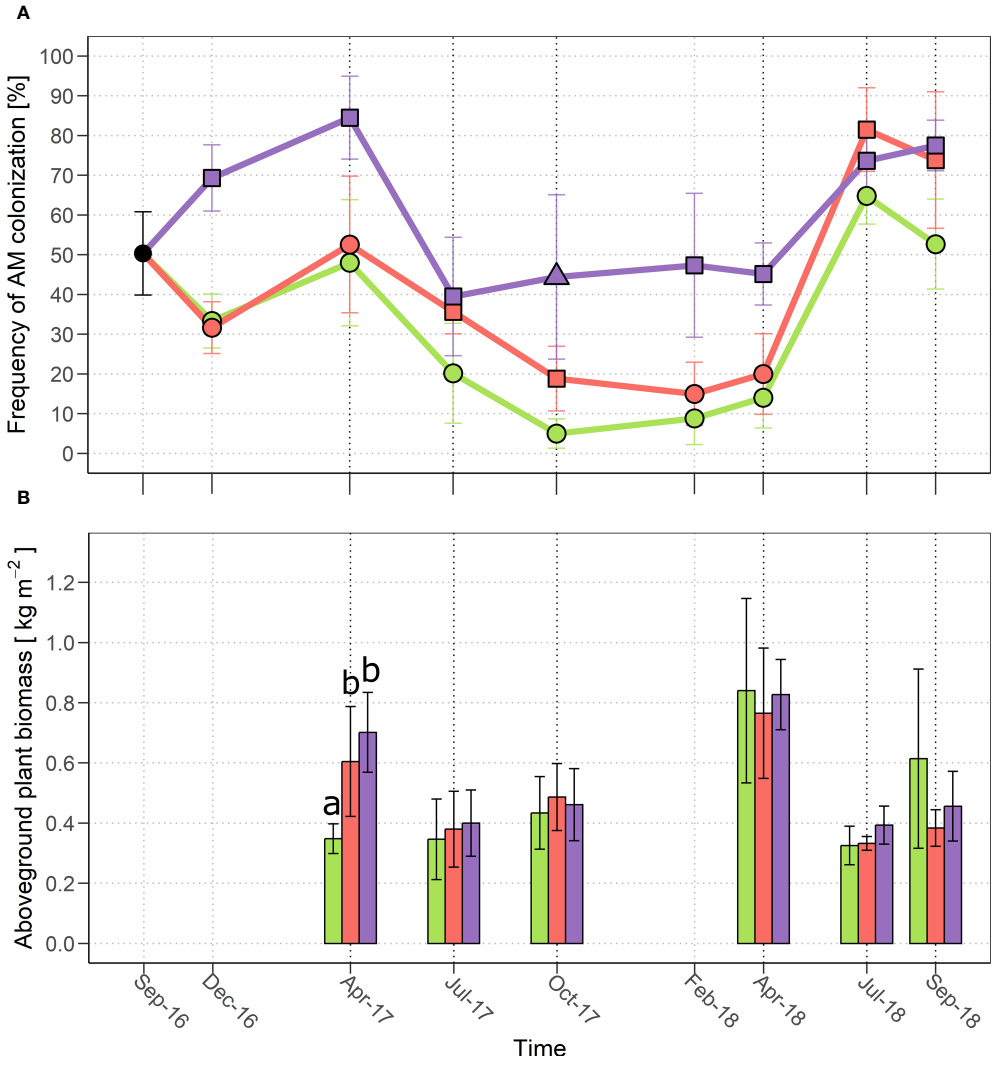

FIGURE 1
(A) Frequency of AM colonization and **(B)** aboveground plant biomass productivity from (October 2016) to September 2018 in the three treatments: control (green), MYC (orange) and MYC+CO (purple). In **(A)** different symbols indicate statistically significant differences among treatments ($p < 0.05$) within a single time point; in **(B)** significant differences among treatments are indicated by different letters. Error bars represent ± SD.

over the summer of both 2017 and 2018, suggesting that microbial inoculation had a positive effect on the AM community and symbiosis development.

By contrast, MYC+CO treatment produced a major increase in AM colonization compared to both MYC and CTR conditions, throughout the initial phase of the project, from December 2016 to April 2017; the samples from July 2017 are the only exception, as the general summer decline lowered root colonization to a level that was equivalent to the other two experimental conditions. In more detail, the most important increase was recorded immediately after sowing, in December 2016 and April 2017, when root colonization in MYC+CO plants exceeded 80%, compared to values close to 50% for CTR and MYC plants. The MYC+CO treatment granted a higher level of mycorrhization also between October 2017 and April 2018 (constantly above 40%, compared to values between 10% and 20% for MYC and CTR). Due to the progressive increase in AM development from 2017 to 2018, all experimental plots reached a comparable level of colonization in July 2018 and a significantly higher colonization level (above 70%) was maintained in MYC and MYC+CO compared to CTR plants (50%) in September 2018.

Lastly, besides the recursive seasonal cycle and irrespectively of the plot treatment, a general increase in AM colonization was observed between the first season (July-October 2017) and the second one (July-October 2018) across all samples. The occurrence of this increase also in the CTR plot, suggests that the mixed meadow management had a positive impact, over time, on the activity of the native AM community also in the absence of any additional treatment.

Plant productivity

Concerning plant productivity, in 2017 MYC (2.98 ± 0.57 kg m^{-2}) and MYC+CO (2.80 ± 0.21 kg m^{-2}) produced a significantly higher

10.3389/fpls.2024.1303750

($p< 0.01$) amount of aboveground biomass compared to CTR (2.30 ± 0.19 kg m^{-2}). Furthermore, a significantly higher production ($p< 0.001$) was observed in MYC (+0.25 kg m^{-2}) and MYC+CO (+0.35 kg m^{-2}) compared to CTR plants in April 2017 (Figure 1B). Nevertheless, this pattern was not recorded in 2018, when the aboveground plant productivity did not differ significantly among treatments.

Plant community composition

The analysis of community alpha diversity showed that the total number of plant species did not significantly differ among the three treatments in 2017 and 2018 (Figure 2A). Concerning the distribution of abundances across the species in the community, a significant ($p< 0.05$) difference was observed after sowing in April 2017, when MYC and MYC+CO showed greater values of Pielou index (Figure 2B) suggesting the absence of a strongly dominating species, which instead was present in the control meadow, where *Festulolium* constituted more than half of the meadow in terms of relative percentage cover. In general, we observed an increase in the number of species as well as in the community evenness from 2017 to 2018, and a homogenization of the samples showed by a decrease in the standard deviation values (Figure 2A, B).

The overall plant community composition significantly differed among all treatments in both 2017 (R^2 = 0.47; F = 6.66,

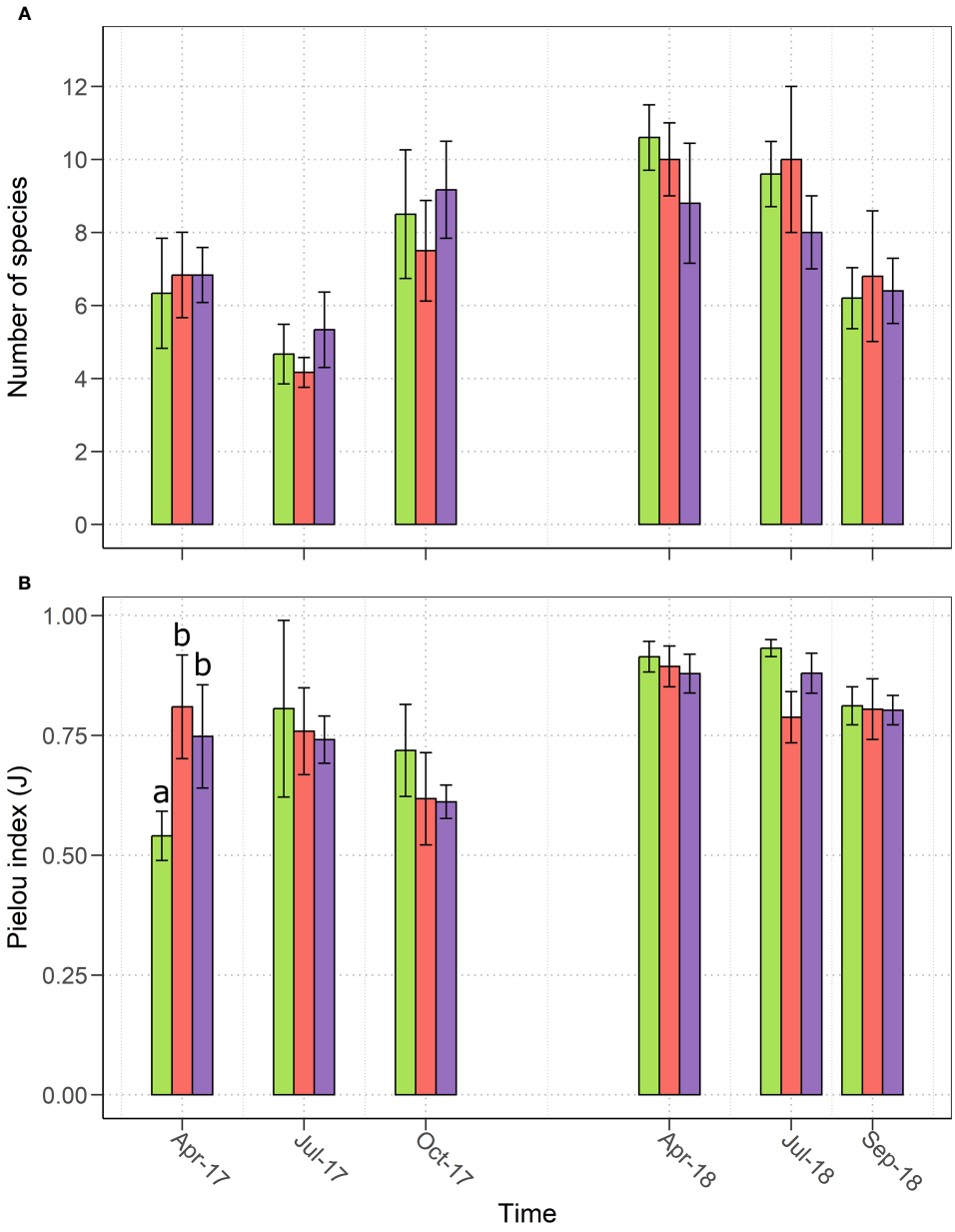

FIGURE 2
(A) Species richness and **(B)** Pielou evenness index **(J)** observed from April 2017 to September 2018 in the three treatments: control (green), MYC (orange) and MYC+CO (purple); significant differences among treatments are indicated by different letters. Error bars represent ± SD.

$p = 0.001$) and 2018 ($R^2 = 0.62$; F = 9.72, $p = 0.001$). In particular, the MYC+CO community was significantly different from both CTR (2017: $p = 0.01$; 2018: $p = 0.04$) and MYC (2017: $p = 0.02$; 2018: $p = 0.03$) treatments throughout the two years of the study.

As summarized in Figure 3A-C, the seasonal pattern in 2017 revealed significant differences in plant species composition among treatments at the beginning (April) and at the end (September-October) of the growing season, whereas plant community composition did not differ significantly among treatments during summer (June-July). By contrast, 2018 was characterized by a constant statistically significant difference among treatments. Moreover, pairwise comparison highlighted that, in 2017, these differences were mainly due to significant differences between CTR and the two inoculated treatments (MYC and MYC+CO) (Figure 3A, B), while in 2018 the three treatments showed consistent differences that were always –significant (Figures 3A-C).

The indicator species analysis (Table 1) showed that, in 2017, *Festulolium* was significantly associated with CTR, whereas *Medicago sativa*, *Trifolium pratense* and were significantly associated with MYC+CO treatment. Remarkably, indicator species association changed in 2018, with *Festulolium* significantly associated with MYC, and *Dactylis glomerata* and *Poa trivialis* associated with MYC+CO.

Biomass composition and pastoral value

The analysis of the biomass composition in terms of plant functional groups highlighted that grass, legume and weed contribution to the aboveground biomass changed in the two seasons (Figure 4). In more detail, grass ($\chi^2 = 9.58$, $p < 0.01$) and legume ($\chi^2 = 6.47$, $p < 0.05$) contribution to the plant biomass composition in 2017 showed significant differences between treatments. Moreover, in 2018 significant differences among treatments were recorded for grass ($\chi^2 = 7.38$, $p < 0.05$), legume ($\chi^2 = 9.98$, $p < 0.01$) and weed ($\chi^2 = 9.55$, $p < 0.01$) contribution to the biomass. Overall, in 2017 the plant biomass produced in the MYC+CO treatment showed a significantly lower ($p < 0.05$) percentage of grasses compared to CTR and MYC, whereas the percentage of legume biomass was significantly higher ($p < 0.05$) in both MYC and MYC+CO compared to CTR (Table 2). In 2018, CTR contained the highest percentage of weeds showing significant differences ($p < 0.01$) with MYC+CO. Lastly, CTR showed the lowest legume contribution to the plant biomass, with significant differences ($p < 0.05$) with both MYC and MYC+CO (Table 2). In conclusion, the MYC+CO treatment displayed a better balance between grass and legume percentage contribution to plant biomass productivity, and the lowest percentage of weeds.

The above-mentioned differences in the plant community composition in terms of species evenness and functional group contribution to the aboveground biomass, led to significant differences in the pastoral value of the forage collected during the growing season (Figure 5), which, in 2018, was significantly ($p < 0.01$) higher in MYC+CO compared to CTR and MYC.

Discussion

The current study provides first evidence that the combined application of CO and a mycorrhizal inoculum during sowing of a mixed meadow promotes AM symbiosis under field conditions, at least in the first year of application, in line with previous studies in controlled laboratory conditions (Volpe et al., 2020; Volpe et al., 2023), and has a major impacts on plant community. However, mixed meadow management had a positive impact, over time, on the activity of the native AM community also in the absence of any additional treatment. Previous studies have demonstrated the CO-dependent promotion of AM under controlled conditions (Volpe et al., 2020). More recent investigations studies, carried out in the model legume *Medicago truncatula*, revealed that the observed acceleration of AM development in CO-treated plants was correlated with the stimulation of pre-symbiotic responses in the host root, including the regulation of gene expression and the triggering of cellular responses that are known to take place during early fungal colonization (Volpe et al., 2023). Our current observation of a comparable promotion of AM colonization under field conditions confirms CO bioactivity and efficiency also in an agricultural context, short of the presence of natural uncontrollable environmental variables, and represents a major advancement toward the use of CO as biostimulants in sustainable agriculture.

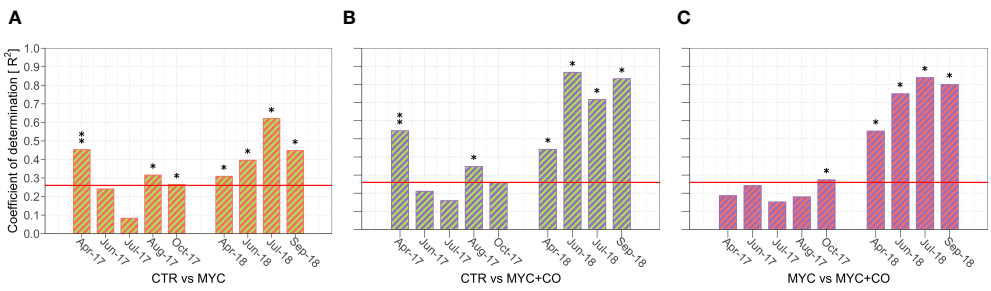

FIGURE 3
(A-C) Results of the pairwise comparison showing the proportion of variance (R^2) in the plant community composition (response variable) explained by the treatment factor (explanatory variable). **(A)** shows the differences between the plant community composition of CTR and MYC, **(B)** between CTR and MYC+CO, and **(C)** between MYC and MYC+CO. The bars overcoming the red horizontal line correspond to significant differences between plant communities: (*) p-value< 0.05 and (**) p-value< 0.001.

10.3389/fpls.2024.1303750

TABLE 1 Results of the indicator species analyses showing the species that were significantly associated with each treatment in 2017 and 2018; only significant *p-values* were reported.

Plant species	CTR		MYC		MYC+CO	
	2017	2018	2017	2018	2017	2018
Festulolium	0.0004			0.0144		
Medicago sativa					0.0074	
Trifolium pratense					0.0069	
Dactylis glomerata						0.0007
Poa trivialis						0.0085

Boosting AM colonization, productivity and plant community composition

In more detail, our results showed that the frequency of AM colonization in plant roots was significantly higher in the meadow treated with a combination of CO and a commercial microbial inoculum (MYC+CO) compared to both the untreated meadow (CTR) and the meadow treated only with the commercial inoculum (MYC), and this increase was most noticeable during the first months following the treatment (April 2017 sampling).

This booster effect of CO application on AM development was not mirrored on the increase of aboveground biomass. A significantly higher productivity was in fact recorded in April 2017 for both MYC+CO and MYC meadow compared to control conditions, the higher average value of MYC+CO samples not being significantly different from the MYC samples. The increase in plant biomass production upon AM inoculation, known as the 'growth effect', is related to both the direct improvement of plant nutrition by AM fungi and - particularly in natural and agronomical ecosystems - the establishment of synergistic interactions with other beneficial microorganisms, such as plant-growth promoting rhizobacteria (PGPRs), nitrogen fixing and phosphate-solubilizing bacteria (Raklami et al., 2019). Furthermore, a faster plant development and/or a greater vegetation density can be the consequence of the improved root system development (Kalamulla et al., 2022) and better seedling establishment in inoculated fields (van der Heijden, 2004; Zhang et al., 2012).

Plant community composition was also affected by our treatments: MYC and MYC+CO meadows showed significantly different species assemblage and a significantly higher species evenness compared to control in April 2017. A lower percentage cover of grasses (especially *Festulolium*), which instead dominated the control, was observed in both inoculated meadows, in favor of a higher cover of forb species, such as *Medicago sativa* and *T. pratense*. This observation is consistent with previous studies establishing that AM colonization tends to increase plant species diversity when the dominant species in the community is a weakly mycotrophic plant, such as annual species and C3 grasses (e.g., *Festulolium*), by increasing the competitive ability of the subordinate species that generally are represented by perennial forbs and legumes such as *M. sativa* and *T. pratense* (Karanika et al., 2008; Bahadur et al., 2019).

Moreover, the increased belowground competitiveness of legume species may generate a positive feedback in the aboveground competition, especially in the case of *M. sativa*, whose extensive canopy can reduce light access by neighboring species (Klabi et al., 2014). Weed suppression through increased functional dispersion represents an additional benefit to the multiple ecosystem services of forage mixtures for sustainable grassland production. Such benefits can arise from positive species interactions and complementary use of resources (Nyfeler et al., 2011; Hoekstra et al., 2016), suggesting that high-yielding mixtures capture and transform increased amounts of resources into biomass (van Ruijven and Berendse, 2005). Moreover, Suter et al. (2017) found that functionally diverse grass-legume

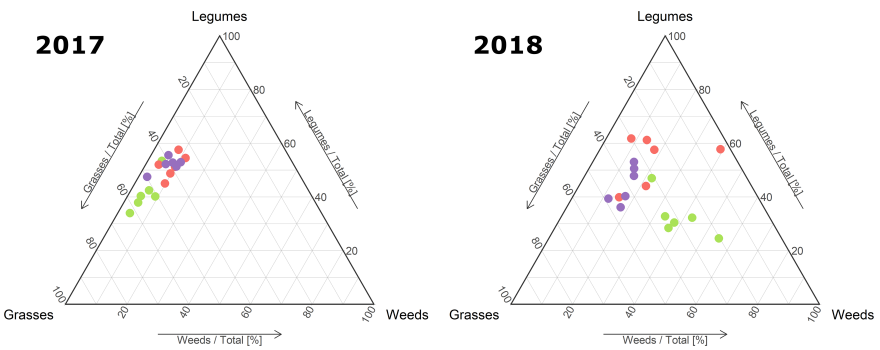

FIGURE 4
Ternary plot of grass, legume and weed contribution [%] to the forage biomass during 2017 and 2018 in the three treatments: CTR (green), MYC (orange) and MYC+CO (purple).

TABLE 2 Mean annual values (± standard deviation) of the percentage contribution to the forage biomass of three plant functional groups during 2017 and 2018; for each functional group, values in bold are significantly different from the other treatments in the same year.

Year	Treatment	Grasses [%]	Legumes [%]	Weeds [%]
2017	CTR	**53.22 ± 6.86**	**41.38 ± 6.58**	5.40 ± 1.91
	MYC	39.61 ± 4.74	51.51 ± 4.38	8.87 ± 2.56
	MYC+CO	40.51 ± 4.80	52.07 ± 2.64	7.42 ± 3.07
2018	CTR	29.43 ± 5.56	**32.60 ± 7.65**	37.97 ± 10.82
	MYC	27.10 ± 13.84	53.73 ± 9.34	19.18 ± 10.71
	MYC+CO	**40.41 ± 6.41**	44.54 ± 6.86	**15.04 ± 2.16**

mixtures can also have direct effects on plant community composition by reducing weed biomass and survival, and consequently the need for herbicide use, in particular when the mixture includes species of different rooting depth (as in the case of the shallow-rooted *Lolium perenne* and the deep-rooted *Trifolium pratense*). Furthermore, the fast development of the sown species in the first months after sowing is critical to reduce weed establishment and reproduction by limiting available resources (light, water, and minerals) (Weisberger et al., 2019), with a direct impact on the community composition over a longer period of time after meadow establishment.

The observed differences in the plant community structure had important implications for forage quality, so that, during the second year of the study, when the three meadows showed the greatest differences in terms of species composition, we found a significantly higher pastoral value in MYC+CO compared to MYC and control. This finding was consistent with the higher contribution of legumes and the lower contribution of weeds to the aboveground biomass of the MYC+CO meadow. Indeed, legume species generally show a higher Index of Specific Quality (ISQ) for their productivity, palatability, and preference by livestock (Cavallero et al., 2007). Furthermore, legumes enrich the forage protein content with positive effects on its quality (French, 2017). A similar effect was observed also for the grass species *Dactylis glomerata*, which in our study was found to be significantly associated with the MYC+CO meadow (French, 2017). Although we did not perform a chemical characterization of the forage, previous studies found increased P levels in forage from AM inoculated plants (Smith et al., 2003; Chippano et al., 2021).

Applicative perspectives

AM fungal development is known to be subject to seasonal cycles that impact on spore germination and mycelial growth in the soil, as well as the colonization of host roots (Jakobsen et al., 2003; Kemmelmeier et al., 2022). Under this respect, the temporal extension of this study (i.e., 24 months) allowed us to investigate the effect of AM inoculation and CO treatment over a markedly longer period of time compared to previous studies. In this frame, while the early boost in AM colonization of MYC+CO plant roots was remarkable, a significant effect was also evident during the July-October 2017 period, while after our second CO application by spray, AM colonization levels were constantly and significantly higher in MYC+CO compared to both MYC and CTR samples but did not show any booster effect. This pattern is in line with the promotion of symbiosis development by exogenous CO application in controlled conditions (Volpe et al., 2020). Nevertheless, the observation of such a marked effect under field conditions - and over a period of several months after each treatment - is particularly significant and reinforces the conclusion that CO application has long term effects on AM symbiosis (Volpe et al., 2023).

The observed rise in AM colonization of MYC and CTR plants during the summer of the second year of this investigation (with root colonization of MYC plants reaching the same level as MYC+CO samples), warrants a distinct, yet equally significant, consideration. Most likely, this is the result of the revitalization of both native and inoculated AM propagules following the establishment of the mixed meadow after decades of monocultures (Johnson et al., 2005; Fester and Sawers, 2011). This effect of plant biodiversity on soil microbial population is well known but does not weaken the usefulness of either AM inoculation or CO application: the combination of these treatments at sowing can in fact support the early development and stabilization of symbiotic associations in the delicate period of meadow establishment.

Altogether, the combined impact of mixed sowing and mixed microbial inoculation on soil microbial activity - of which AM colonization was used here as a proxy - is very promising for regenerative and sustainable agricultural applications. In this scenario, the introduction of CO treatment has been a catalyst for AM development since the early months: a significant advantage for farmers, thanks to the positive effect of AM colonization on plant nutrition and health (Johnson et al., 2005).

Following this first study, focused on the plant community and a single group of beneficial microbes (AM fungi), it will now be very interesting to investigate the effect of microbial inoculation and CO treatment on the whole soil microbiota, through metagenomics analyses revealing the phylogenetic and functional composition of fungal and bacterial communities under each experimental condition. In this sense, it has already been demonstrated as the co-application of CO and AM fungi has an impact on the rhizosphere microecology, favoring the beneficial bacteria community and increasing soil microbial biomass carbon content (Ma et al., 2023). An intriguing aspect to be clarified is the effect of CO-dependent AM promotion on rhizobial infection in legumes, which host both symbionts in a largely unexplored physiological and metabolic balance.

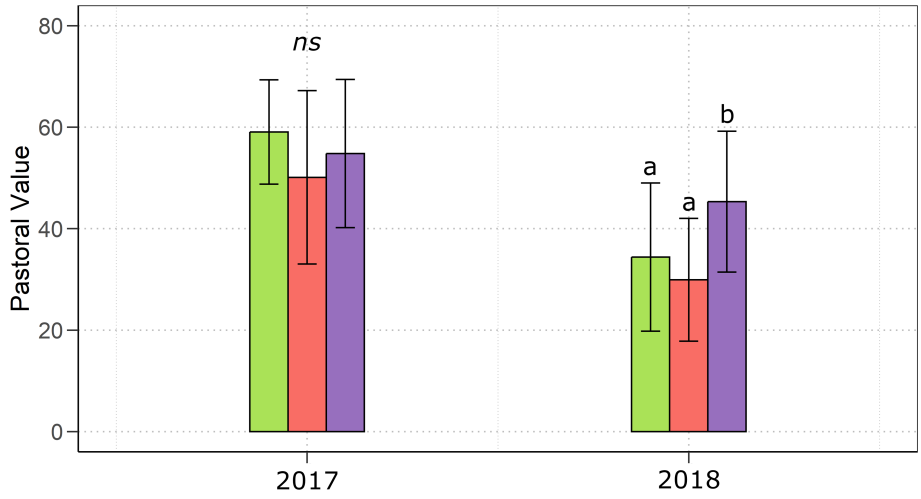

FIGURE 5
Annual mean pastoral value of the mixed meadows during the growing season 2017 and 2018 under the three different treatments: control (green), MYC (orange) and MYC+CO (purple). Error bars represent ± SD. Different letters indicate statistically significant differences; ns = non significant.

Lastly, an analogous approach to the one we used can be developed for the restoration of natural ecosystems with grasslands, another promising field of application for AM symbiosis and plant growth-promoting microbes in general (Singh Rawat et al., 2022).

Data availability statement

The raw data supporting the conclusions of this article will be made available by the authors, without undue reservation.

Author contributions

LO: Conceptualization, Data curation, Formal Analysis, Investigation, Methodology, Software, Supervision, Writing – original draft, Writing – review & editing. VV: Conceptualization, Data curation, Formal Analysis, Investigation, Methodology, Supervision, Writing – original draft, Writing – review & editing. GC: Conceptualization, Data curation, Formal Analysis, Investigation, Methodology, Supervision, Writing – original draft, Writing – review & editing. MP: Data curation, Investigation, Writing – review & editing. EB: Data curation, Investigation, Writing – review & editing. AC: Data curation, Investigation, Writing – review & editing. CS: Conceptualization, Funding acquisition, Investigation, Methodology, Resources, Supervision, Visualization, Writing – original draft, Writing – review & editing. AG: Conceptualization, Funding acquisition, Investigation, Methodology, Project administration, Resources, Supervision, Validation, Visualization, Writing – original draft, Writing – review & editing.

Funding

The author(s) declare financial support was received for the research, authorship, and/or publication of this article. This study was funded by Fondazione Cassa di Risparmio di Cuneo (Bando Ricerca Scientifica 2015 -Project AMforQuality).

Acknowledgments

A special thanks to the owners of 'La Corte' farm, Marco Bergese and Gianfranco Bergese, for being open and willing to help and collaborate in our study. We are grateful to Giusto Giovannetti for donating the inoculum Micosat F (CCS Aosta S.r.l.) that was essential for the study. We particularly appreciate the precious contribution of Andrea Cavallero and Marco Prati for his expertise and assistance during sowing. Finally, we thank all the students of the Department of Life Sciences and Systems Biology, University of Torino, who took part in fieldwork and lab experiments.

Conflict of interest

The authors declare that the research was conducted in the absence of any commercial or financial relationships that could be construed as a potential conflict of interest.

Publisher's note

All claims expressed in this article are solely those of the authors and do not necessarily represent those of their affiliated organizations, or those of the publisher, the editors and the reviewers. Any product that may be evaluated in this article, or claim that may be made by its manufacturer, is not guaranteed or endorsed by the publisher.

Supplementary material

The Supplementary Material for this article can be found online at: https://www.frontiersin.org/articles/10.3389/fpls.2024.1303750/full#supplementary-material

References

Agathokleous, E., Feng, Z., Oksanen, E., Sicard, P., Wang, Q., Saitanis, C. J., et al. (2020). Ozone affects plant, insect, and soil microbial communities: A threat to terrestrial ecosystems and biodiversity. *Sci. Adv.* 12, 1176. doi: 10.1126/sciadv.abc1176

Arihawa, J., and Karasawa, T. (2000). Effect of previous crops on arbuscular mycorrhizal formation and growth of succeeding maize. *Soil. Sci. Plant Nutrit.* 46, 43–51. doi: 10.1080/00380768.2000.10408760

Bahadur, A., Batool, A., Nasir, F., Jiang, S., Mingsen, Q., Zhang, Q., et al. (2019). Mechanistic insights into arbuscular mycorrhizal fungi-mediated drought stress tolerance in plants. *Int. J. Mol. Sci.* 20, 1–18. doi: 10.3390/ijms20174199

Baltruschat, H., and Dehne, H. W. (1988). The occurrence of vesicular–arbuscular mycorrhiza in agro-ecosystems. 1. Influence of nitrogen fertiliser and green manure in continuous monoculture and in crop rotation on the inoculum potential of winter wheat. *Plant Soil* 107, 279–284. doi: 10.1007/BF02370558

Balzergue, C., Chabaud, M., Barker, D. G., Bécard, G., and Rochange, S. F. (2013). High phosphate reduces host ability to develop arbuscular mycorrhizal symbiosis without affecting root calcium spiking responses to the fungus. *Front. Plant Sci.* 29. doi: 10.3389/fpls.2013.00426

Bardgett, R. D. (1996). "Potential effects on the soil mycoflora of changes in the UK agricultural policy for upland grasslands," in *Fungi and environmental change*. Eds. J. C. Frankland, N. Magan and G. M. Gadd (Cambridge: Cambridge University Press), 163–183.

Baslam, M., Antolín, M. C., Gogorcena, Y., Muñoz, F., and Goicoechea, N. (2014). Changes in alfalfa forage quality and stem carbohydrates induced by arbuscular mycorrhizal fungi and elevated atmospheric CO2. *Ann. Appl. Biol.* 164, 190–199. doi: 10.1111/aab.12092

Boval, M., and Dixon, R. M. (2012). The importance of grasslands for animal production and other functions: a review on management and methodological progress in the tropics. *Animal* 6, 748–762. doi: 10.1017/S1751731112000304

Cavallero, A., Aceto, P., Gorlier, A., Lombardi, G., Lonati, M., Martinasso, B., et al. (2007). *I tipi pastorali delle Alpi piemontesi*. (Bologna, Italy: Alberto Perdisa Editore)

Cavallero, A., Rivoira, G., and Talamucci, P. (2002). "Pascoli," in *Coltivazioni erbacee*. Eds. R. Baldoni and L. Giardini (Bologna, Italy: Foraggere e tappeti erbosi. Patron Editore), 239–294.

Cavallero, A., Talamucci, P., Grignani, c., Reyneri, A., Ziliotto, U., Scotton, M., et al. (1992). Caratterizzazione della dinamica produttiva di pascoli naturali italiani. *Riv. di Agron.* 26, 325–343.

Chippano, T., Mendoza, R., Cofré, N., and García, I. (2021). Divergent root P uptake strategies of three temperate grassland forage species. *Rhizosphere* 17, 100312. doi: 10.1016/j.rhisph.2021.100312

Culman, S. W., Young-Mathews, A., Hollander, A. D., Ferris, H., Sánchez-Moreno, S., O'Geen, A. T., et al. (2010). Biodiversity is associated with indicators of soil ecosystem functions over a landscape gradient of agricultural intensification. *Landsc. Ecol.* 25, 1333–1348. doi: 10.1007/s10980-010-9511-0

Daget, P., and Poissonet, J. (1971). Une méthode d'analyse phytologique des prairies. *Annales. Agronomiques.* 22, 5–41.

Douds, D. D., Galvez., L., Franke-Snyder, M., Reider, C., and Drinkwater, L. E. (1997). Effect of compost addition and crop rotation point upon VAM fungi. *Agric. Ecosyst. Environ.* 65, 257–266. doi: 10.1016/S0167-8809(97)00075-3

Douds, D. D., Nagahashi J.R., G., Pfeffer, P. E., Kayser, W. M., and Reider, C. (2005). On-farm production and utilisation of arbuscular mycorrhizal fungus inoculum. *Can. J. Plant Sci.* 85, 15–21. doi: 10.4141/P03-168

Duhamel, M., and Vandenkoornhuyse, P. (2013). Sustainable agriculture: possible trajectories from mutualistic symbiosis and plant neodomestication. *Trends Plant Sci.* 18, 597–600. doi: 10.1016/j.tplants.2013.08.010

Fester, T., and Sawers, R. (2011). Progress and challenges in agricultural applications of arbuscular mycorrhizal fungi. *Crit. Rev. Plant Sci.* 30, 459–470. doi: 10.1080/07352689.2011.605741

Foley, J. A., DeFries, R., Asner, G. P., Barford, C., Bonan, G., Carpenter, S. R., et al. (2005). Global consequences of land use. *Science* 309, 570–574. doi: 10.1126/science.1111772

French, K. E. (2017). Species composition determines forage quality and medicinal value of high diversity grasslands in lowland England. *Agric. Ecosyst. Environ.* 241, 193–204. doi: 10.1016/j.agee.2017.03.012

Genre, A., Chabaud, M., Balzergue, C., Puech-Pagès, V., Novero, M., Rey, T., et al. (2013). Short-chain chitin oligomers from arbuscular mycorrhizal fungi trigger nuclear Ca2+ spiking in *Medicago truncatula* roots and their production is enhanced by strigolactone. *New Phytol.* 198, 190–202. doi: 10.1111/nph.12146

Genre, A., Lanfranco, L., Perotto, S., and Bonfante, P. (2020). Unique and common traits in mycorrhizal symbioses. *Nat. Rev. Microbiol.* 18, 649–660. doi: 10.1038/s41579-020-0402-3

Gosling, P., Hodge, A., Goodlass, G., and Bending, G. (2006). Arbuscular mycorrhizal fungi and organic farming. *Agric. Ecosyst. Env.* 113, 17–35. doi: 10.1016/j.agee.2005.09.009

Griffiths, B. S., and Philippot, L. (2013). Insights into the resistance and resilience of the soil microbial community. *FEMS Microbiol. Rev.* 37, 112–129. doi: 10.1111/j.1574-6976.2012.00343.x

Guldberg, F. T., Broman, N. I., Silva, S. S., Barnes, C. J., Bruun, H. H., and Ejrnæs, R. (2022). The biodiversity effect of reduced tillage on soil microbiota. *Ambio* 51, 1022–1033. doi: 10.1007/s13280-021-01611-0

Hack, C. M., Porta, M., Schäufele, R., and Grimoldi, A. A. (2019). Arbuscular mycorrhiza mediated effects on growth, mineral nutrition and biological nitrogen fixation of *Melilotus alba* Med. in a subtropical grassland soil. *Appl. Soil Ecol.* 134, 38–44. doi: 10.1016/j.apsoil.2018.10.008

Harrier, L. A., and Watson, C. A. (2004). The potential role of arbuscular mycorrhizal (AM) fungi in the bioprotection of plants against soil-borne pathogens in organic and/or other sustainable farming systems. *Pest Manage. Sci.* 60, 149–157. doi: 10.1002/ps.820

Hetrick, B. A. D., Wilson, G. W. T., and Todd, T. C. (1996). Mycorrhizal response in wheat cultivars: relationship to phosphorus. *Canad. J. Bot.* 74, 19–25. doi: 10.1139/b96-003

Hewitt, E. J. (1966). *Sand and water culture methods used in study of plant nutrition* (Farnham Royal, Bucks, England: England: Commonwealth Agricultural Bureaux).

Hoekstra, A. Y., Chapagain, A. K., and Zhang, G. (2016). Water footprints and sustainable water allocation. *Sustainability* 8, 20. doi: 10.3390/su8010020

Hopkins, A., and Holz, B. (2006). Grassland for agriculture and nature conservation: production, quality and multi-functionality. *Agron. Res. 4 (1)* pp, 3–20.

Jakobsen, I., Smith, S. E., and Smith, F. A. (2003). "Function and diversity of arbuscular mycorrhizae in carbon and mineral nutrition," in *Mycorrhizal ecology*. Eds. M. G. A. van der Heijden and I. R. Sanders (Berlin, Heidelberg: Springer), 75–92.

Jiang, Y., Wang, W., Xie, Q., Liu, N., Liu, L., Wang, D., et al. (2017). Plants transfer lipids to sustain colonization by mutualistic mycorrhizal and parasitic fungi. *Science* 356, 1172–1175. doi: 10.1126/science.aam9970

Johnson, D., Jdo, M. I., Genney, D. R., Anderson, I. C., and Alexander, I. J. (2005). How do plants regulate the function, community structure, and diversity of mycorrhizal fungi? *J. Exp. Bot.* 56, 1751–1760. doi: 10.1093/jxb/eri192

Kalamulla, R., Karunarathna, S. C., Tibpromma, S., Galappaththi, M. C. A., Suwannarach, N., Stephenson, S. L., et al. (2022). Arbuscular mycorrhizal fungi in sustainable agriculture. *Sustain* 14, 1–15. doi: 10.3390/su141912250

Karanika, E. D., Mamolos, A. P., Alifragis, D. A., Kalburtji, K. L., and Veresoglou, D. S. (2008). Arbuscular mycorrhizas contribution to nutrition, productivity, structure and diversity of plant community in mountainous herbaceous grassland of northern Greece. *Plant Ecol.* 199 (2), 225–234. doi: 10.1007/s11258-008-9427-9

Kemmelmeier, K., dos Santos, D. A., Grittz, G. S., and Stürmer, S. L. (2022). Composition and seasonal variation of the arbuscular mycorrhizal fungi spore community in litter, root mat, and soil from a subtropical rain forest. *Mycorrhiza* 32, 409–423. doi: 10.1007/s00572-022-01084-3

Keymer, A., Pimprikar, P., Wewer, V., Huber, C., Brands, M., Bucerius, S. L., et al. (2017). Lipid transfer from plants to arbuscular mycorrhiza fungi. *eLIFE* 6, e29107. doi: 10.7554/eLife.29107.051

Klabi, R., Hamel, C., Schellenberg, M. P., Iwaasa, A., Raies, A., and St-Arnaud, M. (2014). Interaction between legume and arbuscular mycorrhizal fungi identity alters the competitive ability of warm-season grass species in a grassland community. *Soil Biol. Biochem.* 70, 176–182. doi: 10.1016/j.soilbio.2013.12.019

Lanfranco, L., Bonfante, P., and Genre, A. (2016). The mutualistic interaction between plants and arbuscular mycorrhizal fungi. *Microbiol. Spectr.* 4 (6). doi: 10.1128/microbiolspec.FUNK-0012-2016

Luginbuehl, L. H., Menard, G. N., Kurup, S., Van Erp, H., Radhakrishnan, G. V., Breakspear, A., et al. (2017). Fatty acids in arbuscular mycorrhizal fungi are synthesized by the host plant. *Science* 356, 1175–1178. doi: 10.1126/science.aan0081

Ma, J., Xie, Y., Sun, J., Zou, P., Ma, S., Yuan, Y., et al. (2023). Co-application of chitooligosaccharides and arbuscular mycorrhiza fungi reduced greenhouse gas fluxes in saline soil by improving the rhizosphere microecology of soybean. *J. Environ. Manage.* 345, 118836. doi: 10.1016/j.jenvman.2023.118836

Milardi, M., Gavioli, A., Soana, E., Lanzoni, M., Fano, E. A., and Castaldelli, G. (2020). The role of species introduction in modifying the functional diversity of native communities. *Sci. Total. Environ.* 10, 134364. doi: 10.1016/j.scitotenv.2019.134364

Nyfeler, D., Huguenin-Elie, O., Suter, M., Frossard, E., and Lüscher, A. (2011). Grass–legume mixtures can yield more nitrogen than legume pure stands due to mutual stimulation of nitrogen uptake from symbiotic and non-symbiotic sources. *Agriculture. Ecosyst. Environ.* 140 (1-2), 155–163. doi: 10.1016/j.agee.2010.11.022

Poschlod, P., Bakker, J. P., and Kahmen, S. (2005). Changing land use and its impact on biodiversity. *Basic. Appl. Ecol.* 6, 93–98. doi: 10.1016/j.baae.2004.12.001

Raklami, A., Bechtaoui, N., Tahiri, A. I., Anli, M., Meddich, A., and Oufdou, K. (2019). Use of rhizobacteria and mycorrhizae consortium in the open field as a strategy for improving crop nutrition, productivity and soil fertility. *Front. Microbiol.* 10. doi: 10.3389/fmicb.2019.01106

R Core Team (2023). *R: A language and environment for statistical computing* (Vienna, Austria: R Foundation for Statistical Computing).

Sala, O. E., Chapin, F. S., Armesto, J. J., Berlow, E., Bloomfield, J., Dirzo, R., et al. (2000). Global biodiversity scenarios for the year 2100. *Science* 287, 1770–1774. doi: 10.1126/science.287.5459.1770

Sanderson, M. A., Brink, G., Ruth, L., and Stout, R. (2012). Grass-legume mixtures suppress weeds during establishment better than monocultures. *Agron. J.* 104, 36–42. doi: 10.2134/agronj2011.0130

Sengl, P., Magnes, M., Weitenthaler, K., Wagner, V., Erdős, L., and Berg, C. (2017). Restoration of lowland meadows in Austria: A comparison of five techniques. *Basic. Appl. Ecol.* 24, 19–29. doi: 10.1016/j.baae.2017.08.004

Shi, J., Wang, X., and Wang, E. (2023). Mycorrhizal symbiosis in plant growth and stress adaptation: from genes to ecosystems. *Annu. Rev. Plant Biol.* 22, 569–607. doi: 10.1146/annurev-arplant-061722-090342

Singh Rawat, V., Kaur, J., Bhagwat, S., Pandit, M. A., and Rawat, C. D. (2022). Deploying microbes as drivers and indicators in ecological restoration. *Restor. Ecol.* 31, e136881of16.

Smith, S. E., Facelli, E., Pope, S., and Smith, F. A. (2010). Plant performance in stressful environments: interpreting new and established knowledge of the roles of arbuscular mycorrhizas. *Plant Soil* 326, 3–20. doi: 10.1007/s11104-009-9981-5

Smith, S., and Read, D. (2008). *Mycorrhizal symbiosis* (London: Academic Press).

Smith, R. S., Shiel, R. S., Bardgett, R. D., Millward, D., Corkhill, P., Rolph, G., et al. (2003). Soil microbial community, fertility, vegetation and diversity as targets in the restoration management of a meadow grassland. *J. Appl. Ecol.* 40, 51–64. doi: 10.1046/j.1365-2664.2003.00780.x

Stoate, C., Báldi, A., Beja, P., Boatman, N. D., Herzon, I., van Doorn, A., et al. (2009). Ecological impacts of early 21st century agricultural change in Europe - A review. *J. Environ. Manage.* 91, 22–46. doi: 10.1016/j.jenvman.2009.07.005

Sun, J., Miller, J. B., Granqvist, E., Wiley-Kalil, A., Gobbato, E., Maillet, F., et al. (2015). Activation of symbiosis signaling by arbuscular mycorrhizal fungi in legumes and rice. *Plant Cell* 27, 823–838. doi: 10.1105/tpc.114.131326

Suter, M., Hofer, D., and Lüscher, A. (2017). Weed suppression enhanced by increasing functional trait dispersion and resource capture in forage ley mixtures. *Agric. Ecosyst. Environ.* 240, 329–339. doi: 10.1016/j.agee.2017.01.007

Trouvelot, A., Kough, J. L., and Gianinazzi-Pearson, V. (1986). "Mesure du taux de mycorhization VA d'un système radiculaire. Recherche de methods d'estimation ayant une signification fonctionnelle," in *Physiological and genetical aspects of mycorrhizae*. Eds. V. Gianinazzi-Pearson and S. Gianinazzi (Paris, France: INRA), 217–221.

van der Heijden, M. G. A. (2004). Arbuscular mycorrhizal fungi as support systems for seedling establishment in grassland. *Ecol. Lett.* 7, 293–303. doi: 10.1111/j.1461-0248.2004.00577.x

van der Heijden, M. G. A., Francis, M., Selosse, M. A., and Sanders, I. R. (2015). Mycorrhizal ecology and evolution: the past, the present, and the future. *New Phytol.* 205, 1406–1423. doi: 10.1111/nph.13288

van Der Putten, W. H., Klironomos, J. N., and Wardle, D. A. (2007). Microbial ecology of biological invasions. *ISME. J.* 1, 28–37. doi: 10.1038/ismej.2007.9

van Ruijven, J., and Berendse, F. (2005). Diversity–productivity relationships: Initial effects, long-term patterns, and underlying mechanisms. *PNAS* 102 ((3)), 695–700. doi: 10.1073/pnas.040752410

Volpe, V., Carotenuto, G., Berzero, C., Cagnina, L., Puech-Pagès, V., and Genre, A. (2020). Short chain chito-oligosaccharides promote arbuscular mycorrhizal colonization in *Medicago truncatula*. *Carbohydr. Polym.* 229, 115505. doi: 10.1016/j.carbpol.2019.115505

Volpe, V., Chialva, M., Mazzarella, T., Crosino, A., Capitanio, S., Costamagna, L., et al. (2023). Long-lasting impact of chitooligosaccharide application on strigolactone biosynthesis and fungal accommodation promotes arbuscular mycorrhiza in *Medicago truncatula*. *New Phytol.* 237, 216–2331. doi: 10.1111/nph.18697

Walker, K. J., Stevens, P. A., Stevens, D. P., Mountford, J. O., Manchester, S. J., and Pywell, R. F. (2004). The restoration and re-creation of species-rich lowland grassland on land formerly managed for intensive agriculture in the UK. *Biol. Conserv.* 119, 1–18. doi: 10.1016/j.biocon.2003.10.020

Wang, W., Shi, J., Xie, Q., Jiang, Y., Yu, N., and Wang, E. (2017). Nutrient exchange and regulation in arbuscular mycorrhizal symbiosis. *Mol. Plant* 12, 1147–1158. doi: 10.1016/j.molp.2017.07.012

Weisberger, D., Nichols, V., and Liebman, M. (2019). Does diversifying crop rotations suppress weeds? A meta-analysis. *PloS One* 14, 1–12. doi: 10.1371/journal.pone.0219847

Wyatt, G. A., Kiers, E. T., Gardner, A., and West, S. A. (2014). A biological market analysis of the plant-mycorrhizal symbiosis. *Evolution* 68, 2603–2618. doi: 10.1111/evo.12466

Zhang, T., Sun, Y., Shi, Z., and Feng, G. (2012). Arbuscular mycorrhizal fungi can accelerate the restoration of degraded spring grassland in Central Asia. *Rangel. Ecol. Manage.* 65, 426–432. doi: 10.2111/REM-D-11-00016.1

frontiers | Frontiers in Sustainable Food Systems

TYPE Original Research
PUBLISHED 04 April 2024
DOI 10.3389/fsufs.2024.1352924

Check for updates

OPEN ACCESS

EDITED BY
Mohamed Ait-El-Mokhtar,
University of Hassan II Casablanca, Morocco

REVIEWED BY
Marco E. Mng'ong'o,
Mbeya University of Science and Technology, Tanzania
Heba Mahmoud Mohammad Abdel-Aziz,
Mansoura University, Egypt
I. Rashmi,
Indian Institute of Soil and Water Conservation (ICAR), India

*CORRESPONDENCE
Yashbir Singh Shivay
✉ ysshivay@hotmail.com

RECEIVED 09 December 2023
ACCEPTED 08 February 2024
PUBLISHED 04 April 2024

CITATION
Baral K, Shivay YS, Prasanna R, Kumar D, Srinivasarao C, Mandi S, Nayak S and Reddy KS (2024) Optimising nitrogen use efficiency of prilled urea through integrated use of nano-ZnO and green manuring for better productivity, quality and nutritional status of *Basmati* rice crop. *Front. Sustain. Food Syst.* 8:1352924. doi: 10.3389/fsufs.2024.1352924

COPYRIGHT
© 2024 Baral, Shivay, Prasanna, Kumar, Srinivasarao, Mandi, Nayak and Reddy. This is an open-access article distributed under the terms of the Creative Commons Attribution License (CC BY). The use, distribution or reproduction in other forums is permitted, provided the original author(s) and the copyright owner(s) are credited and that the original publication in this journal is cited, in accordance with accepted academic practice. No use, distribution or reproduction is permitted which does not comply with these terms.

Optimising nitrogen use efficiency of prilled urea through integrated use of nano-ZnO and green manuring for better productivity, quality and nutritional status of *Basmati* rice crop

Kirttiranjan Baral[1], Yashbir Singh Shivay[1]*, Radha Prasanna[2], Dinesh Kumar[1], Cherukumalli Srinivasarao[3], Sunil Mandi[4], Somanath Nayak[1] and Kadapa Sreenivasa Reddy[1]

[1]Division of Agronomy, Indian Council of Agricultural Research (ICAR)-Indian Agricultural Research Institute, New Delhi, India, [2]Division of Microbiology, ICAR-Indian Agricultural Research Institute, New Delhi, India, [3]ICAR-National Academy of Agricultural Research Management, Hyderabad, India, [4]Division of Natural Resource Management, ICAR-Indian Agricultural Research Institute, Dhemaji, India

In agricultural systems, significant nitrogen (N) losses from traditional fertilizers pose risks to food security and economic stability. An emerging approach to mitigate these losses involves nanoparticles (NPs) coatings onto urea, aiming to enhance N availability and consequently boost crop yields. To explore the most effective and sustainable N management strategies, a field experiment was carried out in *Basmati* rice at the ICAR-Indian Agricultural Research Institute, New Delhi, India over 2020–2021 in a split-plot design, with two summer green manure (GM) types-*Sesbania* (G2) and cowpea (G3) and fallow in the main plot and six nitrogen fertilization (NF) modules, i.e., 0 kg N + 5 kg Zn ha^{-1} through bulk ZnO (N1), N through prilled urea (PU) (N2), N through PU + 5 kg Zn ha^{-1} through bulk ZnO (N3), 1% bulk ZnO-coated urea (1% BZnCU) (N4), 0.1% nano ZnO-coated urea (0.1% NZnCU) (N5) and 0.2% nano ZnO-coated urea (0.2% NZnCU) (N6) in subplots replicated three times. The objectives of the study was to identify the optimal GM crops and the most effective NF modules on enhancing plant height, dry biomass, grain yield, milling quality, and N, P, K nutrition, as well as nitrogen use efficiency (NUE). Our findings demonstrated that, a significant enhancement in plant height (13.34%) and dry biomass (38.1%) at harvest was observed with the combined application of G2 and N6 when juxtaposed against G1 and N1. The pooled analysis revealed that GM enhanced grain yield by 12.75% in comparison to G1, irrespective of the NF modules employed. The *Sesbania* was identified as the top-performing GM, registering a yield 17.5% greater than fallow while it was 8.13% for cowpea. Among NF modules, there was a noted 10.03% yield increase when urea was zinc-coated compared to using only urea (N2), and a 33.75% increase against the N1. The application of N6 modules boosted hulling, milling, and head rice recovery by 3.73, 4.45, and 4.98%, respectively, compared to N1. Moreover, combining zinc with urea raised the N content in milled rice by approximately 9.1% and heightened the N, P, and K concentration in the straw by 22.8, 4.44, and 11.8%, and total N, P, and K uptake by 5.72, 3.33, and 11.7%, in comparison to the combined effect of N1 and N2. Considering the NUE metrics, such as partial factor productivity (PFP), agronomic efficiency (AE), recovery efficiency (RE), and physiological efficiency (PE), the application

of GM showcased superior performance in PFP and RE against the G1, while AE and PE remained unaffected. The G2 as a GM, performed best in PFP and RE. The N5 module delineated the most substantial advancements in NUE indices, despite being comparable to N6. In conclusion, the adoption of *Sesbania* as a green manure crops, coupled with the 0.2% nano ZnO-coated urea module, is identified as an efficient method for maximizing growth, yield, milling attributes, nutrient assimilation, and overall NUE in the *Basmati* rice.

KEYWORDS

grain yield, green manuring, milling quality, nano Zn, NUE

1 Introduction

To meet the food demands of a projected global population nearing 9.7 billion, a considerable 119% increase in edible crop production is anticipated. Essential macronutrients such as nitrogen (N), phosphorus (P), and potassium (K) are fundamental to plant growth, with nitrogen being most crucial. However, insufficient N levels impede plant growth and productivity. Notably, synthetic N fertilizer, primarily urea, is instrumental in half of the global food production, witnessing a significant surge in usage over recent decades (Beig et al., 2020). However, a substantial N from urea is lost, posing environmental and economic challenges. This inefficiency in N utilization jeopardizes crop development and yields, potentially heightening the risks of food insecurity. Hence, an urgent call for efficient N management strategies echoes, aiming to bolster nitrogen use efficiency (NUE) and overall crop quality and yield (Prasad and Hobbs, 2018). Innovative strategies, such as controlled-release fertilizers, have surfaced as promising alternatives (Hou et al., 2019; Sun et al., 2020; Qiong et al., 2021; Liu et al., 2023). The integration of organic and inorganic nutrients, with an emphasis on green manure (GM), has been spotlighted within sustainable agricultural practices, enhancing the availability and efficiency of essential nutrients. The inclusion of critical micronutrients, specifically zinc (Zn), in nitrogenous fertilizers emerges as a beneficial strategy to enhance NUE. Zn holds a significant place in plant nutrition, with its deficiency notably affecting rice production across various Asian regions, causing a decline in yields (Farooq et al., 2018; Zulfiqar et al., 2021; Kandil et al., 2022; Khampuang et al., 2022). Considering rice's substantial contribution to global dietary energy and protein, and with a particular nod to India's remarkable US $ 3.54 billion revenue from *Basmati* rice exports in 2021–2022 (APEDA, 2023), an efficient management of N and Zn becomes essential to sustain and optimize *Basmati* rice productivity.

The type of Zn introduced to the plant environment can markedly influence plant responses. ZnO nanoparticles (NPs) are particularly notable due to their enhanced reactivity, attributed to their nano size, which facilitates improved nutrient delivery (Baral et al., 2019, 2020; Al-Khayri et al., 2023). These NPs swiftly dissolve into ions in soil systems, potentially enabling the reduction of nutrient application rates without diminishing yields, thereby promoting cost-efficiency and a minimized environmental impact (Sadhukhan et al., 2021; Akhtar et al., 2022; Nongbet et al., 2022; Kumar et al., 2023; Yadav et al., 2023). Earlier findings suggest that ZnO NPs contribute to improved nutrient uptake and yields in rice compared to traditional approaches (Adhikary et al., 2022; Sheikhnazari et al., 2023). Furthermore, a study by Yang et al. (2021) demonstrated that ZnO NPs could enrich rice with elevated levels of essential nutrients such as N, P, and K. However, the practical application of NPs in field crop production presents challenges, mainly due to the complexities involved in administering smaller doses effectively. In this context, the concept of nano-coating on conventional fertilizers, like urea, has emerged as a promising solution, leading to the creation of 'nano-enabled fertilizers' (Dimkpa and Bindraban, 2018). This strategy is perceived as a practical advancement for efficient nutrient delivery to crops (Shivay et al., 2019). Specifically, zinc-coated urea has been identified as a potent nutrient source, catering to the essential growth requirements of plants and promoting enhanced NUE (Shivay et al., 2019; Beig et al., 2022).

Despite existing research, a comprehensive understanding of how ZnO NPs coated urea influences plant performance, especially within the context of *Basmati* rice cultivation, remains to be fully explored. Hence, the investigation was motivated by various research gaps, including enquiries into the potential of nano zinc to improve *Basmati* rice growth, quality, and yield at a lower rate, serving as a feasible substitute for bulk Zn fertilizer in the Northwestern Indo-Gangetic Plains (NW IGP) of India. Additionally, the study sought to determine whether the nitrogen use efficiency of *Basmati* rice could be improved through the simultaneous application of nano zinc and urea. Another focus was on identifying the optimal rate of nano zinc and determining which green manuring options would establish the most effective and agronomically efficient strategy for nitrogen management. These questions formed the basis for the experimental design and exploration within the research framework. Thus, this study hypothesizes a potential synergistic interaction between nano-zinc and green manure, aiming to elucidate their collective impact on *Basmati* rice with the following objective, e.g., to evaluate the performance of different green manure sources and ZnO-NPs on *Basmati* rice yield, quality, nutrient uptake and NUE.

2 Materials and methods

2.1 Study area and soil analysis

Over two consecutive years, research was conducted at the ICAR-Indian Agricultural Research Institute in New Delhi, India. These

studies took place during 2020–2021 on sandy clay-loam soil. Initial soil tests showed the presence of 171 kg ha^{-1} of alkaline permanganate oxidizable N (Subbiah and Asija, 1956), 15.9 kg ha^{-1} of available P (Olsen et al., 1954), 309 kg ha^{-1} of exchangeable K (Hanway and Heidel, 1952), an organic carbon content of 0.65%, Zn content of 0.67 mg kg^{-1} (DTPA extractable) and pH of 7.68 (soil: water) (Prasad et al., 2006). The weather parameters observed during the crop growth period has been provided in Supplementary Table S2.

2.2 Details of experimental treatment

In the conducted experiment, diverse treatments were applied to evaluate their effects, categorized into two main segments: green manuring (GM) in the main plot and nitrogen fertilization (NF) modules in subplots. For the GM, three strategies were implemented. The control/fallow group (G1) had no green manuring. In the *Sesbania* (*Sesbania aculeata*) treatment (G2), the plant was integrated into the soil 45 days post-sowing. Similarly, in the Cowpea (*Vigna unguiculata*) treatment (G3), incorporation into the soil was done at 45 days after sowing. The addition of *Sesbania* (G2) and cowpea (G3) green manures resulted in the incorporation of dry biomass at around 5.2 and 3.43 t ha^{-1}, and 4.98 and 3.24 t ha^{-1} during the first and second years of the investigation, respectively. In the subplot consisting of NF modules, varied fertilization strategies were applied. Module N1 involved the application of 5 kg Zn ha^{-1} through bulk ZnO. For N2, nitrogen was administered at a rate of 120 kg N ha^{-1} through prilled urea (PU). Module N3 combined 120 kg N ha^{-1} of nitrogen through PU and 5 kg Zn ha^{-1} through bulk ZnO. In module N4 (1% bulk ZnO-coated urea) (1% BZnCU); N was applied at a rate of 120 kg N ha^{-1} as PU, in conjunction with 2.08 kg Zn ha^{-1} as bulk ZnO. Module N5 entailed the application of 0.1% nano ZnO-coated urea (0.1% NZnCU) with N at 120 kg N ha^{-1} as PU, supplemented by 0.208 kg Zn ha^{-1} as nano ZnO. Lastly, module N6 comprised of 0.2% nano ZnO-coated urea (0.2% NZnCU) at an N rate of 120 kg N ha^{-1} as PU, alongside 0.416 kg Zn ha^{-1} as nano ZnO. The urea used in our experiment was obtained from KRIBHCO, Noida, India. We obtained both nano and bulk ZnO for our experiment from Sigma Aldrich, Mumbai, India. To characterize the particles, both forms underwent particle size analysis using the Zetatrac™ particle size analyzer, utilizing Dynamic Light Scattering (DLS). The analysis indicated that 95% of the nano ZnO particles have a diameter of less than 74 nm, confirming their nanoscale dimensions. In contrast, the bulk ZnO has dimensions exceeding 100 nm, with a diameter less than 3,430 nm.

2.3 Coating protocol

In a controlled lab setting, both nano-structured ZnO and bulk ZnO were added to PU. A mixture of water and gum-acacia, in a 1:1 ratio, was used as the adhesive. This natural binder is derived from the *Acacia* tree. The urea coating was carried out in parts using a hand-operated rotary device for seed treatment. Initially, a specific volume of PU was added to the drum. Then, the gum-acacia solution was introduced, and the drum was rotated for 15 min to ensure the urea granules were uniformly coated with the adhesive (Pooniya et al., 2018; Shivay et al., 2019). Following this, the designated amount of ZnO was added, and the contents were mixed for another 15 min. The zinc-coated urea was spread on plastic trays and dried at room temperature (around 25 ± 5°C) with air circulation systems. It's worth noting that the volume of gum-acacia used remained the same as in the zinc-coated urea process. This urea coating process was typically done 3–4 days before being used in the field.

2.4 Crop management

The GM crops, aged 45 days, were mixed into the experimental field according to specific treatment needs using a tractor-operated disc harrow. The field was heavily irrigated with 10 cm of water before incorporating the GM crops. During the last puddling round, P and K were added in the form of single superphosphate (26 kg P ha^{-1}) and muriate of potash (33 kg K ha^{-1}), respectively. The N was applied in *Basmati* rice using PU and zinc-coated urea, into three parts. One-third of the N was used initially, another one-third at the 50% tillering phase, and the last portion at the panicle initiation phase. The variety used was "Pusa Basmati 6" with plant geometry being 20 cm × 10 cm.

2.5 Determination of plant height, dry matter, grain yield and milling quality

The height of *Basmati* rice was recorded every 30 days up to the harvest using a standard meter stick, marking the distance from the plant's base to the topmost leaf in centimeters. Dry matter accumulation was tracked on five distinct hills at the 30 days interval up to the harvest. After air drying, these samples were placed in a hot air oven at 60 ± 2°C until they reached a steady weight. Measurements were taken with a dry weight scale and noted in g per hill. For computation of grain yield, rice harvested from each plot (each subplot had a size of 17.5m^2) was sun-dried and weighed. To calculate the hulling percentage, 100 g samples of sun-dried paddy from each plot were processed through a miniature "Satake Rice Mill," and the weight of the resulting brown rice was recorded (Satake, 1990). The hulling percentage was calculated using the weight of the brown rice relative to the weight of the rough rice, multiplied by 100. The milling percentage was determined by weighing the polished rice and using it along with the weight of the rough rice in a calculation, multiplied by 100. Head rice recovery was calculated by using the weight of the whole milled rice relative to the weight of the rough rice, and the results were expressed as a percentage.

2.6 Plant nutrient analysis

Basmati rice plant samples, including grain and straw, were thoroughly dried in a hot air oven at a specific temperature range (60°C ± 2°C) until they reached a constant dry weight. For N analysis, a 0.5 g ground sample was mixed with a combination of concentrated sulphuric acid and other chemicals including $CuSO_4$, K_2SO_4, selenium powder, and mercury oxide. After a day,

a white hue indicated digestion was complete. This solution was then diluted to 100 mL with water. Using Kjeldahl's method (Piper, 1966), the samples were distilled, and their N content was determined by titration with a standard sulfuric acid solution, while also using a blank for reference. The N content was then represented as a percentage. For P analysis, plant samples were digested using a mixture of HNO_3 and $HClO_4$. The P content was then determined using the vanado-molybdo-phosphoric acid yellow colour method in a nitric acid medium, as described by Piper (1966). This was measured spectrophotometrically at a wavelength of 470 nm to get the exact percentage. For K analysis, the previously digested samples were used. A flame photometer was used to measure the K content in the plant material. Finally, the uptake values of N, P, and K (kg ha^{-1}) were calculated by multiplying the yield of grain and straw (in kg ha^{-1}) with their respective nutrient concentrations (%).

2.7 Estimation of NUE

The efficiency of N applied through GM and NF modules was evaluated using NUE indices including partial factor productivity (PFP), agronomic efficiency (AE), recovery efficiency (RE), and physiological efficiency (PE). These metrics were determined based on the methods suggested by Fageria and Baligar (2003):

$$PFP = Y_f / N_a$$

$$AE = \left(Y_f - Y_c\right) / N_a$$

$$RE = \left[\left(NU_f - NU_c\right) / N_a\right] \times 100$$

$$PE = \left(Y_f - Y_c\right) / NU_f - NU_c$$

In the formulas utilized, Y_f and Y_c symbolize the yields (kg ha^{-1}) in plots with and without fertilization, respectively. NU_f and NU_c indicate the N uptake by the *Basmati* rice in plots fertilized with NF modules (excluding N1)/GM (G2 & G3) and the control plots (G1/N1), respectively. The N_a represents the quantity of nitrogen applied (kg ha^{-1}).

2.8 Statistical computation

Data collected over 2 years was consolidated and analyzed collectively, with the average values being reported. The statistical analysis was conducted using R (version 4.2.2) along with R-Studio (version 2022.12.0 + 353), leveraging the "agricolae" package (de Mendiburu, 2019). A 5% significance level was used to assess the statistical differences among various treatment groups. Additionally, Duncan's Multiple Range Test (DMRT) was utilized in post-hoc analysis to classify the means of the treatment groups, as per the methodology of Gomez and Gomez (1984).

3 Results

3.1 Plant height and dry matter accumulation

The findings from the current study revealed a significant interaction between GM crops and NF modules in influencing the growth phases of *Basmati* rice, as shown in Figures 1, 2. Specifically, combining *Sesbania* (G2) with 1% BZnCU (N4) considerably increased the plant height throughout its growth stages, outperforming the results achieved with G3 using the same zinc treatment (Figure 1). Over a two-year period, combining G2 with 0.2% NZnCU (N6) resulted in a 13.34% rise in the plant height at harvest compared to fallow fields treated with 5 kg Zn ha^{-1} in the form of bulk ZnO. Similarly, when G3 was combined with N6, there was an 18.75% increase in height at harvest in comparison to fallow fields with the aforementioned Zn treatment. When it comes to dry matter accumulation, G2 paired with N6 boosted it by 38.1% versus fallow fields with N1 (Figure 2). Conversely, the integration of G3 and N6 increased dry matter by 28.21%. Notably, the conjunctive use of G2 with N6 closely mirrored the effectiveness of G2 with N4 in both in plant height and dry matter.

3.2 Grain yield

The green manure crops and nitrogen fertilization modules had a significant effect on the grain yield of *Basmati* rice as evident from Table 1. The pooled data from 2 years revealed that GM led to a 12.75% improvement in grain yield versus fallow fields, regardless of the type of NF modules. *Sesbania* (G2) stood out as the superior GM crop, outdoing cowpea (G1), as shown in Table 1. According to the pooled data, rice grain yield increased by 17.5% when G2 was used as GM, in contrast to a fallow field (G1). Meanwhile, utilizing G3 as GM saw an 8.13% increment in grain yield when compared to G1. The NF modules also had a notable impact on grain yield. When zinc was coated with urea, the yield surged by 10.03% versus using only urea and by 33.75% against the N1, as depicted in Table 1. Among all NF modules, N4 emerged as the most potent, though its results were closely matched by N6, with both outpacing other NF modules.

3.3 Milling quality

Over the 2 years, the pooled data (Table 2) indicated that the mean rates of hulling, milling, and head rice recovery were 75.85, 65.55, and 56%, respectively. While the GM did not show a significant influence on these recovery rates in *Basmati* rice, NF modules showcased a remarkable positive effect. Specifically, the N4 module emerged as the most beneficial, delivering results that were akin to those obtained using N6. The pooled data revealed that utilizing N4 enhanced the hulling, milling, and head rice recovery rates by 4.67, 5.57, and 6.43%, respectively, in comparison to the control group. In contrast, applying the N6 module improved these rates by 3.73, 4.45, and 4.98% relative to N1. Additionally, the

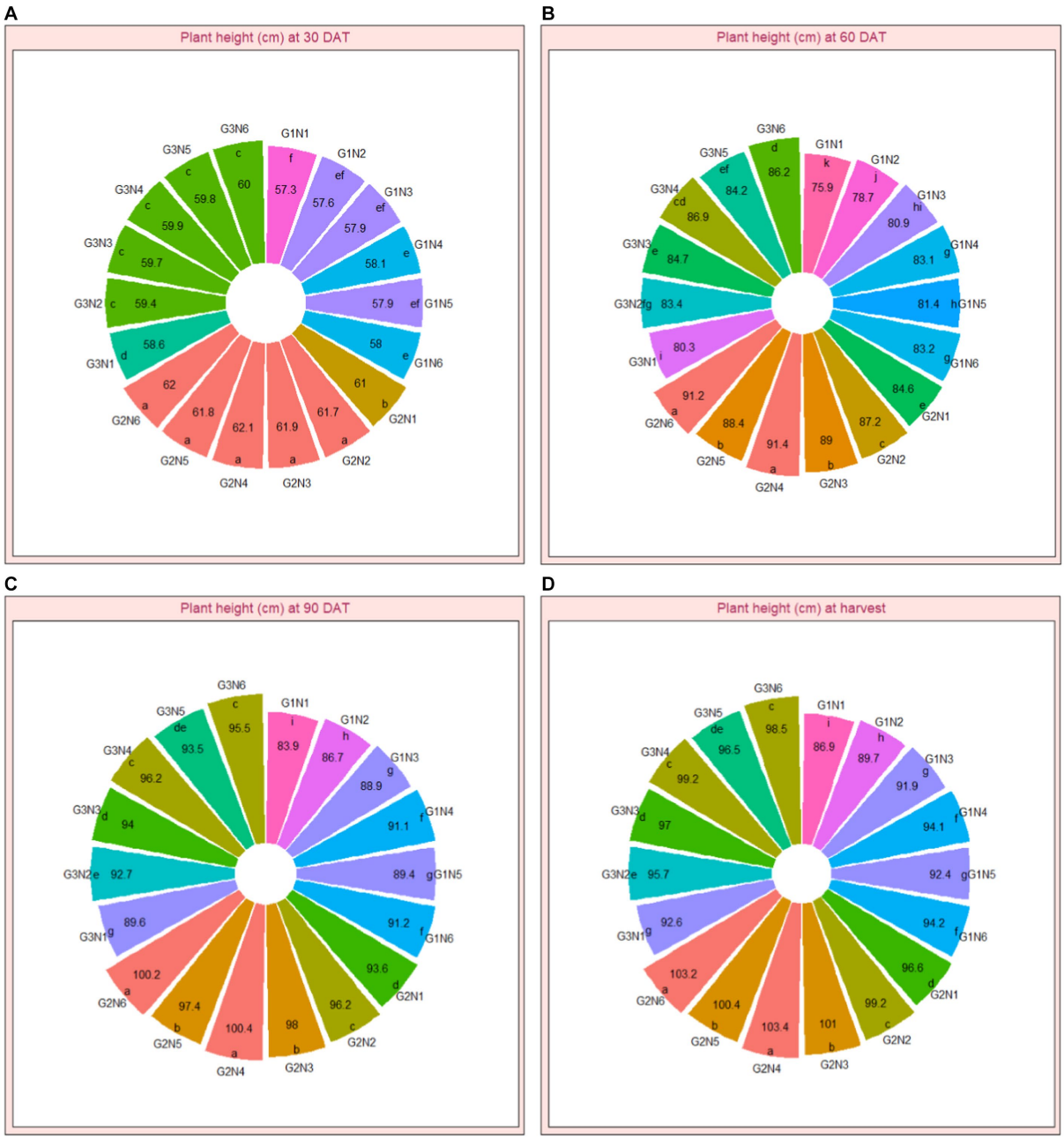

FIGURE 1
(A–D) Interaction effect of green manuring (GM) and N fertilization modules (NF) on the plant height (cm) of *Basmati* rice (pooled data of 2 years). Bar of same letter(s) do not differ significantly at 5% probability level by DMRT. DAT, days after transplanting.

conjoint use of GM with NF modules had a significant impact in elevating the recovery rates (Figure 3).

3.4 Nutrient content and uptake

The Tables 2–4 and Figures 4–6 detail the experimental results exploring the influence of GM and NF modules on the N, P, and K contents in various *Basmati* rice components such as husk, bran, milled grain, and straw. Both GM and NF modules considerably affected the nutrient concentrations. Utilizing G2 residue as a GM yielded the highest concentrations of N, P, and K across the different parts of rice and straw surpassing G3 and G1, with G2 proving to be exceptionally effective among the examined GM crops. The NF modules also had a considerable impact. Moreover, the combined application of zinc and urea significantly enhanced the N, P, and K contents in the rice grain and straw compared to applying N2 or N1. Specifically, the combination of zinc along with urea application improved N content in milled rice by around 9.1% and increased the N, P, and K contents in the straw by 22.8, 4.44, and 11.8%, respectively, when compared to non-zinc coating urea or N1. Conversely, a

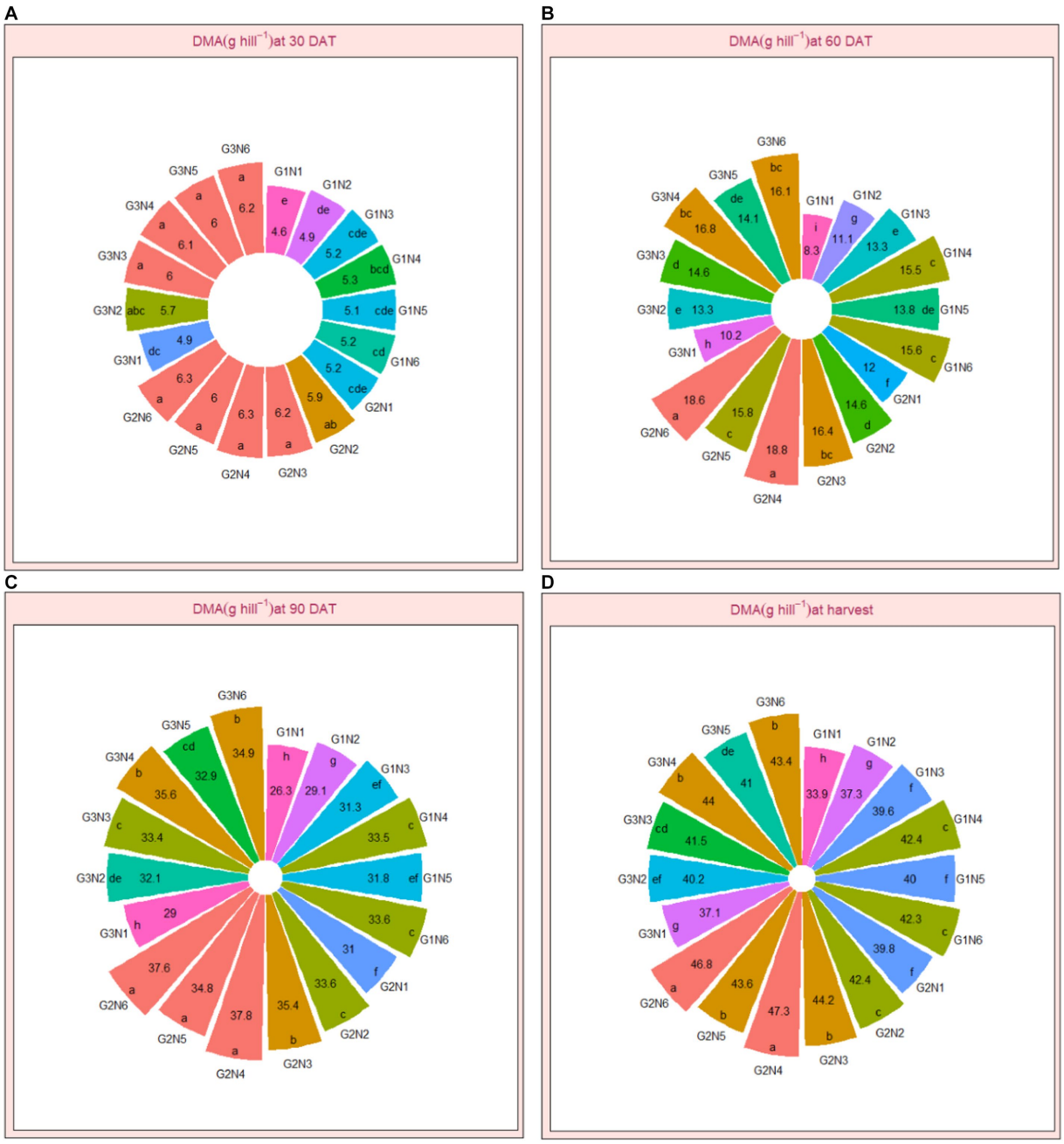

FIGURE 2
(A–D) Interaction effect of green manuring (GM) and N fertilization modules (NF) on the dry matter accumulation (g hill^{-1}) of *Basmati* rice (pooled data of 2 years). Bar of same letter(s) do not differ significantly at 5% probability level by DMRT. DAT, days after transplanting.

higher zinc application saw a minor reduction in P content in both grain and straw (Figure 5). Among the NF modules, N4 was particularly effective, closely trailed by N6 in improving N, P, and K contents in various parts of the rice. Figures 6, 7 showed that both GM and NF significantly affected *Basmati* rice's total N, P, and K uptake over 2 years. The G2 residue's integration into the soil resulted in the highest total absorption of N, P, and K by the rice, superior to G3 and G1. The NF modules also played a pivotal role, where their combination with urea significantly elevated the total N, P, and K absorbed by the rice by 5.72, 3.33, and 11.7%, respectively, compared to N2. Regarding the NF modules, the N4 application was most successful in maximizing *Basmati* rice's overall N, P, and K contents closely followed by N6, both proving more efficient than other NF modules.

3.5 Nitrogen use efficiency

The data from Figure 8 demonstrate that using GM and NF modules significantly affects the *Basmati* rice's partial factor

10.3389/fsufs.2024.1352924

TABLE 1 Effect of green manuring (GM) and N fertilization modules (NF) on productivity and milling attributes of *Basmati* rice (pooled data of 2 years).

Treatment	Grain yield (t ha^{-1})	Hulling (%)	Milling (%)	Head rice recovery (%)
Green manuring (GM)				
G1	3.75^{c}	75.1	64.8	55.25
G2	4.40^{a}	76.5	66.2	56.65
G3	4.06^{b}	76.13	65.83	56.28
S/NS ($p = 0.05$)	S	NS	NS	NS
N fertilization modules (NF)				
N1	3.23^{d}	71.32^{d}	61.02^{d}	51.47^{d}
N2	3.92^{c}	74.99^{c}	64.69^{c}	55.14^{c}
N3	4.19^{b}	76.64^{bc}	66.34^{bc}	56.79^{bc}
N4	4.48^{a}	78.51^{a}	68.21^{a}	58.66^{a}
N5	4.20^{b}	76.23^{bc}	65.93^{bc}	56.38^{bc}
N6	4.42^{a}	77.80^{ab}	67.50^{ab}	57.95^{ab}
S/NS ($p = 0.05$)	S	S	S	S

Means followed by the same letter(s) within a column do not differ significantly at 5% probability level at DMRT. S, significant at $p = 0.05$; NS, non-significant at $p = 0.05$.

TABLE 2 Effect of green manuring (GM) and N fertilization modules (NF) on N uptake by *Basmati* rice (pooled data of 2 years).

Treatment	N uptake by husk (kg ha^{-1})	N uptake by bran (kg ha^{-1})	N uptake by milled rice (kg ha^{-1})	N uptake by straw (kg ha^{-1})
Green manuring (GM)				
G1	5.88^{c}	6.64^{c}	32.37^{c}	53.79^{c}
G2	8.18^{a}	8.60^{a}	43.92^{a}	68.25^{a}
G3	6.88^{b}	7.63^{b}	38.30^{b}	60.86^{b}
S/NS ($p = 0.05$)	S	S	S	S
N fertilization modules (NF)				
N1	5.36^{d}	5.36^{e}	24.14^{d}	46.83^{c}
N2	6.44^{c}	5.90^{d}	34.34^{c}	58.16^{b}
N3	7.18^{b}	6.81^{c}	39.10^{b}	64.17^{a}
N4	7.89^{a}	7.53^{a}	46.69^{a}	66.99^{a}
N5	7.33^{ab}	7.61^{c}	39.91^{b}	64.25^{a}
N6	7.69^{ab}	7.51^{b}	45.01^{a}	65.41^{a}
S/NS ($p = 0.05$)	S	S	S	S

Means followed by the same letter(s) within a column do not differ significantly at 5% probability level at DMRT. S, significant at $p = 0.05$; NS, non-significant at $p = 0.05$.

productivity (PFP), agronomic efficiency (AE), recovery efficiency (RE), and physiological efficiency (PE). Over a 2 years study, regardless of the specific type of GM or NF modules, the PFP was found to be 29.4 kg of grain kg^{-1} N, AE was 7.06 kg of grain increase kg^{-1} N applied, RE was 26.67%, and PE was 22.21 kg of grain increase kg^{-1} N uptake. The GM proved to be more effective than G1 in enhancing PFP and RE. The incorporation of *Sesbania* as a green manure improved the PFP and RE to 32 and 34%, respectively. In contrast, for cowpea, these values were 29% for PFP and 27% for RE. On the other hand, fallow land exhibited PFP and RE value of 26 and 19%, respectively. However, there was no significant difference observed in AE, and PE over two years. Out of the GM used, G2 performed better than G3 in terms of PFP and RE. The NF modules also played a pivotal role in determining the aforementioned parameters. The application of 1% BZnCU proved to be successful in significantly enhancing nitrogen use efficiency (NUE), increasing it from 20 to 40%. This improvement in NUE was statistically comparable with the application of 0.2% NZnCU.

4 Discussion

4.1 Plant height and dry matter accumulation

A noticeable interaction effect has been observed between GM and NF modules, influencing the plant height and dry matter accumulation in *Basmati* rice. The implementation of GM aids synchronized release of nutrients through decomposition, facilitating augmented growth in rice, as substantiated by Meena

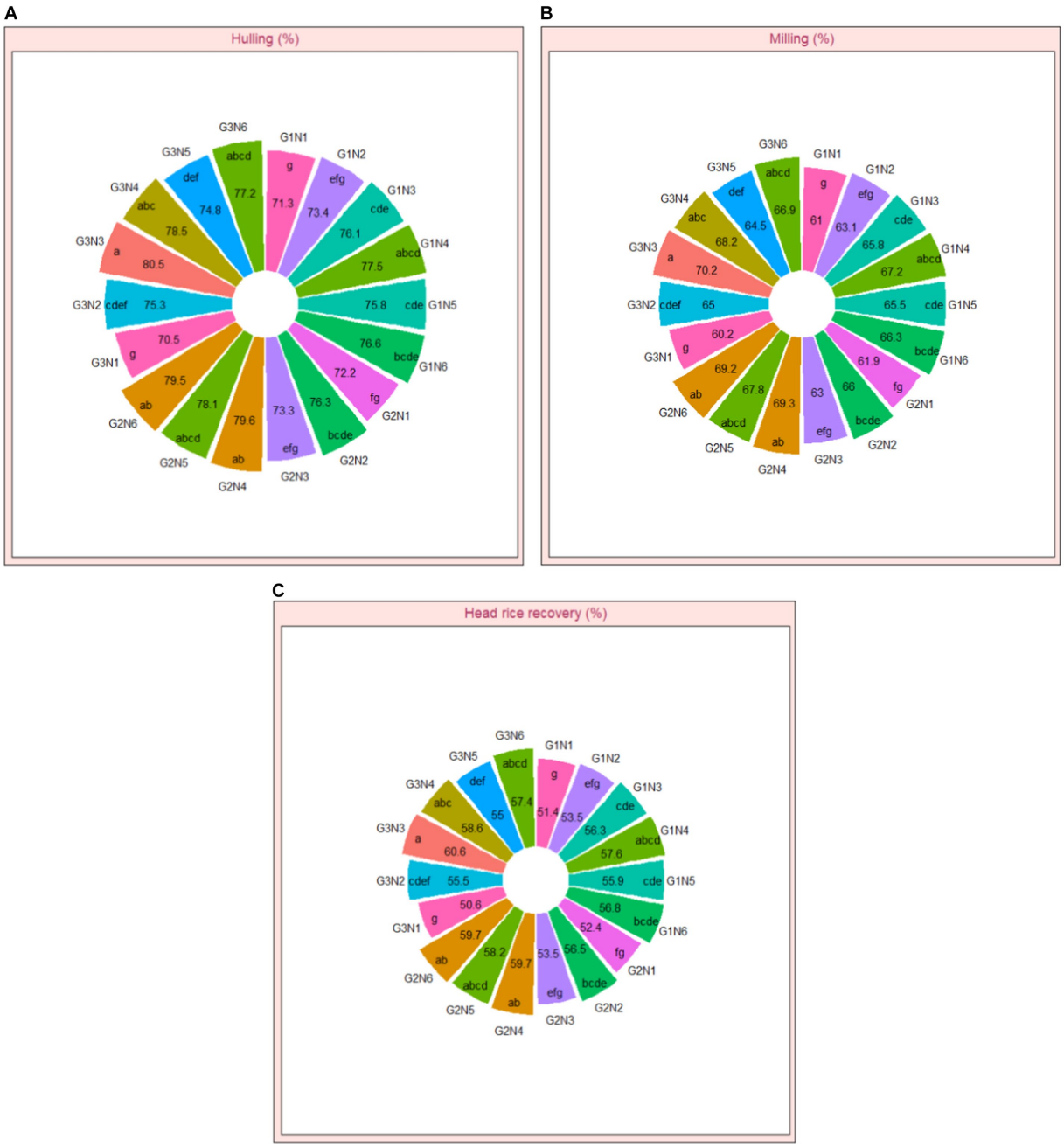

FIGURE 3
(A–C) Interaction effect of green manuring (GM) and N fertilization modules (NF) on hulling (%), milling (%) and head rice recovery (%) of *Basmati* rice (pooled data of 2 years). Bar of same letter(s) do not differ significantly at 5% probability level by DMRT.

et al. (2018). Conforming to these findings, our observations elucidate that GM improved parameters such as plant height and dry biomass. Leguminous GM plays a pivotal role in the atmospheric nitrogen fixation process, enriching soil N content and thereby enhanced crop growth. Beyond N, the decomposition of these green manure recycles other nutrients like P and K fostering soil health. Additionally, GM facilitates better root architectures and optimization of nutrient uptake mechanisms (Mandal and Pal, 2009). The incorporation of GM before the *Basmati* rice is instrumental in improving the organic matter content in the soil. The application of Zn, in combination with N leads to synergistic interplay with the prevailing organic matter, mitigating tendencies of zinc fixation. The application of 0.2% nano zinc oxide coated urea outperformed the 0.1% counterpart in terms of growth parameters. Moreover, the application of ZnO NPs in conjunction with prilled urea (N5/N6) has emerged as a superior strategy, surpassing the performance of conventional bulk ZnO coatings. This elevation in growth is attributed to the enhanced solubility kinetics of NPs in aqueous mediums (Zhang et al., 2021; Prakash et al., 2022), resonating with the earlier

TABLE 3 Effect of green manuring (GM) and N fertilization modules (NF) on P uptake by *Basmati* rice (pooled data of 2 years).

Treatment	P uptake by husk (kg ha^{-1})	P uptake by bran (kg ha^{-1})	P uptake by milled rice (kg ha^{-1})	P uptake by straw (kg ha^{-1})
Green manuring (GM)				
G1	0.18^{c}	2.28^{c}	2.93^{c}	7.71^{c}
G2	0.23^{a}	2.89^{a}	3.86^{a}	9.67^{a}
G3	0.20^{b}	2.55^{b}	3.29^{b}	9.00^{b}
S/NS ($p = 0.05$)	S	S	S	S
N fertilization modules (NF)				
N1	0.18^{c}	1.95^{c}	2.38^{d}	6.98^{c}
N2	0.22^{a}	2.59^{b}	3.28^{c}	9.60^{a}
N3	0.21^{ab}	2.70^{ab}	3.50^{b}	9.61^{a}
N4	0.20^{b}	2.77^{a}	3.78^{a}	8.59^{b}
N5	0.21^{ab}	2.69^{ab}	3.51^{b}	9.28^{a}
N6	0.20^{a}	2.75^{a}	3.70^{a}	8.70^{b}
S/NS ($p = 0.05$)	S	S	S	S

Means followed by the same letter(s) within a column do not differ significantly at 5% probability level at DMRT. S, significant at $p = 0.05$; NS, non-significant at $p = 0.05$.

TABLE 4 Effect of green manuring (GM) and N fertilization modules (NF) on K uptake by *Basmati* rice (pooled data of 2 years).

Treatment	K uptake by grain (kg ha^{-1})	K uptake by straw (kg ha^{-1})
Green manuring (GM)		
G1	9.95^{c}	129.59^{c}
G2	14.13^{a}	151.29^{a}
G3	11.97^{b}	140.97^{b}
S/NS ($p = 0.05$)	S	S
N fertilization modules (NF)		
N1	7.87^{d}	115.90^{d}
N2	10.75^{c}	136.77^{c}
N3	12.25^{b}	146.14^{ab}
N4	14.66^{a}	150.72^{a}
N5	12.44^{b}	145.19^{b}
N6	14.14^{a}	148.97^{ab}
S/NS ($p = 0.05$)	S	S

Means followed by the same letter(s) within a column do not differ significantly at 5% probability level at DMRT. S, significant at $p = 0.05$; NS, non-significant at $p = 0.05$.

insights by Shivay et al. (2008). The integration of both organic and inorganic fertilization strategies, as underscored by Mangaraj et al. (2022), has been manifested as a sustainable approach towards enhancing rice crop growth.

4.2 Grain yield

The incorporation of GM contributed a substantial amount of N, P, and K (Supplementary Table S1). A consistent nutrient release from organic sources like GM perpetuates throughout the crop's developmental stages, enhancing accessibility to essential nutrients and contributing to improved fertile tillers production and subsequently increased yield. Selvi and Kalpana (2009) supported these results, finding similar efficacy between GM with cowpea and *Dhiancha* and the use of conventional fertilizers in increasing the grain yield of transplanted rice. The present study underscores the effectiveness of Zn and N supplementation in improving crop yields (Figure 9). Applying Zn, particularly in the form of ZnO NPs, has been shown to increase grain yields (Hussain et al., 2018; Bala et al., 2019; Elshayb et al., 2021; Yang et al., 2021; Zhang et al., 2021; Parashar et al., 2023). This could be due to crucial role of Zn in enhancing pollination and fertilization, minimizing the likelihood of grain sterility (Khan and Siddiqui, 2020). Additionally, Zn is crucial in increasing biomass (Pooniya et al., 2012), aiding in the effective transfer of

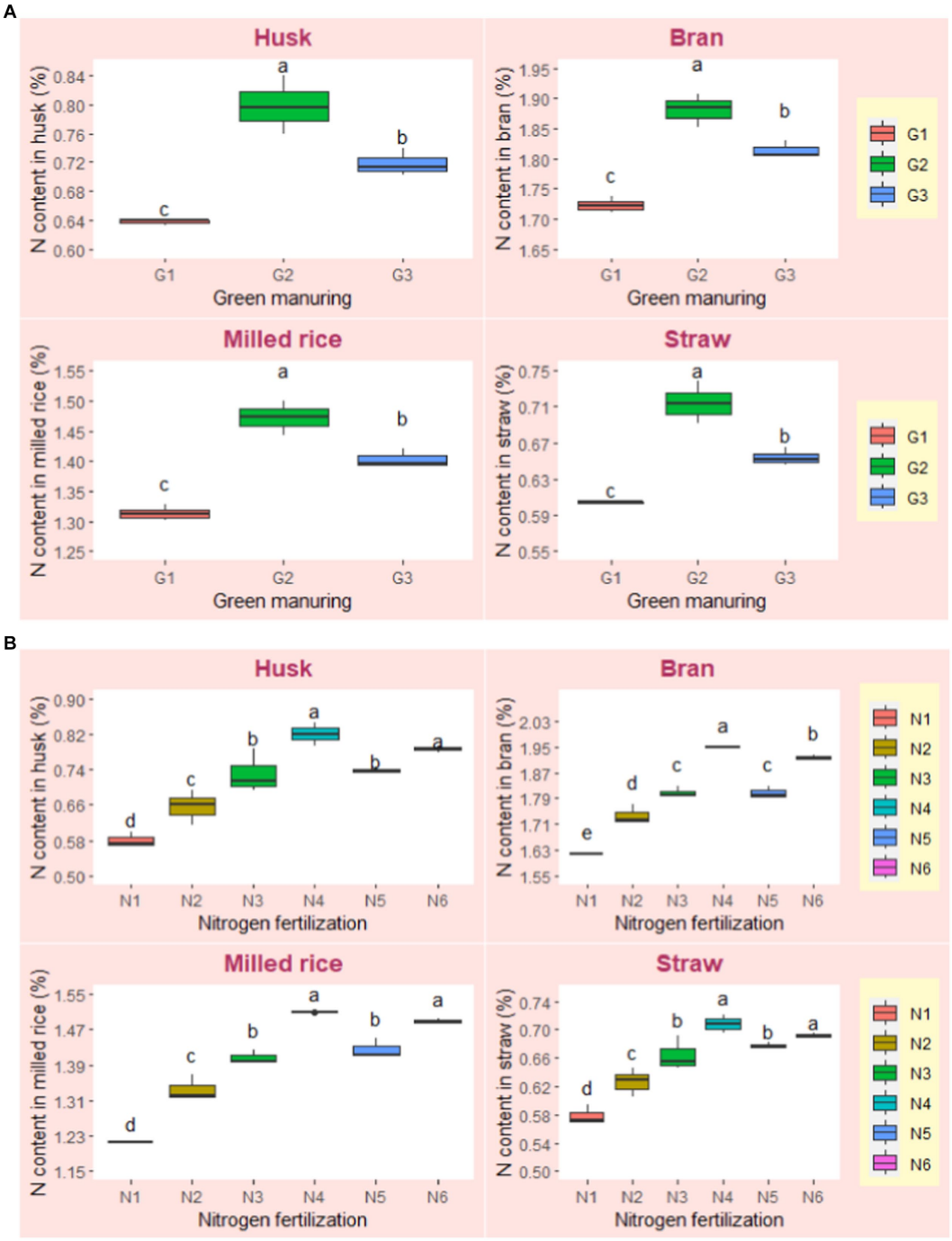

FIGURE 4
(A) Effect of green manuring (GM) on the N content of *Basmati* rice (pooled data of 2 years). **(B)** Effect of N fertilization modules (NF) on the N content of *Basmati* rice (pooled data of 2 years). Boxplot of same letter(s) do not differ significantly at 5% probability level by DMRT.

photosynthates to the reproductive parts of crops. This study reveals that yields improved due to better availability of N (Figure 10), P (Figure 11), and K (Figures 6, 10) when using nano-zinc coated urea, surpassing the conventional forms of zinc. The application of 0.2% nano zinc oxide coated urea outperformed the 0.1% counterpart with respect to grain yield. This improvement is attributed to Zn's essential function as an enzyme cofactor and the advantageous properties of ZnO NPs, such as smaller size and increased solubility and diffusion, ensuring its optimal availability in the soil. Du et al. (2019) also found that Zn application enhances N absorption in rice, subsequently boosting biomass and yield.

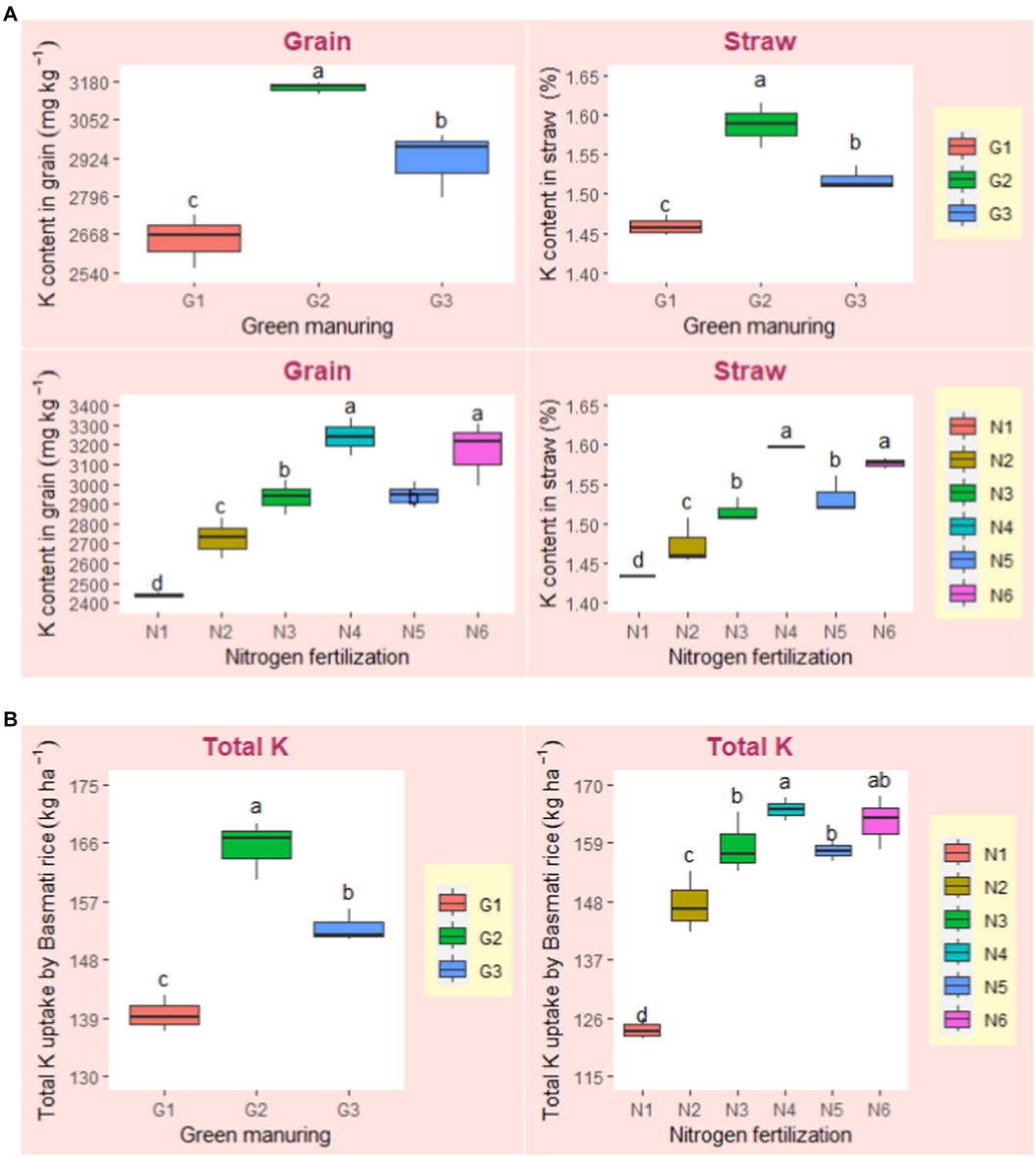

FIGURE 5
(A) Effect of green manuring (GM) and N fertilization modules (NF) on the K content of *Basmati* rice (pooled data of 2years). **(B)** Effect of green manuring (GM) and N fertilization modules (NF) on the total K uptake of *Basmati* rice (pooled data of 2years). Boxplot of same letter(s) do not differ significantly at 5% probability level by DMRT.

4.3 Milling quality

Recent research by Aulakh et al. (2016) has shown that N management can enhance the quality of *Basmati* rice. Specifically, the use of G2 in treatments led to the highest hulling and milling percentages and improved head rice recovery. Similarly, Pooniya and Shivay (2015) found that using *Sesbania* as GM boosted several *Basmati* rice quality indicators, including those aforementioned. The utilization of 0.2% NZnCU resulted in notable enhancements in hulling, milling, and head rice recovery, demonstrating improvements of 3.73, 4.45, and 4.98%, respectively, when compared to the soil application of 5 kg Zn ha^{-1}. These findings strongly suggest that the application of ZnO NPs had a substantial and positive influence on the overall milling quality. Achieving high *Basmati* rice yields with substantial N content necessitates a consistent N supply, as pointed out by Naik and Das (2007). Proper N fertilization can enhance N absorption in rice, thereby activating nitrate reductase, leading to better N distribution in the grains, as noted by Zhu et al. (2022).

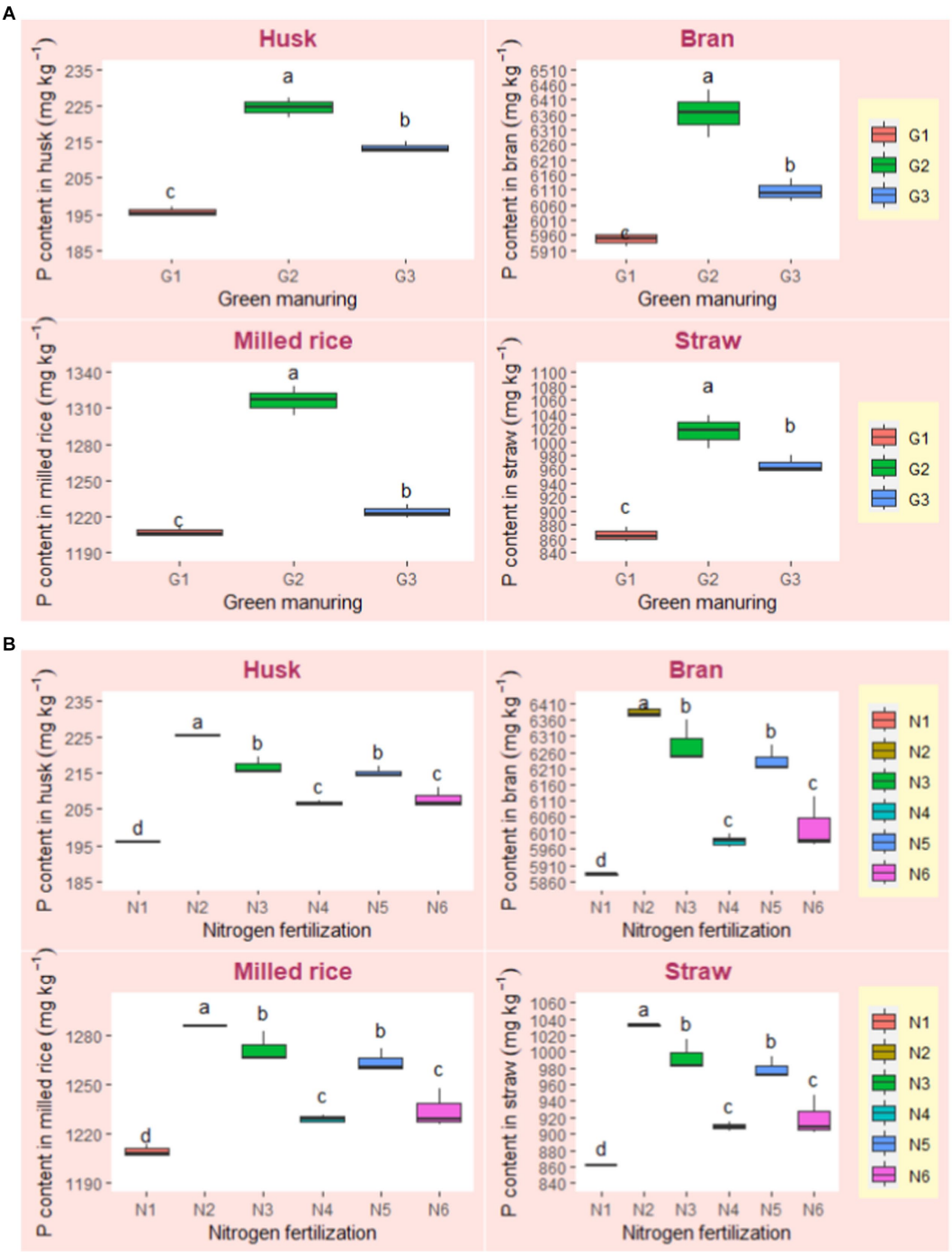

FIGURE 6
(A) Effect of green manuring (GM) on the P content of *Basmati* rice (pooled data of 2 years). **(B)** Effect of N fertilization modules (NF) on the P content of *Basmati* rice (pooled data of 2 years). Boxplot of same letter(s) do not differ significantly at 5% probability level by DMRT.

4.4 Nutrient content and uptake

In our experiment, we observed that green manured *Basmati* rice was found to contain higher N, P and K content in the grain and straw than fallow. Likewise, we noticed that N, P, and K content and uptake was more prominent in *Basmati* rice with G2/G3 than in G1. The higher nutrient content and uptake could be attributed to increased grain yield in the GM-treated plots. In fact, *Basmati* rice with G2 as GM displayed superior grain yield, N, P, and K uptake. This is likely because G2 supplied the soil with more N, P, and K, as shown in Supplementary Table S1. Compared to cowpea; *Sesbania* resulted in richer N, P, and K

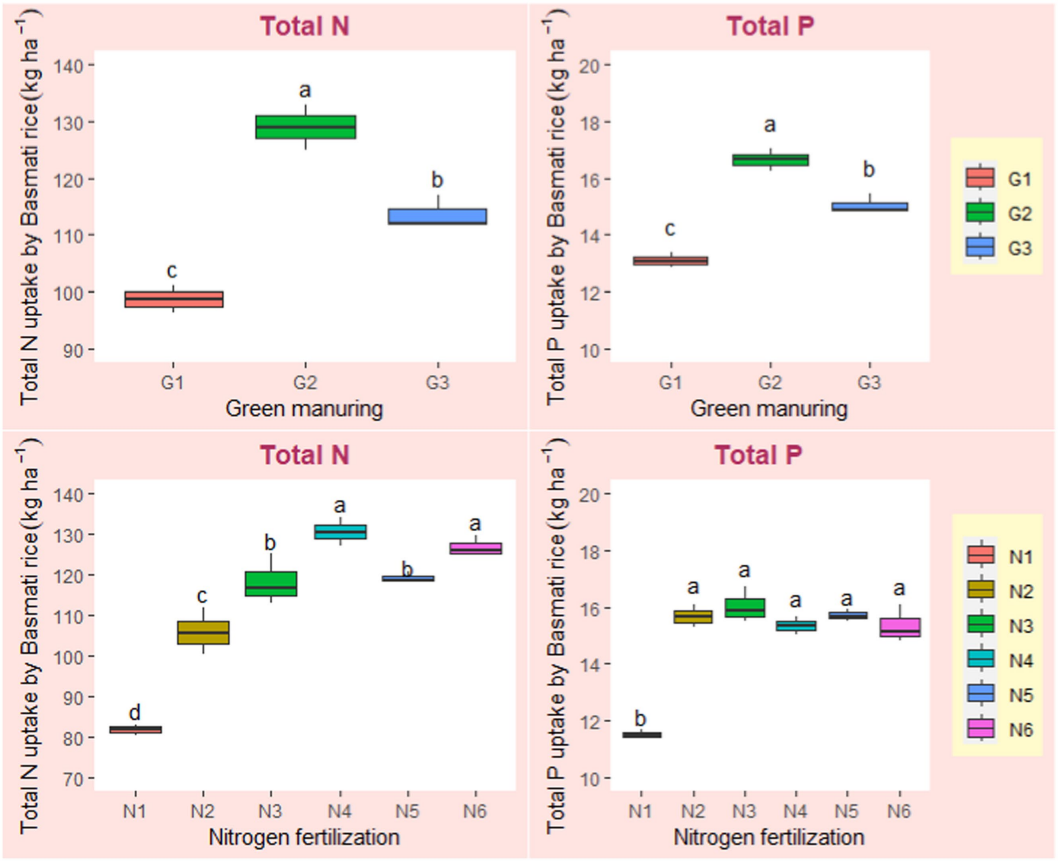

FIGURE 7
Effect of green manuring (GM) and N fertilization modules (NF) on the total N and P uptake of *Basmati* rice (pooled data of 2 years). Boxplot of same letter(s) do not differ significantly at 5% probability level by DMRT.

profiles in *Basmati* rice grain and straw. The GM crops, as Meena et al. (2018) highlighted can enhance soil qualities and nutrient availability. Using ZnO NPs notably increased the content and uptake of N, P, and K over the N1/N2. Zn coatings have been found to enhance the uptake of essential nutrients like N, P, and K in rice, as observed by Panhwar et al. (2015). This improvement can be linked to the positive effects of nano zinc-coated urea on rice growth, leading to increased biomass and subsequent higher N, P, and K uptake. The efficiency of zinc-treated urea is enhanced with greater nano ZnO dosages, consistent with Beig et al. (2023) findings. However, we noticed a reduction in the grain P content when Zn was applied. The minor reductions in P content in both grain and straw, along with the overall uptake of P with elevated Zn levels, could be due to the antagonistic interaction between Zn and P, as pointed out by Ghoneim (2016). Further, it might be due to decreased movement of P from the roots to the shoots and an imbalanced ratio of P-to-Zn in the plant, referred to as the dilution effect (Lonergan et al., 2009). This lowering of P content is also consistent with the findings by Fageria et al. (2011), who noted Zn's antagonistic effect on P absorption due to the probable formation of zinc phosphate, restricting the uptake of P from the cultivated soil. Similar observations were made in rice plants treated with ZnO NPs, displaying considerable inhibition of P accumulation (Bala et al., 2019; Elshayb et al., 2021). Conversely, our data showed that K uptake in both grain and straw increased significantly with the use of ZnO NPs. This enhancement is likely due to the synergistic interaction between Zn and K, facilitating increased availability and movement of K from the roots and shoots to other parts of the plant (Kumar et al., 2016).

4.5 Nitrogen use efficiency

The green manuring practices are known to enhance nitrogen use efficiency (Meng et al., 2019; Bhardwaj et al., 2023). Incorporating GM significantly augmented soil N content, which, upon decomposition, elevated N absorption, as evidenced in Table 2 and Figure 2. Nano ZnO's addition fosters beneficial microbial growth, increasing the mobility of essential nutrients and thus promoting improved crop growth. This is substantiated by the higher N uptake by rice tissue with the application of nano-ZnO as compared to bulk ZnO. This could be attributed to several mechanisms. First, ZnO NPs boost the availability of

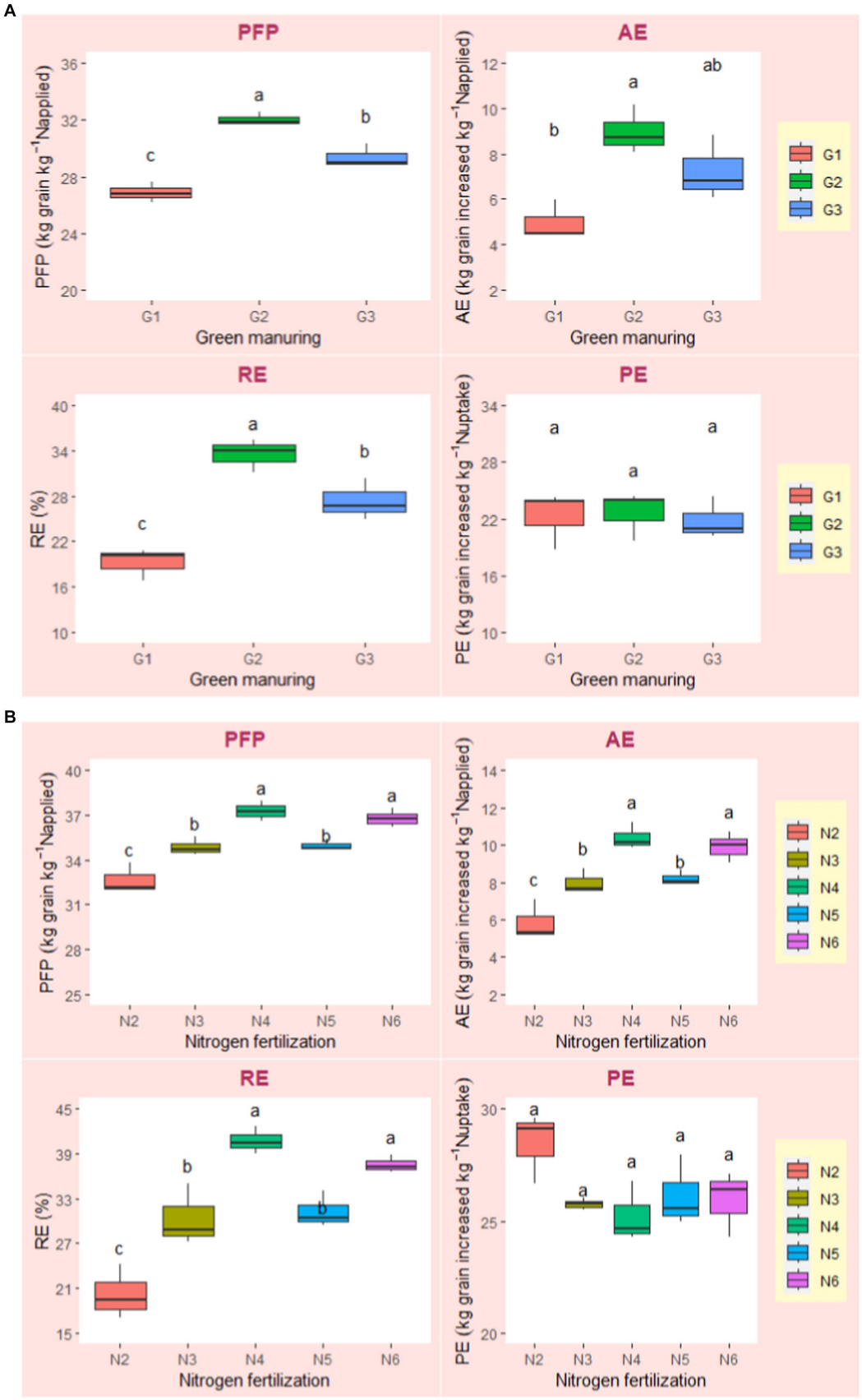

FIGURE 8
(A) Effect of green manuring (GM) on the NUE indices of *Basmati* rice (pooled data of 2 years). **(B)** Effect of N fertilization modules (NF) on the NUE indices of *Basmati* rice (pooled data of 2 years). Boxplot of same letter(s) do not differ significantly at 5% probability level by DMRT.

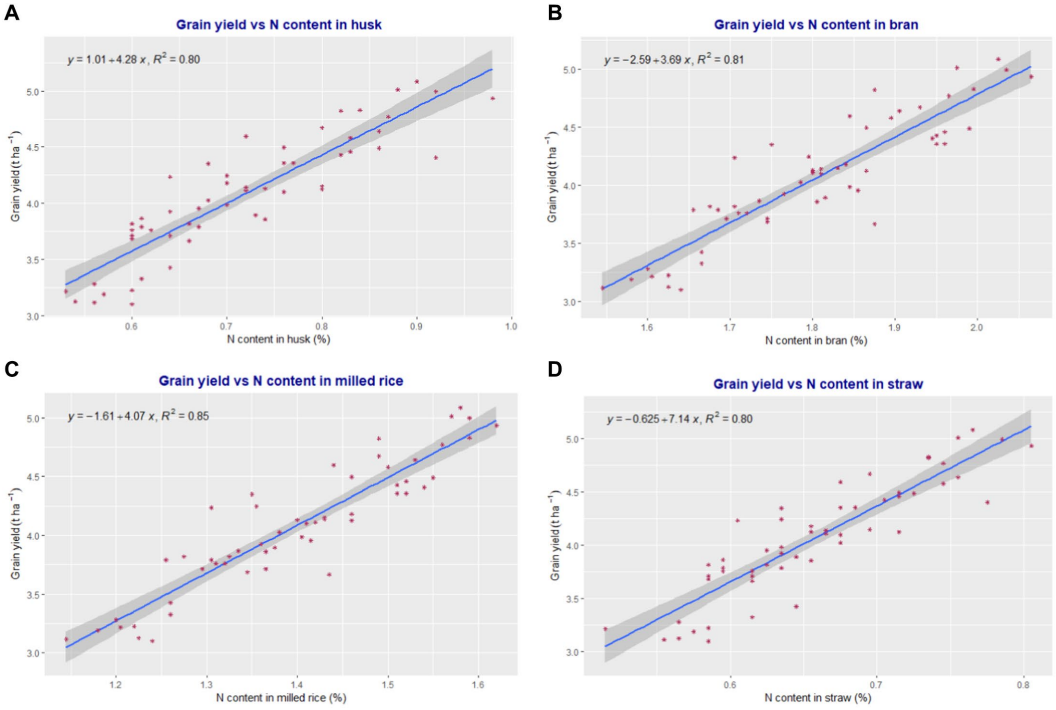

FIGURE 9
(A) Regression between grain yield and N content in husk. **(B)** Regression between grain yield and N content in bran. **(C)** Regression between grain yield and N content in milled rice. **(D)** Regression between grain yield and N content in straw.

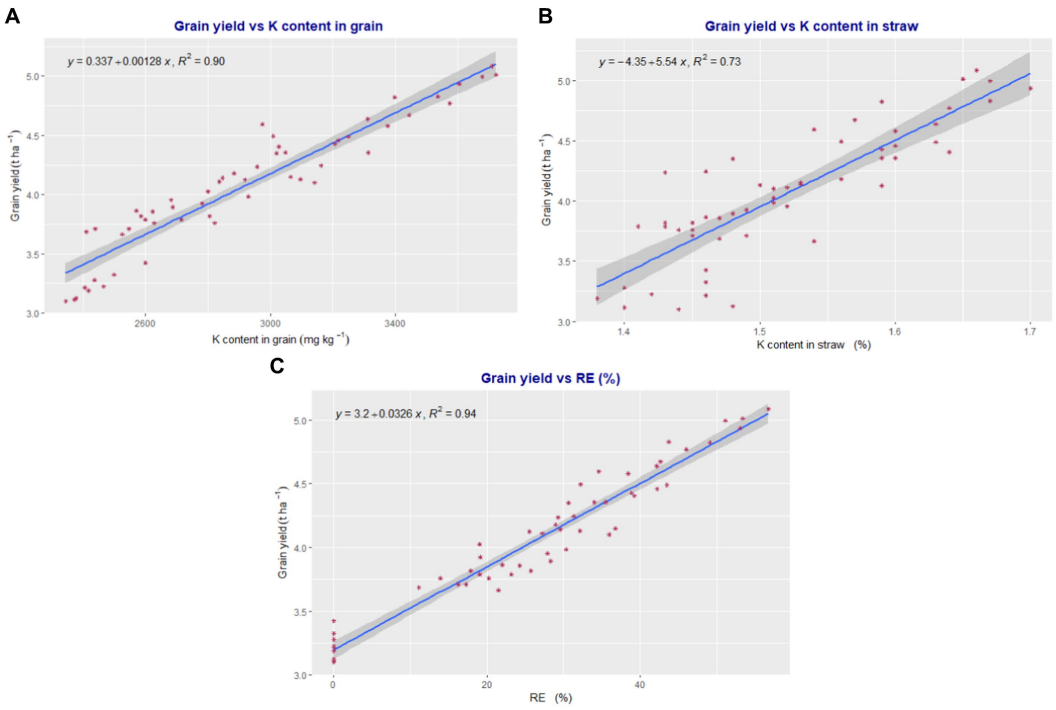

FIGURE 10
(A) Regression between grain yield and K content in grain. **(B)** Regression between grain yield and K content in straw. **(C)** Regression between grain yield and recovery efficiency of N.

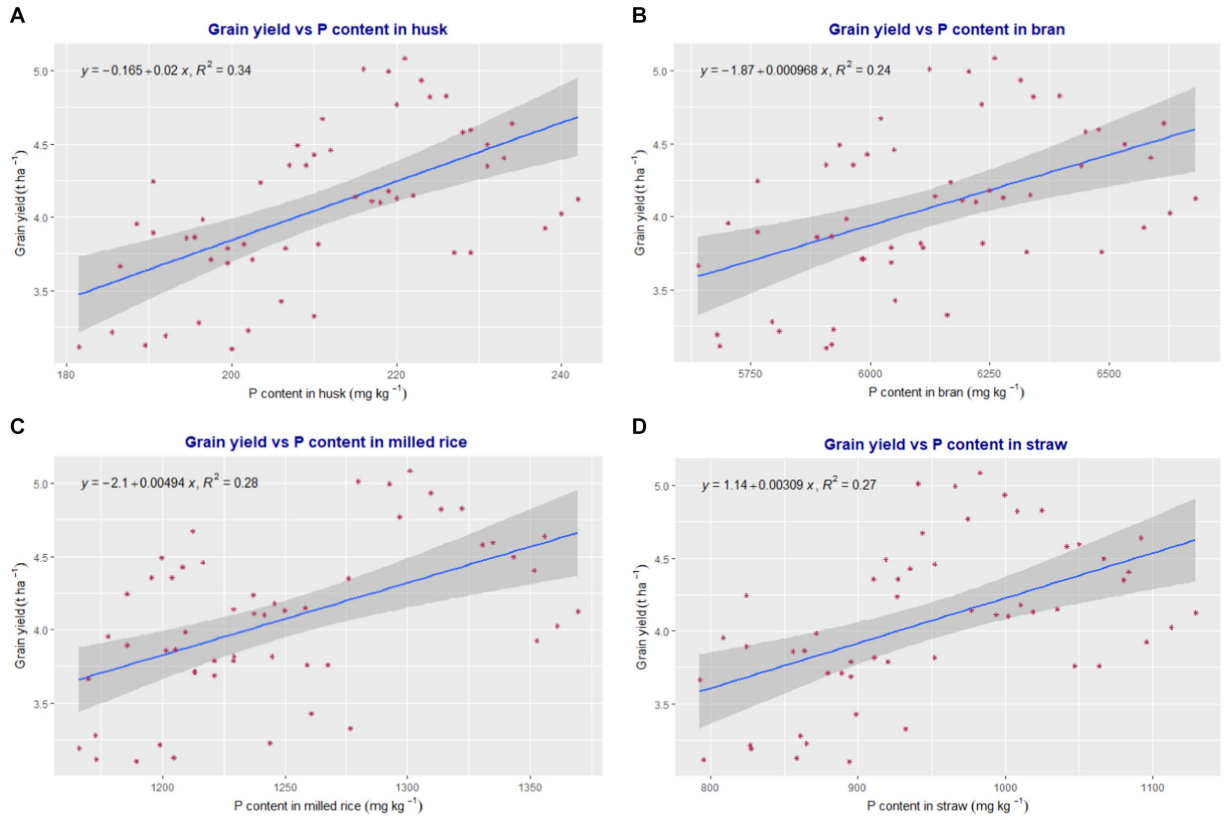

FIGURE 11
(A) Regression between grain yield and P content in husk. **(B)** Regression between grain yield and P content in bran. **(C)** Regression between grain yield and P content in milled rice. **(D)** Regression between grain yield and P content in straw.

essential nutrients like N soil due to enhanced microbial activity in the rhizosphere and stimulation of soil enzymes such as urease (Raliya et al., 2017). Secondly, ZnO NPs foster root growth, likely due to elevated indole acetic acid production, facilitating better nutrient absorption (Adhikari et al., 2015). Moreover, the application of ZnO NPs has been seen to augment the plant's sink capacity, thereby increasing overall biomass and nutrient accumulation in rice plants (Chen et al., 2020). Interestingly, a reverse relationship was observed between the applied Zn amounts and NUE metrics, such as PFP, AE, and RE. the application of 0.2% nano zinc oxide coated urea outperformed the 0.1% counterpart in terms of NUE. Further, nano ZnO-coated urea outperformed traditional bulk ZnO due to its enhanced adsorption, translocation, and gradual release (Zulfiqar et al., 2020). In our study, a prominent positive correlation was noted between N and Zn concentrations in grain (Figure 12). Zn plays a crucial role in aiding N absorption and translocation in rice. The study elucidated the impact of Zn and N synergism, emphasizing the elevation in N uptake due to Zn nutrition, thereby enhancing NUE. Notably, the application of NZnCU (N5/N6) showcased an increase in grain yield and augmented N in both grain and straw, contributing to the enhancement of NUE indices. Further, the use of coated urea is also advantageous due to its capability to slow down urea hydrolysis, minimizing losses and ensuring adequate N availability for crops culminating in better NUE (Yaseen et al., 2021).

5 Conclusion

The utilization of *Sesbania* as a green manure prior to transplanting had a significant positive impact on various aspects of *Basmati* rice, including plant height, dry matter, productivity, and milling qualities. This beneficial influence was further improved when *Sesbania* was combined with 0.2% nano ZnO coated urea. Our study on *Basmati* rice strongly suggests that the combination of nano ZnO coated urea is effective in promoting the transport of essential macronutrients, specifically N, P and K into the edible tissue. Notably, the yield response of *Basmati* rice treated with 0.2% nano ZnO coated urea was comparable to those treated with the conventional fertilization approach, i.e., 1% bulk ZnO coated urea, even with a 20% reduction in zinc application. The successful delivery of optimal macronutrients, particularly nitrogen, to plants through agronomic techniques like summer green manuring and nano zinc oxide coated urea, along with the efficient translocation of these nutrients into the edible grain portions, as demonstrated in our research, shows significant promise in addressing the prevalent nitrogen

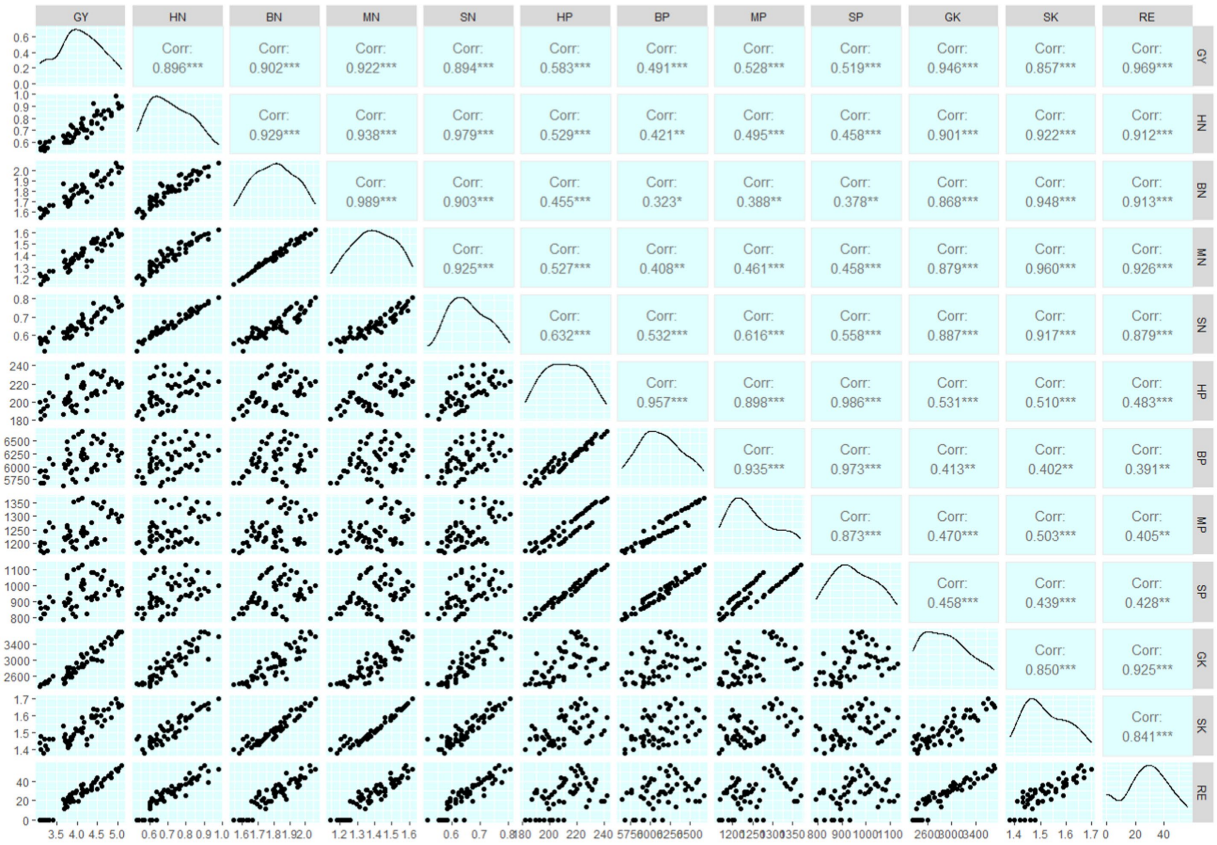

FIGURE 12
Correlation matrix depicting correlation co-efficient (upper half), density plot (diagonal) and scatter plot (lower half). GY, grain yield; HN, husk N content (%); BN, bran N content (%); MN, milled rice N content (%); SN, straw N content (%); HP, husk P content (mg kg^{-1}); BP, bran P content (mg kg^{-1}); MP, milled rice P content (mg kg^{-1}); SP, straw P content (mg kg^{-1}); GK, grain K content (mg kg^{-1}); SK, straw K content (%); RE, recovery efficiency of N (%) *Significant at $p = 0.05$; **Significant at $p = 0.01$; ***Significant at $p = 0.001$.

deficiency in plants. Long term studies are essential to gain a thorough understanding of efficacy of green manure and nano ZnO across various agro-ecology, farming, and cropping systems and fully assessing the long term sustainability of this novel strategy.

Data availability statement

The original contributions presented in the study are included in the article/Supplementary material, further inquiries can be directed to the corresponding author.

Author contributions

KB: Investigation, Data curation, Formal analysis, Methodology, Software, Writing – original draft. YS: Conceptualization, Funding acquisition, Investigation, Supervision, Writing – review & editing. RP: Supervision, Writing – review & editing. DK: Data curation, Supervision, Writing – review & editing. CS: Software, Writing – review & editing. SM: Data curation, Software, Writing – review & editing. SN: Data curation, Software, Writing – review & editing. KR: Data curation, Formal analysis, Software, Writing – review & editing.

Funding

The author(s) declare that no financial support was received for the research, authorship, and/or publication of this article.

Acknowledgments

The authors acknowledge the ICAR-Indian Agricultural Research Institute and the Indian Council of Agricultural Research, New Delhi, India for the financial support and necessary facilities.

Conflict of interest

The authors declare that the research was conducted in the absence of any commercial or financial relationships that could be construed as a potential conflict of interest.

Publisher's note

All claims expressed in this article are solely those of the authors and do not necessarily represent those of their affiliated organizations, or those of the publisher, the editors and the reviewers. Any product that may be evaluated in this article, or claim that may be made by its manufacturer, is not guaranteed or endorsed by the publisher.

Supplementary material

The Supplementary material for this article can be found online at: https://www.frontiersin.org/articles/10.3389/fsufs.2024.1352924/full#supplementary-material

References

Adhikari, T., Kundu, S., Biswas, A. K., Tarafdar, J. C., and Subba Rao, A. (2015). Characterization of zinc oxide nano particles and their effect on growth of maize (*Zea mays* L.) plant. *J. Plant Nutr.* 38, 1505–1515. doi: 10.1080/01904167.2014.992536

Adhikary, S., Biswas, B., Chakraborty, D., Timsina, J., Pal, S., Tarafdar, J. C., et al. (2022). Seed priming with selenium and zinc nanoparticles modifies germination, growth, and yield of direct-seeded rice (*Oryza sativa* L.). *Sci. Rep.* 12:7103. doi: 10.1038/s41598-022-11307-4

Akhtar, N., Ilyas, N., Meraj, T. A., Pour-Aboughadareh, A., Sayyed, R. Z., Mashwani, Z. U. R., et al. (2022). Improvement of plant responses by nanobiofertilizer: a step towards sustainable agriculture. *Nanomaterials* 12:965. doi: 10.3390/nano12060965

Al-Khayri, J. M., Rashmi, R., Surya Ulhas, R., Sudheer, W. N., Banadka, A., Nagella, P., et al. (2023). The role of nanoparticles in response of plants to abiotic stress at physiological, biochemical, and molecular levels. *Plants* 12:292. doi: 10.3390/plants12020292

APEDA. (2023). Available at: https://apeda.gov.in/apedawebsite/SubHead_Products/Basmati_Rice.htm (Accessed January 15, 2023)

Aulakh, C. S., Kaur, P., Walia, S. S., Gill, R. S., Sharma, S., and Buttar, G. S. (2016). Productivity and quality of *Basmati* rice (*Oryza sativa*) in relation to nitrogen management. *Indian J. Agron.* 61, 467–473.

Bala, R., Kalia, A., and Dhaliwal, S. S. (2019). Evaluation of efficacy of ZnO nanoparticles as remedial zinc nano fertilizer for rice. *J. Soil Sci. Plant Nutr.* 19, 379–389. doi: 10.1007/s42729-019-00040-z

Baral, K., Kumar, D., and Shivay, Y. S. (2019). Effects of ZnO nano-particles embedded nitrogen, phosphorus and potassium fertilizer on productivity, physical grain quality and nutrient harvest indices of aromatic rice (*Oryza sativa*). *Indian J. Agron.* 64, 520–523.

Baral, K., Kumar, D., and Shivay, Y. S. (2020). Effect of zinc oxide nanoparticles embedded NPK fertilizer on growth, yield and zinc concentration and uptake of aromatic rice (*Oryza sativa*). *Indian J. Agric. Sci.* 90, 1626–1630. doi: 10.56093/ijas.v90i8.105980

Beig, B., Niazi, M. B. K., Jahan, Z., Hussain, A., Zia, M. H., and Mehran, M. T. (2020). Coating materials for slow release of nitrogen from urea fertilizer: a review. *J. Plant Nutr.* 43, 1510–1533. doi: 10.1080/01904167.2020.1744647

Beig, B., Niazi, M. B. K., Sher, F., Jahan, Z., Malik, U. S., Khan, M. D., et al. (2022). Nanotechnology-based controlled release of sustainable fertilizers. A review. *Environ. Chem. Lett.* 20, 2709–2726. doi: 10.1007/S10311-022-01409-W

Beig, B., Niazi, M. B. K., Ullah, B., Gondal, A. N., Jahan, Z., Zia, M., et al. (2023). Effect of zinc oxide and zinc oxide nanoparticles coating on urea diffusion and its release kinetics for design and development of slow-release fertilizer: an experimental and numerical investigation. *J. Coat. Technol. Res.* 21, 199–213. doi: 10.1007/s11998-023-00810-6

Bhardwaj, A. K., Malik, K., Chejara, S., Rajwar, D., Narjary, B., and Chandra, P. (2023). Integration of organics in nutrient management for rice-wheat system improves nitrogen use efficiency via favorable soil biological and electrochemical responses. *Front. Plant Sci.* 13:1075011. doi: 10.3389/fpls.2022.1075011

Chen, C., Shu, X. W., Xu, J. J., Yu, X. F., Gao, Y. B., Tang, D. N., et al. (2020). Fundamental features of P, K absorption and utilization in rice populations with different sink capacity. *J. Zhejiang Univ. Agric. Life Sci.* 21, 12–28. doi: 10.1631/jzus.B1900452

de Mendiburu, F.. (2019). *Package 'agricolae' statistical procedures for agricultural research*. R Package, version 1.3.1

Dimkpa, C., and Bindraban, P. (2018). Nanofertilizers: new products for the industry? *Agric. Food Chem.* 66, 6462–6473. doi: 10.1021/acs.jafc.7b02150

Du, W., Yang, J., Peng, Q., Liang, X., and Mao, H. (2019). Comparison study of zinc nanoparticles and zinc sulphate on wheat growth: from toxicity and zinc biofortification. *Chemosphere* 227, 109–116. doi: 10.1016/j.chemosphere.2019.03.168

Elshayb, O. M., Farroh, K. Y., Amin, H. E., and Atta, A. M. (2021). Green synthesis of zinc oxide nanoparticles: fortification for rice grain yield and nutrients uptake enhancement. *Molecules* 26:584. doi: 10.3390/molecules26030584

Fageria, N. K., and Baligar, V. C. (2003). Methodology for evaluation of lowland rice genotypes for nitrogen use efficiency. *J. Plant Nutr.* 26, 1315–1333. doi: 10.1081/PLN-120020373

Fageria, N. K., Dos Santos, A. B., and Cobucci, T. (2011). Zinc nutrition of lowland rice. *Commun. Soil Sci. Plant Anal.* 42, 1719–1727. doi: 10.1080/00103624.2011.584591

Farooq, M., Ullah, A., Rehman, A., Nawaz, A., Nadeem, A., Wakeel, A., et al. (2018). Application of zinc improves the productivity and biofortification of fine grain aromatic rice grown in dry seeded and puddled transplanted production systems. *Field Crops Res.* 216, 53–62. doi: 10.1016/j.fcr.2017.11.004

Ghoneim, A. M. (2016). Effect of different methods of Zn application on rice growth, yield and nutrients dynamics in plant and soil. *J. Agric. Ecol. Res. Int.* 6, 1–9. doi: 10.9734/JAERI/2016/22607

Gomez, K. A., and Gomez, A. A. (1984). "Statistical procedures for agricultural research" in *An international rice research institute book. 2nd* ed (New York: John Wiley & Sons)

Hanway, J. J., and Heidel, H. (1952). Soil analysis methods as used in Iowa state college soil testing laboratory. *Iowa State Coll. Agric. Bull.* 57:131.

Hou, P., Xue, L., Zhou, Y., Li, G., Yang, L., and Xue, L. (2019). Yield and N utilization of transplanted and direct-seeded rice with controlled or slow-release fertilizer. *Agron. J.* 111, 1208–1217. doi: 10.2134/agronj2018.03.0192

Hussain, A., Ali, S., Rizwan, M., Rehman, M. Z. U., Javed, M. R., Imran, M., et al. (2018). Zinc oxide nanoparticles alter the wheat physiological response and reduce the cadmium uptake by plants. *Environ. Pollut.* 242, 1518–1526. doi: 10.1016/j.envpol.2018.08.036

Kandil, E. E., El-Banna, A. A., Tabl, D. M., Mackled, M. I., Ghareeb, R. Y., Al-Huqail, A. A., et al. (2022). Zinc nutrition responses to agronomic and yield traits, kernel quality, and pollen viability in rice (*Oryza sativa* L.). *Front. Plant Sci.* 13:791066. doi: 10.3389/fpls.2022.791066

Khampuang, K., Dell, B., Chaiwong, N., Lordkaew, S., Rouached, H., and Prom-U-Thai, C. (2022). Grain zinc and yield responses of two rice varieties to zinc biofortification and water management. *Sustainability* 14:8838. doi: 10.3390/su14148838

Khan, M. R., and Siddiqui, Z. A. (2020). Role of zinc oxide nanoparticles in the management of disease complex of beetroot (*Beta vulgaris* L.) caused by *Pectobacterium betavasculorum*, *Meloidogyne incognita* and *Rhizoctonia solani*. *Hortic. Environ. Biotechnol.* 62, 225–241. doi: 10.1007/s13580-020-00312-z

Kumar, N., Samota, S. R., Venkatesh, K., and Tripathi, S. C. (2023). Global trends in use of nano-fertilizers for crop production: advantages and constraints—a review. *Soil Tillage Res.* 228:105645. doi: 10.1016/j.still.2023.105645

Kumar, D., Uppal, R. S., Ram, H., and Dhaliwal, S. S. (2016). Effect of N, Zn and Fe application on N, P, K content and their total uptake in Parmal rice (*Oryza sativa* L.). *Prog. Agric.* 16, 71–76. doi: 10.5958/0976-4615.2016.00012.0

Liu, Y., Ma, C., Li, G., Jiang, Y., Hou, P., Xue, L., et al. (2023). Lower dose of controlled/slow-release fertilizer with higher rice yield and N utilization in paddies: evidence from a meta-analysis. *Field Crops Res.* 294:108879. doi: 10.1016/j.fcr.2023.108879

Lonergan, P. F., Pallotta, M. A., Lorimer, M., Paull, J. G., Barker, S. J., and Graham, R. D. (2009). Multiple genetic loci for zinc uptake and distribution in barley (*Hordeum vulgare*). *New Phytol.* 184, 168–179. doi: 10.1111/j.1469-8137.2009.02956.x

Mandal, A., and Pal, A. K. (2009). Growth of roots and yield as influenced by green manuring in rice–wheat cropping system. *Agric. Sci. Digest* 29, 32–35.

Mangaraj, S., Paikaray, R. K., Maitra, S., Pradhan, S. R., Garnayak, L. M., Satapathy, M., et al. (2022). Integrated nutrient management improves the growth and yield of rice and green gram in a rice—green gram cropping system under the coastal plain agro-climatic condition. *Plants* 11:142. doi: 10.3390/plants11010142

Meena, B. L., Fagodiy, R. K., Prajapat, K., Dotaniya, M. L., Kaledhonkar, M. J., and Sharma, P. C. (2018). "Legume green manuring: an option for soil sustainability" in *Legumes for soil health and sustainable management*. eds. R. Meena, A. Das, G. Yadav and R. Lal (Singapore: Springer), 387–408.

Meng, X., Li, Y., Zhang, Y., and Yao, H. (2019). Green manure application improves rice growth and urea nitrogen use efficiency assessed using ^{15}N labeling. *Soil Sci. Plant Nutr.* 65, 511–518. doi: 10.1080/00380768.2019.1635872

Naik, S. K., and Das, D. K. (2007). Relative performance of chelated zinc and zinc sulphate for low land rice (*Oryza sativa* L.). *Nutr. Cycling Agroecosyst.* 81, 219–227. doi: 10.1007/s10705-007-9158-7

Nongbet, A., Mishra, A. K., Mohanta, Y. K., Mahanta, S., Ray, M. K., Khan, M., et al. (2022). Nanofertilizers: a smart and sustainable attribute to modern agriculture. *Plants* 11:2587. doi: 10.3390/plants11192587

Olsen, R., Cole, C. V., Watanabe, F. S., and Dean, L. A. (1954). "Estimation of available Q26 phosphorus in soils by extraction with sodium bicarbonate" in *Circular No. 939* (Washington, DC: United States Department of Agriculture)

Panhwar, Q. A., Naher, U. A., Radziah, O., Shashuddin, J., Razi, I. M., Dipti, S. S., et al. (2015). Quality and antioxidant activity of rice grown on alluvial soil amended with Zn, cu and Mo. *S. Afr. J. Bot.* 98, 77–83. doi: 10.1016/j.sajb.2015.01.021

Parashar, R., Afzal, S., Mishra, M., and Singh, N. K. (2023). Improving biofortification success rates and productivity through zinc nanocomposites in rice (*Oryza sativa* L.). *Environ. Sci. Pollut. Res.* 30, 44223–44233. doi: 10.1007/s11356-023-25293-1

Piper, C. S.. (1966). *Soil and plant analysis*. Hans Publishers, Bombay, India. pp. 250–251.

Pooniya, V., and Shivay, Y. S. (2015). Influence of green manuring and zinc fertilization on quality parameters of *Basmati* rice. *Commun. Soil Sci. Plant Anal.* 46, 382–392. doi: 10.1080/00103624.2014.981275

Pooniya, V., Shivay, Y. S., Pal, M., and Bansal, R. (2018). Relative performance of boron, sulphur and zinc coatings onto prilled urea for increasing productivity and nitrogen use efficiency in maize. *Exp. Agric.* 54, 577–591. doi: 10.1017/S0014479717000254

Pooniya, V., Shivay, Y. S., Rana, A., Nain, L., and Prasanna, R. (2012). Enhancing soil nutrient dynamics and productivity of *Basmati* rice through residue incorporation and zinc fertilization. *Eur. J. Agron.* 41, 28–37. doi: 10.1016/j.eja.2012.03.004

Prakash, V., Rai, P., Sharma, N. C., Singh, V. P., Tripathi, D. K., Sharma, S., et al. (2022). Application of zinc oxide nanoparticles as fertilizer boosts growth in rice plant and alleviates chromium stress by regulating genes involved in oxidative stress. *Chemosphere* 303:134554. doi: 10.1016/j.chemosphere.2022.134554

Prasad, R., and Hobbs, P. R. (2018). "Efficient nitrogen management in the tropics and subtropics" in *Soil nitrogen uses and environmental impacts* (CRC Press), 191–232.

Prasad, R., Shivay, Y. S., Kumar, D., and Sharma, S. N. (2006). *Learning by doing exercises in soil fertility (a practical manual for soil fertility)*. Division of Agronomy, Indian Agricultural Research Institute, New Delhi pp, 68.

Qiong, W. U., Wang, Y. H., Ding, Y. F., Tao, W. K., Shen, G. A. O., Li, Q. X., et al. (2021). Effects of different types of slow-and controlled-release fertilizers on rice yield. *J. Integr. Agric.* 20, 1503–1514. doi: 10.1016/S2095-3119(20)63406-2

Raliya, R., Saharan, V., Dimkpa, C., and Biswas, P. (2017). Nanofertilizer for precision and sustainable agriculture: current state and future perspectives. *J. Agric. Food Chem.* 66, 6487–6503. doi: 10.1021/acs.jafc.7b02178

Sadhukhan, R., Sharma, L. D., Sen, S., Karmakar, S., Banerjee, K., and Baral, K. (2021). Enhancing the productivity of field crops through nano-fertilizer. *Agricultural development in asia—potential use of nano-materials and nano-technology*. IntechOpen

Satake, T.. (1990). *Modern Rice milling technology*. University of Tokyo Press, Tokyo.

Selvi, R. V., and Kalpana, R. (2009). Potentials of green manure in integrated nutrient management for rice—a review. *Agric. Rev.* 30, 40–47.

Sheikhnazari, S., Niknezhad, Y., Fallah, H., and Barari Tari, D. (2023). Integrated application of rice husk biochar and ZnO-NPs improves yield components, yield and nutrient uptake in grain of rice under different nitrogen fertilizer levels. *Gesunde Pflanzen* 75, 211–221. doi: 10.1007/s10343-022-00691-6

Shivay, Y. S., Kumar, D., Prasad, R., and Ahlawat, I. P. S. (2008). Relative yield and zinc uptake by rice from zinc sulphate and zinc oxide coatings onto urea. *Nutr. Cycl. Agroecosyst.* 80, 181–188. doi: 10.1007/s10705-007-9131-5

Shivay, Y. S., Pooniya, V., Pal, M., Ghasal, P. C., Bana, R., and Jat, S. L. (2019). Coated urea materials for improving yields, profitability, and nutrient use efficiencies of aromatic rice. *Glob. Chall.* 3:1900013. doi: 10.1002/gch2.201900013

Subbiah, B. V., and Asija, G. L. (1956). A rapid procedure for the estimation of available nitrogen in soils. *Curr. Sci.* 25, 259–260.

Sun, H., Zhou, S., Zhang, J., Zhang, X., and Wang, C. (2020). Effects of controlled-release fertilizer on rice grain yield, nitrogen use efficiency, and greenhouse gas emissions in a paddy field with straw incorporation. *Field Crops Res.* 253:107814. doi: 10.1016/j.fcr.2020.107814

Yadav, A., Yadav, K., and Abd-Elsalam, K. A. (2023). Nanofertilizers: types, delivery and advantages in agricultural sustainability. *Agrochemicals* 2, 296–336. doi: 10.3390/agrochemicals2020019

Yang, G., Yuan, H., Ji, H., Liu, H., Zhang, Y., Wang, G., et al. (2021). Effect of ZnO nanoparticles on the productivity, Zn biofortification, and nutritional quality of rice in a life cycle study. *Plant Physiol. Biochem.* 163, 87–94. doi: 10.1016/j.plaphy.2021.03.053

Yaseen, M., Ahmad, A., Naveed, M., Ali, M. A., Shah, S. S. H., Hasnain, M., et al. (2021). Subsurface-applied coated nitrogen fertilizer enhanced wheat production by improving nutrient-use efficiency with less ammonia volatilization. *Agronomy* 11:2396. doi: 10.3390/agronomy11122396

Zhang, H., Wang, R., Chen, Z., Cui, P., Lu, H., Yang, Y., et al. (2021). The effect of zinc oxide nanoparticles for enhancing rice (*Oryza sativa* L.) yield and quality. *Agriculture* 11:1247. doi: 10.3390/agriculture11121247

Zhu, H., Zhang, T., Zhang, C., He, X., Shi, A., Tan, W., et al. (2022). Optimizing irrigation and nitrogen management to increase yield and nitrogen recovery efficiency in double-cropping rice. *Agronomy* 12:1190. doi: 10.3390/agronomy12051190

Zulfiqar, U., Hussain, S., Ishfaq, M., Matloob, A., Ali, N., Ahmad, M., et al. (2020). Zinc-induced effects on productivity, zinc use efficiency, and grain biofortification of bread wheat under different tillage permutations. *Agronomy* 10:1566. doi: 10.3390/agronomy10101566

Zulfiqar, U., Hussain, S., Maqsood, M., Ishfaq, M., and Ali, N. (2021). Zinc nutrition to enhance rice productivity, zinc use efficiency, and grain biofortification under different production systems. *Crop Sci.* 61, 739–749. doi: 10.1002/csc2.20381

frontiers | Frontiers in Sustainable Food Systems

TYPE Original Research
PUBLISHED 12 September 2024
DOI 10.3389/fsufs.2024.1388916

Check for updates

OPEN ACCESS

EDITED BY
Mohamed Ait-El-Mokhtar,
University of Hassan II Casablanca, Morocco

REVIEWED BY
Marco E. Mng'ong'o,
Mbeya University of Science and Technology, Tanzania
Sudip Sengupta,
Swami Vivekananda University, India
Muhammad Aleem Ashraf,
Khwaja Fareed University of Engineering and Information Technology (KFUEIT), Pakistan

*CORRESPONDENCE
Rajan Bhatt
rajansoils@pau.edu
Akbar Hossain
akbarhossainwrc@gmail.com

RECEIVED 20 February 2024
ACCEPTED 15 August 2024
PUBLISHED 12 September 2024

CITATION
Bhatt R, Imas P, Perelman A, Verma KK, Al-Shuraym LA, Sayed S, Gaber A and Hossain A (2024) Polyhalite improves growth, yield, and quality and reduces insect pest incidence in sugarcane (*Saccharum officinarum* L.) in the semiarid tropics.
Front. Sustain. Food Syst. 8:1388916.
doi: 10.3389/fsufs.2024.1388916

COPYRIGHT
© 2024 Bhatt, Imas, Perelman, Verma, Al-Shuraym, Sayed, Gaber and Hossain. This is an open-access article distributed under the terms of the Creative Commons Attribution License (CC BY). The use, distribution or reproduction in other forums is permitted, provided the original author(s) and the copyright owner(s) are credited and that the original publication in this journal is cited, in accordance with accepted academic practice. No use, distribution or reproduction is permitted which does not comply with these terms.

Polyhalite improves growth, yield, and quality and reduces insect pest incidence in sugarcane (*Saccharum officinarum* L.) in the semiarid tropics

Rajan Bhatt[1]*, Patricia Imas[2], Adi Perelman[2], Krishan K. Verma[3], Laila A. Al-Shuraym[4], Samy Sayed[5], Ahmed Gaber[6] and Akbar Hossain[7]*

[1]PAU–Krishi Vigyan Kendra, Amritsar, India, [2]International Potash Institute (IPI), Industriestrasse, Switzerland, [3]Sugarcane Research Institute, Guangxi Academy of Agricultural Sciences/Key Laboratory of Sugarcane Biotechnology and Genetic Improvement (Guangxi), Ministry of Agriculture and Rural Affairs/Guangxi Key Laboratory of Sugarcane Genetic Improvement, Nanning, China, [4]Department of Biology, College of Science, Princess Nourah Bint Abdulrahman University, Riyadh, Saudi Arabia, [5]Department of Economic Entomology and Pesticides, Faculty of Agriculture, Cairo University, Giza, Egypt, [6]Department of Biology, Faculty of Science, Taif University, Taif, Saudi Arabia, [7]Division of Soil Science, Bangladesh Wheat and Maize Research Institute, Dinajpur, Bangladesh

Introduction: In semiarid tropical locations, polyhalite ($K_2Ca_2Mg(SO_4)4H_2O$) and muriate potash (KCl) were tested for their ability to increase cane growth, yield, and recovery at potash (K)- and calcium (Ca)-deficient sites.

Methods: The treatments involved control plots with no potash fertilizer (T_1); T_2 and T_3 applied potassium through (muriate potash) MOP only at 80 and 120 kg K_2O ha^{-1}, whereas T_4 and T_5 applied potassium with half of MOP and polyhalite at 80 and 120 kg K_2O ha^{-1}, respectively.

Results and discussion: At 35 days after harvest (DAH), T_2 (10.82%), T_3 (24.1%), T_4 (34.9%), and T_5 (34.9%) had a greater ratoon resprouting rate than did the control treatment, where it was just 37.0 out of 100 harvested canes. At 308 DAH, T_2 (–5.9%), T_3 (–5.7%), and T_5 (–6.6%) presented greater leaf chlorophyll contents than did T_1. The K-fertilized plots yielded 64.31 t ha^{-1} in T_2 and 65.97 t ha^{-1} in T_5, whereas the control plot yielded 61.5 t ha^{-1}. Compared with the control plots, the T_5 plots experienced fewer stalk borer (–28.6%), top borer (–23.3%), and early shoot borer (–23.3%) attacks. T_2, T_4, and T_5 presented higher percentages of commercial cane sugar (CCS) (6.82, 8.83, and 8.74%, respectively) than did the control plots. T_1 and T_3 had similar CCSs (10.99 and 11.33%, respectively). The CCS weight per area ranged from 7.98 to 8.47 t ha^{-1} near maturity. T_4 (8.59 t ha^{-1}) and T_5 (8.60 t ha^{-1}) had significantly greater values than did T_1–T_3. Compared with the control, the applied potassium fertilizer increased the economic output by 8,711, 11,687, 13,485, and 13,857 INR ha^{-1} in the T_2, T_3, T_4, and T_5 plots, respectively. The higher cost of polyhalite than MOP has reduced its economic advantages. Thus, the T_4 plots outperformed the other treatments in terms of growth, yield, and quality indices, but their higher values (120 kg K_2O ha^{-1}) were statistically equivalent.

Conclusion: Finally, the study concluded that MOP and polyhalite at a 50% ratio of 80 kg K_2O ha^{-1} may help improve sugarcane growth, yield, and quality in semiarid tropical locations.

KEYWORDS

polyhalite, sugarcane, productivity, quality, insect pest

1 Introduction

As a major industrial crop, sugarcane (*Saccharum* spp.) is cultivated in semiarid regions ranging from 36.7°N to 31.0°S in tropical to subtropical regions of the equator (Bhatt et al., 2021c; Choudhary and Singh, 2016; Bhatt, 2020). Generally, sugarcane is planted for two purposes: to extract sugar, which accounts for 75% of global sugar consumption, and to produce ethanol, which is blended into gasoline (O'Hara et al., 2009; Singh et al., 2011; Bhatt and Singh, 2021). In Punjab, India, the cane area is 91,000 ha, with a land productivity of 800 qt ha^{-1} and a sugar recovery of <10% (PAU, 2022). Among the different claimed reasons for the lower sugar recovery in the region, the major ones are unbalanced fertilizer use with little attention given to potash, upcoming water-stressed conditions, higher insect pest and disease incidence, and poor quality of cane seeds offered to cane farmers, which restricts sugarcane productivity and quality in the region (Bhatt et al., 2021a; Bhatt et al, 2021c).

However, an important barrier to reaching the potential yield of high-quality crops is the uneven use of fertilizers, especially potash (Bhatt et al., 2021b). According to one previous study, 2.08 qt ha^{-1} nitrogen, 0.53 qt ha^{-1} phosphorus, 2.80 qt ha^{-1} potassium, and 0.30 qt ha^{-1} S, as well as relatively low levels of other elements, are required for every 1,000 qt of sugarcane produced (Shukla et al., 2017).

Sugarcane is grown in Indian Punjab on soils that are already low in sulfur (S), magnesium (Mg), calcium (Ca), and potassium (K). Very little soil fertilizer containing potassium is used. Therefore, both sugarcane productivity and recovery are lower than those in neighboring states with solid potash recommendations. To reduce the risk of lodging, insect pests, and disease susceptibility in the canes, potash is needed. The various pools of K present in the soils are as follows: 90–98% of the total is mineral K, 1–2% is exchangeable K, 1–10% is non-exchangeable K, and 0.1–0.2% is soil-soluble K. Potassium ions move across pools in the soil system when the pool equilibrium is changed (Barber, 1995; Wakeel and Ishfaq, 2022). The soluble and exchangeable potassium pools in the soil re-equilibrate quickly. After being transferred from clay exchange sites during flooding, some soils can lose a significant quantity of potassium. In soils with limited cation exchange capacity, potash (K) leakage is a serious problem (Singh et al., 2004; Fageria et al., 1990).

In agricultural soils for enhancing both water and land productivity, muriate potash (KCl) has long been used. to meet crop potassium demands (Bhatt and Singh, 2021). The sustainable dose of MOP in sugarcane agriculture has not been standardized or recommended in the region (Bhatt and Singh, 2021; Bhatt et al., 2021b). However, Bhatt et al. (2021b) attempted to treat plant canes in the region but, to date, have not been tested for ratoon canes. Sugarcane lands where canes have been preferred for decades have been reported to be deficient in nutrients, particularly potash, owing to their high uptake and almost no supply from the outside environment. "Polyhalite" ($K_2Ca_2Mg(SO_4)4H_2O$) is a multinutrient fertilizer (AngloAmerican, 2016) that provides us with many nutrients, *viz.* 14% K, 17% Ca, 6% MgMg, and 48% SS (AngloAmerican, 2016). This nutrient organic fertilizer is being removed 1.2 km deep from the sea of the northeastern coast of England (Garnett, 2021), which has few ecological implications (Pavinato et al., 2020). Compared with typical fertilizer, polyhalite acts as a slow-release nutrient (Vale, 2016), which further leads to less leaching losses and reduces its footprint (Bhatt and Singh, 2021). Previously, many workers evaluated its efficiency in many crops, *viz. Zea mays*, L. (maize) (Fraps, 1932; Tien et al., 2020); *Sorghum bicolor*, L. (sorghum) (Barbarick, 1991); *Actinidia deliciosa* (kiwifruit) (Zhao et al., 2020); *Solanum tuberosum* (potato) (Garnett, 2021); *Solanum Lycopersicum* (tomato) (Sacks et al., 2017); *Brassica oleracea* var. *capitata* (cabbage) (Tien et al., 2021). In comparison to other forms of K fertilizers, including KCl, polyhalite has been shown to produce soil K that is retained by plants for an extended period of time (Lewis et al., 2020). To date, the efficiency of polyhalite in the ratoon crop in semiarid regions of sugarcane (*Saccharum officinarum*) has not been examined (Bhatt et al., 2020), although Bhatt et al. (2021a) evaluated the performance of this plant crop. In the present study, halite, which is composed of hydrated K, Ca, Mg, and S, was studied as a partial substitute for MOP fertilizer.

Polyhalite supplies Ca for membrane stability (Steward, 1974; Kirkby and Pilbeam, 1984; White and Broadley, 2003), as do numerous signal transduction pathways and initiation (Steward, 1974; Kirkby and Pilbeam, 1984; White and Broadley, 2003; Monshausen, 2012). Furthermore, because Ca is transferred in vegetation via xylem sap, canes are unable to remobilize Ca from older tissues, increasing the importance of polyhalite in our Ca-deficient plots, which resulted in greater growth and yield parameters. The Mg provided by polyhalite is necessary for photosynthesis and glucose partitioning (Cakmak and Yazici, 2010; Farhat et al., 2016; Gransee and Führs, 2013). However, S also enhances cane land productivity (Khan and Mobin, 2005; Kovar and Grant, 2011) by commonly interacting with nitrogen (Jamal et al., 2010). Balanced nutrient utilization is required to sustainably increase sugarcane production and quality; ignorance of the optimum nutrient balance could be detrimental (Bhatt, 2020; Bhatt and Singh, 2021). K is important for the morphological and biochemical activity of sugarcane plants: it controls stomatal opening, translocates plant assets from all around the plant, diminishes the prevalence and mortality of insect pest attacks, encourages root development, and enhances nutrient, pesticide, and moisture efficiency improvements while also decreasing crop inputs in agriculture to reduce their respective footprints (Bhatt et al., 2021a; Bhatt et al., 2021b). When K levels are low, photosynthesis products (Hartt, 1969) and their transportation in cane plants are significantly hampered (Quampah et al., 2011). While Bhatt et al. (2021b) attempted to corroborate these findings in the plant crop, the present study also conducted experiments in the ratoon crop using different combinations of MOP and multinutritional fertilizer polyhalite during the 2021–2022 ratoon season. The objectives of this study were to determine (1) a sustainable potash dose for increasing ratoon cane development and land productivity, (2) which was associated with the lowest incidence of insect pests, and (3) which was associated with the greatest cost benefits.

2 Materials and methods

2.1 Investigation location

Investigations were approved from March 2021 to March 2022 during the sugarcane ratoon season at the experimental farm of the PAU–Regional Research Station, Kapurthala, Punjab, India, which is situated at 31° 23.032′ N and 75° 21.647′ E, with an elevation of 0.225 km

above sea level. The ratoon cane crop regenerated from spring 2021 to 2022 after the plant cane crop was harvested on 22 March 2021. The meteorological data during the experiment period from April 2021 to March 2022 are provided in Supplementary Figure S1.

2.2 Soil characteristics

Standard procedures were used to gather representative, repeated soil samples from the site (Bhatt and Sharma, 2014). In March 2021, following the harvesting of sugarcane seed crops via a posthole auger (with an inner diameter of 7.2 cm), 10 surface (0–15 cm) soil samples were collected. The samples of soil were left in the shade for 48 h to dry. Throughout the sampling depths, large roots, trash, and stones were carefully removed from the samples that were obtained. The samples of soil were laid out on an uncontaminated piece of cloth and allowed to dry in the shade for 48 h. After the drying process was finished, the soil clods were broken up with a wooden hammer and passed through a 2 mm sieve. The materials were subsequently placed in sterile polythene bags and appropriately labeled for evaluation of their chemical and physical properties. The texture of the soil was estimated via the feel method. Standard procedures were followed to estimate the pH and EC of the soil in a 1:2 soil:water mixture (Jackson, 1967). The soil organic carbon content was measured via Walkley and Black wet digestion and the fast titration method (Walkley and Black, 1934). The available K and phosphorus (P) contents were measured via 1 N ammonium acetate (pH 7) extract and 0.5 M NaHCO3 extract (Olsen, 1954), respectively (Jackson, 1967). To determine the Ca and Mg contents in the soils, the EDTA method was used (Barrows and Simpson, 1962). The results of the analysis revealed that 65–68% of the samples from the investigated location were loaded with coarse sand and 11–33% with clay, and the topsoil was low in K, Ca, and SOC (%) but high in P and Mg (Table 1).

2.3 Irrigation liquid extraction

The groundwater level at the testing site was 26 m. The quality of the irrigation water used on the crop was determined in triplicate, and the findings are displayed in Table 2.

2.4 Treatments and experimental design

Nitrogen fertilizers were applied to all the plots at the regionally recommended dose (RRD) (PAU, 2022). Potash fertilizers (K_2O ha^{-1}) were broadcast under different treatments: T_2: MOP alone or in combination with polyhalite ($K_2Ca_2Mg(SO_4)4H_2O$) under different doses; T_1: 0 kg of K_2O ha^{-1}; T_2: 80 kg of K_2O ha^{-1} as muriate potash; T_3: 120 kg of K_2O ha^{-1} as muriate potash; T_4: 80 kg of K_2O ha^{-1} as muriate potash + polyhalite (50% each); T_5: 120 kg of K_2O ha^{-1} as muriate potash + polyhalite (50% each). The detailed treatments of the present ratoon sugarcane experiments are summarized in Table 3.

The above combinations were distributed in randomized block designs in 15 plots measuring 6 m × 4.5 m in length, with three replicates, as was done earlier for plant crops, as shown in Figure 1.

TABLE 1 Properties of the 0–15 cm soil layer at the investigation site.

Soil properties	Ideals
Sand	65.1%
Clay	11.7%
pH	8.66
Electrical conductivity	0.22 ds m^{-1}
SOC	0.35%
N	34.4 kg ha^{-1}
P	54.4 kg ha^{-1}
K	135.6 kg ha^{-1}
Mg	553.7 ppm
Ca	140.3 ppm
Bulk density	1.67 Mg m^{-3}

pH, potential of hydrogen; SOC, soil organic carbon; N, available nitrogen; P, available phosphorus; K, available potash; Mg, available magnisium; Ca, available calcium.

TABLE 2 Irrigation water quality parameters of the tube–well water at the investigation site.

Replications	(meq L^{-1})				Residual $NaCO_3$	EC (ds m^{-1})
	$Ca^{2+} + Mg^{2+}$	Cl^{-1}	CO_3^{-2}	HCO_3^-		
R_1	3.8	0.6	0.0	3.6	0.0	0.48
R_2	3.5	0.7	0.0	3.4	0.0	0.52
R_3	3.4	0.7	0.0	3.7	0.0	0.50
Mean ± SE	3.6 ± 0.12	0.7 ± 0.03	0.0	3.7 ± 0.09	0.0	0.51 ± 0.01

$Ca^{2+} + Mg^{2+}$, calcium and magnesium; Cl^{-1}, chloride; CO_3^{-2}, carbonates; HCO_3^-, bicarbonates; Residual $NaCO_3$, residual sodium carbonates; EC, electrical conductivity.

TABLE 3 Different fertilizer combinations in the different investigation plots.

Treatments	Potassium nourishment			
	$(K_2Ca_2Mg(SO_4)4H_2O)$ (%)	$(K_2Ca_2Mg(SO_4)\ 4H_2O)$ (kg K_2O_5 ha^{-1})	KCl (%)	KCl (kg K_2O_5 ha^{-1})
T_1	0.0	0.0	0.0	0.0
T_2	0.0	0.0	66.0	80.0
T_3	0.0	0.0	100.0	120.0
T_4	33.0	40.0	33.0	40.0
T_5	50.0	60.0	50.0	60.0

T_1 = 0 kg of K_2O ha^{-1}; T_2 = 80 kg of K_2O ha^{-1} as a muriate potash (KCl); T_3 = 120 kg of K_2O ha^{-1} as a muriate potash; T_4 = 80 kg of K_2O ha^{-1} as a muriate potash + polyhalite (50% each); T_5 = 120 kg of K_2O ha^{-1} as a muriate potash + polyhalite (50% each).

FIGURE 1
Layout of the experiment carried out at RRS, Kapurthala [T_1: 0 kg of K_2O ha^{-1}; T_2: 80 kg of K_2O ha^{-1} as a muriate potash (KCl); T_3: 120 kg of K_2O ha^{-1} as a muriate potash; T_4: 80 kg of K_2O ha^{-1} as a muriate potash + polyhalite (50% each); T_5: 120 kg of K_2O ha^{-1} as a muriate potash + polyhalite (50% each)].

FIGURE 2
Field view of the ratoon sugarcane crop in the experimental field.

On 26 March 2021, the earlier sugarcane crop of CoPb 93 was harvested for the regrowth of the next ratoon crop in the present study. The best-practice agronomic approaches for ratoon cane production were adopted on the basis of the recommendation of Punjab Agricultural University, Ludhiana (PAU, 2022), and the crop stand is shown in Figure 2.

2.5 Collection of different growth and yield parameters

The proportion of resprouted setts that germinated in each plot 35 days after the plant crop was harvested in each treatment was calculated (Bhatt and Singh, 2021; Bhatt et al., 2021b). To determine the number of tillers in each treatment plot, the total number of tillers from a 5 m^2 area was physically counted at 210 and 310 days after harvesting (DAH) of seed crops (Bhatt and Singh, 2021). A total of 347 DAHs for the milling of sugarcane stalks were reported. From the entire plot area, canes that were suitable for milling were visually examined and numbered. 1,000 ha^{-1} was the unit of expression used to describe the ends (Bhatt and Singh, 2021; Bhatt et al., 2021b). For each plot, five sugarcane stalks were randomly selected and marked. At 128, 144, 172, and 217 days after harvest (DAH), a ruler was used to measure the distance between the highest growth point of the stalks and the soil surface.

Using Vernier calipers, the cane girths of five randomly selected and tagged sugarcane stalks were measured at 116, 171, 198, and 280 DAH. The stalk diameter was calculated by averaging the stalk diameter measurements at the cane's head, center, and lower ends (Bhatt and Singh, 2021; Bhatt et al., 2021b). At 170, 218, 280, and 315, five randomly selected disease-free tagged sugarcane stalks were used for recording the total number of nodes and the average of the five nodes considered. At 238, 277, and 308 DAH, a SPAD-502+ chlorophyll meter was used to measure the leaf chlorophyll content under the different treatments. Additionally, when the sugarcane stalks from each experimental plot were harvested by hand and weighed via a field scale, the weight of all the stalks was recorded as t ha^{-1}, representing the cane yield.

2.6 Ratoon cane quality parameters

At the 10th and 12th months, five disease-free ratoon stalks were randomly selected and removed from each plot for analysis of their juice quality parameters at the Biochemistry Laboratory of the PAU–Regional Research Station, Kapurthala, Punjab, India. Using a cane crusher, the juice was extracted and tested for quality through established procedures (Meade and Chen, 1977). Using a digital refractometer (Optics Technology Delhi 34), the Brix and sugar percentage in the juice were determined as described previously (Meade and Chen, 1977). The following formula (Equation i) was used to estimate the percentage of commercial cane sugar (CCS) consumed:

$$\mathrm{CCS}(\%) = \left[\mathrm{Sucrose}\% - (\mathrm{Brix}\% - \mathrm{Sucrose}\%) \times 0.4\right] \times 0.74 \quad \text{(i)}$$

(Equation i) has crushing and multiplication factors of 0.74 and 0.4, respectively.

The following formula (Equation ii) was used to determine the CCS content in t ha^{-1} via the cane yield and the percentage of total CCS.

$$\mathrm{CCS}\left(\mathrm{t\ ha^{-1}}\right) = [\mathrm{CCS}(\%) \times \mathrm{sugarcane\ yield}\left(\mathrm{t\ ha^{-1}}\right]/100 \quad \text{(ii)}$$

2.7 Insect–pest frequency monitoring

During the 2021–2022 ratoon season, several insect pests of sugarcane were thoroughly documented. These pests, which included the early shoot borer (*Chilo infuscatellus*), top borer (*Scirpophaga excerptalis*), and stalk borer (*Chilo auricilius*), had a detrimental effect on sugarcane yield. In June, the top borer population was counted, the early shoot borer population was counted after 60 DAH in May, and the stalk borer population was counted from 100 plants at harvest to evaluate the impact of irrigation and potash doses on the incidence of insect pests on sugarcane. The % incidence of early shoot borer has been estimated by using the following formula (Equation iii):

$$\%\ \text{incidence of early shoot borer} = \frac{\text{Total number of dead hearts}}{\text{Total number of shoots}} \times 100 \quad \text{(iii)}$$

In June, July, and August, the top borer percentage incidence (Equation iv) was recorded, and the cumulative incidence was computed.

$$\%\ \text{Incidence of top borer} = \frac{\text{Total number of infested canes in 3 m row length}}{\text{Total number of canes observed in 3 m row length}} \times 100 \quad \text{(iv)}$$

The percentage of aged stalks at the time of harvest was recorded.

$$\text{Percent incidence of stalk borer} = \frac{\text{Total number of affected canes}}{100\ \text{canes}} \times 100 \quad \text{(v)}$$

2.8 Benefit-to-cost ratio

The benefits of the different treatments were calculated via the costs of MOP and polyhalite (as applied) as well as the MSP (Bhatt and Singh, 2021; Bhatt et al., 2021b; Kumar et al., 2019) via the following (Equation vi):

$$\mathrm{B:C\ ratio} = \text{Economic benefit from additional K} \left(\mathrm{INR\ ha^{-1}}\right) / \text{Cost of additional K} \left(\mathrm{INR\ ha^{-1}}\right) \quad \text{(vi)}$$

2.9 Data analysis

The online OPSTAT tool was used to assess cane growth, quality, and insect pest data. $p < 0.05$ indicated statistical significance. The correlations between experimental treatment quality measures were also examined via R (Olivoto and Dal'Col Lúcio, 2020).

3 Results

3.1 Ratoon cane performance pertaining to growth and yield parameters

During 2021–2022, the resprouting time, height, girth, number of nodes per plant, number of millable canes, number of tillers per plant, chlorophyll content, and cane weight were greater on the advanced side of the K-fertilized plots than in the control plots (Figure 3; Table 4).

The irrigation water used to irrigate the canes is a good standard (Table 2). At 35 DAH, the resprouted ratoon buds were greater in the T_2 (through 10.82%), T_3 (through 24.1%), T_4 (through 34.9%), and T_5 (through 34.9%) treatments than in the control treatment (Figure 3). At 128 DAH, there was no discernible difference in ratoon cane length between the K treatment and the control treatment. There were no changes in stalk height between any of the treatments at 144 DAH (T_3, T_4, and T_5 had stalks greater than those in the control plots) or 172 DAH (the stalks in the T_5 canes were taller than those in the control

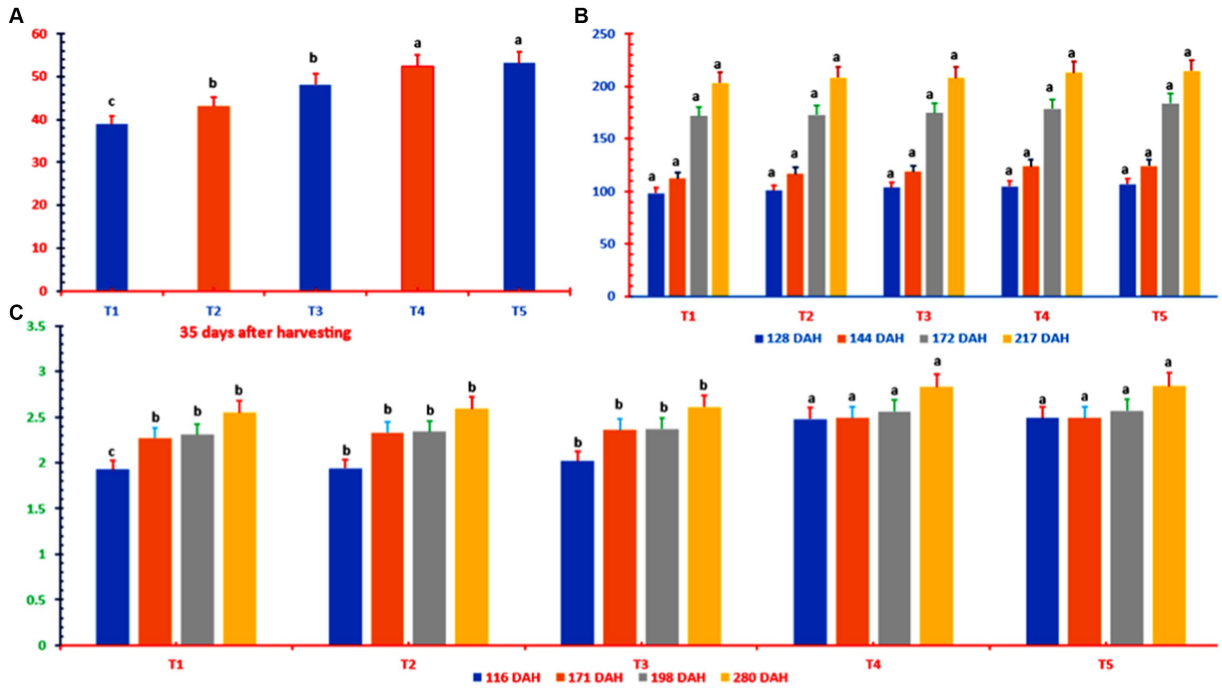

FIGURE 3
Ratoon sugarcane resprouting **(A)**, height **(B)**, and girth **(C)** at different K doses and sources. DAH, days after harvesting; T_1 = 0 kg of K_2O ha^{-1}; T_2 = 80 kg of K_2O ha^{-1} as muriate of potash; T_3 = 120 kg of K_2O ha^{-1} as muriate of potash; T_4 = 80 kg of K_2O ha^{-1} as muriate potash + polyhalite (50% each); T_5 = 120 kg of K_2O ha^{-1} as muriate potash + polyhalite (50% each). In column bars, means with similar letter(s) are identical as per $LSD_{0.05}$.

TABLE 4 Ratoon sugarcane growth and land productivity at different K doses and sources.

Treatments	Per cane nodes				NMC (000 ha^{-1})	Number of tillers		Chlorophyll concentration			Land productivity (t ha^{-1})
	Days after harvesting (DAH)										
	170	218	280	315	347	211	310	238	277	308	
T_1	14.5^a	19.5^a	22.6^a	24.3^a	3.3^c	4.4^a	6.7^b	66.2^a	41.6^a	42.4^a	61.50^c
T_2	14.8^a	19.5^a	22.0^a	22.7^c	3.7^b	5.1^a	7.2^{ab}	60.0^b	34.3^b	39.9^b	64.31^b
T_3	14.5^a	19.5^a	22.1^a	24.1^b	3.9^b	4.9^a	7.6^{ab}	54.6^c	30.0^c	40.0^b	65.27^{ab}
T_4	14.1^a	18.9^a	21.9^a	23.1^{bc}	4.5^a	4.6^a	8.4^a	44.8^d	33.5^b	36.4^c	65.85^a
T_5	14.5^a	19.7^a	22.5^a	23.4^b	4.6^a	5.0^a	8.3^b	45.6^d	30.3^c	39.6^b	65.97^a
CD (≤0.05)	NS	NS	NS	0.53	0.4	NS	NS	2.6	2.6	2.1	1.33
SE (m)	0.62	0.34	0.31	0.16	0.11	0.34	0.51	0.79	0.79	0.63	0.40
CV (%)	7.4	3.0	2.43	1.18	4.6	12.1	11.5	2.5	4.1	2.7	1.10

NMC, number of millable canes; DAH, days after harvesting. T_1 = 0 kg of K_2O ha^{-1}; T_2 = 80 kg of K_2O ha^{-1} as a muriate potash; T_3 = 120 kg of K_2O ha^{-1} as a muriate potash; T_4 = 80 kg of K_2O ha^{-1} as a muriate potash + polyhalite (50% each); T_5 = 120 kg of K_2O ha^{-1} as a muriate potash + polyhalite (50% each; three replicates). In a column, means with similar letter(s) are identical as per $LSD_{0.05}$.

plots). By 217 DAH, however, there were no appreciable differences in stalk height across any of the treatments.

The sugarcane stalk widths for T_4 and T_5 were greater than those for T_1, T_2, or T_3 (Figure 3). At 116 DAH, the difference in stalk diameter was greatest, with an increase over that in T_1 of up to 29% in T_5. At 280 DAH, compared with the control treatment, T_5 resulted in the greatest increase in stalk diameter at 11%. Similarly, the T_4 and T_5 treatments resulted in significantly greater changes from the baseline treatment across all three growth and yield measures and greater changes in stalk diameter than did the T_1, T_2, and T_3 treatments. However, the T_4 and T_5 treatment plots were significantly comparable (Figure 3).

Table 4 clearly shows that the number of nodes or tillers per ratoon cane did not change over time in any way that could be distinguished between the treatments. The K-treated plots had more millable cane per treatment at 347 DAH than did the control plots, where no potash was applied (Table 4). T_4 and T_5, which were MOP plus polyhalite treatments, had 36–39% more NMC than did T_1, whereas T_2 and T_3, which were MOP-only treatments, had 12–18% more NMC than did T_1.

The SPAD meter results indicated that at 238, 277, and 308 DAH, the chlorophyll content of the leaves was lower in all the K treatments than in the reference point control plots (Table 4). The leaf chlorophyll concentrations at 308 DAH were lower in T_2 (−5.9%), T_3 (−5.7%), and T_5 (−6.6%) than in T_1, with T_4 (−14.2%) having the lowest concentration.

The baseline treatment yielded an average of 61.5 t ha^{-1}. All the potash-fertilized plots yielded yields greater than the baseline yield, ranging from 64.31 t ha^{-1} in T_2 to 65.97 t ha^{-1} in T_5, with the T_4 and T_5 plots reporting the highest yields, followed by the T_3 and T_2 plots. This was true regardless of the type of K fertilizer used. The T_2, T_3, T_4, and T_5 plots yielded 4.6, 6.1, 7.1, and 7.3% more pollen, respectively, than did the control T_1 plot (Table 4).

3.2 Quality parameters

The T_4 and T_5 treatment plots presented greater purities (3.2 and 4.3%, respectively) than did the T_1 control treatment after 10 months of cane crop growth (Table 5). In terms of purity, however, T_3 did not differ considerably from T_1. The T_1 and T_3 treatments had statistically similar Pols, whereas the T_2 (5.6%), T_4 (6.8%), and T_5 (7.5%) treatments had greater Pols than did the T_1 control. The percentages of commercial cane sugar (CCS) in T_1 and T_3 were similar (10.987 and 11.332%, respectively), but the percentage of CCS was greater in T_2 (6.82%), T_4 (8.83%), and T_5 (8.74%) than in the control plots.

For all the quality parameters at the 10th month, the T_4 and T_5 plots presented similar values, which were greater than those of the control T_1 plot; however, at a higher dose in the T_5 plot, there was a 3% decrease in the amount of extracted sugar. However, the T_2 and T_4 plots received 80 kg K_2O ha^{-1} potash alone or in combination with 40 kg K_2O ha^{-1} and 40 kg polyhalite ha^{-1}, respectively, while the juice quality parameters were similar. However, on the higher side, *viz.* like in T_3 and T_5, 120 kg K_2O ha^{-1} had some benefit from the T_2 and T_4 plots in terms of quality, but all five quality metrics were similar (Table 5).

Table 6 shows that T_2, T_4, and T_5, which were significantly equivalent in purity (by 2.81, 2.87, and 0.81%, respectively), had germinated from ratoon sugarcane after 12 months compared with T_1 and T_3. On the other hand, the Brix values of the T_2, T_3, T_4, and T_5 plots were 4.58, 0.14, 3.66, and 0.73% lower than those of the T_1 control plots, respectively (Table 6). In treatments T_1 through T_5, the CCS percentage (ranging from 12.99 to 13.05%) was comparable across all the treatment plots. A comparison of the T_2 and T_3 plots to the T_1 plot revealed that the average values were −0.62 and −0.10%, respectively, but the increases in the T_4 and T_5 plots were +0.46 and +0.38%, respectively. In terms of weight per area, the CCS ranged from 7.98 to 8.47 t ha^{-1}, with T_4 (8.59 t ha^{-1}) and T_5 (8.60 t ha^{-1}) having significantly greater CCSs than did any of the T_1–T_3 samples.

Furthermore, Table 6 shows that T_2 (20.83°) and T_4 (21.03°) had lower Brix values than did the T_1 control (21.83°). The percentage of sugar extracted did not differ significantly between treatments, ranging from 48.82% in T_1 to 50.66% in T_4, as previously reported (Filho, 1985; Wood, 1990; Chapman, 1980). In terms of the quality measures investigated, the T_2 and T_4 plots with 80 kg ha^{-1} K exhibited a substantial difference from the T_1 control compared with the treatments with 120 kg ha^{-1} K fertilizer applied, as previously reported (Sudama et al., 1998; Singh et al., 1999).

3.3 Infestation of insect pests

Compared with the control treatment, all K treatments reduced early shoot borer (*Chilo infuscatellus*) attack, as T_5 had the greatest

TABLE 5 Ratoon sugarcane quality parameters at 10 months at different K doses and sources.

Treatments	Brix (°)	Pol (%)	Purity (%)	CCS (%)	Extraction (%)
T_1	18.7^{b}	16.1^{c}	86.1^{c}	10.99^{c}	47.05^{a}
T_2	19.1^{ab}	17.0^{ab}	88.6^{ab}	11.74^{ab}	48.44^{a}
T_3	19.0^{ab}	16.5^{bc}	87.0^{bc}	11.33^{bc}	46.77^{a}
T_4	19.3^{ab}	17.2^{a}	89.3^{a}	11.96^{a}	50.13^{a}
T_5	19.5^{a}	17.3^{a}	88.7^{ab}	11.95^{a}	48.63^{a}
CD (≤0.05)	NS	0.62	2.14	0.51	NS
SE (m)	0.18	0.19	0.65	0.15	1.30
CV (%)	0.14	1.92	1.27	2.30	4.67

CCS, commercial cane sugar content; DAH, days after harvesting; T_1 = 0 kg of K_2O ha^{-1}; T_2 = 80 kg of K_2O ha^{-1} as muriate potash; T_3 = 120 kg of K_2O ha^{-1} as muriate potash; T_4 = 80 kg of K_2O ha^{-1} as muriate + polyhalite (50% each); T_5 = 120 kg of K_2O ha^{-1} as muriate potash + polyhalite (50% each; three replicates). In a column, means with similar letter(s) are identical as per $LSD_{0.05}$.

TABLE 6 Ratoon sugarcane quality parameters at 12 months at different K doses and sources.

Treatments	Brix (°)	Pol (%)	Purity (%)	CCS (%)	Sugar extraction (%)	CCS (t ha^{-1})
T_1	21.83^{a}	18.95^{ab}	86.78^{b}	12.99^{a}	48.82^{a}	7.98^{c}
T_2	20.83^{b}	18.58^{b}	89.22^{a}	12.91^{a}	49.01^{a}	8.30^{b}
T_3	21.80^{a}	18.92^{ab}	86.82^{b}	12.98^{a}	49.23^{a}	8.47^{b}
T_4	21.03^{b}	18.78^{b}	89.27^{a}	13.05^{a}	50.66^{a}	8.59^{a}
T_5	21.67^{a}	18.95^{ab}	87.48^{b}	13.04^{a}	50.01^{a}	8.60^{a}
CD (≤0.05)	0.62	0.46	1.60	NS	NS	0.32
SE (m)	0.186	0.14	0.48	0.11	1.00	0.10
CV (%)	1.50	1.28	0.94	1.40	3.50	1.98

CCS, commercial cane sugar; DAH, days after harvesting; T_1 = 0 kg of K_2O ha^{-1}; T_2 = 80 kg of K_2O ha^{-1} as muriate; T_3 = 120 kg of K_2O ha^{-1} as muriate potash; T_4 = 80 kg of K_2O ha^{-1} as muriate potash + polyhalite (50% each); T_5 = 120 kg of K_2O ha^{-1} as muriate potash + polyhalite (50% each). In a column, means with similar letter(s) are identical as per $LSD_{0.05}$.

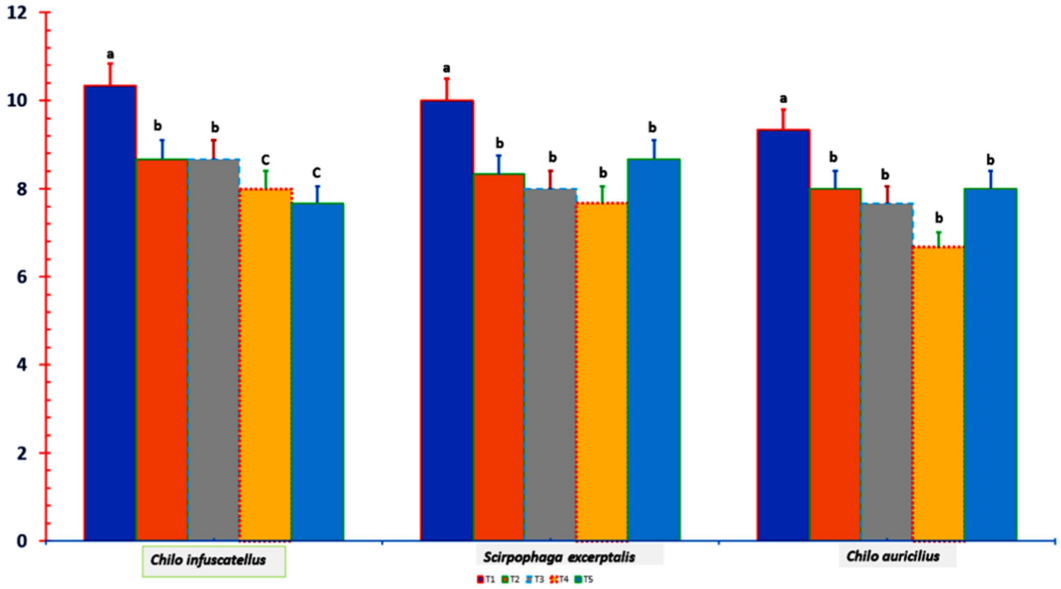

FIGURE 4
Insect pest incidence in ratoon canes at different K doses and sources. In all the treatments, the recommended dose of non-K fertilizers was applied. DAH, days after harvesting; T_1 = 0 kg of K_2O ha^{-1}; T_2 = 80 kg of K_2O ha^{-1} as muriate potash; T_3 = 120 kg of K_2O ha^{-1} as muriate; T_4 = 80 kg of K_2O ha^{-1} as muriate potash + polyhalite (50% each); T_5 = 120 kg of K_2O ha^{-1} as muriate potash + polyhalite (50% each; three replicates). In column bars, means with similar letter(s) are identical as per $LSD_{0.05}$.

reduction (−25.8%), whereas T_2 and T_3 had the least reduction (−16.1%) (Figure 4).

While the stalk borer (*Chilo auricilius*) and top borer (*Scirpophaga excerptalis*) were less common in T_4 than in the control, there was no discernible difference in their occurrence between any of the K_2O treatments and the control (Figure 4). Compared with those in the control plots, T_5 presented the fewest early shoot-borer attacks (−23.3%), whereas T_4 presented the lowest incidence of stalk borer attacks (−28.6%) and top borer assaults (−23.3%). Among the K_2O treatments, T_3 had the highest frequency of stem borer infestation and the greatest occurrence of attack from all three insect pests. The early shoot borer (*Chilo infuscatellus*) and top borer (*Scirpophaga excerptalis*), at 0.0, −8.0, and 13.4%, and the stalk borer (*Chilo auricilius*), at −4.2, −13.0, and 20.0%, respectively, were significantly lower in the T_2, T_3, T_4, and T_5 plots (Figure 4). The T_4 treatment (80 kg K_2O ha^{-1}) had the lowest incidence of insect pest infestations, despite being significantly comparable to the other potash treatments.

3.4 Correlation analysis between quality variables

Correlation analysis between quality variables revealed that Brix was positively correlated with all the other quality parameters, with much stronger correlations with CCS (%) and Pol. Furthermore, CCS (%) had a stronger and more positive relationship with Brix, Pol, purity, and extractable %age. The extractable %age and purity were reported to have strong positive relationships with CCS (%) and Pol, respectively. Finally, Pol was reported to have a strong positive relationship with all the other quality parameters by December (Table 7).

TABLE 7 Investigation of correlations between various quality indices of ratoon sugarcane plants at 10 and 12 months of age with various K sources and dosages.

After 10 months					
	Brix	CCS (%)	Extractable %age	Pol	Purity
Brix	1.00	0.77*	0.47	0.85*	0.37
CCS (%)	0.77*	1.00	0.55*	0.99*	0.88*
Extractable %age	0.47	0.55*	1.00	0.55*	0.45
Pol	0.85*	0.99*	0.55*	1.00	0.81*
Purity	0.37	0.88*	0.45	0.81*	1.00

After 12 months						
	Brix	CCS (%)	CCS (t ha$^{-1)}$	Extractable %age	Pol	Purity
Brix	1.00	0.49	0.13	0.16	0.79*	−0.71*
CCS (%)	0.49	1.00	0.76*	0.28	0.92*	0.27
CCS (t ha^{-1})	0.13	0.76*	1.00	0.37	0.59*	0.47
Extractable %age	0.16	0.28	0.37	1.00	0.27	0.04
Pol	0.79*	0.92*	0.59*	0.27	1.00	−0.12
Purity	−0.71*	0.27	0.47	0.04	0.12	1.00

CCS, commercial cane sugar (%); CCS (t ha^{-1}), commercial cane sugar (t ha^{-1}; three replicates). *Differer significantly at 5% level of probability.

TABLE 8 The benefit-to-cost ratio of ratoon sugarcane at different K doses and sources.

Treatments	Extra potash fertilizer price (US $ ha^{-1})	Cane land productivity (t ha^{-1})	Yield change from the control plot (t ha^{-1})	Economic profit from applied potash (US $ ha^{-1})	Profit over expenditure ratio
T_1	0	61.50	0	0	0.00
T_2	34.3	64.31	2.81	117.8	3.44
T_3	51.4	65.27	3.77	158.1	3.08
T_4	75.0	65.85	4.35	182.4	2.43
T_5	112.6	65.97	4.47	187.4	1.66

INR, Indian rupee; sugarcane price: INR 3,100 t^{-1}; MOP cost: US $257 t^{-1}; polyhalite cost: US $406 t^{-1}; T_1 = 0 kg of K_2O ha^{-1}; T_2 = 80 kg of K_2O ha^{-1} as a muriate potash; T_3 = 120 kg of K_2O ha^{-1} as muriate potash; T_4 = 80 kg of K_2O ha^{-1} as muriate potash + polyhalite (50% each); T_5 = 120 kg of K_2O ha^{-1} as a muriate potash + polyhalite (50% each). The average rate of 2021 US $ is equivalent to 73.94 INR.

For the ratoon crop at 12 months, Brix was positively but weakly related to CCS (%), CCS (t ha^{-1}), and extractable %age but was strongly related to pol (0.79); however, it was strongly but negatively related to purity (−0.71), which was not observed after the 10th month. CCS (%) had both positive and strong relationships with CCS (t ha^{-1}) (0.76) and pol (0.92) but had weak relationships with purity (0.27) and extractable %age (028). However, Pol had positive relationships with Brix (0.79), CCS (%) (0.92), and CCS (t ha^{-1}) (0.59) (Table 7). However, after the 12th month, the extractable %age also had a weaker relationship with the other quality parameters.

3.5 Profit-over-expenditure ratio

The most costly K fertilizers were found in T_5 (120 kg K_2O ha^{-1} applied as KCl and $K_2Ca_2Mg(SO_4)4H_2O$ combined; Table 8), whereas the least expensive fertilizers were found in T_2 (80 kg K_2O ha^{-1} applied as KCl alone). T_5 yielded 65.97 t ha^{-1}, the highest output, whereas T_1 yielded 61.5 t ha^{-1}. For T_2, T_3, T_4, and T_5, the applied K fertilizer produced economic gains of 117.8, 158.1, 182.4, and 187.4 US $ ha^{-1}, respectively (Table 8).

The benefit-to-cost ratios of T_2 (3.44) and T_3 (3.08) were the highest, whereas those of T_4 (2.43) and T_5 (2.43) were the lowest (1.66). Although polyhalite, which is imported from England, is more expensive than other nutrients, it is still a great multinutrient fertilizer for soils that are low in both Ca and K. Benefit reductions of 10.5 and 31.6% were observed after switching from T_2 to T_3 and from T_4 to T_5, respectively. Higher K fertilizer broadcasting did not enhance farmers' economic benefits (Table 8), because greater production costs are associated with greater K fertilizer application. These costs were lower for the combined KCL and $K_2Ca_2Mg(SO_4)4H_2O$ treatments than for the KCl treatment alone. The advantages were not increased but rather diminished by switching from T_2 to T_3 and then from T_4 to T_5 (Table 8). This could have been due to increased insect pest infestations, yield responses, and higher fertilizer prices.

4 Discussion

4.1 Development and yields of ratoon sugarcane

In the deficient K soils, broadcasted potash resulted in enhanced development and land productivity of the ratoon sugarcane plants (Figure 3; Table 4) compared with those in the unfertilized control plots because of the role of the potash in controlling stomatal openings under stressed conditions and sugar translocation (Wood and Schroeder, 2004). Potash plays a role in increasing the rhizosphere zone of cane plants, which helps reduce the negative effects of water stress (Bhatt and Singh, 2021; Bhatt et al., 2020;Bhatt et al.,2021b). Furthermore, the effective H^+/K^+ symport—a protein that simultaneously transports H^+ and K^+ ions across root cell membranes—conveys that K absorption is more efficient than Ca or Mg (Bhatt et al., 2020; Wood and Schroeder, 2004). Potash also catalyzes enzymes, enhances the efficiency of applied inputs such as water and fertilizers such as N fertilizers through interactive effects (Korndörfer and Oliveira, 2005), and improves the extraction of moisture and minerals from soils (Singh et al., 1999; Wood and Schroeder, 2004; Korndörfer and Oliveira, 2005; Schultz et al., 2010; Kwong, 2002; Ashraf et al., 2008; Bhatt et al, 2021c).

Both 80 kg K_2O ha^{-1} pure muriate potash and 120 kg K_2O ha^{-1} pure muriate potash improved the sugarcane yield when mixed with polyhalite at a 50% ratio. Polyhalite augmented the production of dry matter. In combination with polyhalite and muriate potash treatments, there is less competition between Cl^- and SO_4^{2-} for absorption by plant roots. In sole muriate potash treatments, on the other hand, there can be more severe competition due to the presence of Cl^- and the lack of SO_4^{2-} in the soil (Huber et al., 2012; Dordas, 2008). With respect to isolated potash deposits, this competition could be even worse. Ca^{2+}, K^+, and SO_4^{2-} accumulate in the soil in treatments where polyhalite + MOP are both accessible, leading to enhanced cane development and growth. Furthermore, K in KCl binds to clay granules in soils more firmly than does K from polyhalite because of competition between monovalent (K^+) and divalent (Ca^{2+} and Mg^{2+}) cations; as a result, potash from later sources is more easily accessible. Crop performance is impacted by synchronizing the availability of nutrients with periods of crop nutrient need, as well as by inconsistency in the accessibility of Ca, Mg, and S, particularly in treatments where only MOP is present (Pavuluri et al., 2017). At our Ca deficiency site, polyhalite supplied a regular flow of Ca, Mg, and S, which improved sugarcane development and land productivity in the region (Figure 4; Table 4) (Smith et al., 1987; Clark and Smith, 1988).

Reportedly, higher numbers of millable canes at 315 and 347 DAH, chlorophyll concentrations at 238, 277, and 308 DAH, and land productivity (Table 4), followed by quality parameters at the 10th and 12th months (Tables 5, 6), have been regularly reported in control plots than K-fertilized plots. The enhancements reached a maximum when both polyhalite and muriate potash (50% each) were applied at 80 K_2O ha^{-1}, which was also found to be statistically equivalent to 120 K_2O ha^{-1} plots. Furthermore, lower stomatal conductance and higher mesophyll resistance led to a decrease in starch synthase, nitrate reductase, invertase, phosphofructokinase, sucrose phosphate synthase, β-amylase, and pyruvate kinase. However, deficient K supply resulted in wilting and inadequate photosynthetic translocation from leaves to cane stems under stressful conditions, which also reported a higher prevalence of insect pests (Bhatt and Singh, 2021; Bhatt et al., 2021a; Bhatt et al., 2021b).

Under T_4 and T_5 treatments loaded with polyhalite fertilizer, cane plants receive relatively high levels of K, Ca, and Mg, which increases the storage lifetime of reaped ratton plants and decreases losses that occur after harvesting (Yermiyahu et al., 2019). When loaded with a low chloride concentration, polyhalite behaves as a slow-release fertilizer and is further reported to have a relatively high use efficiency (Yermiyahu et al., 2019; Herrera et al., 2022), lowering the danger of saline conditions and indigenous soil K loss. Ca effects of polyhalite are similar to those of gypsum, which are recognized to be significant for sugarcane output (Bhatt et al., 2020; Bhatt et al., 2021b). Because polyhalite is >10 times more soluble than gypsum, the calcium would migrate to the subsurface more quickly than it does for gypsum. Ca would be applied yearly with polyhalite in place of applying gypsum every 5–7 years to reduce subsoil acidity.

Additionally, the benefit-to-cost ratio decreased when the potash dose increased from 40 kg K_2O ha^{-1}. This occurred because of the greater fertilizer costs (Table 8), lower yields (Table 4), and greater incidence of insect pests (Figure 4). Cane growth and land productivity were both increased by the addition of Ca, Mg, and S, which are low in these nutrients, to the experimental soil.

4.2 Sugarcane juice quality

For combinations of muriate potash and polyhalite, even at 80 kg K_2O ha^{-1}, ratoon cane performance standards were superior to those of muriate potash applied alone, even if the dose was the same (Tables 5, 6). This is because polyhalite provides a more steady supply of essential nutrients, including K^+ and Ca^{2+}, which further enhances various juice quality metrics. Compared with Ca^{2+} or Mg^{2+}, K^+ adsorbs less strongly to mineral soil surfaces, and the overall adsorption capacity of soil increases with increasing clay mineral concentration (Mengel and Haeder, 1977; Rabindra and Kumaraswamy, 1978).

In control plots, insufficient potassium upsets the water balance, resulting in poor growth and reduced sucrose accumulation. Potassium aids in maintaining cell turgor pressure, which is necessary for optimum growth. Potassium stimulates several enzymes essential for starch synthesis, protein synthesis, and photosynthesis. The plant's capacity to create and store carbohydrates, which are subsequently transformed into sucrose, is improved by this activation (Elwan et al., 2008). These metabolic processes are less effective in the absence of sufficient potassium, which lowers the sugar concentration and degrades the quality of the harvested cane in control plots. The movement of nutrients and photosynthates, or the byproducts of photosynthesis, from the leaves to the stalks, where they are stored as sucrose, is another process in which potassium is essential (Bhatt and Singh, 2021; Bhatt et al., 2021b; Wood and Schroeder, 2004).

4.3 Prevalence of pest insects

The plant nutrient balance increases crop resistance to most pests and diseases simply because a healthy ratoon cane is less vulnerable to assault (Huber et al., 2012; Dordas, 2008). A single treatment of MOP at 80 kg K_2O ha^{-1} reduced the number of early shoot borers (*Chilo infuscatellus*), top borers (*Scirpophaga*

excerptalis), and stalk borers (*Chilo auricilius*), albeit not significantly. These reductions were further achieved by pairing MOP and polyhalite at the same dose (Figure 4). Potash (potassium) strengthens plant cell walls, increasing their resistance to pest penetration and reducing insect–pest attacks in sugarcane (Hartt, 1969). Additionally, potassium improves the general health of the plant by strengthening its defense systems, such as the synthesis of chemicals that ward off pests. Furthermore, plants that receive enough potassium from their diet experience less stress, which makes them less susceptible to pest infestations. Potassium increases the plant's capacity to heal from wounds, which lessens the possibility that pests may spread and do serious damage. Reduced pest attacks are the result of stronger physical barriers and improved biochemical defenses in sugarcane that has received potassium fertilization (Bhatt and Singh, 2021; Bhatt et al., 2021b; Elwan et al., 2008; Shukla et al., 2009; Bhatt et al, 2021c).

5 Conclusion

From the results and discussion of the study, it can be concluded that in semiarid tropical soils, among the different nutrients involved in sugarcane cultivation, K^+, Ca^{2+}, Mg^{2+}, and SO_4^{2-} are among those in short supply, owing in part to agricultural intensification. Sugarcane output and juice quality are hampered by a shortage of these critical nutrients. The traditionally used muriate potash is inadequate for addressing this issue and meeting plant needs. Polyhalite has potential for use in the sugarcane production region of North India. We discovered that applying muriate potash alone at 80 kg K_2O ha^{-1} improved ratoon cane performance and enhanced benefits, and these enhancements were further significantly amplified when muriate potash was mixed with polyhalite in deficient soils. However, interestingly, these enhancements in ratoon cane plants were reduced when a higher dose of 120 kg K_2O ha^{-1} was tested at the site, which also reduced the benefits due to the higher costs of additional fertilizers than the reported benefits. The addition of Ca to soils that are low in Ca is one of the anticipated benefits of blending polyhalite with muriate potash at 50%. Further attempts are needed to determine the optimal amounts of important nutrients, such as K, Ca, Mg, and S, for developing balanced fertilization schedules with special emphasis on different sources of potash for improving sugarcane performance and the livelihoods of cane farmers in the region.

Data availability statement

The raw data supporting the conclusions of this article will be made available by the authors, without undue reservation.

Ethics statement

Written informed consent was obtained from the individual(s) for the publication of any identifiable images or data included in this article.

Author contributions

RB: Conceptualization, Data curation, Formal analysis, Funding acquisition, Investigation, Methodology, Validation, Visualization, Writing – original draft. PI: Conceptualization, Funding acquisition, Investigation, Project administration, Supervision, Validation, Visualization, Writing – original draft. AP: Conceptualization, Funding acquisition, Investigation, Methodology, Project administration, Supervision, Validation, Visualization, Writing – original draft. KV: Conceptualization, Investigation, Methodology, Validation, Visualization, Writing – original draft. LA-S: Data curation, Formal analysis, Funding acquisition, Project administration, Software, Writing – review & editing. SS: Data curation, Formal analysis, Funding acquisition, Software, Writing – review & editing. AG: Data curation, Formal analysis, Funding acquisition, Software, Writing – review & editing. AH: Data curation, Formal analysis, Funding acquisition, Resources, Software, Supervision, Writing – review & editing.

Funding

The author(s) declare financial support was received for the research, authorship, and/or publication of this article. This research was funded by the Potash Research Institute of India, Gurgaon, and the International Potash Institute, Switzerland, through Project No. Misc. 168 (PC 5034), "Assessment of POLYHALITE in improving yield and quality of sugarcane in Punjab, India," and was also partially funded by Princess Nourah bint Abdulrahman University Researchers Supporting Project number (PNURSP2024R365), Princess Nourah bint Abdulrahman University, Riyadh, Saudi Arabia.

Conflict of interest

The authors declare that the research was conducted in the absence of any commercial or financial relationships that could be construed as a potential conflict of interest.

Publisher's note

All claims expressed in this article are solely those of the authors and do not necessarily represent those of their affiliated organizations, or those of the publisher, the editors and the reviewers. Any product that may be evaluated in this article, or claim that may be made by its manufacturer, is not guaranteed or endorsed by the publisher.

Supplementary material

The Supplementary material for this article can be found online at: https://www.frontiersin.org/articles/10.3389/fsufs.2024.1388916/full#supplementary-material

References

AngloAmerican. (2016) POLY4 brochure. Available at: https://uk.angloamerican.com/our-fertiliser (Accessed December 21, 2016).

Ashraf, M. Y., Hussain, F., Akhter, J., Gul, A., Ross, M., and Ebert, G. (2008). Effect of different sources and rates of nitrogen and supra optimal level of potassium fertilization on growth, yield and nutrient uptake by sugarcane. Grown under saline conditions. *Pak. J. Bot.* 40, 1521–1531.

Barbarick, K. A. (1991). Polyhalite application to sorghum–sudangrass and leaching in soil columns. *Soil Sci.* 151, 159–166. doi: 10.1097/00010694-199102000-00005

Barber, S. A. (1995). Soil nutrient bioavailability: A mechanical approach. *2nd Edn.* New York: Wiley. 432.

Barrows, H. L., and Simpson, E. C. (1962). An EDTA method for the direct routine determination of calcium and magnesium in soils and plant tissue. *Soil Sci. Soc. Am. J.* 26, 443–445. doi: 10.2136/sssaj1962.03615995002600050012x

Bhatt, R. (2020). "Resources management for sustainable sugarcane production" in Resources use efficiency in agriculture. eds. S. Kumar, S. R. Meena and K. M. Jhariya (Singapore: Springer), 650–685. doi: 10.1007/978-981-15-6953-1_18

Bhatt, R., Oliveira, M. W., and Silva, V. S. G. (2021a). Sugarcane nutrition for food and environmental security. *Brazil J. Dev.* 7, 64431–64467. doi: 10.34117/bjdv7n6-701

Bhatt, R., and Sharma, M. (2014). Importance of soil testing and techniques of soil sampling. England: Lap Lambert Academic Publishing, 1–48.

Bhatt, R., and Singh, P. (2021). Sugarcane response to irrigation and potash levels in subtropics. *Agric. Res. J.* 58, 709–715. doi: 10.5958/2395-146X.2021.00100.9

Bhatt, R., and Singh, M. (2021). Comparative efficiency of polymer–coated urea for lowland rice in semiarid tropics. *Commun. Soil Sci. Plant Anal.* 52, 2331–2341. doi: 10.1080/00103624.2021.1925689

Bhatt, R., Singh, P., Ali, O. M., Latef, A. A. H. A., Laing, A. M., and Hossain, A. (2021b). Yield and quality of ratoon sugarcane are improved by applying potassium under irrigation to potassium deficient soils. *Agronomy* 11:1381. doi: 10.3390/agronomy11071381

Bhatt, R., Singh, P., Hussain, A., and Tamsina, J. (2021c). Rice–wheat system in the northwest indo-Gangetic plains of South Asia: issues and technological interventions for increasing productivity and sustainability. *Paddy Water Environ.* 19, 345–365. doi: 10.1007/s10333-021-00846-7

Bhatt, R., Singh, P., and Kumar, R. (2020). Assessment of polyhalite in improving yield and quality of sugarcane in Punjab, India. Gurgaon: Project submitted to Indian Potash Limited (IPL).

Cakmak, I., and Yazici, A. M. (2010). Magnesium: a forgotten element in crop production. *Better Crops* 94, 23–25.

Chapman, L. S. (1980) Long term responses in cane yields and soil analyses from potassium fertilizer. In: Proceedings of the 1980 conference of the Australian Society of Sugar Cane Technologists, pp. 63–68.

Choudhary, H. R., and Singh, R. K. (2016). Effect of sequential application of herbicides on weeds and productivity of spring–planted sugarcane (*Saccharum officinarum* L.). *Bioscan* 11, 687–690.

Clark, C. J., and Smith, G. S. (1988). Seasonal accumulation of mineral nutrients by kiwifruit 2. Fruit. *New Phytol.* 108, 399–409. doi: 10.1111/j.1469-8137.1988.tb04180.x

Dordas, C. (2008). Role of nutrients in controlling plant diseases in sustainable agriculture. A review. *Agron. Sustain. Dev.* 28, 33–46. doi: 10.1051/agro:2007051

Elwan, E. A., Abazied, A. A., Youssef, L. A., and Sakr, H. E. A. (2008). Influence of some agricultural practices on the infestation with lesser sugarcane borer, Chilo Agamemnon Bles. in the autumn plant cane and its 1st ratoon in upper Egypt. *Egypt. J. Agric. Res.* 86, 1801–1826.

Fageria, N. K., Baligar, V. C., Wright, R. J., and Carvalho, J. R. P. (1990). Lowland rice response to potassium fertilization and its effect on N and P uptake. *Fert. Res.* 21, 157–162. doi: 10.1007/BF01087425

Farhat, N., Elkhouni, A., Zorrig, W., Smaoui, A., Abdelly, C., and Rabhi, M. (2016). Effects of magnesium deficiency on photosynthesis and carbohydrate partitioning. *Acta Physiol. Plant* 38:145. doi: 10.1007/s11738-016-2165-z

Filho, J. O. (1985). "Potassium nutrition of sugarcane" in Potassium in agriculture. ed. R. D. Munson (Madison, WI, USA: American Society of Agronomy, Crop Science Society of America, Soil Science Society of America), 1045–1062.

Fraps, G. S. (1932). Availability to plants to potash in polyhalite. College Station, Texas: Texas Agricultural Experiments Station Bulletin No. 449.

Garnett, S. (2021) The potential of polyhalite fertilizers to enhance potato yield and quality in the United Kingdom. E-ifc, International Potash Institute; 63, pp. 18–27.

Gransee, A., and Führs, H. (2013). Magnesium mobility in soils as a challenge for soil and plant analysis, magnesium fertilization and root uptake under adverse growth conditions. *Plant Soil* 368, 5–21. doi: 10.1007/s11104-012-1567-y

Hartt, C. E. (1969). Some effects of potassium upon the amounts of protein and amino forms of nitrogen, sugars and enzyme activity of sugarcane. *Plant Physiol.* 9, 452–490. doi: 10.1104/pp.9.3.452

Herrera, W. F. B., Arruda, B., De Carvalho, H. W. P., and Pavinato, P. S. (2022). Improving potassium use efficiency of sugarcane through the use of polyhalite. *CABI Agric. Biosci.* 3, 1–11. doi: 10.1186/s43170-022-00124-4

Huber, D., Römheld, V., and Weinmann, M. (2012). "Relationship between nutrition, plant diseases and pests" in Marschner's mineral nutrition of higher plants (Academic Press), 283–298.

Jackson, M. (1967). Soil chemical analysis. New Delhi: Prentice Hall of India Private Limited.

Jamal, A., Moon, Y. S., and Abdin, M. Z. (2010). Sulfur – a general overview and interaction with nitrogen. *Australian J. Crop Sci.* 4, 523–529.

Khan, N. A., and Mobin, M. (2005). Samiullah, the influence of gibberellic acid and sulfur fertilization rate on growth and S–use efficiency of mustard (*Brassica juncea*). *Plant Soil* 270, 269–274. doi: 10.1007/s11104-004-1606-4

Kirkby, E. A., and Pilbeam, D. J. (1984). Calcium as a plant nutrient. *Plant Cell Environ.* 7, 397–405. doi: 10.1111/j.1365-3040.1984.tb01429.x

Korndörfer, G. H., and Oliveira, L. A. (2005). "Potassium in sugarcane crops" in Potassium in Brazilian agriculture. eds. T. Yamada and T. L. Roberts (Piracicaba: Esalq/USP).

Kovar, J. L., and Grant, C. A. (2011) Nutrient cycling in soils: Sulfur. Publications from USDA–ARS/UNL Faculty; Paper 1383.

Kumar, A., Babar, L., Mohan, N., and Bansal, S. K. (2019). Effect of potassium application on yield, nutrient uptake and quality of sugarcane and soil health. *Indian J. Fertil.* 15, 782–786.

Kwong, K. F. (2002) The effects of potassium on growth, development, yield and quality of sugarcane. In Potassium for sustainable crop production and food security, proceedings of the first National Potash Symposium, Dar Es Salaam, Tanzania, 28–29 July 2015; International Potash Institute: Zug, Switzerland; pp. 430–444.

Lewis, T. D., Hallett, P. D., Paton, G. I., and Harrold, L. (2020). Retention and release of nutrients from polyhalite to soil. *Soil Use Manag.* 36, 117–122. doi: 10.1111/sum.12548

Meade, G. P., and Chen, J. C. P. (1977). Can Sugar Handbook. *10th* Edn. New York: Wiley–Interscience, Publication, 405.

Mengel, K., and Haeder, H. E. (1977). Effect of potassium supply on the rates of phloem sap exudation and the composition of phloem sap of ricinis communis. *Plant Physiol.* 59, 282–284. doi: 10.1104/pp.59.2.282

Monshausen, G. B. (2012). Visualizing Ca^{2+} signatures in plants. *Curr. Opin. Plant Biol.* 15, 677–682. doi: 10.1016/j.pbi.2012.09.014

O'Hara, I. M., Edye, L. A., and Doherty, W. (2009) Towards a commercial lignocellulosic ethanol industry in Australia: the Mackay renewable bio commodities pilot plant. In Proceedings of the Australian Society of Sugarcane Technologists, Balina, Australia, 5–8, 31, pp. 11–17.

Olivoto, T., and Dal'Col Lúcio, A. (2020). Metan, an R package for multi-environment trial analysis. *Methods Ecol. Evol.* 11, 783–789. doi: 10.1111/2041-210X.13384

Olsen, S. R. (1954) Estimation of available phosphorus in soils by extraction with sodium bicarbonate (No. 939); US Department of Agriculture.

PAU. (2022) Package of practices for crops of Punjab–Kharif; Punjab Agricultural University: Ludhiana, India; pp. 55–66.

Pavinato, P. S., Corá, J. E., Santos, C., Herrera, A., Pavuluri, W. F. B., and Pierce, F. J. (2020). Sugarcane response to polyhalite fertilizer in Brazilian Oxisols. *Agron. J.* 112, 5264–5278. doi: 10.1002/agj2.20452

Pavuluri, K., Malley, Z., Mzimbiri, M. K., Lewis, T. D., and Meakin, R. (2017). Evaluation of polyhalite in comparison to muriate for corn grain yield in the southern highlands of Tanzania. *African J. Agron.* 5, 325–332.

Quampah, A., Wang, R. M., Shamsi, I. H., Jilani, G., Zhang, Q., Hua, S., et al. (2011). Improving water productivity by potassium application in various rice genotypes. *Int. J. Agric. Biol.* 13, 9–17.

Rabindra, B., and Kumaraswamy, S. (1978). Potash and eye spot disease in sugarcane. *Ind. Potash J.* 3, 15–18.

Sacks, M., Gantz, S., Mezuman, U., Peled, L., and Imas, P. (2017) Polyhalite – a multinutrient fertilizer preventing ca. and mg deficiencies in greenhouse tomatoes under desalinized irrigation water. E-ifc, International Potash Institute; 51, pp. 24–30.

Schultz, N., Lima, E., Pereira, M. G., and Zonta, E. (2010). Residual effects of nitrogen, potassium and vinasse, fertilization on cane plant and ratoon harvested with and without straw burning. *Rev. Bras. Ci Solo* 34, 811–820. doi: 10.1590/S0100-06832010000300023

Shukla, S. K., Solomon, S., Sharma, L., Jaiswal, V. P., Pathak, A. D., and Singh, P. (2017). Green technologies for improving cane sugar productivity and sustaining soil fertility in the sugarcane–based cropping system. *Sugar Tech.* 21, 186–196. doi: 10.1007/s12355-019-00706-z

Shukla, S. K., Yadav, R. L., Singh, P. N., and Singh, I. (2009). Potassium nutrition for improving stubble bud sprouting, dry matter partitioning, nutrient uptake and winter initiated sugarcane (Saccharum spp. hybrid complex) ratoon yield. *Eur. J. Agron.* 30, 27–33. doi: 10.1016/j.eja.2008.06.005

Singh, K. D. N., Mishra, G. K., and Ojha, J. B. (1999). Effect of potassium on yield and quality of sugarcane in calciothents. *Ind. Sugar* 49, 499–507.

Singh, J., Singh, R. D., Anwar, S. I., and Solomon, S. (2011). Alternative sweeteners production from sugarcane in India: lump sugar (Jaggery). *Sugar Tech.* 13, 366–371. doi: 10.1007/s12355-011-0110-4

Singh, B., Singh, Y., Imas, P., and Xie, J. (2004). Potassium nutrition of the rice–wheat cropping system. *Adv. Agron.* 81, 203–259. doi: 10.1016/S0065-2113(03)81005-2

Smith, G. S., Clark, C. J., and Henderson, H. V. (1987). Seasonal accumulation of mineral nutrients by kiwifruit I. Leaves. *New Phytol.* 106, 81–100. doi: 10.1111/j.1469-8137.1987.tb04793.x

Steward, F. C. (1974). Mineral nutrition of plants: principles and perspectives, Emanuel Epstein. *Q. Rev. Biol* 49, 353–354. doi: 10.1086/408215

Sudama, S., Tiwari, T. N., Srivastava, R. P., Singh, G. P., and Singh, S. (1998). Effect of potassium on stomatal behaviour, yield and juice quality of sugarcane under moisture stress conditions. *Ind. J. Plant Physiol.* 3, 303–305.

Tien, T. M., Trang, T. T. T., Ha, P. T. N., Chien, D. T., Thai, T. T., Thang, D. T., et al. (2020) Polyhalite effects on winter maize crop performance on degraded soil in northern Vietnam. E-ifc, International Potash Institute; 62, pp. 3–12.

Tien, T. M., Trang, T. T. T., Ha, P. T. N., and Thu, T. T. M. (2021) Effects of polyhalite application on yield and quality of cabbage grown on degraded soils in northern Vietnam. E-ifc, International Potash Institute; 63, pp. 3–10.

Vale, F. (2016) Calcium and magnesium movement in soil profile with polyhalite as potassium fertilizer for soybean crop. Proceedings of FERTBIO 2016, Goiana, Brazil, October 16–20, 2016.

Wakeel, A., and Ishfaq, M. (2022). "Future research perspectives" in Potash use and dynamics in agriculture (Singapore: Springer), 109–119.

Walkley, A., and Black, I. A. (1934). An estimation of the method for determining soil organic matter and a proposed modification of the chromic acid titration method. *Soil Sci.* 37, 29–38. doi: 10.1097/00010694-193401000-00003

White, P. J., and Broadley, M. R. (2003). Calcium in plants. *Ann. Bot.* 92, 487–511. doi: 10.1093/aob/mcg164

Wood, R. A. (1990). The roles of nitrogen, phosphorus and potassium in the production of sugarcane in South Africa. *Fertil. Res.* 26, 89–98. doi: 10.1007/BF01048746

Wood, A. W., and Schroeder, B. L. (2004) Potassium: a critical role in sugarcane production, particularly in drought conditions. In Proceedings of the Australian Society of Sugarcane Technologists, Brisbane, Australia, 4–7 May 2004. Available at: http://www.cabdirect.org/abstracts/20043079912.html (accessed May 7, 2020).

Yermiyahu, U., Zipori, I., Omer, C., and Beer, Y. (2019) Solubility of granular polyhalite under laboratory and field conditions. E-ifc, International Potash Institute; 58, pp. 3–9.

Zhao, N., Guo, H., Suo, J., Lei, Y., Li, G., Imas, P., et al. (2020) Impact of alternative polyhalite fertilizers on 'xu xiang' kiwifruit yield and quality in Shaanxi Province, China. E-ifc, International Potash Institute; 62, pp. 13–23.

frontiers | Frontiers in Sustainable Food Systems

TYPE Original Research
PUBLISHED 31 October 2024
DOI 10.3389/fsufs.2024.1464021

Check for updates

OPEN ACCESS

EDITED BY
Raffaella Balestrini,
National Research Council (CNR), Italy

REVIEWED BY
Muthuraman Yuvaraj,
Tamil Nadu Agricultural University, India
Anand Kumar Chaudhari,
Government Girls' P.G. College, India

*CORRESPONDENCE
Mahmoud F. Seleiman
✉ mseleiman@ksu.edu.sa

RECEIVED 12 July 2024
ACCEPTED 15 October 2024
PUBLISHED 31 October 2024

CITATION
Elshayb OM, Ghazy HA, Wissa MT, Farroh KY, Wasonga DO and Seleiman MF (2024) Chitosan-based NPK nanostructure for reducing synthetic NPK fertilizers and improving rice productivity and nutritional indices.
Front. Sustain. Food Syst. 8:1464021.
doi: 10.3389/fsufs.2024.1464021

COPYRIGHT
© 2024 Elshayb, Ghazy, Wissa, Farroh, Wasonga and Seleiman. This is an open-access article distributed under the terms of the Creative Commons Attribution License (CC BY). The use, distribution or reproduction in other forums is permitted, provided the original author(s) and the copyright owner(s) are credited and that the original publication in this journal is cited, in accordance with accepted academic practice. No use, distribution or reproduction is permitted which does not comply with these terms.

Chitosan-based NPK nanostructure for reducing synthetic NPK fertilizers and improving rice productivity and nutritional indices

Omnia M. Elshayb[1], Hassnaa A. Ghazy[1], Mariam T. Wissa[1], Khaled Y. Farroh[2], Daniel O. Wasonga[3] and Mahmoud F. Seleiman[4]*

[1]Rice Research and Training Center, Field Crops Research Institute, Kafrelsheikh, Egypt, [2]Nanotechnology and Advanced Materials Central Laboratory, Agricultural Research Center, Giza, Egypt, [3]Department of Crop Sciences, University of Illinois Urbana-Champaign, Urbana, IL, United States, [4]Plant Production Department, College of Food and Agriculture Sciences, King Saud University, Riyadh, Saudi Arabia

Researchers have repeatedly emphasized how urgently we have to decrease the massive nitrogen fertilizer consumption to support agricultural productivity and maintain a sustainable ecosystem. Using chitosan (CS) as a carrier for slow release is considered a potential tool for reducing synthetic fertilizer and improving crop productivity. Therefore, two field experiments were arranged in a randomized complete block design to investigate the effects of seven treatments including synthetic fertilizer and exogenous application of chitosan-based NPK nanostructure (Ch/NPs-NPK) on growth, productivity, and nutrient uptake traits of rice as a worldwide strategy crop during 2022 and 2023 growing seasons. The experimental treatments were: T1 = full recommended synthetic NPK (recommended urea, superphosphate, potassium sulfate; control treatment), T2 = 70% of T1 + Ch/NPs-NPK 100 ppm, T3 = 70% of T1+ Ch/NPs-NPK 200 ppm, T4 = 70% of T1+ Ch/NPs-NPK 300 ppm, T5 = 30% of T1+ Ch/NPs-NPK 100 ppm, T6 = 30% of T1+ Ch/NPs-NPK 200 ppm, and T7 = 30% of T1 + Ch/NPs-NPK 300 ppm. The results revealed that T4 (i.e., 70% of recommended NPK+ Ch/NPs-NPK 300 ppm) and T1 (full recommended synthetic NPK) resulted in the highest and most significant growth and yield traits of rice as well as nutrient grain contents compared to other treatments. Therefore, combining 70% of recommended NPK with Ch/NPs-NPK 300 ppm as an exogenous application can be a smart choice for reducing synthetic NPK fertilizers by 30% in paddy fields without producing a significant decline in terms of growth, yield characteristics, or nutrient grain contents when applying the full recommended synthetic NPK.

KEYWORDS

chitosan-based NPK nanostructure, rice, productivity, sustainable agriculture, food security

1 Introduction

Synthetic fertilizers play a fundamental role in guaranteeing food for a growing population (Seleiman et al., 2021). However, many countries overapply fertilizers, resulting in huge ecological problems including contamination of underground water, biodiversity loss, and decreased soil fertility (Seleiman et al., 2020; Zou et al., 2021; Dimkpa et al., 2023). Egypt is an example of a highly fertilizer-consumed country, where, fertilizer consumption increased from 136.2 kg/ha in 1971 up to 473.4 kg/ha in 2020 with an annual increasing rate of 2.98%. Moreover, massive amounts of synthetic fertilizers are lost via leaching, degradation, runoff, and volatilization which has adverse environmental and economic impacts (Vejan et al., 2021; Almutari, 2023). Therefore, deep attention has to be paid to reduce the intensive utilization of agrochemical fertilizers to reinforce sustainable agriculture production (Seleiman et al., 2017).

The main cereals such as wheat, barley, rice, and maize are a daily basis for human food supply and the largest agrochemicals consumers in the agriculture sector (Ladha et al., 2016; Hafez and Seleiman, 2017; Elshayb et al., 2022b; Alhammad et al., 2023; Haydar et al., 2024). Of the major cereals, rice is regarded as an essential crop that provides food for almost half of the global population (Carrijo et al., 2017; Badawy et al., 2021). Rice nutrient requirements are driven by balanced applications among nitrogen, phosphorus, and potassium (NPK) at different rates (Vijayakumar et al., 2024). The synthetic fertilizers of NPK have been the cornerstone of rice production because of the critical role of these nutrients in many physiological pathways such as the photosynthesis process, mitotic activities, root proliferation, tissue growth, and development (Seleiman et al., 2022). Although the growers mostly relied on synthetic fertilizers to increase rice production, the excessive amounts and unbalanced NPK ratios led to several issues with the soil (e.g., soil acidification, decrease in both soil organic matter and salt accumulation, and reduced cation exchange capacity) plus the negative effects on environmental integrity (Upadhyay et al., 2023). Therefore, environmentally friendly solutions that aim to reduce NPK inputs, preserve crop production outcomes, and overcome negative climate perturbations should be considered when considering fertilizer inputs, particularly NPK, in paddy fields.

In such a scenario, nano-fertilizers are one of the most advanced interventions with appropriate formulations with a smart mechanism to achieve optimal plant uptake and avoid nutrient losses (Badawy et al., 2021; Elshayb et al., 2022a; Verma et al., 2022; Devi et al., 2023; Kumar et al., 2023; Tomar et al., 2024). The application of nano-fertilizers to soil or sprayed over the vegetative system greatly enhances plant nutrition (Batool et al., 2024; Mukhtiar et al., 2024; Singh et al., 2024). With lower molecular weights, better bioavailability, longer half-lives, and a higher surface area-to-volume ratio, nanoparticles are more effective (Sarkar et al., 2022; Ferradj et al., 2024). Particularly biological nano fertilizers hold a lot of potential as an instrument for sustainable agriculture. In contrast to mineral fertilizers, these fertilizers may have a high nutrient use efficiency and a slow-release nutrient profile, which means they give plants the nutrients they require over a longer time (Sangwan et al., 2023). Notably, there are various types of nano fertilizers, including those based on macronutrients (N, K, and P) (Chakraborty et al., 2023). As a result of its wide surface area and capability, the macronutrients (N, P, and K) in nanocomposite fertilizer encourage the absorption use of nutrients by crops resulting in increasing plant height, dry matter, leaf area, chlorophyll synthesis, and photosynthesis rate (Sundararajan et al., 2024).

One of these smart nano-formulations, chitosan-based nanostructure (Ch/NPs) has gained more attention from scientists in the past few years owing to its biodegradable and biocompatible features (Abdel-Aziz et al., 2018; Ingle et al., 2022; Devi et al., 2023; Sangwan et al., 2023). It is worth mentioning that chitosan is a polycationic polymer that is isolated from chitin which is the second most abundant polysaccharide globally (a structural polymer in many different types of animals, mollusks, shrimp, fungi, and crabs) after it has been deacetylated (Ingle et al., 2022). One of the major advantages Ch/NPs typically degrade into non-toxic byproducts, reducing the risk of accumulation in the body or plant tissues and minimizing long-term side effects (Devi et al., 2023). In addition to their biocompatibility, Ch/NPs have been shown to stimulate a plant's immune system and aid in biotic and abiotic stress management (Sangwan et al., 2023). As a non-toxic biopolymer, Ch/NPs can be organized and integrated strategically with fertilizer sources (i.e., urea, potassium sulfate, and calcium phosphate) to produce control-release fertilizer of NPK. Loading urea fertilizer into Ch/NPs has proven its efficiency in reducing urea fertilizer quantity and enhancing rice grain productivity as documented in a previous study by Elshayb et al. (2022b). As a result, Corradini et al. (2010) loading NPK fertilizer into Ch/NPs can be a benign approach for making a complex NPK fertilizer with slow-release properties which is known as chitosan-based NPK nano-structure (Ch/NPs-NPK). Prior studies demonstrated the outstanding merits of Ch/NPs-NPK in improving wheat productivity under different soils compared with classical NPK fertilizer (Abdel-Aziz et al., 2018), enhancing both growth and potato tuber (Elshamy et al., 2019), and improving both nutrient uptake and water absorption of French bean (Hasaneen et al., 2016). A prior study by Deshpande et al. (2017) declared that the foliar application of zinc amalgamated with Ch/NPs on two durum wheat cultivars caused a significant increase in zinc grain content by 27 and 42% compared to zinc-deficient control plants. However, the foliar spray of Ch/NPs significantly increased the levels of Fe, Zn, Mn, P, Ca, and Mg in finger millet plants in comparison of the control treatment (Sathiyabama and Manikandan, 2021). However, the application of Ch/NPs-NPK in paddy schedule fertilization and its effect on nutritional grain content has remained unexplored until now.

Looking at the above objectives, this study focused on evaluating the application of chitosan-based NPK nano-structure at a different rate with a combination of T-NPK aiming to determine the optimal dose for enhancing growth properties, minimize T-NPK inputs, and maximize both grain productivity and nutrients (N, P, and K) uptake.

2 Materials and methods

2.1 Site, soil, and climatological properties

In the Agriculture Research Station, Kar El-Sheikh, Egypt's Experimental Farm of Sakha (31°05′17″N, 30°56′44″E), two field tests were carried out in 2022 and 2023 seasons.

The soil samples were taken from topsoil (depth of 0–20 cm), air-dried, and crushed (by passing through a 2-mm screen to remove big particles) before the setup of the experiments. The primary physiological properties were analyzed and recorded as described

before (Ryan et al., 2001). Across the 2022 and 2023 seasons, the analysis data declared that soil type was clayey texture, organic matter (OM%; 6.40 and 7.12), pH (1:2.5 water suspension; 8.16 and 8.35), Ec (dS m^{-1}; 3.08 and 2.90), available N (ppm; 585.4 and 592.3), available P (ppm; 5.68 and 6.00), available K (ppm; 1.44 and 1.65), available Zn^{+2} (ppm; 0.88 and 0.91), available Fe^{+2} (ppm; 4.97 and 5.00), and available Mn^{+2} (ppm; 3.14 and 3.82).

The weather databases were collected from a field observatory near the experimental site. The monthly meteorological particulars were codified annually from a field observatory and recorded in Figure 1.

2.2 Preparation of chitosan-based NPK nano-structure

Chitosan-based NPK nano-structure (Ch/NPs-NPK) was prepared according to Corradini et al. (2010) with some modifications. Briefly, chitosan (Ch) (molecular weight 100,000–300,000 Da, and viscosity: 50 to 200 mPa·s, ACROS, China) aqueous solution (0.2% w/v) was prepared by dissolving Ch in acetic acid solution (1% v/v) (99–100%, Riedel-de Haën) at ambient temperature. The pH of the solutions was adjusted to 5.5 with 0.5 M sodium hydroxide pellets (≥95%, Sigma-Aldrich, US) solution. Subsequently, tripolyphosphate (TPP) (Technical grade, 85%, Sigma-Aldrich, US) as a cross-linking agent solution was dissolved in 10 mL deionized water to a final concentration of 0.6 mg/mL. After 30 min of vigorous magnetic stirring, the TPP solution was added dropwise (0.3 mL/min) to the chitosan solution in the Ch solution. Ch-NPK nano fertilizer was prepared by loading nitrogen (N), phosphorous (P), and potassium (K) into Ch/NPs by dissolving different amounts of NPK into 100 mL of nanoparticle solution under homogenizing at 18,000 rpm for 30 min in the presence of Tween 80 at 25°C. The resulting solution to incorporate NPK into the nanoparticles presents this final concentration: (i) 100, 200, and 400 ppm of N; (ii) 15, 30, and 60 ppm of P; (iii) 100, 200, and 400 ppm of K. The morphology of Ch/NPs-NPK was imaged by a High-Resolution Transmission Electron Microscope (HR-TEM) operating at an accelerating voltage of 200 kV (Tecnai G2, FEI, Netherlands). Diluted Ch-NPK NF solution was ultra-sonicated for 5 min to reduce the particle aggregation. Using a micropipette, three drops from the sonicated solution were deposited on a carbon-coated copper grid and left to dry at room temperature.HR-TEM images of the Ch/NPs-NPK that were deposited on the grid were captured for morphological evaluation. Dynamic light scattering (DLS) measurement of size and Zeta Potential was undertaken using a Nano-zeta sizer (Malvern, ZS Nano, UK). Synthesis and characterization of Ch/NPs-NPK were performed in Nanotechnology & Advanced Materials Central Laboratory (NAMCL), Agricultural Research Center (ARC), Giza, Egypt.

2.3 Plant material, and experimental details

During the dual seasons (2022 and 2023), the uniform size of rice grain (*Oryza sativa* L., Sakha super 300) was used in this study. After the nursery land was prepared, the rice grains at the rate of 120 kg/ha^{-1} were soaked (for 24 h), incubated (for 48 h) to accelerate the germination process, and then the pre-germinated seed broadcasted in the nursery on 20 and 22 of May in both seasons, respectively. The experiments were organized in a randomized complete block design (RCBD) including 3 replicates with 7 treatments. In the permanent field, the 21-day-old seedlings were transplanted in the experimental unit with a size of 12 m^2 (4 m length × 3 m width). The transplanted seedlings (2–3 seedlings/hill) were pulled and organized in the respective units at a 20 × 20 cm distance between hills and rows. The studied treatments comprised factorial combinations among two fertilization levels (i.e., 70, and 30%) of traditional NPK fertilizer and three foliar doses of Ch/NPs-NPK (i.e., 100, 200, and 300 ppm) as well as the full recommended dose treatment (control treatment). The foliar application of Ch/NPs-NPK was applied twice (after transplanting at 20 and 40 D). The experimental treatment details are shown in Table 1.

According to the abovementioned amount of traditional soil application of NPK fertilizer, both potassium sulfate (48% K_2O) and mono-superphosphate (15 %P_2O_5) were applied and integrated into the experimental soil before tillage. However, the amount of urea (CH_4N_2O)

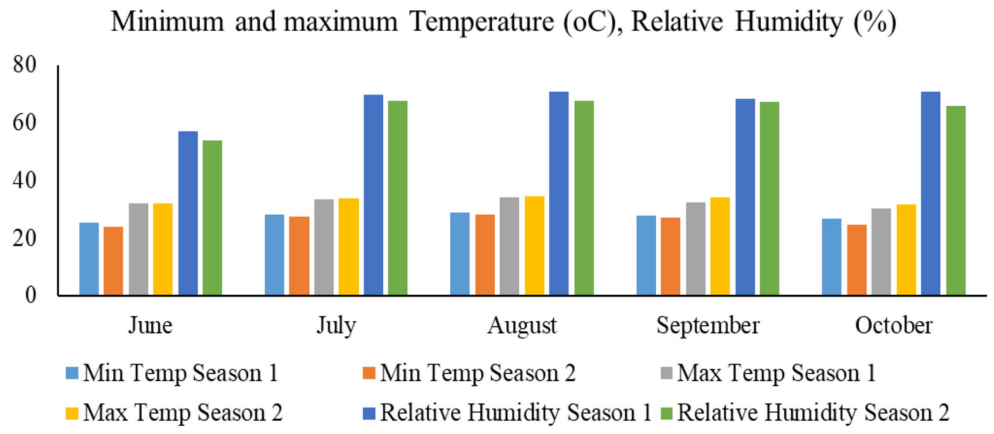

FIGURE 1
Minimum and maximum temperature and relative humidity during the growing seasons of the current experiment.

TABLE 1 The Schedule of the different fertigation treatments.

Treatments	Soil application of traditional NPK	Foliar application of Ch/NPs-NPK	Designation
T1	The full recommended NPK	Without any foliar application	100% NPK (control treatment)
T2	70% of recommended NPK	100 ppm	70% NPK + 100 mg NPK/l
T3	70% of recommended NPK	200 ppm	70% NPK + 200 mg NPK/l
T4	70% of recommended NPK	300 ppm	70% NPK + 300 mg NPK/l
T5	30% of recommended NPK	100 ppm	30% NPK + 100 mg NPK/l
T6	30% of recommended NPK	200 ppm	30% NPK + 200 mg NPK/l
T7	30% of recommended NPK	300 ppm	30% NPK + 300 mg NPK/l

fertilizer was added as previously mentioned (twice at 2/3 as a basal application and 1/3 at panicle initiation). While observing the recommended doses of urea, mono-superphosphate, and potassium sulfate are 165 kg N/ha^{-1}, 36 kg P_2O_5 /ha^{-1}, and 60 kg K_2O /ha^{-1}, respectively. Before seedling transplanting and after puddling, Zinc sulfate was broadcasted and applied at the rate of 24 kg/ha^{-1}. Six days after transplanting, 4.8 L/ha of the herbicide Saturn [S-(4-Chlorophenol methyl) diethyl carbamothioate] was sprayed to control weeds.

2.4 Data gathering

2.4.1 Physiological indicators

Photosynthetic pigments (i.e., chlorophyll a, chlorophyll b, and carotenoids) measured in fresh and fully expanded leaves (5 g) from the upper canopy and will be extracted in acetone (90% v/v) and then filtered to overact a final volume of 50 mL. Estimation of total chlorophyll (i.e., Ch. a and Ch. b) and carotenoid contents (C. content) was evaluated spectrophotometrically from the absorbance of the final extract as mg g^{-11}FW^{-1} agreeing to the protocol given by Wellburn (1994) using Equations 1–3 as follows:

$$\text{Ch.a} = 12.25\text{A663.2} - 2.79\ \text{A646.8} \tag{1}$$

$$\text{Ch.b} = 21.5\ \text{A466.8} - 5.1\text{A663.2} \tag{2}$$

$$\text{C.content} = 1000\ \text{A470} - 1.82\ \text{Ch.a} - 85.02\ \text{Ch.b} / 198 \tag{3}$$

Where, A663.2, A646.8, and A470 represent the absorbance taken at 663.2 nm (Ch. a), 646.8 nm (Ch. b), and 470 nm (carotenoids) respectively.

At the heading stage, from a fixed point of each experimental unit, the rice leaf area index (LAI_S) was estimated from 10 tagged leaves which were randomly sampled and calculated according to the following Equation 4:

$$\text{LAIs} = \text{Leaf area of tagged leaves}\,(\text{cm2}) \div \text{Ground area occupied by these leaves}\,(\text{cm2}) \tag{4}$$

concerning the evaluation of dry matter production per hill (DMP/hill), five hills from each plot were pulled out, air-dried, sealed into a kraft paper bag, and then exposed to oven-dried (70°C for 48 h) and stopped when a steady weight (g/hill) had been obtained according to the methodology proposed by Yoshida et al. (1971).

2.4.2 Yield causative components and yield outcomes

When the experimental field reached maturity, a certain area of the center of each experimental unit (10 m^2) was harvested, well-dried, and mechanically threshed to evaluate the various studied characters. The estimation of plant height (cm^2), number of panicles/m^2 (No. Panicles/m^2), panicle characters (length, weight, filled grains percentage "Equation 5"), 10^3 grain weight (g), biological yield (BY), final grain yield (GY), and harvest index (HIs) percentage "Equation 6" were calculated. During 2 years, both BY and GY weights were converted to t/ha in the results databases noting the adjustment of paddy grains to 14% moisture content as mentioned by Yoshida (1981).

$$\text{Filled grain}\,(\%) = \left[\frac{\text{Total filled grains number}}{\text{The total grains number}} \div\right] \times 100 \tag{5}$$

$$\text{HIs} = \text{final grain yield} \div \text{biological yield} \tag{6}$$

2.4.3 Nutrient uptake indices

The uptake of N (N-uptake) indices was calculated by using the Micro-Kjeldahl methodology. Samples of both grain and straw (5 g of each) in each experimental unit were exposed to oven-dried (70°C) to obtain a constant weight. Thereafter, samples were ground and digested using H_2SO_4-H_2O_2 as the standard given earlier by Jackson (2005). However, the uptake of P (P-uptake) indices was estimated as the methodology indicated by Watanabe and Olsen (1965). About the uptake of K nutrient, (K-uptake) indices were computed by a flame photometer (RHYS international LTD, India) using atomic absorption as described by Peterburgski (1968). Whereby, nutrient uptake in both grains and straw parts was calculated as kg/ha using Equation 7:

$$\text{Nutrient uptake}\left(\frac{\text{kg}}{\text{ha}}\right) = \text{nutrient content}\,(\text{g} / \text{kg}) \times \text{grain or straw yield}\left(\frac{\text{kg}}{\text{ha}}\right) \tag{7}$$

2.5 Statistical analysis

The obtained data was subjected to an analysis of variance (Gomez and Gomez, 1984). The means of different treatments were compared by Turkey's test to clarify the significant difference at $p \leq 0.05$ probability according to Hsu (1996). All statistical analyses were conducted utilizing the analysis of variance technique by the COSTATC computer software package.

3 Results

3.1 The characterization of chitosan-based NPK nano-structure

3.1.1 TEM analysis results

According to the findings displayed in Figure 2, Ch/NPs-NPK had a spherical surface, a uniform size distribution, was stable, and had a finely shaped exterior. The greatest surface area for loading NPK nutrients onto the surface of chitosan nanoparticles is found in their spherical shape, smooth surface, and an average size of about 25.7 nm.

3.1.2 Dynamic light scattering analysis

Hydrodynamic diameter was measured in the nanoscale range using the DLS technique. The zeta potential of Ch/NPs-NPK was +45.4 mV, and its size was 32.7 nm (Figure 3).

3.2 The effects of several rates of traditional NPK fertilizers and their combination with chitosan-based NPK nano-structure as a foliar application on physiological indicators

The physiological indicators of total photosynthetic pigments (Figure 4), LAIs, and DMP/hill were significantly (at $p \leq 0.05$) influenced by several rates of traditional NPK fertilizers and their combination with Ch/NPs-NPK (Table 2). The higher values of total photosynthetic pigments (i.e., Ch. a, Ch. b, and C. content) showed in rice plots that fertilized with T1 (full recommended dosage of conventional NPK) which gave identical statistically with T4 (70% NPK + 300 mg NPK/l) in both seasons. Similar findings were noted for LAIs, where T4 and T3 (4.86 and 5.22) fertilization resulted in statistical conformity with T1 (5.48) in the 1st season. However, in the 2nd season, only T4 (5.37) recorded statistical similarity with T1. As for DMP/hill (g/hill), the highest weight of dry matter was rendered from the application of T1 with no significant difference between this treatment and T4 (81.9, 79.6, and 83.1, 80.3 g/hill respectively) in both cropping seasons. Whilst, the application of T5 gave the lowest values of total photosynthetic pigments (4.105 and 4.387 mg $g^{-1}FW^{-1}$), LAIs (4.12 and 4.32), and DMP/hill (63.8 and 65.2 g/hill) respectively in both sequential seasons.

Various letters (a, b, c, d, etc.) denoted a statistically significant variation in the treatment means at $p < 0.05$. As for treatments abbreviation (see Table 1).

3.3 The effects of several rates of traditional NPK fertilizers and their combination with chitosan-based NPK nano-structure as a foliar application on yield causative components

The appraisal data in Table 3 imparted that a meaningful impact has been made by several treatments concerning plant height, No. panicles/m^2, and panicle length in both seasons. The tallest plants (115.1 and 116.9 cm) were recorded under the T1 treatment without significant differences between this treatment (T1) and both T3 and T4 (115.1, 114.3, and 114.5 cm) treatments in the 2022 season. Whilst, in the 2023 season, T1 treatment gave identical statistically with T4 only. As for the result of counting panicles number /m^2, T1 gave the best value (574.4 and 583.2 panicles/m^2) which was statistically identical with T4 (556.4 panicles/m^2) treatment in the 1st season and

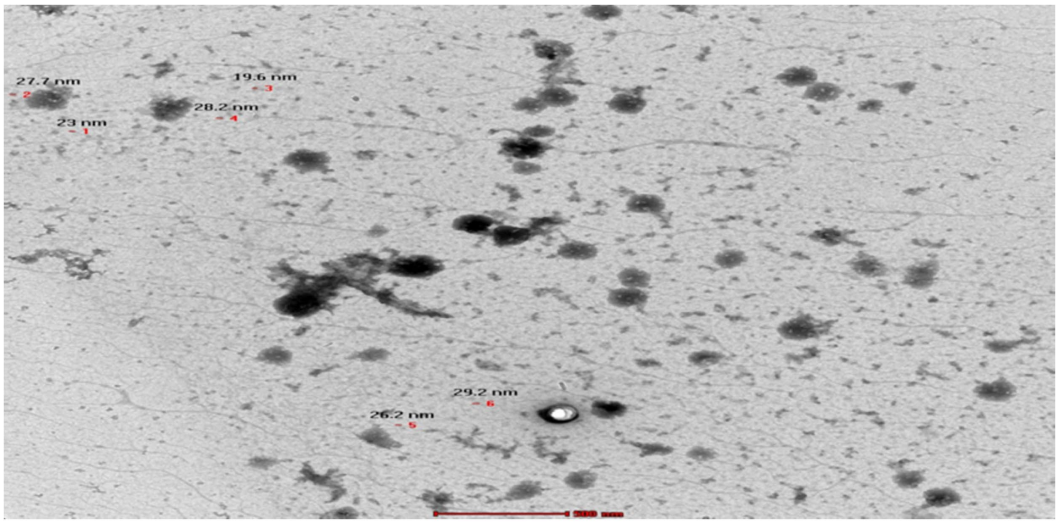

FIGURE 2
TEM image of Ch/NPs-NPK.

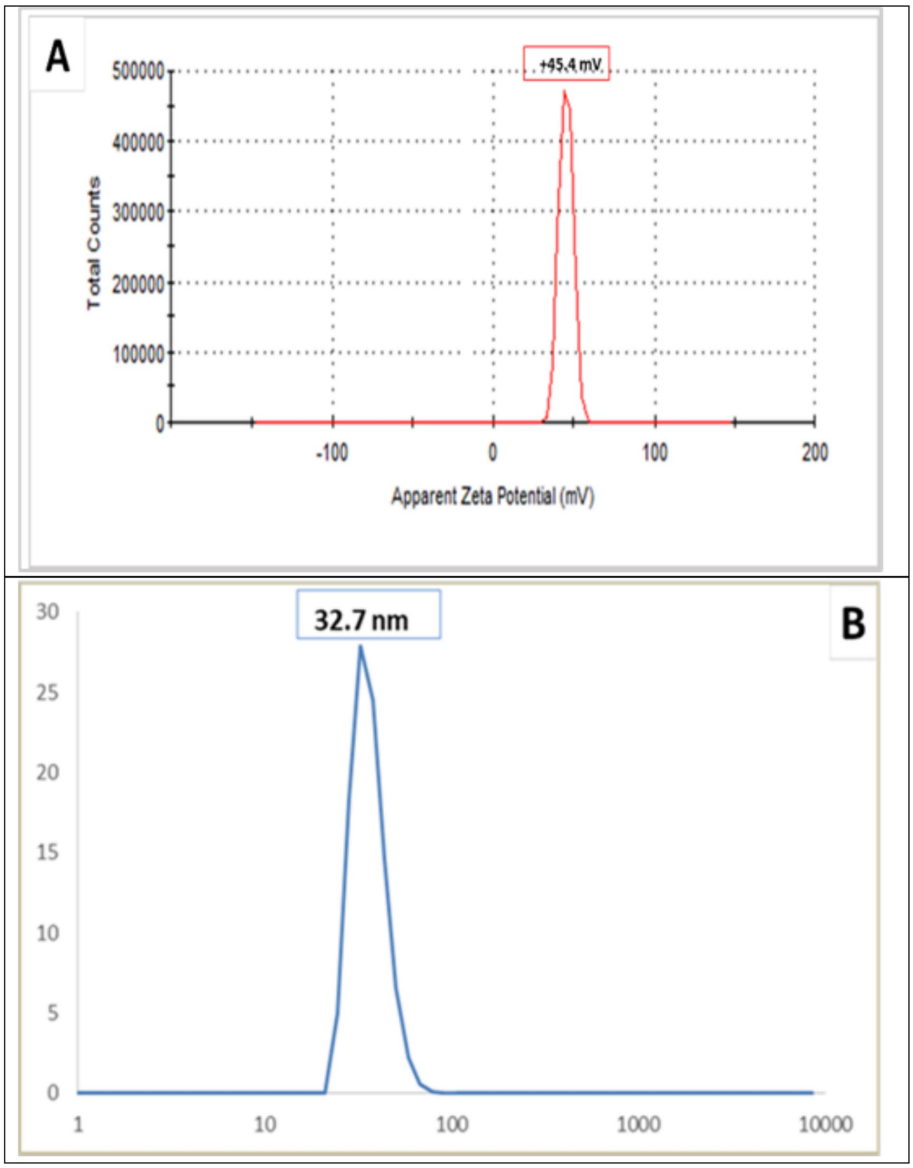

FIGURE 3
DLS analysis of Ch/NPs-NPK. Zeta potential (A) and Particle size (B).

with both T3 and T4 (551.3 and 568.2 panicles/m^2 respectively) treatments in the 2nd season. Likewise, T4 rendered a statistical match with T1 (22.8, and 24.1 cm, respectively in both seasons) concerning the length of the panicle. Again, the lowest values of these characters, i.e., plant height (103.3 and 104.3 cm), No. panicles/m^2 (454.4 and 455.7), and panicle length (18.3, and 18.0 cm) respectively during both planting, seasons were witnessed under T5 treatment.

A different and significant response on panicle weight, filled grains percentage, and 10^3-grain weight characters were observed under various treatments (Table 4). Compared to a traditional application of NPK (control treatment), both T3 and T4 (3.73 and 4.11 g respectively) gave statistical conformity with the T1 (4.12 g) concerning panicle weight in the 2022 season. However, T4 treatment only provided (4.30 g) a statistical match with T1 (4.13 g) in the 2023 season. Concerning the filled grains percentage character, there wasn't a significant difference between T1 and T4 (89.6 and 92.2% respectively) in the 2022 season but in the 2023 season, T3 and T4 (88.6 and 92.6% respectively) treatments gave identical statistics to the application of T1. As regards 10^3-grain weight, the highest weight was observed in both treatments of T1 and T4 (26.93, 28.90, and 27.49, 28.16 g) respectively in the 2022 and 2023 seasons and without significant difference between them. Nevertheless, the lowest values of these characters, i.e., panicle weight (3.03 and 3.11 g), filled grain percentage (77.8 and 79.9%), and 10^3-grain weight (23.20 and 23.49 g) were noted under the treatment of T5.

3.4 The effects of several rates of traditional NPK fertilizers and their combination with chitosan-based NPK nano-structure as a foliar application on yield outcomes

The obtained data about yield outcomes (BY and GY) and HIs are recorded in Table 5. During both cultivated seasons, a significant influence ($p \leq 0.05$) appeared among all treatments related to BY which recorded the highest value (24.16 and 24.93 t/ha^{-1}) respectively

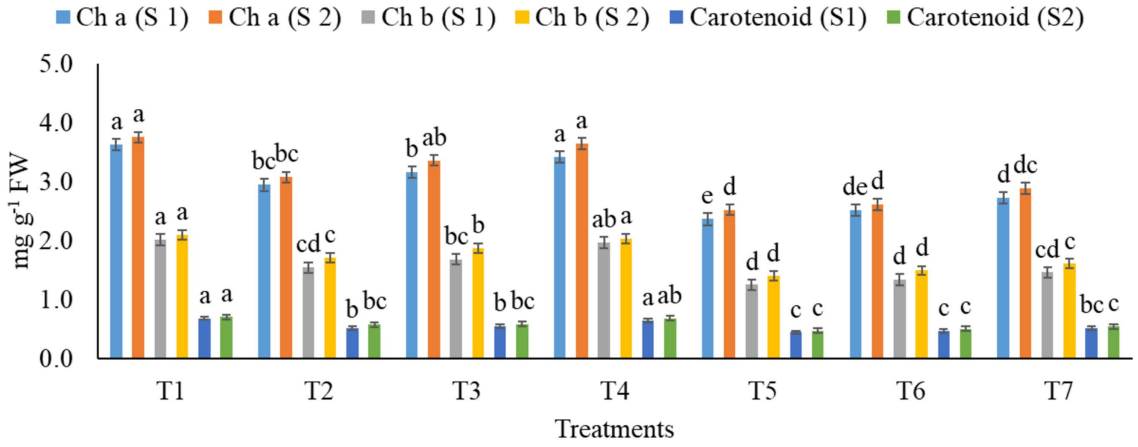

FIGURE 4
The effects of several rates of traditional NPK fertilizers and their combination with chitosan-based NPK nano-structure as a foliar application on total chlorophyll (i.e., Ch. a and Ch. b) and carotenoid contents (C. content). Various letters (a, b, c, d, etc.) denoted a statistically significant variation in the treatment means at $p < 0.05$. As for 366 Treatments treatments abbreviation (see Table 1).

TABLE 2 Effects of synthetic NPK fertilizers and their combination with chitosan-based NPK nano-structure as a foliar application on total pigment contents, leaf area index, and dry matter production.

Traits treatments	Total pigments contents (mg $g^{-1}FW^{-1}$)		Leaf area index (LAIs)		Dry matter production (g/hill)	
	2022	2023	2022	2023	2022	2023
T1	6.326 a	6.558 a	5.48 a	5.82 a	81.9 a	83.1 a
T2	5.009 bc	5.366 c	4.61 bc	4.59 c	72.5 bc	73.1 bc
T3	5.391 bc	5.805 b	4.86 ab	4.98 bc	76.3 ab	75.2 bc
T4	6.028 ab	6.354 a	5.22 a	5.37 ab	79.6 ab	80.3 ab
T5	4.105 d	4.387 d	4.12 d	4.32 d	63.8 d	65.2 d
T6	4.323 d	4.598 cd	4.23 cd	4.60 c	66.1 cd	66.7 d
T4	4.691 cd	5.030 c	4.59 bc	4.76 bc	68.3 cd	70.1 cd
F. test	**	**	**	**	**	**

** implies $p \leq 0.05$; Data followed by the same letter were not significantly different for probability. Each column's various letters (a, b, c, d, etc.) denoted a statistically significant variation in the treatment means at $p < 0.05$. As for treatments abbreviation (see Table 1).

from the T1 treatment and on par with the T4 treatment. Also, the same trend was revealed concerning GY which represented the highest value underlying T1 treatment (10.93 and 11.04 t/ha, respectively, over both seasons). Notably, the T1 and T4 treatments did not significantly differ in either of the two seasons. For HIs during both seasons, the implications exhibited that T1 and T4 contributed the highest HIs value (0.448, 0.451, and 0.447, 0.449 respectively) without significant difference between them. The lowest value of BY (20.83, and 21.27 t/ha), GY (8.35, and 8.56 t/ha), and HIs (0.403 and 0.410) is seen under the application of T5 in the 1st and 2nd seasons.

3.5 The effects of several rates of traditional NPK fertilizers and their combination with chitosan-based NPK nano-structure as a foliar application on nutrient uptake indices

From the results set (Figure 5), a substantial change in nutrient uptake (i.e., N, P, and K nutrients) of rice grain was indicated by the effect of various applications during the 1st and 2nd seasons. Concerning N uptake indices by grains, the control treatment (T1) gave statistics similar to the T4 application in both seasons. Also, the same trend was observed concerning P uptake indices whereby the highest value was recorded by T1 without a significant difference between T1 and T4 in both sequential seasons. Whilst, a variable increase was noted concerning K uptake indices underlying rice plants treated with T3 and T4 applications and with no substantial difference between T1, T3, and T4 in both cropping seasons. Substantial difference between T1, T3, and T4 in both cropping seasons. The lowest values of N, P, and K elements uptake were presented from the plots that fertilized with T5 application in both of 2022 and 2023 seasons.

Concerning nutrient uptake (i.e., N, P, and K nutrients) of rice straw parts, the resultant data set in Figure 6 illustrated a variable significant influence in these indices via the effect of various applications. The control treatment gave the highest rank concerning the indices of N uptake by rice straw without a significant difference between T1 and T4 treatments in both seasons. Once more, T1 reaffirmed superiority in the indices of P uptake by rice straw with

TABLE 3 Effects of synthetic NPK fertilizers and their combination with chitosan-based NPK nano-structure as a foliar application on some yield components traits.

Traits treatments	Plant height (cm)		No. panicles/m^2		Panicle length (cm)	
	2022	2023	2022	2023	2022	2023
T1	115.1 a	117.0 a	574.4 a	583.2 a	23.3 a	23.4 a
T2	111.2 b	112.6 b	616.3 c	529.5 b	20.3 b	20.9 b
T3	114.3 a	111.8 b	541.4 bc	551.3 ab	20.9 b	21.3 b
T4	114.5 a	116.5 a	556.4 ab	568.2 a	22.8 a	24.1 a
T5	103.3 d	104.3 c	454.4 d	455.7 d	18.3 c	18.0 d
T6	105.8 c	107.1 c	467.6 d	474.5 cd	19.7 bc	20.1 c
T4	109.5 b	110.9 b	482.2 cd	488.6 c	1020.1 bc	20.3 c
F. test	**	**	**	**	**	**

** implies $p \leq 0.05$; Data followed by the same letter were not significantly different for probability. Each column's various letters (a, b, c, d, etc.) denoted a statistically significant variation in the treatment means at $p < 0.05$. As for treatments abbreviation (see Table 1).

TABLE 4 Effects of synthetic NPK fertilizers and their combination with chitosan-based NPK nano-structure as a foliar application on some yield components traits.

Traits treatments	Panicle weight (g)		Filled grains (%)		1,000 grain weight (g)	
	2022	2023	2022	2023	2022	2023
T1	4.12 a	4.13 a	89.6 ab	91.1 a	26.93 ab	28.90 a
T2	3.59 bc	3.81 bc	82.7 c	86.8 c	25.33 bc	26.15 b
T3	3.73 ab	3.90 bc	86.2 b	88.6 ab	25.95 b	26.75 b
T4	4.11 a	4.30 a	92.2 a	92.6 a	27.49 a	28.16 a
T5	3.03 c	3.11 d	77.8 d	79.9 d	23.20 d	23.49 d
T6	3.42 bc	3.53 c	80.1 cd	83.7 cd	24.06 d	23.98 cd
T4	3.43 bc	3.70 bc	80.6 cd	84.8 c	24.06 cd	25.10 bc
F. test	**	**	**	**	**	**

** implies $p \leq 0.05$; Data followed by the same letter were not significantly different for probability. Each column's various letters (a, b, c, d, etc.) denoted a statistically significant variation in the treatment means at $p < 0.05$. As for treatments abbreviation (see Table 1).

statistical conformity with the application of T4 in the 1st and 2nd seasons. As for the indices of P uptake by rice straw, the treatment of T1, and T4 occupied the highest rank without significant difference among them in the 1st season. Whilst there was a statistical match between T1, T3, and T4 in the 2nd season. Across both seasons, the treatment of T5 submitted the lowest rank concerning all studied nutrient uptake in rice straw.

4 Discussion

Undoubtedly, crop agrarian productivity necessitates the usage of NPK-containing fertilizers because of their vital role in macronutrient (i.e., N, P, and K) homeostasis that determines biomass synthesis and dry matter production (Moe et al., 2019; Krasilnikov et al., 2022; Sarkar et al., 2022). More critically, the tiny particle size and wide surface area of nano fertilizers lead to an increase in particle number per unit of weight as well as high reactivity, which improves the fertilizer's contact with the plant and boosts both fertilizer use efficacy and nutrient uptake (Abdel-Aziz et al., 2018; Abd-Elrahman et al., 2023; Devi et al., 2023; Elshayb et al., 2022a). Hence, modified NPK fertilizer with nanostructure and slow-release properties has a special potential to enhance the usage and uptake of nutrients.

Photosynthetic pigments have a cardinal role in light energy's absorption, transmission, and transformation processes during photosynthesis (Moe et al., 2019). Numerous investigations have demonstrated that the regulation of photosynthetic pigment synthesis in crop leaves is significantly influenced by nitrogen nutrition (Vijayalakshmi et al., 2015; Peng et al., 2021). Also, an appositive correlation is well-documented between N-level supply and both Ch. content and C. content (Kumari et al., 2024; Srikanth et al., 2023). Therefore, the results in Figure 4 and Table 2 may be due to the different variations of N quantities supply which reflect on total photosynthetic pigments (i.e., chlorophyll a, chlorophyll b, and carotenoids) that were affected positively with several studied traits. The coprecipitation of chemical fertilizer of NPK and exogenous application of Ch/NPs-NPK 300 ppm underlying T4 may give plants adequate P nutrient addition that has a monumental role in several metabolic processes (i.e., photosynthesis, energy storage, and cell division) as a result of an integral constituent of phospholipids, nucleic acid, and co-enzymes that ultimately activate amino acid formation (Bechtaoui et al., 2021; Gao et al., 2023; Vance et al., 2003). On the other side, sufficient K supply plays an influential function in photosynthetic CO_2 fixation and preservation of chloroplast status about enzyme activities, PH, and turgor (Dreyer et al., 2017). In this regard, Sheoran et al. (2021) found that wheat plants sprayed with

TABLE 5 Effects of synthetic NPK fertilizers and their combination with chitosan-based NPK nano-structure as a foliar application on yield outcomes.

Traits treatments	Biological yield (t/ha)		Grain yield (t/ha)		Harvest index (%)	
	2022	2023	2022	2023	2022	2023
T1	24.16 a	24.93 a	10.93 a	11.04 a	0.448 a	0.451 a
T2	22.11 bc	22.20 bc	9.37 c	9.54 bc	0.424 c	0.430 bc
T3	22.72 bc	22.79 bc	9.66 bc	9.93 bc	0.436 bc	0.438 b
T4	23.40 ab	23.92 ab	10.45 ab	10.69 ab	0.447 a	0.449 a
T5	20.83 c	21.27 c	8.35 d	8.55 d	0.403 d	0.410 c
T6	21.36 c	21.86 c	8.58 cd	8.83 cd	0.415 cd	0.414 c
T4	21.94 bc	22.25 bc	8.91 cd	9.27 cd	0.419 cd	0.422 bc
F. test	**	**	**	**	**	**

** implies $p \leq 0.05$; Data followed by the same letter were not significantly different for probability. Each column's various letters (a, b, c, d, etc.) denoted a statistically significant variation in the treatment means at $p < 0.05$. As for treatments abbreviation (see Table 1).

nano-K utilized the exchangeable K in the sandy loam soil to the highest extent possible, resulting in the least amount of K leaching. This may be explained by the increased absorption of K and its related functions in cation-anion balance, energy transfer, stomatal movement, osmoregulation, photosynthesis, enzyme activation, protein synthesis, and phloem transport (Elshamy et al., 2019; Abd-Elrahman et al., 2023). Therefore, applying Ch/NPs-NPK 300 ppm can probably compensate for the missing quantity of chemical NPK fertilizer under the condition of T4 (when T-NPK decreases by up to 30%). Hence, compared to T1 (control), total pigment contents did not give a statistical difference with the T4 treatment (Table 2). Indeed, the higher efficacy of the photosynthesis process reflected positively on cell properties (e.g., elongation, division, and expansion) (Moe et al., 2019). It is obvious that the sole application of Ch/NPs (at the rate of 90 ppm) has been proven beneficial to wheat plants undergoing water stress conditions via enhancing Ch. Content (Behboudi et al., 2019). Another article given by Devi et al. (2023), indicated that Ch/NPs played a versatile growth promoter role by underpinning leaf area and total Ch. Content of rice plants. On the above basis, the higher contents of photosynthesis pigment led to higher values of LAIs which was witnessed clearly under the treatments of T1, and T4 (in both seasons). Consequently, the increase of LAIs values causes a benign utilization and capture of solar energy that leads to more photo-assimilated formation and ultimately generates higher DMP (Moe et al., 2019; Elshayb et al., 2022a; Elshayb et al., 2022b; He et al., 2024). Hereby, the perusal results (Table 2) deduced that the application of Ch/NPs-NPK 300 ppm concerning the treatment of T4 may be synchronized and underpinned with the plant's nutrient needs despite the decrease of traditional NPK fertilizers till 30%.

After Ch/NPs-NPK is applied exogenously, it penetrates the epidermal of plant leaves, allowing for easy absorption through the plant's organs. Due to the noncirculatory system of plant vascular systems, exogenous nanoscale material moves directly into the xylem (the shoot's internal structure) and phloem (the root's internal structure) (Gangwar et al., 2023). Probably, the foliar application of Ch/NPs-NPK (at the proper dose) supported and enhanced the translocation process from paddy shoots to their root. Moreover, a facility of molecule absorption (due to its tiny size) may be reflected favorably on enhancing the physiological processes that work on encouraging meristematic activity, cell division, and both stem and internode elongation Subsequently improving plant height. A previous study by Hasaneen et al. (2016), found that the Ch/NPs-NPK treatment had a significant favorable impact on the growth characteristics of the plants, and they attributed this to an enhanced nutritionally balanced state resulting from an increase in NPK flux within plant tissue.

Indeed, reproductive tiller per unit area is an important morpho-physiological characteristic of paddies and is considered an indicator of high N content (Banayo et al., 2021; Elshayb et al., 2022a; Tyagi et al., 2024). Moreover, the higher reproductive tillers under T4 treatment may be due to P sufficiency status in early stages that perhaps led to encouraging the formation of roots, tillers, and flowering because plants remobilize it within their tissues throughout the advanced growth stages (Miranda-Villagómez et al., 2019). These striking data concerning T1 and T4 treatments (Tables 3, 4) signified that sufficient and adequate absorption of N, P, and K nutrients before the panicle initiation stage perhaps occurred and caused a positive effect on panicle numbers per meter, panicle primordia formation, number of spikelet's per panicle, and panicle branching (Yoshida, 1981). Thus, across both seasons, the increase in N, P, and K nutrients was more predominant with the application of T4. The increase in panicle length is related to the increase concurrently with N addition (Liu et al., 2020; He et al., 2024). This implies that utilization applications of T1 (applying the full recommended dose of NPK), and the T4 (applying 70% of NPK + 300 ppm Ch/NPs-NPK) treatments possibly gave the plants with optimum nitrogen dose. On the other side, chitosan promotes phytohormone formation, especially cytokinin which enhances cell proliferation in the filling stage resulting in the developing sink size (Behboudi et al., 2019; Sangwan et al., 2023). In this sense, the production and translocation of the pre-sorted assimilated output from enriched plant tissues can easily transfer from source to sink, indicating a notable improvement in yield-causative components including panicle qualities (i.e., length and weight), filled grains percentage, and 1,000-grain weights.

Overall, benign DMP is the infrastructure for producing a distinguished yield component and grain outcomes (Abdel-Aziz et al., 2018; Elshayb et al., 2022a; Seleiman et al., 2022; He et al., 2024). The photosynthetic synthesis of leaves (especially flag leaves) is responsible for 90% of rice grain output (Hai-Yan et al., 2009) Also, higher N intake during the vegetative period until panicle initiation is associated

10.3389/fsufs.2024.1464021

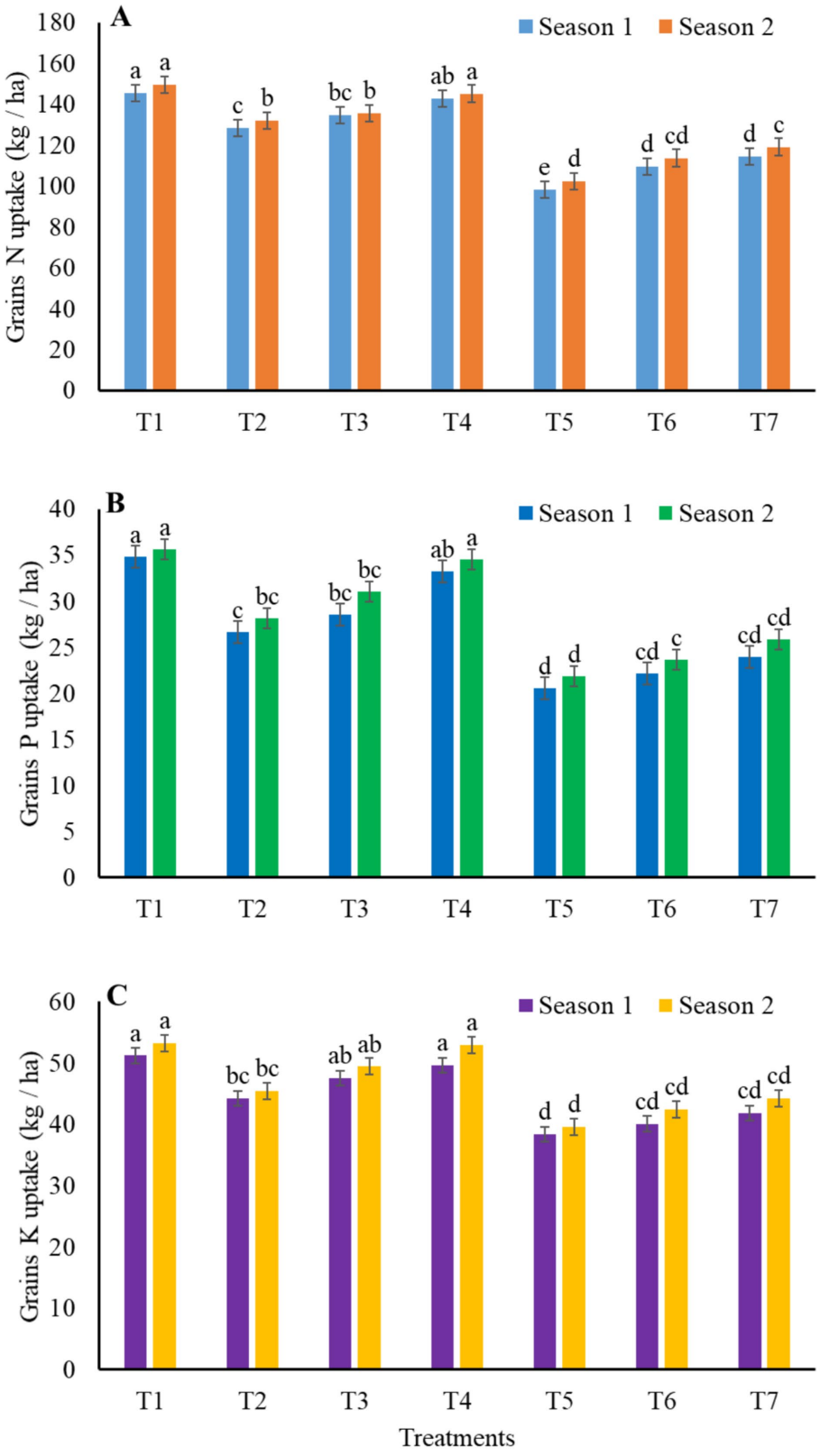

FIGURE 5
Effects of traditional NPK fertilizers and their combination with chitosan-based NPK nano-structure as a foliar application on **(A)** grain N uptake, grain P uptake **(B)**, and grain K uptake **(C)** of rice. Various letters (a, b, c, d, etc.) indicate a statistically significant variation among treatment means at $p < 0.05$. As for treatments abbreviation (see Table 1).

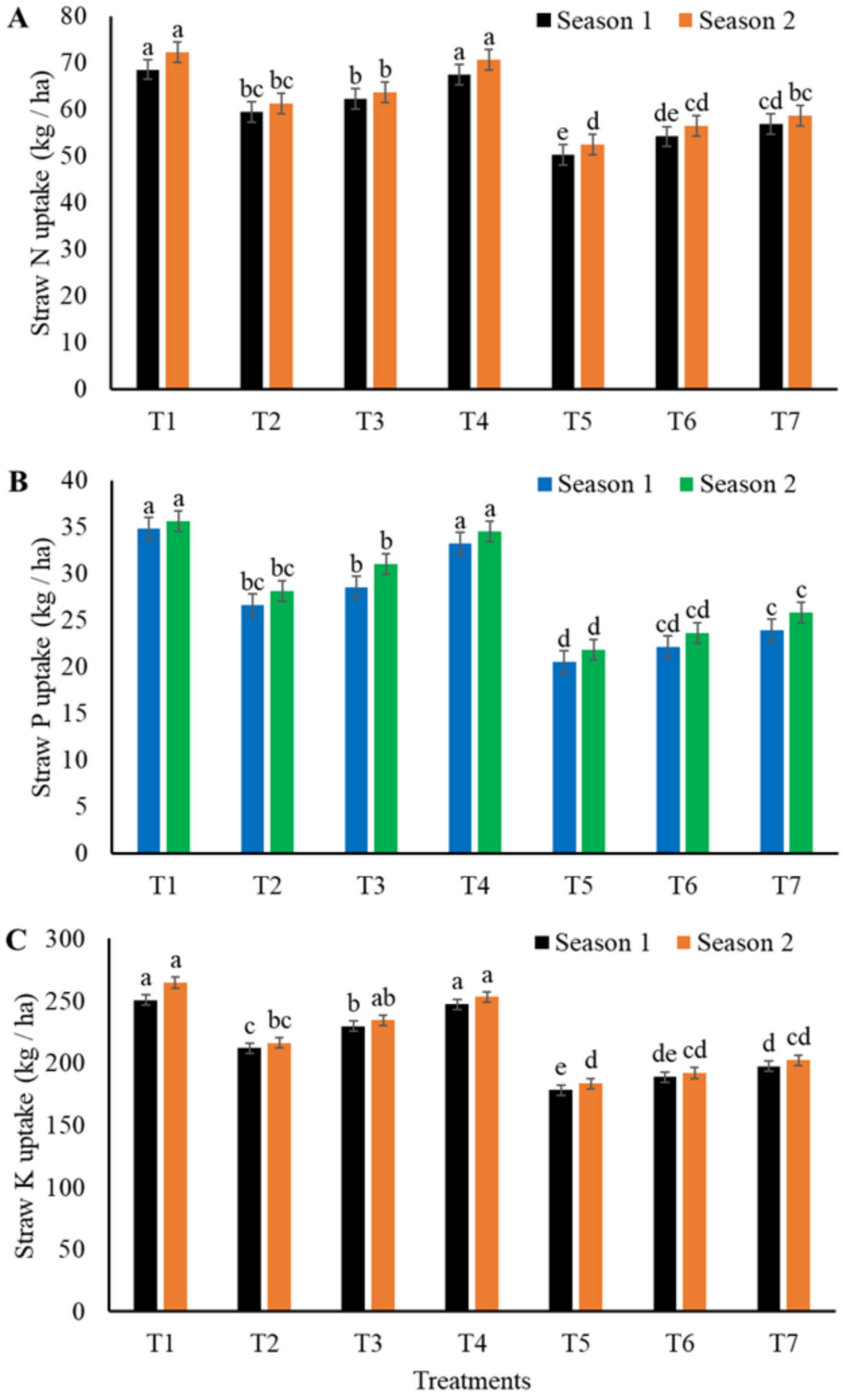

FIGURE 6
Effects of traditional NPK fertilizers and their combination with chitosan-based NPK nano-structure as a foliar application on **(A)** N uptake **(B)** P uptake, and **(C)** K uptake of rice straw. Various letters (a, b, c, d, etc.) indicate a statistically significant variation in the treatment means at $p < 0.05$. As for treatments abbreviation (see Table 1).

with benign carbohydrate buildup which could minimize tiller abortion, enhance reproductive tillers, and eventually maximize GY (Seleiman et al., 2022; Tyagi et al., 2024). Therefore, probably, T1 and T4 provided a benign content of N in rice tissues (Table 5). Previous research by Elshayb et al. (2022a), demonstrated that rice crops GY and BY were optimized and 40% less urea was required in paddy fields when urea chitosan nanoparticles were sprayed instead of the highly recommended traditional approach. On the other side, the presence

of potassium may boost the GY magnitude underlying T1 and T4 treatment (Table 5) because of its vital role in converting photosynthetic products into starch and protein which are transported directly to grains (Al-Shahmani and Al-Juthery, 2021). An earlier investigation by Sirisena et al. (2012), declared that using potassium fertilizer in nanosizing form greatly improved GY outcomes. Also, Poudel et al. (2023), noted that the foliar application of P in the nanoscale form during tillering and panicle initiation stages enhanced some bioprocess that led to increasing rice grain and straw yields.

As for, nutrients (i.e., N, P, and K) uptake indices by grains, the obvious result (Figure 5) was the increase of nutrient uptake with increasing both Ch/NPs-NPK and T-NPK levels which perhaps produced sufficient nutrition for rice production. This study hypothesis was that Ch/NPs were grabbed by NPK nutrients which added a slow-release feature to the composite of Ch/NPs-NPK resulting in higher efficacy concerning nutrient uptake. As per Abdel-Aziz et al. (2018), using Ch/NPs-NPK in wheat fertilization has been able to lower N loss and increase N uptake's effectiveness. Another investigation by Elshayb et al. (2022a), observed that utilizing urea-chitosan nanocomposite by 500 ppm led to optimizing N-uptake in both grain and straw rice yields. Another investigation by Abdel-Hakim et al. (2023) revealed that the leaf tissues of lettuce plants treated with NPK as a nano formulation had the largest accumulation of nutrients (N, P, K, Ca, Mg, Fe, Mn, and Zn). Recent studies pointed to the effective role of Ch/NPs in improving nutrient cycling and providing essential nutrients over an extended period, reducing the frequency of applications (Sarkar et al., 2022; Singh et al., 2024). Therefore, it is possible that the foliar application of Ch/NPs-NPK 300 ppm underlying T4 treatment was a good route to obtain the mechanism of uptake and transport of NPK nutrients into intact plant organs.

An analysis of the current findings showed that the nutrients (i.e., N, P, and K) uptake indices by straw (Figure 6) increased progressively by increasing both Ch/NPs-NPK and T-NPK levels. Meanwhile, T4 treatment gave a substantial increase in nutrient uptake by straw which may be due to the mass flow phenomenon via a pressure differential between the leaves and stems, which is what allows nanoparticles to travel from stomata and make their way to the xylem vessels and then move the phloem tissue where they were carried nutrients to reach all plant tissues (Hasaneen et al., 2016). A prior study by Corradini et al. (2010) pointed to the ability of endosomes (parts of the endocytic membrane transport pathway) to transport the nanoparticles to various sites within the cells. Notably the most important aspect of utilizing Ch/NPs associated with synthetic fertilizers contributes to reducing environmental pollution because it's biodegradable (Sangwan et al., 2023). Consequently, even though T-NPK dropped by up to 30%, the application of T4 improved the status of nutrient (i.e., N, P, and K) absorption indices in grain and straw yields and can be considered a smart and eco-friendly application in paddy fields.

5 Conclusion

The findings of the current study reported that utilizing Ch/NPs-NPK with 300 ppm was considered a significant application to compensate synthetic NPK fertilizers by 30% without a significant reduction in growth, yield, and nutrient content of rice. Therefore, using Ch/NPs-NPK can be recommended as an exogenous application in the paddy fields to reduce the excessive use of synthetic NPK fertilizers and enhance physiological traits that lead to sustaining a satisfactory grain outcome. Accordingly, this approach not only can mitigate the environmental impact associated with excessive fertilizer use but also can enhance the physiological traits of the rice plants, contributing to sustainable agricultural practices. The biodegradable and slow-release feature of Ch/NPs makes it an alternative to smart-safe use in the agriculture sector. Ultimately, utilizing such modern and modified technologies to produce compensatory alternatives for balanced plant nutrition provides environmental and economic usefulness in the ecosystem. Moreover, there's a dire demand to examine and explore the potential of Ch/NPs-NPK on different rice varieties, and other plant species for a deep and thorough evaluation of these materials.

Data availability statement

The raw data supporting the conclusions of this article will be made available by the authors, without undue reservation.

Author contributions

OE: Conceptualization, Funding acquisition, Methodology, Project administration, Resources, Software, Writing – original draft, Writing – review & editing. HG: Conceptualization, Data curation, Formal analysis, Funding acquisition, Methodology, Writing – original draft, Writing – review & editing. MW: Investigation, Methodology, Software, Supervision, Validation, Writing – original draft, Writing – review & editing. KF: Methodology, Software, Supervision, Validation, Visualization, Writing – original draft, Writing – review & editing. DW: Methodology, Software, Writing – original draft, Writing – review & editing. MS: Data curation, Funding acquisition, Investigation, Methodology, Project administration, Resources, Writing – original draft, Writing – review & editing.

Funding

The author(s) declare that financial support was received for the research, authorship, and/or publication of this article. This research was funded by Researchers Supporting Project (RSPD2024R751), King Saud University, Riyadh, Saudi Arabia.

Conflict of interest

The authors declare that the research was conducted in the absence of any commercial or financial relationships that could be construed as a potential conflict of interest.

Publisher's note

All claims expressed in this article are solely those of the authors and do not necessarily represent those of their affiliated organizations, or those of the publisher, the editors and the reviewers. Any product that may be evaluated in this article, or claim that may be made by its manufacturer, is not guaranteed or endorsed by the publisher.

References

Abdel-Aziz, H. M. M., Hasaneen, M., and Omer, A. (2018). Foliar application of nano chitosan NPK fertilizer improves the yield of wheat plants grown on two different soils. *J. Exp. Biol.* 14, 63–72. doi: 10.5455/egyjebb.20180106032701

Abdel-Hakim, S. G., Shehata, A. S. A., Moghannem, S. A., Qadri, M., el-Ghany, M. F. A., Abdeldaym, E. A., et al. (2023). Nanoparticulate fertilizers increase nutrient absorption efficiency and agro-physiological properties of lettuce plant. *Agronomy* 13:691. doi: 10.3390/agronomy13030691

Abd-Elrahman, S. H., El-Gabry, Y. A., Hashem, F. A., Ibrahim, M. F., El-Hallous, E. I., Abbas, Z. K., et al. (2023). Influence of nano-chitosan loaded with potassium on potassium fractionation in sandy soil and strawberry productivity and quality. *Agronomy* 13:1126. doi: 10.3390/agronomy13041126

Alhammad, B. A., Ahmad, A., Seleiman, M. F., and Tola, E. (2023). Seed priming with nanoparticles and 24-epibrassinolide improved seed germination and enzymatic performance of *Zea mays* L. in salt-stressed soil. *Plan. Theory* 12:690. doi: 10.3390/plants12040690

Almutari, M. M. (2023). Synthesis and modification of slow-release fertilizers for sustainable agriculture and environment: a review. *Arab. J. Geosci.* 16:518. doi: 10.1007/s12517-023-11614-8

Al-Shahmani, A., and Al-Juthery, H. (2021). Response of rice (*Oryza sativa* L.) to silica fertilization and spraying with nano-potassium and calcium. *IOP Conf. Ser. Earth Environ. Sci.* 735:012068. doi: 10.1088/1755-1315/735/1/012068

Badawy, S. A., Zayed, B. A., Bassiouni, S. M., Mahdi, A. H., Majrashi, A., Ali, E. F., et al. (2021). Influence of nano silicon and nano selenium on root characters, growth, ion selectivity, yield, and yield components of rice (*Oryza sativa* L.) under salinity conditions. *Plan. Theory* 10:1657. doi: 10.3390/plants10081657

Banayo, N. P., Rahon, R. E., Sta. Cruz, P., and Kato, Y. (2021). Fertilizer responsiveness of high-yielding drought-tolerant rice in rainfed lowlands. *Plant Product. Sci.* 24, 279–286. doi: 10.1080/1343943X.2020.1847668

Batool, A., Azizullah, A., Ullah, K., Shad, S., Khan, F. U., Seleiman, M. F., et al. (2024). Green synthesis of Zn-doped TIO2 nanoparticles from Zanthoxylum armatum. *BMC Plant Biol.* 24:820 (2024). doi: 10.1186/s12870-024-05525-3

Bechtaoui, N., Rabiu, M. K., Raklami, A., Oufdou, K., Hafidi, M., and Jemo, M. (2021). Phosphate-dependent regulation of growth and stresses management in plants. *Front. Plant Sci.* 12:679916. doi: 10.3389/fpls.2021.679916

Behboudi, F., Tahmasebi-Sarvestani, Z., Kassaee, M. Z., Modarres-Sanavy, S. A. M., Sorooshzadeh, A., and Mokhtassi-Bidgoli, A. (2019). Evaluation of chitosan nanoparticles effects with two application methods on wheat under drought stress. *J. Plant Nutr.* 42, 1439–1451. doi: 10.1080/01904167.2019.1617308

Carrijo, D. R., Lundy, M. E., and Linquist, B. (2017). Rice yields and water use under alternate wetting and drying irrigation: a meta-analysis. *Field Crop Res.* 203, 173–180. doi: 10.1016/j.fcr.2016.12.002

Chakraborty, R., Mukhopadhyay, A., Paul, S., Sarkar, S., and Mukhopadhyay, R. (2023). Nanocomposite-based smart fertilizers: a boon to agricultural and environmental sustainability. *Sci. Total Environ.* 863:160859. doi: 10.1016/j.scitotenv.2022.160859

Corradini, E., De Moura, M., and Mattoso, L. (2010). A preliminary study of the incorparation of NPK fertilizer into chitosan nanoparticles. *Express Polym Lett* 4, 509–515. doi: 10.3144/expresspolymlett.2010.64

Deshpande, P., Dapkekar, A., Oak, M. D., Paknikar, K. M., and Rajwade, J. M. (2017). Zinc complexed chitosan/TPP nanoparticles: a promising micronutrient nanocarrier suited for foliar application. *Carbohydr. Polym.* 165, 394–401. doi: 10.1016/j.carbpol.2017.02.061

Devi, O. R., Ojha, N., Laishram, B., Dutta, S., and Kalita, P. (2023). Roles of nano-fertilizers in sustainable agriculture and biosafety. *Environ. Ecol.* 5:100044. doi: 10.1016/j.plana.2023.100044

Dimkpa, C., Adzawla, W., Pandey, R., Atakora, W. K., Kouame, A. K., Jemo, M., et al. (2023). Fertilizers for food and nutrition security in sub-Saharan Africa: an overview of soil health implications. *Front. Soil Sci.* 3:1123931. doi: 10.3389/fsoil.2023.1123931

Dreyer, I., Gomez-Porras, J., and Riedelsberger, J. (2017). The potassium battery: a mobile energy source for transport processes in plant vascular tissues. *New Phytol.* 216, 1049–1053. doi: 10.1111/nph.14667

Elshamy, M. T., El-Khallal, S. M., Husseiny, S. M., and Farroh, K. Y. (2019). Application of nano-chitosan NPK fertilizer on growth and productivity of potato plant. *J. Sci. Res. Sci.* 36, 424–441. doi: 10.21608/jsrs.2019.58522

Elshayb, O. M., Nada, A. M., Farroh, K. Y., Al-Huqail, A. A., Aljabri, M., Binothman, N., et al. (2022a). Utilizing urea–chitosan nanohybrid for minimizing synthetic urea application and maximizing *Oryza sativa* l. productivity and n uptake. *Agriculture* 12:944. doi: 10.3390/agriculture12070944

Elshayb, O. M., Nada, A. M., Sadek, A. H., Ismail, S. H., Shami, A., Alharbi, B. M., et al. (2022b). The integrative effects of biochar and ZnO nanoparticles for enhancing rice productivity and water use efficiency under irrigation deficit conditions. *Plan. Theory* 11:1416. doi: 10.3390/plants11111416

Ferradj, S., Yahoum, M. M., Rebiha, M., Nabi, I., Toumi, S., Lefnaoui, S., et al. (2024). Nanocurcumin-based sugar-free formulation: development and impact on diabetes and oxidative stress reduction. *Nano* 14:1105. doi: 10.3390/nano14131105

Gangwar, J., Kadanthottu Sebastian, J., Puthukulangara Jaison, J., and Kurian, J. (2023). Nano-technological interventions in crop production—a review. *Physiol. Mol. Biol. Plants* 29, 93–107. doi: 10.1007/s12298-022-01274-5

Gao, D., Cheng, R., Kun, D., Xiaolei, W., Yunhe, Z., Yanqiu, G., et al. (2023). Effect of phosphorus, iron, zinc, and their combined deficiencies on photosynthetic characteristics of rice (*Oryza sativa* L.) seedlings. *Agronomy* 13:1657. doi: 10.3390/agronomy13061657

Gomez, K. A., and Gomez, A. A. (1984). Statistical procedures for agricultural research. 2nd Edn. New York, NY: John Wiley & Sons. p. 680–696.

Hafez, E. H., and Seleiman, M. F. (2017). Response of barley quality traits, yield and antioxidant enzymes to water-stress and chemical inducers. *Int. J. Plant Prod.* 11, 477–490. doi: 10.22069/IJPP.2017.3712

Hai-Yan, W., Zhang, H.-C., Qun, M., Qi-Gen, D., Zhong-Yang, H., Ke, X., et al. (2009). Photosynthetic characteristics of flag leaf in rice genotypes with different nitrogen use efficiency. *Acta Agron. Sin.* 35, 2243–2251. doi: 10.1016/S1875-2780(08)60120-0

Hasaneen, M., Abdel-aziz, H. M. M., and Omer, A. M. J. (2016). Effect of foliar application of engineered nanomaterials: carbon nanotubes NPK and chitosan nanoparticles NPK fertilizer on the growth of French bean plant. *Biochem. Biotechnol. Res.* 4, 68–76.

Haydar, M. S., Ghosh, D., and Roy, S. (2024). Slow and controlled release nanofertilizers as an efficient tool for sustainable agriculture: recent understanding and concerns. *Plant Nano Biol.* 7:100058. doi: 10.1016/j.plana.2024.100058

He, X., Zhu, H., Shi, A., and Wang, X. (2024). Optimizing nitrogen fertilizer management enhances Rice yield, dry matter, and nitrogen use efficiency. *Agronomy* 14:919. doi: 10.3390/agronomy14050919

Hsu, J. (1996). Multiple comparisons: Theory and methods. Florida, USA: CRC Press.

Ingle, P. U., Shende, S. S., Shingote, P. R., Mishra, S. S., Sarda, V., Wasule, D. L., et al. (2022). Chitosan nanoparticles (ChNPs): a versatile growth promoter in modern agricultural production. *Heliyon* 8:e11893. doi: 10.1016/j.heliyon.2022.e11893

Jackson, M. L. (2005). Soil chemical analysis: Advanced course: A manual of methods useful for instruction and research in soil chemistry, physical chemistry of soils, soil fertility, and soil genesis. Wisconsin, USA: UW-Madison Libraries Parallel Press.

Krasilnikov, P., Taboada, M., and Amanullah. (2022). Fertilizer use, soil health and agricultural sustainability. *Agriculture* 12:462. doi: 10.3390/agriculture12040462

Kumar, N., Samota, S. R., Venkatesh, K., and Tripathi, S. (2023). Global trends in use of nano-fertilizers for crop production: advantages and constraints–a review. *Soil Tillage Res.* 228:105645. doi: 10.1016/j.still.2023.105645

Kumari, A., Sharma, H., Kumari, A., Sharma, P., Pathak, N., Singh, R., et al. (2024). "Movement and signaling of macronutrients in plant system" in Essential minerals in plant-soil systems" (Elsevier), 1–28.

Ladha, J., Tirol-Padre, A., Reddy, C., Cassman, K., Verma, S., Powlson, D., et al. (2016). Global nitrogen budgets in cereals: a 50-year assessment for maize, rice and wheat production systems. *Sci. Rep.* 6, 1–9. doi: 10.1038/srep19355

Liu, K., Li, T., Chen, Y., Huang, J., Qiu, Y., Li, S., et al. (2020). Effects of root morphology and physiology on the formation and regulation of large panicles in rice. *Field Crop Res.* 258:107946. doi: 10.1016/j.fcr.2020.107946

Miranda-Villagómez, E., Trejo-Téllez, L. I., Gómez-Merino, F. C., Sandoval-Villa, M., Sánchez-García, P., and Aguilar-Méndez, M. Á. (2019). Nanophosphorus fertilizer stimulates growth and photosynthetic activity and improves P status in rice. *J. Nanomater.* 2019, 1–11. doi: 10.1155/2019/5368027

Moe, K., Htwe, A. Z., Thu, T. T., Kajihara, Y., and Yamakawa, T. (2019). Effects on NPK status, growth, dry matter and yield of rice (*Oryza sativa*) by organic fertilizers applied in field condition. *Agriculture* 9:109. doi: 10.3390/agriculture9050109

Mukhtiar, A., Zia, M. A., Alawadi, H. F., Naqve, M., Seleiman, M. F., Mahmood, A., et al. (2024). Role of iron oxide nanoparticles in maize (*Zea mays* L.) to enhance salinity stress tolerance. *Notulae Botanicae Horti Agrobotanici Cluj-Napoca* 52:13695. doi: 10.15835/nbha52313695

Peng, J., Feng, Y., Wang, X., Li, J., Xu, G., Phonenasay, S., et al. (2021). Effects of nitrogen application rate on the photosynthetic pigment, leaf fluorescence characteristics, and yield of indica hybrid rice and their interrelations. *Sci. Rep.* 11:7485. doi: 10.1038/s41598-021-86858-z

Peterburgski, A. (1968). Handbook of agronomic chemistry. Moscow: Kolop Publishing House.

Poudel, A., Singh, S. K., Jiménez-Ballesta, R., Jatav, S. S., Patra, A., and Pandey, A. (2023). Effect of nano-phosphorus formulation on growth, yield and nutritional quality of wheat under semi-arid climate. *Agronomy* 13:768. doi: 10.3390/agronomy13030768

Ryan, J., Estefan, G., and Rashid, A. (2001). Soil and plant analysis laboratory manual: ICARDA Available at: https://repo.mel.cgiar.org/items/149b8091-6d46-4a67-9c1e-733c899b5428.

Sangwan, S., Pankaj, S., Leela, W., and Sahil, M. (2023). "Effect of chitosan nanoparticles on growth and physiology of crop plants" in Engineered nanomaterials for sustainable agricultural production, soil improvement and stress management (Academic Press), 99–123.

Sarkar, M. R., Rashid, M. H., Rahman, A., Kafi, M. A., Hosen, M. I., Rahman, M. S., et al. (2022). Recent advances in nanomaterials based sustainable agriculture: an overview. *Environ. Nanotechnol. Monit. Manag.* 18:100687. doi: 10.1016/j.enmm.2022.100687

Sathiyabama, M., and Manikandan, A. (2021). Foliar application of chitosan nanoparticle improves yield, mineral content and boost innate immunity in finger millet plants. *Carbohydr. Polym.* 258:117691. doi: 10.1016/j.carbpol.2021.117691

Seleiman, M. F., Almutairi, K. F., Alotaibi, M., Shami, A., Alhammad, B. A., and Battaglia, M. L. (2021). Nano-fertilization as an emerging fertilization technique: why can modern agriculture benefit from its use? *Plan. Theory* 10:2. doi: 10.3390/plants10010002

Seleiman, M. F., Elshayb, O. M., Nada, A. M., El-leithy, S. A., Baz, L., Alhammad, B. A., et al. (2022). Azolla compost as an approach for enhancing growth, productivity and nutrient uptake of *Oryza sativa* L. *Agronomy* 12:416. doi: 10.3390/agronomy12020416

Seleiman, M. F., Santanen, A., and Mäkelä, P. (2020). Recycling sludge on cropland as fertilizer-advantages and risks. *Resour. Conserv. Recycling* 155:104647. doi: 10.1016/j.resconrec.2019.104647

Seleiman, M. F., Selim, S., Jaakkola, S., and Mäkelä, P. (2017). Chemical composition and *in vitro* digestibility of whole-crop maize fertilized with synthetic fertilizer or digestate and harvested at two maturity stages in boreal growing conditions. *Agric. Food Sci.* 26, 47–55. doi: 10.23986/afsci.60068

Sheoran, P., Goel, S., Boora, R., Kumari, S., Yashveer, S., and Grewal, S. (2021). Biogenic synthesis of potassium nanoparticles and their evaluation as a growth promoter in wheat. *Plant Gene* 27:100310. doi: 10.1016/j.plgene.2021.100310

Singh, A., Rajput, V. D., Varshney, A., Sharma, R., Ghazaryan, K., Minkina, T., et al. (2024). Revolutionizing crop production: nanoscale wonders-current applications, advances and future Frontiers. *Egypt. J. Soil Sci.* 64, 221–258. doi: 10.21608/ejss.2023.246354.1684

Sirisena, D., Dissanayake, D., Somaweera, K., Karunaratne, V., and Kottegoda, N. (2012). "Use of nano-K fertilizer as a source of potassium in rice cultivation" in First National Nanotechnology Conference, 98.

Srikanth, B., Subrahmanyam, D., Sanjeeva Rao, D., Narender Reddy, S., Supriya, K., Raghuveer Rao, P., et al. (2023). Promising physiological traits associated with nitrogen use efficiency in rice under reduced N application. *Front. Plant Sci.* 14:1268739. doi: 10.3389/fpls.2023.1268739

Sundararajan, N., Habeebsheriff, H. S., Dhanabalan, K., Cong, V. H., Wong, L. S., Rajamani, R., et al. (2024). Mitigating global challenges: harnessing green synthesized nanomaterials for sustainable crop production systems. *Global Chall.* 8:2300187. doi: 10.1002/gch2.202300187

Tomar, B., Tomar, S. S., Parihar, S. S., Patle, T., Patel, H., and Singh, P. (2024). "Advanced and intelligent nanofertilizer base soil management for sustainable agriculture" in Sustainable agriculture Nanotechnology and Biotechnology for Crop Production and Protection, vol. 17.

Tyagi, A., Chakraborty, N., and Raghuram, N. (2024). Morpho-physiological evaluation of Indica Rice genotypes with contrasting crop duration for nitrogen use efficiency under graded urea doses. *J. Plant Growth Regul.*, 1–22. doi: 10.1007/s00344-024-11437-1

Upadhyay, P. K., Singh, V. K., Rajanna, G., Dwivedi, B. S., Dey, A., Singh, R. K., et al. (2023). Unveiling the combined effect of nano fertilizers and conventional fertilizers on crop productivity, profitability, and soil well-being. *Front. Sustain. Food Syst.* 7:1260178. doi: 10.3389/fsufs.2023.1260178

Vance, C. P., Uhde-Stone, C., and Allan, D. (2003). Phosphorus acquisition and use: critical adaptations by plants for securing a nonrenewable resource. *New Phytol.* 157, 423–447. doi: 10.1046/j.1469-8137.2003.00695.x

Vejan, P., Khadiran, T., Abdullah, R., and Ahmad, N. (2021). Controlled release fertilizer: a review on developments, applications and potential in agriculture. *J. Control. Release* 339, 321–334. doi: 10.1016/j.jconrel.2021.10.003

Verma, K. K., Song, X.-P., Joshi, A., Tian, D., Rajput, V. D., Singh, M., et al. (2022). Recent trends in nano-fertilizers for sustainable agriculture under climate change for global food security. *Nano* 12:173. doi: 10.3390/nano12010173

Vijayakumar, S., Kumar, D., Ramesh, K., Bussa, B., Kaje, V., and Shivay, Y. (2024). Effect of split application of potassium on nutrient recovery efficiency, soil nutrient balance, and system productivity under rice-wheat cropping system (RWCS). *J. Plant Nutr.* 47, 1546–1563. doi: 10.1080/01904167.2024.2315974

Vijayalakshmi, P., Vishnukiran, T., Kumari, B. R., Srikanth, B., Rao, I. S., Swamy, K., et al. (2015). Biochemical and physiological characterization for nitrogen use efficiency in aromatic rice genotypes. *Field Crop Res.* 179, 132–143. doi: 10.1016/j.fcr.2015.04.012

Watanabe, F., and Olsen, S. (1965). Test of an ascorbic acid method for determining phosphorus in water and NaHCO3 extracts from soil. *Soil Sci. Soc. Am. J.* 29, 677–678. doi: 10.2136/sssaj1965.03615995002900060025x

Wellburn, A. R. (1994). The spectral determination of chlorophylls a and b, as well as total carotenoids, using various solvents with spectrophotometers of different resolution. *J. Plant Physiol.* 144, 307–313. doi: 10.1016/S0176-1617(11)81192-2

Yoshida, S. (1981). Fundamentals of rice crop science. Los Baños, Philippines: International Rice Research Institute.

Yoshida, S., Forno, D. A., and Cock, J. H. (1971). Laboratory manual for physiological studies of rice. Los Baños, Philippines: International Rice Research Institute.

Zou, Y., Zeng, Q., Li, H., Liu, H., and Lu, Q. (2021). Emerging technologies of algae-based wastewater remediation for bio-fertilizer production: a promising pathway to sustainable agriculture. *J. Chem. Technol. Biotechnol.* 96, 551–563. doi: 10.1002/jctb.6602

frontiers | Frontiers in Sustainable Food Systems

TYPE Original Research
PUBLISHED 14 January 2025
DOI 10.3389/fsufs.2024.1514409

Check for updates

OPEN ACCESS

EDITED BY
Mohamed Ait-El-Mokhtar,
University of Hassan II Casablanca, Morocco

REVIEWED BY
Mushtaq Ahmad Khan,
Hazara University, Pakistan
Nitin Gudadhe,
Navsari Agricultural University, India

*CORRESPONDENCE
Jun Zhang
627085986@qq.com

RECEIVED 20 October 2024
ACCEPTED 30 December 2024
PUBLISHED 14 January 2025

CITATION
Zhang J, He W, Wei Z, Chen Y and Gao W (2025) Integrating green manure and fertilizer reduction strategies to enhance soil carbon sequestration and crop yield: evidence from a two-season pot experiment. *Front. Sustain. Food Syst.* 8:1514409. doi: 10.3389/fsufs.2024.1514409

COPYRIGHT
© 2025 Zhang, He, Wei, Chen and Gao. This is an open-access article distributed under the terms of the Creative Commons Attribution License (CC BY). The use, distribution or reproduction in other forums is permitted, provided the original author(s) and the copyright owner(s) are credited and that the original publication in this journal is cited, in accordance with accepted academic practice. No use, distribution or reproduction is permitted which does not comply with these terms.

Integrating green manure and fertilizer reduction strategies to enhance soil carbon sequestration and crop yield: evidence from a two-season pot experiment

Jun Zhang[1,2,3]*, Wei He[1,2,4], Zheng Wei[1,2], Yifei Chen[1,2] and Weichun Gao[1,2]

[1]Shaanxi Dijian Guantian Investment and Construction Co., Ltd., Baoji, China, [2]Shaanxi Provincial Land Engineering Construction Group Co., Ltd., Xi'an, China, [3]Zhongshan High Standard Farmland Construction Group Baoji Co., Ltd., Baoji, China, [4]School of Water Resources and Hydropower, Xi'an University of Technology, Xi'an, China

The excessive use of chemical fertilizers in agricultural production has led to diminishing returns, necessitating alternative methods to enhance soil fertility and reduce fertilizer dependency. One promising approach is the integration of leguminous green manure, which improves soil structure, enhances nutrient cycling, and supports sustainable farming practices. However, the application of green manure in systems with continuous fertilizer reduction remains underexplored. This study addresses this gap by investigating the effects of reducing nitrogen and phosphorus fertilizers (N-P) by up to 24% in conjunction with multiple cropping of soybean green manure on soil fertility, organic carbon fractions, and wheat yield. The research employed a pot experiment conducted over two wheat-growing seasons (March 2021 to July 2022) at an experimental station in Baoji, China. Treatments included CK (control, no fertilizer), CF (conventional fertilizer), and reduced N-P fertilizer applications by 6% (RF6), 12% (RF12), 18% (RF18), and 24% (RF24). Key findings revealed that RF12 had no significant impact on wheat grain yield compared to CF. The incorporation of soybean green manure significantly improved soil alkaline nitrogen by 22.3% and available phosphorus by 30.7%, while high-labile organic carbon (H-LOC) and microbial biomass carbon (MBC) increased by 34.5 and 29.6%, respectively. Additionally, a notable increase of 12.4% in soil organic carbon content was observed, suggesting enhanced carbon sequestration potential. This study provides valuable insights into sustainable agricultural practices by demonstrating that incorporating leguminous green manure alongside moderate fertilizer reduction can maintain crop yield, improve soil nutrient availability, and increase organic carbon content, thus supporting reduced reliance on chemical fertilizers and promoting long-term soil fertility and carbon sequestration.

KEYWORDS

green manure, fertilizer reduction, soil carbon sequestration, crop yield, sustainable agriculture

1 Introduction

Soil carbon sequestration plays a pivotal role in promoting sustainable agriculture and mitigating climate change, as it underpins soil fertility and ecosystem functionality. Chemical fertilizers, while integral to enhancing crop productivity, have increasingly been associated with environmental concerns such as nutrient leaching, greenhouse gas emissions, and soil acidification, alongside diminishing returns due to excessive use (Liu et al., 2022; Hou et al., 2023). This has necessitated the exploration of alternative strategies, such as the use of green manure, which offers potential benefits for soil organic carbon (SOC) dynamics and sustainable farming systems. Leguminous green manure, in particular, is distinguished by its capacity for biological nitrogen fixation and nutrient release, which not only improve soil structure and fertility but also modulate SOC dynamics (Mandal et al., 2003; Carter et al., 2014). These dynamics are governed by distinct SOC fractions, including highly labile organic carbon (H-LOC), low-labile organic carbon (L-LOC), and recalcitrant organic carbon (ROC), each contributing uniquely to SOC storage and turnover (Rahmati et al., 2020; Rossi et al., 2020). However, the specific effects of green manure incorporation on these SOC fractions remain inadequately understood.

The integration of green manure into soil introduces both organic carbon and nitrogen, which may significantly influence SOC fractions and their cycling. Green manure, as a high-quality residue with a low carbon-to-nitrogen (C/N) ratio, is prone to rapid decomposition, facilitating the release of nutrients and contributing to SOC pools (Xu et al., 2021; Lyu et al., 2024). This contrasts with the effects of synthetic fertilizers, which primarily provide inorganic nutrients and indirectly affect SOC dynamics by altering microbial activity (Li et al., 2018; He et al., 2020). The interplay between green manure and synthetic fertilizers is further complicated by phenomena such as the priming effect, where the addition of fresh organic matter accelerates the decomposition of existing SOC (Liu et al., 2015; Zheng et al., 2022). Such trade-offs raise critical questions about the balance between adding new organic carbon (e.g., cellulose and lignin from green manure) and triggering the mineralization of stable carbon stocks. Understanding these mechanisms is essential for optimizing carbon sequestration strategies while mitigating potential SOC losses due to accelerated turnover.

Leguminous green manure, with its high nitrogen content and low C/N ratio, is hypothesized to stimulate SOC turnover by enhancing microbial activity (Zhou et al., 2021; Fan et al., 2022). Simultaneously, the reduction of synthetic nitrogen (N) and phosphorus (P) fertilizers may moderate these dynamics, potentially limiting microbial decomposition rates and influencing SOC stabilization (Han et al., 2021; Liang et al., 2022). This study seeks to investigate the combined effects of green manure incorporation and reduced synthetic fertilizer inputs on SOC fractions (H-LOC, L-LOC, and ROC) and their turnover. The central hypothesis posits that specific SOC fractions will exhibit differential responses, with some fractions being stimulated while others are stabilized, depending on the balance between nutrient inputs and microbial activity. Additionally, the study aims to elucidate how these practices influence the overall carbon sequestration potential of soils, thereby advancing the understanding of sustainable fertilizer management in monoculture systems.

This investigation addresses critical knowledge gaps through a field experiment examining the impacts of green manure incorporation and fertilizer reductions on SOC fractions, soil nutrient dynamics, and crop productivity. The findings aim to inform sustainable agricultural practices, offering a scientific basis for strategies that enhance SOC sequestration while maintaining agricultural yields.

2 Materials and methods

2.1 Experimental site

The outdoor pot experiment was conducted from March 2021 to July 2022 at the experimental station of the College of Agriculture, Baoji College of Arts and Sciences (107°1' E, 34°4' N). The site is located in the midsection of the northern slope of the Taibai Mountains, characterized by a temperate continental climate, with an average annual temperature of 7.5–8.2°C, annual precipitation ranging from 180 to 270 mm, and annual evaporation of 1,500–2000 mm. The test soil was the topsoil (0–20 cm) from a wheat field where fertilizer reduction had been implemented for three consecutive years. The soil type was irrigated gray desert soil. Before the experiment started (in 2018), the basic physical and chemical properties of the soil were: pH 7.79, organic matter content 19.5 g/kg, alkaline nitrogen 62.13 mg/kg, available phosphorus 29.85 mg/kg, and available potassium 175.95 mg/kg.

2.2 Experimental design

The pot experiment of multiple cropping green manure after wheat harvest included six treatments: no fertilizer (CK), conventional fertilizer (CF) (applying nitrogen and phosphorus fertilizers only), and nitrogen and phosphorus fertilizer reductions of 6, 12, 18, and 24% (RF6, RF12, RF18, and RF24, respectively). Each treatment was replicated three times. Fertilizers were applied during the wheat season, while no fertilizer was applied during the green manure season. Before the experiment, soil samples from each treatment were taken to measure the basic soil properties.

The pots used in the experiment were high-density polyethylene rectangular containers, 46.5 cm long, 35.0 cm wide, and 22.0 cm high, with each pot filled with 40.0 kg of air-dried soil. After aging, the soil layer was about 20 cm deep. The pots were buried flush with the ground to simulate field soil temperatures. During both the wheat and soybean growing seasons, soil moisture content was controlled to maintain 40–60% of the field water-holding capacity using the weighing method. Wheat was sown on April 1, 2021 (variety: Xin Chun 38), with two rows per pot, row spacing of 15 cm, and each row 10 cm away from the pot edge. After sowing, 80 plants per pot were retained. After wheat was harvested on July 6, soil and plant samples were collected to measure wheat yield and soil fertility indicators. Soybean plants were sown on July for green manuring purpose, following the same sowing method as wheat. After emergence, 10 plants per row were retained, and the green manure was plowed under during the full flowering stage, with plant and soil samples collected. At the time of plowing, the aboveground biomass and nutrient contents of the green manure for each treatment are shown in Table 1. The same wheat growing operations were repeated in 2022, with soil

10.3389/fsufs.2024.1514409

TABLE 1 Aboveground biomass, dry matter and nutrient contents of soybean in each treatment.

Treatment	Biomass (g pot^{-1})	Dry matter (g pot^{-1})	Organic carbon (%)	Total nitrogen (%)	Total phosphorus (%)	Total potassium (%)
CK	358.46 ± 6.06 c	100.99 ± 1.33 c	40.01 ± 0.29 b	3.31 ± 0.06 b	0.62 ± 0.01 a	1.54 ± 0.03 a
CF	537.98 ± 7.39 a	166.16 ± 1.96 a	41.68 ± 0.35 a	3.56 ± 0.07 a	0.62 ± 0.02 a	1.53 ± 0.02 a
RF6	538.78 ± 6.87 a	165.24 ± 1.79 a	42.30 ± 0.40 a	3.31 ± 0.06 b	0.53 ± 0.01 c	1.50 ± 0.03 b
RF12	563.94 ± 5.95 a	174.32 ± 1.56 a	42.43 ± 0.29 a	3.38 ± 0.05 a	0.57 ± 0.01 b	1.52 ± 0.03 a
RF18	485.10 ± 5.60 b	154.66 ± 1.67 b	41.76 ± 0.23 a	3.12 ± 0.05 c	0.63 ± 0.01 a	1.53 ± 0.03 a
RF24	478.56 ± 6.47 b	163.14 ± 1.85 a	42.04 ± 0.35 a	3.15 ± 0.06 c	0.57 ± 0.01 b	1.51 ± 0.03 a
Two-factor ANOVA (Significance)						
Year (Y)	ns	ns	ns	ns	**	**
Treatment (T)	ns	ns	**	*	**	**
Interaction (Y × T)	ns	ns	ns	ns	**	**

CK, CF, RF6, RF12, RF18, and RF24 represent the treatments of no fertilizer, conventional nitrogen and phosphorus fertilizer, and nitrogen and phosphorus fertilizer reductions of 6, 12, 18, and 24%, respectively. Different letters in the same column represent significant differences at the 5% significance level following the LSD test. ***, **, and * indicate significance at $p < 0.001$, $p < 0.01$, and $p < 0.05$, respectively; "ns" indicates no significance ($p > 0.05$).

TABLE 2 Fertilizer application dose and fertilization strategy of each treatment.

Treatment	Base fertilizer (kg hm^{-2})		Topdressing (kg hm^{-2})		Total nutrient content (kg hm^{-2})	
	N	P_2O_5	*N*	P_2O_5	*N*	P_2O_5
CK	–	–	–	–	–	–
CF	72.00	32.00	228.00	101.35	300.00	133.35
RF6	67.68	30.08	214.32	95.27	282.00	125.35
RF12	63.36	28.16	200.64	89.18	264.00	117.34
RF18	59.04	26.24	186.96	83.10	246.00	109.34
RF24	54.72	24.32	173.28	77.02	228.00	101.34

CK, CF, RF6, RF12, RF18, and RF24 represent the treatments of no fertilizer, conventional nitrogen and phosphorus fertilizer, and nitrogen and phosphorus fertilizer reductions of 6, 12, 18, and 24%, respectively. The values in the table represent the fertilizer application rates for each treatment.

samples taken before sowing (March 28) and after harvest (July 1) to determine nutrient contents.

The fertilization strategy for the wheat season was as follows: base fertilizer accounted for 24% of the total nutrients, while topdressing accounted for 76% of the total nutrients (with 10% applied during the seedling stage, 30% during the jointing stage, 20% during the booting stage, 10% during the flowering stage, and 6% during the ripening stage). The fertilization amounts for each treatment are shown in Table 2. Urea (N ≥ 46.4%) and superphosphate ($P_2O_5 \geq 46\%$) were used as the nitrogen and phosphorus sources for the base fertilizer. During topdressing, ammonium phosphate (N ≥ 12%, $P_2O_5 \geq 61\%$) was used as the phosphorus source, and urea was used to supply the remaining required nitrogen.

2.3 Measured items and methods

2.3.1 Plant sample collection and measurement

Wheat and green manure samples were collected at the time of harvest and plowing, respectively. After being killed at 105°C for 30 min, the samples were dried at 75°C to a constant weight to measure dry matter. The wheat plants were divided into grain, husk, and straw (stem and leaves), while the soybean plants were divided into stems, leaves, and pods. Each plant part was ground and passed through a 0.5 mm sieve for determining the contents of carbon (C), nitrogen (N), phosphorus (P), and potassium (K). The carbon content of the plants was measured using the potassium dichromate heating method, while nitrogen, phosphorus, and potassium contents were measured using the digestate after H_2SO_4-H_2O_2 digestion. Nitrogen content was determined using the Nessler's reagent colorimetric method, phosphorus using the vanadium molybdenum yellow colorimetric method, and potassium using a flame photometer (Cong et al., 2023).

2.3.2 Soil sample collection and measurement

Soil samples were collected five times: during wheat sowing in 2021 (S1), after wheat harvest (S2), after the plowing of green manure (S3), during wheat sowing in 2022 (S4), and after wheat harvest in 2022 (S5). For each pot, six evenly distributed sampling points were selected, and soil was taken from a depth of 20 cm using a stainless steel soil auger with an inner diameter of 3 cm. The soil samples were then air-dried, ground, and sieved through 1.00 mm (18 mesh) and 0.15 mm (100 mesh) sieves. Soil samples passing through the 1.00 mm sieve were used to measure soil pH, alkaline nitrogen (AN), available phosphorus (AP), and available potassium (AK), while samples passing through the 0.15 mm sieve were used to measure soil organic carbon (SOC) and total nitrogen (TN). Soil pH was measured using a potentiometer with a water-to-soil ratio of 2.5:1. SOC was determined

using the potassium dichromate heating method, and TN was measured using the semi-micro Kjeldahl method. AN was determined using the alkaline diffusion method, AP using the sodium bicarbonate extraction-molybdenum antimony colorimetric method, and AK using the ammonium acetate extraction-flame photometry method (Cong et al., 2023). Soil microbial biomass carbon (MBC) and microbial biomass nitrogen (MBN) (Li et al., 2018) were extracted using the chloroform fumigation method and then determined using the potassium dichromate heating method and semi-micro Kjeldahl method, respectively. Soil organic carbon fractions were measured using the improved acid extraction method as described by Rahmati et al. (2020). The highly labile fraction (H-LOC, g/kg) was extracted with 2.5 mol/L H_2SO_4, and the low-labile fraction (L-LOC, g/kg) was extracted with 13.0 mol/L H_2SO_4. The remaining fraction was considered the recalcitrant fraction (ROC, g/kg). All extracted fractions were measured using the potassium dichromate heating method.

2.3.3 Soil quality evaluation

To evaluate the effects of different fertilizer reduction treatments and the incorporation of green manure on soil quality, the overall data set method based on principal component analysis (PCA) was used (Duan et al., 2024). Thirteen indicators—pH, SOC, TN, C/N ratio, AN, AP, AK, MBC, MBN, MBC/MBN, H-LOC, L-LOC, and ROC—were included to establish the data set and further calculate the soil quality index (SQI). The calculation steps are shown in Equation 1:

$$SQI = \sum_{i=1}^{n} w_i \times S_i \quad (1)$$

where n is the number of soil parameters, W_i is the weight of the i-th parameter, and S_i is the score of the i-th parameter. The weights W_i were derived from PCA. First, components with eigenvalues greater than 1 were retained to determine the number of principal components. Then, factor loadings, variance percentages, and cumulative variance percentages for each principal component were obtained. Finally, the weight for each parameter (W_i) was calculated as the ratio of the communalities of the i-th indicator to the sum of the communalities of all indicators (Iheshiulo et al., 2024). For pH, the score S_i was determined using Equation 3, and for other indicators, Equation 2 was used:

$$S_i = \frac{X_i - X_{\min}}{X_{\max} - X_{\min}} \quad (2)$$

$$S_i = \frac{X_{\max} - X_i}{X_{\max} - X_{\min}} \quad (3)$$

2.4 Data processing and analysis

Analysis of variance (ANOVA) and principal component analysis (PCA) were performed using SPSS 22.0 software. The least significant difference (LSD) method was used to test for significant differences between treatments ($p < 0.05$). Microsoft Excel 2019 and Origin 2022 software were used for data processing and graph creation.

3 Results

3.1 Wheat dry matter and yield

The reduction of different proportions of chemical fertilizers and the replanting of green manure after wheat harvest significantly affected wheat dry matter and yield formation (Table 3). The dry matter, grain yield, 1,000-grain weight, and the number of grains per spike all reached significant levels between the years (Y) ($p < 0.01$), indicating that the incorporation of green manure significantly influenced these four indicators. After the replanting and incorporation of green manure, dry matter, grain yield, and the number of grains per spike increased by 15.9–52.4%, 32.2–40.6%, and 6.1–15.5%, respectively. Before the incorporation of green manure, the yield of CF and RF6 treatments was significantly higher than other treatments. However, after the incorporation of green manure, there were no significant differences in yield among the CF, RF6, and RF12 treatments.

3.2 Changes in annual soil nutrient content

In all treatments, after the incorporation of green manure (after S3), the available soil nutrient content showed an increasing trend, while changes in pH, organic carbon, and total nitrogen content were less pronounced (Figures 1A–C). The soil alkaline nitrogen content exhibited a rapid increase during the green manure growth season (S2 to S3) and after the 175-day incorporation period (S3 to S4) (Figure 1D). The changes in available phosphorus content showed an upward trend during the 175-day (S4) and 272-day (S5) periods after the incorporation of the green manure (Figure 1E), indicating that phosphorus release from the green manure decomposition occurred slowly. The available potassium content increased rapidly after the 175-day incorporation period (S4), while during the second wheat growing season, it showed a rapid decline (Figure 1F). Compared with the wheat harvest season in 2021, the soil alkaline nitrogen content in 2022 increased by 8.0–45.9%, available phosphorus increased by 20.0–57.3%, and available potassium decreased by 8.8–14.2%.

3.3 Soil organic carbon fractions and microbial biomass carbon and nitrogen contents

Compared to 2021, after the wheat harvest in 2022, the soil organic carbon content significantly increased ($p < 0.01$), with an increase range of 10.6–14.5% (Table 4). Among them, the high labile organic carbon fraction (H-LOC) increased by 34.7–44.5% ($p < 0.01$). After the return of green manure to the field, the microbial biomass carbon (MBC) and microbial biomass nitrogen (MBN) contents also significantly increased. The two-factor analysis of variance indicated that there were significant differences among the different fertilizer reduction treatments in all indicators, but the interaction between fertilizer reduction and the return of green manure only had a significant effect on the contents of H-LOC, MBC, and MBN ($p < 0.01$).

10.3389/fsufs.2024.1514409

TABLE 3 Effects of fertilizer reduction and soybean return on wheat dry matter and yield.

Year	Treatment	Dry matter (g pot−1)	Grain yield (g pot−1)	Seeds per spike (seeds ear−1)	1,000-kernel weight (g pot−1)
2021	CK	96.81 ± 3.62 d	53.21 ± 4.44 c	17.73 ± 0.69 d	37.37 ± 0.69 c
	CF	177.68 ± 1.85 a	86.32 ± 5.61 a	23.86 ± 1.10 a	47.58 ± 1.13 a
	RF6	174.49 ± 7.31 ab	82.28 ± 2.53 a	22.80 ± 0.98 a	47.17 ± 1.28 a
	RF12	168.23 ± 3.97 bc	77.18 ± 1.23 b	21.28 ± 0.66 b	42.54 ± 0.84 b
	RF18	159.51 ± 5.10 c	75.60 ± 0.94 b	20.70 ± 0.94 bc	41.99 ± 0.45 b
	RF24	161.38 ± 2.27 c	74.88 ± 3.01 b	20.13 ± 0.66 c	42.06 ± 1.14 b
2022	CK	147.57 ± 3.87 c	90.12 ± 7.36 c	20.89 ± 1.98 c	38.89 ± 0.79 c
	CF	218.53 ± 4.70 a	115.16 ± 2.83 a	25.31 ± 1.02 a	47.95 ± 1.34 a
	RF6	214.34 ± 1.01 a	108.74 ± 0.45 ab	24.33 ± 0.35 ab	47.25 ± 1.63 a
	RF12	212.92 ± 5.86 a	108.54 ± 0.24 ab	24.00 ± 0.84 ab	46.46 ± 0.57 a
	RF18	187.63 ± 3.92 b	105.59 ± 1.65 b	23.26 ± 0.36 b	43.28 ± 0.37 b
	RF24	187.01 ± 13.28 b	101.92 ± 5.08 b	23.24 ± 0.37 b	43.09 ± 0.53 b
Two-factor ANOVA (Significance)					
Year (Y)		**	ns	ns	**
Treatment (T)		**	**	*	**
Interaction (Y × T)		**	ns	ns	**

CK, CF, RF6, RF12, RF18, and RF24 represent the treatments of no fertilizer, conventional nitrogen and phosphorus fertilizer, and nitrogen and phosphorus fertilizer reductions of 6, 12, 18, and 24%, respectively. The values in the table represent the fertilizer application rates for each treatment. Different letters in the same column represent significant differences at the 5% significance level. ***, **, and * indicate significance at $p < 0.001$, $p < 0.01$, and $p < 0.05$, respectively; "ns" indicates no significance ($p > 0.05$).

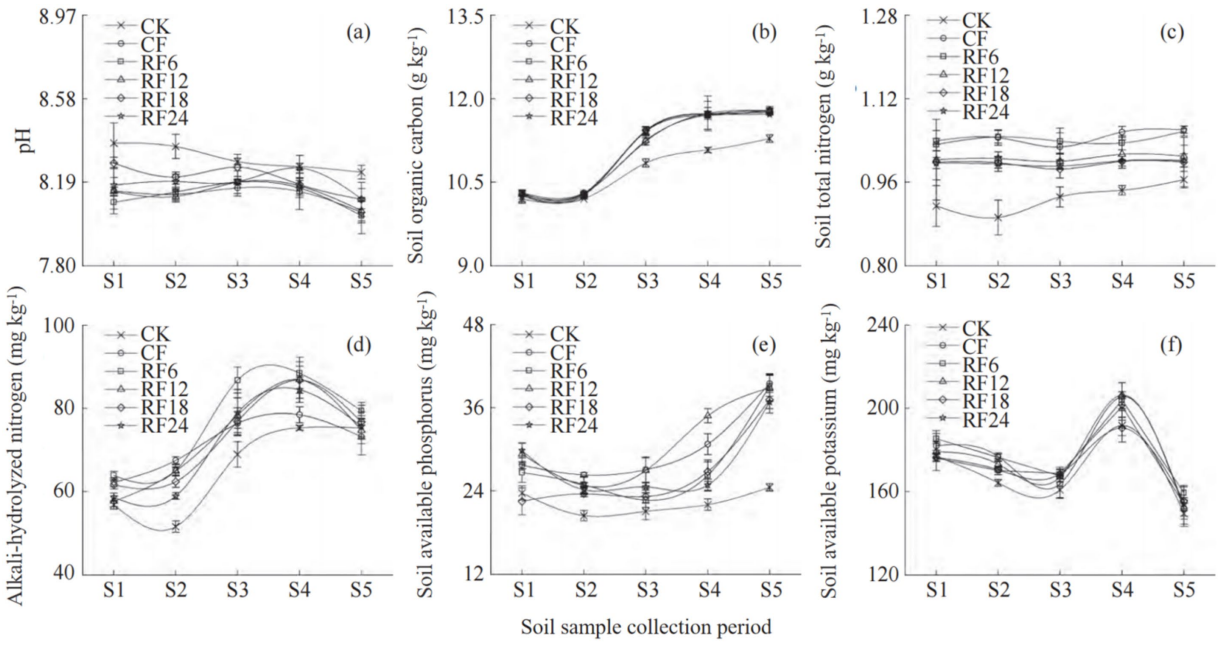

FIGURE 1
Soil nutrient dynamics under reduced application of chemical fertilizer and green manure. **(a)** Soil pH, **(b)** Soil organic carbon (g/kg), **(c)** Soil total nitrogen (g/kg), **(d)** Alkali-hydrolyzed nitrogen (mg/kg), **(e)** Soil available phosphorus (mg/kg), **(f)** Soil available potassium (mg/kg). CK, CF, RF6, RF12, RF18, and RF24 represent the treatments of no fertilizer, conventional nitrogen and phosphorus fertilizer, and nitrogen and phosphorus fertilizer reductions of 6, 12, 18, and 24%, respectively. The values in the table represent the fertilizer application rates for each treatment. S1, S2, S3, S4, and S5 represent the sowing of wheat in 2021 (April 1, 2021), the harvest of wheat in 2021 (July 6, 2021), the green manure of soybean returning to the field in 2021 (September 30, 2021), the sowing of wheat in 2022 (March 28, 2022), and the harvest of wheat in 2022 (July 1, 2022). The values at each point are averages ($n = 3$).

3.4 Soil quality evaluation

Principal component analysis revealed that there were two principal components with eigenvalues greater than 1 in 2021 and four in 2022. The calculated weights (w_i) and soil quality index (SQI) are shown in Table 5 and Figure 2, respectively. There were no significant differences in SQI between treatments in the wheat harvests of 2021 and 2022. In 2021, the treatments showed a trend of

TABLE 4 Effects of fertilizer reduction and green manure incorporation on soil organic carbon fractions and microbial biomass carbon and nitrogen contents.

Year	Treatment	Soil organic carbon (g kg−1)	High-labile fraction (g kg−1)	Low-labile fraction (g kg−1)	Recalcitrant fraction (g kg−1)	Microbial biomass carbon (mg kg−1)	Microbial biomass nitrogen (mg kg−1)
2021	CK	10.20 ± 0.01 c	3.11 ± 0.03 d	2.08 ± 0.03 a	5.02 ± 0.02 b	60.87 ± 2.83 d	18.13 ± 2.05 c
	CF	10.31 ± 0.00 a	3.38 ± 0.02 a	1.88 ± 0.04 b	5.05 ± 0.06 ab	152.97 ± 3.45 a	40.18 ± 1.09 a
	RF6	10.30 ± 0.03 a	3.37 ± 0.00 a	1.88 ± 0.01 b	5.06 ± 0.03 ab	150.08 ± 3.85 a	39.24 ± 1.71 a
	RF12	10.30 ± 0.03 ab	3.35 ± 0.03 ab	1.88 ± 0.04 b	5.07 ± 0.04 ab	133.86 ± 3.32 b	37.87 ± 1.96 ab
	RF18	10.28 ± 0.03 ab	3.31 ± 0.02 bc	1.87 ± 0.01 b	5.10 ± 0.02 a	126.98 ± 3.87 bc	35.22 ± 1.04 b
	RF24	10.26 ± 0.02 b	3.31 ± 0.01 c	1.85 ± 0.01 b	5.10 ± 0.02 a	123.38 ± 6.08 c	35.03 ± 3.07 b
2022	CK	11.28 ± 0.07 b	4.19 ± 0.07 b	2.08 ± 0.07 a	5.02 ± 0.04 b	378.93 ± 8.81 c	47.29 ± 4.26 e
	CF	11.79 ± 0.07 a	4.80 ± 0.05 a	1.92 ± 0.01 b	5.07 ± 0.06 ab	465.11 ± 35.35 b	68.54 ± 1.37 d
	RF6	11.79 ± 0.04 a	4.79 ± 0.04 a	1.92 ± 0.02 b	5.08 ± 0.02 ab	529.11 ± 24.74 a	86.39 ± 3.93 c
	RF12	11.79 ± 0.03 a	4.79 ± 0.01 a	1.89 ± 0.01 b	5.11 ± 0.02 a	520.62 ± 32.14 a	108.48 ± 3.68 a
	RF18	11.76 ± 0.02 a	4.79 ± 0.02 a	1.88 ± 0.01 b	5.09 ± 0.04 a	510.95 ± 22.25 ab	96.36 ± 2.20 b
	RF24	11.72 ± 0.02 a	4.78 ± 0.02 a	1.86 ± 0.02 b	5.07 ± 0.02 ab	496.44 ± 18.47 ab	91.69 ± 6.94 bc
Two-factor ANOVA (Significance)							
Year (Y)		**	**	ns	ns	**	**
Treatment (T)		**	**	**	*	**	**
Interaction (Y × T)		ns	**	ns	ns	**	**

Different letters in the same column represent significant differences at the 5% significance level following the LSD test. CK, CF, RF6, RF12, RF18, and RF24 represent the treatments of no fertilizer, conventional nitrogen and phosphorus fertilizer, and nitrogen and phosphorus fertilizer reductions of 6, 12, 18, and 24%, respectively. The values in the table represent the fertilizer application rates for each treatment. ***, **, and * indicate significance at $p < 0.001$, $p < 0.01$, and $p < 0.05$, respectively; "ns" indicates no significance ($p > 0.05$).

CF > RF6 > RF12 > RF18 > RF24 > CK ($p < 0.05$), while in 2022, all fertilizer reduction treatments had higher SQIs than CK. The two-factor analysis of variance showed that both fertilizer reduction treatments and the interaction with green manure return had significant effects on SQI ($p < 0.01$).

4 Discussion

4.1 Effects of fertilizer reduction and multiple cropping of green manure on wheat yield

Nitrogen fertilizer plays a crucial role in wheat yield formation, contributing the most to yield compared to phosphorus and potassium fertilizers (Hou et al., 2023). Therefore, most studies on fertilizer reduction focus on nitrogen reduction. Due to differences in soil fertility, the potential for nitrogen reduction varies across studies. For example, in fields with high soil fertility, nitrogen reduction of 20 to 60% (Du et al., 2020; Han et al., 2021; Wang et al., 2021) had no significant effect on yield, while in fields with lower soil fertility, reducing nitrogen by 25% (Lu et al., 2021) or 50% (Bonanomi et al., 2020) resulted in yield reduction. Shi et al. (2021) provided suggestions for nitrogen and phosphorus reduction in dryland wheat through long-term experiments, recommending an application of 144 kg hm^{-2} P_2O_5 when the pre-sowing soil available phosphorus level was 16.9 mg/kg. A three-year positioning experiment conducted in the early stage of this research showed that when nitrogen input was 300 kg hm^{-2} and phosphorus input was 133 kg hm^{-2}, reducing nitrogen and phosphorus fertilizers by 6% had no significant effect on spring wheat yield, but higher reduction ratios resulted in decreased yields. The yield reduction trend became more pronounced with time, indicating that the potential for fertilizer reduction in low-fertility soils is lower. Therefore, improving soil fertility through green manure return may be an effective way to reduce chemical fertilizer input.

In this study, after multiple cropping of green manure followed by its incorporation into the soil, treatments with nitrogen and phosphorus fertilizer reductions of 6 and 12% showed no significant differences in grain yield, 1,000-grain weight, and the number of grains per spike compared to conventional fertilizer treatments. These findings are consistent with the research of Wei et al. (2024) and Qiao et al. (2021), who found that reducing nitrogen fertilizer by 15% and multiple cropping of hairy vetch increased wheat's maximum growth rate, 1,000-grain weight, average leaf area index, and total photosynthetic potential, thus increasing grain yield. The results of reducing nitrogen and phosphorus fertilizers and incorporating green manure in this study suggest that short-term incorporation of green manure does not significantly affect the number of grains per spike but mainly affects 1,000-grain weight and dry matter. This is similar to the findings of Zhang et al. (2022), who also observed this phenomenon. The reason may be that the nitrogen fixation characteristics of leguminous green manure, along with the release of nutrients during decomposition, enhanced the soil's nitrogen and phosphorus supply capacity, which affected the source-to-sink transformation in the crop. Additionally, the nutrient release cycle of green manure decomposition is relatively long, providing nutrients throughout the next crop's growing season (He et al., 2020; Amede

TABLE 5 Principal component analysis parameters of soil nutrient indices during wheat harvest in 2021 and 2022.

Soil property	2021				2022					
	Principal component 1	Principal component 2	Communalities	Wi	Principal component 1	Principal component 2	Principal component 3	Principal component 4	Communalities	Wi
	PC1	PC2			PC1	PC2	PC3	PC4		
pH	−0.916	0.131	0.856	0.076	−0.770	0.158	0.062	0.050	0.625	0.055
SOC	0.882	0.021	0.778	0.069	0.766	−0.113	−0.072	0.473	0.828	0.072
TN	0.874	0.369	0.900	0.080	0.542	−0.832	−0.010	0.063	0.990	0.087
C/N	−0.844	−0.382	0.858	0.076	−0.163	0.924	−0.030	0.230	0.935	0.082
AN	0.952	0.001	0.905	0.080	0.164	−0.022	0.877	0.379	0.940	0.082
AP	0.969	−0.128	0.955	0.085	0.948	−0.239	−0.079	0.000	0.962	0.084
AK	0.916	0.207	0.882	0.078	0.328	0.158	0.592	−0.579	0.818	0.072
MBC	0.985	0.006	0.971	0.086	0.914	−0.018	0.191	0.073	0.877	0.077
MBN	0.959	−0.139	0.938	0.083	0.865	0.379	0.009	−0.016	0.893	0.078
MBC/MBN	0.588	0.413	0.516	0.046	−0.824	−0.450	0.079	0.188	0.923	0.081
H-LOC	0.977	−0.034	0.955	0.085	0.958	−0.124	−0.084	−0.038	0.941	0.082
L-LOC	−0.868	0.460	0.965	0.086	−0.846	−0.184	0.149	0.371	0.910	0.080
ROC	0.361	−0.816	0.797	0.071	0.703	0.381	−0.102	0.369	0.786	0.069
Eigenvalue	9.846	1.429			6.925	2.208	1.219	1.078		
Percent variance	75.742	10.989			53.266	16.982	9.373	8.292		
Cumulative percent variance	75.742	86.731			53.266	70.248	79.621	87.913		

SOC, Soil Organic Carbon, TN, Total Nitrogen, C/N, Carbon-to-Nitrogen ratio, AN, Available Nitrogen, AP, Available Phosphorus, AK, Available Potassium, MBC, Microbial Biomass Carbon, MBN, Microbial Biomass Nitrogen, MBC/MBN, Ratio of Microbial Biomass Carbon to Microbial Biomass Nitrogen, H-LOC, Hydrophobic Light Organic Carbon, L-LOC, Labile Light Organic Carbon, ROC, Readily Oxidizable Carbon, Wi, Contribution rate of each soil property in the principal component analysis. The eigenvalue indicates the amount of variance explained by each principal component, with the percent variance and cumulative percent variance reflecting the explained proportion.

10.3389/fsufs.2024.1514409

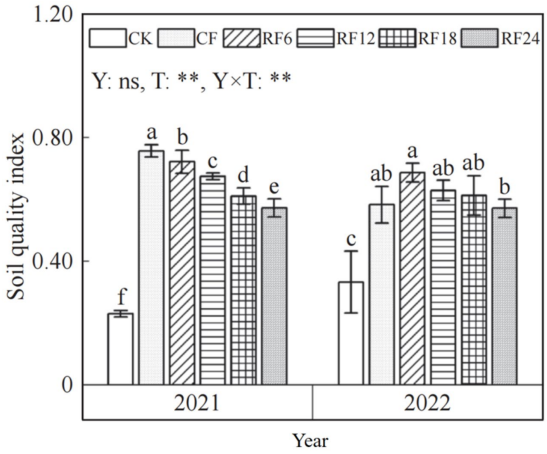

FIGURE 2
Soil quality index under reduced application of chemical fertilizer and green manure in wheat harvest period. Different letters in the same column represent significant differences at the 5% significance level following the LSD test. CK, CF, RF6, RF12, RF18, and RF24 represent the treatments of no fertilizer, conventional nitrogen and phosphorus fertilizer, and nitrogen and phosphorus fertilizer reductions of 6, 12, 18, and 24%, respectively. The values in the table represent the fertilizer application rates for each treatment. ***, **, and * indicate significance at $p < 0.001$, $p < 0.01$, and $p < 0.05$, respectively; "ns" indicates no significance ($p > 0.05$).

et al., 2021). This further suggests that green manure incorporation supplies additional nutrients during the growing season of subsequent crops, increasing yield and thus enhancing the potential for fertilizer reduction.

4.2 Effects of green manure decomposition on soil nutrients

This study found that incorporating green manure into soil resulted in a notable increase in soil nutrient availability, although changes in pH, organic carbon, and total nitrogen were less pronounced. Nitrogen and potassium exhibited synchronized release patterns during green manure decomposition, whereas phosphorus was released more gradually. Such findings align with prior research, including Zhou et al. (2021) and Yang et al. (2024), which demonstrated that legume green manure decomposition follows a rapid initial release phase, contributing significantly to nutrient availability within 180 days.

The decomposition and incorporation of approximately 24,000 kg/ha of green manure led to substantial increases in soil alkaline nitrogen (8.0–45.9%) and available phosphorus (20.0–57.3%) after 272 days. These results are consistent with long-term studies, such as those by Lyu et al. (2024), highlighting how legume green manure boosts nitrogen and phosphorus contents over extended periods. Conversely, available potassium levels declined (8.8–14.2%), a phenomenon explained by the activation and utilization of soil potassium reserves, as previously reported by Wang et al. (2000).

The role of green manure in improving soil quality became evident in the study's soil quality index (SQI) assessment, which showed that the incorporation of green manure compensated for nutrient deficiencies caused by reduced chemical fertilizers. Treatments with a 12% reduction in nitrogen and phosphorus fertilizers demonstrated comparable SQI levels to conventional practices, indicating the potential of green manure to sustain soil health under lower fertilizer inputs. Previous research, such as Fan et al. (2022), supports these findings by emphasizing the interaction between legume green manure and fertilizer reduction in enhancing soil nutrient reserves.

The data demonstrate that incorporating green manure improves soil nutrient availability and mitigates the potential adverse effects of chemical fertilizer reduction. These improvements suggest that green manure plays a pivotal role in sustainable nutrient management, enabling reduced reliance on synthetic fertilizers without compromising soil fertility.

4.3 Effects of multiple cropping of green manure on soil organic carbon fractions under fertilizer reduction conditions

Green manure, as an external source of organic carbon, helps to sequester organic carbon in farmland (Liu et al., 2015). The results of this study show that reducing chemical fertilizer while incorporating green manure significantly increased the soil organic carbon content. This could be due to the addition of external carbon from green manure, which directly influenced the increase in both labile and recalcitrant soil organic carbon (SOC) fractions and promoted the decomposition and cycling of SOC (Zheng et al., 2022). In this study, the increase in SOC was significantly correlated with the increase in high-labile organic carbon (H-LOC). The improvement in wheat dry matter after green manure incorporation indirectly increased the return of straw and roots, further contributing to carbon input. The continuous three-year application of chemical fertilizers provided additional nitrogen sources for soil microorganisms, which in turn increased microbial activity and accelerated the decomposition of existing organic matter in the soil (Guo et al., 2017; Shi et al., 2021). This acceleration occurs because nitrogen fertilizers stimulate microbial biomass and activity, enhancing the breakdown of organic matter to release nutrients (Liu et al., 2022). However, this process can deplete soil organic matter stocks over time if not balanced with organic inputs such as green manure (Xu et al., 2021).

The two-factor analysis of variance results (Table 4) indicate that as the fertilizer reduction ratio increased under green manure incorporation conditions, the content of high-labile organic carbon decreased (similar trends were observed for microbial biomass carbon and nitrogen), while there were no significant differences in the low-labile and recalcitrant organic carbon fractions. This may be because, under no fertilizer or low fertilizer conditions, the distribution of organic carbon fractions tends to be stable. The corresponding labile fractions will be both sequestered and decomposed, and the turnover rate within the same soil is considered fixed. Therefore, under no or low fertilizer application, the carbon sequestration efficiency is low, while treatments with higher fertilizer applications have higher labile fractions, and their resistance to decomposition is stronger than that of the former. Some studies have suggested that the quality of organic carbon affects its sequestration in the soil, and different organic materials have different impacts on the soil carbon pool (Chang et al., 2024). Plant residues with a low carbon-to-nitrogen (C/N) ratio and low lignin content are

considered high-quality carbon sources and are more likely to form relatively stable SOC. This is because when soil nitrogen availability is high, nutrient-rich microbial communities gradually become dominant and regulate the intensity of SOC decomposition. Therefore, in this study, it is believed that the introduction of low C/N external organic matter from green manure provided carbon and nitrogen sources for soil microorganisms, which increased microbial biomass carbon (MBC) and microbial biomass nitrogen (MBN). By increasing H-LOC, this process alleviated the decomposition of other fractions, changed the turnover of soil carbon, and increased SOC content.

5 Conclusion

In this pot experiment, conducted over two wheat-growing seasons, incorporating green manure alongside a moderate reduction of synthetic nitrogen and phosphorus fertilizers effectively maintained wheat yields while improving soil quality. The study found significant increases in soil nutrient availability, with soil alkaline nitrogen and available phosphorus rising by 22.3 and 30.7%, respectively. Additionally, soil organic carbon content increased by 12.4%, driven by a boost in both labile and microbial biomass carbon fractions. These findings highlight the potential of integrating green manure with reduced fertilizer inputs as a sustainable strategy for enhancing soil carbon sequestration, improving soil fertility, and reducing dependence on chemical fertilizers. The results support the long-term viability of this approach for sustainable agricultural intensification. In summary, on irrigated gray desert soil, the return of approximately 24,000 kg ha^{-1} of green manure, in conjunction with a 12% reduction in conventional nitrogen and phosphorus fertilizer application (N 300 kg ha^{-1} and P_2O_5 133 kg ha^{-1}), was able to maintain wheat yields and increase soil organic carbon content.

Data availability statement

The original contributions presented in the study are included in the article/supplementary material, further inquiries can be directed to the corresponding author.

Author contributions

JZ: Conceptualization, Data curation, Formal analysis, Funding acquisition, Investigation, Methodology, Project administration, Resources, Software, Supervision, Validation, Visualization, Writing – original draft, Writing – review & editing. WH: Conceptualization, Data curation, Formal analysis, Funding acquisition, Investigation, Methodology, Project administration, Resources, Software, Supervision, Validation, Visualization, Writing – original draft, Writing – review & editing. ZW: Formal analysis, Funding acquisition, Project administration, Software, Supervision, Validation, Visualization, Writing – original draft, Writing – review & editing. YC: Conceptualization, Data curation, Investigation, Methodology, Project administration, Resources, Writing – original draft, Writing – review & editing. WG: Conceptualization, Data curation, Formal analysis, Funding acquisition, Writing – original draft, Writing – review & editing.

Funding

The author(s) declare that financial support was received for the research, authorship, and/or publication of this article. This paper was funded by 2023 annual Shaanxi Province State Capital Operation Budget Science and Technology Innovation Special Fund Project "Guanzhong Area Green Farmland Construction Key Technology Research and Demonstration Promotion Project," Technology Innovation Center for Land Engineering and Human Settlements, Shaanxi Land Engineering Construction Group Co., Ltd. and Xi'an Jiaotong University (Grant no. 2024WHZ0234).

Conflict of interest

JZ, WH, ZW, YC, and WG were employed by Shaanxi Dijian Guantian Investment and Construction Co., Ltd. JZ, WH, ZW, YC, and WG were employed by Shaanxi Provincial Land Engineering Construction Group Co., Ltd. JZ was employed by Zhongshan High Standard Farmland Construction Group Baoji Co., Ltd.

Generative AI statement

The author(s) declare that no Gen AI was used in the creation of this manuscript.

Publisher's note

All claims expressed in this article are solely those of the authors and do not necessarily represent those of their affiliated organizations, or those of the publisher, the editors and the reviewers. Any product that may be evaluated in this article, or claim that may be made by its manufacturer, is not guaranteed or endorsed by the publisher.

References

Amede, T., Legesse, G., Agegnehu, G., Gashaw, T., Degefu, T., Desta, G., et al. (2021). Short term fallow and partitioning effects of green manures on wheat systems in east African highlands. *Field Crop Res.* 269:108175. doi: 10.1016/j.fcr.2021.108175

Bonanomi, G., De Filippis, F., Zotti, M., Idbella, M., Cesarano, G., Al-Rowaily, S., et al. (2020). Repeated applications of organic amendments promote beneficial microbiota, improve soil fertility and increase crop yield. *Appl. Soil Ecol.* 156:103714. doi: 10.1016/j.apsoil.2020.103714

Carter, M. S., Sørensen, P., Petersen, S. O., Ma, X., and Ambus, P. (2014). Effects of green manure storage and incorporation methods on nitrogen release and N_2O emissions after soil application. *Biol. Fertil. Soils* 50, 1233–1246. doi: 10.1007/s00374-014-0936-5

Chang, F., Zhang, H., Zhao, N., Zhao, P., Song, J., Yu, R., et al. (2024). Green manure removal with reduced nitrogen improves saline-alkali soil organic carbon storage in a wheat-green manure cropping system. *Sci. Total Environ.* 926:171827. doi: 10.1016/j.scitotenv.2024.171827

Cong, M., Hu, Y., Sun, X., Yan, H., Yu, G., Tang, G., et al. (2023). Long-term effects of biochar application on the growth and physiological characteristics of maize. *Front. Plant Sci.* 14:425. doi: 10.3389/fpls.2023.1172425

Du, Q., Zhou, L., Chen, P., Liu, X., Song, C., Yang, F., et al. (2020). Relay-intercropping soybean with maize maintains soil fertility and increases nitrogen recovery efficiency by reducing nitrogen input. *Crop J.* 8, 140–152. doi: 10.1016/j.cj.2019.06.010

Duan, Y., Wang, T., Lei, X., Cao, Y., Liu, L., Zou, Z., et al. (2024). Leguminous green manure intercropping changes the soil microbial community and increases soil nutrients and key quality components of tea leaves. *Hortic. Res.* 11:uhae018. doi: 10.1093/hr/uhae018

Fan, M., Liu, X., Zhou, Y., Núñez-Delgado, A., Luo, L., Long, S., et al. (2022). Effects of the combined application of Chinese Milk vetch (*Astragalus sinicus* L.) and red mud to remediate the cadmium-polluted acidic Paddy soil. *Sustain. For.* 14:13192. doi: 10.3390/su142013192

Guo, H., Ye, C., Zhang, H., Pan, S., Ji, Y., Li, Z., et al. (2017). Long-term nitrogen & phosphorus additions reduce soil microbial respiration but increase its temperature sensitivity in a Tibetan alpine meadow. *Soil Biol. Biochem.* 113, 26–34. doi: 10.1016/j.soilbio.2017.05.024

Han, J., Dong, Y., and Zhang, M. (2021). Chemical fertilizer reduction with organic fertilizer effectively improve soil fertility and microbial community from newly cultivated land in the loess plateau of China. *Appl. Soil Ecol.* 165:103966. doi: 10.1016/j.apsoil.2021.103966

He, H.-B., Li, W.-X., Zhang, Y.-W., Cheng, J.-K., Jia, X.-Y., Li, S., et al. (2020). Effects of Italian ryegrass residues as green manure on soil properties and bacterial communities under an Italian ryegrass (*Lolium multiflorum* L.)-rice (*Oryza sativa* L.) rotation. *Soil Tillage Res.* 196:104487. doi: 10.1016/j.still.2019.104487

Hou, S., Dang, H., Huang, T., Huang, Q., Li, C., Li, X., et al. (2023). Targeting high nutrient efficiency to reduce fertilizer input in wheat production of China. *Field Crop Res.* 292:108809. doi: 10.1016/j.fcr.2023.108809

Iheshiulo, E. M.-A., Larney, F. J., Hernandez-Ramirez, G., St Luce, M., Chau, H. W., and Liu, K. (2024). Quantitative evaluation of soil health based on a minimum dataset under various short-term crop rotations on the Canadian prairies. *Sci. Total Environ.* 935:173335. doi: 10.1016/j.scitotenv.2024.173335

Li, L.-J., Zhu-Barker, X., Ye, R., Doane, T. A., and Horwath, W. R. (2018). Soil microbial biomass size and soil carbon influence the priming effect from carbon inputs depending on nitrogen availability. *Soil Biol. Biochem.* 119, 41–49. doi: 10.1016/j.soilbio.2018.01.003

Liang, X., Jin, X., Han, B., Sun, R., Xu, W., Li, H., et al. (2022). China's food security situation and key questions in the new era: a perspective of farmland protection. *J. Geogr. Sci.* 32, 1001–1019. doi: 10.1007/s11442-022-1982-9

Liu, H., Li, J., Li, X., Zheng, Y., Feng, S., and Jiang, G. (2015). Mitigating greenhouse gas emissions through replacement of chemical fertilizer with organic manure in a temperate farmland. *Sci. Bull.* 60, 598–606. doi: 10.1007/s11434-014-0679-6

Liu, X., Peng, C., Zhang, W., Li, S., An, T., Xu, Y., et al. (2022). Subsoiling tillage with straw incorporation improves soil microbial community characteristics in the whole cultivated layers: a one-year study. *Soil Tillage Res.* 215:105188. doi: 10.1016/j.still.2021.105188

Lu, J., Hu, T., Zhang, B., Wang, L., Yang, S., Fan, J., et al. (2021). Nitrogen fertilizer management effects on soil nitrate leaching, grain yield and economic benefit of summer maize in Northwest China. *Agric. Water Manag.* 247:106739. doi: 10.1016/j.agwat.2021.106739

Lyu, H., Li, Y., Wang, Y., Wang, P., Shang, Y., Yang, X., et al. (2024). Drive soil nitrogen transformation and improve crop nitrogen absorption and utilization - a review of green manure applications. *Front. Plant Sci.* 14:600. doi: 10.3389/fpls.2023.1305600

Mandal, U. K., Singh, G., Victor, U. S., and Sharma, K. L. (2003). Green manuring: its effect on soil properties and crop growth under rice–wheat cropping system. *Eur. J. Agron.* 19, 225–237. doi: 10.1016/S1161-0301(02)00037-0

Qiao, J., Zhao, D., Zhou, W., Yan, T., and Yang, L. (2021). Sustained rice yields and decreased N runoff in a rice-wheat cropping system by replacing wheat with Chinese milk vetch and sharply reducing fertilizer use. *Environ. Pollut.* 288:117722. doi: 10.1016/j.envpol.2021.117722

Rahmati, M., Eskandari, I., Kouselou, M., Feiziasl, V., Mahdavinia, G. R., Aliasgharzad, N., et al. (2020). Changes in soil organic carbon fractions and residence time five years after implementing conventional and conservation tillage practices. *Soil Tillage Res.* 200:104632. doi: 10.1016/j.still.2020.104632

Rossi, L. M. W., Mao, Z., Merino-Martín, L., Roumet, C., Fort, F., Taugourdeau, O., et al. (2020). Pathways to persistence: plant root traits alter carbon accumulation in different soil carbon pools. *Plant Soil* 452, 457–478. doi: 10.1007/s11104-020-04469-5

Shi, Z., Liu, D., Liu, M., Hafeez, M. B., Wen, P., Wang, X., et al. (2021). Optimized fertilizer recommendation method for nitrate residue control in a wheat–maize double cropping system in dryland farming. *Field Crop Res.* 271:108258. doi: 10.1016/j.fcr.2021.108258

Wang, J. L., Liu, K. L., Zhao, X. Q., Zhang, H. Q., Li, D., Li, J. J., et al. (2021). Balanced fertilization over four decades has sustained soil microbial communities and improved soil fertility and rice productivity in red paddy soil. *Sci. Total Environ.* 793:148664. doi: 10.1016/j.scitotenv.2021.148664

Wang, J. G., Zhang, F. S., Zhang, X. L., and Cao, Y. P. (2000). Release of potassium from K-bearing minerals: effect of plant roots under P deficiency. *Nutr. Cycl. Agroecosyst.* 56, 45–52. doi: 10.1023/A:1009894427550

Wei, J., Fan, Z., Hu, F., Mao, S., Yin, F., Wang, Q., et al. (2024). Legume green manure can intensify the function of chemical nitrogen fertilizer substitution via increasing nitrogen supply and uptake of wheat. *Crop J.* 12, 1222–1232. doi: 10.1016/j.cj.2024.07.004

Xu, P., Wu, J., Wang, H., Han, S., Zhu, J., Fu, Q., et al. (2021). Long-term partial substitution of chemical fertilizer with green manure regulated organic matter mineralization in paddy soil dominantly by modulating organic carbon quality. *Plant Soil* 468, 459–473. doi: 10.1007/s11104-021-05130-5

Yang, L., Zhou, J., Zamanian, K., Zhang, K., Zhao, J., Zang, H., et al. (2024). Peanut straw application rate had a greater effect on decomposition and nitrogen, potassium and phosphorus release than irrigation. *Plant Soil* 499, 193–205. doi: 10.1007/s11104-022-05614-y

Zhang, X., Hua, Y., Liu, Y., He, M., Ju, Z., and Dai, X. (2022). Wide belt sowing improves the grain yield of bread wheat by maintaining grain weight at the backdrop of increases in spike number. *Front. Plant Sci.* 13:772. doi: 10.3389/fpls.2022.992772

Zheng, H., Liu, D., Liao, X., Miao, Y., Li, Y., Li, J., et al. (2022). Field-aged biochar enhances soil organic carbon by increasing recalcitrant organic carbon fractions and making microbial communities more conducive to carbon sequestration. *Agric. Ecosyst. Environ.* 340:108177. doi: 10.1016/j.agee.2022.108177

Zhou, G., Chang, D., Gao, S., Liang, T., Liu, R., and Cao, W. (2021). Co-incorporating leguminous green manure and rice straw drives the synergistic release of carbon and nitrogen, increases hydrolase activities, and changes the composition of main microbial groups. *Biol. Fertil. Soils* 57, 547–561. doi: 10.1007/s00374-021-01547-3

frontiers | Frontiers in Sustainable Food Systems

TYPE Original Research
PUBLISHED 12 February 2025
DOI 10.3389/fsufs.2025.1505001

Check for updates

OPEN ACCESS

EDITED BY
Raffaella Balestrini,
National Research Council (CNR), Italy

REVIEWED BY
Huiqiao Pan,
Carnegie Institution for Science, United States
Mushtaq Ahmad Khan,
Hazara University, Pakistan

*CORRESPONDENCE
Everlon Cid Rigobelo
everlon.cid@unesp.br

RECEIVED 01 October 2024
ACCEPTED 27 January 2025
PUBLISHED 12 February 2025

CITATION
de Andrade da Silva MSR, de Carvalho LAL, Santos CHB, Frezarin ET, da Silva CGN, Pinheiro DG, Zonta E, Babalola OO and Rigobelo EC (2025) Effect of co-inoculation with plant growth-promoting bacteria on the microbiome of soybean roots.
Front. Sustain. Food Syst. 9:1505001.
doi: 10.3389/fsufs.2025.1505001

COPYRIGHT
© 2025 de Andrade da Silva, de Carvalho, Santos, Frezarin, da Silva, Pinheiro, Zonta, Babalola and Rigobelo. This is an open-access article distributed under the terms of the Creative Commons Attribution License (CC BY). The use, distribution or reproduction in other forums is permitted, provided the original author(s) and the copyright owner(s) are credited and that the original publication in this journal is cited, in accordance with accepted academic practice. No use, distribution or reproduction is permitted which does not comply with these terms.

Effect of co-inoculation with plant growth-promoting bacteria on the microbiome of soybean roots

Maura Santos Reis de Andrade da Silva[1,2], Lucas Amoroso Lopes de Carvalho[1], Carlos Henrique Barbosa Santos[3], Edvan Teciano Frezarin[1], Cleudison Gabriel Nascimento da Silva[4], Daniel Guariz Pinheiro[1], Everaldo Zonta[2], Olubukola Oluranti Babalola[5] and Everlon Cid Rigobelo[1]*

[1]Agricultural and Livestock Microbiology Postgraduate Program, School of Agricultural and Veterinarian Sciences, São Paulo State University (UNESP), São Paulo, Brazil, [2]Departamento de Solos Instituto de Agronomia, Universidade Federal Rural do Rio de Janeiro, Rio de Janeiro, Brazil, [3]Faculty of Agrarian and Veterinary Sciences, State University of São Paulo (UNESP), São Paulo, Brazil, [4]Department of Agricultural, University of Federal of Lavras, Lavras, Brazil, [5]Food Security and Safety Niche Area, Faculty of Natural and Agricultural Sciences, North-West University, Mmabatho, South Africa

Introduction: The effect of co-inoculation with plant growth-promoting bacteria on the microbiome of soybean roots was investigated in a field experiment. Soybean plants were inoculated with *Bacillus subtilis*, *Bacillus aryabhattai*, *Streptomyces* sp., and *Saccharopolyspora spinosa* and compared to a control treatment that received mineral fertilization.

Methods: The yield parameters and endophytic microbiome of soybean roots were evaluated.

Results: No significant differences in yield were observed among the treatments, suggesting that microbial inoculation can serve as an alternative to mineral fertilization without compromising productivity. Among the most abundant genera, there was a high prevalence of members of the phylum Proteobacteria (21 of the top 25 genera). Overall, the genera of these phyla represented 88.61% of the samples on average. There were also genera in the phyla Bacteroidetes (2/25), Actinobacteria (1/25), and Firmicutes (1/25). The massive presence of *Bradyrhizobium*, which represented 71.22% of the sequences at the genus level, was remarkable. *Bradyrhizobium* was the most abundant genus in all samples, except for *Saccharopolyspora spinosa* (ST treatment), whose abundance was only 12.66%. Co-occurrence network analysis revealed changes in the microbial community structure and genera considered as hubs.

Discussion: These findings demonstrate the potential of co-inoculation with plant growth-promoting bacteria to modulate the root microbiome and enhance the colonization of *B. japonicum*, which may contribute to improving the efficiency of this symbiont in promoting plant growth. Further research is required to elucidate the mechanisms underlying these interactions and their implications for soybean productivity.

KEYWORDS

microbiome, *Saccharopolyspora spinosa*, *Streptomyces*, metagenomic, plant growth

Introduction

Plant growth-promoting rhizobacteria (PGPR) are beneficial soil bacteria that inhabit the rhizosphere and colonize the root surface and surrounding soil (Khoso et al., 2024). They play crucial roles in enhancing plant growth and development through various direct and indirect mechanisms. PGPR directly promote plant growth by assisting in resource acquisition, such as nitrogen fixation, phosphate solubilization, and essential mineral uptake, and by modulating plant hormone levels (Paulus and Tooy, 2024). They act as biocontrol agents, thereby reducing the inhibitory effects of pathogens on plant growth and development (Gu et al., 2020).

Interestingly, PGPR can form biofilms at nutrient- and moisture-rich sites, which further enhances their ability to promote plant growth, improve nutrient and water uptake, and increase plant stress tolerance (Kumar et al., 2024). Additionally, PGPR have been found to alleviate various environmental stresses in plants, including salinity, flooding, heavy metals, drought, and cold, through mechanisms such as the production of osmolytes, exopolysaccharides, and activation of antioxidant defense systems in plants (Mun et al., 2024). Notably, these effects on plant growth may be attributed to alterations in the plant microbiome caused by bacterial inoculation.

Bacterial inoculation has significant effects on the soybean plant microbiome, influencing both the rhizosphere and root-associated bacterial communities. Inoculation with rhizobia and plant growth-promoting bacteria (PGPB) can alter the diversity and composition of soybean root endophytic bacteria throughout the growing season (Verma et al., 2024). Co-inoculation with multiple bacterial strains can promote synergistic effects on plant growth and stress tolerance (Wang et al., 2024). The origin of the microbial inoculants also plays a role in shaping the rhizosphere bacterial community structure and influencing plant growth (Khosravi et al., 2024). There are several mechanisms by which bacterial inoculation changes the plant microbiome, including competition for resources (Verma et al., 2024; Wahab et al., 2024). Introduced bacteria compete with existing microorganisms for nutrients and space, potentially altering microbiome composition (Ikiz et al., 2024). Modification of root exudates by ample-inoculated bacteria can influence plant physiology, leading to changes in root exudates. This, in turn, attracts or repels different microbial species and reshapes the microbiome. Members of the plant microbiome can interact with each other in a synergistic manner. Synergistic interactions may form beneficial relationships with existing microbes, enhancing their collective effects on plant health and microbiome structure (Gu et al., 2020).

Interestingly, bacterial inoculation can also help soybean plants cope with environmental stresses. For instance, co-inoculation with bacteria improved plant growth and nodulation under arsenic stress, while also reducing As translocation to the aerial parts (Armendariz et al., 2019). Additionally, composite bacterial inoculants containing multiple PGPR strains can coordinately modulate rhizosphere microbial community structure, improve soil nutrient availability, and enhance soybean growth (Paulus and Tooy, 2024).

Although some studies have demonstrated changes induced by bacterial inoculation, there is limited information regarding the effects of these specific bacterial strains on the plant microbiome. Therefore, the objective of this study was to evaluate the effects of inoculation with four different bacterial species on the microbiome of soybean plants.

Materials and methods

Field methodology

Location

The experiment was carried out in an agricultural area belonging to the Teaching, Research and Extension Farm (FEPE) of UNESP—Campus of Jaboticabal, starting in November 2019 and ending in March 2020. The climate of the Jaboticabal region is Cwa, according to the Köppen classification, with wet summers and dry winters. The UNESP unit is located in the northwestern region of São Paulo state (21° 15′ 22″ S, 48° 18′ 58″ W, and an altitude of 605 m).

Experiment setup

Plots in the field condition of 30 m^2 (6 m × 5 m) were established, with a spacing of 0.5 m between rows and 0.1 m between plants. The soil of the area was of the latosol type, and sowing was carried out mechanically at a depth of 5 cm. Chemical analysis of the soil was previously carried out to evaluate its acidity and nutrient availability. The nitrogen dose, urea corresponding to the control treatment was applied manually by repetitions, row by row, after the emergence of the plants. Due to the history of having successive crops with soybean inoculated with strains of *Bradyrhizobium*, there was no need for reinoculation of this inoculant in this area.

Inoculum preparation and applications

The microorganisms used in this study were sourced from diverse sources. Specifically, *Bacillus subtilis* was obtained from soil and identified through sequencing and was deposited in the bank under the accession number MZ133755. *Bacillus aryabhattai* CCT4005 and *Streptomyces* sp. 244 were provided by André Tosello, and *Saccharopolyspora spinosa* ATCC 49460 was obtained from the American Type Culture Collection (ATCC). The bacterial strains belong to Laboratory of Soil Microbiology (LSM) of FCAV/UNESP in Jaboticabal. Microorganisms were inoculated in suitable culture media for growth. The inoculants *B. subtilis* and *B. aryabhattai* were prepared in nutrient broth, *Streptomyces* sp. in SM medium (1% glucose, 3% casein peptone, 1.0% yeast extract, 0.05% potassium dihydrogen phosphate, and 0.2% magnesium sulfate heptahydrate) and *S. spinosa* in Jensen's medium (2% sucrose, 0.1% dipotassium phosphate, 0.05% magnesium sulfate, 0.05% sodium chloride, 0.01% ferrous sulfate, 0.0005% sodium molybdate, 0.2% calcium carbonate and 1.5% agar). All the strains were grown in a BOD chamber for 72 h, after which a final concentration of 1×10^8 colony forming units (CFU) mL^{-1} was applied. In total, two applications were carried out, the first 15 days after planting (DAP) and the second 30 days after planting. The applications of the inoculants were carried out using 1000 mL ha^{-1} backpack sprayers via foliar way.

Experimental design

In the field, the plots were arranged in randomized blocks, with five treatments and four replications. The treatments are detailed in Table 1. Description of control treatment.

The control treatment received the same fertilization as the other treatments, with the addition of 200 kg ha^{-1} of urea (a nitrogen source). No bacterial inoculation was performed in the control group.

TABLE 1 Description of the treatments carried out with several microorganisms inoculated into soybean under field conditions.

Treatment	Inoculant	Accession number	Applications
CT	Control		200 kg he^{-1} (N)
BS	*Bacillus subtilis*	MZ133755	1,000 mL he^{-1}
BA	*Bacillus aryabhattai*	CCT4005	1,000 mL he^{-1}
ST	*Streptomyces* sp.	2444	1,000 mL he^{-1}
SS	*Saccharopolyspora spinosa*	ATCC 49460	1,000 mL he^{-1}

In contrast, the other treatments were subjected to bacterial inoculation, but did not receive urea supplementation.

Harvest

After the physiological maturity of the grains, which were obtained at 120 days after sowing, the soybean was harvested by means of a specialized parcel harvester, and the grains were then packed in paper bags and stored at room temperature until drying.

Data recorded

Shoot dry mass

The dry mass of the aerial part was determined at the beginning of the flowering of the soybean crop. Five randomly chosen plants were collected from each plot during this period, placed in paper bags and dried in an oven with forced air circulation at 65°C for 72 h. After this period, the dry matter was obtained by weighing the material on a semianalytical balance (Lobo et al., 2019).

Determination of nitrogen and phosphorus in shoots and roots

Five hundred micrograms of dried and ground plant samples were weighed and placed into 50 mL digestion tubes, which were left to decouple at room temperature for 1.5 h. The tubes were then positioned in a digestion block, initially heated to 80°C for 20 min before the temperature was increased to 160°C. The tubes were monitored and removed once the material ascended the tube walls, and most of the HNO_3 evaporated, leaving a clear solution. After cooling, 1.3 mL the concentrated $HClO_4$ was added to each tube. The tubes were returned to the block, the temperature was increased to 210°C, and digestion was deemed complete when the solution turned colorless with dense white vapor of $HClO_4$ and H_2O formed above the dissolved material. The tubes were cooled and the contents were diluted to 25 mL with water in a snap-cap glass (Wan et al., 2020).

For phosphorus analysis, 1 mL of the digested sample was transferred to a test tube, to which 4 mL of water and 2 mL of reagent mix (comprising equal parts of 5% ammonium molybdate and 0.25% vanadate) were added. The mixture was allowed to rest for 15 min before measuring the absorbance at 420 nm using a UV VIS spectrophotometer (Meier et al., 2020).

Thousand grain dough

Using a box with holes adapted for the simultaneous counting of 100 grains of the crop, the mass of 1000 grains was determined by weighing eight subsamples with 100 grains each on a semianalytical scale.

Production and yield

At the end of the field experiment, the soybeans were harvested by a specialized plot harvester, stored at room temperature for drying and later weighed on a semianalytical scale to determine the total grain yield. The productivity in kg ha^{-1} relative to the production per unit of area was also determined.

Data analysis

Data normality and heteroscedasticity were assessed by the Shapiro–Wilk and Bartlett tests, respectively. Analysis of variance (ANOVA) was performed for each experiment to detect differences, and Tukey's multiple comparison test was used to compare the means at the 5% significance level. PCA was performed after data standardization (to avoid the influence of different units for the means of response variables), and all the statistical analyses were performed with R software (R Core Team, 2023).

DNA extraction

Roots were manually harvested using surgical gloves and immediately stored in sterilized plastic containers. To dislodge the rhizospheric soil, roots were placed in a 50 mL conical tube containing 35 mL of phosphate buffer and 0.02% Tween 20 and vortexed for 2 min. The roots were then transferred to sterile paper towels using sterilized forceps and subsequently transferred to 50 mL centrifuge tubes for superficial sterilization. The sterilization involved treating the plant tissues were sterilized with 100% ethanol for 3 min, 2% sodium hypochlorite for 2 min, and 70% ethanol for 3 min, based on a modified protocol from Cao et al. (2005). To confirm the sterilization efficacy, the final wash was cultured on nutrient agar plates and checked for the absence of microbial growth. Following sterilization, the roots were pooled by treatment and macerated using a sterile mortar and pestle in liquid nitrogen. Genomic DNA was extracted from these samples using the PowerMax Soil DNA Extraction Kit (Mo Bio Laboratories, Carlsbad, CA, United States), according to the manufacturer's specifications. DNA concentration and purity were assessed using fluorometry (Qubit™ 3.0, Invitrogen) and spectrophotometry (NanoDrop™ 1000, Thermo Fisher Scientific), respectively, to determine the A260/A280 ratio.

Sequencing of the samples

Sterilized roots were macerated using a sterile mortar and pestle with liquid nitrogen. The PowerMax Soil DNA Extraction Kit (Mo Bio Laboratories, Carlsbad, CA) was used to extract the genomic DNA according to the Manufacturer's instructions. The concentration of the extracted DNA was determined by fluorometry (Qubit™ 3.0, Invitrogen), and purity was estimated by calculating the A260/A280 ratio via spectrophotometry (NanoDrop™ 1000, Thermo Fisher Scientific) (de Souza et al., 2016). The hypervariable region V4 of the 16S rRNA gene was amplified using the primers 515F (5′-GTGCCAGCMGCCGCGGTAA-3′) and 806R (5′-GGACTACHV GGGTWTCTAAT-3′). Three forward primers were used for amplification. These were modified by adding degenerate nucleotides (Ns) to the 5′ region to increase the diversity of target sequences

(de Souza et al., 2016). PCR was performed in 30 cycles using the HotStarTaq Plus Master Mix Kit (Qiagen) under the following conditions: 94°C for 3 min, followed by 28 cycles at 94°C for 30 s, 53°C for 40 s, and 72°C for 1 min, and a final elongation step at 72°C for 5 min. PNA clamp sequences (PNA Bio) were added to block amplification of the 16S rRNA gene from the ribosomes and mitochondria. The amplification products were analyzed on a 2% agarose gel to determine the amplification success and relative intensity of the bands. Amplicon sequencing was performed on the Illumina MiSeq platform (Lundberg et al., 2013).

Sequence data processing

The initial data quality was assessed using the "FastQC" program (Version: 0.11.9; Andrews, 2010). Then, the parameters for quality processing were determined through the "USEARCH" program (Version: 11.0.667), where the thresholds for quality pruning ("-fastx_info") and size ("-fastq_eestats2"), as well as the position of the primers used for amplification of the target region ("-search_oligodb"). The detected primers (515F. 5′-GTGCCAGCMGCCGCGGTAA; 806R 5′-GGACTACHVGGGTWTCTAAT) were then removed by the "Atropos" program (Version: 1.1.31; Didion et al., 2017). The low-quality ends were pruned by the "PRINSEQ-lite" program (Version: 0.20.4; Schmieder and Edwards, 2011), removing bases whose average quality window was less than Q20 (read forward) or Q18 (read reverse) ("-trim_qual_window 3"; "-trim_qual_right 20/18"), as well as complete sequences with a mean quality lower than Q20 ("-min_qual_mean 20"). The processed reads were submitted to the "DADA2" pipeline (Version: 1.22.0; Callahan et al., 2016) through its package for the statistical program "R" (Version: 4.1.2; R Core Team, 2020). The reads were subjected to a quality control process ("filterAndTrim"), where size truncation ("truncLen = 250") and quality filtering ("maxEE = 2") were performed based on the values stipulated by the "USEARCH." Then, the exact amplicon sequence variants (ASVs) were designated for each sample, which was later filtered to retain possible chimeric sequences ("removeBimeraDenovo") and then taxonomically classified ("assignTaxonomy") based on the NCBI RefSeq 16S rRNA database supplemented by RDP (Version: 16; Cole et al., 2014). The taxonomic annotations of the ASVs, as well as their per-sample counts, were exported into a "phyloseq" object (R package "phyloseq"; Version: 1.38.0; McMurdie and Holmes, 2013) and transformed into compositional data (function "phyloseq_standardize_otu_abundance" from the R package "metagMisc"; Version: 0.0.4; Tedersoo et al., 2022). The datasets generated for this study were deposited in the NCBI: Sequence Read Archive (SRA), under the accession number PRJNA1086858.

Descriptive and statistical analysis of the microbiome

The extent of sequencing coverage per sample was inferred through rarefaction curves obtained by the "amp_rarecurve" function of the R package "ampvis2" (version 2.7.17; Andersen et al., 2004). Richness (Chao1) and diversity (Shannon and Gini-Simpson indices) indices were calculated using the "alpha" function of the R package "microbiome" (Version: 1.10.0). The means of these measurements were compared pairwise, using the Student/Wilcoxon *t*-test (depending on the adherence of the data to normality and homoscedasticity, measured by the Shapiro–Wilk and Bartlett tests, respectively). For beta diversity, the dissimilarities were calculated using the Bray–Curtis index ("distance" function of the R package "phyloseq"), which was used for principal coordinate analysis (PCoA). The statistical significance of the separation of the evaluated treatments was determined through a PERMANOVA, considering a *p*-value of 0.05. Finally, the taxa whose abundances significantly changed were identified. For this purpose, the "DESeq2" approach (Version: 1.34.0; Love et al., 2014), which models the data assuming a negative binomial distribution and implements the Wald test to compare the means (*p*-value adjusted <0.05), was used. The taxonomic profiles and other graphical representations were generated in R using the "ggplot2" package (Version 3.3.5). The networks of each treatment were established based on the classified genera of each treatment. A minimum abundance filter was used to avoid spurious correlations (minimum relative abundance of 0.1%). The relationships between genera were inferred through Pearson's correlation coefficients. For the calculation of correlations, the tables of counts of ASVs aggregated at the sex level were submitted to the function "corr.test" of the "psych" R package (Version: 2.2.5), considering a minimum correlation threshold of 0.75 (strongly positive or negative relationships) at a confidence level of 95% (*p*-value <0.05). Correlation values were provided to the function "graph_from_data_frame" of the R package "igraph" (Version: 1.3.1; Csardi, 2005) to construct the network graph. Centrality and topological measures were obtained from the graphs. The numbers of co-occurring genera (nodes), relationships between them (edges), and the formation of modules were evaluated. The number of connections (degree), intermediation ability (betweenness), and tendency to form dense clusters (clustering coefficient) were also estimated. The most important genera (Hubs) were determined from the computation of Kleinberg's hubbiness score (Kleinberg, 2000).

Results

BA inoculation with soybean enriches taxonomic diversity

High-throughput sequencing of the 20 samples generated 1,639,843 reads, which were relatively well distributed across treatments (Table 2). The generated sequences were of good quality, reflecting a low loss during the quality control and processing steps (Table 2). However, there was high contamination with sequences from the host plant, such as mitochondria and chloroplasts. Filtering these contaminating sequences caused a considerable decrease in usable reads (average: 70.2%), which was particularly severe in the BA treatment (84.3%) (Table 2).

Despite the substantial reduction in the number of sequenced reads, the rarefaction curves showed that the remaining usable reads had enough coverage to represent the bacterial communities present in the samples (Figure 1). The graphs show that in all samples, there was a tendency to form an asymptotic curve, thus reflecting the stabilization of the encounter of new sequences as the sampling effort increased (i.e., an increase in the number of reads).

Taxonomic assignment of the sequences revealed a total of 2 domains, 18 phyla, 35 classes, 68 orders, 115 families, 239 genera, and 94 species of unique prokaryotes. The vast majority of usable reads could be assigned to the genus level (average: 95.9%) (Table 3). The BA and ST treatments had greater numbers of unique genera and species (Table 3). The BA treatment also had greater numbers of

10.3389/fsufs.2025.1505001

TABLE 2 The number of reads per processing step was counted.

Treatment	Raw	After QC	Merged	Processed	Usable
CT	333,653	329,379	329,372	320,279	110,784
BS	318,841	314,829	314,817	305,450	121,835
BA	348,161	343,871	343,863	335,083	54,758
ST	316,819	312,708	312,694	304,478	96,235
SS	322,369	318,199	318,189	308,482	100,944

Each step corresponds to one or more processes of transformation and quality filtering of the sequences obtained via high-throughput sequencing.

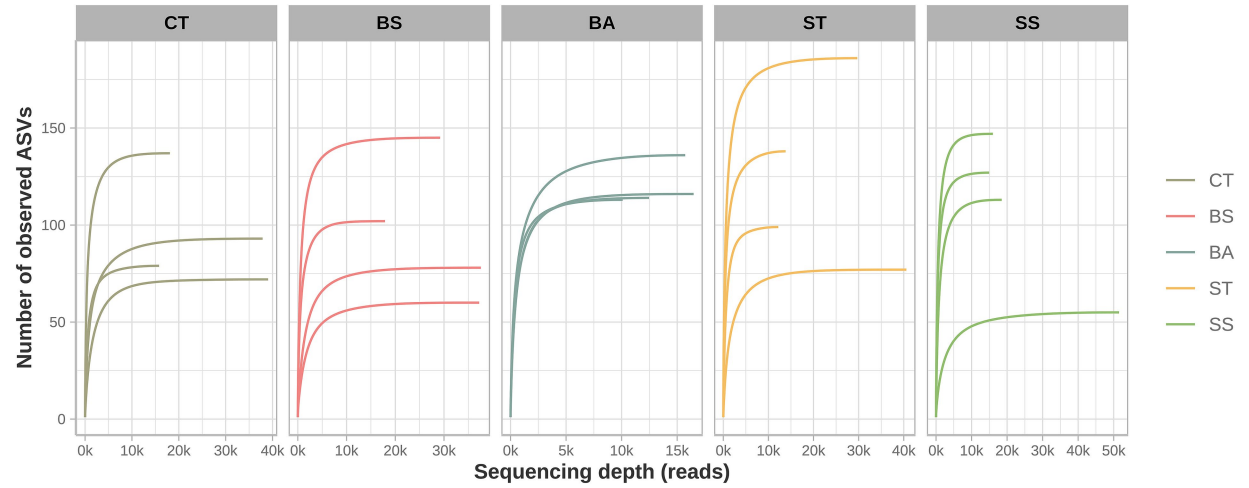

FIGURE 1
Rarefaction curves. The stabilization of the curves indicated a reduction in the detection of new ASVs as the number of reads increased.

families, classes, orders, and phyla than did the other treatments (Table 3). Members of the prokaryotic kingdom "Archaea" were observed only in samples from the BA, ST, and SS treatments but in very low abundance (mean relative abundance >0.01%).

Increase in *Bradyrhizobium* frequency

The microbial communities were mostly dominated by the phylum Proteobacteria (Figure 2A). This phylum represented, on average, 93.75% of the relative abundance. The BS treatment had the greatest relative abundance of Proteobacteria in the samples (average: 95.41%). Sequences derived from other phyla of lower abundance were concentrated in Bacteroidetes (average: 2.82%), Actinobacteria (average: 2.01%), and Firmicutes (average: 1.09%). On average, sequences unclassified at the phylum level represented 0.16% of the relative abundance of the samples.

Among the most abundant genera (Figure 2B), there was a high prevalence of members of the Proteobacteria phylum (21 of the top 25; Figure 2B). Together, the genera of these phyla represented, on average, 88.61% of the samples. There were also genera of the phyla Bacteroidetes (2/25), Actinobacteria (1/25), and Firmicutes (1/25). The massive presence of the genus *Bradyrhizobium*, which represented, on average, 71.22% of the sequences at the genus level, is remarkable. *Bradyrhizobium* was the most abundant genus in all the samples, except for sample ST (ST treatment), whose abundance was only 12.66%. Four ASVs of the genus *Bradyrhizobium* were detected; however, none of them were classified at the species level. The second most abundant genus throughout the samples was *Salmonella* (average: 1.94%), corresponding to a single ASV whose species was not classified. The third most abundant genus, *Massilia* (average: 1.59%), presented nine different ASVs, six of which were from unclassified species and three of which were assigned to the species *M. agri* strain K-3-1, *M. phosphatilytica* strain 12-OD1, and *M. kyonggiensis* strain TSA1.

The bacterial inoculation promoted slight changes in the microbiome

The taxonomic profiles revealed that the BA treatment had greater consistency in the presence of different genera. This can be seen in the high average abundance of genera other than *Bradyrhizobium* (average 38.77%) and in the higher percentage of less abundant genera ("Others"; average 12.67%) (Figure 2B). In the other treatments, there were occasional samples with less dominance of the genus *Bradyrhizobium*; however, this was not consistent throughout the entire treatment (Figure 2B).

Despite the noticeable differences observed in the proportions of the taxonomic profiles (Figure 2), alpha diversity measures were similar between treatments since there was no significant difference in pairwise comparisons between the different indices evaluated (Table 4). In the measurement of the richness of ASVs, inferred by the Chao1 index, there was an increase in the values of the treatments inoculated with microorganisms (BS, BA, ST, and SS; Table 1); however, the variance of these values in the samples did not allow us to identify statistical differences when compared with the control. Similarly, for the diversity indices (Shannon and

TABLE 3 The number of successful assignments up to each taxonomic rank was counted.

Treatment	Kingdom	Phylum	Class	Order	Family	Genus	Species
CT	110,784	110,644	110,530	110,366	109,260	108,718	2,683
	(1)	(11)	(21)	(40)	(66)	(123)	(33)
BS	121,835	121,770	120,459	120,278	119,738	118,646	3,379
	(1)	(11)	(23)	(44)	(71)	(121)	(36)
BA	54,758	54,603	54,418	54,214	53,158	52,440	2,668
	(2)	(16)	(29)	(52)	(84)	(145)	(36)
ST	96,235	96,130	94,720	94,147	92,275	87,447	3,797
	(2)	(13)	(23)	(47)	(78)	(141)	(50)
SS	100,944	100,851	100,698	100,531	99,104	98,384	2,646
	(2)	(15)	(25)	(49)	(79)	(128)	(34)

The number of unique taxa from each taxonomic level found in each treatment is shown in parentheses.

Gini-Simpson), the BA and ST treatments had greater values but were not significantly different from the control treatment (Table 4).

The similarity in sample compositions was also reinforced by beta diversity analysis. The Bray–Curtis distances between the samples did not show any separation between the treatments (PERMANOVA: p-value >0.05), although the composition can explain most of the variation found within them (first two axes = 78.64% of the variation; Figure 3).

Slight changes in the structure of microbiome and co-occurrence networks

Although the prokaryotic communities present in the treatments were narrowly similar, some significant differences were found when prospecting for differentially abundant taxa (DATs). In total, 30 DATs were found, 24 of which were unique. The measures of differences (fold changes), p-values, and relative abundances in the treatments. Differences were concentrated on more specific taxonomic ranks, such as family, genus, and species (Figure 4). Compared with the control treatment (CT), the ST treatment caused the most shifts at 14 DAT (Figure 4C). Of these, 12 were found in greater abundance in the ST samples, while two other species were more prevalent in the CT samples.

The SS treatment had the least number of shifts (4 DAT), mainly reductions in the abundance of taxa present in the CT treatment (Figure 4D). The abundances of the *Sphingobacterium mucilaginosum* strain THG-SQA8 and the *Stenotrophomonas maltophilia* strain ATCC-13637 seemed to be most affected by inoculation since their abundances decreased after 4 and 3 of the treatments, respectively.

The microbial community structure was explored through co-occurrence networks (Figure 5 and Table 5). The relationships of taxa at the genus level seemed to be affected by the treatments, as structural shifts were observed (Figure 5). The CT network had intermediate centrality measures in general comparison with other networks.

The BS and BA treatments had greater tendencies to form larger modules, with modularity values of 0.524 and 0.687, respectively (Table 5). Additionally, the BA treatment group presented a greater number of modules (7; Table 5). Notably, this treatment had strong negative correlations (Figure 5 and Table 5). The modularity values of the ST and SS treatments were considerably lower than those of the CT network, at 0.074 and 0.081, respectively. The SS had only two modules.

Another aspect noted in the structuring is the density of the modules. The ST treatment presented a module composed of strongly correlated genera (Figure 5), with a high number of edges and a high mean degree of connections per node (Table 5). This resulted in a high clustering coefficient (0.995; Table 5). The same observations apply—to a lesser extent—to the BS treatment. The BA and SS treatments, on the other hand, had opposite trends, as they had a lower number of edges and mean degree by genus. Thus, their clustering coefficients were lower than those of CT (Table 5). Another consequent effect of the greater number of rarefied modules in the BA and SS treatment networks was the greater dependence on intermediate taxa to maintain the internal links of the modules. This can be verified by the highest means and maximums of betweenness of these treatments (Table 5). Finally, changes are observed in the genera considered hubs since the results differed between treatments (except for the BS treatment, whose taxa are present in the densest submodule tied in this measure) (Table 5). However, considering the same exception, all hub taxa belonged to the phylum Proteobacteria (Figure 5 and Table 5).

Productivity and nitrogen content increase

The data show statistical significance at a significance level of 5% based on the ANOVA. Figure 6 demonstrates that all bacterial treatments exhibited similar or superior performance in productivity and production compared to the control and *S. spinosa* (SS), which demonstrated the highest mean productivity (4407.32 kg/ha) in contrast to the control (4201.32 kg/ha). For the productivity parameter, the highest value was observed in the SS treatment compared with the control, whereas no statistically significant difference was found between the other treatments and the control. Regarding nitrogen content, only the ST treatment did not exhibit a statistically significant difference from the control, whereas the other treatments demonstrated higher values than the control.

Discussion

Many microorganisms are associated with plants and have a significant effect on various aspects of plant growth and development.

10.3389/fsufs.2025.1505001

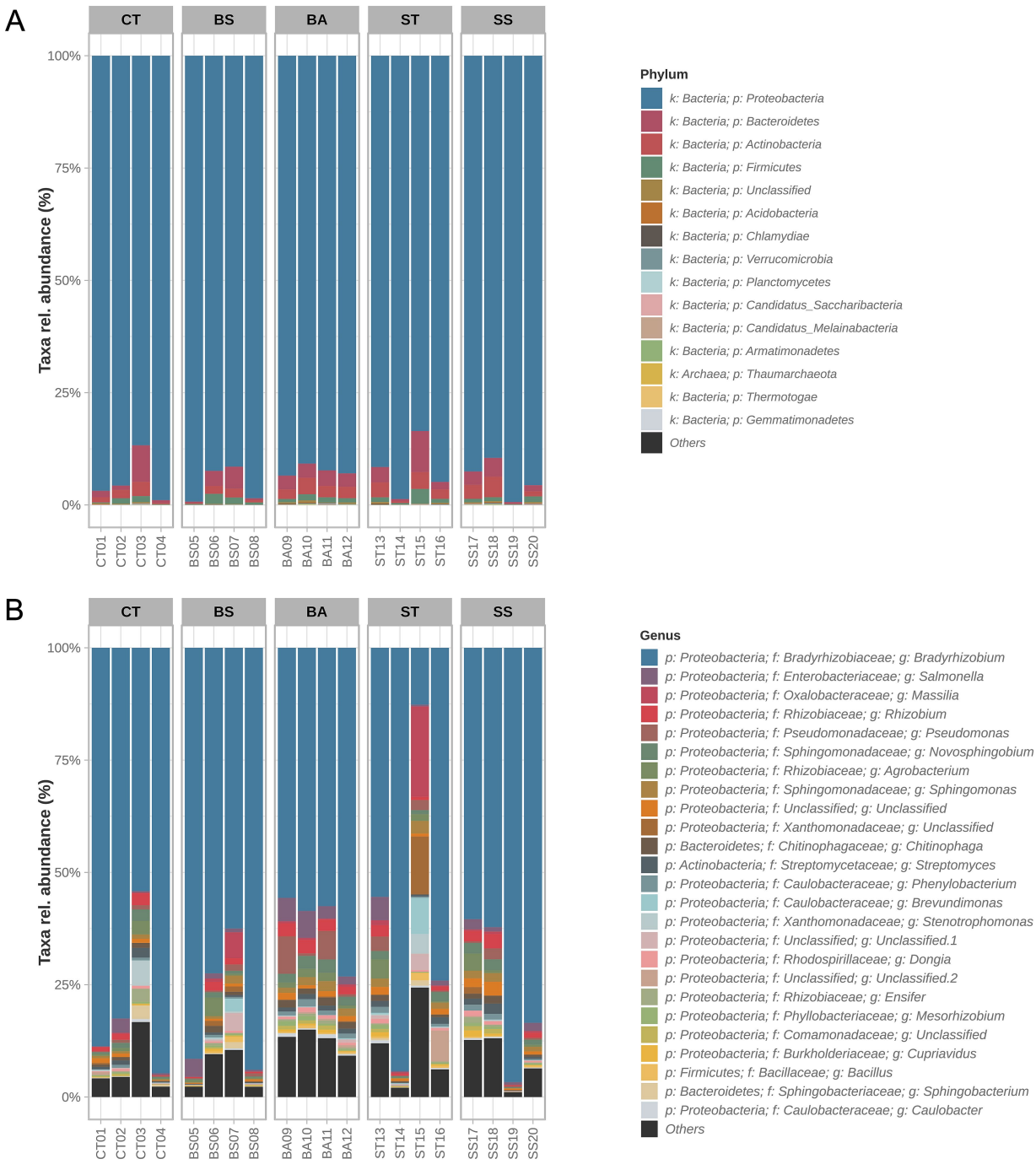

FIGURE 2
Taxonomic profiles of the samples. Relative abundances of the 15 most prevalent phyla **(A)** and 25 most prevalent genera **(B)**. The taxa with the highest prevalence were aggregated in the "others" category.

These associated microorganisms can enhance nutrient availability in the soil and improve the ability of a plant to absorb nutrients and water. In addition, they can produce phytohormones such as auxins, gibberellins, and cytokinins, which promote root and shoot development, increase a plant's ability to explore the soil, and enhance its photosynthetic efficiency. Interactions between microorganisms can sometimes be detrimental because they may produce antimicrobial molecules to eliminate one another or compete for the same niche of colonization and nutrient resources. However, these interactions can also be synergistic, where one species of microorganism assists another in colonizing and establishing itself in the soil or host plant (Wallis and Galarneau, 2020; Nakano et al., 2022).

As demonstrated in other studies, the process of inoculating endogenous microorganisms can significantly alter soil and root microbiomes, thereby promoting growth and enhancing the capacity of plants to thrive (Mitter et al., 2016; Nadarajah and Abdul Rahman, 2021).

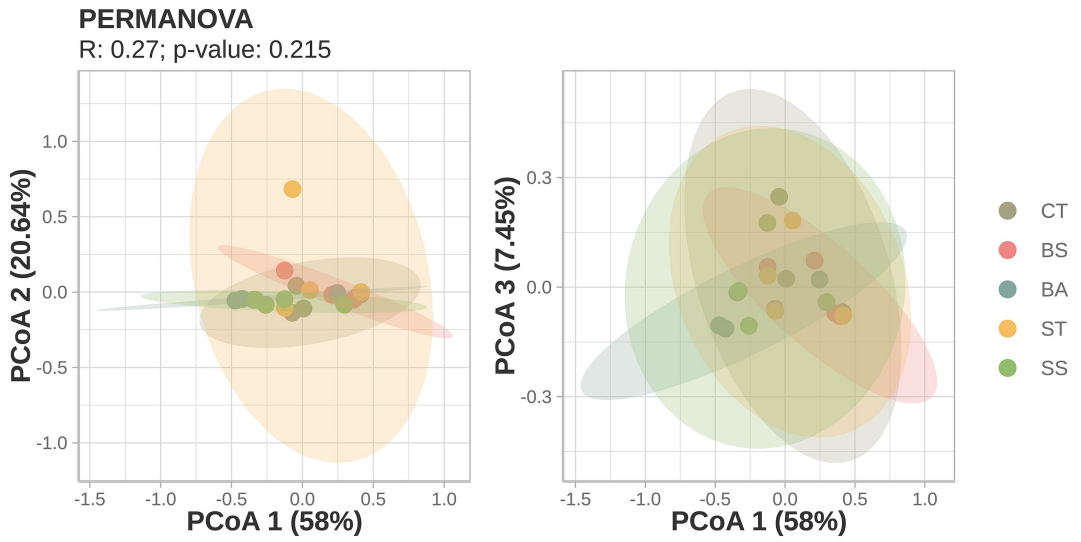

FIGURE 3
Principal coordinates analysis (PCoA) of Bray–Curtis dissimilarity distances. Axes and variance: the axes represent principal components (PCs) or dimensions that explain variation in the data. Higher percentages on the axes indicate a greater explanation for the variance in community differences. Clustering: points close together indicate similar microbial communities, whereas points farther apart show distinct communities.

TABLE 4 Alpha diversity measures.

Treatment	Chao1	Shannon	Gini-Simpson
CT	95.25 ± 29.17	1.66 ± 0.97	0.57 ± 0.28
BS	96.25 ± 36.77	1.49 ± 0.97	0.47 ± 0.28
BA	119.75 ± 10.90	2.42 ± 0.34	0.69 ± 0.11
ST	125.00 ± 47.85	2.26 ± 1.32	0.65 ± 0.34
SS	110.50 ± 39.54	1.93 ± 0.98	0.62 ± 0.23

The values represent the means of each treatment, followed by the standard deviation.

In this study, the objective was to determine which bacteria would stimulate soybean growth and how the inoculation of these bacteria would impact the root microbiome compared to the control, which did not receive bacterial inoculation. To achieve this goal, several bacteria were inoculated into the soybean crop, including *B. subtilis* (BS), *B. aryabhattai* (BA), *Streptomyces* sp. (ST), and *S. spinosa* (SS). Interestingly, in terms of promoting plant growth, no significant differences were observed among the treatments, indicating that none of the bacterial strains enhanced soybean productivity. However, according to the PCA analysis, inoculation with *S. spinosa* and *B. aryabhattai* showed the potential to improve plant yield. Variables related to nitrogen content in the grains and aboveground parts showed a stronger correlation with *S. spinosa* inoculation. These results suggest that *S. spinosa* may play a significant role in increasing nitrogen availability and utilization in plants. *Saccharopolyspora spinosa* is a bacterium belonging to the Actinobacteria phylum. It is a naturally occurring organism used to produce spinosad, an insect-control agent (Breslin et al., 2000). This organism is involved in a fermentation process that results in spinosad, which has been widely used to control several caterpillars that cause yield losses in many different crops, such as chickpea, corn, cotton, wheat, peanut, soybean, and other valuable agricultural crops (Yang et al., 2019; Mihretie et al., 2020; Qu et al., 2020) because of its low mammalian toxicity, ecotoxicology, and minimal environmental impact.

There is currently no published research indicating that the bacterium *S. spinosa* exhibits plant growth-promoting properties, nor is there any evidence suggesting that inoculation with this bacterium has any impact on the nitrogen content of soybean grains. However, inoculation with SS may have changed the rhizospheric microbiome, favoring nitrogen absorption by plants.

Phosphorus content in the dry mass was influenced more by *B. aryabhattai*. This indicated that *B. aryabhattai* may have a particular impact on phosphorus availability and plant biomass accumulation. Several studies have demonstrated the capacity of bacteria from the genus *Bacillus* to solubilize phosphorus and increase the phosphorus content in plants (Emami et al., 2020; Pathania et al., 2020; Torres et al., 2024). At present, there is no evidence to suggest that *B. arayabhattai* can enhance the phosphorus content in soybeans. According to a study by Kang et al. (2023), *B. arayabhattai* has the capacity to eliminate excess nitrogen from soil through two processes: the conversion of ammonia to other nitrogen forms and the reduction of those forms into harmless nitrogen gas. However, this finding has raised concerns, as the inoculation of this bacterium could potentially harm soybean plants by hindering their ability to absorb nitrogen. Although this effect may occur, Kang et al. (2012) reported that it only occurs under specific circumstances such as cold temperatures and highly alkaline environments, which are typically challenging for other bacteria. Conversely, the control treatment, which received mineral fertilization, did not differ from the treatments. These findings suggest that mineral fertilization can be replaced with the inoculation of these bacteria without any reduction in yield or the need for *B. japonicum* inoculation in areas where soybeans are consistently produced.

Several studies have demonstrated the capacity of the inoculation of indigenous bacteria to modulate the rhizospheric and root

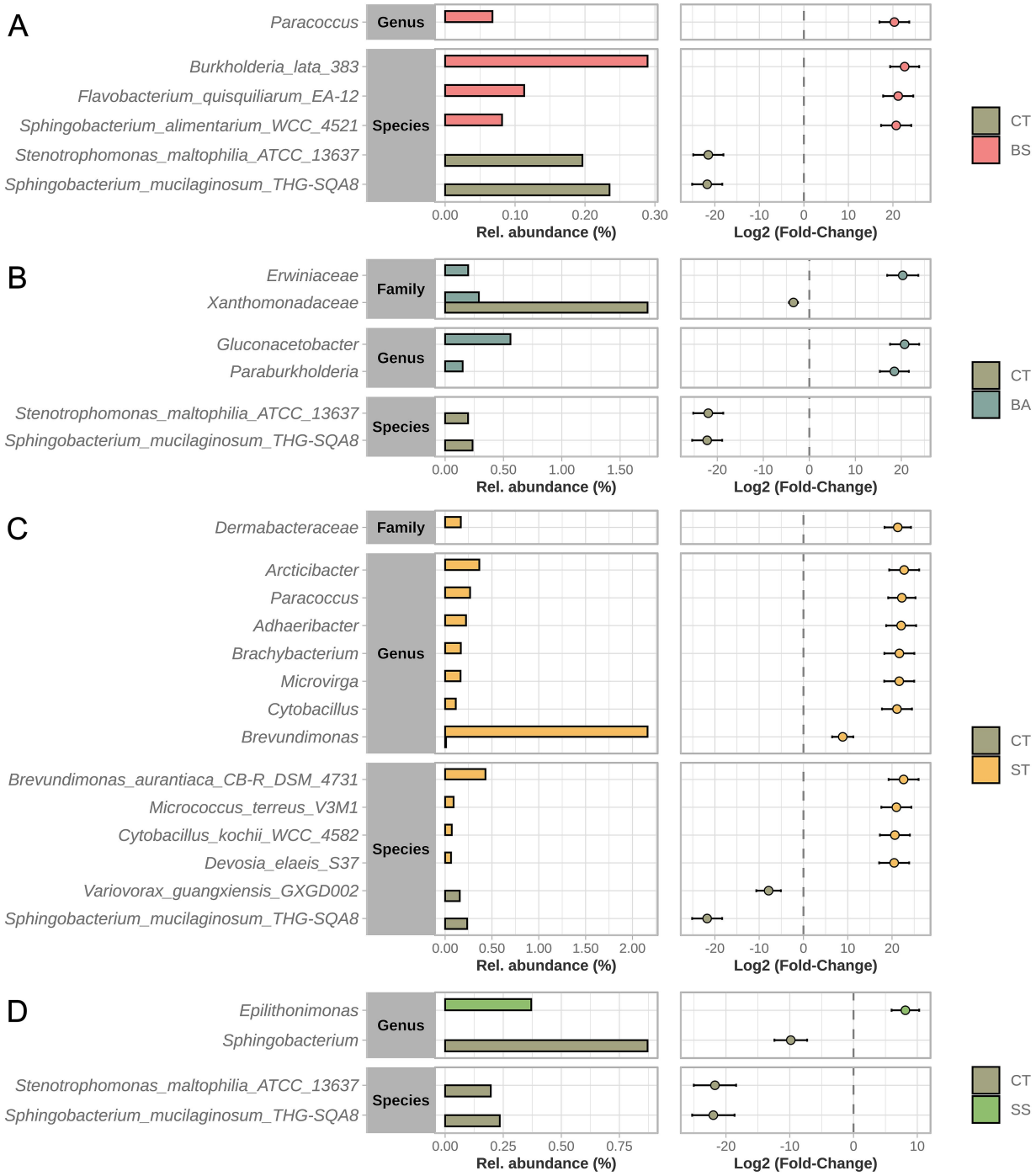

FIGURE 4
Differentially abundant taxa (DAT). Comparisons were made between each treatment and the control **(A–D)**. All the taxonomic ranks were tested. The bar graph (left) represents the comparison of relative abundances, and the dot-and-whisker graph (right) represents the intensity of the difference (fold-change) and its variation in the samples.

microbiomes to promote plant growth (Dastogeer et al., 2020). However, little information is available on how to manipulate the microbiome to promote plant growth. In the present study, inoculation with four types of bacterial strains influenced the root microbiome in different ways; however, *B. japonicum* was the most abundant genus in all samples, except for ST (ST treatment), with an abundance of only 12.66%.

The introduction of a bacterium may result in an increase in the population of other bacteria. This increase in population was attributed to the altered environment caused by the introduced bacteria or their influence on the roots of the plant. This phenomenon occurred for all the evaluated strains, except for ST.

Despite the noticeable differences observed in the proportions of the taxonomic profiles (Figure 2), alpha diversity measures were similar

10.3389/fsufs.2025.1505001

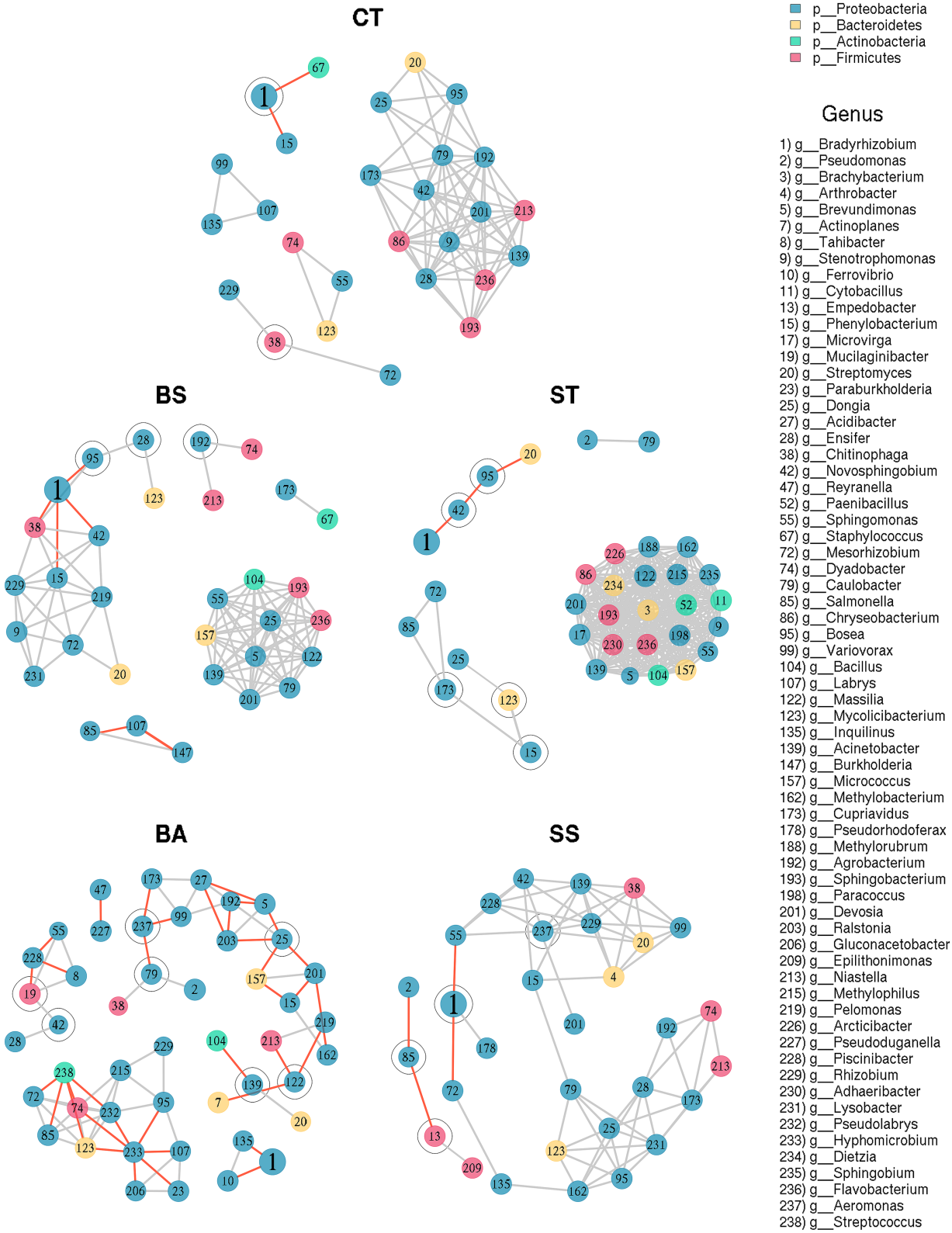

FIGURE 5
Co-occurrence network graphs of treatments at genus rank. The networks were established using strong Pearson's correlation coefficients ($r = \pm 0.75$) of the relationships at a confidence level of 95% ($p < 0.05$). Negative relationships are depicted in red, whereas positive relationships are represented in light gray. Articulation points (taxa that generated additional modules in their absence) are denoted by an outer circle.

TABLE 5 Topological features and centrality measures of correlation networks.

Attribute	CT	BS	BA	ST	SS
No. of nodes	27	32	46	35	31
No. of edges (±)	80 (78/2)	91 (85/6)	76 (40/36)	262 (259/3)	71 (67/4)
No. of. modules (sizes)	5 (15, 3, 3, 3, 3)	5 (11, 3, 13, 3, 2)	7 (15, 3, 4, 13, 3, 6, 2)	4 (23, 4, 2, 6)	2 (27, 4)
Modularity	0.23	0.524	0.687	0.074	0.081
Clustering Coefficient	0.811	0.925	0.639	0.995	0.63
Mean degree	5.926	5.688	3.304	14.971	4.581
Max. degree	13 (ID: 192, 79)	10 (ID: 139, 104, 5, 79, 201, 25, 236, 122, 157, 193, 55)	8 (ID: 232)	22 (ID: 230, 226, 104, 3, 5, 86, 11, 201, 234, 236, 122, 215, 188, 157, 17, 52, 198, 193, 235, 55, 9)	9 (ID: 139)
Mean betweenness	1.481	2.75	6.174	0.6	24.677
Max. betweenness	10.506 (ID: 192, 79)	20 (ID: 95)	40 (ID: 25)	6 (ID: 173, 15)	123.956 (ID: 15)
Main hubs	ID: 192, 79	ID: 139, 104, 5, 79, 201, 25, 236, 122, 157, 193, 55	ID: 232	ID: 55, 9	ID: 139

Some attributes refer to specific genera. These attributes are preceded by "ID" and present the identifiers informed in the legend of the networks (Figure 5).

between the treatments, as there was no significant difference in pairwise comparisons between the different indices evaluated (Table 4). Some results have shown no differences in alpha diversity between the treatments and have also shown an effect on plant growth (Bueno et al., 2022; dos Santos et al., 2022). When the bacterial inoculant was applied, indigenous bacteria could promote modifications in the microbiome, resulting in both alterations and benefits to the plant. However, these changes were short-lived, and the microbiome returned to its previous state, rendering microbiome evaluation unable to detect any differences. Another study that provided this evidence was conducted by Lobo et al. (2019). In this study, four strains of *B. subtilis* were inoculated into maize crops under field conditions. Notably, only the treatment that showed a higher yield than the control had fewer *B. subtilis*-covered roots than the other treatments. This suggests that the set of abilities of bacteria to interact with plants is more important than the number of bacteria in promoting plant growth.

All inoculated strains demonstrated the ability enhanced the population of *B. japonicum* in the roots of plants. This phenomenon appears to be primarily influenced by the behavior of *B. japonicum* rather than the inoculated microorganisms themselves.

A study demonstrated that co-inoculation with *Trichoderma harzianum* did not increase the number of *B. japonicum* bacteria but helped soybean plants to form nodules even in the presence of nitrate, which usually stops nodule formation (Iturralde et al., 2020). Co-inoculation of *Azospirillum baldaniorum* with *B. japonicum* improves root nodule fixation in lima bean nitrogen (Lopes et al., 2022). Groppa et al. (1998) inoculated *B. japonicum* with *A. brasilense* in soybean and verified that nodule number and nodule dry weight were not affected by dual inoculation; however, co-inoculated plants showed a significantly higher proportion of nodules attached to the main root and located in the upper of the root system. The results showed that co-inoculation with *B. japonicum* and *A. brasilense* led to an increase in the number of the most active nodules, resulting in greater nitrogen fixation and assimilation.

Compared with the control treatment (CT), the ST treatment caused the greatest shifts at 14 DAT (Figure 4C). Of these, 12 were found to be more abundant in the ST samples, whereas two other species were more prevalent in the CT samples.

Various studies have demonstrated a correlation between high microbial diversity and soil, which is suppressive. The suppressive effect of soil is attributed to the intense competition among microorganisms, which may be a result of high microbial diversity, making it difficult for pathogens to establish and thereby reduce the incidence of diseases (Kotsou et al., 2004; Zhao et al., 2018; dos Santos Souza et al., 2019). Although the effect of high DAT on plant growth remains inconclusive, further research is necessary to determine whether a higher number of DAT is beneficial for promoting plant growth. The results of such studies will be crucial for providing a clearer understanding of this phenomenon.

Conclusion

Co-inoculation of soybean with plant growth-promoting bacteria did not significantly increase the yield compared to mineral fertilization. However, microbial inoculation serves as a viable alternative to mineral fertilization without compromising productivity. Although bacterial inoculation did not enhance the yield, it promoted the growth of *B. japonicum* in plant roots, with the exception of *Streptomyces* treatment. This suggests that co-inoculation may be an effective strategy for improving the efficiency of *B. japonicum* in promoting plant growth. The inoculated strains influenced the root microbiome in different ways, with *B. japonicum* being the most abundant genus in most of the samples. Further research is required to fully understand the mechanisms underlying these microbial interactions and their implications for soybean productivity. Overall, this study demonstrates the potential of co-inoculation with plant growth-promoting bacteria to modulate the root microbiome and enhance beneficial microbial colonization in soybean.

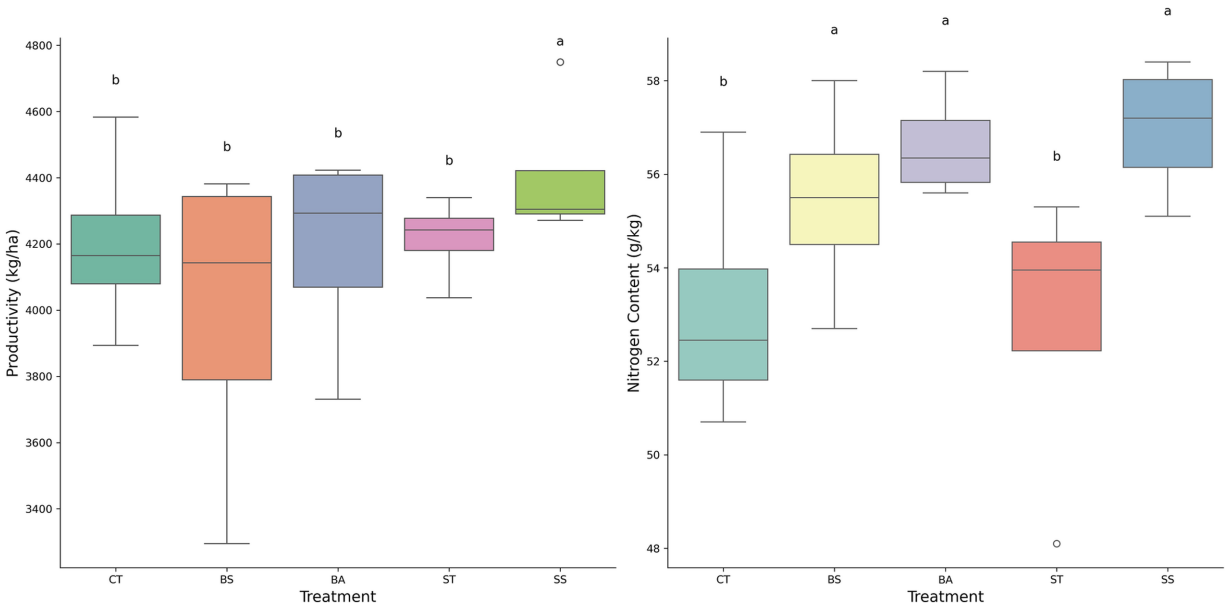

FIGURE 6
This consisted of two box plots comparing the effects of different treatments (CT, BS, BA, ST, and SS) on two parameters: productivity (kg/ha) on the left and nitrogen content (g/kg) on the right. The SS treatment had the highest value for productivity, whereas the BS, BA, and SS treatments had the highest values for nitrogen content. The same letters indicate no statistical difference between treatments according to Tukey 5%.

Data availability statement

The datasets presented in this study can be found in online repositories. The names of the repository/repositories and accession number(s) can be found in the article/supplementary material.

Author contributions

MA: Writing – original draft, Writing – review & editing. LC: Writing – original draft, Writing – review & editing. CSa: Writing – original draft, Writing – review & editing. EF: Writing – original draft, Writing – review & editing. CSi: Writing – original draft, Writing – review & editing. DP: Writing – original draft, Writing – review & editing. EZ: Writing – original draft, Writing – review & editing. OB: Writing – original draft, Writing – review & editing. ER: Writing – original draft, Writing – review & editing.

Funding

The author(s) declare that financial support was received for the research, authorship, and/or publication of this article. This study was financed in part by the Coordination for the Improvement of Higher Education Personnel (CAPES), Brazil, Finance Code 001.

Acknowledgments

The authors thank FAPESP for financial support Process number 21/10821-8 CNPQ—Process: 302234/2022-5.

Conflict of interest

The authors declare that the research was conducted in the absence of any commercial or financial relationships that could be construed as potential conflicts of interest.

Generative AI statement

No Generative AI was used in the preparation of this manuscript.

Publisher's note

All claims expressed in this article are solely those of the authors and do not necessarily represent those of their affiliated organizations, or those of the publisher, the editors and the reviewers. Any product that may be evaluated in this article, or claim that may be made by its manufacturer, is not guaranteed or endorsed by the publisher.

References

Andersen, K., Kirkegaard, R., Karst, S., and Albertsen, M. (2004). ampvis2: an R package to analyse and visualise 16S rRNA amplicon data. bioRxiv.

Andrews, S. (2010). *FastQC: a quality control tool for high throughput sequence data*. Babraham Institute, Cambridge, United Kingdom: Babraham Bioinformatics.

Armendariz, A. L., Talano, M. A., Olmos Nicotra, M. F., Escudero, L., Breser, M. L., Porporatto, C., et al. (2019). Impact of double inoculation with *Bradyrhizobium japonicum* E109 and *Azospirillum brasilense* Az39 on soybean plants grown under arsenic stress. *Plant Physiol. Biochem.* 138, 26–35. doi: 10.1016/j.plaphy.2019.02.018

Breslin, W. J., Marty, M. S., Vedula, U., Liberacki, A. B., and Yano, B. L. (2000). Developmental toxicity of spinosad administered by gavage to CD 1 rats and New Zealand white rabbits. *Food Chem. Toxicol.* 38, 1103–1112. doi: 10.1016/S0278-6915(00)00108-3

Bueno, C. B., dos Santos, R. M., de Souza Buzo, F., de Andrade da Silva, M. S. R., and Rigobelo, E. C. (2022). Effects of chemical fertilization and microbial inoculum on *Bacillus subtilis* colonization in soybean and maize plants. *Front. Microbiol.* 13:901157. doi: 10.3389/fmicb.2022.901157

Callahan, B. J., McMurdie, P. J., Rosen, M. J., Han, A. W., Johnson, A. J. A., and Holmes, S. P. (2016). DADA2: high-resolution sample inference from Illumina amplicon data. *Nat. Methods* 13:581. doi: 10.1038/nmeth.3869

Cao, L., Qiu, Z., You, J., Tan, H., and Zhou, S. (2005). Isolation and characterization of endophytic streptomycete antagonists of *Fusarium* wilt pathogen from surface-sterilized banana roots. *FEMS Microbiol. Lett.* 247, 147–152. doi: 10.1016/j.femsle.2005.05.006

Cole, J. R., Wang, Q., Fish, J. A., Chai, B., McGarrell, D. M., Sun, Y., et al. (2014). Ribosomal Database Project: Data and tools for high throughput rRNA analysis. *Nucleic Acids Res.* 42. doi: 10.1093/nar/gkt1244

Csardi, G. (2005). The igraph software package for complex network research. Available at: https://www.researchgate.net/publication/221995787 (Accessed February 11, 2024).

Dastogeer, K. M. G., Tumpa, F. H., Sultana, A., Akter, M. A., and Chakraborty, A. (2020). Plant microbiome—an account of the factors that shape community composition and diversity. *Curr. Plant Biol.* 23:100161. doi: 10.1016/j.cpb.2020.100161

de Souza, R. S. C., Okura, V. K., Armanhi, J. S. L., Jorrín, B., Lozano, N., da Silva, M. J., et al. (2016). Unlocking the bacterial and fungal communities assemblages of sugarcane microbiome. *Sci. Rep.* 6:28744. doi: 10.1038/srep28774

Didion, J. P., Martin, M., and Collins, F. S. (2017). Atropos: specific, sensitive, and speedy trimming of sequencing reads. *PeerJ* 5:e3720. doi: 10.7717/peerj.3720

dos Santos, R. M., Cueva-Yesquén, L. G., Garboggini, F. F., Desoignies, N., and Rigobelo, E. C. (2022). Inoculum concentration and mineral fertilization: effects on the endophytic microbiome of soybean. *Front. Microbiol.* 13:900980. doi: 10.3389/fmicb.2022.900980

dos Santos Souza, C. R., de Oliveira Barbosa, A. C., Ferreira, C. F., Souza, F. V. D., de Souza Rocha, L., de Souza, E. H., et al. (2019). Diversity of microorganisms associated to *Ananas* spp. from natural environment, cultivated and ex situ conservation areas. *Sci. Hortic.* 243, 544–551. doi: 10.1016/J.SCIENTA.2018.09.015

Emami, S., Alikhani, H. A., Pourbabaee, A. A., Etesami, H., Motasharezadeh, B., and Sarmadian, F. (2020). Consortium of endophyte and rhizosphere phosphate solubilizing bacteria improves phosphorous use efficiency in wheat cultivars in phosphorus deficient soils. *Rhizosphere* 14:100196. doi: 10.1016/j.rhisph.2020.100196

Groppa, M. D., Zawoznik, M. S., and Tomaro, M. L. (1998). Effect of co-inoculation with *Bradyrhizobium japonicum* and *Azospirillum brasilense* on soybean plants. *Eur. J. Soil Biol.* 34, 75–80. doi: 10.1016/S1164-5563(99)90004-3

Gu, Y., Dong, K., Geisen, S., Yang, W., Yan, Y., Gu, D., et al. (2020). The effect of microbial inoculant origin on the rhizosphere bacterial community composition and plant growth-promotion. *Plant Soil* 452, 105–117. doi: 10.1007/s11104-020-04545-w

Ikiz, B., Dasgan, H. Y., and Gruda, N. S. (2024). Utilizing the power of plant growth promoting rhizobacteria on reducing mineral fertilizer, improved yield, and nutritional quality of *Batavia lettuce* in a floating culture. *Sci. Rep.* 14:1616. doi: 10.1038/s41598-024-51818-w

Iturralde, E. T., Stocco, M. C., Faura, A., Mónaco, C. I., Cordo, C., Pérez-Giménez, J., et al. (2020). Coinoculation of soybean plants with *Bradyrhizobium japonicum* and *Trichoderma harzianum*: coexistence of both microbes and relief of nitrate inhibition of nodulation. *Biotechnol. Rep.* 26:e00461. doi: 10.1016/j.btre.2020.e00461

Kang, S. M., Khan, A. L., Hamayun, M., Hussain, J., Joo, G. J., You, Y. H., et al. (2012). Gibberellin-producing *Promicromonospora* sp. SE188 improves *Solanum lycopersicum* plant growth and influences endogenous plant hormones. *J. Microbiol.* 50, 902–909. doi: 10.1007/s12275-012-2273-4

Kang, X., Zhao, X., Song, X., Wang, D., Shi, G., Duan, X., et al. (2023). Nitrogen removal by a novel strain *Priestia aryabhattai* KX-3 from East Antarctica under alkaline pH and low-temperature conditions. *Process Biochem.* 130, 674–684. doi: 10.1016/j.procbio.2023.05.030

Khoso, M. A., Wagan, S., Alam, I., Hussain, A., Ali, Q., Saha, S., et al. (2024). Impact of plant growth-promoting rhizobacteria (PGPR) on plant nutrition and root characteristics: current perspective. *Plant Stress* 11:100341. doi: 10.1016/j.stress.2023.100341

Khosravi, H., Khoshru, B., Nosratabad, A. F., and Mitra, D. (2024). Exploring the landscape of biofertilizers containing plant growth-promoting rhizobacteria in Iran: progress and research prospects. *Curr. Res. Microb. Sci.* 7:100268. doi: 10.1016/j.crmicr.2024.100268

Kleinberg, J. M. (2000). Hubs, Authorities, and Communities.

Kotsou, M., Mari, I., Lasaridi, K., Chatzipavlidis, I., Balis, C., and Kyriacou, A. (2004). The effect of olive oil mill wastewater (OMW) on soil microbial communities and suppressiveness against *Rhizoctonia solani*. *Appl. Soil Ecol.* 26, 113–121. doi: 10.1016/J.APSOIL.2003.12.001

Kumar, V., Chourasia, H. K., Rajani, K., and Kumar, R. R. (2024). Exploration and characterization of high-efficiency phosphate-solubilizing bacteria isolates from chickpea rhizospheric soil. *Int. J. Bio-Resour. Stress Manag.* 15, 01–09. doi: 10.23910/1.2024.4987a

Lobo, L. L. B., dos Santos, R. M., and Rigobelo, E. C. (2019). Promotion of maize growth using endophytic bacteria under greenhouse and field conditions. *Aust. J. Crop. Sci.* 13, 2067–2074. doi: 10.21475/ajcs.19.13.12.p2077

Lopes, Á., Setubal, I., Costa, V., Zilli, J., Rodrigues, A., and Bonifacio, A. (2022). Synergism of *Bradyrhizobium* and *Azospirillum baldaniorum* improves growth and symbiotic performance in lima bean under salinity by positive modulations in leaf nitrogen compounds. *Appl. Soil Ecol.* 180:104603. doi: 10.1016/J.APSOIL.2022.104603

Love, M. I., Huber, W., and Anders, S. (2014). Moderated estimation of fold change and dispersion for RNA-seq data with DESeq2. *Genome Biol.* 15:550. doi: 10.1186/s13059-014-0550-8

Lundberg, D. S., Yourstone, S., Mieczkowski, P., Jones, C. D., and Dangl, J. L. (2013). Practical innovations for high-throughput amplicon sequencing. *Nat. Methods* 10, 999–1002. doi: 10.1038/nmeth.2634

McMurdie, P. J., and Holmes, S. (2013). Phyloseq: an R package for reproducible interactive analysis and graphics of microbiome census data. *PLoS One* 8:e61217. doi: 10.1371/journal.pone.0061217

Meier, M., Liu, Y., Lay-Pruitt, K. S., Takahashi, H., and von Wirén, N. (2020). Auxin-mediated root branching is determined by the form of available nitrogen. *Nat. Plants* 6, 1136–1145. doi: 10.1038/s41477-020-00756-2

Mihretie, A., Yimer, D., Wudu, E., and Kassaw, A. (2020). Efficacy of insecticides against African bollworm (*Helicoverpa armigera* Hubner) on chickpea (*Cicer arietinum*) in the lowlands of Wollo, Northeastern Ethiopia. *Cogent Food Agric.* 6:1833818. doi: 10.1080/23311932.2020.1833818

Mitter, B., Pfaffenbichler, N., and Sessitsch, A. (2016). Plant-microbe partnerships in 2020. *Microb. Biotechnol.* 9, 635–640. doi: 10.1111/1751-7915.12382

Mun, B. G., Hussain, A., Park, Y. G., Kang, S. M., Lee, I. J., and Yun, B. W. (2024). The PGPR *Bacillus aryabhattai* promotes soybean growth via nutrient and chlorophyll maintenance and the production of butanoic acid. *Front. Plant Sci.* 15:1341993. doi: 10.3389/fpls.2024.1341993

Nadarajah, K., and Abdul Rahman, N. S. N. (2021). Plant-microbe interaction: aboveground to belowground, from the good to the bad. *Int. J. Mol. Sci.* 22:10388. doi: 10.3390/ijms221910388

Nakano, M., Omae, N., and Tsuda, K. (2022). Inter-organismal phytohormone networks in plant-microbe interactions. *Curr. Opin. Plant Biol.* 68:102258. doi: 10.1016/j.pbi.2022.102258

Pathania, P., Bhatia, R., and Khatri, M. (2020). Cross-competence and affectivity of maize rhizosphere bacteria *Bacillus* sp. MT7 in tomato rhizosphere. *Sci. Hortic.* 272:109480. doi: 10.1016/j.scienta.2020.109480

Paulus, J. M., and Tooy, D. (2024). Effect of plant growth promoting rhizobacteria (PGPR) on growth and yield of soybean. *J. Agric.* 3, 30–38. doi: 10.47709/joa.v3i01.3613

Qu, Q., Zhang, Z., Peijnenburg, W. J. G. M., Liu, W., Lu, T., Hu, B., et al. (2020). Rhizosphere microbiome assembly and its impact on plant growth. *J. Agric. Food Chem.* 68, 5024–5038. doi: 10.1021/ACS.JAFC.0C00073

R Core Team (2020). *R: A Language and Environment for Statistical Computing. R Foundation for Statistical Computing.* Available at: https://www.R-project.org/.

R Core Team (2023). *R: A language and environment for statistical computing.* Vienna, Austria: R Foundation for Statistical Computing. Available at: https://www.R-project.org/

Schmieder, R., and Edwards, R. (2011). Quality control and preprocessing of metagenomic datasets. *Bioinformatics* 27, 863–864. doi: 10.1093/bioinformatics/btr026

Tedersoo, L., Bahram, M., Zinger, L., Nilsson, R. H., Kennedy, P. G., Yang, T., et al. (2022). Best practices in metabarcoding of fungi: from experimental design to results. *Mol. Ecol.* 31, 2769–2795. doi: 10.1111/mec.16460

Torres, P., Altier, N., Beyhaut, E., Fresia, P., Garaycochea, S., and Abreo, E. (2024). Phenotypic, genomic and in planta characterization of *Bacillus sensu lato* for their phosphorus biofertilization and plant growth promotion features in soybean. *Microbiol. Res.* 280:127566. doi: 10.1016/j.micres.2023.127566

Verma, K. K., Joshi, A., Song, X. P., Singh, S., Kumari, A., Arora, J., et al. (2024). Synergistic interactions of nanoparticles and plant growth promoting rhizobacteria enhancing soil-plant systems: a multigenerational perspective. *Front. Plant Sci.* 15:1376214. doi: 10.3389/fpls.2024.1376214

Wahab, A., Bibi, H., Batool, F., Muhammad, M., Ullah, S., Zaman, W., et al. (2024). Plant growth-promoting rhizobacteria biochemical pathways and their environmental impact: a review of sustainable farming practices. *Plant Growth Regul.* 104, 637–662. doi: 10.1007/s10725-024-01218-x

Wallis, C. M., and Galarneau, E. R. A. (2020). Phenolic compound induction in plant-microbe and plant-insect interactions: a meta-analysis. *Front. Plant Sci.* 11:5870753. doi: 10.3389/fpls.2020.580753

Wang, M., Ge, A. H., Ma, X., Wang, X., Xie, Q., Wang, L., et al. (2024). Dynamic root microbiome sustains soybean productivity under unbalanced fertilization. *Nat. Commun.* 15:1668. doi: 10.1038/s41467-024-45925-5

Wan, W., Qin, Y., Wu, H., Zuo, W., He, H., Tan, J., et al. (2020). Isolation and characterization of phosphorus solubilizing bacteria with multiple phosphorus sources utilizing capability and their potential for lead immobilization in soil. *Front. Microbiol.* 11:752. doi: 10.3389/fmicb.2020.00752

Yang, X., Chen, X., and Yang, X. (2019). Effect of organic matter on phosphorus adsorption and desorption in a black soil from Northeast China. *Soil Tillage Res.* 187, 85–91. doi: 10.1016/J.STILL.2018.11.016

Zhao, M., Yuan, J., Zhang, R., Dong, M., Deng, X., Zhu, C., et al. (2018). Microflora that harbor the NRPS gene are responsible for *Fusarium* wilt disease-suppressive soil. *Appl. Soil Ecol.* 132, 83–90. doi: 10.1016/J.APSOIL.2018.08.022

frontiers | Frontiers in Sustainable Food Systems

TYPE Original Research
PUBLISHED 19 March 2025
DOI 10.3389/fsufs.2025.1550106

Check for updates

OPEN ACCESS

EDITED BY
Marouane Baslam,
Niigata University, Japan

REVIEWED BY
Raj Majumdar,
Agricultural Research Service (USDA), United States
Arafat Abdel Hamed Abdel Latef,
South Valley University, Egypt

*CORRESPONDENCE
Tika B. Adhikari
tbadhika@ncsu.edu

RECEIVED 22 December 2024
ACCEPTED 25 February 2025
PUBLISHED 19 March 2025

CITATION
Adhikari TB, Philbrick AN and Louws FJ (2025) Elucidating the impact of organic amendments on soil bacterial communities and strawberry yield in North Carolina. *Front. Sustain. Food Syst.* 9:1550106. doi: 10.3389/fsufs.2025.1550106

COPYRIGHT
© 2025 Adhikari, Philbrick and Louws. This is an open-access article distributed under the terms of the Creative Commons Attribution License (CC BY). The use, distribution or reproduction in other forums is permitted, provided the original author(s) and the copyright owner(s) are credited and that the original publication in this journal is cited, in accordance with accepted academic practice. No use, distribution or reproduction is permitted which does not comply with these terms.

Elucidating the impact of organic amendments on soil bacterial communities and strawberry yield in North Carolina

Tika B. Adhikari[1]*, Ashley N. Philbrick[1] and Frank J. Louws[1,2]

[1]Department of Entomology and Plant Pathology, North Carolina State University, Raleigh, NC, United States, [2]Department of Horticultural Science, North Carolina State University, Raleigh, NC, United States

Strawberry (*Fragaria* × *ananassa* Duchesne ex Rozier) is an important small fruit grown worldwide. Organic amendments can alter microbial communities and increase crop productivity. While research on organic amendments in strawberry cultivation has primarily focused on various regions in the U.S., especially the West Coast, there has been little to no investigation into their potential benefits in North Carolina (NC). A three-year trial was conducted from 2019 to 2022 at the Horticultural Crops Research Station in Castle Hayne, NC, U. S. A. The main objective of the study was to examine the effects of reduced rates of dried molasses (5.60 t/ha) and mustard meal (2.24 t/ha), a half-rate combination of both, a positive control (Pic Clor 60), and a negative control (no fumigated and no amended) on soil bacterial communities and strawberry yield. Our results from 16S microbiome amplicon sequencing showed significant variations in the composition of the soil bacterial community over time between the organic amendment treatments and the controls. The alpha diversity indices (Shannon index) of the soil bacterial microbiome were generally higher in plots with organic amendments than those treated with Pic Clor 60. Taxonomic classification revealed that the two phyla, *Proteobacteria* and *Actinobacteriota*, were prominent in the organic amendment treatments. The total marketable yield rankings for the three organic amendment treatments (dried molasses, mustard meal, and the half-rate combination of both) were comparable to those achieved through fumigation. The results indicated that bacterial structure and yield improved in the organic amendment plots, while microbial diversity decreased in the fumigation plots, and yields were lower in the untreated plots. This study will inform the selection of organic amendments to enhance microbial diversity and promote sustainability in strawberry farming in NC.

KEYWORDS

***Fragaria* × *ananassa*, microbiome, soil, 16S rRNA, organic amendments, strawberry**

1 Introduction

Strawberry (*Fragaria* × *ananassa* Duchesne ex Rozier) is a highly nutritious and vital crop (Hannum, 2004). The continuous cultivation of strawberries in fields for an extended period has decreased the diversity of bacterial communities and soil health parameters, while the presence of pathogenic fungi has increased (Li and Liu, 2019; Yang et al., 2023). Organic amendments provide essential nutrients, enhance the quality of soil, and impact microbial communities, disease management, and crop productivity in various regions (Oldfield et al., 2018; Strauss and Kluepfel, 2015). An organic amendment refers to any material that increases the organic matter content of soil and improves its chemical, physical, and biological properties (Goss et al., 2013; Rosskopf et al., 2020).

Soil management practices such as cover crops, reduced tillage, mulches, and organic amendments can improve sustainable soil quality, health, and crop productivity (Abawi and Widmer, 2000; Louws et al., 2000; Pankhurst, 1997; Rosskopf et al., 2020). Cover crops like ryegrass, pearl millet, oats, white clover, cowpea, and hairy vetch can be used as green manure crops before planting. They contribute to improved soil health and crop yield, erosion prevention, reduction of plant-parasitic nematode populations, and the addition of organic matter or nitrogen (e.g., legumes) to subsequent cash crops (Fageria et al., 2005). Two common organic amendments, dried molasses, and mustard meal are frequently used in combination with anaerobic soil disinfestation (ASD) to reduce soil-borne diseases and enhance microbial communities in strawberry and tomato production systems across the West Coast, Southeastern, and Midwestern regions (Mazzola et al., 2015; Testen and Miller, 2018; Vincent et al., 2022; Wang and Mazzola, 2019). Dried molasses is a byproduct of the sugar-making process obtained from crushed sugar cane and contains high sugar content which positively impacts soil microbiomes, improves soil structure and moisture retention; functions as a biopesticide, and promotes plant growth and high yields (Expósito et al., 2022). On the other hand, various Brassicaceae seed meals (SMs) like *Sinapis alba* L., *Brassica juncea* L., and *B. carinata* have been utilized as soil amendments in agricultural production systems (Mazzola and Brown, 2010; Mazzola et al., 2015). Among these, a commercial *Brassica* pellet called BioFence (Triumph Italia SPA) was incorporated into the soil to suppress soil-borne pathogens significantly, attributed to a chemically-derived mechanism by releasing biologically active glucosinolate hydrolysis products such as isothiocyanates (Matthiessen and Kirkegaard, 2006). Organic amendments must be effective, affordable, readily available, and biodegradable for soil microbiomes (Daugovish et al., 2021, 2023). It is crucial to evaluate how different organic amendments affect beneficial microbiomes and crop productivity in a new area (Mazzola et al., 2018; Larkin, 2015; Liu et al., 2021; Shu et al., 2022). This is necessary because soil, weather conditions, soil-borne pathogens, microbial communities, and cropping systems vary across regions (Strauss and Kluepfel, 2015).

California's climate and soil composition are unique, making it possible for strawberries to grow throughout the year. Several studies conducted on the West Coast indicate that organic amendments as carbon sources impact soil microbial communities (Deng et al., 2019; Hewavitharana et al., 2014, 2019; Poret-Peterson et al., 2019, 2020). For example, rice bran used resulted in microbial communities with a distinct composition compared to those obtained from molasses (Mazzola et al., 2018). The main strawberry growing season in North Carolina typically occurs from October to early June. However, it may vary depending on geographic locations, soil types, strawberry genotypes, growing seasons, and weather conditions (Bandara and Janaranjana, 2021; Poling, 1993; Samtani et al., 2019; Rana and Gu, 2020). Strawberry growers use raised beds with black plastic mulch and buried drip irrigation lines. Plugs (rooted strawberry tips) are transplanted in the beds in mid-October and managed throughout the winter. Harvesting takes place from early April to early June, and marketable yields can range from 16.8 t/ha to 33.63 t/ha, with net returns from $4,856 t/ha to $6,475/ha (Rysin et al., 2015; Sydorovych et al., 2006). Intensive cropping systems have led to low soil carbon inputs and reduced soil fertility. Additionally, the lack of crop rotation and high dependence on fumigants have caused soil deterioration. Although various management practices such as organic amendments, cover crops, crop rotations, and biofumigation were evaluated in North Carolina (NC), U. S. A. (Louws, 2009; Welker et al., 2008), strawberry growers encounter unique challenges, like distinct pest problems, limited access to high-yield varieties, and the impact of climate change on disease outbreaks (Bandara and Janaranjana, 2021). Importantly, the findings from studies on organic amendments conducted on the West Coast may not be directly applicable to the East Coast, such as NC. Consequently, there is a knowledge gap in conducting a comprehensive assessment of the impacts of organic amendments on soil microbiome composition and structure, and their effect on strawberry production in NC. Depending on organic amendments, they can either increase or decrease soil microbial diversity compared to chemical fertilizers (Ahn et al., 2012; Bebber and Richards, 2020; Bonanomi et al., 2020; Feng et al., 2018; Shu et al., 2022). Soil microbiomes are a vital part of soil biodiversity and contribute to various ecosystem processes such as the decomposition of organic matter, nutrient cycling, and enhancement of plant productivity (Bernard et al., 2014; Bender et al., 2016; Bonanomi et al., 2020; Saleem et al., 2019; Shu et al., 2022; Xia et al., 2020). Overusing mineral fertilizers in the past depleted microbial diversity in agricultural soils (Zhou et al., 2020). On the other hand, organic amendments, including livestock manure, crop residue, cereal brans, molasses, mustard meal, and green manure, not only improve soil microbial activities but also alter microbial composition and diversity (Gravuer et al., 2019; Li et al., 2021; Liu et al., 2021; Rosskopf et al., 2020; Xia et al., 2020; Zhou et al., 2020).

We hypothesize that organic amendments could positively shift bacterial community assembly and improve strawberry yield, as this could be a critical and unexplored aspect in North Carolina. This study aimed to fill the gaps in our knowledge about the effects of two organic amendments: dried molasses and mustard meal on bacterial abundance, composition, and diversity in the soil, and on crop yield in NC. To achieve this, we conducted three-year field trials, extracted DNA from the soil, sequenced the V3-V4 region of the 16S ribosomal RNA (rRNA), and monitored the yield over time.

2 Materials and methods

2.1 Experimental site description

Field experiments were conducted from 2019 to 2022 at the Horticultural Crops Research Station in Castle Hayne, NC, U. S. A. The experimental site is situated at a latitude of 34° 21′ 20" N and a longitude of 77°53′ 59" W, and its elevation is nine meters above sea level. The climate of this area is mild, with warm summers and cool winters. The average daily temperature varies between 32°C in the summer and 15°C in the winter. The rainfall is evenly distributed throughout the year, with an average annual precipitation of 1,118 mm (Robinson, 2005). The baseline soil conditions, recorded during land preparation in 2019, consisted of a clay sandy loam with a pH of 5.9. The soil had an organic carbon content of 1.16%, a cation exchange capacity of 4.5 meq/100 cm^2, and the following nutrient levels: phosphorus at 90 mg/kg, potash at 14 mg/kg, magnesium at 8 mg/kg, and calcium at 63 mg/kg. Soil depth varies depending on soil types, compactness, and crop root growth. For example, strawberry is a shallow-rooted crop, and our experimental site has clay sandy loam soil. Thus, we collected soils at a 12 to 15 cm depth to assess soil nutrients and microbiomes.

TABLE 1 Ten treatments were used in field experiments between 2019 and 2021, and five promising treatments/controls were selected and evaluated in 2022.

Serial No[a]	Treatment	Plastic-type used	Rate
1*	Pic-Clor 60 (Pic 60 or PC)	Black	196.15 kg/ha
2*	No fumigation and no organic amendments or non-treated control (NTC)	Black	
3	Cover crop (cowpeas: pearl millet) + compost (CC + Comp)	Black	Cover crops (cowpea: 112 kg/ha: pearl millet 11.2 kg/ha) + compost 16.8 t/ha
4*	Dried molasses full rate (MS)	Black	Dried molasses full rate (MS) Black 5.60 t/ha
5	Dried molasses half-rate (½MS)	Black	Dried molasses half-rate (½MS) Black 2.8 t/ha
6	Mustard meal half-rate (½MM)	Black	Mustard meal half-rate (½MM) Black 1.12 t/ha
7	Mustard meal full rate (MM)	Clear	Mustard meal full rate (MM) Clear 2.24 t/ha
8	No fumigation	Clear	
9*	Mustard meal full rate (MM)	Black	Mustard meal full rate (MM) Black 2.24 t/ha
10*	Dried molasses half-rate + mustard half-rate (½ MS + ½ MM)	Black	Dried molasses half-rate + mustard half-rate (1/2 MS + 1/2 MM) Black 2.8 t/ha + 1.12 t/ha

[a]Ten treatments were evaluated in 2020 and 2021 while five treatments (*) were implemented in 2022 based on their effectiveness from the previous 2 years.

2.2 Field plot preparation and experimental design

In mid-September of the years 2019, 2020, and 2021, three raised beds were created for each treatment plot, each 9.2 m long, 0.61 m wide, and 0.2 m high, with 1.5 m from the center of one bed to the other. Beds were pre-formed, and the organic amendment was added to the top of each bed and mixed with the soil at 15 cm soil depth as recommended previously (Murphy, 2020) using a rototiller to ensure even distribution. The beds were pulled and covered with a 0.025 mm black VaporSafe® totally impermeable film (TIF) made of polyethylene plastic mulch (Raven Industries, Inc., Sioux Falls, SD, U. S. A.). The experiment was arranged using a randomized block design, with each block or replication being the same size as the number of treatments (i.e., factor). Additionally, each treatment was assigned to one experimental unit within each block. The same design with four blocks was used each year. Each block consisted of 10 experimental units (plots) in 2020 and 2021, and 5 in 2022 and treatments were applied annually to the same plot area. Each treatment was applied to one experimental unit within the block were typically considered as random effects. For microbiome analysis, three replications per treatment were utilized to minimize sequencing costs, while four replications per treatment were used for yield data analysis.

2.3 Treatments selection

Ten experimental treatments using black or clear plastic mulch were evaluated in 2020 and 2021 (Table 1). Only five effective treatments for higher yield in 2020 and 2021 were further selected and evaluated in 2022.

The following materials were used in these experiments. During the summer, a mixture of cowpea and pearl millet cover crops were seeded to promote optimal growth. Before seeding in June, a standard compost application rate of 16.8 metric tons per hectare was applied, as reported by a local waste management consortium (Nuova Amit, 2007) and previous experience (McWhirt et al., 2014). After this, the vegetation was flail-mowed early September to evenly distribute the cut residue across the cover crop plots. The residue from the cover crops was then incorporated into the soil to a depth of 20 to 30 cm using a PTO-driven rototiller, as recommended by McWhirt et al. (2014).

To reduce production costs, we purchased dried molasses (5.60 t/ha) from Agricultural Carbon Source in Plant City, FL, U. S. A. and mustard meal (MM) in the form of BioFence™ (2.24 t/ha) from *Brassica carinata* at Volunteer Ag Products in Greenfield, TN, U. S. A. A half rate of MS and MM (½ MS + ½ MM) was also prepared. Two control treatments were used: pre-plant chemical fumigation using Pic-Clor 60 (60% chloropicrin and 40% 1, 3-dichloro propene; 196.15 kg/ha) from TriEst Ag Group, Inc., (Greenville, NC, U. S. A.) as a positive control and no fumigation and no amendment as a negative control. Fumigant beds were prepared by injecting Pic-Clor 60 with two knives per bed evenly spaced (12 to 15 cm soil depth). Two drip lines were placed about 2.5 cm beneath the soil surface and spaced approximately 0.3 m apart. The beds were covered with 0.025 mm black VaporSafe® TIF plastic mulch (Raven Industries, Inc., Sioux Falls, SD, U. S. A.). As reported previously (Shennan et al., 2014), all beds treated with organic amendments were saturated to a depth of 20 to 30 cm. This saturation was achieved by applying water at a pressure of 83 kPa for up to 6 hours or until beds were saturated, which facilitated the rapid breakdown of the organic amendments.

2.4 Planting

The application of readily biodegradable organic amendments is followed by irrigating the soil to its field capacity and maintaining anaerobic conditions for a specific duration known as the incubation period, which typically lasts from 3 to 6 weeks (Meshram et al., 2024; Shennan et al., 2014). This process influences the composition of the soil microbial community. The standard wait time after fumigation is three weeks before planting to prevent crop damage due to chemical residues. Therefore, 3 weeks after adding the organic amendments, the beds were aerated by puncturing holes in the plastic. The beds were planted with five-week-old seedlings, known as plugs, from the commercial strawberry variety 'Chandler' (Poling, 1993). This variety is commonly grown in North Carolina, USA (Samtani et al., 2019), and the seedlings were sourced from Aarons Creek Farms Inc. in Junction, VA, or Fresh-Pik Produce Inc. in Wilson, NC, U. S. A. between October 17 and 18 each year. Sixty plants were planted on each bed with offset twin rows at ~0.30 m between each plant. Subsequently, plants were watered and fertilized according to

standard production practices (Hoffmann et al., 2021). After the June harvest, the strawberry beds were broken up; the same treatment was applied to each plot and treated the same way every year.

2.5 Soil sampling

Soil samples for microbiome analysis were collected from the harvesting area of each plot, covering approximately 1.9 m^2 from the entrance of the central bed. To prevent plot interference across the years, all data were secured from the central beds of the three-bed plot. In 2019, soil samples (20 cores/plot) were collected from each treatment after applying organic amendments and Pic-Clor 60 and just one day before planting. For the second collection, soil samples were collected between the first and second week of April each year. A handheld soil probe (1.75 cm internal diameter) was used to collect 20 cores from the rhizosphere soil in the harvesting area at a depth of 15 cm. Approximately 500 grams of soil per replicate per treatment were collected and mixed well in a 10-liter bucket to create a bulk sample. In this study, the term "microbiome" pertains to the bacterial communities associated with this soil sample.

2.6 Marketable yield and data analysis

The yield data were collected from the inner 20-plant zone of the inner bed. The total marketable yield was recorded weekly in 2020 but semi-weekly in 2021 and 2022. Marketable yields were calculated in kilograms per hectare (kg/ha). The data was analyzed using the Statistical Analysis Software (SAS) Version 9.4 (SAS Institute, 2016) through analysis of variance (ANOVA). Two-way ANOVA was used to compare the effects of 10 treatments (Table 1) on strawberry yield. Mean values were then compared using Tukey's HSD test at $p \leq 0.05$ level. Spearman's rank correlation coefficient analysis was performed to determine the strength and direction (negative or positive) and to assess the r and *p*-values for the slope of the relationship between the 2020 and 2021 yield data. Based on these results, five treatments: the full rate of dried molasses (MS), the full rate of mustard meal (MM), half the rate of dried molasses, and half the rate of mustard meal (½ MS + ½ MM), fumigation treatment with Pic-Clor 60 and a control treatment without fumigation were selected and evaluated in 2022.

2.7 DNA extraction

DNA was extracted from 0.25 g of rhizosphere soil using the DNeasy PowerSoil® Pro kit (QIAGEN Sciences, Germantown, MD, U.S.A). The DNA was quantified using a Nanodrop 2000 spectrophotometer (Thermo Fisher Scientific, Waltham, MA, U.S.A). The final DNA concentration was adjusted to 20 ng/μl for each sample and then shipped to Novogene Corporation, Sacramento, CA, U.S.A.

2.8 Amplicon sequencing

The bacterial 16S ribosomal RNA (16S rRNA) gene amplicons were generated using the forward primer 515F and the reverse primer 806R, which target the V4 variable region (Caporaso et al., 2011). This approach enhances community clustering with the specified read length (Janssen, 2006; Klindworth et al., 2013; Liu et al., 2007). Standardized quantities of PCR products from each DNA sample were pooled and ligated with adapters following the manufacturer's guidelines (Illumina, San Diego, CA, U.S.A.). Sequencing was performed on the Illumina MiSeq platform using the MiSeq reagent kit v2 for 250 bp paired-end runs (Novogene Corporation, Sacramento, CA, U.S.A.).

2.9 Sequence data processing and bioinformatics

The sequencing data was processed using a Novogene proprietary pipeline.[1] The Quantitative Insights Into Microbial Ecology (QIIME) software Version 1.7.0 (Caporaso et al., 2010) was used to filter the raw sequence and obtain a high-quality clean sequence (Bokulich et al., 2013). Aligned clean sequences with SILVA Version 128 (Quast et al., 2013) using a confidence threshold of 80%. Sequences of barcodes, primers, and short sequences containing ambiguous base calls and homopolymer runs exceeding 6 bp were removed. Sequences that were unassigned or classified as Eukaryota, Archaea, mitochondria, and chloroplasts were excluded. The aligned sequences were examined for chimeric sequences using UCHIME (Edgar et al., 2011), and any chimeric sequences were removed. The processed sequences were then clustered into operational taxonomic units (OTUs) at a 97% similarity level using UPARSE software (Edgar, 2013) and BLASTn from NCBI.[2]

2.10 Sequence data analysis

Sequence data were analyzed using phyloseq Version 1.20.0 (McMurdie and Holmes, 2013) and an R software Version 4. 2.0 (R Core Team, 2022) and normalized using cumulative sum scaling in metagenomeSeq Version 1.18.0 (Paulson et al., 2014). The 16S rRNA training set from the Ribosomal Database Project Version 1.20 (Cole et al., 2014) was used to assign taxonomy to each OTU. Representative sequences were identified at the genus and species level, and the OTUs were utilized to compare bacterial communities in the soil across different treatments (Supplementary Table S1). Rarefaction curves were created based on the observed OTUs (Caporaso et al., 2010). The number of sequences was normalized across all samples to 9,999 reads using the random subsample method. The Shannon's diversity index (H′) was used to assess bacterial community α-diversity (diversity within treatment) using mother Version 1. 34.1 (Schloss et al., 2009) using the minimum library size as the default with 1,000-bootstrap resampling. These indices were computed for treatments and years, and means were compared using Tukey's Honest Significant Difference (HSD) test ($p \leq 0.001$) to determine significant differences between treatments.

Venn diagrams (Heberle et al., 2015) were generated to compare OTU data of three organic amendment treatments (MS, MM, and ½ MS + ½ MM) with Pic-Clor 60 and NTC. The relative abundance of taxonomic ranks, such as phylum, genus, and species, were analyzed to identify the most abundant OTUs (greater than 0.3%) in each treatment. The two-part testing using a nonparametric Wilcoxon

1 https://www.novogene.com/
2 https://www.ncbi.nih.gov/

rank-based approach was used to compare the bacterial communities across different treatments and years (Wagner et al., 2011). Histograms were created to compare the common bacterial phyla with different organic amendment treatments and sampling years. They were selected to compare the abundance across treatments based on cumulative subsampling (CSS). Evolutionary trees were generated to compare the common bacterial genera using MUSCLE Version 3.8.31 (Edgar, 2004). Differentially enriched genera were visualized using ternary plots to identify the predominant bacterial species (Bulgarelli et al., 2015). This approach allowed for a comparison of individual organic amendments with Pic-Clor 60 and the negative control (NTC). The density of circles observed in the plots represents the relative abundance and distribution patterns of different bacterial species.

The β-diversity of the bacterial community was analyzed to generate Bray–Curtis dissimilarity using PAST software Version 4.03 (Hammer et al., 2001). After normalization, we examined the relative abundances of OTUs across each taxonomic rank in every sample to assess community dissimilarity coefficients between pairwise treatments using the R package metagenomeSeq Version 1.18.0 (Paulson et al., 2014). Heatmaps were employed to visualize the data, and a value of 0.00 indicated that the two treatments were identical. Tukey's HSD test assessed mean differences using a significance level ($p \leq 0.05$). To determine if bacterial community composition clustered according to treatments, non-metric multidimensional scaling (NMDS) was conducted using the Bray–Curtis dissimilarity index with PAST software Version 4.03 (Hammer et al., 2001). Additionally, a stress value greater than 0.3 indicates a poor representation, while a stress value below 0.01 signifies a uniform or excellent representation of the bacterial community composition. Normalized data were used to assess variations in bacterial taxa across treatments. The detected community of taxa in each sample was compared to those in all other samples using analysis of similarity (ANOSIM) (Hammer et al., 2001). In ANOSIM data analysis, a probability value (P_{ANOSIM}) of ≤0.01 and an average correlation coefficient (R_{ANOSIM}) of 0.98 indicates a strong relationship or significant similarities between the two treatments. In contrast, a high p value, such as $P_{ANOSIM} = 0.5$, along with a low R_{ANOSIM} (ranging from 0.2 to 0.4), suggests a weak correlation or notable dissimilarities between the two treatments.

3 Results

3.1 Sequencing and reads associated with the soil microbiomes

Refraction curves typically reached a plateau, indicating that most of the community diversity had been sequenced and was sufficient for analysis (*data not shown*). Regardless of treatments, in 2020, amplified soil DNA showed the highest total raw and effective sequence (Supplementary Figures 1A–D).

3.2 Total OTUs associated with the soil microbiomes

The distribution of bacterial communities varied across treatments and years. The bacterial shared total OTUs in soil treated with MS, MM, and ½ MS + ½ MM differed significantly ($p \leq 0.0001$) from Pic-Clor 60 and NTC each year (Supplementary Figures S2A–L). Overall, the total number of shared OTUs was significantly higher by 35 to 45% in the soil following all organic amendment treatments. The lowest total number of shared OTUs across all treatments occurred in 2019, with counts ranging from 3,078 to 3,265 (Supplementary Figures S2A–F). In contrast, all treatments achieved the highest number of shared OTUs in 2021, with counts ranging from 8,194 to 8,258 (Supplementary Figures S2G–L). The total shared OTUs for MS showed greater significance in 2019 and 2022, but not in the intervening years.

3.3 Bacterial abundance changes over time

The CSS-normalized OTU data analysis of bacterial relative abundance indicated that eight phyla were prevalent across the treatments (Figures 1A–D). These predominant phyla included *Acidobacteria*, *Actinobacteria*, *Bacteroidota*, *Chloroflexi*, *Firmicutes*, *Patescibacteria*, *Planctomycetes*, and *Proteobacteria*, were common to all year soils sampled. The impact of organic amendments on the relative abundance of bacterial communities varied based on the treatments applied and the years examined. For example, significant differences were observed each year in the abundance of the bacterial phyla *Actinobacteria* and *Proteobacteria* between the organic amendment treatments (MS, MM, and ½ MS + ½ MM) and the positive control (Pic-Clor 60) (Figures 1A–D). Generally, the dominant bacterial phyla across all treatments were *Firmicutes*, *Proteobacteria*, and *Actinobacteria*, among others. *Proteobacteria* was more abundant in the plots treated with Pic-Clor 60 in 2022 than in other sampling years. *Firmicutes* were less abundant in the control treatments in 2019 and 2020 than those that received organic amendments. *Proteobacteria* showed a slight increase in abundance across all years following organic amendment treatments. *Chloroflexota* (specifically *Chloroflexi*) was more abundant in the MM and MS + MM treatments than in the others in 2021 (Figure 1C).

Phylogenetic evolutionary trees were analyzed to determine the relationships among key bacterial genera under various treatments. For example, the genus *Bacillus* was found to be predominantly present in all three organic amendments across the years (Figures 2A–D). Similarly, regardless of the organic amendment treatments, *Sphingomonas* was observed in 2020, KD4-96 in 2021, and *Burkholderia* in 2022. The assembled reads were further analyzed using a ternary plot to confirm the effects of organic amendments on bacterial functional enrichment categories at the species level, which helped identify the bacterial species that support microbial establishment in the strawberry rhizosphere. The average abundance of the dominant bacterial species associated with the OTUs found in soil varied with different organic amendments and across the sampling years (Figures 3A–L). Ternary plots indicated that in 2019, the most frequently detected species included *Chitophagaceae bacterium* and *Rhodanobacter.* In 2020, *Microcoleus* spp., *Bacillus aryabhattai*, *Terrabacter*, and *Clostridium saccharoperbutylaceto* were predominant. In 2021, *C. saccharoperbutylaceto* and *Bacillus funiculus* were the most common, while in 2022; the frequently detected species included *Bradyrhizobium alkalii*, *Komagataeibacter saccharivora*, and *Bacillus azotoformans* (Figures 3A–L). Overall, the presence of these

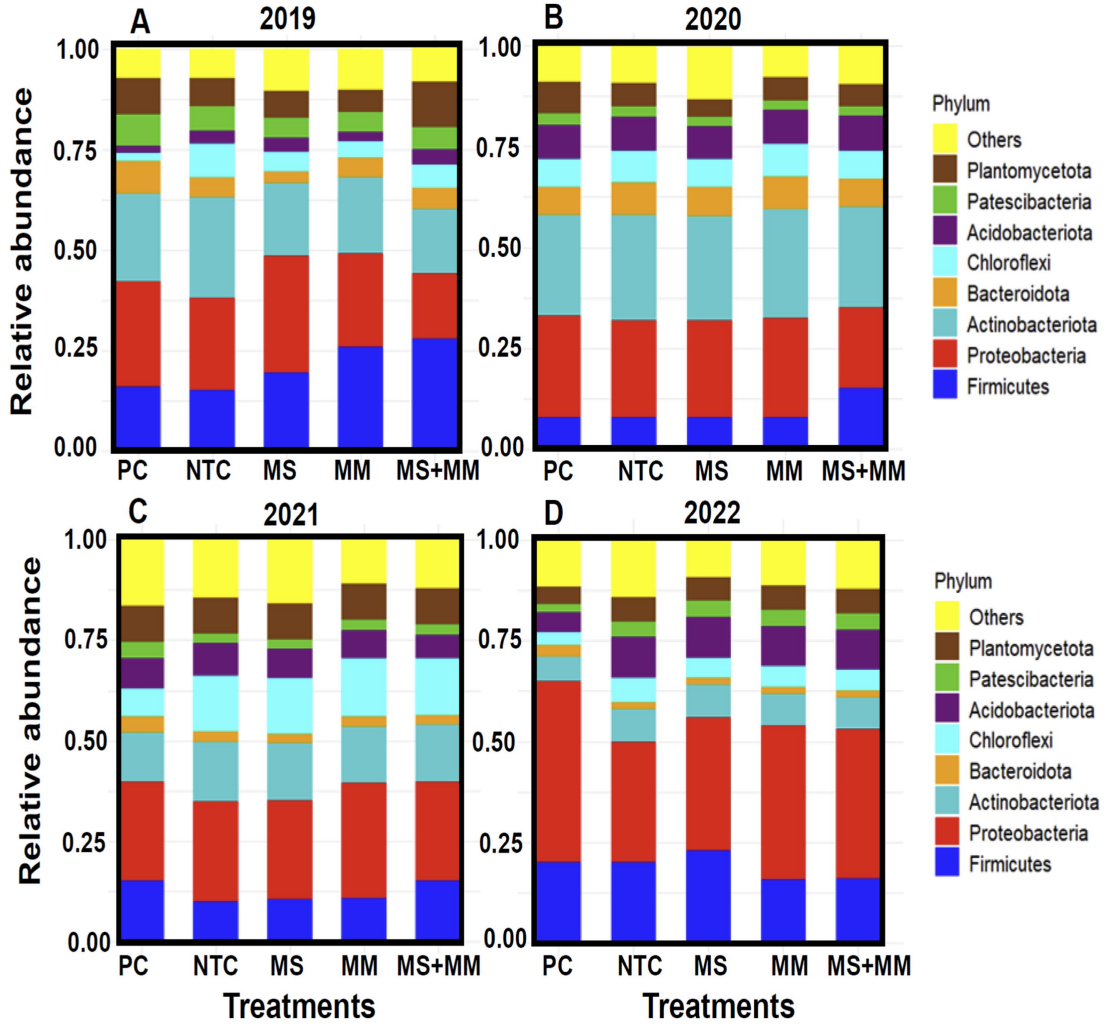

FIGURE 1
Stacked bar charts display the relative abundance of predominant bacteria at the phylum level (Y-axis) in soil samples collected over 4 years: 2019 **(A)**, 2020 **(B)**, 2021 **(C)**, and 2022 **(D)**. Sequence data from three replications in each treatment for 2019 to 2022 were used to determine the relative abundance of the top eight bacteria at the phylum level. Unknownphyla are categorized as "others." Each bacterial phylum in each treatment isrepresented by the same color for each year, corresponding to three organic amendments (X-axis): dried molasses (MS), mustard meal (MM), and a combination of half-rate of both (½ MS + ½ MM). The control treatments included a non-amended control (NTC) and chemical soil fumigation with Pic-Clor 60 (PC).

potentially beneficial bacteria demonstrated resilience across all the experiments.

3.4 Effects of organic amendments on the α-diversity of bacterial communities

The α-diversity for each sample using the Shannon diversity index (H′) was used to assess the diversity of bacterial communities in the soil. The results indicated that α-diversity varied significantly among treatments over the years (Figures 4A–D). Notably, the α-diversity in soil treated with Pic-Clor 60 was significantly lower ($p \leq 0.001$) than in the other treatments. The lowest H′ ranging from 8.2 to 8.5, was recorded in 2019 with the application of Pic-Clor 60. Furthermore, the reduction in H′ was more pronounced across all treatments in 2019 compared to other years. In all organic treatments, H′ in 2021 was higher, falling between 11 and 11.5, compared to the range of 10 to 10.5 observed in 2019, 2020, and 2022 (Figures 4A–D). Additionally, the α-diversity of bacterial communities showed no significant differences in soil treated with MS, MM, and NTC in 2021, with H′ values ranging from 9.5 to 11.5.

3.5 Effects of organic amendment treatments on the β-diversity of bacterial communities

β-diversity analysis was performed to assess the differences in bacterial diversity among the treatments (Figures 5A–D). The results indicated that Pic-Clor 60 significantly influenced bacterial β-diversity in the soil (Tukey's HSD test, $p \leq 0.001$), with dissimilarity coefficients ranging from 0.329 in 2019 to 0.133 in 2020. Most samples from the respective treatments displayed low coefficient values and did not differ significantly from each other or negative control (NTC),

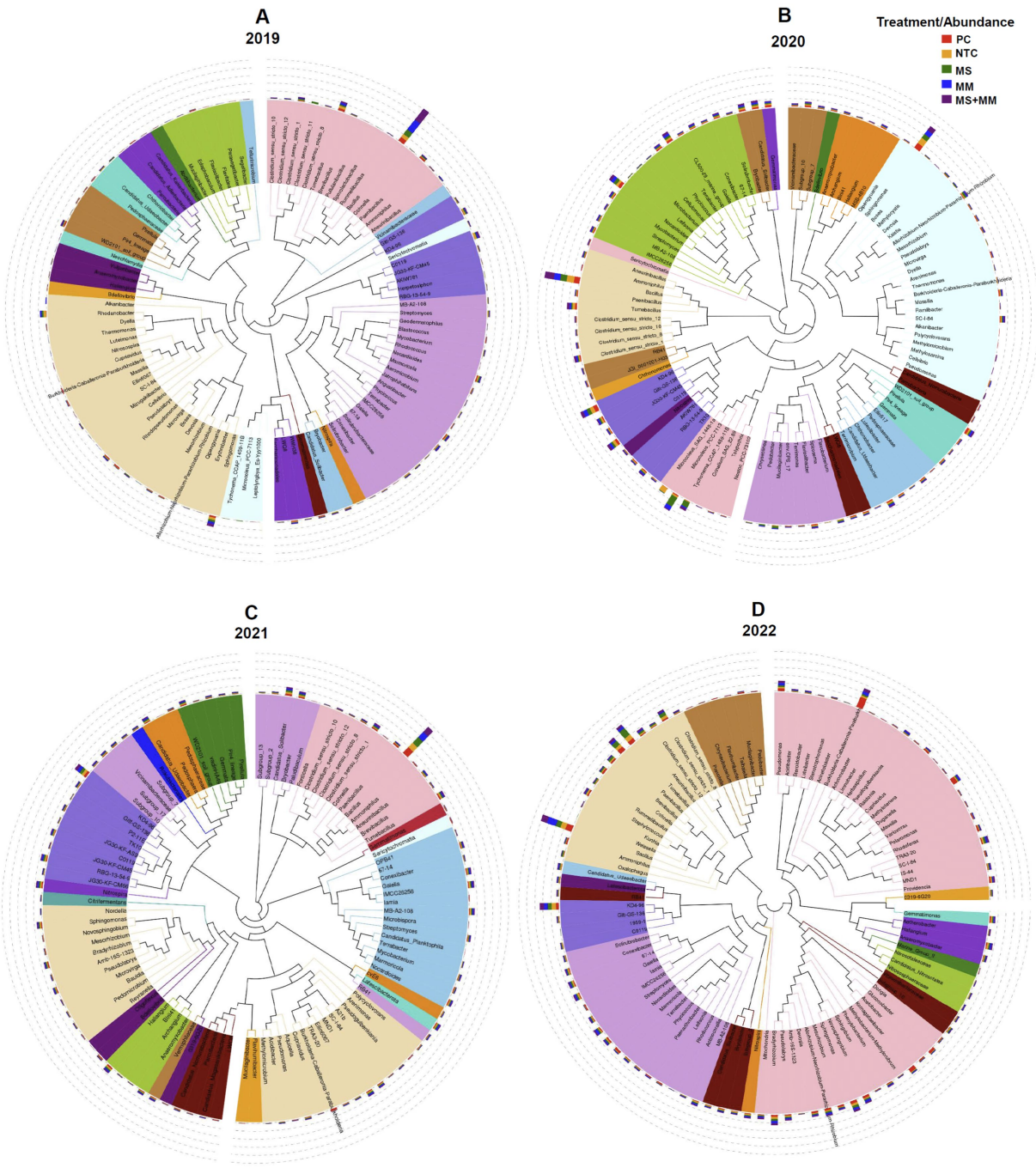

FIGURE 2
The evolutionary phylogenetic trees of the most abundant bacterial genera in soil samples collected over 4 years: 2019 **(A)**, 2020 **(B)**, 2021 **(C)**, and 2022 **(D)** are presented in response to three organic amendments: dried molasses (MS), mustard meal (MM), and a combination of half-rate of both (½ MS + ½ MM). The controls included non-amended control (NTC) and chemical soil fumigation with Pic-Clor 60 (PC). The sequence data from three replications in each treatment were utilized for bacterial community analysis to construct the trees. In the innermost circle, different branches with colors represent bacterial phyla. The outermost circle with a stacked bar graph displays the relative abundance of the bacterial genus in each treatment. The same color for each year represents each treatment.

indicating a high degree of similarity among them. For example, the dissimilarity coefficients for all organic amendment treatments (MS, MM, and ½ MS + ½ MM) and NTC were consistently below 0.1 and showed no significant differences across years (Figures 5A–D).

To assess the variation in bacterial communities across different treatments and sampling years, we visualized the OTU data using Non-metric Multidimensional Scaling (NMDS) plots (Figures 6A–D). In both 2019 and 2022, the soil bacterial communities in plots treated with Pic-Clor 60 displayed distinct clustering and significantly different bacterial composition ($p < 0.0001$), indicating the highest degree of dissimilarity compared to other treatments (Figures 6A–D). In contrast, the bacterial communities in plots treated with organic

10.3389/fsufs.2025.1550106

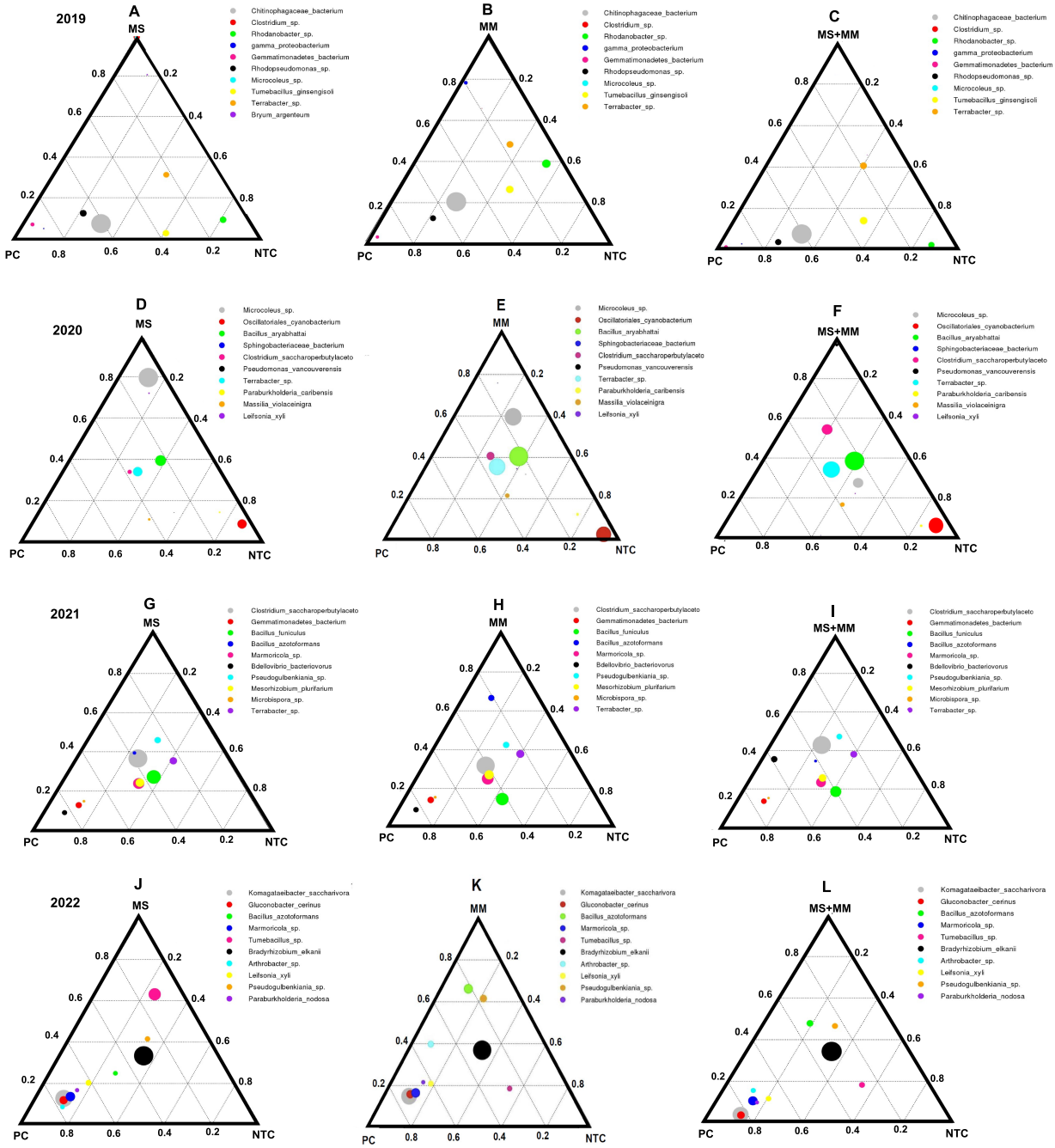

FIGURE 3
Ternary plots illustrate the average abundance of the dominant bacterial species found in soil samples collected over 4 years: 2019 **(A)**, 2020 **(B)**, 2021 **(C)**, and 2022 **(D)**. The sequence data from three replications in each treatment from 2019 to 2022 were used for the bacterial community analysis. Each ternary plot is represented as a triangle with sides scaled from zero to one, and the data can be expressed in terms of either proportions or absolute values. Each side of the triangle corresponds to one of the three measured components. The axes are arranged as follows: the X-axis is at the bottom of the plot, the Y-axis is on the right, and the Z-axis is on the left. A point is plotted on the triangle so that a line drawn perpendicular to each side from the point intersects at the respective component values. The impacts of three organic amendments were examined: dried molasses (MS), mustard meal (MM), and a combined half-rate of both (½ MS + ½ MM), along with a non-amended control (NTC) and a chemical soil fumigation treatment using Pic-Clor 60 (PC). The proportions of the three components in the plots are unconstrained, varying from zero to one. The size of each circle and color in the plots indicates the abundance of specific bacterial species in the soil.

amendments (e.g., MM, MS, or a combination of ½ MS and ½ MM) did not show significant differences in composition when compared to those treated with Pic-Clor 60 and the negative control (NTC) during 2020 and 2021. During these years, clustering by treatment was less distinct (Figures 6A–D). The stress values remained low throughout the years (i.e., < 0.3), ranging from 0.124 to 0.183. This indicates a strong representation of the bacterial community composition and a shift towards more stress-tolerant species. Overall, communities in soil amended with organic treatments were significantly different in composition from those in soil treated with

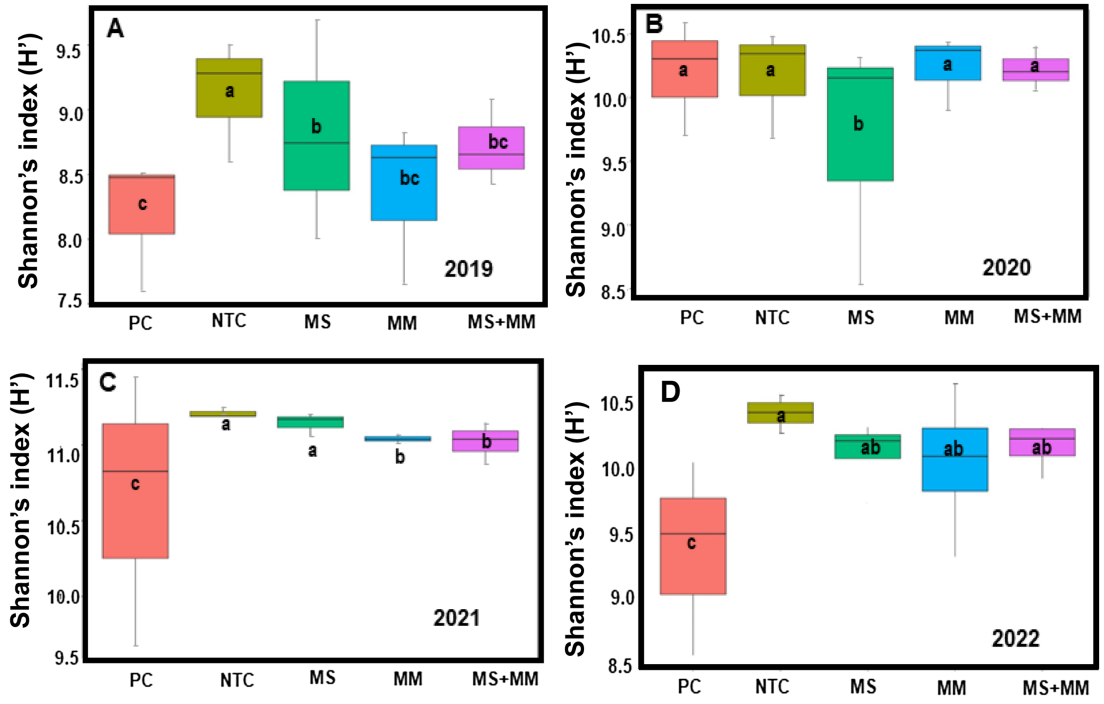

FIGURE 4
Comparison of the α-diversity of bacterial communities found in soil samples collected over 4 years: 2019 **(A)**, 2020 **(B)**, 2021 **(C)**, and 2022 **(D)** in response to three organic amendments: dried molasses (MS), mustard meal (MM), and a combination half-rate of both (½ MS + ½ MM). The controls included non-amended control (NTC) and chemical soil fumigation with Pic-Clor 60 (PC). The sequence data from three replications in each treatment from 2019 to 2022 were used for bacterial community analysis in the soil. The boxplots display Shannon's index (H') on the Y-axis and treatments on the X-axis. The same color for each year represents each treatment. Mean values followed by the same letter are not significantly different based on Tukey's honest significant difference test ($p \leq 0.05$).

Pic-Clor 60 in 2022 ($P_{ANOSIM} \leq 0.07$ and $R_{ANOSIM} \geq 0.42$). However, the bacterial communities observed in 2019 ($P_{ANOSIM} \leq 0.24$ and $R_{ANOSIM} \geq 0.49$) and 2020 ($P_{ANOSIM} \leq 0.73$ and $R_{ANOSIM} \geq -0.13$), and in 2021 ($P_{ANOSIM} \leq 0.78$ and $R_{ANOSIM} \geq -0.14$) suggested some degree of overlap between the bacterial compositions across treatments (Supplementary Table S2).

3.6 Effects of organic amendment treatments on strawberry yield

Across 3 years, the total marketable yield fluctuated annually, with the lowest yield observed in 2020. Generally, cumulative marketable yields ranged from 4,775 kg/ha to 29,815 kg/ha (Figures 7A–C). Plots covered with clear plastic (NTC-CLR) in 2020 and 2021 displayed low marketable yields. Similarly, plots using compost/cover crop (CC + Comp) and plots covered with clear plastic (CLR), whether amended with MM full rate (MM-CLR) or not amended (NTC-CLR), also reported the lowest yields in both years. In 2021, all non-CLR treatments were similar (Figure 7B). Spearman's correlation coefficient was used to examine organic amendments' positive or negative influence on yield and the relationship between yields in 2020 and 2021. The coefficient value of 0.98 was highly significant ($p \leq 0.0001$) (Supplementary Figure S3), indicating that the treatments that resulted in the highest yield in 2020 also led to the highest yield in 2021. The MS at full rate, the MM at half rate (½ MM), and the ½ MS + ½ MM combination produced higher yields than the NTC and showed similar yields as the Pic-Clor 60 in 2020 (Figure 7A). In 2022, the ½ MS + ½ MM combination and MS full rate amendments generated higher yields compared to both the NTC and Pic-Clor 60, while the MM full rate produced marketable berries equivalent to the Pic-Clor 60 treatment and higher than the NTC (Figure 7C).

4 Discussion

The experiments examine the association of bacterial communities with strawberry soil in North Carolina, USA. The results indicate that organic amendments can alter the bacterial microbiome in strawberry fields and increase crop yield. This effect selectively enriches certain bacteria populations known to be beneficial in plant production systems, aligning with previous studies that examined various organic amendments and agricultural byproducts used with anaerobic soil disinfestation (ASD) in different states across the United States (Adhikari and Louws, 2022; Adhikari et al., 2023; Bernard et al., 2014; Rosskopf et al., 2020; Strauss and Kluepfel, 2015; Testen et al., 2021). Therefore, investigating the interactions of the factors that shape the bacterial microbiome is crucial.

This study investigates the effects of two common organic amendments, molasses, and mustard meal on bacterial community composition, diversity, and strawberry yield. The results suggest that these treatments increased yields compared to the non-treated control (NTC) in two out of 3 years. They performed similarly to, or even better than, the fumigation treatment in all three years.

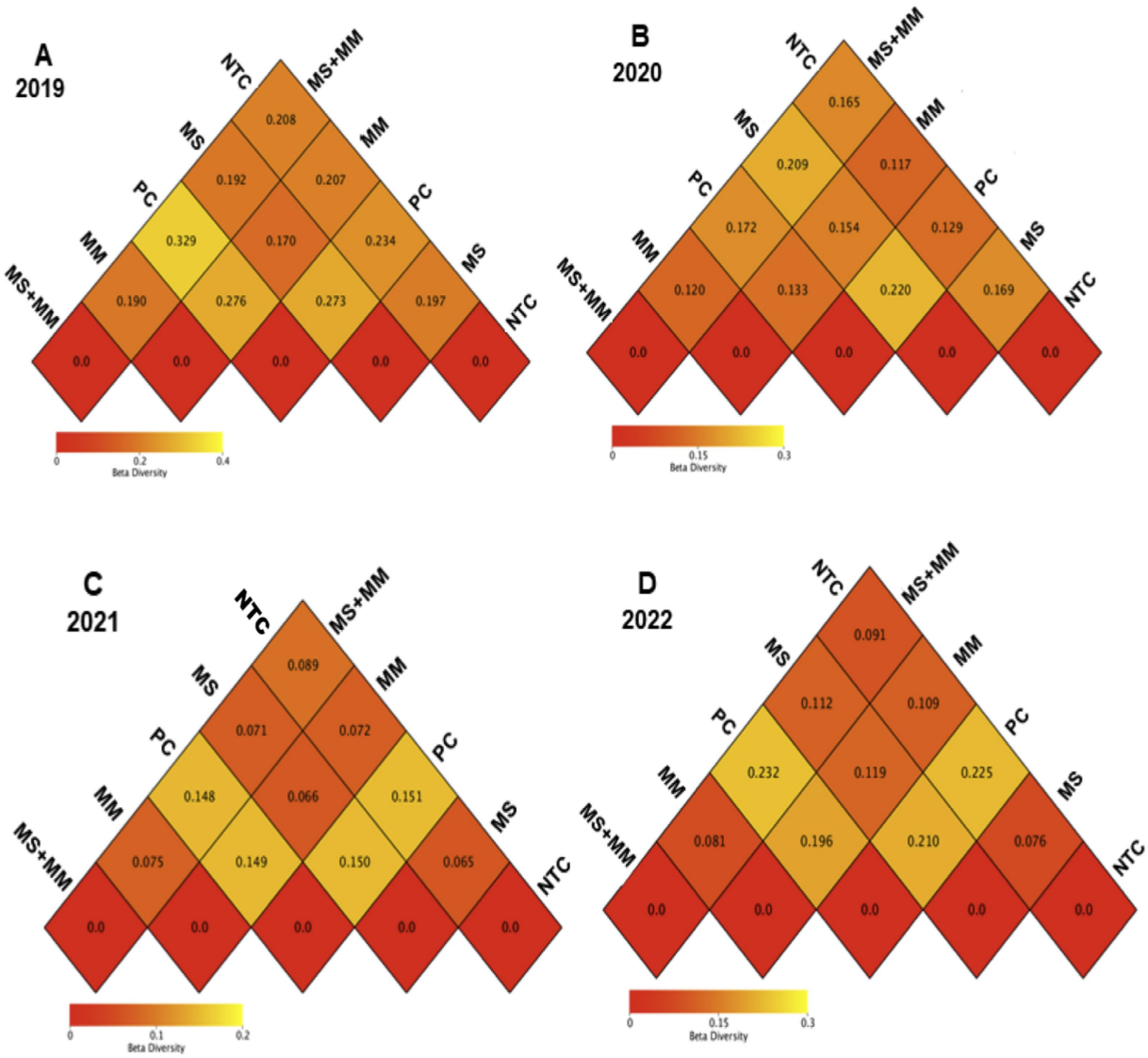

FIGURE 5
Comparison of the β-diversity of bacterial communities found in soil samples collected over 4 years: 2019 **(A)**, 2020 **(B)**, 2021 **(C)**, and 2022 **(D)** in response to three organic amendments: dried molasses (MS), mustard meal (MM), and a combination half-rate of both (½ MS + ½ MM). The controls included non-amended control (NTC) and chemical soil fumigation with Pic-Clor 60 (PC). The sequence data from three replications in each treatment from 2019 to 2022 were used for bacterial community analysis in soil. Heatmaps were created to compare the dissimilarity coefficients and compared according to Tukey's honest significant difference test ($p \leq 0.001$). The dissimilarity coefficient score shows red for a decrease and green for an increase in bacterial β-diversity in treatment-paired comparisons.

This supports our hypothesis that organic amendments can positively impact microbial communities and enhance crop yields. A previous study demonstrated that organic amendments positively influenced bacterial diversity, which can enhance nutrient turnover and provide additional nutrients for plant growth (Fan et al., 2021). These amendments are essential for maintaining soil microbial communities and offer various benefits, including improved organic matter decomposition, enhanced soil structure, and health, increased crop yields, and suppression of soilborne pathogens (Bonilla et al., 2012; Liu et al., 2021; Luo et al., 2018; Thangarajan et al., 2013; Shu et al., 2022). Specifically, the application of mustard meal at rates of 4.4 to 6.6 tons per hectare and molasses at 20 to 25 tons per hectare has been shown to positively alter microbial communities and impact crop yields (Mazzola et al., 2015, 2018; Poret-Peterson et al., 2019; Testen and Miller, 2018).

Application different rates of the mustard meal (2.2, 4.4, and 6.6 t/ha) were compared on specific rootstock genotypes to manage apple replant disease in the Pacific region (Wang and Mazzola, 2019). Another organic amendment, dried molasses, has been applied at a rate of 20 to 22 t/ha to mitigate soil-borne pathogens in tomatoes in Florida and Ohio (Testen and Miller, 2018; Vincent et al., 2022). Liquid or dried MS has also been used at a rate of 20 to 22 t/ha in tomatoes in Florida and Ohio (Testen and Miller, 2018; Vincent et al., 2022). Although using higher rates of MS and MM has been shown to affect soil microbial communities positively (Mazzola et al., 2015; Testen and Miller, 2018; Vincent et al., 2022; Wang and Mazzola, 2019), excessive application of organic amendments can lead to

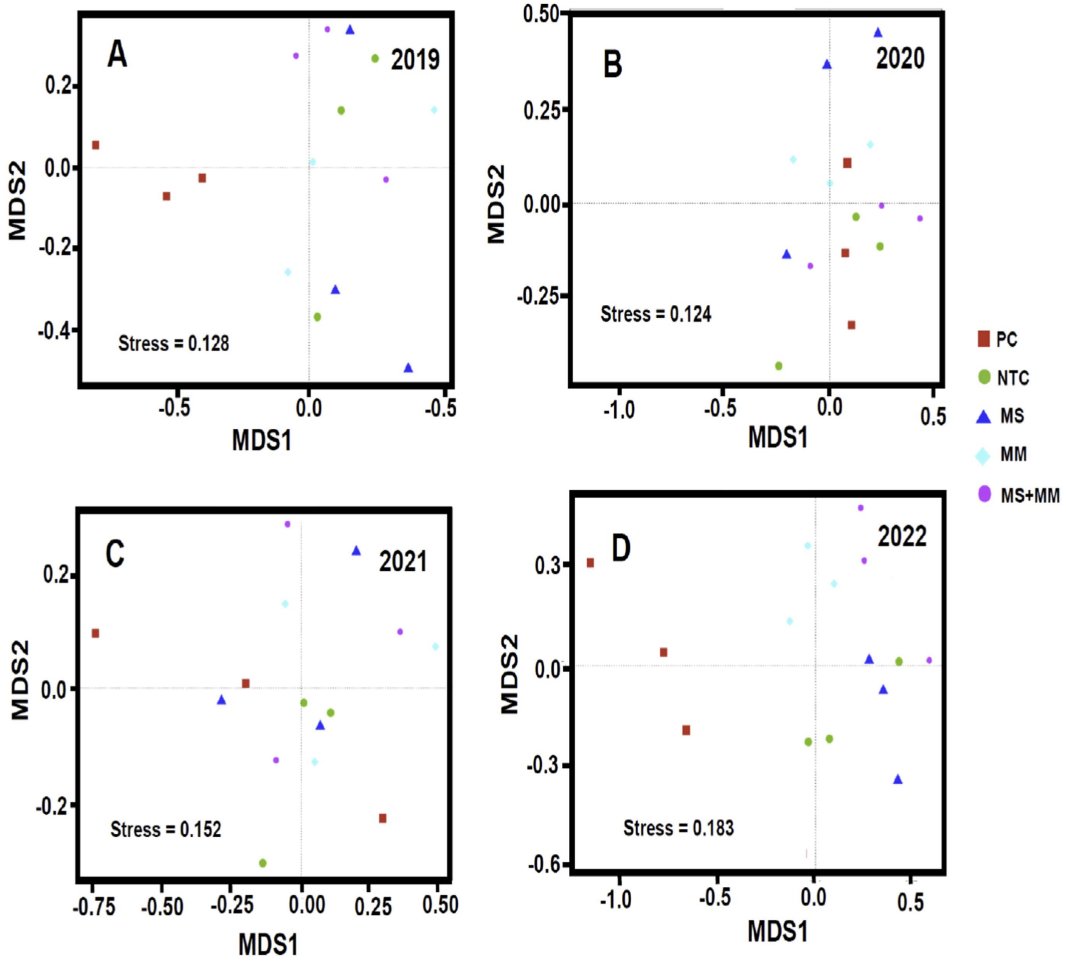

FIGURE 6
Ordination was conducted using nonmetric multidimensional scaling (NMDS) of operational taxonomic units, accompanied by the analysis of similarity (ANOSIM) (Hammer et al., 2001). This analysis was performed on soil samples collected over four years: 2019 **(A)**, 2020 **(B)**, 2021 **(C)**, and 2022 **(D)**. The study investigated the impact of three organic amendments: dried molasses (MS), mustard meal (MM), and a combination of half-rates of both (½ MS + ½ MM), along with a non-amended control (NTC) and chemical soil fumigation using Pic-Clor 60 (PC). Each treatment is represented by a symbol and organized by the same color for each year. The sequence data from three replications in each treatment from 2019 to 2022 were combined and used for bacterial community analysis. In ANOSIM data analysis, a probability value (P_{ANOSIM}) of ≤0.01 and an average correlation coefficient (R_{ANOSIM}) of 0.98 indicate a strong relationship or significant similarities between the two treatments. In contrast, a high *p* value, such as P_{ANOSIM} = 0.5, and a low R_{ANOSIM} (ranging from 0.2 to 0.4) suggests a weak correlation or dissimilarities between the two treatments.

increased production costs. Therefore, we determined whether dried molasses (5.60 t/ha) and mustard meal (2.24 t/ha) and a combination of half the rate of both (1:1 ratio), would still be effective in treating the bacterial communities over three years during strawberry production. These rates were lower than those used in previous studies in other states (Mazzola et al., 2015; Testen and Miller, 2018; Vincent et al., 2022). Specific bacterial and fungal phyla were found to be more abundant in MM-treated soil compared to the control (Wang and Mazzola, 2019).

Some dominant taxa, e.g., *Actinobacteria* and *Proteobacteria*, were identified in this study in response to organic amendments. The application of MS and composted poultry litter to the soil can significantly enhance the microbial communities, including actinomycetes, arbuscular mycorrhizal fungi, Gram-positive and Gram-negative bacteria, and protozoa (Welbaum et al., 2004). Additionally, MS contains free sugars that support microbial communities (Bonanomi et al., 2020) and members of the *Bacteroidetes* and *Proteobacteria* quickly flourish in nutrient-rich environments (Fierer et al., 2007). Intriguingly, the members of *Firmicutes* phylum exhibited low abundance in the soil initially, but it became more prevalent following all organic amendment treatments in the subsequent years. Previous investigations also suggest that members of *Firmicutes* were enriched in soils treated with organic amendments (Poret-Peterson et al., 2019; Strauss and Kluepfel, 2015). In contrast, soil treated with rice bran did not show the presence of the *Firmicutes* phylum (Mazzola et al., 2018). Field crops like rice (Edwards et al., 2015), wheat (Ai et al., 2015), and smooth cordgrass (Hong et al., 2015) have indicated an increase in the relative abundance of *Proteobacteria*. Evidence from several studies suggested that management practices (Edwards et al., 2015; Wipf et al., 2021), soil depths (Schlatter et al., 2018, 2020), host genotypes (Hassani et al., 2023; Peiffer et al., 2013), geographic sites (Edwards et al., 2015, 2018), and microenvironments, and soil physiochemical properties near the rhizoplane of plants play critical roles in plant-microbe associations (Singh et al., 2004; Trivedi

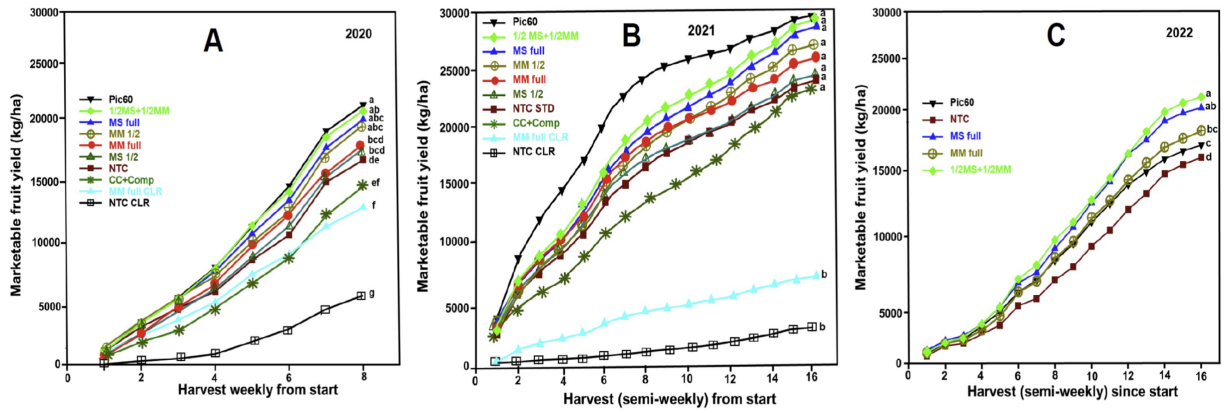

FIGURE 7
Impacts of organic amendments on strawberry yield in North Carolina, U. S. A. In 2020 and 2021, 10 treatments were evaluated, and each treatment was represented by a line graph and organized in the same color for each year. Acronyms for treatments are defined in materials and methods (Table 1). **(A)** The cumulative yield (Y-axis) was harvested over eight weekly harvests (X-axis) in 2020. As denoted by the same letter, the cumulative marketable yield progress was not significantly different based on repeated measures analysis and the Fisher Protected LSD ($p \leq 0.05$). **(B)** The cumulative marketable yield progress curves at semi-weekly harvests in 2021 revealed that each curve when followed by the same letter, exhibited no significant difference based on repeated measures analysis and the Fisher Protected LSD ($p \leq 0.05$). An independence analysis indicated a significant correlation between the 10 treatment ranking of total yield in 2020 and the yield in 2021 (Supplementary Figure S3). **(C)** Three promising organic amendments treatments: dried molasses (MS), mustard meal (MM), and a combination half-rate of both (½ MS + ½ MM), and the controls included non-amended control (NTC) and chemical soil fumigation with Pic-Clor 60 (PC) were selected and further evaluated in 2022. The cumulative marketable yield progress curves at semi-weekly harvests showed each amendment increased yield compared to the NTC, and yields were greater or similar to the fumigation treatment denoted by the same letter based on repeated measures analysis and the Fisher Protected LSD ($p \leq 0.05$).

et al., 2020). The differences in bacterial community composition observed across years in this study could be attributed to micro-environmental conditions in the soil, plant growth, and interactions between plants and microbiomes (Mowlick et al., 2013, 2014; Robinson, 2005; Stremińska et al., 2014; Stromberger et al., 2005).

Cumulative marketable yields varied considerably between years, but yields in 2020 and 2022 were lower than in 2021. Due to the COVID-19 pandemic during harvest in 2020, movement restrictions led to a lack of timely crop and pest management practices, resulting in irreversible losses at different crop stages and affecting the quantity and quality of the harvest. Variation in yield is frequently a function of fall and winter conditions that impact plant growth and yield potential (Poling, 1993). Throughout the study, only one strawberry cultivar., 'Chandler' was used. When plating soil suspensions on semi-selective media from various treatments, we observed several novel strains of beneficial Gram-positive and Gram-negative bacteria associated with strawberry plants. For example, one such strain is *Bacillus aryabhattai*, which can dissolve phosphate, synthesize siderophores, produce plant growth hormones, and enhance salt tolerance (Bhattacharyya et al., 2017; Liu et al., 2020; Park et al., 2017; Shahid et al., 2022). Although these organic amendments positively affected bacterial composition and strawberry yield, it is essential to note that the experiments were conducted in just one location. Conducting additional studies in different places in the future can help mitigate potential biases and offer a more comprehensive understanding of how microbial diversity responds to organic amendments.

In conclusion, low MS and MM rates, each at half the usual amount, can enhance beneficial bacterial microbiomes and marketable yield in field-grown strawberries. This approach can also lower production costs compared to the high rates used in other studies. These findings have practical implications for improving agricultural practices and increasing strawberry yield. Next-generation sequencing technologies and culturomics can provide further insights into microbiome functions and plant-microbiome interactions. Ultimately, these findings could lead to biologically based solutions for improving soil and plant health and increasing crop yield in conventional and organic strawberry production systems.

Data availability statement

The original contributions presented in the study are included in the article/Supplementary material, further inquiries can be directed to the corresponding author.

Author contributions

TA: Conceptualization, Data curation, Formal analysis, Investigation, Methodology, Project administration, Resources, Supervision, Validation, Funding acquisition, Writing – original draft, Writing – review & editing. AP: Methodology, Writing – review & editing. FL: Funding acquisition, Writing – review & editing.

Funding

The author(s) declare that financial support was received for the research and/or publication of this article. The North Carolina Strawberry Association, the Southern Region Small Fruit Consortium, and USDA-NIFA-SCRI Grant # 2017-51181-26832 funded this study.

Acknowledgments

The authors thank John Garner and Jonathan Francki and other staff at Horticultural Crops Research Station, Castle Hayne, NC; David Baltzegar and other staff at Genomic Sciences Laboratory (GSL), North Carolina State University, Raleigh, NC; and Mohd Zubair and Cassidy Hardaway Novogene Corporation, Inc., Sacramento, CA, U. S. A. for their technical support.

Conflict of interest

The authors declare that the research was conducted in the absence of any commercial or financial relationships that could be construed as a potential conflict of interest.

The author(s) declared that they were an editorial board member of Frontiers, at the time of submission. This had no impact on the peer review process and the final decision.

Generative AI statement

The author(s) declare that no Gen AI was used in the creation of this manuscript.

Publisher's note

All claims expressed in this article are solely those of the authors and do not necessarily represent those of their affiliated organizations, or those of the publisher, the editors and the reviewers. Any product that may be evaluated in this article, or claim that may be made by its manufacturer, is not guaranteed or endorsed by the publisher.

Supplementary material

The Supplementary material for this article can be found online at: https://www.frontiersin.org/articles/10.3389/fsufs.2025.1550106/full#supplementary-material

References

Abawi, G. S., and Widmer, T. L. (2000). Impact of soil health management practices on soilborne pathogens, nematodes and root diseases of vegetable crops. *Appl. Soil Ecol.* 15, 37–47. doi: 10.1016/S0929-1393(00)00070-6

Adhikari, T. B., and Louws, F. J. (2022). Improving soil health for strawberry production in the southeast: providing tools for growers. Project #: 2021-R-09. Submitted to the Southern Region Small Fruit Consortium (SRSFC), Raleigh, North Carolina, USA.

Adhikari, T. B., Philbrick, A., and Louws, F. J. (2023). Deciphering the active strawberry microbiome associated with roots and rhizosphere soil. The paper was presented at the 12th International Society of Plant Pathology at the Satellite event Phytobiomes Research for Plant Health, held from August 19-25, 2023, in Lyon, France.

Ahn, J.-H., Song, J., Kim, B.-Y., Kim, M.-S., Joa, J.-H., and Weon, H.-Y. (2012). Characterization of the bacterial and archaeal communities in rice field soils subjected to long-term fertilization practices. *J. Microbiol.* 50, 754–765. doi: 10.1007/s12275-012-2409-6

Ai, C., Liang, G., Sun, J., Wang, X., He, P., Zhou, W., et al. (2015). Reduced dependence of rhizosphere microbiome on plant-derived carbon in 32-year long-term inorganic and organic fertilized soils. *Soil Biol. Biochem.* 80, 70–78. doi: 10.1016/j.soilbio.2014.09.028

Bandara, B., and Janaranjana, S. (2021). Understanding the economic sustainability of strawberry farming in North Carolina. *Int. J. Food Agric. Eco.* 9, 191–202. doi: 10.2139/ssrn.4319525

Bebber, D. P., and Richards, V. R. (2020). A meta-analysis of the effect of organic and mineral fertilizers on soil microbial diversity. *Ecology*. 175:104450. doi: 10.1101/2020.10.04.325373

Bender, S. F., Wagg, C., and van der Heijden, M. G. A. (2016). An underground revolution: biodiversity and soil ecological engineering for agricultural sustainability. *Trends Ecol. Evol.* 31, 440–452. doi: 10.1016/j.tree.2016.02.016

Bernard, E., Larkin, R. P., Tavantzis, S., Erich, M. S., Alyokhin, A., and Gross, S. (2014). Rapeseed rotation, compost, and biocontrol amendments reduce soilborne diseases and increase tuber yield inorganic and conventional potato production systems. *Plant Soil* 374, 611–627. doi: 10.1007/s11104-013-1909-4

Bhattacharyya, C., Bakshi, U., Mallick, I., Mukherji, S., Bera, B., and Ghosh, A. (2017). Genome-guided insights into the plant growth promotion capabilities of the physiologically versatile *Bacillus aryabhattai* strain AB211. *Front. Microbiol.* 8:41. doi: 10.3389/fmicb.2017.00411

Bokulich, N. A., Subramanian, S., Faith, J. J., Gevers, D., Gordon, J. I., Knight, R., et al. (2013). Quality filtering vastly improves diversity estimates from Illumina amplicon sequencing. *Nat. Methods* 10, 57–59. doi: 10.1038/nmeth.2276

Bonanomi, G., De Filippis, F., Zotti, M., Idbella, M., Cesarano, G., Al-Rowaily, S., et al. (2020). Repeated applications of organic amendments promote beneficial microbiota, improve soil fertility, and increase crop yield. *Appl. Soil Ecol.* 156:103714. doi: 10.1016/j.apsoil.2020.103714

Bonilla, N., Gutiérrez-Barranquero, J. A., De Vicente, A., and Cazorla, F. M. (2012). Enhancing soil quality and plant health through suppressive organic amendments. *Diversity* 4, 475–491. doi: 10.3390/d4040475

Bulgarelli, D., Garrido-Oter, R., Münch, P. C., Weiman, A., Dröge, J., Pan, Y., et al. (2015). Structure and function of the bacterial root microbiota in wild and domesticated barley. *Cell Host Microbe* 17, 392–403. doi: 10.1016/j.chom.2015.01.011

Caporaso, J. G., Kuczynski, J., Stombaugh, J., Bittinger, K., Bushman, F. D., Costello, E. K., et al. (2010). QIIME allows analysis of high-throughput community sequencing data. *Nat. Methods* 7, 335–336. doi: 10.1038/nmeth.f.303

Caporaso, J. G., Lauber, C. L., Walters, W. A., Berg-Lyons, D., Lozupone, C. A., Turnbaugh, P. J., et al. (2011). Global patterns of 16S rRNA diversity at a depth of millions of sequences per sample. *Proc. Natl. Acad. Sci. USA* 108, 4516–4522. doi: 10.1073/pnas.1000080107

Cole, J. R., Wang, Q., Fish, J. A., Chai, B., McGarrell, D. M., Sun, Y., et al. (2014). Ribosomal database project: data and tools for high throughput rRNA analysis. *Nucleic Acids Res.* 42, D633–D642. doi: 10.1093/nar/gkt1244

Daugovish, O., Muramoto, J., Shennan, C., and Zavatta, M. (2021). Plant-derived carbon sources for anaerobic soil disinfestation in Southern California. *Glob. J. Agric. Innov. Res. Dev.* 8, 169–175. doi: 10.15377/2409-9813.2021.08.13

Daugovish, O., Valdes-Berriz, M., Muramoto, J., Shennan, C., Zavatta, M., and Henry, P. (2023). Carbon sources for anaerobic soil disinfestation in Southern California strawberry. *Agronomy* 13:1635. doi: 10.3390/agronomy13061635

Deng, S., Wipf, H. M. L., Pierroz, G., Raab, T. K., Khanna, R., and Coleman-Derr, D. (2019). A plant growth-promoting microbial soil amendment dynamically alters the strawberry root bacterial microbiome. *Sci. Rep.* 9:17677. doi: 10.1038/s41598-019-53623-2

Edgar, R. C. (2004). MUSCLE: multiple sequence alignment with high accuracy and high throughput. *Nucleic Acids Res.* 32, 1792–1797. doi: 10.1093/nar/gkh340

Edgar, R. (2013). UPARSE: highly accurate OTU sequences from microbial amplicon reads. *Nat. Methods* 10, 996–998. doi: 10.1038/nmeth.2604

Edgar, R. C., Haas, B. J., Clemente, J. C., Quince, C., and Knight, R. (2011). UCHIME improves the sensitivity and speed of chimera detection. *Bioinformatics* 27, 2194–2200. doi: 10.1093/bioinformatics/btr381

Edwards, J., Johnson, C., Santos-Medellín, C., Lurie, E., Podishetty, N. K., Bhatnagar, S., et al. (2015). Structure, variation, and assembly of the root-associated microbiomes of rice. *Proc. Natl. Acad. Sci. USA* 112, 911–920. doi: 10.1073/pnas.1414592112

Edwards, J. A., Santos-Medellín, C. M., Liechty, Z. S., Nguyen, B., Lurie, E., Eason, S., et al. (2018). Compositional shifts in root-associated bacterial and archaeal microbiota track the plant life cycle in field-grown rice. *PLoS Biol.* 16, 1–28. doi: 10.1371/journal.pbio.2003862

Expósito, A., García, S., Giné, A., Escudero, N., Herranz, S., Pocurull, M., et al. (2022). Effect of molasses application alone or combined with *Trichoderma asperellum* T-34 on *Meloidogyne* spp. management and soil microbial activity in organic production systems. *Agronomy* 12:1508. doi: 10.3390/agronomy12071508

Fageria, N. K., Baligar, V. C., and Bailey, B. A. (2005). Role of cover crops in improving soil and row crop productivity. *Comm. Soil Sci. Plant Anal.* 36, 2733–2757. doi: 10.1080/00103620500303939

Fan, K., Delgado-Baquerizo, M., Guo, X., Wang, D., Zhu, Y., and Chu, H. (2021). Biodiversity of keystone phylotypes determines crop production in a 4-decade fertilization experiment. *ISME J.* 15, 550–561. doi: 10.1038/s41396-020-00796-8

Feng, M., Adams, J. M., Fan, K., Shi, Y., Sun, R., Wang, D., et al. (2018). Long-term fertilization influences community assembly processes of soil diazotrophs. *Soil Biol. Biochem.* 126, 151–158. doi: 10.1016/j.soilbio.2018.08.021

Fierer, N., Bradford, M. A., and Jackson, R. B. (2007). Toward an ecological classification of soil bacteria. *Ecology* 88, 1354–1364. doi: 10.1890/05-1839

Goss, M. J., Tubeileh, A., and Goorahoo, D. (2013). A review of the use of organic amendments and the risk to human health. *Adv. Agron.* 120, 275–379. doi: 10.1016/B978-0-12-407686-0.00005-1

Gravuer, K., Gennet, S., and Throop, H. L. (2019). Organic amendment additions to rangelands: a meta-analysis of multiple ecosystem outcomes. *Glob. Chang. Biol.* 25, 1152–1170. doi: 10.1111/gcb.14535

Hammer, O., Harper, D. A., and Ryan, P. D. (2001). PAST: paleontological statistics software package for education and data analysis. *Palaeontol. Electron.* 4:9. Available at: http://palaeo-electronica.org/2001_1/past/issue1_01.htm

Hannum, S. M. (2004). Potential impact of strawberries on- human health: a review of the science. *Crit. Rev. Food Sci. Nutr.* 44, 1–17. doi: 10.1080/10408690490263756

Hassani, M.-A., Gonzalez, O., Hunter, S. S., Holmes, G., Hewavitharana, S., Ivors, K., et al. (2023). Microbiome network connectivity and composition linked to disease resistance in strawberry plants. *Phytobiomes* 7, 298–311. doi: 10.1094/PBIOMES-10-22-0069-R

Heberle, H., Meirelles, G. V., da Silva, F. R., Telles, G. P., and Minghim, R. (2015). Interacti Venn: a web-based tool for the analysis of sets through Venn diagrams. *BMC Bioinform.* 16, 1–7. doi: 10.1186/s12859-015-0611-3

Hewavitharana, S. S., Klarer, E., Reed, A. J., Leisson, R., Poirier, B., Honaas, L., et al. (2019). Temporal dynamics of the soil metabolome and microbiome during simulated anaerobic soil disinfestation. *Front. Microbiol.* 10:2365. doi: 10.3389/fmicb.2019.02365

Hewavitharana, S. S., Ruddell, D., and Mazzola, M. (2014). Carbon source-dependent antifungal and nematicidal volatiles derived during anaerobic soil disinfestation. *Eur. J. Plant Pathol.* 140, 39–52. doi: 10.1007/s10658-014-0442-5

Hoffmann, M., Volk, E., and Peres, N. (2021). Strawberry plasticulture producers guide. Gen. Tech. Rep. SRS-260r. Asheville, NC: U.S. Department of Agriculture Forest Service, Southern Research Station. 53 p. Nulty, Steven; Gavazzi, Michael, eds. Hurricane preparation and recovery in the Southeastern United States.

Hong, Y., Liao, D., Hu, A., Wang, H., Chen, J., Khan, S., et al. (2015). Diversity of endophytic and rhizoplane bacterial communities associated with exotic *Spartina alterniflora* and native mangrove using Illumina amplicon sequencing. *Can. J. Microbiol.* 61, 723–733. doi: 10.1139/cjm-2015-0079

Janssen, P. H. (2006). Identifying the dominant soil bacterial taxa in libraries of 16S rRNA and 16S rRNA genes. *Appl. Environ. Microbiol.* 72, 1719–1728. doi: 10.1128/AEM.72.3.1719-1728.2006

Klindworth, A., Pruesse, E., Schweer, T., Peplies, J., Quast, C., Horn, M., et al. (2013). Evaluation of general 16S ribosomal RNA gene PCR primers for classical and next-generation sequencing-based diversity studies. *Nucleic Acids Res.* 41:e1. doi: 10.1093/nar/gks808

Larkin, R. P. (2015). Soil health paradigms and implications for disease management. *Annu. Rev. Phytopathol.* 53, 199–221. doi: 10.1146/annurev-phyto-080614-120357

Li, P., Li, Y., Xu, L., Zhang, H., Shen, X., Xu, H., et al. (2021). Crop yield-soil quality balance in double cropping in China's upland by organic amendments: a meta-analysis. *Geoderma* 403:115197. doi: 10.1016/j.geoderma.2021.115197

Li, W., and Liu, Q. (2019). Changes in fungal community and diversity in strawberry rhizosphere soil after 12 years in the greenhouse. *J. Integ. Agric.* 18, 677–687. doi: 10.1016/S2095-3119(18)62003-9

Liu, H., Brettell, L. E., Qiu, Z., and Singh, B. K. (2020). Microbiome-mediated stress resistance in plants. *Trends Plant Sci.* 25, 733–743. doi: 10.1016/j.tplants.2020.03.014

Liu, S., Khan, M. H., Yuan, Z., Hussain, S., Cao, H., and Liu, Y. (2021). Response of soil microbiome structure and network profiles to four soil amendments in mono-cropping strawberry greenhouse. *PLoS One* 16:e0245180. doi: 10.1371/journal.pone.0245180

Liu, Z., Lozupone, C., Hamady, M., Bushman, F. D., and Knight, R. (2007). Short pyrosequencing reads suffice for accurate microbial community analysis. *Nucleic Acids Res.* 35:e12. doi: 10.1093/nar/gkm541

Louws, F. J. (2009). "IPM for soilborne disease management for vegetable and strawberry crops in SE" in Plant pathology in the 21st century: Contributions to the 9th international congress. eds. U. Gisi, I. Chet and M. L. Gullino (New York: Springer), 217–227.

Louws, F. J., Grabowski, M. A., Fernandez, G. E., and Vollmer, J. B. (2000). Compost as an alternative to methyl bromide in plasticulture strawberry production. Proc. Intl. Res. Conf. Methyl Bromide Alternatives and Emissions Reduction 33/1–33/2.

Luo, G., Li, L., Friman, V.-P., Guo, J., Guo, S., Shen, Q., et al. (2018). Organic amendments increase crop yields by improving microbe-mediated soil functioning of agroecosystems: a meta-analysis. *Soil Biol. Biochem.* 124, 105–115. doi: 10.1016/j.soilbio.2018.06.002

Matthiessen, J. N., and Kirkegaard, J. A. (2006). Biofumigation and enhanced biodegradation: opportunity and challenge in soilborne pest and disease management. *Crit. Rev. Plant Sci.* 25, 235–265. doi: 10.1080/07352680600611543

Mazzola, M., and Brown, J. (2010). Efficacy of brassicaceous seed meal formulations for the control of apple replant disease in organic and conventional orchard production systems. *Plant Dis.* 94, 835–842. doi: 10.1094/PDIS-94-7-0835

Mazzola, M., Hewavitharana, S. S., and Strauss, S. L. (2015). Brassica seed meal soil amendments transform the rhizosphere microbiome and improve apple production through resistance to pathogen reinfestation. *Phytopathology* 105, 460–469. doi: 10.1094/PHYTO-09-14-0247-R

Mazzola, M., Muramoto, J., and Shennan, C. (2018). In California field trials, anaerobic disinfestation induced changes to the soil microbiome, disease incidence, and strawberry fruit yields. *Appl. Soil Ecol.* 127, 74–86. doi: 10.1016/j.apsoil.2018.03.009

McMurdie, P. J., and Holmes, S. (2013). Phyloseq: an R package for reproducible interactive analysis and graphics of microbiome census data. *PLoS One* 8:e61217. doi: 10.1371/journal.pone.0061217

McWhirt, A., Fernandez, G., and Schroeder-Moreno, M. (2014). Sustainable practices for Plasticulture strawberry production in the southeast. NC Cooperative Extension Publication. Available online at: http://content.ces.ncsu.edu/sustainable-practices-for-plasticulturestrawberry-production-in-the-southeast/ (Accessed September 20, 2024).

Meshram, S., Philbrick, A. N., and Adhikari, T. B. (2024). Anaerobic soil disinfestation: a biologically-based solution for sustainable crop production. *Front. Hortic.* 3:1436782. doi: 10.3389/fhort.2024.1436782

Mowlick, S., Inoue, T., Takehara, T., Tonouchi, A., Kaku, N., Ueki, K., et al. (2014). Usefulness of Japanese-radish residue in biological soil disinfestation to suppress spinach wilt disease accompanying with proliferation of soil bacteria in the Firmicutes. *Crop Prot.* 61, 64–73. doi: 10.1016/j.cropro.2014.03.010

Mowlick, S., Yasukawa, H., Inoue, T., Takehara, T., Kaku, N., Ueki, K., et al. (2013). Suppression of spinach wilt disease by biological soil disinfestation incorporated with Brassica juncea plants in association with changes in soil bacterial communities. Crop protect. 54, 185-193.

Murphy, S. (2020). FS1328 Soil for raised beds. Rutgers Cooperative Extension Fact Sheet FS1328. (Accessed February 16, 2025).

Nuova Amit (2007). Company material published in the yearbook 2007 by CIC - consortium of Italian composters. Available online at: http://compost.it/schede_soci/nuovaamit.pdf.

Oldfield, E. E., Wood, S. A., and Bradford, M. A. (2018). Direct effects of soil organic matter on productivity mirror those observed with organic amendments. *Plant Soil* 423, 363–373. doi: 10.1007/s11104-017-3513-5

Pankhurst, C. E. (1997). "Biodiversity of soil organisms as an indicator of soil health" in Biological indicators of soil health. eds. C. E. Pankhurst, B. M. Doube and V. V. S. R. Gupta (Wallingford: CAB International), 297–324.

Park, Y. G., Mun, B. G., Kang, S. M., Hussain, A., Shahzad, R., Seo, C. W., et al. (2017). *Bacillus aryabhattai* SRB02 tolerates oxidative and nitrosative stress and promotes the growth of soybean by modulating the production of phytohormones. *PLoS One* 12:e0173203. doi: 10.1371/journal.pone.0173203

Paulson, J. N., Talukder, H., Pop, M., and Bravo, H. C. (2014). metagenomeSeq: Statistical analysis for sparse high-throughput sequencing. Bioconductor. Available online at http://cbcb.umd.edu/software/metagenomeSeq (Accessed November 20, 2023).

Peiffer, J. A., Spor, A., Koren, O., Jin, Z., Tringe, S. G., Dangl, J. L., et al. (2013). Diversity and heritability of the maize rhizosphere microbiome under field conditions. *Proc. Natl. Acad. Sci. USA* 110, 6548–6553. doi: 10.1073/pnas.1302837110

Poling, E. B. (1993). Strawberry plasticulture in North Carolina: II. Preplant, planting, and postplant considerations for growing Chandler strawberry on black plastic mulch. *Hort Technol.* 3, 383–393. doi: 10.21273/HORTTECH.3.4.383

Poret-Peterson, A. T., Albu, S., McClean, A. E., and Kluepfel, D. A. (2019). Shifts in soil bacterial communities as a function of carbon source used during anaerobic soil disinfestation. *Front. Environ. Sci.* 6:60. doi: 10.3389/fenvs.2018.00160

Poret-Peterson, A. T., Sayed, N., Glyzewski, N., Forbes, H., González-Orta, E. T., and Kluepfel, D. A. (2020). Temporal responses of microbial communities to anaerobic soil disinfestation. *Microb. Ecol.* 80, 191–201. doi: 10.1007/s00248-019-01477-6

Quast, C., Pruesse, E., Yilmaz, P., Gerken, J., Schweer, T., Yarza, P., et al. (2013). The SILVA ribosomal RNA gene database project: improved data processing and web-based tools. *Nucleic Acids Res.* 41, D590–D596. doi: 10.1093/nar/gks1219

R Core Team (2022). A language and environment for statistical computing. Vienna, Austria: R Foundation for Statistical Computing.

Rana, T. S., and Gu, S. (2020). Growth and yield of organic day-neutral strawberries in low tunnels inside high tunnels in North Carolina. *Hort Sci.* 55, 336–343. doi: 10.21273/HORTSCI14491-19

Robinson, P. J. (2005). North Carolina weather and climate. North Carolina: University of North Carolina Press, Chapel Hill, 256.

Rosskopf, E., Di Gioia, F., Hong, J. C., Pisani, C., and Kokalis-Burelle, N. (2020). Organic amendments for pathogen and nematode control. *Annu. Rev. Phytopathol.* 58, 277–311. doi: 10.1146/annurev-phyto-080516-035608

Rysin, O., McWhirt, A., Fernandez, G., Louws, F. J., and Schroeder-Moreno, M. (2015). Economic viability and environmental impact assessment of three different strawberry production systems in the southeastern United States. *Hort Technol.* 25, 585–594. doi: 10.21273/HORTTECH.25.4.585

Saleem, M., Hu, J., and Jousset, A. (2019). More than the sum of its parts: microbiome biodiversity as a driver of plant growth and soil health. *Annu. Rev. Ecol. Evol. Syst.* 50, 145–168. doi: 10.1146/annurev-ecolsys-110617-062605

Samtani, J. B., Rom, C. R., Friedrich, H., Fennimore, S. A., Finn, C. E., and Petran, A. (2019). The status and future of the strawberry industry in the United States. *Hort Technol.* 29, 11–24. doi: 10.21273/HORTTECH04135-18

SAS Institute (2016). Statistical analysis software (SAS) User's guide version 9.4. Cary, NC, USA: SAS Institute, Inc.

Schlatter, D. C., Kahl, K., Carlson, B., Huggins, D. R., and Paulitz, T. (2018). Fungal community composition and diversity vary with soil depth and landscape position in a no-till wheat-based cropping system. *FEMS Microbiol. Ecol.* 94:94. doi: 10.1093/femsec/fiy098

Schlatter, D. C., Kahl, K., Carlson, B. R., Huggins, D. R., and Paulitz, T. C. (2020). Soil acidification modifies soil depth-microbiome relationships in a no-till wheat cropping system. *Soil Biol. Biochem.* 149:107939. doi: 10.1016/j.soilbio.2020.107939

Schloss, P. D., Westcott, S. L., Ryabin, T., Hall, J. R., Hartmann, M., Hollister, E. B., et al. (2009). Introducing mothur: open-source, platform-independent, community-supported software for describing and comparing microbial communities. *Appl. Environ. Microbiol.* 75, 7537–7541. doi: 10.1128/AEM.01541-09

Shahid, M., Zeyad, M. T., Syed, A., Singh, U. B., Mohamed, A., Bahkali, A. H., et al. (2022). Stress-tolerant endophytic isolate *Priestia aryabhattai* BPR-9 modulates physio-biochemical mechanisms in wheat (*Triticum aestivum* L.) for enhanced salt tolerance. *Int. J. Environ. Res. Public Health* 19:10883. doi: 10.3390/ijerph191710883

Shennan, C., Muramoto, J., Lamers, J., Mazzola, M., Rosskopf, E. N., Kokalis-Burelle, N., et al. (2014). Anaerobic soil disinfestation for soilborne disease control in strawberry and vegetable systems: current knowledge and future directions. *Acta Hortic.* 1044, 165–175. doi: 10.17660/ActaHortic.2014.1044.20

Shu, X., He, J., Zhou, Z., Xia, L., Hu, Y., Zhang, Y., et al. (2022). Organic amendments enhance soil microbial diversity, microbial functionality and crop yields: a meta-analysis. *Sci. Total Environ.* 829:154627. doi: 10.1016/j.scitotenv.2022.154627

Singh, B. K., Millard, P., Whiteley, A. S., and Murrell, J. C. (2004). Unraveling rhizosphere–microbial interactions: opportunities and limitations. *Trends Microbiol.* 12, 386–393. doi: 10.1016/j.tim.2004.06.008

Strauss, S. L., and Kluepfel, D. A. (2015). Anaerobic soil disinfestation: a chemical-independent approach to pre-plant control of plant pathogens. *J. Integr. Agric.* 14, 2309–2318. doi: 10.1016/S2095-3119(15)61118-2

Stremińska, M. A., Runia, W. T., Termorshuizen, A. J., Feil, H., and van der Wurff, A. W. G. (2014). Anaerobic soil disinfestation in microcosms of two sandy soils. *Commun. Agric. Appl. Biol. Sci.* 79, 15–19

Stromberger, M. E., Klose, S., Ajwa, H., Trout, T., and Fennimore, S. (2005). Microbial populations and enzyme activities in soils fumigated with methyl bromide alternatives. *Soil Sci. Soc. Am.* 69, 1987–1999. doi: 10.2136/sssaj2005.0076

Sydorovych, O., Safley, C. D., Ferguson, L. M., Poling, E. B., Fernandez, G. E., Brannen, P. M., et al. (2006). Economic evaluation of the methyl bromide alternatives for the production of strawberries in the southeastern US. *Hort Technol.* 16, 118–128. doi: 10.21273/HORTTECH.16.1.0118

Testen, A. L., and Miller, S. A. (2018). Carbon source and soil origin shape soil microbiomes and tomato soilborne pathogen populations during anaerobic soil disinfestation. *Phytobiomes* 2, 138–150. doi: 10.1094/PBIOMES-02-18-0007-R

Testen, A. L., Rotondo, F., Mills, M. P., Horvat, M. M., and Miller, S. A. (2021). Evaluation of agricultural byproducts and cover crops as anaerobic soil disinfestation carbon sources for managing a soilborne disease complex in high tunnel tomatoes. *Front. Sustain. Food Syst.* 5:645197. doi: 10.3389/fsufs.2021.645197

Thangarajan, R., Bolan, N. S., Tian, G., Naidu, R., and Kunhikrishnan, A. (2013). Role of organic amendment application on greenhouse gas emission from soil. *Sci. Total Environ.* 465, 72–96. doi: 10.1016/j.scitotenv.2013.01.031

Trivedi, P., Leach, J. E., Tringe, S. G., Sa, T., and Singh, B. K. (2020). Plant–microbiome interactions: from community assembly to plant health. *Nat. Rev. Microbiol.* 18, 607–621. doi: 10.1038/s41579-020-0412-1

Vincent, I. R., Paudel, B. R., Guo, H., Rosskopf, E. N., Di Gioia, F., Hong, J. C., et al. (2022). Spatial and temporal changes of soil microbial communities in field tomato production as affected by anaerobic soil disinfestation. *Front. Sustain. Food Syst.* 6:838635. doi: 10.3389/fsufs.2022.838635

Wagner, B. D., Robertson, C. E., and Harris, J. K. (2011). Application of two-part of statistics for comparison of sequence variant counts. *PLoS One* 6:e20296. doi: 10.1371/journal.pone.0020296

Wang, L., and Mazzola, M. (2019). Field evaluation of reduced rate Brassicaceae seed meal amendment and rootstock genotype on the microbiome and control of apple replant disease. *Phytopathology* 109, 1378–1391. doi: 10.1094/PHYTO-02-19-0045-R

Welbaum, G. E., Sturz, A. V., Dong, Z., and Nowak, J. (2004). Managing soil microorganisms to improve productivity of agro-ecosystems. *Crit. Rev. Plant Sci.* 23, 175–193. doi: 10.1080/07352680490433295

Welker, R. M., Louws, F. J., Driver, J. G. Smith, and Schiemann, C. A. (2008). On-farm research and extension activities to implement MB alternatives: an area-wide initiative update. Proc. of the Int. Res. Conf. on Methyl Bromide Alternatives and Emissions Reduction. 9/1–9/3. Available online at: http://mbao.org/2008/Proceedings/009WelkerRMBAOAREAWIDEFJL.pdf (Accessed July 12, 2023).

Wipf, H. M. L., Xu, L., Gao, C., Spinner, H. B., Taylor, J., Lemaux, P., et al. (2021). Agricultural soil management practices differentially shape the bacterial and fungal microbiomes of *Sorghum bicolor*. *Appl. Environ. Microbiol.* 87, e02345–e02320. doi: 10.1128/AEM.02345-20

Xia, Q., Rufty, T., and Shi, W. (2020). Soil microbial diversity and composition: links to soil texture and associated properties. *Soil Biol. Biochem.* 149:107953. doi: 10.1016/j.soilbio.2020.107953

Yang, H., Zhang, X., Qiu, X., Chen, J., Wang, Y., Zhang, G., et al. (2023). *Fusarium* wilt invasion results in a strong impact on strawberry microbiomes. *Plants (Basel).* 12:4153. doi: 10.3390/plants12244153

Zhou, Z., Wang, C., and Luo, Y. (2020). Meta-analysis of the impacts of global change factors on soil microbial diversity and functionality. *Nat. Commun.* 11:3072. doi: 10.1038/s41467-020-16881-7

frontiers | Frontiers in Sustainable Food Systems

TYPE Review
PUBLISHED 26 March 2025
DOI 10.3389/fsufs.2025.1549048

Check for updates

OPEN ACCESS

EDITED BY
Raffaella Balestrini,
National Research Council (CNR), Italy

REVIEWED BY
V. S. Saravanan,
Pondicherry University, India
Marika Pellegrini,
University of L'Aquila, Italy

*CORRESPONDENCE
Elizabeth Temitope Alori
aloritope@yahoo.com

RECEIVED 20 December 2024
ACCEPTED 10 March 2025
PUBLISHED 26 March 2025

CITATION
Alori ET, Onaolapo AO and Ibaba AL (2025) Cell free supernatant for sustainable crop production.
Front. Sustain. Food Syst. 9:1549048.
doi: 10.3389/fsufs.2025.1549048

COPYRIGHT
© 2025 Alori, Onaolapo and Ibaba. This is an open-access article distributed under the terms of the Creative Commons Attribution License (CC BY). The use, distribution or reproduction in other forums is permitted, provided the original author(s) and the copyright owner(s) are credited and that the original publication in this journal is cited, in accordance with accepted academic practice. No use, distribution or reproduction is permitted which does not comply with these terms.

Cell free supernatant for sustainable crop production

Elizabeth Temitope Alori[1,2,3]*, Abidemi Olubusayo Onaolapo[1,2,3] and Ayibanoa Lekoo Ibaba[1,2,3]

[1]Department of Crop and Soil Sciences, Landmark University, Omu-Aran, Nigeria, [2]SDG 2 (Zero Hunger) Research Group, Landmark University, Omu-Aran, Nigeria, [3]SDG 15 (Life on Land) Research Group, Landmark University, Omu-Aran, Nigeria

The increase in demand for food production due to the ever-increasing human population across the world requires that food production should grow exponentially. For agricultural food production to meet the needs of human requirements and demands there is a need for sustainable practices that will ensure production and availability of food without affecting soil health, soil biota and soil fertility. Over the years, many plant growth promoting bacteria (PGPB) strains have been identified and reported to provide a number of benefits to plants, including enhanced nutrient uptake, growth, and development as well as increased resistance to biotic and abiotic stress. However only a small number of them, are sold today, mostly due to the formulations' inability to support bacterial survival both during and after application in agroecosystems. PGPB strains that present these difficult constraints can be employed in the production of cell-free supernatants (CFSs), which are broth cultures that have undergone various mechanical and physical procedures to eliminate cells. The available literature suggests that CFS may be a reliable source of secondary metabolites for sustainable agriculture. This review therefore discusses cell free supernatant of various soil microorganisms that have been used in crop production and offered pertinent information about CFS for upcoming studies on CFSs as bio stimulant and biocontrol agents in sustainable agriculture. The significance, sources, applications, mechanisms of action of CFS and benefits of studies on CFS agricultural applications—both as a bio fertilizer and a biocontrol agent were studied.

KEYWORDS

agrobiotechnology, biofertilizers, bioinoculants, bioremediation, sustainable food production

Introduction

Conventional agriculture employed to increase agricultural production and meet the food demand of the ever-increasing human population heavily relies on excessive use of agrochemicals such as fertilizers, herbicides and pesticides (Li et al., 2022). However, this agricultural system, although increasing production, has proven unsustainable in the long run. Further nutrient input for instance, can result in a decline in soil fertility (Kopittke et al., 2019). The excessive and inappropriate use of agrochemicals pollute soil, air and water through nutrient leaching, causing a chemical imbalance across multiple ecosystems (Chandini et al., 2019). These chemical fertilizers and pesticides can also lead to soil acidification, greenhouse gas emissions, negative impacts on human health and harm to non-target organisms resulting in a loss of biodiversity (Li et al., 2020). Chemical fertilizers have considerable deleterious effects on soil, plants, humans and environmental sustainability increasing the costs and reducing profitability (Alori et al., 2019).

Therefore, there is a need for a more eco-friendly and sustainable methods that may be practiced without health hazards. The use of microbial inoculants holds great promise to improve crop yield without negative environmental and health risks (Alori et al., 2019). However, under harsh environmental condition, the impact of microbial inoculant diminishes (Naamala et al., 2023).

Cell-free supernatant is a liquid fraction obtained from microorganism cultures after centrifugation. It contains various plant growth-promoting compounds, enzymes and secondary metabolites such as antibiotics (Naamala et al., 2023). Microbial cell-free supernatant (CFS) has been reported to be associated with the strong proliferation of resident beneficial soil microbes that activate beneficial soil microorganisms; therefore, it is a safe, efficient and environmentally friendly approach to minimize shortfalls related to the technology of microbial inoculation (Morcillo et al., 2020).

The use of cell-free supernatant in sustainable crop production has garnered attention for its potential to promote plant growth, increase yield, and reduce the negative impact of chemical fertilizers and pesticides on the environment. The compounds are less likely to experience diminished effects under harsh environmental conditions. Additionally, they are generally required in low concentrations and are easier to store compared to live microbial cells (Naamala et al., 2022).

Cell-free supernatants can be extracted via several methods depending on the purpose of use of the supernatant. These methods include centrifugation and filtration that are appropriate for general applications (Subramanian et al., 2021; Zhou et al., 2022), solvent extraction and precipitation are useful for isolating specific metabolites (Gudiña et al., 2015; Santoyo et al., 2021), and Lyophilization method which is preferred for long-term storage (Sornsenee et al., 2021).

Extracted CFS has been stored by several researchers using various techniques. The following methods have reported. Refrigeration (4°C) Storage (Koohestani et al., 2018). Freezing (−20°C to −80°C) (Gunal Köroglu et al., 2024). Lyophilization (Freeze-Drying) Storage Technique: Šuchová et al. (2022) Spray Drying (Gullifa et al., 2023). Storage in Preservative Solutions (Hamad et al., 2022). Encapsulation Technique (Bassani et al., 2019).

Several researchers have reported the use of CFS in medicine and food. For example, Arrioja-Bretón et al. (2020), investigated the antimicrobial activity and storage stability of CFS from lactic acid bacteria and its applications with fresh beef. Mani-López et al. (2022) studied CFS production, composition, and the antimicrobial activity of CFS from LAB *in vitro*, on foods, and in active packaging. Mao et al. (2023) explored the impact of CFS of lactic acid bacteria on *Staphylococcus aureus* biofilm and its metabolites.

In agriculture, Wang et al. (2018) examined the application and mechanism of Bacillus subtilis in biocontrol of plant disease. Khamsuk et al. (2024) investigated the anti-microbial activities of CFS of plant growth promoting bacteria from rhizospheric soil of rice plant. Li et al. (2023), studied if the application of Bacillus subtilis promotes growth and quality of cucumber. Pellegrini et al. (2020) reviewed the application of CFS from plant growth-promoting bacteria in sustainable agriculture.

However, there is limited information on the comprehensive application of microbial CFS (from both bacteria and fungi) in agriculture and environmental remediation. This research aims to discuss the application of microbial CFS to various soil microorganisms for crop growth and yield improvement, crop protection, and crop response to abiotic stressors including the remediation of polluted soils. It emphasizes the significance of CFS in sustainable crop production. Sources of CFS, mechanisms of action, challenges and limitations were thoroughly explained.

Significance of cell-free supernatant in sustainable crop production

Cell-Free Supernatants are significantly important in sustainable crop production as follows:

Improving soil health

Cell-free supernatant contains various secondary metabolites, including organic acids, enzymes, and siderophores, which can enhance soil health. These compounds can stimulate the growth of beneficial microorganisms such as mycorrhizal fungi, rhizobia, and other nitrogen-fixing bacteria, ultimately improving soil fertility (Pellegrini et al., 2020). Microbial CFS supports the proliferation of resident beneficial soil microbes (Morcillo et al., 2022).

Enhancing plant growth and yield

Cell-free supernatant contains various plant growth-promoting compounds, including indole-3-acetic acid (IAA), gibberellins, cytokinins, and auxins. These compounds can enhance plant growth by promoting cell division, elongation, and differentiation (Naamala et al., 2023). Additionally, cell-free supernatant can improve nutrient uptake by plants by increasing the solubility and availability of essential minerals such as nitrogen, phosphorus, and potassium (Islam et al., 2016). *Bacillus subtilis* and *Bacillus licheniformis* can enhance plant growth and biomass production through the synthesis of various phytohormones, nitrogen fixation, phosphate solubilization, and ammonium ion production (Khan et al., 2018). Moreover, microbial CFS can suppress the growth of plant pathogens, thereby reducing the need for chemical pesticides (Islam et al., 2016). Plants treated with CFS exhibited a higher fruit yield than control plants (Imran et al., 2023).

Sources of cell-free supernatants

Cell free supernatants as shown in Figure 1 are obtained from bacteria, fungi, plant tissue, and animal tissue cultures. Bacterial cultures are the most common source of cell-free supernatant. Bacteria produce various secondary metabolites such as antibiotics, enzymes, and plant growth-promoting compounds, which are present in the cell-free supernatant (Kumar et al., 2020).

Fungal cultures are another source of cell-free supernatants. Fungi produce various secondary metabolites such as mycotoxins, antibiotics, and enzymes, which are present in the cell-free supernatant (Dozolme and Moukha, 2020; Nasrollahzadeh et al., 2022). These compounds are secreted by these microorganisms into the surrounding environment. Plant tissue cultures are also a potential source of cell-free supernatants. Plant cells produce various secondary metabolites such as phenolics, flavonoids, and alkaloids, which are present in the cell-free supernatant (Yadav and Yadav, 2023). These compounds are secreted by plant cells into the surrounding environment to defend against herbivores or pathogens.

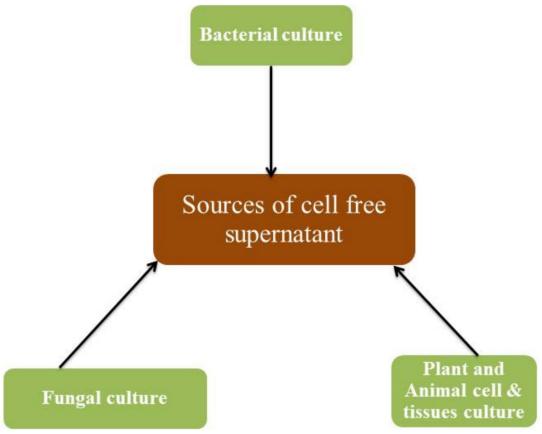

FIGURE 1
Sources of cell free supernatant.

Animal cell cultures are another potential source of cell-free supernatant. Animal cells produce various secondary metabolites such as cytokines, growth factors, and antibodies, which can be found in the cell-free supernatant (Feder-Mengus et al., 2008; Bourebaba et al., 2022). Figure 1 illustrates the various sources of cell free supernatant for agricultural purposes.

Methods for extracting microbial cell-free supernatants

To ensure only extracellular metabolites are obtained without microbial cell contamination, the extraction method of culturing the desired microorganism in the appropriate growth medium is critical. The type of bioactive compounds, desired purity, and intended application of CFS determine the choice of extraction method.

The first step is to culture the desired microorganism in the appropriate growth medium. The cells in culture can then be removed or separated using various methods.

For general applications, centrifugation and filtration are sufficient, while solvent extraction and precipitation are useful for isolating specific metabolites. For long-term storage, Lyophilization will be more appropriate.

i Centrifugation: The culture is centrifuged at 5,000–10,000 rpm for 10–20 min to pellet microbial cells (Majeedras et al., 2018). Differences in density allow centrifugation to separate cells from the liquid culture. The supernatant is then carefully collected without disturbing the pellet (Subramanian et al., 2021). This method is simple, cost-effective and fast. However, some microbial cells may remain in the supernatant, requiring additional filtration.

ii Filtration: This process involves using a membrane filter with an appropriate pore size to eliminate microbial cells and debris. Following centrifugation, the supernatant is filtered through 0.22 µm or 0.45 µm membrane filters to eliminate any remaining cells (Zhou et al., 2022). Sterile filtration guarantees the absence of live microorganisms, ensuring complete removal of microbial cells. This method is ideal for heat-sensitive compounds (Rashid et al., 2021). However some bioactive molecules may adhere to the filter membrane, and highly viscous cultures can lead to filter clogging.

iii Dialysis and ultrafiltration: This method allow for the removal of small molecules or concentrated-bioactive compounds using semipermeable membranes. The CFS is placed in a dialysis bag with a molecular weight cutoff (MWCO) to eliminate salts and low-molecular-weight impurities. Ultrafiltration membranes, with MWCOs (such as 3 kDa, 10 kDa, or 30 kDa) can selectively concentrate larger bioactive molecules (Khan et al., 2020). This process effectively eliminates unwanted small molecules while retaining bioactive compounds, and ultrafiltration enables the fractionation of compounds based on molecular weight. However this technique can be time-consuming and may result in the loss of some metabolites during dialysis.

iv Solvent extraction: This method involves using organic solvents to extract bioactive compounds based on polarity differences. The CFS is combined with an organic solvent like ethyl acetate, methanol, or chloroform at a 1:1 ratio. The mixture is then shaken and allowed to separate into two phases. The organic phase, which contains bioactive metabolites, is collected and evaporated under reduced pressure (Singh et al., 2016). The technique is effective for extracting non-polar bioactive compounds such as antibiotics and secondary metabolites. It can be utilized for selective extraction of various classes of metabolites. However, it's important to note that organic solvents may degrade heat-sensitive compounds, and some solvents can be toxic and should be handled with caution.

v Precipitation (ammonium sulfate or ethanol precipitation): In this method, salts or alcohol are used to precipitate proteinaceous bioactive molecules by altering their solubility. Ammonium sulfate is added to the CFS to achieve 40–80% saturation, leading to protein precipitation (Gudiña et al., 2015). The precipitate is collected by centrifugation and dissolved in buffer for further analysis. Ethanol or acetone can also be used to precipitate extracellular proteins and peptides (Santoyo et al., 2021). This method is suitable for purifying enzymes and antimicrobial peptides as well as concentrating bioactive molecules. However, it requires optimization of precipitation conditions and some bioactive molecules may be lost in the process.

vi Lyophilization (freeze-drying) is a process where water is removed from supernatants through sublimation under vacuum while preserving bioactive compounds. The CFS is frozen at −80°C or in liquid nitrogen before being subjected to a vacuum in a lyophilizer to remove ice through sublimation. The resulting dry powder can be stored for future use, maintaining bioactivity for long-term storage and being suitable for thermostable compounds. However, this method can be expensive and time-consuming, and there is a risk of losing some volatile compounds.

Applications of cell-free supernatant in agriculture and environmental remediation

Cell-free supernatant has various potential applications in agriculture, and environmental remediation. In agriculture, it can

be used as a natural substitute for chemical fertilizers and pesticides, because it contains plant growth-promoting compounds and can suppress the spread of plant diseases (Kaewchomphunuch et al., 2022).

CFS as bio-fertilizer

Several microbial CFS have been reported to enhance plant growth. This technology is desirable amidst the threat of climate change because it is sustainable and environmentally friendly. CFS obtained from *Lactobacillus helveticus* EL2006H enhanced the growth of corn, soybean and potato (Naamala et al., 2023). *Azospirillum brasilense* CFS increased the number of root branches and nodules in soybean (Rondina et al., 2020). According to Posada et al. (2016), CFS of *Bacillus subtilis* EA-CB0575 significantly increased the dry weight of banana plants. The inclusion of CFS from *Bradyrhizobium diazoefficiens* strain USDA 110 and *Rhizobium tropici* strain CIAT 889 increased root diameter by up to 1.6%, root length by 28.5%, root volume by 19.7%, root surface area by 17.8%, number of nodules by 29%, nodule dry weight by 27.2%, root dry weight by 13.5%, and shoot dry weight by 3.8% resulting in a yield increase of by 485 kg ha^{-1} (Moretti et al., 2020). The soil biostimulant products CFS obtained from *Lactobacillus rhamnosus* are made up of lactic acid, peptides, and free amino acids modified by microbial biodiversity, favoring bacterial genera recognized as growth plant promoters (Caballero et al., 2020). CFSs of *Bacillus* sp. strains (U35, U47, U48, U49, and U50) increased all the growth traits of corn (Yaghoubian et al., 2022).

CFS as bio-control agents

CFS containing lipopeptides from *Bacillus subtilis* have shown potent inhibitory activity against plant pathogenic fungus *Fusarium oxysporum* even at very low concentration. They inhibited spore germination by up to 26% and mycelium growth by up to 49% compared to the control (Mihalache et al., 2018). In environmental remediation, cell-free supernatant can be used to degrade pollutants or promote the growth of beneficial microorganisms (Xu et al., 2021). Soil biostimulant products such as (CFS obtained from *Lactobacillus rhamnosus*) consist of lactic acid, peptides, free amino acids, and protein hydrolysates, exhibiting biocontrol activity against some phytopathogenic microorganisms (Caballero et al., 2020). When applied to potato tubers, the filtrated supernatant of *Streptomyces* TN258 24 h before significantly decreased pathogen penetration (*Pythium ultimum*) by 62% and reduced the percentage of weight loss by 59.43% (Sellem et al., 2017). CFS from *Bacillus subtilis* GLB191 containing cyclic lipopeptides fengycin and surfactin is highly active against downy mildew in grapevines through the induction of defense gene expression and callose production (Li et al., 2019).

CFS as abiotic stress ameliorator

Globally, abiotic stresses such as drought, salinity, extreme pH, and heavy metals pose a significant threat to crop productivity. Improving crop tolerance to abiotic stress with microbial CFS is a sustainable strategy to meet the increasing demand for food. Cell-free supernatant may also mitigate abiotic stressors including heavy metal toxicity, salinity, and drought (Ibitoye and Kolawole, 2022). This can occur through various mechanisms such as osmotic adjustment, ion homeostasis, and antioxidant defense. For example, some bacteria can produce exopolysaccharides that protect plants from drought stress by increasing water retention in soil and improving soil structure. CFS produced from *Acinetobacter calcoaceticus* AC06 and *Bacillus amyloliquefaciens* BA01 contains biostimulants that induce osmotic tolerance and metabolic changes in groundnuts under drought stress (Eswaran et al., 2024).

CFS can also be used for bioremediation, which is the process of using microorganisms to degrade or remove environmental contaminants (Pacwa-Płociniczak et al., 2011). Many bacteria in the rhizosphere have the ability to degrade pollutants, such as heavy metals, organic compounds, and pesticides (Alori and Fawole, 2017). These bacteria can be cultured to produce CFS containing enzymes and other molecules that can degrade pollutants. Some examples of bacteria associated with the remediation of environmental pollutants include *Pseudomonas fluorescens* F113, *P. cepacia* ATCC 29351 (Alori and Babalola, 2018), and *Rhodopseudomonas palustris* (Sravya and Sangeetha, 2022). Additionally, CFS also stimulate the growth of indigenous microorganisms, enhancing the natural attenuation of contaminants. Table 1 shows some microorganisms whose CFS has been used to remediate polluted soil. The CFS of these soil microorganisms consists of various types of biosurfactants, glycolipids, exopolymeric substances, and siderophores, which have the potential to reduce and remove soil pollutants ranging from hydrocarbons to heavy metals. The percentage of pollutants removed ranged from 24 to 93%.

Mechanisms of action of microbial cell-free supernatants

Cell-free supernatant exerts various effects including pest and disease control, plant-growth-promoting, bioremediation of polluted soil and defense against abiotic stressors (such as acidity, and salinity) through various mechanisms. Detailed examples of these mechanisms are provided below.

Mechanisms of CFS as bio-control agents (disease control)

Antibiosis mechanism

Cell-free supernatant contains various antibiotics that can inhibit the growth of bacterial and fungal pathogens. These antibiotics can act by inhibiting protein synthesis, cell wall synthesis, DNA replication, or cell membrane integrity of the target microorganism (Borges et al., 2021). The mechanism of action depends on the specific antibiotic present in the cell-free supernatant. The growth inhibition of *Rhizopus oryzae* by CFS from *Trichoderma* spp. could be due to the secretion of harmful extra-cellular compounds like antibiotics such as gliotoxin, and glyoviridin (Alka and Prajapati, 2017).

Many antibiotics exert their antimicrobial activity by inhibiting the synthesis of cell wall components such as peptidoglycan or chitin. This can lead to the weakening or rupture of the cell wall, causing the death of the microorganism (Borges et al., 2021). Additionally, many antibiotics can inhibit the synthesis of bacterial proteins by binding to bacterial ribosomes and preventing the formation of peptide bonds between

amino acids. This can lead to the disruption of essential cellular processes such as DNA replication, transcription, and translation, ultimately causing the death of the microorganism (Sarathy et al., 2019). Moreover, cell-free supernatant may also modulate plant-microbe interactions, leading to improved plant health and yield (Santoyo et al., 2021).

Some bacteria can produce siderophores, which bind iron and make it unavailable to pathogenic fungi (Zhang et al., 2023). The antifungal activity of *Lactobacillus* spp. is associated with the synthesis of organic acids, fatty acids, esters of fatty acids, hydrogen peroxide, bacteriocins, and other secondary metabolites (Perczak et al., 2018). The antifungal activity of CFS containing lipopeptides produced by *Bacillus subtilis* is related to the inhibition of spore germination and the irreversible damage of the hyphae cell wall of plant pathogenic fungi *Fusarium oxysporum* (Mihalache et al., 2018). Microbial CFS activates plants and protects them against harmful bacteria and fungi (Pellegrini et al., 2020). The bioactive compounds in CFS inhibit fungal and bacterial pathogens by disrupting cell membranes (Kumar S. et al., 2021). The presence of amino acids, vitamins, and other nutrients in the supernatant can also contribute to its efficacy in disease resistance (Kumar S. et al., 2020).

CFS from *Trichoderma simmonsii, Aspergillus westerdijkiae*, and *Bacillus* sp. prevents dieback disease on apple rootstocks both when applied and in combination. This suggest additive or synergistic effects between the two biocontrol agents (M'henni et al., 2022).

Enzymatic activity

Lactobacillus plantarum CFS can prevent spore development of pathogenic fungi Fusarium oxysporum for up to 6 days by producing extracellular hydrolytic enzymes (Di Rico et al., 2025). Some CFS contain chitinases or glucanases, which degrade the cell walls of fungi (Veliz et al., 2017). The growth inhibition of *Rhizopus oryzae* could be due to the secretion of cell wall-degrading enzymes such as glucanases, endochitinases, and chitinases (Alka and Prajapati, 2017). The production of hydrolytic enzymes (such as chitinase, glucanase, protease, and cellulase; and antibiotics such as 2,4-diacetyl phloroglucinol, amphisin, oomycin A, hydrogen cyanide, phenazine, pyoluteorin, pyrrolnitrin, cyclic lipopeptides, oligomycin A, zwittermicin A, kanosamine, and xanthobaccin) by beneficial microbes is an important mechanism against phytopathogens for sustainable plant disease management. These enzymes break down the cell wall of fungal pathogens, leading to cell death (Jadhav et al., 2017).

Quorum sensing inhibition

Cell-free supernatant contains various compounds that can interfere with quorum sensing (QS), a mechanism of communication among bacteria that regulates gene expression in response to cell population density and virulence. This mechanism is relied upon by many pathogenic bacteria to control virulence, biofilm formation, and antibiotic resistance. These compounds n CFS can either block the synthesis of quorum sensing molecules or inhibit their binding to receptors, thus disrupting the quorum sensing network (Escobar-Muciño et al., 2022). The bioactive compounds in microbial CFS inhibit fungal and bacterial pathogens by interfering with quorum sensing and inducing systemic resistance in plants (Kumar S. et al., 2021). Mechanisms of Quorum Sensing Inhibition by Microbial CFS include the following:

a Enzymatic degradation of QS signals

Enzymes such as lactonases, acylases, and oxidoreductases found in microbial CFS produced by certain microbes can breakdown or alter quorum sensing signals (autoinducers). For example, AHL-lactonases produced by *Bacillus* and *Pseudomonas* species can breakdown acyl-homoserine lactones (AHLs), which are important QS signals in Gram-negative bacteria (Uroz et al., 2009). Some *Pseudomonas* species can also produce enzymes that can breakdown N-acyl homoserine lactones (AHLs), a QS signaling molecule, effectively disrupting QS communication, and thereby reducing the virulence of plant pathogens (Dong et al., 2000).

b Disruption of biofilm formation

Some microbial CFS disrupts biofilms by interfering with QS pathways. Biofilms are structured bacterial communities that contribute to antimicrobial resistance. For example CFS from *Bacillus subtilis*, produces surfactin, this inhibits *Pseudomonas aeruginosa* biofilm formation. This alters cell adhesion and signaling (Bodini et al., 2007).

c Competitive binding to QS receptors

Certain metabolites in CFS can prevent native autoinducers from activating virulence pathways mimic QS signals by competitively binding to bacterial QS receptors. For example, phenolic compounds in CFS from *Lactobacillus* spp. interfere with QS-controlled biofilm formation in *Pseudomonas aeruginosa* (Rasamiravaka et al., 2015).

d Downregulation of QS gene expression

CFS from *Streptomyces* spp. have been reported to down regulate luxI/R genes in *Chromobacterium violaceum*. This disruption affects QS-regulated pigment production and biofilm formation ultimately reducing virulence and biofilm formation (Lade et al., 2014).

Induction of systemic resistance

Cell-free supernatant can induce systemic resistance in plants, which is a heightened defense response to subsequent pathogen infections (Sivojiene et al., 2021). This can enhance plant resistance to a wide range of pathogens, leading to improved crop health and yield. It is a mechanism by which plants can boost their resistance to a broad range of plant pathogens by activating plant defense pathways, resulting in the accumulation of phytohormones and other defense-related compounds.

For example, treatment with cell-free supernatant of *Trichoderma asperellum* SKT-1 induces systemic resistance against cucumber mosaic virus (CMV) by regulating the expression of various pathogen-related genes, enhancing the defense mechanism against CMV infection (Elsharkawy et al., 2013). Cell free supernatant may contain plant signal molecules such as lipo-chitooligosaccharides (LCO), chitooligosaccharides (CO), chitinous compounds, flavonoids, jasmonic acid, linoleic acid, linolenic acid, and karrikins (Bywater Ekegard and Fitzsimmons, 2020).

Certain compounds derived from CFS can trigger induced systemic resistance (ISR) and systemic acquired resistance (SAR) in plants, making them more resilient against biotic and abiotic stresses (Köhl et al., 2019). This preemptive defense mechanism enhances plant immunity, reducing disease incidence and improving overall crop health. ISR requires jasmonic acid (JA), ethylene (ET) signaling pathways, and nonexpressor of pathogenesis-related protein 1 (NPR1)

(Pieterse and Van Loon, 2007). The two major branches of the JA signaling pathways are controlled by the transcription factor MYC2 and the ethylene response factor (ERF). The ERF branch of the JA pathway is associated with enhanced resistance to necrotrophic pathogens that is regulated by members of the APETALA2/ethylene response factor (AP2/ERF) family, including the JA-responsive marker gene plant defensin1.2 (PDF1.2) (Lorenzo et al., 2003). JA also mediates resistance against herbivores (HIR). After leaf wounding, an increase in the JA derivative Jasmonoyl-isoleucine (JA-Ile) is perceived by a complex consisting of the protein Coronatine insensitive1 (COI1) and Jasmonate ZIM-domain (JAZ) protein. When the hormone is perceived, JAZ repressors are degraded by the proteasome releasing MYC2 and allowing the activation of JA responses such as the accumulation of vegetative storage protein2 (VSP2) (Pieterse et al., 2014). It has been demonstrated that volatiles derived from the linoleic pathway increase sensitivity to methyl jasmonate and induce several defense-related genes, such as chalcone synthase (CHS), allene oxide synthase (AOS), hydroperoxide lyase (HPL), and lipoxygenase 2 (LOX2) (Hirao et al., 2012).

Table 1 summarizes the application and implication of CFS used as biocontrol agents against pests and diseases. It shows that CFS has been studied on various crops including cereal crops like maize, legumes such as soybeans, Lotus japonicas, and chickpeas; vegetables like pepper, tomato, and potato, tuber crops like cassava, and ornamental crops. CFS has been produced from both bacteria, such as the genus Streptomyces, Bacillus, etc., and fungi, such as the genus *Penicillium, Trichoderma*, etc. Components of such CFS include harzianic acid, linoleic acid, hydroxymethylfurfural, gliotoxin, glyoviridin, siderophores, lipopeptides, enzymes such as glucanases, endochitinases, chitinases, etc.

Mechanisms of CFS as bio-fertilizer (plant growth-promotion)

Table 2 summarizes the use and application of CFS for plant growth promotion. It shows that CFS as biofertilizers has been studied on cereal crops such as maize, legumes including soybeans, Lotus japonicas, and chickpeas; vegetables such as pepper, tomato, and potato; tuber crops like cassava; and ornamental crops. CFS has been produced from both bacteria such as genus Lactobacillus, Bacillus etc.

TABLE 1 Microorganisms and their CFS as bio-control agents.

Crop	Organism	Effects	Active component of CFS/mechanism	References
Tomato	*Streptomyces rimosus*	Induces resistance in tomato against *Fusarium oxysporum* f. sp. Lycopersici	By activating the phenylpropanoid pathway	Abbasi et al. (2019)
Tomato	*Trichoderma* spp.	Reduced disease severity	Gliotoxin, glyoviridin, glucanases, endochitinases, chitinases	Alka and Prajapati (2017)
Peanut and maize	*Bacillus albus strains*	reducing disease incidence (DI) and disease severity index (DSI)	Diketopiperazines, macrolactins, siderophores lipopeptides,	Trinh et al. (2025)
Maize (*Zea mays*)	*Bacillus subtilis MF497446* and *Pseudomonas koreensis MG209738*	Controlling *Cephalosporium maydis* in Maize Plant	Siderophore	Ghazy and El-Nahrawy (2021)
Lotus japonicas	*Pantoea eucalypti M91*	Promote morphological and biochemical changes and induce improved photosynthesis and iron translocation	Siderophores	Campestre et al. (2016)
Ornamental bulb plants	*Bacillus subtilis*	Disease suppression	Lipopeptides	Mihalache et al. (2018)
Chili	*Trichoderma* spp.	Inhibits the growth of pathogen	Unknown	Nurbailis et al. (2019)
Tomato	*Trichoderma* sp.	Reduced the disease severity (%)	Harzianic acid, linoleic acid, hydroxymethylfurfural	Imran et al. (2023)
Tomato	*Bacillus amyloliquefaciens*	Reduction in disease incidence (70.00%) and disease severity	IAA production, siderophore production, lytic enzyme	Gautam et al. (2020)
Sugar beet	*Bacillus amyloliquefacien*	Inhibited the appearance of tissue necrosis (up to 92%)	Lipopeptide extracts	Nikolić et al. (2019)
Banana	*Bacillus* sp. EA-CB0959	Reduced incidence of Moko disease for up to 35%	Lipopeptides (surfactins, iturins and fengycins)	Villegas-escobar et al. (2018)
Grape	*Bacillus subtilis*	Reduced the leaf sporulating area by 97%	Surfactin and fengycin	Li et al. (2019)

TABLE 2 Microorganisms and their CFS as plant growth promoter (bio-fertilizers).

Crop	Organism	Effects	Active component of CFS	References
Maize (*Zea mays*), Soybean (*Glycine max*) L. Merill and Potato (*Solanum tuberosum*)	*Lactobacillus helveticus* EL2006H	Enhanced radicle length in corn, mean percentage germination in soybean and photosynthetic rate, greenness and mean fresh weight in potato	Unknown	Naamala et al. (2023)
Pepper (*Capsicum annuum*)	*Alternaria alternate*	Stimulated root growth, induced fruit development, and enhanced the number fruits per plant and yield	Volatile organic compounds	Baroja-Fernández et al. (2021)
Cassava	*Bacillus* sp. *CaSUT007*	Increased root and shoot lengths and total biomass of cassava stalks	Extracellular proteins	Buensanteai et al. (2013)
Maize (*Zea mays*)	*Bacillus Strains* (U35, U47, U48, U49, and U50)	CFSs of Bacillus strains increased all the growth traits of corn seeds and reduced the negative effects of salinity, especially severe salinity		Yaghoubian et al. (2022)
Banana	*Bacillus. subtilis EA-CB0575*	Enhanced dry weight of banana plants	Lipopeptides and siderophores	Posada et al. (2016)
Soybean	*Bacillus. amyloliquefaciens strain KPS46*	Promoted soybean growth	Antibiotic surfactin and proteins	Buensanteai et al. (2008)
Sesame	*Penicillium* spp.	Enhanced shoot and root length as well as the biomass	Enriched in amino acids	Radhakrishnan et al. (2014)
Pepper	*Trichoderma. Harzianum*	Promoted root growth, enhanced fruit yield and altered composition of fruits	Volatile organic compounds (VOCs)	Baroja-Fernández et al. (2021)
Chickpea	*Trichoderma* species	Enhanced germination percentage and increased fresh and dry weight	Unknown	Ali et al. (2014)
Arabidopsis thaliana	*Bradyrhizobium japonicum*	Stimulus effect on root growth and development	Lipo-chitooligosaccharides	Khan et al. (2011)
Lotus japonicas	*Pantoea eucalypti M91*	promote morphological and biochemical changes and induce improved photosynthesis and iron translocation	Siderophores	Campestre et al. (2016)
Soybean	*Bacillus amyloliquefaciens*	Increased root and shoot lengths and plant biomass	Indole-3-acetic acid and surfactin	Buensanteai et al. (2008)
Helianthus annuus	*Pseudomonas citronellolis* strain SLP6 H	Enhance the chlorophyll content, production of antioxidant enzymes, and plant growth	Hydroxamate siderophore	Silambarasan et al. (2020)
Maize	*Bacillus amyloliquefaciens and Bacillus subtilis*	Significantly enhanced length growth of maize seedlings	Indole-3-acetic acid (IAA)	Idris et al. (2004)
Cassava	*Bacillus* sp. CaSUT007	Enhanced growth	Phytohormone and extracellular proteins	Buensanteai et al. (2013)
Alfalfa	*Sinorhizobium meliloti* U143 and *Delftia* sp. JD2	Increased shoot and root matter and hence increased yield	Phenolic compounds (including flavonoids), organic acids, and volatile compounds	Morel et al. (2015)
Pigeon pea	*Bradyrhizobium* strain IC-4059	Significant enhancement in shoot length, root length, dry weight, protein content, and nodule number	Phosphatidylserine, phosphatidylcholine, FMC-5, pantoic acid, ascorbic acid, benzoic acid, 4-pentyl-4-formylphenyl ester, benzimidazole, and phosphatidylethanolamine	Tewari et al. (2020)

and fungi such as genus Penicillium, Trichoderma etc. Mechanisms of action of CFS as a biofertilizer are as follows:

Production of growth hormones

Cell-free supernatant contains various plant growth-promoting compounds such as auxins, cytokinins, and gibberellins. These compounds can stimulate plant growth and development by promoting cell division, elongation, and differentiation (Naamala et al., 2023). They can also enhance nutrient uptake, water retention, and stress tolerance of plants, thus improving their productivity and quality (Kumar S. et al., 2021). For example, some bacteria can produce indole acetic acid (IAA), which promotes root growth and lateral root formation. CFS contains phytohormones that can promote the expansion and maturation of plants, including gibberellins, cytokinins, and auxins. Phytohormones regulate numerous processes, such as cell division, elongation, and differentiation, leading to improved shoot and root growth, nutrient uptake, and stress tolerance (El Sabagh et al., 2022).

Cell-free supernatants that promote plant growth may contain biostimulants that enhance metabolic or physiological processes such as respiration, photosynthesis, nucleic acid uptake, ion uptake, and nutrient delivery. Examples of biostimulants found in CFS include humic acids, fulvic acids, myo-inositol, and glycine (Bywater Ekegard and Fitzsimmons, 2020). Additionally, organic acids and siderophores in CFS improve nutrient solubilization and uptake, ultimately enhancing plant nutrition and yield (Patel and Saraf, 2017).

According to Glick (2020), plant growth-promoting substances like auxins, gibberellins, and cytokinin-like compounds, which can stimulate root elongation, seed germination, and overall plant vigor, are often present in microbial CFS. Cell-free supernatant can also enhance nutrient uptake by plants by increasing the solubility and availability of essential minerals such as nitrogen, phosphorus, and potassium (Yuan et al., 2020). The presence of amino acids, vitamins, and other nutrients in the supernatant can also contribute to its efficacy in promoting plant growth (Kumar S. et al., 2020).

Improvement of soil structure

CFS can also contain exopolysaccharides (EPS) or biofilms, which can increase soil aggregation and water holding capacity. This can improve soil aeration, water infiltration, and nutrient retention, leading to improved plant growth and yield (Ibitoye and Kolawole, 2022).

Enzymatic activity

Cell-free supernatant contains various enzymes such as lipases, amylases, and proteases. These catalysts can hydrolyze different macromolecules like proteins, lipids, and carbohydrates, releasing nutrients that can be utilized by microorganisms or plants (Cruz-Casas et al., 2021).

Regulation of gene expression

Cell-free supernatant may also regulate gene expression in plants, leading to improved plant growth and yield (Kumar S. et al., 2021). For example, some bacteria can produce small RNA molecules that can target specific plant genes and regulate their expression. This can affect various plant processes such as photosynthesis, nutrient uptake, and stress response, leading to improved plant performance.

Mechanism of CFS in the mitigation of abiotic stresses

Table 3 shows some microorganisms that mitigate the effects of abiotic stresses such as drought, salinity, and heavy metals on crops and their components. The active components in these CFS include growth hormones, antioxidants, proteins, amino acids, vitamins, and osmolytes.

Advantages of microbial cell-free supernatants in crop production

Microbial cell-free supernatants (CFS) have emerged as a promising alternative to traditional agricultural inputs due to their bioactive properties and hence exhibit the following advantages:

Reduction in dependence on chemical inputs

By acting as biofertilizers and biostimulants, CFS can reduce the reliance on synthetic fertilizers and pesticides. This contributes to sustainable agriculture by minimizing chemical residues in the soil and preventing environmental pollution (Chowdhury et al., 2015). Furthermore, CFS-based treatments are often compatible with organic farming practices. The incorporation of natural resistance inducers in pest management programs of woody crops, alone or in combination with classical methods, could be a reliable method for reducing the amount of chemical residues in the environment. Cell-free supernatant can reduce the use of agrochemicals by promoting natural plant growth and suppressing the growth of plant pathogens (Yuan et al., 2020).

Compatibility with soil and rhizosphere microbiota

Unlike synthetic agrochemicals that may disrupt soil microbial communities, CFS typically supports beneficial rhizosphere interactions. The absence of live microbial cells reduces competition and interference with native soil microbiota while still promoting beneficial interactions, such as increased phosphate solubilization and nitrogen fixation (Garg et al., 2020). CFS contains antimicrobial compounds such as lipopeptides, enzymes, and volatile organic compounds that effectively suppress plant pathogens without harming beneficial microbes (Olanrewaju et al., 2019). This makes CFS an eco-friendly alternative to synthetic pesticides.

Improving soil health

The compounds present in them can promote the growth of beneficial microorganisms such as mycorrhizal fungi, rhizobia, and other nitrogen-fixing bacteria, which can enhance soil fertility (Kumar S. et al., 2020).

Potential for scalable and cost-effective production

Compared to live microbial inoculants, CFS offers a more stable and easily scalable solution for agricultural applications. It

TABLE 3 CFS of soil microorganisms that mitigate crop abiotic stresses.

S/N	Microorganism	Component of CFS	Stress type	Effect of the CFS	References
1	*Pseudomonas* and *Stenotrophomonas* spp.	Biosurfactant	Heavy metal (As)	24.6% of As removal (678 mg.kg^{1})	Araújo et al. (2021)
2	*Bacillus Strains* (U35, U47, U48, U49, and U50)	Unknown	Salinity	Increased growth traits and reduced the negative effects of salinity	Yaghoubian et al. (2022)
3	*Aspergillus tubingensis* (STSP 25)	Not known	Heavy metals [Pb (II), Ni (II), Cu (II), and Zn (II)]	Removed more than 90% of heavy metals	Mahanty et al. (2020)
4	*Aspergillus carneus* and *Aspergillus niger*	Biosurfactant	Heavy metala (Polyaromatic hydrocarbons)	Removed the lubricating oil from contaminated soil	Mahmoud et al. (2024)
5	*Acinetobacter calcoaceticus AC06* and *Bacillus amyloliquefaciens*	Osmolytes (including proline, salicylic acid, trehalose and glycine betaine)	Drought-stress	Displayed distinct osmotic-adjustment abilities groundnut during drought-stress	Eswaran et al. (2024)
6	*Lysinibacillus* sp. NOSK	Not known	Heavy metals (Ni(II), Cr(VI) and Reactive black 5)	Removed Ni(II) by 70 ± 0.2%, Cr(VI) by 58 ± 1.4% and Reactive black 5 by 82 ± 0.8	San Keskin et al. (2018)
7	*Nocardiopsis* sp.	Biosurfactant (glycopeptide type)	Oil-Contaminated Soils (Hydroarbon)	29 and 35% decrease in the content of hydrocarbons	Biktasheva et al. (2024)
8	*Pseudomonas aeruginosa*	Not known	Tetracycline adsorption	Adsorption of 526.32 mg/g	Debnath et al. (2020)
9	*P. ostreatus*	Not known	Bisphenol-A and carbamazepine	Degradation of bisphenol-A = 90% and carbamazepine	Ji et al. (2017)
10	*Lactobacillus helveticus*	Unknown	Salinity	Enhance mean percentage germination and mean radicle length in the presence of NaCl stress	Naamala et al. (2023)
11	*Pseudomonas aeruginosa*	Glycolipids	Hydrocarbons	Emulsification of hydrocarbons and vegetable oils; removal of metals from soil	Sifour et al. (2007)
12	*Devosia* sp. *(strain SL43)*	Hormones, antioxidants, amino acids, and vitamins	Salinity	Mitigates the adverse effects of salt stress on soybean (*Glycine max* L.) seed vigor index	Monjezi et al. (2023)
13	*Mycobacterium tuberculosis, Rhodococcus erythropolis, Arthrobacter* sp., *Nocardia* sp., *Corynebacterium* sp.	Glycolipids	Hydrocarbons	Enhancement of the bioavailability of hydrocarbons	Franzetti et al. (2010)
14	*Bacillus subtilis SNW3*	Lipopeptides	Crude oil	Displayed great physicochemical properties of surface tension reduction value in bioremediation of crude oil	Umar et al. (2021)
15	*Pseudomonas aeruginosa* and *Pseudomonas putida*	Exopolymeric substances containing alginic, glucuronic acid, galacturonic acid, and uronic acid	Heavy metals (Chromium)	Chromium bioavailability, solubility, and transport or sorption behavior in subsurface system	Kantar et al. (2010)
16	*P. azotoformans*	Siderophores	Arsenic	Detoxify heavy metals	Nair et al. (2007)
17	*Pseudomonas aeruginosa*	Siderophores (ferric iron chelating compounds)	Heavy metals	Detoxify heavy metals such as Cr^{3+}, Al^{3+}, Cu^{2+}, Eu^{3+}, and Pb^{2+}	O'Brien et al. (2014)
18	*Azotobacter chroococcum*	Siderophores	Heavy metals	Alleviate heavy metals	Rizvi and Khan (2018)

(Continued)

TABLE 3 (Continued)

S/N	Microorganism	Component of CFS	Stress type	Effect of the CFS	References
19	*Agrobacterium radiobacter*	Siderophores	Arsenic	Removing 54% of arsenic from polluted sites	Wang et al. (2011)
20	*Bacillus subtilis BL-27*	Lipopeptides	Hydrocarbons, heavy metals	Enhanced biodegradation of hydrocarbons and chlorinated pesticides; removed heavy metals from a contaminated soil	Wang et al. (2018)
21	*Brevibacillus* sp.	Biosurfactant	Phenanthrene	Degraded 93% of phenanthrene in 6 days	Reddy et al. (2010)
22	*Pseudomonas citronellolis*	Biosurfactant	hydrocarbon	Collapsed oil drop within the interval of 10–20 min	Ismail et al. (2018)

eliminates concerns regarding microbial survival, colonization, and environmental adaptability (Patel and Saraf, 2017). Additionally, CFS formulations can be stored and transported more efficiently than live microbial cultures, making them more practical for commercial use.

Ease of application

CFS can be easily applied to plants through foliar sprays or soil drenches, making them convenient for farmers to use.

Shelf life

CFS can be stored and transported more easily than live microbial cultures, making them more practical for large-scale applications.

Storage techniques for cell-free supernatants

To maintain the biological activity and stability of the bioactive compounds contained in CFS, proper storage techniques are essential. The choice of storage method depends on the nature of the bioactive compounds, the intended application, and the duration of storage. The following are some storage technique options that can be explored in the storage of CFS.

Refrigeration (4°C) storage

Refrigeration at 4°C is a commonly used method for short-term storage (up to a few weeks). This method slows down microbial contamination and enzymatic degradation and is hence effective at preserving heat-sensitive compounds. CFS containing organic acids, bacteriocins, and quorum sensing inhibitors can remain stable for 1–2 weeks under refrigeration (Koohestani et al., 2018).

Freezing (−20°C to −80°C)

Freezing is a widely used method to store CFS containing proteins, enzymes, and other temperature-sensitive metabolites. Standard freezing −20°C is suitable for antimicrobial peptides, biosurfactants, and quorum sensing inhibitors (Simpson, 2010). However, repeated freeze–thaw cycles can lead to protein degradation. Ultra-low freezing at −80°C preserves heat-sensitive biomolecules like bacteriocins and enzymes without significant loss of activity (Simpson, 2010).

Lyophilization (freeze-drying) storage technique

Lyophilization also known as freeze-drying removes water from CFS while preserving bioactive compounds. CFS is frozen at −80°C and then subjected to vacuum sublimation to remove ice without affecting bioactivity (Ge et al., 2024). This process prevents degradation of heat-sensitive compounds and extends their shelf life to months or years at room temperature (Kristensen et al., 2020). Lyophilized powder is stored in airtight vials at room temperature or 4°C. Šuchová et al. (2022) used the lyophilization storage technique for bacteriocins, biosurfactants, plant growth-promoting compounds, and quorum sensing inhibitors. Lyophilized bacteriocins from *Lactobacillus* spp. retain activity for over 12 months at 4°C (Cheikhyoussef et al., 2009).

Spray drying

This method is suitable and cost-effective for industrial-scale storage. CFS is atomized into fine droplets and rapidly dried using heated air (80–150°C) (Huang et al., 2017). It can also be encapsulated with maltodextrin or gum arabic to enhance stability (Barcelos et al., 2014). It can be used for probiotic metabolites, biosurfactants, and microbial fertilizers (Gullifa et al., 2023). Biosurfactants from *Bacillus* spp. stored via spray drying remain stable for over a year at room temperature (Marchant and Banat, 2012).

Storage in preservative solutions

Preservatives such as glycerol (10–30%) will protect proteins and bacteriocins during freezing (Corral et al., 2014). Ethyl alcohol (10–50%) was used for organic solvent-stable metabolites such as quorum sensing inhibitors (Hamad et al., 2022).

Encapsulation technique

To protect CFS bioactive compounds from environmental degradation, they can be microencapsulated with polymers (such as alginate and chitosan) (Bassani et al., 2019). Gunal Köroglu et al. (2024) discussed encapsulation of hydrophobic compounds in yeast cells for use in food industries.

Challenges and limitations

Several limitations hinder the widespread adoption of microbial cell-free supernatants (CFS) in sustainable crop production despite their promising applications.

i **Variability in composition**: CFS is a complex mixture of different compounds, and its composition can vary significantly depending on the microbial strain, growth conditions, and extraction methods used. This variability makes it difficult to standardize CFS formulations for large-scale agricultural applications and ensure consistent performance (Compant et al., 2005; Olanrewaju et al., 2019). Standardization and optimization remain critical issues for ensuring reproducibility in field applications.

ii **Inadequate understanding of the mode of action**: The incomplete full understanding of the mode of action makes it difficult to optimize CFS formulations for specific applications and to predict their efficacy in different environmental conditions (Santos et al., 2017).

iii **Compatibility with other inputs**: The compatibility of CFS with other agricultural inputs, such as fertilizers and pesticides, is not well understood. CFS may enhance the efficacy of other inputs, while in other cases, it may have an antagonistic effect, reducing the efficacy of other inputs (Kudjordjie et al., 2019).

iv **Concentration and dosage:** The concentration and dosage of CFS required to achieve optimal effects are not well understood. Some studies have reported that lower concentrations of CFS can be more effective than higher concentrations, while others have reported the opposite (Santos et al., 2017).

v **Shelf-life and storage:** The shelf life and storage conditions of CFS can also be a limitation, as the bioactive compounds such as antimicrobial peptides, enzymes, and secondary metabolites in CFS can degrade over time or under inappropriate storage conditions due to factors such as temperature, pH, and UV radiation (Garg et al., 2020). This degradation can reduce the efficacy of CFS and make it difficult to transport and use CFS in remote areas (Borges et al., 2021). Furthermore, compared to chemical agro-inputs, the shelf life of microbial CFS-based formulations is shorter, necessitating frequent application or the use of stabilizing agents (Chowdhury et al., 2015).

vi **Potential phytotoxicity and environmental concerns**: Although CFS is generally considered environmentally friendly, the potential environmental impact of widespread CFS application needs to be carefully assessed. Some microbial metabolites in CFS, when applied in high concentrations, may exhibit phytotoxic effects, which could result in growth inhibition or stress responses in certain crops (Kumar S. et al., 2021). Furthermore, the long-term impact of repeated CFS applications on soil microbial communities and ecosystem balance is not fully understood, warranting further investigation.

vii **Economic and scalability challenges**: The cost of producing CFS at an industrial scale may not be competitive with conventional fertilizers and pesticides which can be cost-prohibitive for some farmers unless optimized biotechnological approaches are adopted (Patel and Saraf, 2017). Additionally, regulatory hurdles in different countries may delay commercialization and adoption. It is crucial to develop cost-effective production and delivery methods for the widespread adoption of CFS technology.

viii **Limited field efficacy**: Although CFS has demonstrated strong efficacy in controlled environments and laboratory settings, its performance in open-field conditions remains unpredictable. Factors such as soil microbiome interactions, climatic variations, and plant genotype can influence the bioactivity of CFS, potentially reducing its effectiveness compared to synthetic agrochemicals (Köhl et al., 2019).

Conclusion

Cell-free supernatant has emerged as a promising tool for sustainable crop production. Sources of microbial CFS used in crop production include bacteria and fungi. Its applications include plant growth promotion, biocontrol of plant diseases, and mitigation of the effects of abiotic stresses, including heavy metal remediation. By harnessing the power of CFS, we can reduce our reliance on synthetic chemicals and promote a more sustainable and environmentally friendly approach to crop production.

Author contributions

EA: Conceptualization, Writing – original draft, Writing – review & editing, Supervision. AO: Writing – original draft. AI: Writing – original draft.

Funding

The author(s) declare that no financial support was received for the research and/or publication of this article.

Acknowledgments

Authors would like to acknowledge Landmark University for providing enabling environment for this research.

Conflict of interest

The authors declare that the research was conducted in the absence of any commercial or financial relationships that could be construed as a potential conflict of interest.

Generative AI statement

The authors declare that no Gen AI was used in the creation of this manuscript.

Publisher's note

All claims expressed in this article are solely those of the authors and do not necessarily represent those of their affiliated organizations, or those of the publisher, the editors and the reviewers. Any product that may be evaluated in this article, or claim that may be made by its manufacturer, is not guaranteed or endorsed by the publisher.

References

Abbasi, S., Safaie, N., Sadeghi, A., and Shamsbakhsh, M. (2019). Streptomyces Strains Induce Resistance to Fusarium oxysporum f. sp. lycopersici Race 3 in Tomato Through Different Molecular Mechanisms. *Frontiers in microbiology* 10:1505. doi: 10.3389/fmicb.2019.01505

Ali, A., Haider, M. S., Ashfaq, M., and Hanif, S. (2014). Effect of culture filtrates of *Trichoderma* spp. on seed germination and seedling growth in chickpea–an *in-vitro* study. *Pak. J. Phytopathol.* 26, 01–05. Available at: https://www.pjp.pakps.com/index.php/PJP/article/view/55

Alka, R. K., and Prajapati, B. K. (2017). Effect of *Trichoderma* spp. and its culture filtrate antagonists on growth and management of rhizopus rot of tomato fruit *in vitro* and *in vivo*. *J. Pharmacogn. Phytochem.* 6, 394–398. Available at: https://www.phytojournal.com/archives/2017/vol6issue4/PartF/6-3-204-831.pdf

Alori, E. T., and Babalola, O. O. (2018). Microbial inoculants for improving crop quality and human health in Africa. *Front. Microbiol.* 9:02213. doi: 10.3389/fmicb.2018.02213

Alori, E. T., Babalola, O. O., and Prigent-Combaret, C. (2019). Impacts of microbial inoculants on the growth and yield of maize plant. *Open Agricult. J.* 13, 1–8. doi: 10.2174/1874331501913010001

Alori, E. T., and Fawole, O. B. (2017). "Microbial inoculants-assisted phytoremediation for sustainable soil management" in Phytoremediation: Management of Environmental Contaminants. eds. A. A. Ansari, S. S. Gill R, G. G. R. Lanza and L. Newman, vol. 5 (Switzerland: Springer International Publishing), 3–17.

Araújo, L. S. S., Silva, S. Q., and Teixeira, M. C. (2021). Developing a biosurfactant to attenuate arsenic contamination in mining tailings. *Heliyon* 7:e06093. doi: 10.1016/j.heliyon.2021.e06093

Arrioja-Bretón, D., Mani-López, E., Palou, E., and López-Malo, A. (2020). Antimicrobial activity and storage stability of cell-free supernatants from lactic acid bacteria and their applications with fresh beef. *Food Control* 115:107286. doi: 10.1016/j.foodcont.2020.107286

Baroja-Fernández, E., Almagro, G., Sánchez-López, Á. M., Bahaji, A., Gámez-Arcas, S., De Diego, N., et al. (2021). Enhanced yield of pepper plants promoted by soil application of volatiles from cell-free fungal culture filtrates is associated with activation of the beneficial soil microbiota. *Front. Plant Sci.* 12:752653. doi: 10.3389/fpls.2021.752653

Barcelos, G. S., Dias, L. C., Fernandes, P. L., Fernandes Rde, C., Borges, A. C., Kalks, K. H., et al. (2014). Spray drying as a strategy for biosurfactant recovery, concentration and storage. *Springerplus.* 24, 3–49. doi: 10.1186/2193-1801-3-49

Bassani, J. C., Queiroz Santos, V. A., Barbosa-Dekker, A. M., Dekker, R. F. H., Da-Cunha, M. A. A., and Pereira, E. A. (2019). Microbial cell encapsulation as a strategy for the maintenance of stock cultures. *LWT.* 102, 411–417. doi: 10.1016/j.lwt.2018.12.058

Biktasheva, L., Gordeev, A., Usova, A., Kirichenko, A., Kuryntseva, P., and Selivanovskaya, S. (2024). Bioremediation of oil-contaminated soils using biosurfactants produced by Bacteria of the genus *Nocardiopsis* sp. *Microbiol. Res.* 15, 2575–2592. doi: 10.3390/microbiolres15040171

Bodini, S. F., Manfredini, S., Eppis, F., Valentini, F., Santori, F., and Maestri, A. (2007). Quorum sensing inhibition activity of *Bacillus* sp. natural isolates and their plant growth-promoting effect. *J. Biotechnol.* 132, 44–48. doi: 10.1016/j.jbiotec.2007.08.024

Borges, A., Ferreira, C., Saavedra, M. J., and Simões, M. (2021). Antibacterial activity and mechanisms of action of natural compounds isolated from lichens: a review. *Molecules* 26:347. doi: 10.3390/molecules190914496

Bourebaba, Y., Marycz, K., Mularczyk, M., and Bourebaba, L. (2022). Postbiotics as potential new therapeutic agents for metabolic disorders management. *Biomed. Pharmacother.* 153:113138. doi: 10.1016/j.biopha.2022.113138

Buensanteai, N., Sompong, M., Thamnu, K., Athinuwat, D., Brauman, A., and Plassard, C. (2013). The plant growth promoting bacterium *Bacillus* sp. CaSUT007 produces phytohormone and extracellular proteins for enhanced growth of cassava. *Afr. J. Microbiol. Res.* 7, 4949–4954. doi: 10.5897/AJMR12.1839

Buensanteai, N., Yuen, G. Y., and Prathuangwong, S. (2008). The biocontrol bacterium *Bacillus amyloliquefaciens* KPS46 produces auxin, surfactin and extracellular proteins for enhanced growth of soybean plant. *Thai J. Agricult. Sci.* 41, 101–116. Available at: https://www.thaiscience.info/journals/Article/TJAS/10469537.pdf

Bywater Ekegard, M., and Fitzsimmons, A. (2020). Supernatant composition of microbial culture for agricultural use. United States Patent website. Available online at: https://patents.google.com/patent/US10588320B2/en (Accessed February 9, 2025).

Caballero, P., Rodríguez-Morgado, B., Macías, S., Tejada, M., and Parrado, J. (2020). Obtaining plant and soil biostimulants by waste whey fermentation. *Waste Biomass Valorizat.* 11, 3281–3292. doi: 10.1007/s12649-019-00660-7

Campestre, M. P., Castagno, L. N., Estrella, M. J., and Ruiz, O. A. (2016). *Lotus japonicus* plants of the Gifu B-129 ecotype subjected to alkaline stress improve their Fe2+ bio-availability through inoculation with *Pantoea eucalypti* M91. *J. Plant Physiol.* 192, 47–55. doi: 10.1016/j.jplph.2016.01.001

Chandini, R. K., Kumar, R., and Om, P. (2019). The impact of chemical fertilizers on our environment and ecosystem. In: Research trends in environmental sciences, 2, pp. 71–86. Available online at: https://www.researchgate.net/publication/331132826.

Cheikhyoussef, A., Pogori, N., and Chen, H. (2009). Lyophilization of lactic acid bacteria-derived bacteriocins for prolonged shelf-life. *Biotechnol. Lett.* 31, 695–700. doi: 10.1007/s10529-009-9923-8

Chowdhury, S. P., Hartmann, A., Gao, X., and Borriss, R. (2015). Biocontrol mechanism by root-associated Bacillus species with a focus on secondary metabolites. *Microb. Ecol.* 69, 459–470. doi: 10.1007/s00248-014-0533-3

Compant, S., Duffy, B., Nowak, J., Clément, C., and Barka, E. A. (2005). Use of plant growth-promoting bacteria for biocontrol of plant diseases: principles, mechanisms of action, and future prospects. *Appl. Environ. Microbiol.* 71, 4951–4959. doi: 10.1128/AEM.71.9.4951-4959.2005

Corral, S., Salvador, A., Belloch, C., and Flores, M. (2014). Effect of fat and salt reduction on the sensory quality of slow fermented sausages inoculated with Debaryomyces hansenii yeast. *Food Control* 45, 1–7. doi: 10.1016/j.foodcont.2014.04.013

Cruz-Casas, D. E., Aguilar, C. N., Ascacio-Valdés, J. A., Rodríguez-Herrera, R., Chávez-González, M. L., and Flores-Gallegos, A. C. (2021). Enzymatic hydrolysis and microbial fermentation: the most favorable biotechnological methods for the release of bioactive peptides. *Food Chem. Mol. Sci.* 3:100047. doi: 10.1016/j.fochms.2021.100047

Debnath, B., Majumdar, M., Bhowmik, M., Bhowmik, K. L., Debnath, A., and Roy, D. N. (2020). The effective adsorption of tetracycline onto zirconia nanoparticles synthesized by novel microbial green technology. *J. Environ. Manag.* 261:110235. doi: 10.1016/j.jenvman.2020.110235

Di Rico, F., Vuolo, F., and Puglisi, E. (2025). Evaluating the role of viable cells, heat-killed cells or cell-free supernatants in bacterial biocontrol of fungi: a comparison between lactic acid bacteria and *Pseudomonas*. *Microorganisms* 13:105. doi: 10.3390/microorganisms13010105

Dong, Y.-H., Zhang, Q., Xu, J.-L., Li, X.-Z., and Zhang, L.-H. (2000). Quenching quorum sensing signal molecule by N-acyl homoserine lactonases. *FEMS Microbiol. Lett.* 184, 81–88.

Dozolme, P. M. A., and Moukha, S. M. (2020). The *in vitro* production potentialities of secondary toxic metabolites by the fungal factory *Fusarium verticillioides* is, fortunately, largely underestimated in fields: pioneering study on Fumonisins. *Front. Microbiol.* 11:562754. doi: 10.3389/fmicb.2020.562754

El Sabagh, A., Islam, M. S., Hossain, A., Iqbal, M. A., Mubeen, M., Waleed, M., et al. (2022). Phytohormones as growth regulators during abiotic stress tolerance in plants. *Front. Agron.* 4:765068. doi: 10.3389/fagro.2022.765068

Elsharkawy, M. M., Shimizu, M., Takahashi, H., Ozaki, K., and Hyakumachi, M. (2013). Induction of systemic resistance against cucumber mosaic virus in *Arabidopsis thaliana* by *Trichoderma asperellum* SKT-1. *Plant Pathol. J.* 29, 193–200. doi: 10.5423/PPJ.SI.07.2012.0117

Escobar-Muciño, E., Arenas-Hernández, M. M. P., and Luna-Guevara, M. L. (2022). Mechanisms of inhibition of quorum sensing as an alternative for the control of *E. coli* and Salmonella. *Microorganisms* 10:884. doi: 10.3390/microorganisms10050884

Eswaran, S. U. D., Sundaram, L., Perveen, K., Bukhari, N. A., and Sayyed, R. Z. (2024). Osmolyte-producing microbial biostimulants regulate the growth of *Arachis hypogaea* L. under drought stress. *BMC Microbiol.* 24:165. doi: 10.1186/s12866-024-03320-6

Feder-Mengus, C., Ghosh, S., Reschner, A., Martin, I., and Spagnoli, G. C. (2008). New dimensions in tumor immunology: what does 3D culture reveal? *Trends Mol. Med.* 14, 333–340. doi: 10.1016/j.molmed.2008.06.001. PMID: 18614399

Franzetti, A., Gandolfi, I., Bestetti, G., Smyth, T. J., and Banat, I. M. (2010). Production and applications of trehalose lipid biosurfactants. *Eur. J. Lipid Sci. Tech.* 112, 617–627. doi: 10.1002/ejlt.200900162

Garg, A., Gupta, D., and Sharma, S. (2020). Stability and shelf life of microbial biopesticides: challenges and advancements. *Biol. Control* 143:104209. doi: 10.1016/j.biocontrol.2020.104209

Gautam, S., Sharma, R., Chauhan, A., Shirkot, C. K., and Kaushal, R. (2020). Biocontrol activities of rhizobacteria associated with apple, apricot and kiwi rhizosphere against bacterial canker caused by *Clavibacter michiganensis*. *Indian Phytopathol.* 73, 45–56. doi: 10.1007/s42360-019-00172-3

Ge, S., Han, J., Sun, Q., Ye, Z., Zhou, Q., Li, P., et al. (2024). Optimization of cryoprotectants for improving the freeze-dried survival rate of potential probiotic *Lactococcus lactis* ZFM559 and evaluation of its storage stability. *LWT* 198:116052. doi: 10.1016/j.lwt.2024.116052

Ghazy, N., and El-Nahrawy, S. (2021). Siderophore production by *Bacillus subtilis* MF497446 and *Pseudomonas koreensis* MG209738 and their efficacy in *controlling Cephalosporium* maydis in maize plant. *Arch. Microbiol.* 203, 1195–1209. doi: 10.1007/s00203-020-02113-5

Glick, B. R. (2020). "Introduction to Plant Growth-Promoting Bacteria" in Beneficial Plant-Bacterial Interactions (Cham: Springer), 1–37. doi: 10.1007/978-3-030-44368-9_1

Gudiña, E. J., Teixeira, J. A., and Rodrigues, L. R. (2015). Biosurfactant production by Bacillus strains isolated from dairy industries. *Biochem. Eng. J.* 101, 108–118. doi: 10.1016/j.bej.2015.05.006

Gullifa, G., Risoluti, R., Mazzoni, C., Barone, L., Papa, E., Battistini, A., et al. (2023). Microencapsulation by a spray drying approach to produce innovative probiotics-based

products extending the shelf-life in non-refrigerated conditions. *Molecules* 28:860. doi: 10.3390/molecules28020860

Gunal Köroglu, D., Bilgin, A., Karabulut, G., Saricaoglu, B., and Capanoglu, E. (2024). Encapsulation of hydrophobic compounds in yeast cells: methods, characterization, and applications:252-74. doi: 10.37349/eff.2024.00037

Hamad, S., et al. (2022). Ethanol stabilization of quorum sensing inhibitors from *Pseudomonas* spp. *Microb. Biotechnol.* 15, 874–885. doi: 10.1111/1751-7915.14005

Hirao, T., Okazawa, A., Harada, K., Kobayashi, A., Muranaka, T., and Hirata, K. (2012). Green leaf volatiles enhance methyl jasmonate response in Arabidopsis. *J. Biosci. Bioeng.* 114, 540–545. doi: 10.1016/j.jbiosc.2012.06.010

Huang, S., Vignolles, M.-L., Chen, X. D., Le Loir, Y., Jan, G., Schuck, P., et al. (2017). Spray drying of probiotics and other food-grade bacteria: a review. *Trends Food Sci. Technol.* 63, 1–17. doi: 10.1016/j.tifs.2017.02.007

Ibitoye, D. O., and Kolawole, A. O. (2022). Farmers' appraisal on okra [*Abelmoschus esculentus* (L.)] production and phenotypic characterization: a synergistic approach for improvement. *Front. Plant Sci.* 13, 1–9. doi: 10.3389/fpls.2022.787577

Idris, E. E., Bochow, H., Ross, H., and Borriss, R. (2004). Use of *Bacillus subtilis* as biocontrol agent. VI. Phytohormonelike action of culture filtrates prepared from plant growth-promoting *Bacillus amyloliquefaciens* FZB24, FZB42, FZB45 and *Bacillus subtilis* FZB37/Nutzung von Bacillus subtilis als Mittel für den biologischen Pflanzenschutz. VI. Phytohormonartige Wirkung von Kulturfiltraten von pflanzenwachstumsfördernden Bacillus amyloliquefaciens FZB24, FZB42, FZB45 und *Bacillus subtilis* FZB37. *J. Plant Dis. Protect.* 111, 583–597. Available at: https://www.jstor.org/stable/43215615

Imran, M., Abo-Elyousr, K. A. M., Mousa, M. A. A., and Saad, M. M. (2023). Use of Trichoderma culture filtrates as a sustainable approach to mitigate early blight disease of tomato and their influence on plant biomarkers and antioxidants production. *Front. Plant Sci.* 14:1192818. doi: 10.3389/fpls.2023.1192818

Islam, S., Akanda, A. M., Prova, A., Islam, M. T., and Hossain, M. M. (2016). Isolation and Identification of Plant Growth Promoting Rhizobacteria from Cucumber Rhizosphere and Their Effect on Plant Growth Promotion and Disease Suppression. *Frontiers in microbiology* 6:1360. doi: 10.3389/fmicb.2015.01360

Ismail, H. Y., Isa, T., Ngoshe, I. Y., and Gajere, H. M. (2018). Biosurfactant production by Bacteria isolated from hydrocarbon impacted soil. *Bioremed. Sci. Technol. Res.* 6, 1–4. doi: 10.54987/bstr.v6i2.430

Jadhav, H. P., Shaikh, S. S., and Sayyed, R. Z. (2017). "Role of hydrolytic enzymes of rhizoflora in biocontrol of fungal phytopathogens: an overview" in Rhizotrophs: Plant growth promotion to bioremediation, microorganisms for sustainability. ed. S. Mehnaz, vol. 2, 183–203.

Ji, C., Nguyen, L. N., Hou, J., Hai, F. I., and Chen, V. (2017). Direct immobilization of laccase on titania nanoparticles from crude enzyme extracts of *P. ostreatus* culture for micro-pollutant degradation. *Sep. Purif. Technol.* 178, 215–223. doi: 10.1016/j.seppur.2017.01.043

Kaewchomphunuch, T., Charoenpichitnunt, T., Thongbaiyai, V., Ngamwongsatit, N., and Kaeoket, K. (2022). Cell-free culture supernatants of *Lactobacillus* spp. and *Pediococcus* spp. inhibit growth of pathogenic *Escherichia coli* isolated from pigs in Thailand. *BMC Vet. Res.* 18, 60–13. doi: 10.1186/s12917-022-03140-8

Kantar, C., Demiray, H., and Dogan, N. M. (2010). Role of microbial exopolymeric substances on chromium sorption and transport in heterogeneous subsurface soil. II. Binding of Cr(III) in EPS/soil system. *Chemosphere* 82, 1489–1495. doi: 10.1016/j.chemosphere.2011.01.009

Khamsuk, K., Dell, B., Pathom-Aree, W., Pathaichindachote, W., Suphrom, N., Nakaew, N., et al. (2024). Screening Plant Growth-Promoting Bacteria with Antimicrobial Properties for Upland Rice. *Journal of microbiology and biotechnology* 34, 1029–1039. doi: 10.4014/jmb.2402.02008

Khan, W., Costa, C., Souleimanov, A., Prithiviraj, B., and Smith, D. L. (2011). Response of *Arabidopsis thaliana* roots to lipo-chitooligosaccharide from Bradyrhizobium japonicum and other chitin-like compounds. *Plant Growth Regul.* 63, 243–249. doi: 10.1007/s10725-010-9521-6

Khan, N., Martínez-Hidalgo, P., Ice, T. A., Maymon, M., Humm, E. A., Nejat, N., et al. (2018). Antifungal activity of *Bacillus* species against *Fusarium* and analysis of the potential mechanisms used in biocontrol. *Front. Microbiol.* 9:2363. doi: 10.3389/fmicb.2018.02363

Khan, N., Maymon, M., Hirsch, A. M., and Dasgupta, P. R. (2020). Isolation and characterization of plant growth-promoting rhizobacteria (PGPR) from agricultural fields. *Appl. Soil Ecol.* 150:103457. doi: 10.1016/j.apsoil.2019.103457

Köhl, J., Kolnaar, R., and Ravensberg, W. J. (2019). Mode of action of microbial biological control agents against plant diseases: relevance beyond efficacy. *Front. Plant Sci.* 10:845. doi: 10.3389/fpls.2019.00845

Koohestani, M., Moradi, M., Tajik, H., and Badali, A. (2018). Effects of cell-free supernatant of *Lactobacillus acidophilus* LA5 and *Lactobacillus casei* 431 against planktonic form and biofilm of *Staphylococcus aureus*. *Vet. Res. Forum Fall* 9, 301–306. doi: 10.30466/vrf.2018.33086

Kopittke, P. M., Menzies, N. W., Wang, P., McKenna, B. A., and Lombi, E. (2019). Soil and the intensification of agriculture for global food security. *Environ. Int.* 132:105078. doi: 10.1016/j.envint.2019.105078

Kristensen, M. F., Leonhardt, D., Neland, M. L. B., and Schlafer, S. (2020). A 3D printed microfluidic flow-cell for microscopy analysis of in situ-grown biofilms. *J. Microbiol. Methods* 172:105876. doi: 10.1016/j.mimet.2020.105876

Kudjordjie, E. N., Sapkota, R., Steffensen, S. K., Fomsgaard, I. S., and Nicolaisen, M. (2019). Maize synthesized benzoxazinoids affect the host associated microbiome. *Microbiome* 7:151. doi: 10.1186/s40168-019-0765-8

Kumar, S., Mishra, A., Sharma, S., and Vishwakarma, R. K. (2020). Plant growth promoting rhizobacteria: diversity and applications in agriculture. *Environ. Sustain.* 3, 15–27. doi: 10.1007/s42398-019-00113-3

Kumar, S., Patel, J. S., and Meena, R. S. (2021). Biostimulants in sustainable agriculture: advances and future outlook. *Agronomy* 11:199. doi: 10.3390/agronomy11020199

Lade, H., Paul, D., Kweon, J. H., and Yang, Y. H. (2014). Quorum sensing regulation and inhibition of virulence gene expression in *Chromobacterium violaceum*, an opportunistic human pathogen. *Sci. Rep.* 4:6839. doi: 10.1038/srep06839

Li, Y., Héloir, M., Zhang, X., Geissler, M., Trouvelot, S., Jacquens, L., et al. (2019). Surfactin and fengycin contribute to the protection of a *Bacillus subtilis* strain against grape downy mildew by both direct effect and defence stimulation. *Mol. Plant Pathol.* 20, 1037–1050. doi: 10.1111/mpp.12809

Li, P., Su, R., Yin, R., Lai, D., Wang, M., Liu, Y., et al. (2020). Detoxification of mycotoxins through biotransformation. *Toxins* 12, 1–37. doi: 10.3390/toxins12020121

Li, J., Wang, J., Liu, H., Macdonald, C. A., and Singh, B. K. (2022). Application of microbial inoculants significantly enhances crop productivity: a meta-analysis of studies from 2010 to 2020. *J. Sustain. Agric. Environ.* 1, 216–225. doi: 10.1002/sae2.12028

Li, B., Zhao, L., Liu, D., Zhang, Y., Wang, W., Miao, Y., et al. (2023). Bacillus subtilis Promotes Cucumber Growth and Quality under Higher Nutrient Solution by Altering the Rhizospheric Microbial Community. *Plants (Basel, Switzerland)* 12:298. doi: 10.3390/plants12020298

Lorenzo, O., Piqueras, R., Sánchez-Serrano, J. J., and Solano, R. (2003). Ethylene response factor1 integrates signals from ethylene and jasmonate pathways in plant defense. *Plant Cell Online* 15, 165–178. doi: 10.1105/tpc.007468

Mahanty, S., Chatterjee, S., Ghosh, S., Tudu, P., Gaine, T., Bakshi, M., et al. (2020). Synergistic approach towards the sustainable management of heavy metals in wastewater using mycosynthesized iron oxide nanoparticles: biofabrication, adsorptive dynamics and chemometric modeling study. *J. Water Proces Eng.* 37:101426. doi: 10.1016/j.jwpe.2020.101426

Mahmoud, Y. A. G., El-Halmouch, Y. H., Nasr, E. E., Al-Sodany, Y. M., El-Nogoumy, B. A., Ali, S. S., et al. (2024). Exploring the potential of biosurfactants produced by fungi found in soil contaminated with petrochemical wastes. *Sci. Rep.* 14:25733. doi: 10.1038/s41598-024-75865-5

Majeedras, H., Gill, B., and Bhanot, R. (2018). A comparative study on microbial supernatant extraction methods. *Microb. Biotechnol. J.* 5, 34–42. doi: 10.1007/s12355-018-0093-1

Mani-López, E., Arrioja-Bretón, D., and López-Malo, A. (2022). The impacts of antimicrobial and antifungal activity of cell-free supernatants from lactic acid bacteria *in vitro* and foods. *Compr. Rev. Food Sci. Food Saf.* 21, 604–641. doi: 10.1111/1541-4337.12872

Mao, Y., Wang, Y., Luo, X., Chen, X., and Wang, G. (2023). Impact of cell-free supernatant of lactic acid bacteria on *Staphylococcus aureus* biofilm and its metabolites. *Front. Vet. Sci.* 10:1184989. doi: 10.3389/fvets.2023.1184989

Marchant, R., and Banat, I. M. (2012). Biosurfactants: a sustainable replacement for chemical surfactants? *Biotechnol. Lett.* 34, 1597–1605. doi: 10.1007/s10529-012-0956-x

M'henni, Y. B., Salem, I. B., Souli, M., Tounsi, S., Debieu, D., Fillinger, S., et al. (2022). Biocontrol and growth promotion potential of combined application of *Trichoderma simmonsii* and aspergillus westerdijkiae against apple tree dieback disease. *PhytoFrontiers* 2, 268–279. doi: 10.1094/PHYTOFR-01-22-0005-R

Mihalache, G., Balaes, T., Gostin, I., Stefan, M., Coutte, F., and Krier, F. (2018). Lipopeptides produced by *Bacillus subtilis* as new biocontrol products against fusariosis in ornamental plants. *Environ. Sci. Pollut. Res.* 25, 29784–29793. doi: 10.1007/s11356-017-9162-7

Monjezi, N., Yaghoubian, I., and Smith, D. L. (2023). Cell-free supernatant of *Devosia* sp. (strain SL43) mitigates the adverse effects of salt stress on soybean (*Glycine max* L.) seed vigor index. *Front. Plant Sci.* 14:1071346. doi: 10.3389/fpls.2023.1071346

Morcillo, R. J., Singh, S. K., He, D., An, G., Vílchez, J. I., Tang, K., et al. (2020). Rhizobacterium-derived diacetyl modulates plant immunity in a phosphate-dependent manner. *EMBO J.* 39:e102602. doi: 10.15252/EMBJ.2019102602

Morcillo, R. J. L., Baroja-Fernández, E., López-Serrano, L., Leal-López, J., Muñoz, F. J., Bahaji, A., et al. (2022). Cell-free microbial culture filtrates as candidate biostimulants to enhance plant growth and yield and activate soil- and plant-associated beneficial microbiota. *Front. Plant Sci.* 13:1040515. doi: 10.3389/fpls.2022.1040515

Morel, M. A., Cagide, C., Minteguiaga, M. A., Dardanelli, M. S., and Castro-Sowinski, S. (2015). The pattern of secreted molecules during the co-inoculation of alfalfa plants with *Sinorhizobium meliloti* and *Delftia* sp. strain JD2: an interaction that improves plant yield. *Mol. Plant-Microbe Interact.* 28, 134–142. doi: 10.1094/MPMI-08-14-0229-R

Moretti, L. G., Crusciol, C. A. C., Kuramae, E. E., Bossolani, J. W., Moreira, A., Costa, N. R., et al. (2020). Effects of growth-promoting bacteria on soybean root activity, plant development, and yield. *Agron. J.* 112, 418–428. doi: 10.1002/agj2.20010

Naamala, J., Msimbira, L. A., Antar, M., Subramanian, S., and Smith, D. L. (2022). Cell-free supernatant obtained from a salt tolerant *Bacillus amyloliquefaciens* strain enhances germination and radicle length under NaCl stressed and optimal conditions. *Front. Sustain. Food Syst.* 6:788939. doi: 10.3389/fsufs.2022.788939

Naamala, J., Msimbira, L. A., Subramanian, S., and Smith, D. L. (2023). *Lactobacillus helveticus* EL2006H cell-free supernatant enhances growth variables in *Zea mays* (maize), *Glycine max* L. Merill (soybean) and *Solanum tuberosum* (potato) exposed to NaCl stress. *Front. Microbiol.* 13, 1–12. doi: 10.3389/fmicb.2022.1075633

Nair, A., Juwarkar, A. A., and Singh, S. K. (2007). Production and characterization of siderophores and its application in arsenic removal from contaminated soil. *Water Air Soil Pollut.* 180, 199–212. doi: 10.1007/s11270-006-9263-2

Nasrollahzadeh, A., Mokhtari, S., Khomeiri, M., and Saris, P. (2022). Mycotoxin detoxification of food by lactic acid bacteria. *Food Contamination* 9:1. doi: 10.1186/s40550-021-00087-w

Nikolić, I., Berić, T., Dimkić, I., Popović, T., Lozo, J., Fira, D., et al. (2019). Biological control of *Pseudomonas syringae* pv. Aptata on sugar beet with *Bacillus pumilus* SS-10.7 and *Bacillus amyloliquefaciens* (SS-12.6 and SS-38.4) strains. *J. Appl. Microbiol.* 126, 165–176. doi: 10.1111/jam.14070

Nurbailis, N., Djamaan, A., Rahma, H., and Liswarni, Y. (2019). Potential of culture filtrate from Trichoderma spp. as biofungicide to Colletotrichum gloeosporioides causing anthracnose disease in chili. *Biodiversitas Journal of Biological Diversity.* 20. doi: 10.13057/biodiv/d201020

O'Brien, S., Hodgson, D. J., and Buckling, A. (2014). Social evolution of toxic metal bioremediation in *Pseudomonas aeruginosa*. *Proc. R. Soc. B Biol. Sci.* 281:20140858. doi: 10.1098/rspb.2014.0858

Olanrewaju, O. S., Glick, B. R., and Babalola, O. O. (2019). Mechanisms of action of plant growth promoting bacteria. *World J. Microbiol. Biotechnol.* 35:33. doi: 10.1007/s11274-019-2604-1

Pacwa-Płociniczak, M., Płaza, G. A., Piotrowska-Seget, Z., and Cameotra, S. S. (2011). Environmental applications of biosurfactants: recent advances. *Int. J. Mol. Sci.* 12, 633–654. doi: 10.3390/ijms12010633

Patel, S., and Saraf, M. (2017). Applications of bioactive compounds in agriculture: their role in biotic stress management and crop productivity. *Biotechnol. Rep.* 15, 63–69. doi: 10.1016/j.btre.2017.06.001

Pellegrini, M., Pagnani, G., Bernardi, M., Mattedi, A., Spera, D. M., and Gallo, M. D. (2020). Cell-free supernatants of plant growth-promoting Bacteria: a review of their use as biostimulant and microbial biocontrol agents in sustainable agriculture. *Sustain. For.* 12:9917. doi: 10.3390/su12239917

Perczak, A., Goliński, P., Bryła, M., and Waśkiewicz, A. (2018). The efficiency of lactic acid bacteria against pathogenic fungi and mycotoxins. *Arch. Ind. Hyg. Toxicol.* 69, 32–45. doi: 10.2478/aiht-2018-69-3051

Pieterse, C. M. J., and Van Loon, L. C. (2007). "Signalling cascades involved in induced resistance" in Induced resistance for plant defence. eds. D. Walters, A. C. Newton and G. Lyon (London: Blackwell), 65–88.

Pieterse, C. M. J., Zamioudis, C., Berendsen, R. L., Weller, D. M., Van Wees, S. C. M., and Bakker, P. A. H. M. (2014). Induced systemic resistance by beneficial microbes. *Annu. Rev. Phytopathol.* 52, 347–375. doi: 10.1146/annurev-phyto-082712-102340

Posada, L. F., Ramírez, M., Ochoa-Gómez, N., Cuellar-Gaviria, T. Z., Argel-Roldan, L. E., Ramírez, C. A., et al. (2016). Bioprospecting of aerobic endospore-forming bacteria with biotechnological potential for growth promotion of banana plants. *Sci. Hortic.* 212, 81–90. doi: 10.1016/j.scienta.2016.09.040

Radhakrishnan, R., Kang, S. M., Baek, I. Y., and Lee, I. J. (2014). Characterization of plant growth-promoting traits of Penicillium species against the effects of high soil salinity and root disease. *J. Plant Interact.* 9, 754–762. doi: 10.1080/17429145.2014.930524

Rasamiravaka, T., Vandeputte, O. M., Pottier, L., Huet, J., Rabemanantsoa, C., Kiendrebeogo, M., et al. (2015). *Pseudomonas aeruginosa* biofilm formation and quorum sensing are positively regulated by plant secondary metabolites. *Microbes Environ.* 30, 1, 58–66. doi: 10.1264/jsme2.ME14144

Rashid, R., Chelliah, R., and Rahman, S. (2021). Biosurfactant production and quorum sensing inhibition by *Pseudomonas aeruginosa*. *J. Appl. Microbiol.* 130, 785–797. doi: 10.1111/jam.14896

Reddy, M. S., Naresh, B., Leela, T., Prashanthi, M., Madhusudhan, N. C., Dhanasri, G., et al. (2010). Biodegradation of phenanthrene with biosurfactant production by a new strain of *Brevibacillus* sp. *Bioresour. Technol.* 101, 7980–7983. doi: 10.1016/j.biortech.2010.04.054

Rizvi, A., and Khan, M. S. (2018). Heavy metal-induced oxidative damage and root morphology alterations of maize (*Zea mays* L.) plants and stress mitigation by metal tolerant nitrogen-fixing *Azotobacter chroococcum*. *Ecotoxicol. Environ. Saf.* 157, 9–20. doi: 10.1016/j.ecoenv.2018.03.063

Rondina, A. B. L., dos Santos Sanzovo, A. W., Guimarães, G. S., Wendling, J. R., Nogueira, M. A., and Hungria, M. (2020). Changes in root morphological traits in soybean co-inoculated with *Bradyrhizobium* spp. and *Azospirillum brasilense* or treated with *A. brasilense* exudates. *Biol. Fertil. Soils* 56, 537–549. doi: 10.1007/s00374-020-01453-0

San Keskin, N. O., Celebioglu, A., Sarioglu, O. F., Uyar, T., and Tekinay, T. (2018). Encapsulation of living bacteria in electrospuncyclodextrin ultrathin fibers for bioremediation of heavy metals and reactive dye from waste water. *Colloids Surf. B* 161, 169–176. doi: 10.1016/j.colsurfb.2017.10.047

Santos, V. B., and Araújo, W. L.Plant growth promoting rhizobacteria (2017). "Fundamentals and applications" in Plant-microbe interactions in agro-ecological perspectives. eds. D. Singh, H. B. Singh and R. Prabha (Singapore: Springer), 145–168.

Santoyo, G., Moreno-Hagelsieb, G., del Carmen, O.-M. M., and Glick, B. R. (2021). Plant growth-promoting bacterial endophytes. *Microbiol. Res.* 240:126549. doi: 10.1016/j.micres.2020.126549

Sarathy, J. P., Gruber, G., and Dick, T. (2019). Re-understanding the mechanisms of action of the anti-mycobacterial drug Bedaquiline. *Antibiotics* 8:261. doi: 10.3390/antibiotics8040261

Sellem, I., Triki, M. A., Elleuch, L., Cheffi, M., Chakchouk, A., Smaoui, S., et al. (2017). The use of newly isolated Streptomyces strain TN258 as potential biocontrol agent of potato tubers leak caused by *Pythium ultimum*. *J. Basic Microbiol.* 57, 393–401. doi: 10.1002/jobm.201600604

Sifour, M., Al-Jilawi, M. H., and Aziz, G. M. (2007). Emulsification properties of biosurfactant produced from *Pseudomonas aeruginosa* RB 28. *Pak. J. Biol. Sci.* 10, 1331–1335. doi: 10.3923/pjbs.2007.1331.1335

Silambarasan, S., Logeswari, P., Valentine, A., Cornejo, P., and Kannan, V. R. (2020). *Pseudomonas citronellolis* strain SLP6 enhances the phytoremediation efficiency of *Helianthus annuus* in copper contaminated soils under salinity stress. *Plant Soil* 457, 241–253. doi: 10.1007/s11104-020-04734-7

Simpson, R. (2010). Stabilization of Proteins for Storage. Cold Spring Harbor protocols 2010:pdb.top79. doi: 10.1101/pdb.top79

Singh, P., Kim, Y. J., Zhang, D., and Yang, D. C. (2016). Biological synthesis of nanoparticles from plants and microorganisms. *Trends Biotechnol.* 34, 588–599. doi: 10.1016/j.tibtech.2016.02.006

Sivojiene, D., Kacergius, A., Baksiene, E., Maseviciene, A., and Zickiene, L. (2021). The Influence of organic fertilizers on the abundance of soil microorganism communities, agrochemical indicators, and yield in east Lithuanian light soils. *Plants* 10:2648. doi: 10.3390/plants10122648

Sornsenee, P., Chatatikun, M., Mitsuwan, W., Kongpol, K., Kooltheat, N., Sohbenalee, S., et al. (2021). Lyophilized cell-free supernatants of Lactobacillus isolates exhibited antibiofilm, antioxidant, and reduces nitric oxide activity in lipopolysaccharide-stimulated RAW 264.7 cells. *PeerJ* 9:e12586. doi: 10.7717/peerj.12586

Sravya, K., and Sangeetha, S. (2022). Feasibility study on bioremediation techniques to contaminated soils. *Proc. Mater. Today* 51, 2556–2560. doi: 10.1016/j.matpr.2021.12.364

Subramanian, S., Souleimanov, A., and Smith, D. L. (2021). Thuricin17 production and proteome differences in *Bacillus thuringiensis* NEB17 cell-free supernatant under NaCl stress. *Front. Sustain. Food Syst.* 5:630628. doi: 10.3389/fsufs.2021.630628

Šuchová, K., Fehér, C., Ravn, J. L., Bedő, S., Biely, P., and Geijer, C. (2022). Cellulose- and xylan-degrading yeasts: Enzymes, applications and biotechnological potential. *Biotechnol. Adv.* 59:107981. doi: 10.1016/j.biotechadv.2022.107981

Tewari, S., Pooniya, V., and Sharma, S. (2020). Next generation bioformulation prepared by amalgamating Bradyrhizobium, cell free culture supernatant, and exopolysaccharides enhances the indigenous rhizospheric rhizobial population, nodulation, and productivity of pigeon pea. *Appl. Soil Ecol.* 147:103363. doi: 10.1016/j.apsoil.2019.103363

Trinh, L. L., Le, K. N., Le Lam, H. A., and Nguyen, H. H. (2025). Cell-free supernatants from plant growth-promoting rhizobacteria *Bacillus albus* strains control *aspergillus flavus* disease in peanut and maize seedlings. *Beni-Suef Univ. J. Basic Appl. Sci.* 14:4. doi: 10.1186/s43088-025-00594-1

Umar, A., Zafar, A., Wali, H., Siddique, M. P., Qazi, M. A., Naeem, A. H., et al. (2021). Low-cost production and application of lipopeptide for bioremediation and plant growth by *Bacillus subtilis* SNW3. *AMB Express* 11:165. doi: 10.1186/s13568-021-01327-0

Uroz, S., Dessaux, Y., and Oger, P. (2009). Quorum sensing and quorum quenching: the yin and yang of bacterial communication. *Chembiochem* 10, 205–216. doi: 10.1002/cbic.200800521

Veliz, E. A., Martínez-Hidalgo, P., and Hirsch, A. M. (2017). Chitinase-producing bacteria and their role in biocontrol. *AIMS microbiology* 3, 689–705. doi: 10.3934/microbiol.2017.3.689

Villegas-escobar, V., González-jaramillo, L. M., Ramírez, M., Natalia, R., Sierra-zapata, L., Orduz, S., et al. (2018). Lipopeptides from *Bacillus* sp. EA-CB0959: active metabolites responsible for *in vitro* and *in vivo* control of *Ralstonia solanacearum* biol. *Control* 125, 20–28. doi: 10.1016/j.scienta.2017.07.034

Wang, Q., Xiong, D., Zhao, P., Yu, X., Tu, B., and Wang, G. (2011). Effect of applying an arsenic-resistant and plant growth-promoting rhizobacterium to enhance soil arsenic phytoremediation by *Populus deltoides* LH05-17. *J. Appl. Microbiol.* 111, 1065–1074. doi: 10.1111/j.1365-2672.2011.05142.x

Wang, X. Q., Zhao, D. L., Shen, L. L., Jing, C. L., and Zhang, C. S. (2018). "Application and mechanisms of *Bacillus subtilis* in biological control of plant disease" in Role of Rhizospheric microbes in soil. ed. V. Meena (Singapore: Springer), 225–250. doi: 10.1007/978-981-10-8402-7_9

Xu, Y., Yu, Y., Shen, Y., Li, Q., Lan, J., Wu, Y., et al. (2021). Effects of *Bacillus subtilis* and *Bacillus licheniformis* on growth performance, immunity, short chain fatty acid production, antioxidant capacity, and cecal microflora in broilers. *Poult. Sci.* 100:101358. doi: 10.1016/j.psj.2021.101358

Yaghoubian, I., Msimbira, L. A., and Smith, D. L. (2022). Cell-free supernatant of Bacillus strains canImprove seed vigor index of corn (*Zea mays* L.) under salinity stress. *Front. Sustain. Food Syst.* 6:857643. doi: 10.3389/fsufs.2022.857643

Yuan, Y., Wu, K., Liu, F., and Dong, X. (2020). Isolation and identification of plant growth-promoting bacteria and their effects on sustainable crop production. *J. Plant Nutr.* 43, 1447–1464.

Yadav, R., and Yadav, N. (2023). Secondary Metabolites Production in Plant Tissue Culture: A Review. *International Educational Scientific Research Journal* 2, 63–64. Available at: https://www.researchgate.net/publication/367284273_SECONDARY METABOLITESPRODUCTIONINPLANT_TISSUECULTUREAREVIEW/link/63ca67c6d9fb5967c2ee8beb/download?_tp=eyJjb250ZXh0Ijp7InBhZ2U iOiJwdWJsaWNhdGlvbiIsInByZXZpb3VzUGFnZSI6bnVsbCwic3ViUGFnZSI6bnVsbH19

Zhang, S., Deng, Z., Borham, A., Ma, Y., Wang, Y., Hu, J., et al. (2023). Significance of Soil Siderophore-Producing Bacteria in Evaluation and Elevation of Crop Yield. *Horticulturae* 9:370. doi: 10.3390/horticulturae9030370

Zhou, J., Li, J., Wang, J., and Wang, S. (2022). Advances in membrane filtration for microbial supernatant processing. *Trends Biotechnol.* 40, 882–895. doi: 10.1016/j.tibtech.2022.01.005

frontiers | Frontiers in Sustainable Food Systems

TYPE Original Research
PUBLISHED 22 May 2025
DOI 10.3389/fsufs.2025.1581883

Check for updates

OPEN ACCESS

EDITED BY
Mohamed Ait-El-Mokhtar,
University of Hassan II Casablanca, Morocco

REVIEWED BY
Soner Soylu,
Mustafa Kemal University, Türkiye
Talwinder Kaur,
Guru Nanak Dev University, India
Jubair Al-Rashid,
Chinese Academy of Sciences (CAS), China

*CORRESPONDENCE
Muhammad Afzal
mafzal.kust@gmail.com

RECEIVED 23 February 2025
ACCEPTED 02 May 2025
PUBLISHED 22 May 2025

CITATION
Khattak AA, Chen X, AbdAlamer IS, Tomah AA, Hussein RA, Al Farraj DA, Elshikh MS and Afzal M (2025) Isolation and characterization of *Bacillus velezensis*: investigating its mechanisms as an effective biocontrol agent against *Verticillium* wilt in eggplants. *Front. Sustain. Food Syst.* 9:1581883. doi: 10.3389/fsufs.2025.1581883

COPYRIGHT
© 2025 Khattak, Chen, AbdAlamer, Tomah, Hussein, Al Farraj, Elshikh and Afzal. This is an open-access article distributed under the terms of the Creative Commons Attribution License (CC BY). The use, distribution or reproduction in other forums is permitted, provided the original author(s) and the copyright owner(s) are credited and that the original publication in this journal is cited, in accordance with accepted academic practice. No use, distribution or reproduction is permitted which does not comply with these terms.

Isolation and characterization of *Bacillus velezensis*: investigating its mechanisms as an effective biocontrol agent against *Verticillium* wilt in eggplants

Arif Ali Khattak[1], Xiaoyuan Chen[2], Iman Sabah AbdAlamer[3], Ali Athafah Tomah[4], Rasha Abed Hussein[5], Dunia A. Al Farraj[6], Mohamed Soliman Elshikh[6] and Muhammad Afzal[1,2]*

[1]College of Agriculture, South China Agricultural University, Guangzhou, China, [2]Guangdong Provincial Key Laboratory of Utilization and Conservation of Food and Medicinal Resources in Northern Region, Shaoguan University, Shaoguan, China, [3]Department of Biology, College of science, University of Basrah, Basrah, Iraq, [4]Plant Protection, College of Agriculture, University of Misan, AL-amarah, Iraq, [5]Al-Manara College for Medical Sciences, Maysan, AL-Amarah, Iraq, [6]Department of Botany and Microbiology, College of Science, King Saud University, Riyadh, Saudi Arabia

Eggplant production in China is significantly impacted by *Verticillium* wilt caused by *Verticillium dahliae*, leading to substantial yield losses. This study was designed to investigate the potential of rhizobacterial species for the biocontrol of *Verticillium* wilt in eggplant. Among the 42 bacterial isolates tested, strain ARF4 demonstrated the strongest antagonistic effect by inhibiting *V. dahliae* growth by 84.49%, in addition to showing antifungal properties against four other plant pathogens. We found the strain ARF4 is closely related to *Bacillus velezensis* with high bootstrap values (100) through a phylogenetic tree based on 16S, *rpoB*, and *gyrA* gene sequences. The ARF4 produces important antifungal compounds such as chitinase, protease, β-glucosidase, and lipopeptide bacillomycin D, which contribute to its antifungal properties. The extracted lipopeptide of the ARF4 exhibited strong inhibition of conidial germination in *V. dahliae*. Scanning Electron Microscopy (SEM) showed that hyphae treated with the extracted lipopeptide exhibited considerable deformation. Transmission electron microscopy results revealed lysis of the cell walls and plasma membrane, a decreased inner cytoplasmic matrix and a number of mitochondria, and disintegration of internal organelles. Greenhouse trials demonstrated that eggplants treated with strain ARF4 experienced a significant disease severity reduction of 68.45%. This study offers *B. velezensis* ARF4 biological approach to *Verticillium* wilt control in eggplants as an alternative to chemical fungicides and contributes to sustainable agriculture practices.

KEYWORDS

biocontrol, phytopathogenic, bacteria, green technology, sustainable agriculture

1 Introduction

Eggplant (*Solanum melongena*) is a vital agricultural crop in China due to its significant contribution to both the economy and diet. China is the largest producer of eggplant globally, accounting for over 60% of global production. In 2023, China produced approximately 38 million tons of eggplant, showcasing its dominance in the market (Canton, 2021). Zhejiang

province stands out as a major hub for producing eggplants in China, with its cultivated area expanding to 26,666 ha by 2018, "according to data from the Agriculture Department, Zhejiang Province." Eggplant is not only a dietary staple rich in vitamins, minerals, and antioxidants but also a crucial export commodity, enhancing China's agricultural income (Lyu et al., 2024). Its usefulness in cooking makes it an important component of many traditional Chinese dishes. Despite high production, eggplant farming in China meets major challenges due to various diseases. One of the common diseases impacting eggplant crops includes *Verticillium* wilt caused by *Verticillium dahliae* (*V. dahliae*), which has main symptoms such as yellowing leaves, wilting, and yield loss (Ibanga et al., 2023; Scholz et al., 2018; Yang et al., 2019; Zhang et al., 2024).

Verticillium dahliae, the causative agent of *Verticillium* wilt, is a soil-borne fungus that is considered a major threat to eggplant production in China, leading to considerable economic losses (Tomah et al., 2023). The occurrence of *Verticillium* wilt in eggplant cultivation areas in China is responsible for yield losses ranging from 34.1 to 42.5%, which is a major blow to the agricultural economy and causes significant economy impact (Zhu et al., 2021). Urgent research is required to produce resilient, sustainable, and eco-friendly approaches for handling soil-borne diseases affecting eggplant, such as *Verticillium* wilt. Biological control is considered being widely recognized eco-friendly alternative to traditional chemical methods. It plays a crucial role in integrated pest management by employing natural predators to regulate pest populations. This approach offers several significant economic and ecological advantages, making it an important approach to sustainable agriculture (Barzman et al., 2015; Lahlali et al., 2022). Biocontrol offers a sustainable and economical pest management solution, reducing the risk of pesticide resistance while maintaining long-term effectiveness at minimal cost (Pandit et al., 2022; Shang et al., 2024). This method may decrease our dependency on chemical pesticides, which can harm non-target species such as birds, beneficial insects, and aquatic life (Wan et al., 2025). Implementing biological control to minimize reliance on chemical pesticides can offer substantial environmental and health benefits, as chemical pesticides enhance agricultural productivity, while their improper or excessive use can lead to severe environmental damage, polluting soil, air, and water. While also threatening human health with long-term effects like cancer, endocrine disorders, and poisoning. By minimizing the need for these chemicals, biocontrol endorses safer food production and supports healthier ecosystems (Farah et al., 2024; Munir et al., 2024). Rhizobacteria are important biocontrol agents and play a crucial rule, extensively used against *Verticillium* wilt diseases, which infect several plants, such as tomatoes and olives as well. Additionally, they are also effective in the management of other plant diseases such as pepper gray mold, apple bitter rot, and tobacco bacterial wilt (Chen and Wang, 2022; Dhouib et al., 2019; Jiang et al., 2018; Kim et al., 2021; Triki et al., 2006; Wang et al., 2023). Studies have shown that some rhizobacteria species produce a variety of antimicrobial compounds, including lipopeptides and polyketides, which prevent the growth of pathogens and induce systemic resistance in plants (Fazle Rabbee and Baek, 2020). Furthermore, the application of rhizobacteria as a biocontrol agent not only reduces the occurrence of diseases but also increases plant health. Rhizobacteria with antifungal properties can provide promising and sustainable approach to the control of *Verticillium* wilt diseases. The current study was carried out with the objectives to isolate and screen antifungal rhizobacteria strains against *V. dahliae* and to assess their *in vivo* effectiveness in reducing *Verticillium* wilt in eggplant.

2 Materials and methods

2.1 Fungus pathogen and bacterial strain isolation

The highly pathogenic fungus *V. dahliae* H6 was obtained from the Plant Pathology Laboratory, Agriculture and Biotechnology College, Zhejiang University, Hangzhou, China (Tomah et al., 2023). The fields infestated with *Verticillium* wilt prolonged in Yongle Township, Youjiang District, Guangxi, China, in June 2023 were selected. Rhizosphere soil samples were collected from healthy eggplants. Totally 10 samples, each from a distinct field, were collected and analyzed in the laboratory. Soil samples were serially diluted in order to extract bacterial strains and cultured on Lysogeny broth agar (comprising of 5-g yeast extract, 10-g tryptone, 10-g NaCl, and 15-g agar, with a pH range of 7.0–7.5). Bacterial colonies were selected based on morphological characteristics, including color, size, shape, and surface texture. Each colony was then subcultured three times for further isolation and stored in 30% glycerol. The isolated strains were subsequently preserved in the Culture Collection facility at South China Agricultural University, China.

2.2 Screening of rhizobacterial isolates for antifungal activity against the *Verticillium dahliae*

The antifungal activity of all the isolated rhizobacterial strains was evaluated against the *V. dahliae* growth *via* direct confrontation through the dual-culture plate method, as outlined by Meena et al. (2024). Petri plates of 90-mm diameter containing solidified and sterile potato dextrose agar (PDA) medium were prepared in a fume hood. The center of the PDA plate was inoculated with the disc of a pathogenic fungus (0.5 cm in diameter) which was taken from a 15-day-old colony. A 30-µL aliquot of each bacterial suspension previously grown in Luria Bertani broth (LB broth) in a ZWY-211B rotary shaker at 200 rpm at 30°C for 8 h was put on four of the 5-mm diameter paper discs put around the *V. dahliae* inocula at a distance of 25 mm. The plates inoculated with a pathogenic fungus and without bacteria were regarded as the control treatment. All the plates were incubated at 25°C. The *V. dahliae* colonies' growth diameters (mm) in the antagonistic and control treatments were measured after 8 days of incubation. The percentage inhibition of radial growth (PIRG) was calculated through the formula: $PIRG = [(Ct - Vt)/Ct] \times 100$, where Ct is the growth in the control treatment, while Vt is the growth with cell suspensions of the rhizobacteria strain's treatment. The values were determined as the mean of four replicates, while every experiment was repeated at least three times. The rhizobacteria strain demonstrating the strongest antagonistic activity was selected for further investigations.

2.3 Evaluation of the broad-spectrum antifungal activity of strain ARF4

A highly effective strain ARF4 was assayed for its impact toward radial growth of highly aggressive plant pathogenic fungi, viz. *V. dahliae* H6, *Fusarium oxysporum* f. sp. *niveum* ZJ1 (Huang et al., 2023) *Phytophthora capsici* HZ07 (Tomah et al., 2020a), and Sclerotinia sclerotiorum YY01 (Tomah et al., 2020b), obtained from the plant pathology lab, previously identified and placed in the Culture Collection facility of Institute of Biotechnology, Zhejiang University, Zhejiang, China. The strain ARF4 was routinely reactivated at 37°C in LB broth, while the plant pathogens were reactivated on PDA, at 25°C, in dark. To detect the direct activity of an antifungal strain ARF4 *in vitro*, the disc diffusion technique was applied as described by Meena et al. (2024). In brief, the sterile PDA media were poured into 90 mm a diameter Petri dish plates and left to solidify in a fume hood. The 5-mm diameter mycelial plugs were places at the center of the plates (taken from the edge of colonies of 5-day-old plant-pathogen), and then the four of the 5-mm diameter paper discs were put around the fungal inocula at a distance of 25 mm. The paper discs were inoculated with 30 µL of the bacterial cell suspension which had been cultured on LB broth using a ZWY-211B rotary shaker at 200 rpm at 30°C for 12 h.

To evaluate the indirect antagonistic activity of strain ARF4, the poisoned food method was followed as described by Swati Verma et al. (2020). The bacteria were cultured in LB broth in a ZWY-211B rotary shaker at 200 rpm at 25°C for 48 h. Cell-free culture supernatant (CFCS) was obtained after centrifugation at 6000 rpm for 10 min and filtration using a Millipore filter paper of 0.22-µm diameters. The CFCS was incorporated into the molten PDA at 50%, mixed well, and immediately, 10 mL were poured into the Petri plates. After the medium was solidified in the plates inside a fume hood, the mycelial plugs measuring 5 mm in diameter, carefully excised from the 5-day-old plant-pathogen culture, were positioned centrally on plates. Parafilm strips were used to seal the plates. *V. dahlias* plates were incubated for 14 days in the dark at 25°C, while other plant pathogens were incubated for 5 days only. The plant pathogen colonies' growth diameters (mm) in both direct and indirect antagonistic tests were measured, and the PIRG was determined by applying the formula: $PIRG = [(Ct - Cf)/Ct] \times 100$; where Ct; the growth in control treatments while the *Cf*; the growth in CFCS treatments. The recorded values represent the average of three repeats, and the entire experiment was repeated at least three times.

2.4 Identification of bacterial strains

The ARF4 bacterial strain was selected for further experiments, grown on LB agar for 20–24 h at 30°C and characterized following the procedures outlined by Zhang et al. (2018). For 16S ribosomal RNA (*rRNA*) genes analysis, universal primers 27F (5'-AGAGTTTGAT CMTGGCTCAG-3′) and 1492R (5'-TACGGYTACCTTGTTA CGACTT-3′) were used. The Polymerase Chain Reaction (PCR) products were analyzed by separating them on a 1% agarose gel and visualizing them under ultraviolet light, using a transilluminator (GenoSens 1850, Clinx Science Instruments Co., Ltd., China) after staining with ethidium bromide, in order to verify the presence and size of the amplified 16S *rRNA* gene fragments (da Silva et al., 2013; Hayward, 2000). The PCR products were subsequently forwarded for sequencing to Sangon Biotech Company Limited (Shanghai, China) *via* the Sanger method on an automated DNA sequencer (ABI 3730xl, Applied Biosystems, USA). To identify bacterial species, *rpoB* gene was amplified using primers *rpoB*-f (5′-AGGTCAACTAGTTCAGTATGGAC-3′) and *rpoB*-r (5′-AAGAACCGTAACCGGCAACTT-3′) (Qiu et al., 2018), whereas the *gyrA* gene was amplified with primer pair *gyrA*-f (5′-CAGTCAGGAAATGCGTACGTCCTT-3′) and *gyrA*-r (5′-CAAG GTAATGCTCCAGGCATTGCT-′3) (Chun and Bae, 2000). The resulted amplified sequences were edited by BioEdit 7.19, aligned with ClustalX 1.83, and Basic Local Alignment Search Tools (BLAST) against the GenBank database to identify the closely related sequences. Representative strain sequences were deposited in the GenBank in order to acquire accession numbers. These representative sequences were then used to build a phylogenetic tree, with a neighbor-joining/maximum-likelihood (NJ/ML) approach using the MEGA 7.0 (Kumar et al., 2016), with bootstrap analysis (1,000 replication) conducted to evaluate statistical support of the tree nodes in the phylogenetic trees. Bayesian inference of posterior probability (BIPP) analyses are performed with MrBayes v. 3.2.6 (Ronquist et al., 2012). This method was used to analyze evolutionary connections between the identified bacterial strains and other known species.

2.5 Detection and production of β-glucosidase, chitinase, and protease enzymes

To explore the production of some extracellular hydrolytic enzymes by bacterium strain ARF4 which may be related to antagonism toward pathogen growth, the minimal salt medium (MSM) was used with contents following KH_2PO_4 0.2 g, $(NH_4)_2SO_4$ 1 g, $MgSO_4 \bullet 7H_2O$ 0.2 g, K_2HPO_4 1.6 g, $FeSO_4 \bullet 7H_2O$ 0.01 g, $CaCl_2 \bullet 2H_2O$ 0.02, g, and NaCl 0.1 g. For glucanase activity, the MSM medium was supplemented with 0.5% β-1,3-glucan (Howard et al., 2003; Renwick et al., 1991). The MSM medium was prepared by adding 1% (w/v) colloidal chitin and 1.5% (w/v) agar, with the final pH adjusted to 7.0 for the chitinase activity test (Alsalman et al., 2022), while for protease activity, the medium supplemented with 1% skim milk was used. The 10 µL of suspension of bacteria (standardized to 1×10^8 CFU/mL) and 10 µL of LB broth as control were dropped in the center of the plate and incubated for 2–3 days at 30°C. The chitin plates were treated with 0.1% (w/v) Congo red stain and washed with 1% NaCl. The presence of bacterial hydrolytic enzyme activities was revealed by clear zones of hydrolysis around the bacterial colonies.

2.6 Characterization of lipopeptides of strain ARF4

The inhibition zone in the direct antifungal trial was targeted to collect and identify lipopeptides involved in *V. dahliae* inhibition. The inhibition zone located between the ARF4 strain colony and the *V. dahliae* colony was identified on fifty of the LBA media plates. The sections of the LBA media were carefully cut out from the inhibition zone using a sterile scalpel, ensuring to avoid contamination from other areas. The parts of the media around strain ARF4 that grew alone

without *V. dahliae* were collected as a control. An amount of 100 g of cut sections of the medium was added to a 500-ml flask, followed by the addition of 200 mL of ethyl acetate. The mixture was mechanically shaken overnight at 25°C. The ethyl acetate extract obtained from LBA medium sections was filtered using the Whatman filter paper. Subsequently, the ethyl acetate was evaporated under reduced pressure using an evaporator vacuum shaker at 40°C to obtain a dry extract, which was dissolved in a methanol solvent of 40% for analysis.

The ethyl acetate extract was rinsed through a silica gel column using different ratios of methanol and methylene chloride (1:2, 3:1, and 5:1, respectively).

After drying, the extract was purified further with the reversed-phase high-performance liquid chromatography (RP-HPLC) device. The dry extract was dissolved in 40% methanol and filtered using a 0.22-µm pore. A 10-µl aliquot was put into an Inert Sustain C18 column (5 µm, 250 mm × 4.6 mm) in the HPLC system. Mobile phase A was acetonitrile with 0.1% (vol/vol) trifluoroacetic acid (TFA), and mobile phase B was Milli-Q water with 0.1% (vol/vol) TFA. Purification was performed using a solvent containing 45% mobile phase A and 55% mobile phase B at a flow rate of 8 mL/min. The UV absorption at 220 nm was recorded at running times between 0 min and 35 min for detection. The extract of RP-HPLC-purified and bacillomycin D (CAS:76012–17-4, Guangzhou Yaoguang Technology Co., Ltd., China), as a standard, was subjected to a preparative silica gel thin-layer chromatography (TLC) plate (GF254) using n-butanol–methanol–water (39: 10: 20, v/v/v) as the mobile phase. The TLC plate was visualized under the wavelength of 254 nm.

The extract of RP-HPLC-purified was analyzed using matrix-assisted laser desorption/ionization time-of-flight (MALDI-TOF) mass spectrometry (Bruker, Bremen, Germany) equipped with a 337-nm smart laser beam for desorption and ionization. The study focused on detecting and characterizing lipopeptides by analyzing their mass-to-charge (m/z) ratios using MALDI-TOF mass spectrometry. The analysis was conducted using a Bruker instrument (Bremen, Germany) equipped with a 337-nm smart laser beam for desorption and ionization (Ayed et al., 2014).

2.7 Effect of the extracted lipopeptide of strain ARF4 on conidia germination of *Verticillium dahliae*

The extracted lipopeptide of strain ARF4 was tested for its inhibitory effect on the conidial germination of *V. dahliae* using the agar well diffusion technique. A 0.5 mL of conidia suspension of *V. dahliae* (10^6 spores/mL) was evenly spread onto pre-prepared PDA plates (90-mm diameter). Wells (5-mm diameter) were created in the center of the plate by a sterilized cork borer. The extracted lipopeptide (50 µg/mL prepared in 50% w/v DMSO) was added to wells, while 50 µL of DMSO was added to wells as control. The plates were kept at 25°C for two 48 h, and antifungal activity was assessed by measuring the inhibition zone around the wells.

2.8 Structural change assays in SEM and TEM

SEM was used to observe the morphological changes in the fungal hyphae treated with extracted lipopeptide of strain ARF4. The fungal hyphae were treated with 50 µg/mL of extracted lipopeptide using the agar well diffusion technique for 2 days. The 10-mm diameters of mycelial plugs were taken from the inhibition zone and control (50 µL of DMSO). Both samples were fixed in a 2.5% glutaraldehyde solution for 12 h, following the method outlined by Pretorius et al. (2015) and Xiao et al. (2021). After fixation, the samples were washed three times with 100-mM phosphate buffer, each lasting 10 min. Subsequently, the samples were post-fixed in 1% osmium tetroxide for 3 h. Dehydration was then carried out using a graded ethanol series, ranging from 50 to 100%. After mounting onto an aluminium stub, the samples were sputter-coated with a layer of gold particles and examined using a scanning electron microscope (SEM, SU8010, HITACHI, Japan), followed by imaging. For ultrastructural analysis of extracted lipopeptide effect on hyphae, transmission electron microscopy (TEM) was used. Prior to TEM, mycelial plugs were fixed for 12 h in 2.5% glutaraldehyde solution at 4°C. The 100-mM phosphate buffer was used to rinse for 10 min, and the 1% osmium tetroxide solution for 3 h was used to fix the cells and the gradient of ethanol to dehydrate. With the help of LKB-V Ultratome, the gold-coated samples were cut into ultra-thin sections and stained with uranyl acetate for examination under TEM (H-600, Hitachi, Japan) at 15-kV voltage.

2.9 Management of *Verticillium* wilt disease by ARF4 strain

The potential of the selected rhizobacteria strain ARF4 as a biocontrol agent against *Verticillium* wilt disease was evaluated in susceptible eggplant plants (cv. Zheqie 3, an eggplant F1 hybrid) grown in potted soil under greenhouse conditions. Plastic pots were filled with sterilized soil composed of a mixture of peat, vermiculite, and farmyard soil in a 2:1:1 ratio. The conidial suspension of *V. dahliae* was prepared from a liquid culture grown in Potato Dextrose broth for 7 days at a temperature of 24°C and 130 rpm. The conidia were gently scraped from a sporulating fungal culture using a sterile loop. Then, the spores were suspended in a sterile diluent (distilled water, 0.01% Tween 80) to prevent clumping. Conidia were then filtered through sterile cheesecloth (40 µm) to remove hyphal debris, and its concentration was adjusted to (10^7 conidia/mL). A 5 µL of the conidial suspension was loaded onto a hemocytometer. Spore counts were conducted on the central grid under a microscope (40 × magnification). To calculate the conidia concentration, the following formula was used: Conidia/mL = Average count per square × Dilution factor × 10^4 (Gayoso et al., 2010). The cell suspension of bacterium strain ARF4 was cultured in LB medium at a concentration of 10^7 CFU/mL and incubated on a rotary shaker at 130 rpm and 30 ± 2°C for 24 h, then adjusted to a final concentration of 10^7 conidia/mL. The experiment was done using a completely randomized design with three replicates, 10 plants per replicate. The experimental treatments were carried out as follows: the soil of a group of pots was inoculated with 20 mL of conidia suspension of *Verticillium* and 20 mL of a suspension of bacterial cells. The soil of a group of pots was inoculated with 20 mL of conidia suspension of *Verticillium* only, as negative controls, while the soil of a group of pots was left without inoculation with suspensions of bacterial cells and conidia of *Verticillium*, as positive controls. The three-leaf-old eggplant seedlings previously prepared were transplanted into the inoculated pots. The pots were placed in the greenhouse under controlled conditions, maintaining the humidity level to 70–80% and temperatures of 25 ± 3°C with a light, dark

10.3389/fsufs.2025.1581883

cycle of 16/8 h and light intensity of 500 μmol/m^2 was used (Yang et al., 2023). To assess the potential of a bacterial biocontrol agent, the symptoms of the development of *Verticillium* wilt disease on seedlings were monitored after 20-day post-pathogen inoculation. Assessment of disease severity was applied using a 0–5 scale based on foliar symptoms: 0, no diseased leaf; 1, <10%; 2, 11–25%; 3, 26–50%; 4, >50%; and 5, plant killed (Li et al., 2024). The disease severity (%) and the biological control efficacy (%) were evaluated.

2.10 Statistical analysis

The data analysis was performed using IBM SPSS statistics 21 (Georgia, USA). The data presented in the results represent the average value along with the standard error, which is calculated from a minimum of three values obtained in each independent experiment. The significant differences between groups are determined by the least significant difference test, one-way analysis of variance (ANOVA), and Duncan's test.

3 Results

3.1 Bacterial isolations and antifungal test

In the current study, 42 bacterial isolates were isolated from the rhizosphere of eggplant plants. The bacterial isolates were purified and designated sequentially as ARF1 to ARF42 (Table 1). The antifungal effect of these bacterial strains was evaluated against the radial growth of *V. dahliae* using the dual-culture plate method. One-way ANOVA and Duncan's test were used to show the differences among tested bacterial strains in the rates of radial growth inhibition of *V. dahliae* (Table 1). Among these bacterial strains, ARF4 was found to be the most proficient antagonistic strain, showing the maximum *in vitro* inhibition rate of 84.49% against radial growth of *V. dahliae*. Furthermore, 10 of the bacterial strains isolated had caused growth inhibition of *V. dahliae*, ranging from 18.60 to 18.87%. With a lower inhibition rate, 11 of the bacterial strains isolated caused growth inhibition of *V. dahliae*, ranging from 16.07 to 16.92%. Also, eight of the bacterially produced inhibition zones were between 15.07 and 15.99%. While three of the bacterial strains had recorded the zone of inhibition, ranging from 12.03 to 12.66%, five of the bacterial strains had recorded the zone of inhibition, ranging from 11.17 to 11.96%, and four bacterial strains recorded the zone of inhibition from 10.16 to 10.86%. Overall, although most isolates demonstrated only slight antifungal activity, strain ARF4 outperformed other isolates against *V. dahliae*.

TABLE 1 Antifungal activity on *Verticillium dahliae* by rhizobacteria strains isolated from rhizosphere zone of eggplant plants.

Isolate name	PIRG
ARF1	15.22 ± 1.47 ^{d}
ARF2	18.65 ± 1.77 ^{bc}
ARF3	12.66 ± 1.13 ^{e}
ARF4	84.49 ± 3.15 ^{a}
ARF5	16.07 ± 1.82 ^{d}
ARF6	18.64 ± 0.45 ^{bc}
ARF7	15.07 ± 0.67 ^{d}
ARF8	18.61 ± 1.22 ^{bc}
ARF9	11.17 ± 0.18 ^{ef}
ARF10	15.63 ± 1.09 ^{d}
ARF11	18.63 ± 1.21 ^{bc}
ARF12	10.32 ± 1.08 ^{f}
ARF13	16.91 ± 1.11 ^{bcd}
ARF14	16.77 ± 1.72 ^{bcd}
ARF15	18.62 ± 1.17 ^{bc}
ARF16	15.99 ± 0.43 ^{d}
ARF17	16.90 ± 1.13 ^{bcd}
ARF18	16.92 ± 1.27 ^{bcd}
ARF19	10.75 ± 1.22 ^{ef}
ARF20	18.63 ± 0.29 ^{bc}
ARF21	16.17 ± 1.09 ^{d}
ARF22	15.23 ± 1.47 ^{d}
ARF23	18.61 ± 0.69 ^{bc}
ARF24	11.86 ± 0.88 ^{ef}
ARF25	16.09 ± 1.13 ^{d}
ARF26	15.58 ± 1.14 ^{d}
ARF27	12.03 ± 0.53 ^{ef}
ARF28	18.60 ± 1.57 ^{bc}
ARF29	16.27 ± 0.32 ^{d}
ARF30	11.96 ± 1.12 ^{ef}
ARF31	16.87 ± 0.77 ^{bcd}
ARF32	18.87 ± 1.87 ^{b}
ARF33	10.86 ± 1.16 ^{ef}
ARF34	15.46 ± 0.47 ^{d}
ARF35	12.33 ± 0.17 ^{ef}
ARF36	16.39 ± 0.55 ^{cd}
ARF37	11.26 ± 1.23 ^{ef}
ARF38	18.60 ± 0.33 ^{bc}
ARF39	15.21 ± 0.57 ^{d}
ARF40	11.96 ± 1.68 ^{ef}
ARF41	16.63 ± 0.67 ^{bcd}
ARF42	10.16 ± 0.93 ^{f}

The superscript (abcdef) in table shows significant value ($p < 0.05$).

3.2 Broad spectrum antifungal activity

The inhibitory activity of rhizobacteria strain ARF4 was assessed against four plant pathogens *in vitro*. In the disc diffusion assay, bacterial strain ARF4 exhibited a strong direct antagonistic effect and inhibited all tested plant pathogen radial growth compared to the control (Figure 1). Similarly, in the poisoned food method, indirect antagonism using the cell-free culture supernatant (CFCS) of strain ARF4 (55%) also exhibited significant inhibition of radial growth in all pathogens (Figure 1). Visual assessments indicated that the highest inhibition was recorded against *V. dahliae* in both direct and indirect assays. Based on these results, strain ARF4 is considered an effective antagonist in inhibiting the growth of tested plant pathogens.

Statistical analysis of PIRG revealed that strain ARF4 exhibited strong inhibitory potential against plant pathogens with significant difference ($p < 0.05$) observed among them (Table 2). In the disc diffusion assay, the strain ARF4 strain showed the highest PIRG against *V. dahliae* (80.21 ± 0.58%) while the least recorded was against *F. o.* f. sp. *niveum* was (48.88 ± 0.95%). The PIRG values were found to be (64.67 ± 0.88%) and (57.49 ± 0.97%) against *P. capsici* and *S. sclerotiorum*, respectively. In the

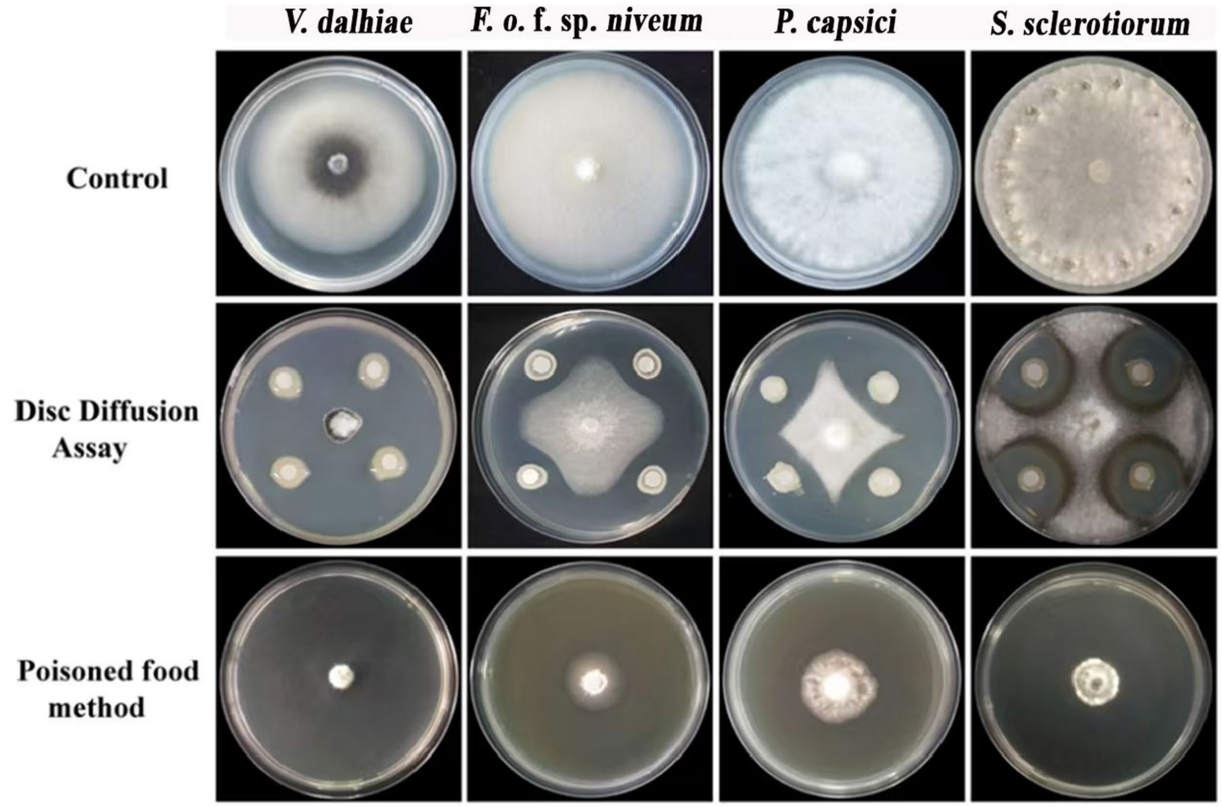

FIGURE 1
In vitro antagonistic activity of strain ARF4 against four plant pathogens. Disc diffusion and poisoned food assays show inhibition of radial growth with maximal suppression against *V. dahliae* (vs. control).

poisoned food method, the CFCS of the bacterial strain ARF4 recorded significant inhibition differences in the radial growth among the plant pathogens. The highest PIRG was again recorded against *V. dahliae* (86.57 ± 0.60%), while the lowest inhibition was recorded against *P. capsici* (67.29 ± 0.92%). However, the high values of PIRG (79.60 ± 0.96%) and (69.19 ± 0.64%) were also recorded against *S. sclerotiorum* and *F. o.* f. sp. *niveum*, respectively.

3.3 Identification of bacterial strains

The DNA of strain ARF4 was amplified by the 16S gene, and a sequence of 1,420 bp was obtained. The BLAST results showed that the strain belongs to the genus *Bacillus* spp. The *rpoB* and *gyrA* genes were amplified to determine a species, and 959 and 546 bp of sequences were obtained, respectively. The BLAST results showed that the species identity of the two genes was aligned 100% with the species of *B. velezensis* of strain BY6 and strain LPL061, respectively. In a phylogenetic tree, the topology of the scoring NJ/ML bootstrap tree analysis was congruent with the BIPP tree for the concatenated three-locus dataset. Strain ARF4 is grouped with *B. velezensis* BY6 and *B. velezensis* LPL061 with a bootstrap support of NJ/ML = 98 and BIPP = 0.99 (Figure 2). This high bootstrap value indicates strong support for the grouping, suggesting that strain ARF4 is closely related to these strains of *B. velezensis*. Strain ARF4 was submitted to GenBank under accession numbers OQ918063.1, OQ920283.1, and OQ920284.1 for 16S, *rpoB*, and *gyrA* genes.

TABLE 2 Antifungal activity of strain ARF4 against four of the plant pathogens using disc diffusion assay and poisoned food method.

Plant pathogens	Percentage inhibition of radial growth (PIRG)	
	Disc diffusion technique	Poisoned food method
V. dahliae	80.21 ± 0.58 a	86.57 ± 0.60 a
F. o. f. sp. *niveum*	48.88 ± 0.95 d	69.19 ± 0.64 c
P. capsici	64.67 ± 0.88 b	67.29 ± 0.92 d
S. sclerotiorum	57.49 ± 0.97 c	79.60 ± 0.96 b
Average of inhibition	62.81	75.66

The superscript (abcd) in table shows significant value ($p < 0.05$).

3.4 Detection production of enzymes of β-glucosidase, chitinase, and protease

The lytic enzymes produced by bacteria play crucial role in the biological transformation of nitrogen, hydrogen, and carbon. These enzymes deform pathogenic fungi's cell walls and act as critical mechanisms of eco-friendly soil-borne pathogen control. ARF4

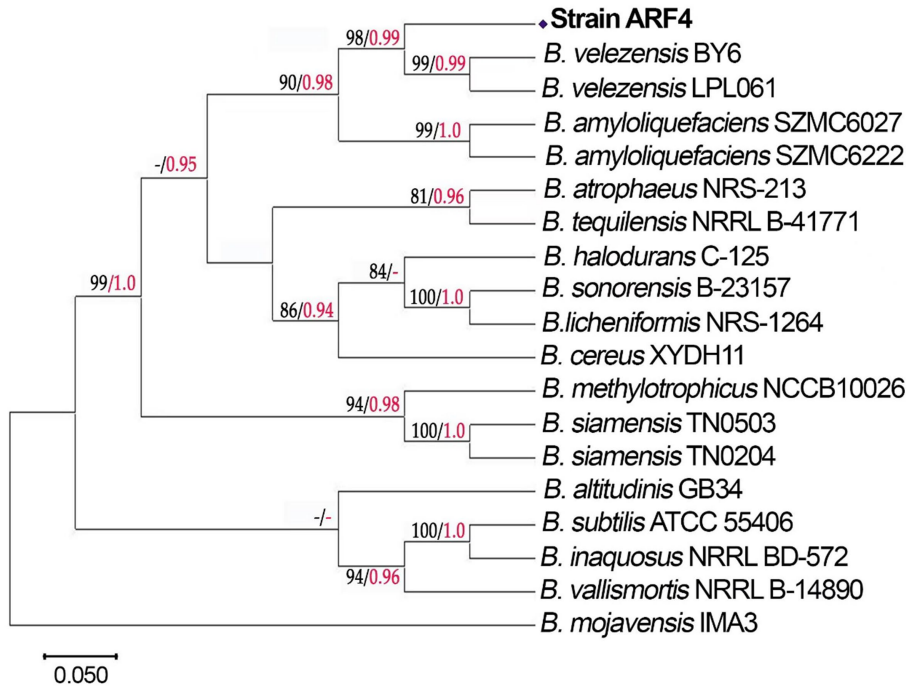

FIGURE 2
The phylogenetic tree of the Strain ARF4 was built based on 16S rRNA, *rpoB*, and *gyrA* gene sequences using MEGA version X with neighbor-joining and maximum-likelihood and Bayesian inference (BI) methods. NJ/ML bootstrap values are indicated by black numbers, while BIPP values are indicated by red. Dashes indicate support values lower than 80% NJ/ML and 0.95 BIPP.

strain produced a halo zone of 1.6 cm around its colony on MSM with 1% skim milk, indicating its capability to produce protease enzyme (Figure 3A). Similarly, ARF4 also exhibited the potential to produce chitinase and β-glucosidase hydrolytic enzymes as indicated by clear halo zones of 1.7- and 1.5-cm diameters on chitin agar and MSM amended with glucan media, respectively (Figures 3B,C).

3.5 Identification of lipopeptides from strain ARF4 extract

The production of specialized lipopeptide by the *B. velezensis* ARF4 cultured on a solid LB medium was analyzed. RP-HPLC analysis showed only one large peak appeared at a retention time19.023 min (Figure 4A). Characterization of the extract produced by strain ARF4 was carried out by TLC. Results obtained by TLC indicate the lipopeptide nature of the bacillomycin D produced, which was observed against standard bacillomycin D (Figure 4B).

Using MALDI-TOF, the resulted mass spectrometry data were compared with the known *Bacillus* metabolite, confirming the presence of a cyclic lipopeptides compound of the iturin family. This compound was homologous to bacillomycin D (m/z 1081.336 $[M + Na]^+$), which includes a heptapeptide molecule attached to a β-amino fatty acid chain consisting of 15 carbon atoms (Table 3; Figures 5A,B). The results of MALDI-TOF mass spectra of strain ARF4, which was grown alone (without *V. dahliae*) as a control, also showed the same lipopeptide indicating polymyxin, which was separated but with shorter peaks (Figure 5C).

3.6 Effect of extracted lipopeptides of the ARF4 on germination *Verticillium dahliae* spores and hyphae structure

The antifungal activity of extracted lipopeptides of strain ARF4 was assessed using the agar well diffusion technique. The extract exhibited strong inhibition of conidial germination in *V. dahliae*, as evidenced by the presence of inhibition zones around the wells, compared to the DMSO control (Figures 6A,B).

In order to study the effects of the extracted lipopeptide on the morphology of *V. dahliae* hyphae, scanning electron microscopy (SEM) was conducted. Agar slices of 0.5 cm^2 from hyphal zones treated with the extract and from regions treated with Dimethylsulfoxide (DMSO) were prepared, and the resulted morphological variations were examined by SEM. The morphology of *V. dahliae* hyphae treated with extracted lipopeptide was significantly different from that of DMSO-treated control. The hyphae treated with extracted lipopeptide exhibited considerable deformation, appearing irregular with extensive collapse, and the normal plump cylindrical shape of the hyphae was lost, likely due to the outflow of cytoplasm, which may have led to cell death (Figure 6C). In contrast, the hyphae from the DMSO-treated control group displayed regular, plump, intact cylindrical structures (Figure 6D).

The cell wall and plasma membrane treated with DMSO showed uniform and typical cellular morphology, with a clear and intact cell wall. The cytoplasmic matrix was dense, and essential organelles, such as the nucleus and mitochondria, exhibited normal and well-defined structures (Figures 7A,C). In contrast, the hyphae treated with the extracted lipopeptide displayed a reduced cytoplasmic matrix and

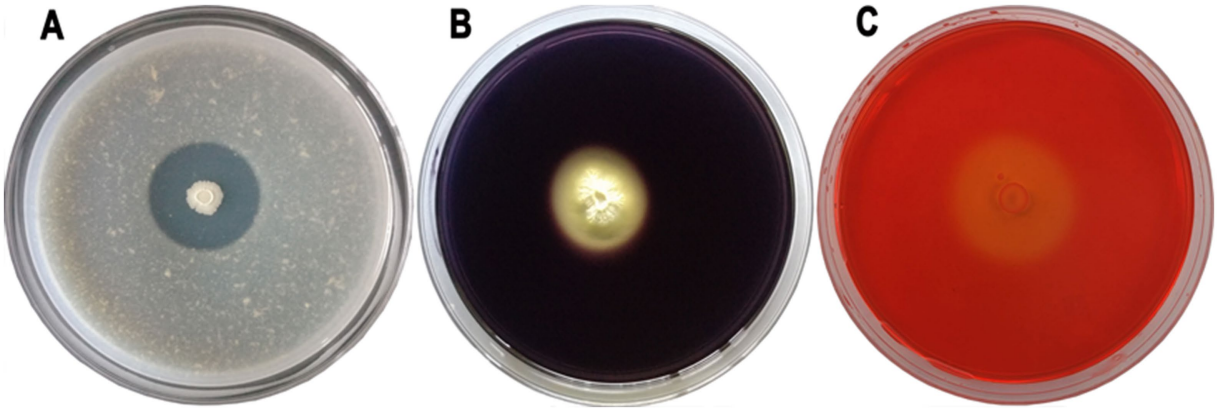

FIGURE 3
The image displays enzyme activity on agar plates incubated with the ARF4 strain. These results highlight the ability of the ARF4 strain to produce enzymes, **(A)** protease, **(B)** β-glucosidase, and **(C)** chitinase, as observed through distinct color changes and clear zones on the agar plates.

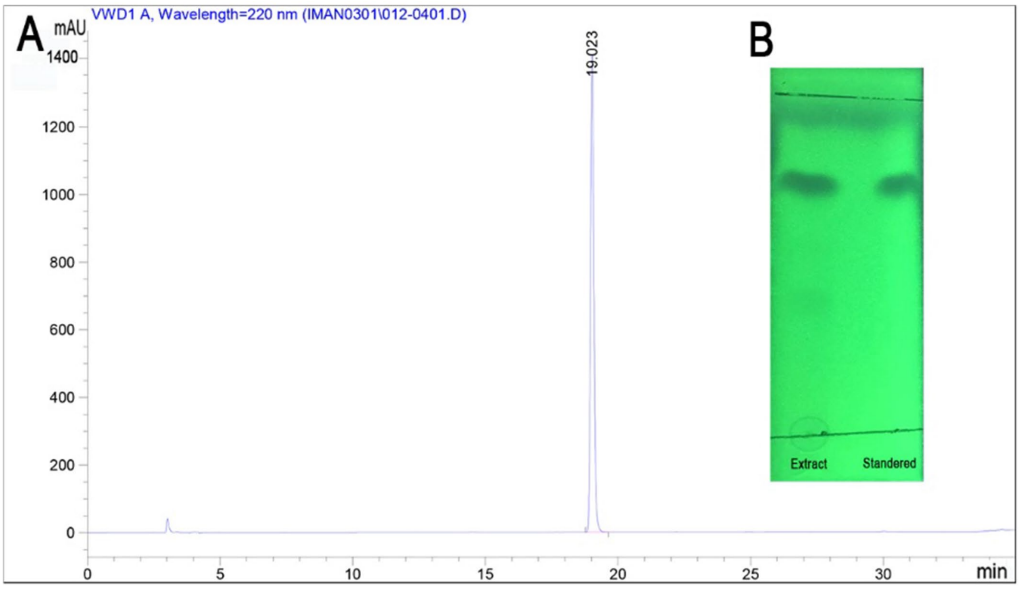

FIGURE 4
Reversed-phase high-performance liquid chromatography (RP-HPLC) and preparative silica gel TLC plate (GF254) analyses. **(A)** RP-HPLC analysis of extract-product by *B. velezensis* strain ARF4. A single peak was observed at 220 nm with a retention time of 19.02 min. **(B)** TLC profile of extract-product in comparison to standard bacillomycin D.

unclear ultrastructure, with a reduced number of mitochondria, and the internal organelles appeared disintegrated (Figure 7B). Additionally, the cell walls and plasma membrane of the treated hyphae were rough and blurred, with visible signs of cell wall lysis (Figure 7D).

3.7 Management of *Verticillium* wilt disease by ARF4 strain

The potential of the ARF4 strain in controlling *Verticillium* wilt disease was rigorously evaluated through a series of pot experiments designed to simulate real-world conditions. The results of these assays were highly promising, indicating that inoculation with the ARF4 strain significantly reduced both the incidence and severity of *Verticillium* wilt in eggplants compared to negative controls (Figure 8). Specifically, the seedling's inoculation with conidia of *V. dahliae* led to the appearance of a major infection, represented by yellowing and wilting of most leaves (Figure 8A). While the yellowing and wilting were observed to be reduced on the leaves of plants co-inoculated with ARF4 strain and conidia of *V. dahliae* (Figure 8B). While no symptoms of yellowing and wilt were observed in the positive control (Figure 8C). Statistically, the disease severity observed in eggplants inoculated solely with *V. dahliae* reached 73.28 ± 1.87 after 20 days, reflecting substantial infection. In contrast, eggplants treated with both *V. dahliae* and the ARF4 strain showed a markedly reduced disease severity of 23.05 ± 0.72 (Figure 8D), corresponding to a control efficacy of 68.45 ± 0.85% (Figure 8E).

TABLE 3 Specialized extracted lipopeptide from the *B. velezensis* ARF4, extracted from the inhibition zone on the PDA medium, detected by MALDI-TOF.

m/z	Putative Assigned Lipopeptide	Lipopeptide Family	References
1053.3	Bacillomycin D C14 $[M + Na]^+$	Iturin	Platel et al. (2021)
1067.3	Bacillomycin D C15 $[M + Na]^+$	Iturin	Platel et al. (2021)
1081.3	Bacillomycin D C15 $[M + K]^+$	Iturin	Platel et al. (2021)
1083.3	Bacillomycin D C16 $[M + Na]^+$	Iturin	Platel et al. (2021)
1095.3	Bacillomycin D C17 $[M + Na]^+$	Iturin	Platel et al. (2021)
1111.3	Bacillomycin D C17 $[M + K]^+$	Iturin	Athukorala et al. (2009)

4 Discussion

In the present study, overall, 42 rhizospheric isolates were extracted from healthy eggplant rhizosphere soil samples, and their antagonistic potential was evaluated using the dual-culture plate method as described by Meena et al. (2024) and Soylu et al. (2021). The PIRG was estimated, and the bacterial strain with strong antagonistic activity was chosen for further experiments. The strain ARF4 had the highest PIRG percentage, which was 84.49%. These results align with other studies where antagonists from the *Bacillus* genus exhibit comparable inhibition against different pathogens (Fira et al., 2018; Soylu et al., 2021). Phylogenetic analysis revealed that strain ARF4 is closely related to these strains of *Bacillus velezensis* (Figure 2). *B. velezensis* (ARF4) was further tested for broad-spectrum antifungal activity against *V. dahliae*, *F. oxysporum* f. sp. *niveum*, *P. capsici*, and *S. sclerotiorum* YY0 through disc diffusion assay, as well as poisoned food method and the results showed that it is considered being an effective antagonist in inhibiting the growth of tested plant pathogens (Figure 1). The dual-culture assay used in this study is in line with the previous studies conducted by Prom and Shi, who effectively demonstrated the antagonistic potential of *B. velezensis* against a range of pathogens like *F. o*. f. sp. *niveum* and *V. dahliae* (Prom et al., 2023; Shi et al., 2024). In our study, the identified strain *B. velezensis* ARF4 has potent biocontrol activity, particularly in managing *Verticillium* wilt, a significant disease affecting eggplant (*Solanum melongena*). This bacterium is highly effective against a broader range of plant pathogens, especially *V. dahliae,* due to its broad-spectrum antifungal activity. These bacteria produce various enzymes such as *β*-glucosidase, chitinase, and protease, as well as the antifungal lipopeptide bacillomycin D (Figures 3, 4). Bacillomycin D is produced by several *Bacillus* strains using fermentative production in liquid media, such as *B. amyloliquefaciens* (Gu et al., 2017; Lv et al., 2024), *B. subtilis* (Gong et al., 2014), and *B. velezensis* HN-2 (Jin et al., 2020). Primary extraction for bacillomycin D produced by *B. velezensis* ARF4 was carried out by using solid LBA media, purification by RH-HPLC, and characterization for bacillomycin D was carried out by using TLC using bacillomycin D as a standard.

While TLC and MALDI-TOF MS analyses provided useful insights, it is important to acknowledge that these techniques yield only preliminary evidence for the identification of bacillomycin D. The lack of structural validation *via* advanced techniques such as nuclear magnetic resonance (NMR) spectroscopy or tandem mass spectrometry (MS–MS) represents a limitation of the current study. Therefore, we explicitly recognize that the identification of bacillomycin D in this study remains tentative. Future studies should incorporate NMR-based structural elucidation and comparative antifungal bioassays using purified standards to confirm the identity and bioactivity of bacillomycin D and its homologs with higher precision.

Bioactive metabolites and lipopeptides are typically extracted from cell-free culture filtrates. However, Zihalirwa Kulimushi et al. (2017) demonstrated, they can also be extracted directly from inhibition zones. While this method may offer practical advantages, such as ease of isolation from actively antagonistic regions, it presents the drawback of potential co-extraction of contaminants. These contaminants may obscure the true efficacy of the antimicrobial agents by introducing other compounds that could interfere with the inhibition zone, leading to an inaccurate assessment of bioactivity. We include this caveat upon the reviewer's request to clarify limitations inherent in our current extraction approach.

Chitinases are key enzymatic players in the antifungal arsenal of *Bacillus* species, targeting chitin found in fungal cell walls. Their antifungal efficacy is attributed to hydrolyzing chitin, leading to morphological distortions and stunted growth of fungi (Nazeer, 2023; Toufiq et al., 2018). This hydrolytic action is crucial in biocontrol strategies, as chitinase production has been correlated with notable antifungal activity (Abdelmoteleb et al., 2017; Zhang et al., 2021). Similarly, proteases contribute to this antifungal action by degrading proteins within the fungal cell wall, further facilitating cell lysis (Allioui et al., 2021). Together, these enzymes disrupt the structural integrity of fungal cells, enhancing the overall antifungal potential of the *Bacillus* species. On the other hand, lipopeptides such as iturin, fengycin, and surfactin emerge as versatile antimicrobial agents that exhibit broad-spectrum antifungal activity. These compounds can disrupt fungal cell membranes, leading to cell lysis and death through mechanisms distinct from those of chitinases and proteases (Guillén-Navarro et al., 2023; Liu et al., 2020). The evidence suggesting that viable *Bacillus* cultures showcase superior antifungal effects compared to individually applied lipopeptides suggests that additional metabolites or a collaborative interaction may be at play (Deng et al., 2023; Jumpathong et al., 2022). The interplay between these components points toward a synergistic mechanism. The simultaneous action of chitinases, proteases, and lipopeptides could create a multipronged approach to fungal inhibition. For example, while lipopeptides compromise the fungal membrane, chitinases and proteases could facilitate further degradation of cellular architecture. This was illustrated in experiments where the combined action of hydrolytic enzymes and lipopeptides led to enhanced antifungal effects compared to

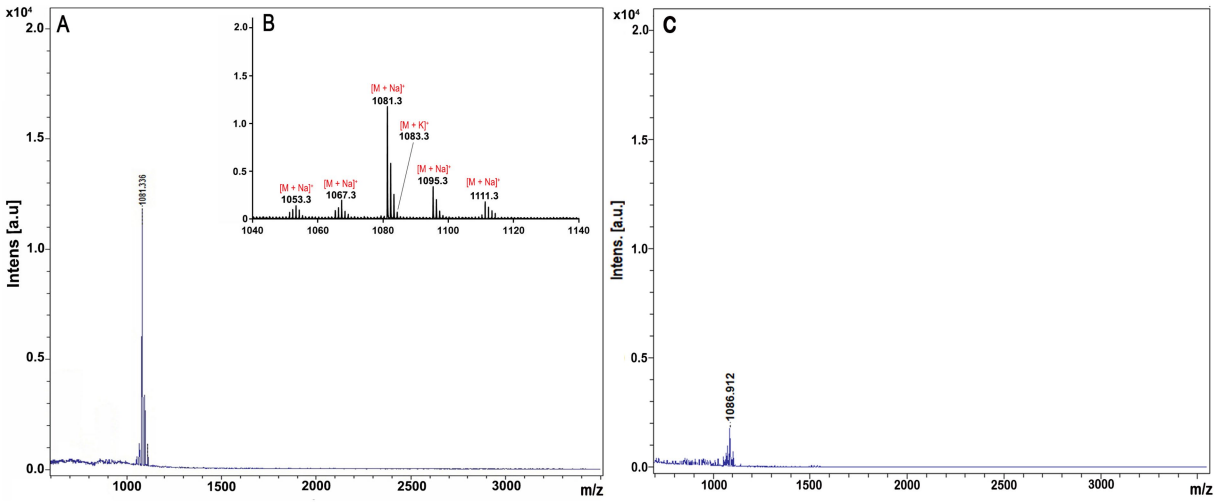

FIGURE 5
MALDI-TOF MS analysis of the extracted lipopeptides produced by the ARF4 strain. **(A)** High mass intensity in the m/z range 500–3,500 is proposed to contain bacillomycin D. **(B)** High mass intensity at m/z 1,040–1,140 is proposed to contain bacillomycin D. **(C)** Lipopeptide was detected in a sample of strain ARF4 without fungi as a control.

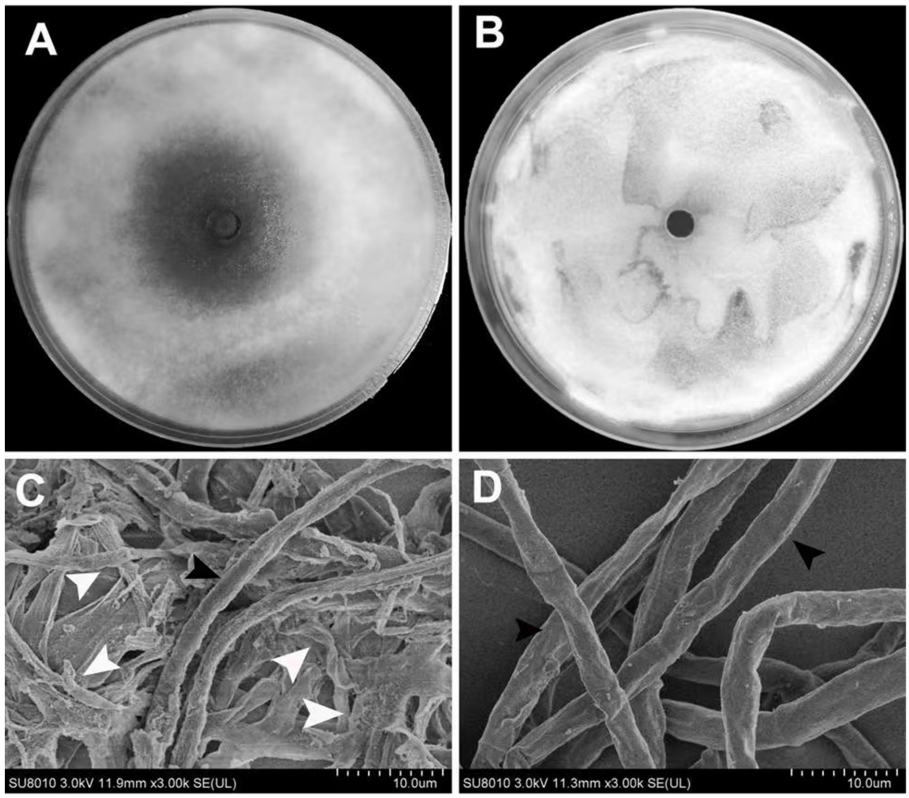

FIGURE 6
Antifungal activity of extracted lipopeptide of the strain ARF4 against *V. dahliae*. **(A)** Antifungal activity of extracted lipopeptide on conidia germination and **(B)** Control treatment using DMSO. **(C)** Scanning electron microscopy images of *V. dahliae* hyphae were treated with extracted lipopeptide of ARF4 and **(D)** were hyphae treated with DMSO (control). White arrows point to hyphae deterioration. Black arrowheads point to plump and intact hyphae.

either component alone (Abdelmoteleb et al., 2017; Al-Mutar et al., 2023; Soylu et al., 2022). The evidence suggests that these factors do not act in isolation but rather synergistically enhance the overall antifungal potential, allowing *Bacillus* species to effectively combat a spectrum of phytopathogenic fungi as well as in the enhancement of plant health.

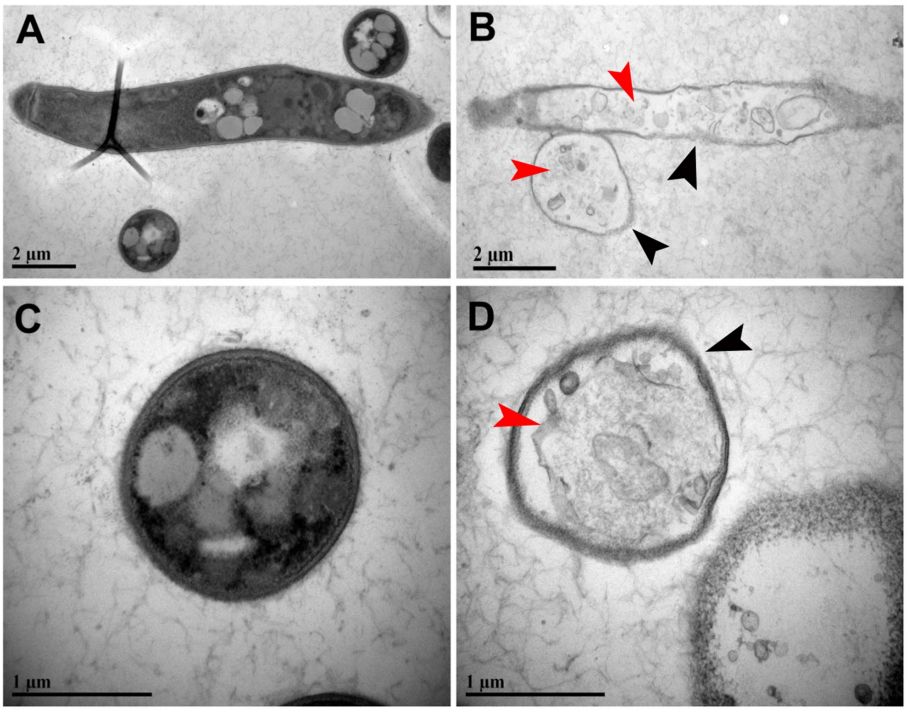

FIGURE 7
Transmission electron microscopy (TEM) analysis showing the effect of lipopeptide produced by the ARF4 strain on the ultrastructure of *V. dahliae* hyphae. **(A,C)** Hyphal cells were treated with 40 µg/mL of DMSO (control). **(B,D)** Hyphal cells were treated with 40 µg/mL of the extracted lipopeptide. Black arrowheads point to the cell wall and plasma membrane lysis of hyphae. Red arrowheads point to a reduced cytoplasmic matrix and unclear ultrastructure, as well as a reduced number of mitochondria, with the internal organelles appearing disintegrated.

In this research, the analysis of MALDI-TOF MS showed that antimicrobial lipopeptides produced by rhizobacteria strain ARF4 against *V. dahliae* were of itrurin family having cyclic structure and homologs to bacillomycin D. These lipopeptides suppress the germination of fungal spores and destroy the fungal cell membrane. Bacillomycin D has been reported to effectively destroy the hyphal structure of *V. dahliae* and, thereby, its pathogenicity (Figure 6; Hammad et al., 2023). In addition, bacillomycin D extracted from *B. velezensis* ARF4 strain has also been shown to inhibit the germination of the *V. dahliae* spores, which further highlights its biocontrol potential (Prom et al., 2023). The biological role of these lipopeptides in biocontrol is well documented, but comprehensive structure–function studies are needed to delineate their specific mechanisms and interactions. The activity of the β-glucosidase and chitinase enzymes also add to the antagonism of this bacterium as they are essential in the breakdown of cell walls of fungal pathogens (Bayisa et al., 2021). Moreover, these enzymes, in addition to antifungal properties, increase nutrient bioavailability in the rhizosphere and promote plant growth and disease resistance (Khan et al., 2020; Songwattana et al., 2023).

Furthermore, a genomic study on *B. velezensis* has revealed that it contains multiple gene clusters related to the biosynthesis of antimicrobial compounds, including non-ribosomal peptide synthetases responsible for lipopeptide production (Hammad et al., 2023; Nakkeeran et al., 2021). This genetic potential highlights the adaptability of *B. velezensis* as a biocontrol agent, capable of combating multiple pathogens effectively in a range of environmental conditions. Also, the targeting of specific strains with improved antifungal activities is a step toward the efficient implementation of *B. velezensis* in agriculture (Grady et al., 2019; Vahidinasab et al., 2022). Field and greenhouse studies have demonstrated that inoculation with *B. velezensis* significantly reduces both the incidence and severity of *Verticillium* wilt in eggplants compared to untreated controls. For example, research indicates that *B. velezensis* strains can effectively lower disease severity by inhibiting the mycelial growth of *V. dahliae* and enhancing plant defense mechanisms (Hasan et al., 2020; Prom et al., 2023). The presence of *B. velezensis* in the rhizosphere stimulates the plant's immune response, leading to increased production of defense-related compounds and improved overall plant health (Ying et al., 2024). This biocontrol strategy not only alleviates *Verticillium* wilt impact but also maintains sustainable agricultural practices by reducing the reliance on chemical fungicides.

5 Conclusion

Bacillus velezensis, with its multiple mechanisms of action, such as the production of antifungal compounds and hydrolytic enzymes, might be considered an important biocontrol agent against *Verticillium* wilt in eggplant. The disease incidence and severity were significantly reduced with the inoculation *B. velezensis*, proving its potential as a sustainable alternative to chemical fungicides in crop protection strategies. Continued

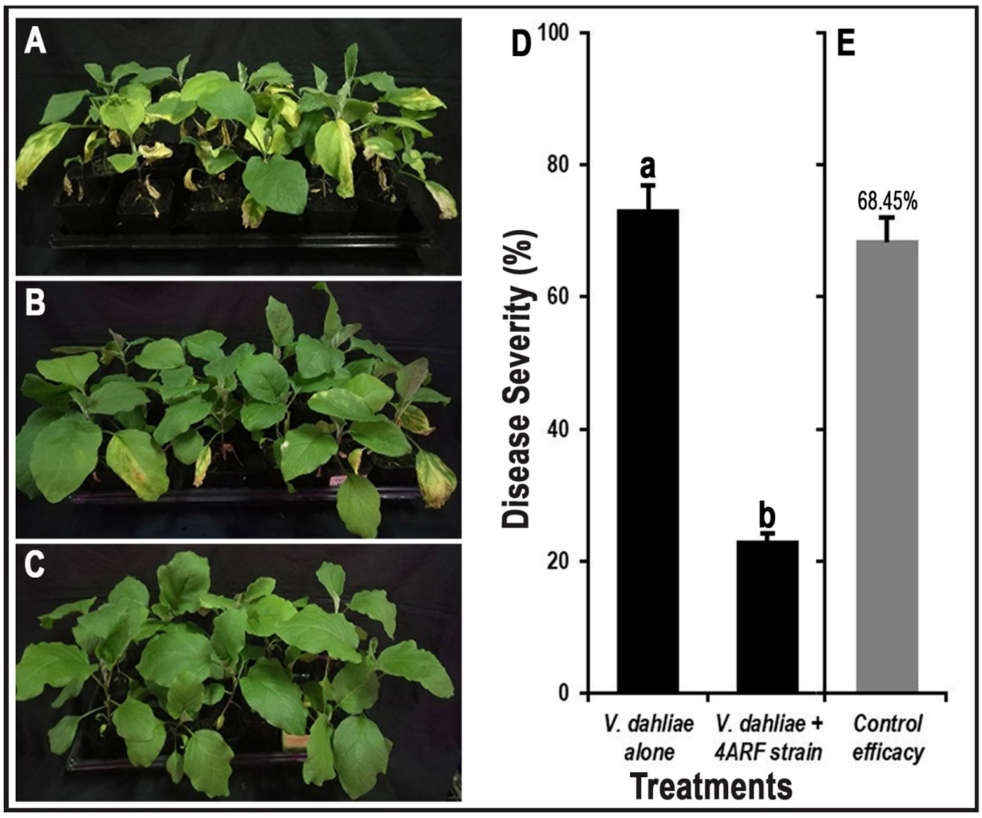

FIGURE 8
Inhibitory efficacy of rhizobacteria strain ARF4 against eggplant *Verticillium* wilt. **(A)** Inoculation with conidia suspension of *V. dahliae*. **(B)** Coinoculation with strain ARF4 and conidia suspension of *V. dahliae*. **(C)** Without inoculation with *V. dahliae* and strain ARF4 (control). **(D)** The disease severity of a *Verticillium* wilt after 20 days. **(E)** Control efficacy to the strain ARF4.

research into the specific mechanisms and optimal application methods will further enhance the efficacy and increase its effectiveness in environmentally friendly disease management strategies of *B. velezensis* in agricultural practices.

Data availability statement

The datasets presented in this study can be found in online repositories. The names of the repository/repositories and accession number(s) can be found at: GenBank accession numbers OQ918063.1, OQ920283.1, and OQ920284.1.

Author contributions

AK: Conceptualization, Data curation, Formal analysis, Investigation, Methodology, Software, Writing – original draft, Writing – review & editing. XC: Writing – review & editing, Supervision, Funding acquisition, Resources. IA: Methodology, Writing – review & editing. AT: Software, Writing – review & editing. RH: Writing – review & editing, Software. DA: Writing – review & editing, Supervision, Project administration, Funding acquisition. ME: Writing – review & editing, Funding acquisition. MA: Writing – review & editing, Data curation, Formal analysis, Project administration, Software, Supervision.

Funding

The author(s) declare that financial support was received for the research and/or publication of this article. This study was supported by King Saud University, Riyadh, Saudi Arabia (RSP2025R190).

Acknowledgments

The authors extend their appreciation to the Researchers supporting project number (RSP2025R190), King Saud University, Riyadh, Saudi Arabia.

Conflict of interest

The authors declare that the research was conducted in the absence of any commercial or financial relationships that could be construed as a potential conflict of interest.

Generative AI statement

The author(s) declare that Gen AI was used in the creation of this manuscript. ChatGPT4o and DeepSeek were used for rephrasing of the article.

Publisher's note

All claims expressed in this article are solely those of the authors and do not necessarily represent those of their affiliated organizations, or those of the publisher, the editors and the reviewers. Any product that may be evaluated in this article, or claim that may be made by its manufacturer, is not guaranteed or endorsed by the publisher.

References

Abdelmoteleb, A., Troncoso-Rojas, R., Gonzalez-Soto, T., and González-Mendoza, D. (2017). Antifungical activity of autochthonous *Bacillus subtilis* isolated from *Prosopis juliflora* against phytopathogenic fungi. *Mycobiology* 45, 385–391. doi: 10.5941/MYCO.2017.45.4.385

Allioui, N., Driss, F., Dhouib, H., Jlail, L., Tounsi, S., and Frikha-Gargouri, O. (2021). Two novel *Bacillus* strains (*subtilis* and simplex species) with promising potential for the biocontrol of *Zymoseptoria tritici*, the causal agent of *Septoria tritici* blotch of wheat. *Biomed. Res. Int.* 2021:6611657. doi: 10.1155/2021/6611657

Al-Mutar, D. M. K., Alzawar, N. S. A., Noman, M., Azizullah Li, D., and Song, F. (2023). Suppression of *Fusarium* wilt in watermelon by *Bacillus amyloliquefaciens* DHA55 through extracellular production of antifungal Lipopeptides. *J. Fungi* 9:336. doi: 10.3390/jof9030336

Alsalman, A. J., Farid, A., Al Mohaini, M., Muzammal, M., Khan, M. H., Dadrasnia, A., et al. (2022). Chitinase activity by chitin degrading strain (*Bacillus Salmalaya*) in shrimp waste. *Int. J. Curr. Res. Rev.* 14, 11–17. doi: 10.31782/IJCRR.2022.141107

Athukorala, S. N., Fernando, W. D., and Rashid, K. Y. (2009). Identification of antifungal antibiotics of *Bacillus* species isolated from different microhabitats using polymerase chain reaction and MALDI-TOF mass spectrometry. *Can. J. Microbiol.* 55, 1021–1032. doi: 10.1139/W09-067

Ayed, H. B., Hmidet, N., Béchet, M., Chollet, M., Chataigné, G., Leclère, V., et al. (2014). Identification and biochemical characteristics of lipopeptides from *Bacillus mojavensis* A21. *Process Biochem.* 49, 1699–1707. doi: 10.1016/j.procbio.2014.07.001

Barzman, M., Bàrberi, P., Birch, A. N. E., Boonekamp, P., Dachbrodt-Saaydeh, S., Graf, B., et al. (2015). Eight principles of integrated pest management. *Agron. Sustain. Dev.* 35, 1199–1215. doi: 10.1007/s13593-015-0327-9

Bayisa, R. A., Cho, J. Y., and Kim, K. Y. (2021). Purification and identification of a new antifungal dipeptide from *Bacillus velezensis* AR1 culture supernatant. *Pest Manag. Sci.* 77, 775–779. doi: 10.1002/ps.6078

Canton, H. (2021). "Food and agriculture organization of the United Nations—FAO" in The Europa directory of international organizations 2021, 297–305.

Chen, Q., and Wang, H. (2022). Biocontrol activity and action mechanism of *Bacillus velezensis* strain SDTB038 against *Fusarium* crown and root rot of tomato. *Front. Microbiol.* 13:994716. doi: 10.3389/fmicb.2022.994716

Chun, J., and Bae, K. S. (2000). Phylogenetic analysis of *Bacillus subtilis* and related taxa based on partial *gyrA* gene sequences. *Antonie Van Leeuwenhoek* 78, 123–127. doi: 10.1023/A:1026555830014

da Silva, M. A. C., Cavalett, A., Spinner, A., Rosa, D. C., Jasper, R. B., Quecine, M. C., et al. (2013). Phylogenetic identification of marine bacteria isolated from deep-sea sediments of the eastern South Atlantic Ocean. *Springerplus* 2, 1–10. doi: 10.1186/2193-1801-2-127

Deng, Y. J., Chen, Z., Ruan, C. Q., Xiao, R. F., Lian, H. P., Liu, B., et al. (2023). Antifungal activities of *Bacillus velezensis* FJAT-52631 and its lipopeptides against anthracnose pathogen *Colletotrichum acutatum*. *J. Basic Microbiol.* 63, 594–603. doi: 10.1002/jobm.202200489

Dhouib, H., Zouari, I., Abdallah, D. B., Belbahri, L., Taktak, W., Triki, M. A., et al. (2019). Potential of a novel endophytic *Bacillus velezensis* in tomato growth promotion and protection against *Verticillium* wilt disease. *Biol. Control* 139:104092. doi: 10.1016/j.biocontrol.2019.104092

Farah, I. F., dos Santos, C. R., Pinto, M. C. F., Araújo, C. R., and Amaral, M. C. S. (2024). Pesticides in aquatic environment: occurrence, ecological implications and legal framework. *J. Environ. Chem. Eng.* 12:114072. doi: 10.1016/j.jece.2024.114072

Fazle Rabbee, M., and Baek, K.-H. (2020). Antimicrobial activities of lipopeptides and polyketides of *Bacillus velezensis* for agricultural applications. *Molecules* 25:4973. doi: 10.3390/molecules25214973

Fira, D., Dimkić, I., Lozo, J., and Stanković, S. (2018). Biological control of plant pathogens by Bacillus species. *J. Biotechnol.* 285, 44–55.

Gayoso, C., Pomar, F., Novo-Uzal, E., Merino, F., and Martínez de Ilárduya, Ó. (2010). The Ve-mediated resistance response of the tomato to *Verticillium dahliae* involves H2O2, peroxidase and lignins and drives PALgene expression. *BMC Plant Biol.* 10:232. doi: 10.1186/1471-2229-10-232

Gong, Q., Zhang, C., Lu, F., Zhao, H., Bie, X., and Lu, Z. (2014). Identification of bacillomycin D from *Bacillus subtilis* fmbJ and its inhibition effects against *Aspergillus flavus*. *Food Control* 36, 8–14. doi: 10.1016/j.foodcont.2013.07.034

Grady, E. N., MacDonald, J., Ho, M. T., Weselowski, B., McDowell, T., Solomon, O., et al. (2019). Characterization and complete genome analysis of the surfactin-producing, plant-protecting bacterium *Bacillus velezensis* 9D-6. *BMC Microbiol.* 19, 1–14. doi: 10.1186/s12866-018-1380-8

Gu, Q., Yang, Y., Yuan, Q., Shi, G., Wu, L., Lou, Z., et al. (2017). Bacillomycin D produced by *Bacillus amyloliquefaciens* is involved in the antagonistic interaction with the plant-pathogenic fungus *Fusarium graminearum*. *Appl. Environ. Microbiol.* 83, e01075–e01017. doi: 10.1128/AEM.01075-17

Guillén-Navarro, K., López-Gutiérrez, T., García-Fajardo, V., Gómez-Cornelio, S., Zarza, E., De la Rosa-García, S., et al. (2023). Broad-spectrum antifungal, biosurfactants and bioemulsifier activity of *Bacillus subtilis* subsp. *spizizenii*—a potential biocontrol and bioremediation agent in agriculture. *Plan. Theory* 12:1374. doi: 10.3390/plants12061374

Hammad, M., Ali, H., Hassan, N., Tawab, A., Salman, M., Jawad, I., et al. (2023). Food safety and biological control; genomic insights and antimicrobial potential of *Bacillus velezensis* FB2 against agricultural fungal pathogens. *PLoS One* 18:e0291975. doi: 10.1371/journal.pone.0291975

Hasan, N., Farzand, A., Heng, Z., Khan, I. U., Moosa, A., Zubair, M., et al. (2020). Antagonistic potential of novel endophytic *Bacillus* strains and mediation of plant defense against *Verticillium* wilt in upland cotton. *Plan. Theory* 9:1438. doi: 10.3390/plants9111438

Hayward, A. (2000). *Ralstonia solanacearum*. Encyclopedia of microbiology, vol. *4*. Cambridge, MA: Academic Press.

Howard, M. B., Ekborg, N. A., Weiner, R. M., and Hutcheson, S. W. (2003). Detection and characterization of chitinases and other chitin-modifying enzymes. *J. Ind. Microbiol. Biotechnol.* 30, 627–635. doi: 10.1007/s10295-003-0096-3

Huang, Z., Lou, J., Gao, Y., Noman, M., Li, D., and Song, F. (2023). FonTup1 functions in growth, conidiogenesis and pathogenicity of *Fusarium oxysporum* f.sp. *niveum* through modulating the expression of the tricarboxylic acid cycle genes. *Microbiol. Res.* 272:127389. doi: 10.1016/j.micres.2023.127389

Ibanga, U. P., Otobong, U. F., Anthony, E. O., Effiong, U. E., and Udo, N. N. (2023). Effect of application of palm bunch ash on the growth and yield of eggplant (*Solanum melongena L.*) in a pineapple orchard. *Am. J. Life Sci.* 12, 50–55. doi: 10.11648/j.ajls.20231104.11

Jiang, C.-H., Liao, M.-J., Wang, H.-K., Zheng, M.-Z., Xu, J.-J., and Guo, J.-H. (2018). *Bacillus velezensis*, a potential and efficient biocontrol agent in control of pepper gray mold caused by *Botrytis cinerea*. *Biol. Control* 126, 147–157. doi: 10.1016/j.biocontrol.2018.07.017

Jin, P., Wang, H., Tan, Z., Xuan, Z., Dahar, G. Y., Li, Q. X., et al. (2020). Antifungal mechanism of bacillomycin D from *Bacillus velezensis* HN-2 against *Colletotrichum gloeosporioides Penz. Pestic. Biochem. Physiol.* 163, 102–107. doi: 10.1016/j.pestbp.2019.11.004

Jumpathong, W., Intra, B., Euanorasetr, J., and Wanapaisan, P. (2022). Biosurfactant-producing *Bacillus velezensis* PW192 as an anti-fungal biocontrol agent against *Colletotrichum gloeosporioides* and *Colletotrichum musae*. *Microorganisms* 10:1017. doi: 10.3390/microorganisms10051017

Khan, M. S., Gao, J., Chen, X., Zhang, M., Yang, F., Du, Y., et al. (2020). The endophytic bacteria *Bacillus velezensis* Lle-9, isolated from *Lilium leucanthum*, harbors antifungal activity and plant growth-promoting effects. *J. Microbiol. Biotechnol.* 30, 668–680. doi: 10.4014/jmb.1910.10021

Kim, Y. S., Lee, Y., Cheon, W., Park, J., Kwon, H.-T., Balaraju, K., et al. (2021). Characterization of *Bacillus velezensis* AK-0 as a biocontrol agent against apple bitter rot caused by *Colletotrichum gloeosporioides*. *Sci. Rep.* 11:626. doi: 10.1038/s41598-020-80231-2

Kumar, S., Stecher, G., and Tamura, K. (2016). MEGA7: molecular evolutionary genetics analysis version 7.0 for bigger datasets. *Mol. Biol. Evol.* 33, 1870–1874. doi: 10.1093/molbev/msw054

Lahlali, R., Ezrari, S., Radouane, N., Kenfaoui, J., Esmaeel, Q., El Hamss, H., et al. (2022). Biological control of plant pathogens: a global perspective. *Microorganisms* 10:596. doi: 10.3390/microorganisms10030596

Li, X., Liang, Z., Yang, G., Lin, T., and Liu, B. (2024). Assessing the severity of *Verticillium* wilt in cotton fields and constructing pesticide application prescription maps using unmanned aerial vehicle (UAV) multispectral images. *Drones* 8:176. doi: 10.3390/drones8050176

Liu, Y., Teng, K., Wang, T., Dong, E., Zhang, M., Tao, Y., et al. (2020). Antimicrobial *Bacillus velezensis* HC6: production of three kinds of lipopeptides and biocontrol potential in maize. *J. Appl. Microbiol.* 128, 242–254. doi: 10.1111/jam.14459

Lv, Z., Li, R., Shi, C., Lu, Z., Meng, F., and Bie, X. (2024). The efficient synthesis strategy of bacillomycin D in *Bacillus amyloliquefaciens* fmbJ. *Process Biochem.* 145, 131–138. doi: 10.1016/j.procbio.2024.06.026

Lyu, J., Jin, N., Ma, X., Yin, X., Jin, L., Wang, S., et al. (2024). A comprehensive evaluation of nutritional quality and antioxidant capacity of different Chinese eggplant varieties based on multivariate statistical analysis. *Antioxidants* 14:10. doi: 10.3390/antiox14010010

Meena, P. N., Meena, A. K., Tiwari, R. K., Lal, M. K., and Kumar, R. (2024). Biological control of stem rot of groundnut induced by *Sclerotium rolfsii sacc*. *Pathogens* 13:632. doi: 10.3390/pathogens13080632

Munir, S., Azeem, A., Zaman, M. S., and Haq, M. Z. U. (2024). From field to table: ensuring food safety by reducing pesticide residues in food. *Sci. Total Environ.* 922:171382. doi: 10.1016/j.scitotenv.2024.171382

Nakkeeran, S., Saranya, N., Senthilraja, C., Renukadevi, P., Krishnamoorthy, A., El Enshasy, H. A., et al. (2021). Mining the genome of *Bacillus velezensis* VB7 (CP047587) for MAMP genes and non-ribosomal peptide synthetase gene clusters conferring antiviral and antifungal activity. *Microorganisms* 9:2511. doi: 10.3390/microorganisms9122511

Nazeer, W. W. (2023). Isolation, purification and characterization of antifungal Chitinase from *Phaseolus vulgaris* Var. *paulista*. *Egyptian Acad. J. Biol. Sci.* 14, 69–79. doi: 10.21608/eajbsh.2023.297612

Pandit, M. A., Kumar, J., Gulati, S., Bhandari, N., Mehta, P., Katyal, R., et al. (2022). Major biological control strategies for plant pathogens. *Pathogens* 11:273. doi: 10.3390/pathogens11020273

Platel, R., Sawicki, M., Esmaeel, Q., Randoux, B., Trapet, P., El Guilli, M., et al. (2021). Isolation and identification of lipopeptide-producing *Bacillus velezensis* strains from wheat phyllosphere with antifungal activity against the wheat pathogen *Zymoseptoria tritici*. *Agronomy* 12:95. doi: 10.3390/agronomy12010095

Pretorius, D., Van Rooyen, J., and Clarke, K. (2015). Enhanced production of antifungal lipopeptides by *Bacillus amyloliquefaciens* for biocontrol of postharvest disease. *New Biotechnol.* 32, 243–252. doi: 10.1016/j.nbt.2014.12.003

Prom, L. K., Medrano, E. G., and Liu, J. (2023). *In vitro* antagonistic action by *Bacillus velezensis* strain LP16S against cotton wilt pathogens. *J. Agric. Crops* 9, 372–375. doi: 10.32861/jac.93.372.375

Qiu, Z., Lu, X., Li, N., Zhang, M., and Qiao, X. (2018). Characterization of garlic endophytes isolated from the black garlic processing. *Microbiol. Open* 7:e00547. doi: 10.1002/mbo3.547

Renwick, A., Campbell, R., and Coe, S. (1991). Assessment of *in vivo* screening systems for potential biocontrol agents of *Gaeumannomyces graminis*. *Plant Pathol.* 40, 524–532. doi: 10.1111/j.1365-3059.1991.tb02415.x

Ronquist, F., Teslenko, M., Van Der Mark, P., Ayres, D. L., Darling, A., Höhna, S., et al. (2012). MrBayes 3.2: efficient Bayesian phylogenetic inference and model choice across a large model space. *Syst. Biol.* 61, 539–542. doi: 10.1093/sysbio/sys029

Scholz, S. S., Schmidt-Heck, W., Guthke, R., Furch, A. C., Reichelt, M., Gershenzon, J., et al. (2018). *Verticillium dahliae*-Arabidopsis interaction causes changes in gene expression profiles and jasmonate levels on different time scales. *Front. Microbiol.* 9:217. doi: 10.3389/fmicb.2018.00217

Shang, H., He, D., Li, B., Chen, X., Luo, K., and Li, G. (2024). Environmentally friendly and effective alternative approaches to pest management: recent advances and challenges. *Agronomy* 14:1807. doi: 10.3390/agronomy14081807

Shi, Y., Niu, X., Yang, H., Chu, M., Wang, N., Bao, H., et al. (2024). Optimization of the fermentation media and growth conditions of *Bacillus velezensis* BHZ-29 using a Plackett–Burman design experiment combined with response surface methodology. *Front. Microbiol.* 15:1355369. doi: 10.3389/fmicb.2024.1355369

Songwattana, P., Boonchuen, P., Piromyou, P., Wongdee, J., Greetatorn, T., Inthaisong, S., et al. (2023). Insights into antifungal mechanisms of *Bacillus velezensis* S141 against *Cercospora* leaf spot in mungbean (*V. radiata*). *Microbes Environ.* 38:ME22079. doi: 10.1264/jsme2.ME22079

Soylu, S., Kara, M., Soylu, E. M., Uysal, A., and Kurt, Ş. (2022). Determination of biocontrol potentials of Endophytic Bacteria in biological control of *Citrus* sour rot disease caused by *Geotrichum citri-aurantii*. *Tekirdağ Ziraat Fakültesi Dergisi* 19, 177–191. doi: 10.33462/jotaf.944704

Soylu, S., Kara, M., Uysal, A., Kurt, Ş., and Soylu, E. (2021). Determination of antagonistic potential of endophytic bacteria isolated from lettuce against lettuce white mould disease caused by *Sclerotinia sclerotiorum*. *Zemdirbyste-Agriculture* 108, 303–312. doi: 10.13080/z-a.2021.108.039

Swati Verma, R., Chauhan, A., Shandilya, M., Li, X., Kumar, R., and Kulshrestha, S. (2020). Antimicrobial potential of ag-doped ZnO nanostructure synthesized by the green method using *Moringa oleifera* extract. *J. Environ. Chem. Eng.* 8:103730. doi: 10.1016/j.jece.2020.103730

Tomah, A. A., Abd Alamer, I. S., Li, B., and Zhang, J.-Z. (2020a). A new species of *Trichoderma* and gliotoxin role: a new observation in enhancing biocontrol potential of *T. virens* against *Phytophthora capsi*c on chili pepper. *Biol. Control* 145:104261. doi: 10.1016/j.biocontrol.2020.104261

Tomah, A. A., Alamer, I. S. A., Khattak, A. A., Ahmed, T., Hatamleh, A. A., Al-Dosary, M. A., et al. (2023). Potential of *Trichoderma virens* HZA14 in controlling *Verticillium* wilt disease of eggplant and analysis of its genes responsible for *Microsclerotial degradation*. *Plan. Theory* 12:3761. doi: 10.3390/plants12213761

Tomah, A. A., Alamer, I. S. A., Li, B., and Zhang, J.-Z. (2020b). Mycosynthesis of silver nanoparticles using screened *Trichoderma* isolates and their antifungal activity against *Sclerotinia sclerotiorum*. *Nano* 10:1955. doi: 10.3390/nano10101955

Toufiq, N., Tabassum, B., Bhatti, M. U., Khan, A., Tariq, M., Shahid, N., et al. (2018). Improved antifungal activity of barley derived chitinase I gene that overexpress a 32 kDa recombinant chitinase in *Escherichia coli* host. *Braz. J. Microbiol.* 49, 414–421. doi: 10.1016/j.bjm.2017.05.007

Triki, M., Hassaïri, A., and Mahjoub, M. (2006). Premières observations de *Verticillium dahliae* sur olivier en Tunisie. *EPPO Bulletin* 36, 69–71. doi: 10.1111/j.1365-2338.2006.00941.x

Vahidinasab, M., Adiek, I., Hosseini, B., Akintayo, S. O., Abrishamchi, B., Pfannstiel, J., et al. (2022). Characterization of *Bacillus velezensis* UTB96, demonstrating improved lipopeptide production compared to the strain *B. velezensis* FZB42. *Microorganisms* 10:2225. doi: 10.3390/microorganisms10112225

Wan, N.-F., Fu, L., Dainese, M., Kiær, L. P., Hu, Y.-Q., Xin, F., et al. (2025). Pesticides have negative effects on non-target organisms. *Nat. Commun.* 16:1360. doi: 10.1038/s41467-025-56732-x

Wang, J., Peng, Y., Xie, S., Yu, X., Bian, C., Wu, H., et al. (2023). Biocontrol and molecular characterization of *Bacillus velezensis* D against tobacco bacterial wilt. *Phytopathol. Res.* 5:50. doi: 10.1186/s42483-023-00204-x

Xiao, J., Guo, X., Qiao, X., Zhang, X., Chen, X., and Zhang, D. (2021). Activity of fengycin and iturin A isolated from *Bacillus subtilis* Z-14 on *Gaeumannomyces graminis* Var. *tritici* and soil microbial diversity. *Front. Microbiol.* 12:682437. doi: 10.3389/fmicb.2021.682437

Yang, H., Wang, T., Ji, F., Zhou, Q., and Wang, J. (2023). Effects of LED light spectrum on the growth and energy use efficiency of eggplant transplants. *Int. J. Agric. Biol. Eng.* 16, 23–29. doi: 10.25165/j.ijabe.20231603.7260

Yang, X., Zhang, Y., Cheng, Y., and Chen, X. (2019). Transcriptome analysis reveals multiple signal network contributing to the *Verticillium* wilt resistance in eggplant. *Sci. Hortic.* 256:108576. doi: 10.1016/j.scienta.2019.108576

Ying, Y., Zhang, N., Li, B., Liu, D., Zhang, Q., Yang, Z., et al. (2024). Biocontrol potential of *Bacillus velezensis* ZF-10 inhibiting potato virus Y and promoting growth of tobacco plant. *J. Phytopathol.* 172:e70002. doi: 10.1111/jph.70002

Zhang, F., Li, X.-L., Zhu, S.-J., Ojaghian, M. R., and Zhang, J.-Z. (2018). Biocontrol potential of *Paenibacillus polymyxa* against *Verticillium dahliae* infecting cotton plants. *Biol. Control* 127, 70–77. doi: 10.1016/j.biocontrol.2018.08.021

Zhang, D., Xiong, X., Wang, Y., Gao, Y., Ren, Y., Wang, Q., et al. (2021). *Bacillus velezensis* WLYS23 strain possesses antagonistic activity against hybrid snakehead bacterial pathogens. *J. Appl. Microbiol.* 131, 3056–3068. doi: 10.1111/jam.15162

Zhang, Y., Zhang, D., Zhang, Y., Cheng, F., Zhao, X., Wang, M., et al. (2024). Early detection of *verticillium* wilt in eggplant leaves by fusing five image channels: a deep learning approach. *Plant Methods* 20:173. doi: 10.1186/s13007-024-01291-3

Zhu, W., Liu, X., Chen, M., Tao, N., Tendu, A., and Yang, Q. (2021). A new miRNA miRm0002 in eggplant participates in the regulation of defense responses to *Verticillium* wilt. *Plan. Theory* 10:2274. doi: 10.3390/plants10112274

Zihalirwa Kulimushi, P., Argüelles Arias, A., Franzil, L., Steels, S., and Ongena, M. (2017). Stimulation of fengycin-type antifungal lipopeptides in *Bacillus amyloliquefaciens* in the presence of the maize fungal pathogen *Rhizomucor variabilis*. *Front. Microbiol.* 8:850. doi: 10.3389/fmicb.2017.00850

Frontiers in
Sustainable Food Systems

Exploring sustainable solutions to global food security

Aligned with the UN Sustainable Development Goals, this journal explores the intersection of food systems, science and practice of sustainability including its environmental, economic and social justice dimensions.

Discover the latest Research Topics

See more →

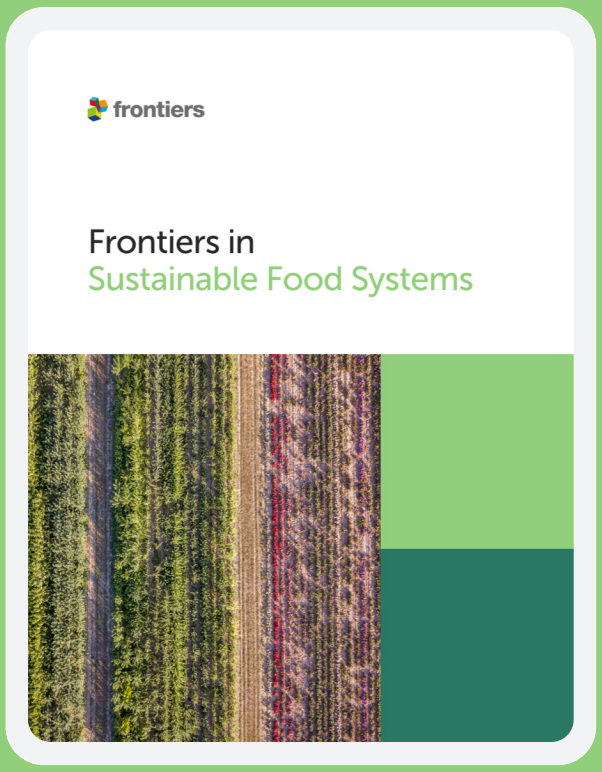

Frontiers

Avenue du Tribunal-Fédéral 34
1005 Lausanne, Switzerland
frontiersin.org

Contact us

+41 (0)21 510 17 00
frontiersin.org/about/contact